frontiers | Research Topics

Unraveling the molecular mechanisms of cytokine signaling in regulating inflammatory diseases

Edited by
Wai Po Chong, Jian Zheng and Huawei Mao

Published in
Frontiers in Immunology

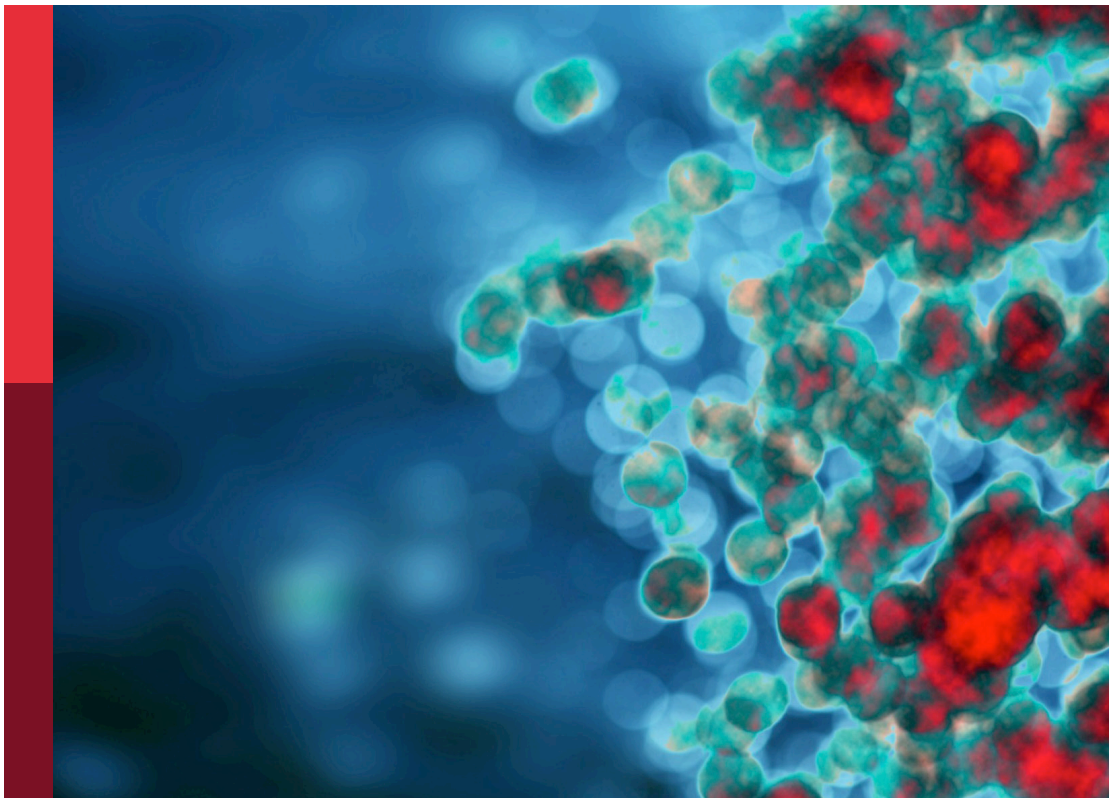

ISSN 1664-8714
ISBN 978-2-8325-6041-9
DOI 10.3389/978-2-8325-6041-9

About Frontiers

Frontiers is more than just an open access publisher of scholarly articles: it is a pioneering approach to the world of academia, radically improving the way scholarly research is managed. The grand vision of Frontiers is a world where all people have an equal opportunity to seek, share and generate knowledge. Frontiers provides immediate and permanent online open access to all its publications, but this alone is not enough to realize our grand goals.

Frontiers journal series

The Frontiers journal series is a multi-tier and interdisciplinary set of open-access, online journals, promising a paradigm shift from the current review, selection and dissemination processes in academic publishing. All Frontiers journals are driven by researchers for researchers; therefore, they constitute a service to the scholarly community. At the same time, the *Frontiers journal series* operates on a revolutionary invention, the tiered publishing system, initially addressing specific communities of scholars, and gradually climbing up to broader public understanding, thus serving the interests of the lay society, too.

Dedication to quality

Each Frontiers article is a landmark of the highest quality, thanks to genuinely collaborative interactions between authors and review editors, who include some of the world's best academicians. Research must be certified by peers before entering a stream of knowledge that may eventually reach the public - and shape society; therefore, Frontiers only applies the most rigorous and unbiased reviews. Frontiers revolutionizes research publishing by freely delivering the most outstanding research, evaluated with no bias from both the academic and social point of view. By applying the most advanced information technologies, Frontiers is catapulting scholarly publishing into a new generation.

What are Frontiers Research Topics?

Frontiers Research Topics are very popular trademarks of the *Frontiers journals series*: they are collections of at least ten articles, all centered on a particular subject. With their unique mix of varied contributions from Original Research to Review Articles, Frontiers Research Topics unify the most influential researchers, the latest key findings and historical advances in a hot research area.

Find out more on how to host your own Frontiers Research Topic or contribute to one as an author by contacting the Frontiers editorial office: frontiersin.org/about/contact

Unraveling the molecular mechanisms of cytokine signaling in regulating inflammatory diseases

Topic editors

Wai Po Chong — Hong Kong Baptist University, China

Jian Zheng — University of Louisville, United States

Huawei Mao — Capital Medical University, China

Citation

Chong, W. P., Zheng, J., Mao, H., eds. (2025). *Unraveling the molecular mechanisms of cytokine signaling in regulating inflammatory diseases*. Lausanne: Frontiers Media SA. doi: 10.3389/978-2-8325-6041-9

Table of contents

frontiers | Frontiers in Immunology

TYPE Editorial
PUBLISHED 11 February 2025
DOI 10.3389/fimmu.2025.1563469

OPEN ACCESS

EDITED AND REVIEWED BY
Silvano Sozzani,
Sapienza University of Rome, Italy

*CORRESPONDENCE
Jian Zheng
jian.zheng.1@louisville.edu
Huawei Mao
maohwei@qq.com
Wai Po Chong
chongwp@hkbu.edu.hk

RECEIVED 20 January 2025
ACCEPTED 27 January 2025
PUBLISHED 11 February 2025

CITATION
Zheng J, Mao H and Chong WP (2025) Editorial: Unraveling the molecular mechanisms of cytokine signaling in regulating inflammatory diseases. *Front. Immunol.* 16:1563469. doi: 10.3389/fimmu.2025.1563469

Editorial: Unraveling the molecular mechanisms of cytokine signaling in regulating inflammatory diseases

Jian Zheng[1,2]*, Huawei Mao[3,4,5]* and Wai Po Chong[6,7]*

[1]Department of Microbiology and Immunology, University of Louisville, Louisville, KY, United States, [2]Center for Predictive Medicine, University of Louisville, Louisville, KY, United States, [3]Department of Immunology, Ministry of Education Key Laboratory of Major Diseases in Children, Beijing Children's Hospital, Capital Medical University, Beijing, China, [4]National Center for Children's Health, Beijing Key Laboratory for Genetics of Birth Defects, Beijing, China, [5]Department of Nephrology and Rheumatology, Children's Hospital of Xinjiang Uygur Autonomous Region, Xinjiang Hospital of Beijing Children's Hospital, Xinjiang, China, [6]School of Chinese Medicine, Hong Kong Baptist University, Hong Kong, Hong Kong SAR, China, [7]Institute for Research and Continuing Education, Hong Kong Baptist University, Shenzhen, China

KEYWORDS

cytokin, inflammation, autoimmunity, infection - immunology, signaling pathway

Editorial on the Research Topic
Unraveling the molecular mechanisms of cytokine signaling in regulating inflammatory diseases

1 Background

Chronic and dysregulated inflammation is a hallmark of many autoimmune and inflammatory diseases, significantly impacting patient health and quality of life. Despite their prevalence, the intricate molecular mechanisms underlying cytokine regulation in these conditions remain poorly understood. This Research Topic aims to bridge this knowledge gap by exploring the complex network of cytokine signaling pathways and their role in immune regulation during inflammatory diseases. Through a collection of nine research articles and six review articles, we delve into the latest discoveries and insights, providing a comprehensive overview of the current state of research in this critical area.

2 Cytokine regulation in infection and associated inflammatory responses

Cambon et al. investigated cytokine profiles in the lung compartment of COVID-19 patients, particularly those with acute respiratory distress syndrome (C-ARDS). The authors evaluated caspase-1 activation, IL-1 signature, and other inflammatory cytokine pathways using post-mortem lung tissue, bronchoalveolar lavage fluid (BALF), and serum. Their findings revealed elevated levels of proinflammatory molecules such as caspase-1, IL-1β, IL-1Ra, IL-6, IFN-γ, and CXCL-10 in BALF from steroid-treated C-ARDS patients, highlighting the predominant IL-1β/IL-6 signature and IFN-γ-associated chemokines

despite steroid treatment. This study underscores the potential of targeting these pathways to improve treatment response and limit lung damage in ARDS.

In another study, Vorobyeva et al. developed an ex vivo model of SARS-CoV-2 lung infection to study cytokine production. Their findings revealed elevated concentrations of proinflammatory mediators, namely G-CSF, GM-CSF, GRO-α, IFN-γ, IL-6, IL-8, IP-10, MCP-3, MIP-1α, PDGF-AA, and VEGF in infected lung tissue, reflecting the cytokine alterations observed in COVID-19 patients. This model provides a valuable platform to investigate the mechanisms of SARS-CoV-2 infection and to test antiviral drugs.

The study by Bédard-Matteau J. et al. identified IL-17F as a key cytokine associated with severe COVID-19. Elevated IL-17F levels were found in severe cases, promoting neutrophil adhesion to endothelial cells via ERK1/2 and p38 MAPK-dependent pathways. These findings highlight the potential of targeting IL-17F signaling to mitigate neutrophilic inflammation and immunothrombosis in severe COVID-19.

Von Stemann et al. examined the association of cytokine autoantibodies (c-aAbs) with community-acquired pneumonia (CAP). They measured c-aAbs targeting various cytokines in plasma samples from 665 CAP patients. The results indicated that high-titer type 1 IFN c-aAb is more prevalent in men with SARS-CoV-2 infection, while GM-CSF c-aAb is associated with asthma and bronchiectasis comorbidities in men. These findings suggest that c-aAb specificity, comorbidity, and sex influence clinical outcomes in CAP, providing insights for personalized treatment strategies.

3 Cytokine signaling in autoimmune and inflammatory conditions

The study by Yang et al. investigated the therapeutic potential of myeloid-derived growth factor (MYDGF) in primary Sjögren's syndrome (pSS). Using a mouse model, the authors demonstrated that MYDGF treatment alleviates pSS symptoms by increasing salivary flow rate, reducing lymphocyte infiltration, and promoting M2 macrophage polarization. The study identifies the suppression of the CX3CL1/CX3CR1 axis as a key mechanism, suggesting MYDGF as a promising therapeutic target for pSS.

Lee et al. explored the role of the pregnane X receptor (PXR) in particulate matter (PM)-induced inflammation in atopic dermatitis (AD). Their findings indicated that PXR activation reduces type 17 inflammation by inhibiting the NF-κB pathway, suggesting PXR as a therapeutic target for controlling PM-induced AD aggravation. In addition, Xu et al. review the emerging role of protease-activated receptor 2 (PAR2) in various skin conditions, such as atopic dermatitis, psoriasis, vitiligo, and melasma. The review highlights the involvement of PAR2 in the cutaneous microenvironment and associated comorbidities, proposing it as a key target for therapeutic intervention.

Ouyang and Dai employed Mendelian randomization to explore the causal relationships between systemic inflammatory cytokines and adhesive capsulitis (AC). Their findings established causal associations between IP-10, RANTES, SDF-1α, TNF-α levels, and AC risk, offering new avenues for understanding AC pathogenesis and developing clinical management strategies.

Liu et al. identified MCP-3 as a significant prognostic biomarker for severe fever with thrombocytopenia syndrome (SFTS). Elevated MCP-3 levels were found to correlate with adverse outcomes. These findings provide a valuable tool for predicting prognosis and understanding the cytokine-mediated pathogenesis of SFTS.

The bibliometric review by Liu et. al. focused on leukocyte cell-derived chemotaxin-2 (LECT2). The study identified liver diseases, systemic inflammatory diseases, and amyloidosis as current research focuses, highlighting the potential of LECT2 for clinical diagnosis and treatment.

In another review, Guo et al. explored the role of the CCL2/CCR2 signaling axis in inflammatory and fibrotic diseases. CCL2, a key cytokine, binds to its receptor CCR2, modulating the recruitment and activation of immune cells and influencing the progression of fibrosis in various organs. The paper highlights recent advances in diagnosing and treating fibrotic diseases linked to this pathway and calls for further research to elucidate its clinical significance in different organ systems.

4 Advances in asthma immunology

In their review, Xie et al. discussed recent advances in asthma immunology, emphasizing the heterogeneity of immune processes and phenotypes. The paper explored the key cellular and molecular mediators involved in type 2-high and type 2-low asthma endotypes and reviews innovative biological and targeted therapies. Understanding the dynamic and complex immunopathology of asthma is crucial for the development of personalized interventions.

5 Regulatory mechanisms of cytokine signaling

Chen et al. investigated the role of LTβR signaling in chemotherapy-induced mucosal damage. The authors' suggested that LIGHT produced by T cells activates LTβR-RelB signaling in intestinal epithelial cells, promoting mucosal repair and offering insights into therapeutic strategies for chemotherapy-induced damage.

The review by Zong et al. explored the cytokine signaling pathways that regulate Treg cells and their implications for autoimmune diseases, transplant rejection, and cancer. Understanding these pathways offers potential for the development of Treg-based immunotherapies to restore immune balance.

Huang et al. examined the bidirectional regulation of the TRPM2 channel in oxidative stress, inflammation, and ischemia-reperfusion (I/R) injury. The role of the TRPM2 channel in exacerbating or protecting against cellular damage under different conditions provides insights into potential therapeutic strategies for related diseases.

6 Conclusion

This Research Topic highlights the critical role of cytokine regulation in chronic inflammatory and autoimmune diseases. By unraveling the molecular mechanisms underlying cytokine signaling pathways, we gain valuable insights into disease progression and identify potential therapeutic targets. This research contributes to the advancement of precision medicine and the development of novel treatments, ultimately improving patient outcomes in autoimmune and inflammatory diseases.

Author contributions

JZ: Writing – review & editing. HM: Writing – review & editing. WC: Writing – original draft, Writing – review & editing.

Funding

The author(s) declare financial support was received for the research, authorship, and/or publication of this article. JZ is supported by University of Louisville startup grants (F1256, F1260) and NIH-COBRE (GB180729A5). HM is supported by the Chinese Institutes for Medical Research, Beijing (CX24PY26), Beijing Hospitals Authority's Ascent Plan (DFL20221001) and Tianchi Talent Program of Xinjiang Uygur Autonomous Region. WC is supported by the National Natural Science Foundation of China (32370959), Natural Science Foundation of Guangdong province (2021A1515010569, 2022A1515012450), Hong Kong Baptist University (167664) and Innovation and Technology Fund of Hong Kong (ITS/057/23MS).

Conflict of interest

The authors declare that the research was conducted in the absence of any commercial or financial relationships that could be construed as a potential conflict of interest.

Publisher's note

frontiers | Frontiers in Immunology

TYPE Review
PUBLISHED 13 May 2024
DOI 10.3389/fimmu.2024.1387975

OPEN ACCESS

EDITED BY
Laura Maggi,
University of Florence, Italy

REVIEWED BY
Michal Kuczma,
Georgia State University, United States
Anette S. B. Wolff,
University of Bergen, Norway
Stanislaw Stepkowski,
University of Toledo, United States

*CORRESPONDENCE
Wai Po Chong
chongwp@hkbu.edu.hk

RECEIVED 19 February 2024
ACCEPTED 29 April 2024
PUBLISHED 13 May 2024

CITATION
Zong Y, Deng K and Chong WP (2024) Regulation of Treg cells by cytokine signaling and co-stimulatory molecules.
Front. Immunol. 15:1387975.
doi: 10.3389/fimmu.2024.1387975

Regulation of Treg cells by cytokine signaling and co-stimulatory molecules

Yuan Zong[1,2], Kaihang Deng[1] and Wai Po Chong[1,2]*

[1]School of Chinese Medicine, Hong Kong Baptist University, Hong Kong, China, [2]Institute for Research and Continuing Education, Hong Kong Baptist University, Shenzhen, China

$CD4^+CD25^+Foxp3^+$ regulatory T cells (Tregs), a vital component of the immune system, are responsible for maintaining immune homeostasis and preventing excessive immune responses. This review explores the signaling pathways of the cytokines that regulate Treg cells, including transforming growth factor beta (TGF-β), interleukin (IL)-2, IL-10, and IL-35, which foster the differentiation and enhance the immunosuppressive capabilities of Tregs. It also examines how, conversely, signals mediated by IL-6 and tumor necrosis factor -alpha (TNF-α) can undermine Treg suppressive functions or even drive their reprogramming into effector T cells. The B7 family comprises indispensable co-stimulators for T cell activation. Among its members, this review focuses on the capacity of CTLA-4 and PD-1 to regulate the differentiation, function, and survival of Tregs. As Tregs play an essential role in maintaining immune homeostasis, their dysfunction contributes to the pathogenesis of autoimmune diseases. This review delves into the potential of employing Treg-based immunotherapy for the treatment of autoimmune diseases, transplant rejection, and cancer. By shedding light on these topics, this article aims to enhance our understanding of the regulation of Tregs by cytokines and their therapeutic potential for various pathological conditions.

KEYWORDS

regulatory T cells, cytokines, signaling pathways, autoimmune diseases, tumors

1 Introduction

$CD4^+CD25^+Foxp3^+$ regulatory T cells (Tregs) are immunoregulatory cells that express the master transcription factor forkhead box protein 3 (Foxp3) (1). Tregs exhibit persistent and high expression of the interleukin (IL)-2 receptor alpha chain or CD25, as IL-2 is crucial for their survival and proper functioning (2). Tregs refer to those T cell subsets that can regulate or suppress the overreaction of the immune system. Although Tregs account for only 3–10% of the peripheral $CD4^+$ T cell population, they are crucial for maintaining immune tolerance by suppressing the activation, proliferation, and function of effector immune cells. They secrete anti-inflammatory cytokines such as IL-10, IL-35, and transforming growth factor beta (TGF-β) to inhibit immune cells in a contact-

independent manner (3, 4). Additionally, Tregs possess a high level of CD25 surface expression, which leads to the consumption of IL-2 in the surrounding environment. This consumption helps restrict the proliferation and activation of effector T cells (Teffs) (5). Tregs also suppress immune cells through contact-dependent mechanisms involving co-stimulatory molecules, such as cytotoxic T lymphocyte–associated protein 4 (CTLA-4), programmed cell death protein 1 (PD-1), and programmed death ligand 1 (PD-L1) (6–10). Through these regulatory mechanisms, Tregs play a crucial role in inhibiting the activity of immune cells, ensuring the balance of the immune system, and preventing the occurrence of excessive immune responses and the development of autoimmune diseases (11, 12).

Tregs can be classified based on their developmental origins (13). Thymus-derived Tregs (tTregs) develop in the thymus, while a small proportion of Tregs is derived from conventional T cells (Tconvs) or peripherally derived Tregs (pTregs) and matures under specific conditions, such as exposure to microbial antigens in the intestinal mucosa (14). In the presence of specific cytokines (i.e., TGF-β and IL-2), antigen stimulation *in vitro* can induce the expression of Foxp3 in Tconvs, which exhibit phenotypic and functional characteristics similar to those of tTregs and pTregs and are called inducible Tregs (iTregs) (15). Subsets of Tregs in peripheral blood exhibit T helper–like characteristics, meaning they share chemokine receptor and transcription factor expression with T helper cells (16). Examples include Th1-Tregs ($CXCR3^+$ $T\text{-}BET^+$ $Foxp3^+$ Tregs) and Th2-Tregs ($CCR8^+$ $GATA3^+$ $Foxp3^+$ Tregs) (17). Another type of T helper–like Treg cell is the follicular regulatory T (Tfr) cell, which suppresses follicular helper T (Tfh) cells. Tfr cells play a critical role in germinal center reactions and antibody production, and defects in Tfr cells lead to antibody accumulation and the occurrence of widespread autoimmune diseases (18–20). These Treg subsets are summarized in Table 1.

The complex interactions among T cell subsets are characterized by diverse functional dynamics. Both iTregs and pTregs typically differentiate from Tconvs, a step critical for peripheral tolerance. It is essential to distinguish tTregs from pTregs and iTregs as they display distinct roles in maintaining central tolerance. The transcription factor Helios has been identified as a biomarker for stable tTregs (32). Additionally, research has uncovered specialized subsets of Tregs, such as Th1-Tregs and Th2-Tregs, each characterized by distinct functions tailored to modulate Th1 and Th2 responses, respectively (33, 34). Indeed, the Treg compartment exhibits a degree of plasticity that enables Tregs to modulate their suppressive functions according to the surrounding microenvironment. For example, interferon gamma (IFN-γ) or IL-27 induce Th1-Tregs with expression of Th1-related molecules, namely chemokine (C-X-C motif) receptor 3 (CXCR3) and T-box gene expressed in T cells (T-bet) (35), which can migrate to sites of Th1 inflammation and suppress Th1 cells effectively (36). Th2-specific Tregs are tailored to suppress Th2 responses, which are associated with allergic inflammation and characterized by Th2 cytokines like IL-4, IL-5, and IL-13, as well as GATA binding protein 3(GATA3) (37, 38).

The development and function of Tregs are heavily reliant on cytokines and co-stimulatory molecules. Exploring their regulatory mechanisms in Tregs is essential for gaining a deeper understanding of immune regulation, the development of related diseases, and the potential for new immunotherapeutic approaches. This review focuses on the role of these signaling pathways in Tregs and their potential implications for future therapeutic strategies.

2 Treg-promoting cytokines

2.1 TGF-β

TGF-β is a multifunctional cytokine produced by macrophages and T cells that plays a critical role in immune regulation. TGF-β exerts its immunoregulatory effects primarily by modulating the development and function of T cell subsets (39). TGF-β induces the expression of Foxp3, a key transcription factor for Tregs, by activating the suppressor of mothers against decapentaplegic (SMAD) signaling pathway (40). This promotes the generation of Tregs, which suppress inflammation and prevent autoimmune reactions. Members of the TGF-β family cooperate with receptors as ligands to form receptor complexes and activate receptor-regulated SMAD (R-SMAD), which cooperates with common mediator SMAD (Co-SMAD) to enter the nucleus. By identifying different SMAD-binding proteins and forming complexes, the specific expression of various target genes is regulated, and multiple biological effects of TGF-β ultimately occur (41). The SMAD family of proteins is the first set of signaling molecules involved in TGF-β signal transduction (40), and this signaling is tightly regulated by inhibitory SMAD (I-SMAD i.e., SMAD6 and SMAD7). The N-terminal domains of SMAD6 and SMAD7 share only 37% homology, while chimeras containing the SMAD7 N-terminal domain and SMAD6 MH2 domain inhibit TGF-β signaling pathways in the same manner as SMAD7 (42). SMAD6 is biased to inhibit signaling pathways induced by the BMP type I receptors ALK-3 and ALK-6. $SMAD6^{-/-}$ mice can develop a variety of cardiovascular diseases (43). SMAD7 inhibits the formation of SMAD complexes and prevents the phosphorylation of SMAD2 and SMAD3, thereby interrupting the signaling cascade and influencing TGF-β signaling and Treg induction (Figure 1) (44).

TGF-β also plays an important regulatory role in the balance between Treg and Th17 cell differentiation (45). Endogenous TGF-

TABLE 1 Treg subtypes and their specific markers and characteristics.

Treg Subtype	Origin	Main Markers
pTregs (21, 22)	Peripheral	GATA3, IRF4, RORC, TBX21, HELIOS
tTregs (21, 23)	Thymus	CCR7, CD45RA, CD31, SELL, NRP1
iTregs (21, 24, 25)	Peripheral	Treg-specific demethylated region (TSDR)
Th1-Tregs (26)	Peripheral	CXCR, Tbet
Th2-Tregs (27, 28)	Peripheral	IL-4, IL-13, IRF4 CCR6-, CXCR3-, CCR4, GATA3
Tr1 (29, 30)	Peripheral	IL-10, CD49b, Lag3, Foxp3-
Tr35 (31)	Peripheral	IL-35, Foxp3-

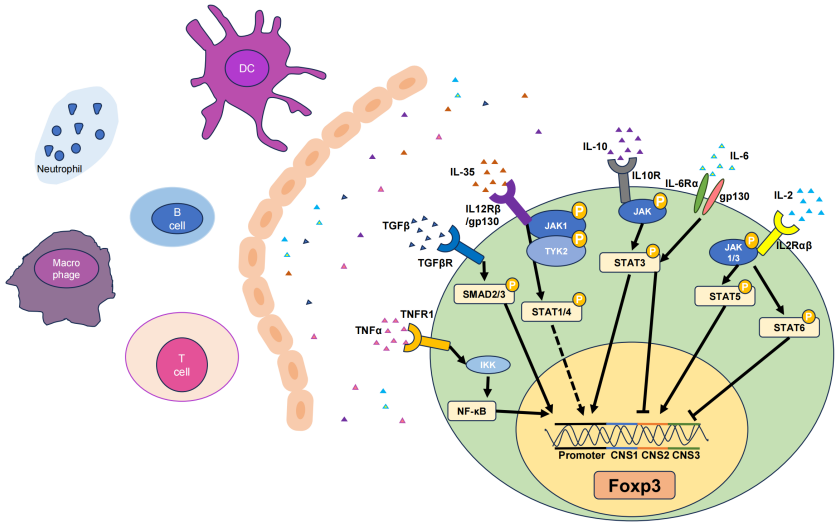

FIGURE 1
Six cytokines that promote Tregs. The TNF-α, TGF-β, IL-6, IL-35, IL-10, and IL-2 pathways can influence their respective receptors to varying degrees, thereby activating different signaling pathways and ultimately upregulating the transcription levels of Foxp3, resulting in increases in the number and stability of Tregs. Among them, there are gene loci that represent the corresponding signaling pathways and functions of different cytokines. Solid lines indicate pathways that have been functionally analysed, while dashed lines represent the effect on the Foxp3 gene without specific key loci identified. JAK, Janus-family tyrosine kinase; CNS, non-coding sequence; TYK2, tyrosine kinase 2. Arrows represent signal path direction, dashed lines represent ambiguity, and horizontal lines represent suppression.

β, along with inflammatory mediators such as IL-6, IL-21, and IL-23, inhibits Foxp3 expression and initiates the differentiation pathway of retinoic acid receptor–related orphan receptor gamma-t (RORγt)–mediated Th17 cells (46). As IL-6 levels decrease during the late phase of inflammation, TGF-β alone promotes the expression of Foxp3 for Treg differentiation and suppresses RORγt to limit Th17 cells, thus maintaining Treg function and controlling the effector cell response for the termination of the immune response (47, 48). Within the cell, the TGF-β/SMAD signaling pathway promotes the expression of Foxp3. SMAD3 can cooperate with nuclear factor of activated T cells (NFAT) to enhance histone acetylation in the Foxp3 enhancer region, thereby inducing Foxp3 transcription (49). Compared to controls, $SMAD3^{-/-}$ mice exhibit a significant reduction in the quantity of Foxp3 induced by TGF-β (50).

The combination of TGF-β and the immunosuppressant rapamycin can significantly promote the proliferation of Tregs, indicating that rapamycin relies largely on TGF-β to exert its immunosuppressive effect (51). Rapamycin is a 32-ring azotriene-containing macrolide that inhibits immunity by inhibiting IL-2 signal transduction by blocking mTOR which is important in IL-2 receptor signaling (52). The IL-2 receptor signaling also leads to the activation of the PI3K/Akt pathway. Akt then activates mTOR by inhibiting the tuberous sclerosis complex (TSC1/TSC2), which normally suppresses mTOR activity. The rapamycin the FK506-binding protein 12 (FKBP12) complex binds to mechanistic target of rapamycin complex1 (mTORC1), inhibits the mammalian target protein of rapamycin (mTOR) pathway, and induces immunosuppression (53). By inhibiting mTORC1, rapamycin effectively blocks the downstream effects of mTOR activation, including protein synthesis and cell cycle progression, which are necessary for T cell proliferation. High-dose rapamycin can promote the proliferation of Tregs by inhibiting the mTOR signaling pathway, thereby significantly inhibiting the progression of experimental autoimmune encephalomyelitis (EAE) in a model and eventually mitigating the incidence and EAE clinical scores of each stage (early onset, peak, and remission) (54).

Many preclinical studies have shown that blocking TGF-β signaling is an effective anti-tumor treatment that can reduce Treg-mediated immunosuppression, increase $CD8^+$ T cell cytotoxicity, promote T cell penetration into the center of the tumor, and thus contribute to strong anti-tumor immunity and tumor regression (55). TGF-β suppresses the immune system by modulating the function of immune cell classes in the tumor microenvironment (TME) (56, 57).

2.2 IL-2

IL-2 is a cytokine mainly produced by activated $CD4^+$ T cells, particularly Th1 subsets (58). In the thymus and peripheral lymphoid organs, IL-2 signaling promotes the differentiation and development of Tregs by binding to the high-affinity IL-2 receptor (IL-2R), which is a heterotrimer consisting of the IL-2R(α/β/γ) subunits. This leads to an increase in Foxp3 gene expression in T cells, promoting the differentiation of $Foxp3^+$ Tregs (59). Upon IL-2 binding to its receptor, the receptor-associated JAKs, specifically JAK1 and JAK3, are activated. JAK1 is associated with the IL-2Rβ chain, and JAK3 is closely linked with the IL-2Rγ chain (60). The activation of JAK kinases is initiated by their phosphorylation, which subsequently enables them to phosphorylate IL-2Rβ and other downstream signaling molecules. This phosphorylation creates docking sites for

signaling molecules containing SH2 domains. Specifically, STAT5 is attracted to the phosphorylated IL-2Rβ chain. Within the STAT5 family, there are two distinct proteins, STAT5A and STAT5B, both of which undergo phosphorylation by the action of JAK kinases (61). Once phosphorylated, STAT5 proteins form homodimers or heterodimers, dissociate from the receptor, and translocate to the nucleus where they bind to specific DNA elements and promote the transcription of target genes (62). Previous studies have revealed that IL-2 signaling activates STAT5 and promotes Foxp3 expression by binding to the intronic enhancer element within conserved non-coding sequence 2 (CNS2) of the Foxp3 gene cluster (Figure 1) (63). This process is essential for maintaining Foxp3 expression in mature Treg cells. Phosphatase 2A (PP2A) is a negative regulator of IL-2 production in Teffs (64) and prevents IL-2Rβ from being clipped from the cell surface by restricting the activity of ADAM metallopeptidase domain 10 (ADAM10) in Tregs, thereby achieving effective IL-2R signaling and ultimately affecting Tregs (65).

IL-2 and IL-2/anti–IL-2 mAb immunocomplexes have been shown to have therapeutic efficacy against autoimmune diseases in preclinical studies via Treg promotions. The complex of IL-2/JES6 (IL-2 and JES6–1 mAb) can selectively expand Tregs for the suppression of autoimmune diseases in EAE (66). With increasing research on the immune regulatory mechanism of low-dose IL-2, IL-2 has gained attention as a potential treatment for various immunological diseases, such as graft-versus-host disease (GvHD) (67), hepatitis C–related vasculitis (68), and type 1 diabetes (69). Low-dose IL-2 promotes a balance between Treg and Th17 cells in patients with Sjögren's syndrome (SS), a condition characterized by dryness (70). In patients with inflammatory myopathy who received 500,000 IU of IL-2 therapy for 5 days, Treg cell numbers significantly increased, while erythrocyte sedimentation rates, muscle enzyme levels, and pain scores significantly decreased (71). Recent clinical studies have shown that low-dose IL-2 is safe and effective against 11 autoimmune diseases, including rheumatoid arthritis (RA) and ankylosing spondylitis (72). Overall, the IL-2 signaling pathway moderates the role of Tregs in immune regulation and self-tolerance by affecting their development, proliferation, survival, and function.

2.3 IL-10

IL-10 is produced by macrophages, monocytes, and T cells and is considered a Th2 cytokine and an anti-inflammatory cytokine. IL-10 signaling requires the presence of cell surface–expressed IL-10 receptors (IL-10R) (73). IL-10 induces STAT3 signaling by phosphorylating the cytoplasmic tails of IL-10R1 and IL-10R2 through Janus-family tyrosine kinase 1 (JAK1) and non-receptor tyrosine-protein kinase (Tyk2), respectively (74). IL-10$^{-/-}$ mice exhibit more severe inflammatory damage, as IL-10 can regulate the function of Tregs through the activation of STAT3, and the lack of IL-10 leads to a significant decrease in STAT3 phosphorylation in microglia. Although the IL-10 promoter lacks binding sites for Foxp3, it does contain binding sites for STAT3, suggesting that Foxp3 may modulate IL-10 expression indirectly through STAT3 signaling. Indeed, Foxp3 is involved in the transcriptional activation of IL-10 by acetylating STAT3 through histone acetyltransferases (HATs), forming the most important connection between IL-10 and Foxp3 (Figure 1) (75). Although IL-10 signaling is not required for the induction of Tregs, it is required for Tregs to mediate their suppressive function. For example, IL-10R is indispensable for Tregs to suppress the autoreactive Th17 response (PMID: 21511185). IL-10 may auto-regulate its expression through a negative feedback loop, which involves the autocrine stimulation of IL-10R and inhibition of the p38 signaling pathway (76). Additionally, IL-10 expression is widely regulated at the post-transcriptional level, possibly involving AU-rich element (77), let-7 (78), or miR-106 (79). Under normal conditions, human iTreg cells produce low levels of IL-10. Inhibiting glycogen synthase kinase-3 (GSK3) can significantly upregulate IL-10 expression in Tregs and promote the generation of IL-10^{+} Foxp3^{+} iTreg cells (80).

IL-10 is predominantly secreted by type 1 regulatory T cells (Tr1 cells). Tr1 cells are typically induced from naïve T cells in the periphery, their differentiation can be driven by several factors, including IL-10, IL-27, and TGF-β (81). The transcription factors (TFs) *c-Maf* interacts with *AhR* to synergistically transactivate the IL-10 and IL-21 promoters, thereby promoting IL-27-induced differentiation of murine Tr1 cells (82). Tr1 cells are characterized by their lack of Foxp3 expression and are identified by the co-expression of CD49b and LAG-3, which serve as distinctive markers in both humans and mice (83). Tr1 cells play a critical immunoregulatory role in promoting tolerance in transplant scenarios, such as renal and pancreatic islet transplantation in humans and mice, and in reducing GvHD following hematopoietic stem cell transplantation, largely through their IL-10 mediated activities and antigen-specific actions (84–86). Tr1 cells have also been shown to ameliorate autoimmune diseases by inhibiting pathogenic Th17 response in experimental autoimmune encephalomyelitis and experimental autoimmune uveitis (87, 88).

IL-10 is a major cytokine involved in Treg-mediated immune regulation and immunosuppression (89). It primarily acts on monocytes and macrophages. IL-10 can inhibit the secretion of the pro-inflammatory cytokines TNF-α and IL-1β by monocytes and macrophages (90). IL-10 also inhibits IL-12 synthesis, hindering the differentiation of Th1 cells (73, 91). Blocking the Treg-mediated suppression of Teffs can be achieved by using anti–IL-10 neutralizing antibodies (92). Treg cells regulate the expression of IL-10 through the transcription factor B-lymphocyte-induced maturation protein-1 (Blimp-1). Mice lacking Blimp-1 in peripheral effector CD4^{+} and CD8^{+} T cells show increased cell numbers, while the overexpression of Blimp-1 in T cells promotes the differentiation of Treg cells and enhances their inhibitory effect on T cell proliferation (93). This highlights the importance of IL-10 in mediating the immunosuppressive function of Treg cells.

In addition, IL-10 has various other regulatory functions. It can induce the differentiation of Th0 cells into helper T cells (Th2), while inhibiting Th1 differentiation, thereby affecting the balance between Th1 and Th2 immune responses (94). IL-10 can also inhibit antigen presentation and prevent monocytes and macrophages from producing pro-inflammatory cytokines. IL-10 can inhibit the secretion of IL-6 and IL-12 by dendritic cells (DCs), thereby suppressing Th17 differentiation (95–97). Compared to

wild-type mice, IL-10$^{-/-}$ mice exhibit more severe arthritis, decreased numbers of Tregs, decreased expression of Foxp3, and increased numbers of Th1 and Th17 cells. This further confirms that IL-10 may work in coordination with Tregs and other immune cells to inhibit the differentiation and development of Th1 and Th17 cells, exerting negative immune regulatory effects (98). The immunostimulatory capacity of IL-10 in the context of immunoregulation has been demonstrated. IL-10 expression in tumor cell lines transfected from IL-10 transgenic mice controls primary tumor growth and reduces the burden of metastasis (99). Recombinant mouse IL-10 has been shown to induce IFN-γ and CD8$^+$ T cell–dependent anti-tumor immunity *in vivo* (100, 101).

2.4 IL-35

IL-35, a member of the IL-12 family, is a heterodimeric protein that consists of p35 and Epstein-barr virus-induced gene 3 (EBI3) (102). It can be secreted by Tregs. IL-35 can be expressed in various tissues and environments, such as the thymus, peripheral lymphoid organs, and inflammatory sites, and influences the generation and maintenance of Tregs by activating the IL-35 receptor (IL-35R) (103). IL-35 not only suppresses effector T cells but also promotes the conversion of CD4$^+$ T cells into IL35-producing induced regulatory T cells (iTr35). IL-35 triggers signal transduction by binding to IL-35R, which is composed of two subunits (i.e. IL-12Rβ2 and IL-27Rα) and subsequently activates the JAK family (102). Specifically, IL-35 induces the phosphorylation and activation of the JAK1 and Tyk2 kinases (104). Activated JAK further phosphorylates and activates STAT proteins, including STAT1 and STAT4 (Figure 1) (105). These phosphorylated STAT proteins undergo conformational changes, form dimers or multimers, and then translocate to the cell nucleus, where they can activate the transcription of the Foxp3.

The function of Tregs proved effective in EBI3$^{-/-}$ and p35$^{-/-}$ mice, that is, IL-35 subunit knockout models, suggesting that IL-35 plays an important role in maintaining the function of Tregs (106). The immunosuppressive capacity of Tregs in EBI3$^{-/-}$ and p35$^{-/-}$ mice was significantly diminished compared to that of Tregs in wild-type mice. In cases of human colon cancer, the expression level of IL-35 in tumor tissues was positively correlated with the degree of malignancy and clinical stage of the tumor. Additionally, a strong positive correlation between the level of IL-35 expression and the number of Tregs in peripheral blood has been noted (107). Therefore, tumor-derived IL-35 may promote tumor growth by recruiting Tregs into the TME (108). Another study conducted by Meghan et al. demonstrated that targeting IL-35 can potentially serve as a therapeutic strategy for tumor suppression. Their research findings revealed that the neutralization of IL-35 led to enhanced tumor control in wild-type C57BL/6 mice when compared to control mice (109).

In summary, IL-35 plays an important role in immune regulation and immune balance by regulating the development of Tregs, enhancing Foxp3 expression and function, and exerting immunosuppressive effects.

3 Treg-inhibitory cytokines

3.1 IL-6

IL-6 is an inflammatory cytokine linked to autoimmune and inflammatory diseases (110). It can be produced by lymphoid and some non-lymphoid cells. It can also be secreted by fibroblasts, endothelial cells, keratinocytes, mesangial cells, and tumor cells. The pro-inflammatory properties of IL-6 include inhibition of the immunosuppressive capacity of Tregs and interference with their differentiation from naïve T cells (111). Studies have shown that high levels of IL-6 and IFN-γ inhibited the expression of Foxp3 during the differentiation of Tregs (112, 113). In early pregnancy, C57BL/6 models, which are susceptible to congenital toxoplasmosis, exhibited elevated IL-6 but reduced expression of Foxp3 in response to congenital toxoplasmosis infection when compared to the infection-resistant Balb/c models (114). *In vitro* activation of purified mouse CD4$^+$ CD25$^+$ Foxp3$^+$ T cells caused their differentiation into Th17 in the presence of IL-6 (47, 115, 116). Therefore, IL-6 is the key factor determining whether naïve CD4$^+$ T cells differentiate into Treg or Th17 cells (117). The deletion of IL-6 and TGF-β in mice contributes to the depletion of Th17 cells, which leads to the failure of EAE modeling (118–120). When IL-6 is present at inflammatory sites, such as sites of mucosal inflammation, it can cause phosphorylation of the downstream STAT3 through tyrosine (121). Hyperactivity of p-STAT3 can increase the expression of the transcription factor RORγt in T cells, followed by a decrease in Foxp3 expression, thus causing CD4$^+$ T cells to differentiate into Th17 cells instead of Tregs (120, 122). Another study reported that when co-cultured with multiple myeloma (MM) cells, bone marrow stromal cells could secrete IL-6 and thereby transform Tregs into Th17 cells, a finding further verified in animal models (123, 124). In preclinical studies, IL-6 monoclonal antibodies demonstrated positive drug synergies (e.g., between bortezomib, melphalan, and dexamethasone), thereby enhancing the effectiveness of MM treatment. This improvement may be attributed to the Treg/Th17 ratio (125, 126). Interestingly, retinoic acid, a metabolite of vitamin A, could regulate TGF-β–dependent immune responses and prevent IL-6 from inducing pro-inflammatory Th17 cells and promoting the differentiation of anti-inflammatory Tregs (127), indicating the complexity of the balance of Th17 cells and Tregs.

3.2 TNF-α

TNF-α is an inflammatory cytokine that mediates inflammation and may cause tissue damage. It is secreted by macrophages, monocytes, neutrophils, CD4$^+$ T cells, and natural killer (NK) cells. While TNF-α is typically known for enhancing immune responses and promoting inflammation, it has also been shown to inhibit Treg function (128). TNF-α suppresses the differentiation and development of Tregs, leading to a reduction in their numbers (129). During Treg differentiation, the presence of TNF-α interferes with the TGF-β signaling pathways. This involves

disruption of the activation and transduction of downstream signaling molecules, such as the phosphorylation and nuclear translocation of the SMAD protein family, subsequently affecting Foxp3 expression and Treg differentiation (129). Previous studies have reported that TNF-α, through tumor necrosis factor receptor 2 (TNFR2) activation, played a role in the expansion and amplification of Tregs (130). Approximately 30–40% of peripheral blood Tregs express TNFR2, which can be upregulated by TNF-α (131). Interestingly, only Tregs that express TNFR2 exhibit strong immunosuppressive activity, while Tregs lacking TNFR2 display minimal to no immunosuppressive activity. Therefore, the TNF–TNFR2 signaling pathway is necessary for maintaining the function and phenotypic stability of Tregs in the body (132). When compared to conventional CD4 single-positive cells, members of the TNF receptor superfamily, including glucocorticoid-induced TNFR-related (GITR), CD134, and TNFR2, are overexpressed on Treg precursor cells. These receptors enhance T cell receptor (TCR) signaling through TGF-β–activated kinase 1 (TAK1) and CD28-dependent signaling pathways. Treg precursor cells lacking TAK1 and CD28 cannot express GITR, CD134, or TNFR2, resulting in the inhibition of $Foxp3^+$ Treg maturation (133).

The systemic injection of an anti–TNF-α neutralizing antibody, such as infliximab, can induce IL-10 in $CD4^+$ T cells and Th17 cells, as well as Aiolos binding of conserved regions of IL-10. However, in the treatment of Crohn's disease with anti–TNF-α therapy, $IL\text{-}17^+$ cells in the intestines of patients decreased significantly after 3 months of treatment, and $Foxp3^+$ cells were unstable. However, the $IL\text{-}17^+/CD4^+$ and $IL\text{-}17^+/Foxp3^+$ ratios were both decreased, suggesting that TNF-α and a balanced relationship between Th17 cells and Tregs are key factors in the treatment of the disease (134–136). TNF-α can damage the function of T cells by enhancing the dephosphorylation of Foxp3; and their function can be restored by TNF-α antagonist therapy, thereby indirectly regulating the interaction between T cells and Th17 and Th1 cells, which affects autoimmune inflammation in RA (137). It is important to note that the inhibitory effects of TNF-α on Tregs may be beneficial in certain contexts, such as enhancing anti-tumor immune responses by reducing the suppressive effects of Tregs (138). The accumulation of Tregs in the TME has been identified as one of the major factors in the initiation and development of immune checkpoint inhibitor resistance (139). The CC motif chemokine receptor 8 (CCR8) is a marker of activated inhibitory Tregs and has a significant impact on the function of Tregs in the TME (140). High levels of TNF-α in the colorectal cancer (CRC) TME upregulate CCR8 expression in Tregs via the TNFR2/NF-κB signaling pathway and Foxp3 transcription factor. Depletion or blockade of TNFR2 inhibits gastrointestinal tumor progression by reducing $CCR8^+$ Treg infiltration, thereby enhancing the efficacy of anti–PD-1 therapy (140, 141).

4 Co-stimulatory molecules

Co-stimulatory molecules, such as CTLA-4 and PD-1 are also crucial for Treg cell activation and function (Figure 2). The B7 family is composed of a group of cell-surface molecules primarily found on antigen-presenting cells (APCs), such as DCs, macrophages, and B cells (142). These molecules provide co-stimulatory or co-inhibitory signals that are crucial for the activation, differentiation, and survival of T cells, thereby playing an essential role in the regulation of T cell–mediated immune responses, especially in the field of immuno-oncology (143). CTLA-4, PD-1, and PD-L1 are the most extensively studied and clinically applied immune checkpoint molecules to date (144). Some clinical trials and studies have shown that the combined use of nivolumab (a PD-1 inhibitor) and ipilimumab (a CTLA-4 blocker) is more effective for patients with advanced melanoma (145). The use of immune checkpoints has ushered in a new era in tumor treatment.

4.1 CTLA-4

CTLA-4 is a co-stimulatory molecule expressed on the surface of effector T cells (146). Interestingly, Treg cells also constitutively

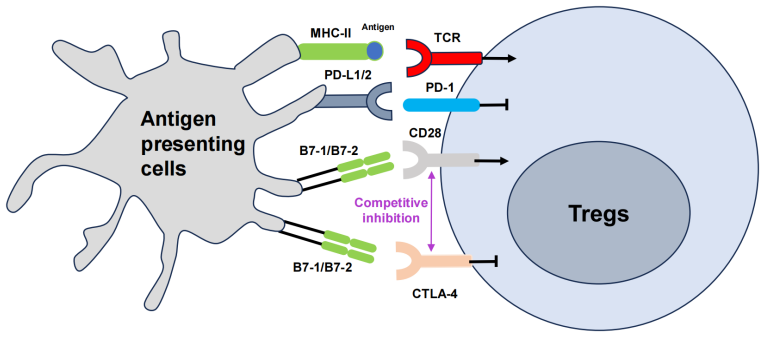

FIGURE 2
The role of co-stimulatory molecules in Treg cells, namely CTLA-4 and PD-1. The T cell receptor (TCR) engages the major histocompatibility complex (MHC)-peptide complex on APCs. The interaction between CD28 on T cells and B7 on APCs triggers costimulatory signaling, which is vital for T cell activation. Cytotoxic T lymphocyte-associated antigen 4 (CTLA-4) mitigates this activation by outcompeting CD28 for its ligands B7, thus attenuating the costimulatory signal. Concurrently, the interaction of programmed cell death protein 1 (PD-1) on T cells with its ligands PD-L1 or PD-L2 also transmitted by APCs, further modulates immune responses, generally by dampening T cell activity. The arrows represent positive regulation of the Tregs response, and the horizontal lines represent negative regulation.

express CTLA-4 for fine tuning T cell activation through the obstruction of co-stimulatory signals (147). CTLA-4 exhibits higher binding affinity for the co-stimulatory molecules CD80/CD86 than CD28, thereby effectively outcompeting it (148). Additionally, CTLA-4 is involved in the 'trans-endocytosis' of CD80 and CD86 from APCs, further inhibiting their availability for co-stimulatory interactions (147). These actions are crucial for Treg cells to exert control over T cell activation and to prevent autoimmune responses (149). The absence of CTLA-4 disrupts Treg cell function, leading to unchecked proliferation and activation of Tconvs, which can result in autoimmune pathology (150). Researchers have shown that introducing the extracellular domain of CTLA-4 (cdCTLA-4) into mice lacking CTLA-4 fully restores Treg activity, suggesting that cdCTLA-4 is sufficient to provide inhibitory function (151). This implies that CTLA-4 function may not necessarily involve a signal transduction process. In another study, the expression of CTLA-4 in $CD4^+$ $CD25^+$ $Foxp3^+$ Treg cells was elevated both in the blood of patients with pulmonary tuberculosis and in the pleural cavity of individuals with tuberculosis pleurisy. Blocking CTLA-4 weakened the ability of $Foxp3^+$ Tregs to suppress the IFN-γ T effector response to the effect of purified protein derivative (PPD) stimulation, and this reversal effect was not consistent with the decrease in IL-10. Blocking CTLA-4 reversed the ability of Tregs to inhibit PPD-driven IFN-γ and IL-2 responses at the mRNA level, while IL-10 and TGF-β did not show significant changes. Blocking CTLA-4 significantly eliminated the inhibitory effect of $Foxp3^+$ Tregs on the PPD-specific T cell proliferation response (152). Therefore, CTLA-4 is a promising new target for immunotherapy for active tuberculosis (153).

Research on CTLA-4 is still in the stage of determining its physical activity. However, although the mechanism is currently obscure, it does not affect the positive clinical effects of anti–CTLA-4 drugs in arousing an immune response and treating tumorigenicity. CTLA-4-targeting agents serve various immunomodulatory roles. Abatacept (Orencia), which includes the CTLA-4 domain, is employed for treating RA and is used to prevent organ transplant rejection, as seen with belatacept (Nulojix). Distinct from ipilimumab (Yervoy), an FDA-approved melanoma treatment that blocks CTLA-4 to stimulate the immune response, abatacept mimics CTLA-4 on T cells. It competes with CD28 for binding to B7 molecules on APCs, thereby blocking the co-stimulatory signal required for T cell activation (154). Belatacept, a derivative of abatacept, with an alteration of merely two amino acids, exhibits a tenfold increase in activity compared to its precursor, more effectively inhibiting the CD28-mediated co-stimulatory signaling of T cells (155). The idea of CTLA-4 target druggability is mainly based on the high-affinity binding of anti-CTLA-4 antibodies to CTLA-4 molecules, mediating Treg depletion or functional blockade, thereby enhancing T cell activation and the immune response to cancer (156). CTLA-4 is involved in maintaining tolerance to autoimmune diseases, such as diabetes, as well as spontaneous abortion tendencies (157–159). Single nucleotide polymorphisms in exon 1 of CTLA-4 have been linked to susceptibility to several autoimmune diseases, including multiple sclerosis (160). The antibody-mediated blocking of CTLA-4 prevents the development of tolerance, enhances the anti-tumor response, and exacerbates autoimmune disease (161). In clinical trials, CTLA-4 development is mainly divided into two treatment modalities: monoclonal antibody or combined with PD-1/PD-L1 monoclonal antibody. Bispecific antibodies have also been constructed by association with other popular targets (162).

4.2 PD-1

PD-1 is a co-inhibitory receptor primarily expressed on activated T cells, B cells, and APCs. PD-1, through binding to its ligands PD-L1 and PD-L2, inhibits T cell activation and function to prevent excessive immune responses (163). Tregs express higher levels of PD-1 on their surfaces compared to $CD4^+$ Th cells (164). This indicates that PD-1 plays an important role in the regulation of Tregs. When PD-1 binds to its ligands, PD-L1 or PD-L2, it exerts inhibitory effects (163). PD-1 activation suppresses signal transduction pathways that activate T cells, leading to reduced cell proliferation and cytokine production, thereby limiting the intensity and duration of immune responses (165). The PD-1 signaling pathway in Tregs can regulate their suppressive function and immune regulatory roles. Evidence from multiple studies indicates that PD-1 inhibits the suppressive abilities of Tregs (166). Isolation of $PD\text{-}1^{hi}$ and $PD\text{-}1^-$ cells from the peripheral blood of healthy individuals has revealed that Tregs with higher levels of PD-1 show diminished suppressive function and elevate production of IFN-γ (167). Mouse model experiments further demonstrate that Tregs lacking PD-1, or those from mice treated with PD-1 blocking antibodies, exhibit enhanced suppressive capabilities (168). In tumor environments, blocking PD-1 not only improves the function of $PD\text{-}1^+$ $CD8^+$ T cells but also intensifies the immunosuppressive effects of $PD\text{-}1^+$ Tregs (169). As a result, the effectiveness of PD-1 inhibitors in treating patients is determined by their complex interplay with both effector T cells and Tregs, which highlights the crucial role of the PD-1 in controlling Tregs.

An *in vivo* mouse MC38 (CRC cell line) subcutaneous transplantation tumor model and an azoxymethane (AOM)/dextran sodium sulfate (DSS)–induced spontaneous CRC model both confirmed that gallic acid can affect Foxp3 protein levels by targeting the expression of ubiquitin specific peptidase 21 (Usp21) in Tregs, inducing the formation of Th1-like Tregs and reducing their immunosuppressive function (170). Simultaneously, gallic acid can enhance the anti-tumor effect of anti–PD-1 immune checkpoint blocking and downregulate the expression of PD-L1 protein in Tregs, indicating that the deubiquitinating enzyme Usp21 can deubiquitinate and stabilize the PD-L1 protein. PD-1 was also expressed on $CD4^+$ $Foxp3^+$ $CXCR5^-$ Tregs and inhibited the activity of lymphocytes by downregulating then maintaining the expression level of Foxp3 protein (171). Neuropilin-1 (NRP-1) plays an essential role in maintaining the stability and function of Tregs within tumors (172). On the one hand, an increase in the NRP-1 phenotype induces the production of IFN-γ in the tumor,

which increases the vulnerability of Tregs, weakens tumor immunosuppression, and enhances antitumor immunity, which is related to the prognosis of melanoma (173) and head and neck squamous cell carcinoma (174). On the other hand, the susceptibility of Treg cells to IFN-γ, which is induced by anti–PD-1 therapy, is a potential mechanism underlying the effectiveness of anti–PD-1 drugs. These drugs stimulate the production of significant quantities of IFN-γ (175). Recently, several studies have reported correlations between tumor PD-L1 expression, objective response rate, and PD-1/PD-L1 inhibitors, suggesting that PD-L1 may become an effective biomarker (176, 177).

5 Potential of Treg-based immunotherapy

The overall outcome of these interactions between Treg subpopulations, cytokines, and co-stimulatory molecules is a finely-tuned immune system that can respond to pathogens aggressively. Based on the characteristics of different subsets of Tregs, different strategies can be utilized to treat autoimmune diseases (178, 179). To date, early clinical trials using Treg cell therapy have shown great promise in the fields of transplantation rejection (180), GvHD (181), and autoimmune diseases (179). However, one of the main challenges in these studies is the isolation of pure Tregs and their expansion to a sufficient clinical dose. The principle of Treg cell therapy is to restore the balance between Teffs and immune regulatory cells by injecting an effective dose of Tregs into the patient's body, thus promoting immunological tolerance (182).

5.1 Autoimmune diseases

Tregs play a pivotal role in upholding immune tolerance to self-antigens, thereby preventing the activation and proliferation of self-reactive T cells that may not be eliminated during thymic selection. They also inhibit APCs, such as DCs, which are instrumental in triggering immune responses (183). Furthermore, Tregs interact with other immune cells, including B cells and NK cells, establishing a balanced immune system (184).

Autoimmune diseases include systemic autoimmune diseases and organ-specific autoimmune diseases. Representative diseases of the former type include systemic lupus erythematosus, SS, and RA (185), and the latter include, for example, type 1 diabetes (186), pemphigus (187), and Hashimoto thyroiditis (188). Treg therapy can alleviate arthritis symptoms by suppressing inflammatory responses and regulating the immune system. In addition, It can regulate intestinal immune balance and reduce intestinal inflammation and tissue damage, thus alleviating inflammatory bowel diseases (such as Crohn's disease and ulcerative colitis) (189, 190). Treg therapy can also alleviate autoimmune hepatitis and improve liver function (191) and systemic lupus erythematosus (192). Finally, Treg therapy can be used for other autoimmune diseases, such as multiple sclerosis (193), myasthenia gravis (194), and autoimmune thyroid diseases (195).

Our recent studies revealed that the intravitreal injection of Tregs resolved ocular inflammation in experimental autoimmune uveitis (116). In patients with RA, synovial Tregs lose their suppressive functions. They fail to inhibit the production of pro-inflammatory cytokines, such as TNF-α and IFN-γ, by other $CD4^+$ T cells and monocytes and to inhibit the proliferation of Teffs (196). In animal models, the adoptive transfer of Tregs significantly reduces disease severity, highlighting the importance of Tregs in controlling abnormal joint inflammatory responses (197). Tregs can also suppress the activity of other immune cells through immunoregulatory molecules, for example, TGF-β and IL–10 produced by Tr1 cells, to inhibit inflammatory reactions and reduce self-attack on joint tissues, thereby alleviating symptoms of RA (198). Other autoimmune diseases, such as inflammatory bowel disease (199), systemic lupus erythematosus (200), and autoimmune thyroid diseases (201), including thyroid nodules, thyroiditis, Graves' disease, and autoimmune hypothyroidism, can all be alleviated by enhancing the immunosuppressive function of Tregs. Today, adoptive Treg therapy has been widely used and tested in autoimmune diseases (Table 2).

5.2 Transplantation

In transplantation, Tregs are critical for promoting graft tolerance and reducing transplant rejection rates. In a study of immune rejection therapy for kidney transplantation, 11 patients were followed for 60 weeks after transplantation to assess immune response, rejection, and renal function. Of these patients, eight were successfully maintained on monotherapy immunosuppression. Additionally, 10 patients who received Tregs treatment could be weaned off immunosuppression to low dose tacrolimus monotherapy within 48 weeks, although eight patients later experienced failure of tacrolimus monotherapy. Despite the need for additional immunosuppressive treatments, all 11 patients in the trial maintained good graft function at the 3-year follow-up time point. The study's authors successfully developed a method for isolating and expanding autologous polyclonal Tregs from a small blood sample and demonstrated the feasibility of this treatment (211).

Graft rejection reactions may occur after bone marrow transplantation, leading to transplant failure. Treg therapy can regulate the immune response after transplantation, reducing the occurrence of graft rejection (212). Amarnath et al. (213) found that Tregs could promote the generation of bone marrow DCs and reduce their ability to stimulate the generation of efficient T cells in GvHD. Tregs have high surface expression levels of PD-L1, which can bind to PD-L1 of DCs, thus inhibiting the activation of T cells and alleviating GvHD (214, 215). In addition, Tregs can express inhibitory molecules (e.g. CTLA-4, LAG-3, and NRP-1) to inhibit T cell activation (216). Tregs can also express CD62L and CCR5, maintain *in vivo* homing characteristics, inhibit the activation of early Teffs, and induce transplantation immune tolerance (217). The development of CAR-T technology has promoted the development of clinical trials using CAR Tregs to treat transplantation immune rejection (218). HLA-A2 is the main

TABLE 2 Animal models of autoimmune disease and inflammation.

Disease	Type	Treg-based immunotherapeutic effects	Influence
Connective tissue autoimmune disease	Systemic lupus erythematosus (202)	Activated Tregs	IFN-γ↓ IL-17↑
	Rheumatoid arthritis (203)	$CD4^+$ $CD25^-$ T & mature tolerant DCs promote $CD4^+$ $CD25^+$ Tregs	TNF-α↓ IL-17↓ IL-6↓ IFN-γ↑ IL-10↑ TGF-β↑
Neuromuscular autoimmune disease	Experimental autoimmune encephalomyelitis (204)	CCL1–Ig promotes $CCR8^+$ Tregs	CD39↑ GranB↑ IL-10↑
	Experimental autoimmune myasthenia gravis (205)	EAMG $CD4^+$ & marrow DCs promote DC EAMG Tregs	Clinical score↓ AChR↓
Endocrine autoimmune disease	Type 1 diabetes (206)	Antigen-specific Tregs	IL-10↑ TGF-β↑ $CD8^+$ T↓ $CD8^+$/$CD4^+$ T↓
	Premature ovarian insufficiency (207)	Activated Tregs	Follicle-stimulating hormone↓ Luteinizing hormone↓ Anti-zona pellucida antibody↓ Estradiol↑ Anti-Müllerian hormone↑
Autoimmune diseases of the digestive system	Autoimmune hepatitis (208)	$CD4^+$ $CD25^+$ Tregs & HSCs promote HSC Tregs	AST↓ ALT↓ Treg/Th17 -
	Ulcerative colitis (209)	Activated Tregs	IL-1↓ TNF-α↓ NO↓ PGE2↓
Other autoimmune diseases	Graft-versus-host disease (210)	Tr1 cells promote Tregs	Th2/Th1↑ Treg/Th17↑

molecular target that causes immune rejection (219). CAR HLA-A2 Tregs can significantly reduce the inflammation and rejection caused by grafts, can promote the immune tolerance of grafts, and are superior to polyclonal Tregs in preventing GvHD caused by donor T cells (220). CAR Treg cell therapy likely has the advantage of avoiding transplant rejection. Early treatment may help prevent the occurrence of rejection reactions, while later treatment may be more suitable for the management of existing rejection reactions.

5.3 Cancer treatment

Tregs, although vital for preserving immune tolerance and preventing autoimmune diseases, can be counterproductive in cancer by inhibiting anti-tumor responses and enabling cancer cells to escape immune surveillance. Consequently, restricting Treg activity is essential for enhancing the immune system's ability to combat cancer. Targeting Tregs also has potential applications in cancer treatment. The goal of targeting Tregs for cancer treatment is to enhance the tumor immune response and suppress tumor growth by modulating the activity of the immune system (221). Immune checkpoint inhibitors have become an important strategy in cancer treatment (222). In this treatment approach, the suppressive effects of Tregs may inhibit the efficacy of immune checkpoint inhibitors. Therefore, reducing or modulating the immunosuppressive effects of Tregs can enhance the efficacy of immune checkpoint inhibitors (182). CpG combined with low-dose anti-OX40/CTLA-4 triple immunotherapy can eliminate Tregs in a tumor and has a curative effect on central nervous system lymphoma in mice (223). In patients with tumors that did not respond to PD-1 monotherapy, the combination of the partial deletion of CARD-containing MAGUK protein 1 (CARMA1) and the sterol regulatory element binding protein (SREBP) inhibitor fatostatin produced a strong antitumor effect (224). This is because, upon the destruction of the CARMA1–BCL10–MALT1 semaphore complex, most tumor-infiltrating Tregs inhibit IFN-γ derived from $CD8^+$ T cells, which inhibits the growth of immunosuppressive M2-like tumor-associated macrophages (TAMs) (225). Fatostatin inhibits SREBP1-mediated fatty acid synthesis, inhibits the occurrence and development of TAMs, and then controls tumor growth.

Chemokine pathway blocking and specific target blocking have also been used to suppress tumors (Table 3) (226). Blocking the migration of Tregs to the TME is a new direction of tumor immunotherapy (227). Tregs in a canine bladder cancer model entered tumor tissue through the CCL17–CCR4 axis, and anti-CCR4 treatment significantly inhibited tumor growth and improved the survival rate. In addition, CCR4 was highly expressed in tumor-infiltrating Tregs (TITRs) in human bladder cancer (228). Another study showed that the number of TITRs in $CD36^{-/-}$ Treg mice was decreased, the anti-tumor activity of tumor-infiltrating lymphocytes was enhanced, and tumor growth was inhibited (229). Neuropilin 1 $(Nrp1)^{-/-}$ Tregs in mice with a partial Nrp1 knockout can prevent wild-type ($Nrp1^{+/+}$) Tregs from performing their immunosuppressive function by secreting IFN-γ, thus promoting the clearance of melanoma (10). New drugs are continuously being developed to inhibit cancers. Some of the difficulties of tumor immunotherapy include eliminating the immunosuppressive effect of the TME and enhancing the specific anti-tumor response. Further effective differentiation between TITRs and tissue-resident Treg

TABLE 3 Methods of Treg-targeted therapy for tumors and their corresponding cytokines.

No.	Therapeutic effect	Drug	Target
1	Treg depletion in the TME	Kinase inhibitor, cyclophosphamide, anti-CD25	IL-2 signaling
2	Halting Treg migration	Anti-CCR4, anti-CCR8	CCR4, CCR8
3	Sensitizing intertumoral Tregs to checkpoint blockade	Anti-TIGIT, anti–LAG-3, LAG-3–Ig fusion protein, nonfucosylated anti–CTLA-4	LAG-3, TIM3, TIGIT, CTLA-4
4	Targeting the co-stimulation of Tregs	GITR agonist, OX40 agonist, ICOS agonist and antagonist, TNFR2 antagonist	GITR, ICOS, OX40, TNFR2, NRP-1
5	Targeting Treg cytokines	Anti–IL-10, anti-GARP, anti–IL-35	IL-10, TGF-β, IL-35
6	Altering Treg fragility	PI3Kδ inhibitor, anti–NRP-1	NRP-1, IFN-γ
7	Targeting Treg metabolism	Meformin, IDO inhibitor, A2AR inhibitor, Orencia, Nulojix	IL-10, CTLA-4, FOXP3

*IL, Interleukin; CD, Cluster of differentiation; CCR, Hemokine (C-C motif) receptor; LAG, Lymphocyte activation gene; TIM, T cell immunoglobulin domain and mucin domain; TIGIT, T cell immunoreceptor with Ig and immunoreceptor tyrosine-based inhibitory motif (ITIM) domains; CTLA, Cytotoxic T lymphocyte-associated antigen; GITR, Glucocorticoid-induced tumor necrosis factor receptor; ICOS, Inducible synergistic co-stimulation molecules; OX40, CD134 & TNF receptor superfamily member 4 (TNFRSF4); TNFR2, Tumor necrosis factor receptor; NRP, Neuropilin; TGF, Transforming growth factor; IFN, Interferon; FOX, Forkhead box protein.

phenotypes or transcription levels, as well as a continuous reduction in the dynamic differences in Tregs between preclinical models and patient-derived samples, can provide more therapeutic bases for immunotherapy based on Treg targets.

The exploration and deployment of therapeutics targeting Tregs are extensive, chiefly because these cells express an array of receptors on their surface. The most utilized are agonists of the TNFR superfamily and antagonists of immune checkpoint inhibitors (230, 231). These modulators alleviate autoimmune conditions and bolster anti-tumor responses by influencing Treg function. Next-generation Treg interventions focus on directing Tregs to selectively recognize tissue or organ-specific antigens by incorporating a chimeric antigen receptor (CAR) structure. Engineered CAR-Tregs are also being designed to convert pro-inflammatory cytokine signals into those of IL-2 or IL-10, which intensifies the suppression of inflammation (232).

6 Conclusion

The study of Treg signaling pathways provides a theoretical basis for immune balance and the treatment of autoimmune diseases. By modulating the quantity and function of Tregs, immune system activity can be balanced, inflammation can be alleviated, and the development and progression of autoimmune diseases can be prevented and treated. Preliminary results from clinical trials demonstrate the potential of Treg therapy in the fields of transplant rejection, autoimmune diseases, and cancer. Although the application of Treg therapy poses challenges, personalized treatment strategies and the optimization and monitoring of treatment processes will contribute to improving its safety and efficacy and promoting its further clinical implementation.

Conflicts of Interest

The authors declare that the research was conducted in the absence of any commercial or financial relationships that could be construed as a potential conflict of interest.

Author contributions

ZY: Writing – original draft, Writing – review & editing. KD: Writing – original draft, Investigation, Software. WC: Writing – original draft, Writing – review & editing.

Funding

The author(s) declare financial support was received for the research, authorship, and/or publication of this article. This research was funded by the National Natural Science Foundation of China (32370959), Natural Science Foundation of Guangdong province and Institute for Research and Continuing Education, Hong Kong Baptist University (2021A1515010569, 2022A1515012450).

Conflict of interest

The authors declare that the research was conducted in the absence of any commercial or financial relationships that could be construed as a potential conflict of interest.

Publisher's note

References

1. Sakaguchi S, Sakaguchi N, Asano M, Itoh M, Toda M. Immunologic self-tolerance maintained by activated T cells expressing il-2 receptor alpha-chains (Cd25). Breakdown of a single mechanism of self-tolerance causes various autoimmune diseases. *J Immunol.* (1995) 155:1151–64.

2. Boehm F, Martin M, Kesselring R, Schiechl G, Geissler EK, Schlitt HJ, et al. Deletion of foxp3+ Regulatory T cells in genetically targeted mice supports development of intestinal inflammation. *BMC Gastroenterol.* (2012) 12:97. doi: 10.1186/1471–230X-12–97

3. Collison LW, Pillai MR, Chaturvedi V, Vignali DA. Regulatory T cell suppression is potentiated by target T cells in a cell contact, il-35- and il-10-dependent manner. *J Immunol.* (2009) 182:6121–8. doi: 10.4049/jimmunol.0803646

4. Nakamura K, Kitani A, Strober W. Cell contact-dependent immunosuppression by cd4(+)Cd25(+) regulatory T cells is mediated by cell surface-bound transforming growth factor beta. *J Exp Med.* (2001) 194:629–44. doi: 10.1084/jem.194.5.629

5. Pandiyan P, Zheng L, Ishihara S, Reed J, Lenardo MJ. Cd4+Cd25+Foxp3+ Regulatory T cells induce cytokine deprivation-mediated apoptosis of effector cd4+ T cells. *Nat Immunol.* (2007) 8:1353–62. doi: 10.1038/ni1536

6. Tekguc M, Wing JB, Osaki M, Long J, Sakaguchi S. Treg-expressed ctla-4 depletes cd80/cd86 by trogocytosis, releasing free pd-L1 on antigen-presenting cells. *Proc Natl Acad Sci U.S.A.* (2021) 118:e2023739118. doi: 10.1073/pnas.2023739118

7. Kazanova A, Rudd CE. Programmed cell death 1 ligand (Pd-L1) on T cells generates treg suppression from memory. *PloS Biol.* (2021) 19:e3001272. doi: 10.1371/journal.pbio.3001272

8. Cross AR, Lion J, Poussin K, Glotz D, Mooney N. Inflammation determines the capacity of allogenic endothelial cells to regulate human treg expansion. *Front Immunol.* (2021) 12:666531. doi: 10.3389/fimmu.2021.666531

9. Zhang L, Zhang M, Xu J, Li S, Chen Y, Wang W, et al. The role of the programmed cell death protein-1/programmed death-ligand 1 pathway, regulatory T cells and T helper 17 cells in tumor immunity: A narrative review. *Ann Transl Med.* (2020) 8:1526. doi: 10.21037/atm-20–6719

10. Overacre-Delgoffe AE, Chikina M, Dadey RE, Yano H, Brunazzi EA, Shayan G, et al. Interferon-gamma drives T(Reg) fragility to promote anti-tumor immunity. *Cell.* (2017) 169:1130–41 e11. doi: 10.1016/j.cell.2017.05.005

11. Kondelkova K, Vokurkova D, Krejsek J, Borska L, Fiala Z, Ctirad A. Regulatory T cells (Treg) and their roles in immune system with respect to immunopathological disorders. *Acta Med (Hradec Kralove).* (2010) 53:73–7. doi: 10.14712/18059694.2016.63

12. Rocamora-Reverte L, Melzer FL, Wurzner R, Weinberger B. The complex role of regulatory T cells in immunity and aging. *Front Immunol.* (2020) 11:616949. doi: 10.3389/fimmu.2020.616949

13. Workman CJ, Szymczak-Workman AL, Collison LW, Pillai MR, Vignali DA. The development and function of regulatory T cells. *Cell Mol Life Sci.* (2009) 66:2603–22. doi: 10.1007/s00018–009-0026–2

14. Russler-Germain EV, Rengarajan S, Hsieh CS. Antigen-specific regulatory T-cell responses to intestinal microbiota. *Mucosal Immunol.* (2017) 10:1375–86. doi: 10.1038/mi.2017.65

15. Chen W, Jin W, Hardegen N, Lei KJ, Li L, Marinos N, et al. Conversion of peripheral cd4+Cd25- naive T cells to cd4+Cd25+ Regulatory T cells by tgf-beta induction of transcription factor foxp3. *J Exp Med.* (2003) 198:1875–86. doi: 10.1084/jem.20030152

16. Duhen T, Duhen R, Lanzavecchia A, Sallusto F, Campbell DJ. Functionally distinct subsets of human foxp3+ Treg cells that phenotypically mirror effector th cells. *Blood.* (2012) 119:4430–40. doi: 10.1182/blood-2011–11-392324

17. Halim L, Romano M, McGregor R, Correa I, Pavlidis P, Grageda N, et al. An atlas of human regulatory T helper-like cells reveals features of th2-like tregs that support a tumorigenic environment. *Cell Rep.* (2017) 20:757–70. doi: 10.1016/j.celrep.2017.06.079

18. Chung Y, Tanaka S, Chu F, Nurieva RI, Martinez GJ, Rawal S, et al. Follicular regulatory T cells expressing foxp3 and bcl-6 suppress germinal center reactions. *Nat Med.* (2011) 17:983–8. doi: 10.1038/nm.2426

19. Reinhardt RL, Liang HE, Locksley RM. Cytokine-secreting follicular T cells shape the antibody repertoire. *Nat Immunol.* (2009) 10:385–93. doi: 10.1038/ni.1715

20. Fu W, Liu X, Lin X, Feng H, Sun L, Li S, et al. Deficiency in T follicular regulatory cells promotes autoimmunity. *J Exp Med.* (2018) 215:815–25. doi: 10.1084/jem.20170901

21. Shevach EM, Thornton AM. Ttregs, ptregs, and itregs: similarities and differences. *Immunol Rev.* (2014) 259:88–102. doi: 10.1111/imr.12160

22. Gottschalk RA, Corse E, Allison JP. Expression of helios in peripherally induced foxp3+ Regulatory T cells. *J Immunol.* (2012) 188:976–80. doi: 10.4049/jimmunol.1102964

23. Yadav M, Louvet C, Davini D, Gardner JM, Martinez-Llordella M, Bailey-Bucktrout S, et al. Neuropilin-1 distinguishes natural and inducible regulatory T cells among regulatory T cell subsets in vivo. *J Exp Med.* (2012) 209:1713–22, S1–19. doi: 10.1084/jem.20120822

24. Kim YC, Bhairavabhotla R, Yoon J, Golding A, Thornton AM, Tran DQ, et al. Oligodeoxynucleotides stabilize helios-expressing foxp3+ Human T regulatory cells during in vitro expansion. *Blood.* (2012) 119:2810–8. doi: 10.1182/blood-2011–09-377895

25. Koch MA, Tucker-Heard G, Perdue NR, Killebrew JR, Urdahl KB, Campbell DJ. The transcription factor T-bet controls regulatory T cell homeostasis and function during type 1 inflammation. *Nat Immunol.* (2009) 10:595–602. doi: 10.1038/ni.1731

26. Kitz A, Dominguez-Villar M. Molecular mechanisms underlying th1-like treg generation and function. *Cell Mol Life Sci.* (2017) 74:4059–75. doi: 10.1007/s00018–017-2569-y

27. Krishnamoorthy N, Khare A, Oriss TB, Raundhal M, Morse C, Yarlagadda M, et al. Early infection with respiratory syncytial virus impairs regulatory T cell function and increases susceptibility to allergic asthma. *Nat Med.* (2012) 18:1525–30. doi: 10.1038/nm.2896

28. Noval Rivas M, Burton OT, Wise P, Charbonnier LM, Georgiev P, Oettgen HC, et al. Regulatory T cell reprogramming toward a th2-cell-like lineage impairs oral tolerance and promotes food allergy. *Immunity.* (2015) 42:512–23. doi: 10.1016/j.immuni.2015.02.004

29. Yao Y, Vent-Schmidt J, McGeough MD, Wong M, Hoffman HM, Steiner TS, et al. Tr1 cells, but not foxp3+ Regulatory T cells, suppress nlrp3 inflammasome activation via an il-10-dependent mechanism. *J Immunol.* (2015) 195:488–97. doi: 10.4049/jimmunol.1403225

30. Song Y, Wang N, Chen L, Fang L. Tr1 cells as a key regulator for maintaining immune homeostasis in transplantation. *Front Immunol.* (2021) 12:671579. doi: 10.3389/fimmu.2021.671579

31. Chaturvedi V, Collison LW, Guy CS, Workman CJ, Vignali DA. Cutting edge: human regulatory T cells require il-35 to mediate suppression and infectious tolerance. *J Immunol.* (2011) 186:6661–6. doi: 10.4049/jimmunol.1100315

32. Thornton AM, Lu J, Korty PE, Kim YC, Martens C, Sun PD, et al. Helios(+) and helios(-) treg subpopulations are phenotypically and functionally distinct and express dissimilar tcr repertoires. *Eur J Immunol.* (2019) 49:398–412. doi: 10.1002/eji.201847935

33. Wang J, Zhao X, Wan YY. Intricacies of tgf-beta signaling in treg and th17 cell biology. *Cell Mol Immunol.* (2023) 20:1002–22. doi: 10.1038/s41423–023-01036–7

34. Venuprasad K, Kong YC, Farrar MA. Control of th2-mediated inflammation by regulatory T cells. *Am J Pathol.* (2010) 177:525–31. doi: 10.2353/ajpath.2010.090936

35. Gocher-Demske AM, Cui J, Szymczak-Workman AL, Vignali KM, Latini JN, Pieklo GP, et al. Ifngamma-induction of T(H)1-like regulatory T cells controls antiviral responses. *Nat Immunol.* (2023) 24:841–54. doi: 10.1038/s41590–023-01453-w

36. Paust HJ, Riedel JH, Krebs CF, Turner JE, Brix SR, Krohn S, et al. Cxcr3+ Regulatory T cells control th1 responses in crescentic gn. *J Am Soc Nephrol.* (2016) 27:1933–42. doi: 10.1681/ASN.2015020203

37. Butcher MJ, Zhu J. Recent advances in understanding the th1/th2 effector choice. *Fac Rev.* (2021) 10:30. doi: 10.12703/r/10–30

38. Chapoval S, Dasgupta P, Dorsey NJ, Keegan AD. Regulation of the T helper cell type 2 (Th2)/T regulatory cell (Treg) balance by il-4 and stat6. *J Leukoc Biol.* (2010) 87:1011–8. doi: 10.1189/jlb.1209772

39. Travis MA, Sheppard D. Tgf-beta activation and function in immunity. *Annu Rev Immunol.* (2014) 32:51–82. doi: 10.1146/annurev-immunol-032713–120257

40. Hata A, Chen YG. Tgf-beta signaling from receptors to smads. *Cold Spring Harb Perspect Biol.* (2016) 8:a022061. doi: 10.1101/cshperspect.a022061

41. Itoh S, ten Dijke P. Negative regulation of tgf-beta receptor/smad signal transduction. *Curr Opin Cell Biol.* (2007) 19:176–84. doi: 10.1016/j.ceb.2007.02.015

42. Hanyu A, Ishidou Y, Ebisawa T, Shimanuki T, Imamura T, Miyazono K. The N domain of smad7 is essential for specific inhibition of transforming growth factor-beta signaling. *J Cell Biol.* (2001) 155:1017–27. doi: 10.1083/jcb.200106023

43. Galvin KM, Donovan MJ, Lynch CA, Meyer RI, Paul RJ, Lorenz JN, et al. A role for smad6 in development and homeostasis of the cardiovascular system. *Nat Genet.* (2000) 24:171–4. doi: 10.1038/72835

44. Laudisi F, Stolfi C, Monteleone I, Monteleone G. Tgf-beta1 signaling and smad7 control T-cell responses in health and immune-mediated disorders. *Eur J Immunol.* (2023) 53:e2350460. doi: 10.1002/eji.202350460

45. Lee GR. The balance of th17 versus treg cells in autoimmunity. *Int J Mol Sci.* (2018) 19:730. doi: 10.3390/ijms19030730

46. Ivanov II, Zhou L, Littman DR. Transcriptional regulation of th17 cell differentiation. *Semin Immunol.* (2007) 19:409–17. doi: 10.1016/j.smim.2007.10.011

47. Yang XO, Nurieva R, Martinez GJ, Kang HS, Chung Y, Pappu BP, et al. Molecular antagonism and plasticity of regulatory and inflammatory T cell programs. *Immunity.* (2008) 29:44–56. doi: 10.1016/j.immuni.2008.05.007

48. Zhou L, Lopes JE, Chong MM, Ivanov II, Min R, Victora GD, et al. Tgf-beta-induced foxp3 inhibits T(H)17 cell differentiation by antagonizing rorgammat function. *Nature.* (2008) 453:236–40. doi: 10.1038/nature06878

49. Tone Y, Furuuchi K, Kojima Y, Tykocinski ML, Greene MI, Tone M. Smad3 and nfat cooperate to induce foxp3 expression through its enhancer. *Nat Immunol.* (2008) 9:194–202. doi: 10.1038/ni1549

50. Gu AD, Wang Y, Lin L, Zhang SS, Wan YY. Requirements of transcription factor smad-dependent and -independent tgf-beta signaling to control discrete T-cell functions. *Proc Natl Acad Sci U.S.A.* (2012) 109:905–10. doi: 10.1073/pnas.1108352109

51. Zhang W, Zhang D, Shen M, Liu Y, Tian Y, Thomson AW, et al. Combined administration of a mutant tgf-beta1/fc and rapamycin promotes induction of regulatory T cells and islet allograft tolerance. *J Immunol*. (2010) 185:4750–9. doi: 10.4049/jimmunol.1000769

52. Kay JE, Kromwel L, Doe SE, Denyer M. Inhibition of T and B lymphocyte proliferation by rapamycin. *Immunology*. (1991) 72:544–9.

53. Zhang F, Cheng T, Zhang SX. Mechanistic target of rapamycin (Mtor): A potential new therapeutic target for rheumatoid arthritis. *Arthritis Res Ther*. (2023) 25:187. doi: 10.1186/s13075–023-03181-w

54. Li Z, Nie L, Chen L, Sun Y, Li G. Rapamycin relieves inflammation of experimental autoimmune encephalomyelitis by altering the balance of treg/th17 in a mouse model. *Neurosci Lett*. (2019) 705:39–45. doi: 10.1016/j.neulet.2019.04.035

55. Chen SY, Mamai O, Akhurst RJ. Tgfbeta: signaling blockade for cancer immunotherapy. *Annu Rev Cancer Biol*. (2022) 6:123–46. doi: 10.1146/annurev-cancerbio-070620–103554

56. Luo Q, Hu Z, Zhao H, Fan Y, Tu X, Wang Y, et al. The role of tgf-beta in the tumor microenvironment of pancreatic cancer. *Genes Dis*. (2023) 10:1513–24. doi: 10.1016/j.gendis.2022.10.019

57. Tao B, Yi C, Ma Y, Li Y, Zhang B, Geng Y, et al. A novel tgf-beta-related signature for predicting prognosis, tumor microenvironment, and therapeutic response in colorectal cancer. *Biochem Genet*. (2023). doi: 10.1007/s10528–023-10591–7 [Epub ahead of print]

58. Bachmann MF, Oxenius A. Interleukin 2: from immunostimulation to immunoregulation and back again. *EMBO Rep*. (2007) 8:1142–8. doi: 10.1038/sj.embor.7401099

59. Abbas AK, Trotta E D, Marson A, Bluestone JA. Revisiting il-2: biology and therapeutic prospects. *Sci Immunol*. (2018) 3:eaat1482. doi: 10.1126/sciimmunol.aat1482

60. Smith GA, Uchida K, Weiss A, Taunton J. Essential biphasic role for jak3 catalytic activity in il-2 receptor signaling. *Nat Chem Biol*. (2016) 12:373–9. doi: 10.1038/nchembio.2056

61. Ross SH, Cantrell DA. Signaling and function of interleukin-2 in T lymphocytes. *Annu Rev Immunol*. (2018) 36:411–33. doi: 10.1146/annurev-immunol-042617–053352

62. Liao W, Lin JX, Leonard WJ. Interleukin-2 at the crossroads of effector responses, tolerance, and immunotherapy. *Immunity*. (2013) 38:13–25. doi: 10.1016/j.immuni.2013.01.004

63. Feng Y, Arvey A, Chinen T, van der Veeken J, Gasteiger G, Rudensky AY. Control of the inheritance of regulatory T cell identity by a cis element in the foxp3 locus. *Cell*. (2014) 158:749–63. doi: 10.1016/j.cell.2014.07.031

64. Yu A, Snowhite I, Vendrame F, Rosenzwajg M, Klatzmann D, Pugliese A, et al. Selective il-2 responsiveness of regulatory T cells through multiple intrinsic mechanisms supports the use of low-dose il-2 therapy in type 1 diabetes. *Diabetes*. (2015) 64:2172–83. doi: 10.2337/db14–1322

65. Sezin T, Selvakumar B, Scheffold A. The role of a disintegrin and metalloproteinase (Adam)-10 in T helper cell biology. *Biochim Biophys Acta Mol Cell Res*. (2022) 1869:119192. doi: 10.1016/j.bbamcr.2021.119192

66. Tomala J, Weberova P, Tomalova B, Jiraskova Zakostelska Z, Sivak L, Kovarova J, et al. Il-2/jes6–1 mab complexes dramatically increase sensitivity to lps through ifn-gamma production by cd25(+)Foxp3(-) T cells. *Elife*. (2021) 10:e62432. doi: 10.7554/eLife.62432

67. Betts BC, Pidala J, Kim J, Mishra A, Nishihori T, Perez L, et al. Il-2 promotes early treg reconstitution after allogeneic hematopoietic cell transplantation. *Haematologica*. (2017) 102:948–57. doi: 10.3324/haematol.2016.153072

68. Saadoun D, Rosenzwajg M, Joly F, Six A, Carrat F, Thibault V, et al. Regulatory T-cell responses to low-dose interleukin-2 in hcv-induced vasculitis. *N Engl J Med*. (2011) 365:2067–77. doi: 10.1056/NEJMoa1105143

69. Hartemann A, Bensimon G, Payan CA, Jacqueminet S, Bourron O, Nicolas N, et al. Low-dose interleukin 2 in patients with type 1 diabetes: A phase 1/2 randomised, double-blind, placebo-controlled trial. *Lancet Diabetes Endocrinol*. (2013) 1:295–305. doi: 10.1016/S2213–8587(13)70113-X

70. Miao M, Hao Z, Guo Y, Zhang X, Zhang S, Luo J, et al. Short-term and low-dose il-2 therapy restores the th17/treg balance in the peripheral blood of patients with primary Sjogren's syndrome. *Ann Rheum Dis*. (2018) 77:1838–40. doi: 10.1136/annrheumdis-2018–213036

71. Zhang SX, Wang J, Sun HH, Zhang JQ, Liu GY, Luo J, et al. Circulating regulatory T cells were absolutely decreased in dermatomyositis/polymyositis patients and restored by low-dose il-2. *Ann Rheum Dis*. (2021) 80:e130. doi: 10.1136/annrheumdis-2019–216246

72. Rosenzwajg M, Lorenzon R, Cacoub P, Pham HP, Pitoiset F, El Soufi K, et al. Immunological and clinical effects of low-dose interleukin-2 across 11 autoimmune diseases in a single, open clinical trial. *Ann Rheum Dis*. (2019) 78:209–17. doi: 10.1136/annrheumdis-2018–214229

73. Moore KW, de Waal Malefyt R, Coffman RL, O'Garra A. Interleukin-10 and the interleukin-10 receptor. *Annu Rev Immunol*. (2001) 19:683–765. doi: 10.1146/annurev.immunol.19.1.683

74. Riley JK, Takeda K, Akira S, Schreiber RD. Interleukin-10 receptor signaling through the jak-stat pathway. Requirement for two distinct receptor-derived signals for anti-inflammatory action. *J Biol Chem*. (1999) 274:16513–21. doi: 10.1074/jbc.274.23.16513

75. Wingelhofer B, Neubauer HA, Valent P, Han X, Constantinescu SN, Gunning PT, et al. Implications of stat3 and stat5 signaling on gene regulation and chromatin remodeling in hematopoietic cancer. *Leukemia*. (2018) 32:1713–26. doi: 10.1038/s41375–018-0117-x

76. Hammer M, Mages J, Dietrich H, Schmitz F, Striebel F, Murray PJ, et al. Control of dual-specificity phosphatase-1 expression in activated macrophages by il-10. *Eur J Immunol*. (2005) 35:2991–3001. doi: 10.1002/eji.200526192

77. Powell MJ, Thompson SA, Tone Y, Waldmann H, Tone M. Posttranscriptional regulation of il-10 gene expression through sequences in the 3'-untranslated region. *J Immunol*. (2000) 165:292–6. doi: 10.4049/jimmunol.165.1.292

78. Schulte LN, Eulalio A, Mollenkopf HJ, Reinhardt R, Vogel J. Analysis of the host microrna response to salmonella uncovers the control of major cytokines by the let-7 family. *EMBO J*. (2011) 30:1977–89. doi: 10.1038/emboj.2011.94

79. Sharma A, Kumar M, Aich J, Hariharan M, Brahmachari SK, Agrawal A, et al. Posttranscriptional regulation of interleukin-10 expression by hsa-mir-106a. *Proc Natl Acad Sci U.S.A*. (2009) 106:5761–6. doi: 10.1073/pnas.0808743106

80. Cheng H, Wang L, Yang B, Li D, Wang X, Liu X, et al. Cutting edge: inhibition of glycogen synthase kinase 3 activity induces the generation and enhanced suppressive function of human il-10(+) foxp3(+)-induced regulatory T cells. *J Immunol*. (2020) 205:1497–502. doi: 10.4049/jimmunol.2000136

81. Chihara N, Madi A, Karwacz K, Awasthi A, Kuchroo VK. Differentiation and characterization of tr1 cells. *Curr Protoc Immunol*. (2016) 113:3 27 1–3 10. doi: 10.1002/0471142735.im0327s113

82. Apetoh L, Quintana FJ, Pot C, Joller N, Xiao S, Kumar D, et al. The aryl hydrocarbon receptor interacts with C-maf to promote the differentiation of type 1 regulatory T cells induced by il-27. *Nat Immunol*. (2010) 11:854–61. doi: 10.1038/ni.1912

83. Brockmann L, Soukou S, Steglich B, Czarnewski P, Zhao L, Wende S, et al. Molecular and functional heterogeneity of il-10-producing cd4(+) T cells. *Nat Commun*. (2018) 9:5457. doi: 10.1038/s41467–018-07581–4

84. Ranjbar M, Solgi G, Mohammadnia M, Nikbin B, Pourmand G, Ansaripour B, et al. Regulatory T-cell subset analysis and profile of interleukin (Il)-10, il-17 and interferon-gamma cytokine-producing cells in kidney allograft recipients with donor cells infusion. *Clin Exp Nephrol*. (2012) 16:636–46. doi: 10.1007/s10157–012-0591–9

85. Singh A, Ramachandran S, Graham ML, Daneshmandi S, Heller D, Suarez-Pinzon WL, et al. Long-term tolerance of islet allografts in nonhuman primates induced by apoptotic donor leukocytes. *Nat Commun*. (2019) 10:3495. doi: 10.1038/s41467–019-11338-y

86. Riley JS, McClain LE, Stratigis JD, Coons BE, Ahn NJ, Li H, et al. Regulatory T cells promote alloengraftment in a model of late-gestation in utero hematopoietic cell transplantation. *Blood Adv*. (2020) 4:1102–14. doi: 10.1182/bloodadvances.2019001208

87. Fitzgerald DC, Zhang GX, El-Behi M, Fonseca-Kelly Z, Li H, Yu S, et al. Suppression of autoimmune inflammation of the central nervous system by interleukin 10 secreted by interleukin 27-stimulated T cells. *Nat Immunol*. (2007) 8:1372–9. doi: 10.1038/ni1540

88. Chong WP, van Panhuys N, Chen J, Silver PB, Jittayasothorn Y, Mattapallil MJ, et al. Nk-dc crosstalk controls the autopathogenic th17 response through an innate ifn-gamma-il-27 axis. *J Exp Med*. (2015) 212:1739–52. doi: 10.1084/jem.20141678

89. Saraiva M, Vieira P, O'Garra A. Biology and therapeutic potential of interleukin-10. *J Exp Med*. (2020) 217:e20190418. doi: 10.1084/jem.20190418

90. Armstrong L, Jordan N, Millar A. Interleukin 10 (Il-10) regulation of tumour necrosis factor alpha (Tnf-alpha) from human alveolar macrophages and peripheral blood monocytes. *Thorax*. (1996) 51:143–9. doi: 10.1136/thx.51.2.143

91. Saraiva M, O'Garra A. The regulation of il-10 production by immune cells. *Nat Rev Immunol*. (2010) 10:170–81. doi: 10.1038/nri2711

92. Rivas JR, Liu Y, Alhakeem SS, Eckenrode JM, Marti F, Collard JP, et al. Interleukin-10 suppression enhances T-cell antitumor immunity and responses to checkpoint blockade in chronic lymphocytic leukemia. *Leukemia*. (2021) 35:3188–200. doi: 10.1038/s41375–021-01217–1

93. Beppu LY, Mooli RGR, Qu X, Marrero GJ, Finley CA, Fooks AN, et al. Tregs facilitate obesity and insulin resistance via a blimp-1/il-10 axis. *JCI Insight*. (2021) 6:e140644. doi: 10.1172/jci.insight.140644

94. Mosmann TR, Moore KW. The role of il-10 in crossregulation of th1 and th2 responses. *Immunol Today*. (1991) 12:A49–53. doi: 10.1016/S0167–5699(05)80015–5

95. Allavena P, Piemonti L, Longoni D, Bernasconi S, Stoppacciaro A, Ruco L, et al. Il-10 prevents the differentiation of monocytes to dendritic cells but promotes their maturation to macrophages. *Eur J Immunol*. (1998) 28:359–69. doi: 10.1002/(SICI)1521–4141(199801)28:01<359::AID-IMMU359>3.0.CO;2–4

96. Koch F, Stanzl U, Jennewein P, Janke K, Heufler C, Kampgen E, et al. High level il-12 production by murine dendritic cells: upregulation via mhc class ii and cd40 molecules and downregulation by il-4 and il-10. *J Exp Med*. (1996) 184:741–6. doi: 10.1084/jem.184.2.741

97. Mittal SK, Roche PA. Suppression of antigen presentation by il-10. *Curr Opin Immunol*. (2015) 34:22–7. doi: 10.1016/j.coi.2014.12.009

98. Carter NA, Vasconcellos R, Rosser EC, Tulone C, Munoz-Suano A, Kamanaka M, et al. Mice lacking endogenous il-10-producing regulatory B cells develop exacerbated disease and present with an increased frequency of th1/th17 but a decrease in regulatory T cells. *J Immunol*. (2011) 186:5569–79. doi: 10.4049/jimmunol.1100284

99. Groux H, Cottrez F, Rouleau M, Mauze S, Antonenko S, Hurst S, et al. A transgenic model to analyze the immunoregulatory role of il-10 secreted by antigen-presenting cells. *J Immunol*. (1999) 162:1723–9.

100. Fujii S, Shimizu K, Shimizu T, Lotze MT. Interleukin-10 promotes the maintenance of antitumor cd8(+) T-cell effector function in situ. *Blood*. (2001) 98:2143–51. doi: 10.1182/blood.v98.7.2143

101. Emmerich J, Mumm JB, Chan IH, LaFace D, Truong H, McClanahan T, et al. Il-10 directly activates and expands tumor-resident cd8(+) T cells without *de novo* infiltration from secondary lymphoid organs. *Cancer Res*. (2012) 72:3570–81. doi: 10.1158/0008–5472.CAN-12–0721

102. Collison LW, Delgoffe GM, Guy CS, Vignali KM, Chaturvedi V, Fairweather D, et al. The composition and signaling of the il-35 receptor are unconventional. *Nat Immunol*. (2012) 13:290–9. doi: 10.1038/ni.2227

103. Zhang J, Zhang Y, Wang Q, Li C, Deng H, Si C, et al. Interleukin-35 in immune-related diseases: protection or destruction. *Immunology*. (2019) 157:13–20. doi: 10.1111/imm.13044

104. Dong Y, Li X, Yu Y, Lv F, Chen Y. Jak/stat signaling is involved in il-35-induced inhibition of hepatitis B virus antigen-specific cytotoxic T cell exhaustion in chronic hepatitis B. *Life Sci*. (2020) 252:117663. doi: 10.1016/j.lfs.2020.117663

105. Zysk W, Glen J, Trzeciak M. Current insight into the role of il-35 and its potential involvement in the pathogenesis and therapy of atopic dermatitis. *Int J Mol Sci*. (2022) 23:15709. doi: 10.3390/ijms232415709

106. Collison LW, Workman CJ, Kuo TT, Boyd K, Wang Y, Vignali KM, et al. The inhibitory cytokine il-35 contributes to regulatory T-cell function. *Nature*. (2007) 450:566–9. doi: 10.1038/nature06306

107. Zeng JC, Zhang Z, Li TY, Liang YF, Wang HM, Bao JJ, et al. Assessing the role of il-35 in colorectal cancer progression and prognosis. *Int J Clin Exp Pathol*. (2013) 6:1806–16.

108. Wang Z, Liu JQ, Liu Z, Shen R, Zhang G, Xu J, et al. Tumor-derived il-35 promotes tumor growth by enhancing myeloid cell accumulation and angiogenesis. *J Immunol*. (2013) 190:2415–23. doi: 10.4049/jimmunol.1202535

109. Turnis ME, Sawant DV, Szymczak-Workman AL, Andrews LP, Delgoffe GM, Yano H, et al. Interleukin-35 limits anti-tumor immunity. *Immunity*. (2016) 44:316–29. doi: 10.1016/j.immuni.2016.01.013

110. Tanaka T, Narazaki M, Kishimoto T. Il-6 in inflammation, immunity, and disease. *Cold Spring Harb Perspect Biol*. (2014) 6:a016295. doi: 10.1101/cshperspect.a016295

111. Fujimoto M, Nakano M, Terabe F, Kawahata H, Ohkawara T, Han Y, et al. The influence of excessive il-6 production in vivo on the development and function of foxp3 + Regulatory T cells. *J Immunol*. (2011) 186:32–40. doi: 10.4049/jimmunol.0903314

112. Koenecke C, Lee CW, Thamm K, Fohse L, Schafferus M, Mittrucker HW, et al. Ifn-gamma production by allogeneic foxp3+ Regulatory T cells is essential for preventing experimental graft-versus-host disease. *J Immunol*. (2012) 189:2890–6. doi: 10.4049/jimmunol.1200413

113. Bettelli E, Carrier Y, Gao W, Korn T, Strom TB, Oukka M, et al. Reciprocal developmental pathways for the generation of pathogenic effector th17 and regulatory T cells. *Nature*. (2006) 441:235–8. doi: 10.1038/nature04753

114. Sousa RO, Cariaco Y, Almeida MPO, Nascimento LAC, Coutinho LB, Ferreira-Junior AA, et al. The imbalance of tnf and il-6 levels and foxp3 expression at the maternal-fetal interface is involved in adverse pregnancy outcomes in a susceptible murine model of congenital toxoplasmosis. *Cytokine*. (2021) 143:155517. doi: 10.1016/j.cyto.2021.155517

115. Xu L, Kitani A, Fuss I, Strober W. Cutting edge: regulatory T cells induce cd4 +Cd25-foxp3- T cells or are self-induced to become th17 cells in the absence of exogenous tgf-beta. *J Immunol*. (2007) 178:6725–9. doi: 10.4049/jimmunol.178.11.6725

116. Zhang T, Han X, Zhong Y, Kam HT, Qiao D, Chen Z, et al. Regulatory T cell intravitreal delivery using hyaluronan methylcellulose hydrogel improves therapeutic efficacy in experimental autoimmune uveitis. *Biomater Adv*. (2023) 151:213496. doi: 10.1016/j.bioadv.2023.213496

117. Kimura A, Kishimoto T. Il-6: regulator of treg/th17 balance. *Eur J Immunol*. (2010) 40:1830–5. doi: 10.1002/eji.201040391

118. Bettelli E, Korn T, Oukka M, Kuchroo VK. Induction and effector functions of T(H)17 cells. *Nature*. (2008) 453:1051–7. doi: 10.1038/nature07036

119. Ogura H, Murakami M, Okuyama Y, Tsuruoka M, Kitabayashi C, Kanamoto M, et al. Interleukin-17 promotes autoimmunity by triggering a positive-feedback loop via interleukin-6 induction. *Immunity*. (2008) 29:628–36. doi: 10.1016/j.immuni.2008.07.018

120. Yang XO, Panopoulos AD, Nurieva R, Chang SH, Wang D, Watowich SS, et al. Stat3 regulates cytokine-mediated generation of inflammatory helper T cells. *J Biol Chem*. (2007) 282:9358–63. doi: 10.1074/jbc.C600321200

121. Wang Y, van Boxel-Dezaire AH, Cheon H, Yang J, Stark GR. Stat3 activation in response to il-6 is prolonged by the binding of il-6 receptor to egf receptor. *Proc Natl Acad Sci U.S.A*. (2013) 110:16975–80. doi: 10.1073/pnas.1315862110

122. Zhang W, Liu X, Zhu Y, Liu X, Gu Y, Dai X, et al. Transcriptional and posttranslational regulation of th17/treg balance in health and disease. *Eur J Immunol*. (2021) 51:2137–50. doi: 10.1002/eji.202048794

123. Iliopoulos D, Hirsch HA, Struhl K. An epigenetic switch involving nf-kappab, lin28, let-7 microrna, and il6 links inflammation to cell transformation. *Cell*. (2009) 139:693–706. doi: 10.1016/j.cell.2009.10.014

124. Guichelaar T, Emmelot ME, Rozemuller H, Martini B, Groen RW, Storm G, et al. Human regulatory T cells do not suppress the antitumor immunity in the bone marrow: A role for bone marrow stromal cells in neutralizing regulatory T cells. *Clin Cancer Res*. (2013) 19:1467–75. doi: 10.1158/1078–0432.CCR-12–2177

125. Lonial S, Durie B, Palumbo A, San-Miguel J. Monoclonal antibodies in the treatment of multiple myeloma: current status and future perspectives. *Leukemia*. (2016) 30:526–35. doi: 10.1038/leu.2015.223

126. Hunsucker SA, Magarotto V, Kuhn DJ, Kornblau SM, Wang M, Weber DM, et al. Blockade of interleukin-6 signalling with siltuximab enhances melphalan cytotoxicity in preclinical models of multiple myeloma. *Br J Haematol*. (2011) 152:579–92. doi: 10.1111/j.1365–2141.2010.08533.x

127. Xiao S, Jin H, Korn T, Liu SM, Oukka M, Lim B, et al. Retinoic acid increases foxp3+ Regulatory T cells and inhibits development of th17 cells by enhancing tgf-beta-driven smad3 signaling and inhibiting il-6 and il-23 receptor expression. *J Immunol*. (2008) 181:2277–84. doi: 10.4049/jimmunol.181.4.2277

128. Valencia X, Stephens G, Goldbach-Mansky R, Wilson M, Shevach EM, Lipsky PE. Tnf downmodulates the function of human cd4+Cd25hi T-regulatory cells. *Blood*. (2006) 108:253–61. doi: 10.1182/blood-2005–11-4567

129. Zhang Q, Cui F, Fang L, Hong J, Zheng B, Zhang JZ. Tnf-alpha impairs differentiation and function of tgf-beta-induced treg cells in autoimmune diseases through akt and smad3 signaling pathway. *J Mol Cell Biol*. (2013) 5:85–98. doi: 10.1093/jmcb/mjs063

130. Chen X, Baumel M, Mannel DN, Howard OM, Oppenheim JJ. Interaction of tnf with tnf receptor type 2 promotes expansion and function of mouse cd4+Cd25+ T regulatory cells. *J Immunol*. (2007) 179:154–61. doi: 10.4049/jimmunol.179.1.154

131. Hamano R, Huang J, Yoshimura T, Oppenheim JJ, Chen X. Tnf optimally activatives regulatory T cells by inducing tnf receptor superfamily members tnfr2, 4–1bb and ox40. *Eur J Immunol*. (2011) 41:2010–20. doi: 10.1002/eji.201041205

132. Chen X, Wu X, Zhou Q, Howard O, Netea MG, Oppenheim JJ. Tnfr2 is critical for the stabilization of the cd4+ Foxp3+ Regulatory T cell phenotype in the inflammatory environment. *J Immunol*. (2013) 190:1076–84. doi: 10.4049/jimmunol.1202659

133. Mahmud SA, Manlove LS, Schmitz HM, Xing Y, Wang Y, Owen DL, et al. Costimulation via the tumor-necrosis factor receptor superfamily couples tcr signal strength to the thymic differentiation of regulatory T cells. *Nat Immunol*. (2014) 15:473–81. doi: 10.1038/ni.2849

134. Evans HG, Roostalu U, Walter GJ, Gullick NJ, Frederiksen KS, Roberts CA, et al. Tnf-alpha blockade induces il-10 expression in human cd4+ T cells. *Nat Commun*. (2014) 5:3199. doi: 10.1038/ncomms4199

135. Holtta V, Sipponen T, Westerholm-Ormio M, Salo HM, Kolho KL, Farkkila M, et al. In crohn's disease, anti-tnf-alpha treatment changes the balance between mucosal il-17, foxp3, and cd4 cells. *ISRN Gastroenterol*. (2012) 2012:505432. doi: 10.5402/2012/505432

136. Ternant D, Pfister M, Le Tilly O, Mulleman D, Picon L, Willot S, et al. Infliximab treatment does not lead to full tnf-alpha inhibition: A target-mediated drug disposition model. *Clin Pharmacokinet*. (2022) 61:143–54. doi: 10.1007/s40262–021-01057–3

137. Nie H, Zheng Y, Li R, Guo TB, He D, Fang L, et al. Phosphorylation of foxp3 controls regulatory T cell function and is inhibited by tnf-alpha in rheumatoid arthritis. *Nat Med*. (2013) 19:322–8. doi: 10.1038/nm.3085

138. Dwivedi M, Tiwari S, Kemp EH, Begum R. Implications of regulatory T cells in anti-cancer immunity: from pathogenesis to therapeutics. *Heliyon*. (2022) 8:e10450. doi: 10.1016/j.heliyon.2022.e10450

139. Iglesias-Escudero M, Arias-Gonzalez N, Martinez-Caceres E. Regulatory cells and the effect of cancer immunotherapy. *Mol Cancer*. (2023) 22:26. doi: 10.1186/s12943–023-01714–0

140. Guo Y, Xie F, Liu X, Ke S, Chen J, Zhao Y, et al. Blockade of tnf-alpha/tnfr2 signalling suppresses colorectal cancer and enhances the efficacy of anti-pd1 immunotherapy by decreasing ccr8+ T regulatory cells. *J Mol Cell Biol*. (2023). doi: 10.1093/jmcb/mjad067 [Epub ahead of print]

141. Qu Y, Wang X, Bai S, Niu L, Zhao G, Yao Y, et al. The effects of tnf-alpha/tnfr2 in regulatory T cells on the microenvironment and progression of gastric cancer. *Int J Cancer*. (2022) 150:1373–91. doi: 10.1002/ijc.33873

142. Greenwald RJ, Freeman GJ, Sharpe AH. The B7 family revisited. *Annu Rev Immunol*. (2005) 23:515–48. doi: 10.1146/annurev.immunol.23.021704.115611

143. Zang X, Allison JP. The B7 family and cancer therapy: costimulation and coinhibition. *Clin Cancer Res*. (2007) 13:5271–9. doi: 10.1158/1078–0432.CCR-07–1030

144. Wang Y, Zhang H, Liu C, Wang Z, Wu W, Zhang N, et al. Immune checkpoint modulators in cancer immunotherapy: recent advances and emerging concepts. *J Hematol Oncol*. (2022) 15:111. doi: 10.1186/s13045–022-01325–0

145. Larkin J, Chiarion-Sileni V, Gonzalez R, Grob JJ, Rutkowski P, Lao CD, et al. Five-year survival with combined nivolumab and ipilimumab in advanced melanoma. *N Engl J Med*. (2019) 381:1535–46. doi: 10.1056/NEJMoa1910836

146. Babamohamadi M, Mohammadi N, Faryadi E, Haddadi M, Merati A, Ghobadinezhad F, et al. Anti-ctla-4 nanobody as a promising approach in cancer immunotherapy. *Cell Death Dis*. (2024) 15:17. doi: 10.1038/s41419-023-06391-x

147. Qureshi OS, Zheng Y, Nakamura K, Attridge K, Manzotti C, Schmidt EM, et al. Trans-endocytosis of cd80 and cd86: A molecular basis for the cell-extrinsic function of ctla-4. *Science*. (2011) 332:600–3. doi: 10.1126/science.1202947

148. Waldman AD, Fritz JM, Lenardo MJ. A guide to cancer immunotherapy: from T cell basic science to clinical practice. *Nat Rev Immunol*. (2020) 20:651–68. doi: 10.1038/s41577–020-0306–5

149. Paterson AM, Lovitch SB, Sage PT, Juneja VR, Lee Y, Trombley JD, et al. Deletion of ctla-4 on regulatory T cells during adulthood leads to resistance to autoimmunity. *J Exp Med*. (2015) 212:1603–21. doi: 10.1084/jem.20141030

150. Jain N, Nguyen H, Chambers C, Kang J. Dual function of ctla-4 in regulatory T cells and conventional T cells to prevent multiorgan autoimmunity. *Proc Natl Acad Sci U.S.A*. (2010) 107:1524–8. doi: 10.1073/pnas.0910341107

151. Hossen MM, Ma Y, Yin Z, Xia Y, Du J, Huang JY, et al. Current understanding of ctla-4: from mechanism to autoimmune diseases. *Front Immunol*. (2023) 14:1198365. doi: 10.3389/fimmu.2023.1198365

152. Shao L, Gao Y, Shao X, Ou Q, Zhang S, Liu Q, et al. Ctla-4 blockade reverses the foxp3+ T-regulatory-cell suppression of anti-tuberculosis T-cell effector responses. *bioRxiV* [Preprint] (2020). doi: 10.1101/2020.05.11.089946

153. Sun HL, Du XF, Tang YX, Li GQ, Yang SY, Wang LH, et al. Impact of immune checkpoint molecules on foxp3(+) treg cells and related cytokines in patients with acute and chronic brucellosis. *BMC Infect Dis*. (2021) 21:1025. doi: 10.1186/s12879–021-06730–3

154. Dhunputh C, Ducassou S, Fernandes H, Picard C, Rieux-Laucat F, Viallard JF, et al. Abatacept is useful in autoimmune cytopenia with immunopathologic manifestations caused by ctla-4 defects. *Blood*. (2022) 139:300–4. doi: 10.1182/blood.2021013496

155. Krummey SM, Cheeseman JA, Conger JA, Jang PS, Mehta AK, Kirk AD, et al. High ctla-4 expression on th17 cells results in increased sensitivity to ctla-4 coinhibition and resistance to belatacept. *Am J Transplant*. (2014) 14:607–14. doi: 10.1111/ajt.12600

156. Sobhani N, Tardiel-Cyril DR, Davtyan A, Generali D, Roudi R, Li Y. Ctla-4 in regulatory T cells for cancer immunotherapy. *Cancers (Basel)*. (2021) 13:1440. doi: 10.3390/cancers13061440

157. Stumpf M, Zhou X, Bluestone JA. The B7-independent isoform of ctla-4 functions to regulate autoimmune diabetes. *J Immunol*. (2013) 190:961–9. doi: 10.4049/jimmunol.1201362

158. Vasu C, Gorla SR, Prabhakar BS, Holterman MJ. Targeted engagement of ctla-4 prevents autoimmune thyroiditis. *Int Immunol*. (2003) 15:641–54. doi: 10.1093/intimm/dxg061

159. Fan Q, Zhang J, Cui Y, Wang C, Xie Y, Wang Q, et al. The synergic effects of ctla-4/foxp3-related genotypes and chromosomal aberrations on the risk of recurrent spontaneous abortion among a Chinese han population. *J Hum Genet*. (2018) 63:579–87. doi: 10.1038/s10038–018-0414–2

160. Masterman T, Ligers A, Zhang Z, Hellgren D, Salter H, Anvret M, et al. Ctla4 dimorphisms and the multiple sclerosis phenotype. *J Neuroimmunol*. (2002) 131:208–12. doi: 10.1016/s0165–5728(02)00274–6

161. Parry RV, Chemnitz JM, Frauwirth KA, Lanfranco AR, Braunstein I, Kobayashi SV, et al. Ctla-4 and pd-1 receptors inhibit T-cell activation by distinct mechanisms. *Mol Cell Biol*. (2005) 25:9543–53. doi: 10.1128/MCB.25.21.9543–9553.2005

162. Farhangnia P, Ghomi SM, Akbarpour M, Delbandi AA. Bispecific antibodies targeting ctla-4: game-changer troopers in cancer immunotherapy. *Front Immunol*. (2023) 14:1155778. doi: 10.3389/fimmu.2023.1155778

163. Chen RY, Zhu Y, Shen YY, Xu QY, Tang HY, Cui NX, et al. The role of pd-1 signaling in health and immune-related diseases. *Front Immunol*. (2023) 14:1163633. doi: 10.3389/fimmu.2023.1163633

164. Gianchecchi E, Fierabracci A. Inhibitory receptors and pathways of lymphocytes: the role of pd-1 in treg development and their involvement in autoimmunity onset and cancer progression. *Front Immunol*. (2018) 9:2374. doi: 10.3389/fimmu.2018.02374

165. Yamaguchi H, Hsu JM, Yang WH, Hung MC. Mechanisms regulating pd-L1 expression in cancers and associated opportunities for novel small-molecule therapeutics. *Nat Rev Clin Oncol*. (2022) 19:287–305. doi: 10.1038/s41571–022-00601–9

166. Pauken KE, Torchia JA, Chaudhri A, Sharpe AH, Freeman GJ. Emerging concepts in pd-1 checkpoint biology. *Semin Immunol*. (2021) 52:101480. doi: 10.1016/j.smim.2021.101480

167. Lowther DE, Goods BA, Lucca LE, Lerner BA, Raddassi K, van Dijk D, et al. Pd-1 marks dysfunctional regulatory T cells in Malignant gliomas. *JCI Insight*. (2016) 1: e85935. doi: 10.1172/jci.insight.85935

168. Tan CL, Kuchroo JR, Sage PT, Liang D, Francisco LM, Buck J, et al. Pd-1 restraint of regulatory T cell suppressive activity is critical for immune tolerance. *J Exp Med*. (2021) 218:e20182232. doi: 10.1084/jem.20182232

169. Kumagai S, Togashi Y, Kamada T, Sugiyama E, Nishinakamura H, Takeuchi Y, et al. The pd-1 expression balance between effector and regulatory T cells predicts the clinical efficacy of pd-1 blockade therapies. *Nat Immunol*. (2020) 21:1346–58. doi: 10.1038/s41590–020-0769–3

170. Deng B, Yang B, Chen J, Wang S, Zhang W, Guo Y, et al. Gallic acid induces T-helper-1-like T(Reg) cells and strengthens immune checkpoint blockade efficacy. *J Immunother Cancer*. (2022) 10:e004037. doi: 10.1136/jitc-2021–004037

171. Sage PT, Francisco LM, Carman CV, Sharpe AH. The receptor pd-1 controls follicular regulatory T cells in the lymph nodes and blood. *Nat Immunol*. (2013) 14:152–61. doi: 10.1038/ni.2496

172. Chuckran CA, Liu C, Bruno TC, Workman CJ, Vignali DA. Neuropilin-1: A checkpoint target with unique implications for cancer immunology and immunotherapy. *J Immunother Cancer*. (2020) 8:e000967. doi: 10.1136/jitc-2020–000967

173. Graziani G, Lacal PM. Neuropilin-1 as therapeutic target for Malignant melanoma. *Front Oncol*. (2015) 5:125. doi: 10.3389/fonc.2015.00125

174. Yang X, Xu T, Song X, Wu Y. Overexpression of nrp1 is associated with poor prognosis via accelerating immunosuppression in head and neck squamous cell carcinoma. *Int J Gen Med*. (2023) 16:2819–29. doi: 10.2147/IJGM.S409336

175. Liu Z, McMichael EL, Shayan G, Li J, Chen K, Srivastava R, et al. Novel effector phenotype of tim-3(+) regulatory T cells leads to enhanced suppressive function in head and neck cancer patients. *Clin Cancer Res*. (2018) 24:4529–38. doi: 10.1158/1078–0432.CCR-17–1350

176. Khunger M, Hernandez AV, Pasupuleti V, Rakshit S, Pennell NA, Stevenson J, et al. Programmed cell death 1 (Pd-1) ligand (Pd-L1) expression in solid tumors as a predictive biomarker of benefit from pd-1/pd-L1 axis inhibitors: A systematic review and meta-analysis. *JCO Precis Oncol*. (2017) 1:1–15. doi: 10.1200/PO.16.00030

177. Zhang B, Liu Y, Zhou S, Jiang H, Zhu K, Wang R. Predictive effect of pd-L1 expression for immune checkpoint inhibitor (Pd-1/pd-L1 inhibitors) treatment for non-small cell lung cancer: A meta-analysis. *Int Immunopharmacol*. (2020) 80:106214. doi: 10.1016/j.intimp.2020.106214

178. Ghobadinezhad F, Ebrahimi N, Mozaffari F, Moradi N, Beiranvand S, Pournazari M, et al. The emerging role of regulatory cell-based therapy in autoimmune disease. *Front Immunol*. (2022) 13:1075813. doi: 10.3389/fimmu.2022.1075813

179. Spence A, Klementowicz JE, Bluestone JA, Tang Q. Targeting treg signaling for the treatment of autoimmune diseases. *Curr Opin Immunol*. (2015) 37:11–20. doi: 10.1016/j.coi.2015.09.002

180. Park TY, Jeon J, Lee N, Kim J, Song B, Kim JH, et al. Co-transplantation of autologous T(Reg) cells in a cell therapy for Parkinson's disease. *Nature*. (2023) 619:606–15. doi: 10.1038/s41586–023-06300–4

181. Daenthanasanmak A, Iamsawat S, Chakraborty P, Nguyen HD, Bastian D, Liu C, et al. Targeting sirt-1 controls gvhd by inhibiting T-cell allo-response and promoting treg stability in mice. *Blood*. (2019) 133:266–79. doi: 10.1182/blood-2018–07-863233

182. Hosseinalizadeh H, Rabiee F, Eghbalifard N, Rajabi H, Klionsky DJ, Rezaee A. Regulating the regulatory T cells as cell therapies in autoimmunity and cancer. *Front Med (Lausanne)*. (2023) 10:1244298. doi: 10.3389/fmed.2023.1244298

183. Andre S, Tough DF, Lacroix-Desmazes S, Kaveri SV, Bayry J. Surveillance of antigen-presenting cells by cd4+ Cd25+ Regulatory T cells in autoimmunity: immunopathogenesis and therapeutic implications. *Am J Pathol*. (2009) 174:1575–87. doi: 10.2353/ajpath.2009.080987

184. Pedroza-Pacheco I, Madrigal A, Saudemont A. Interaction between natural killer cells and regulatory T cells: perspectives for immunotherapy. *Cell Mol Immunol*. (2013) 10:222–9. doi: 10.1038/cmi.2013.2

185. Ohlsson M, Hellmark T, Bengtsson AA, Theander E, Turesson C, Klint C, et al. Proteomic data analysis for differential profiling of the autoimmune diseases sle, ra, ss, and anca-associated vasculitis. *J Proteome Res*. (2021) 20:1252–60. doi: 10.1021/acs.jproteome.0c00657

186. Alsaeed A. Comment on: autoimmune diseases and their prevalence in Saudi Arabian patients with type 1 diabetes mellitus. *Saudi Med J*. (2023) 44:1310. doi: 10.15537/smj.2023.44.12.20230818

187. Dmochowski M, Jalowska M, Bowszyc-Dmochowska M. Issues occupying our minds: nomenclature of autoimmune blistering diseases requires updating, pemphigus vulgaris propensity to affect areas adjacent to natural body orifices unifies seemingly diverse clinical features of this disease. *Front Immunol*. (2022) 13:1103375. doi: 10.3389/fimmu.2022.1103375

188. Boutzios G, Koukoulioti E, Goules AV, Kalliakmanis I, Giovannopoulos I, Vlachoyiannopoulos P, et al. Hashimoto thyroiditis, anti-parietal cell antibodies: associations with autoimmune diseases and Malignancies. *Front Endocrinol (Lausanne)*. (2022) 13:860880. doi: 10.3389/fendo.2022.860880

189. McLarnon A. Ibd: regulatory T-cell therapy is a safe and well-tolerated potential approach for treating refractory Crohn's disease. *Nat Rev Gastroenterol Hepatol*. (2012) 9:559. doi: 10.1038/nrgastro.2012.167

190. Clough JN, Omer OS, Tasker S, Lord GM, Irving PM. Regulatory T-cell therapy in Crohn's disease: challenges and advances. *Gut*. (2020) 69:942–52. doi: 10.1136/gutjnl-2019–319850

191. Diestelhorst J, Junge N, Schlue J, Falk CS, Manns MP, Baumann U, et al. Pediatric autoimmune hepatitis shows a disproportionate decline of regulatory T cells in the liver and of il-2 in the blood of patients undergoing therapy. *PloS One*. (2017) 12: e0181107. doi: 10.1371/journal.pone.0181107

192. Shin JI. The beneficial effect of leflunomide on systemic lupus erythematosus: the role of tregs repopulation?: comment on: leflunomide: friend or foe for systemic lupus erythematosus? *Rheumatol Int*. (2013) 33:273–6. doi: 10.1007/s00296–013-2795-z

193. Shariati M, Shaygannejad V, Abbasirad F, Hosseininasab F, Kazemi M, Mirmosayyeb O, et al. Silymarin restores regulatory T cells (Tregs) function in multiple sclerosis (Ms) patients in vitro. *Inflammation*. (2019) 42:1203–14. doi: 10.1007/s10753–019-00980–9

194. Zhang Y, Wang HB, Chi LJ, Wang WZ. The role of foxp3+Cd4+Cd25hi tregs in the pathogenesis of myasthenia gravis. *Immunol Lett*. (2009) 122:52–7. doi: 10.1016/j.imlet.2008.11.015

195. Chen Z, Wang Y, Ding X, Zhang M, He M, Zhao Y, et al. The proportion of peripheral blood tregs among the cd4+ T cells of autoimmune thyroid disease patients: A meta-analysis. *Endocr J*. (2020) 67:317–26. doi: 10.1507/endocrj.EJ19–0307

196. Biton J, Semerano L, Delavallee L, Lemeiter D, Laborie M, Grouard-Vogel G, et al. Interplay between tnf and regulatory T cells in a tnf-driven murine model of arthritis. *J Immunol*. (2011) 186:3899–910. doi: 10.4049/jimmunol.1003372

197. Chavele KM, Ehrenstein MR. Regulatory T-cells in systemic lupus erythematosus and rheumatoid arthritis. *FEBS Lett*. (2011) 585:3603–10. doi: 10.1016/j.febslet.2011.07.043

198. Grover P, Goel PN, Greene MI. Regulatory T cells: regulation of identity and function. *Front Immunol*. (2021) 12:750542. doi: 10.3389/fimmu.2021.750542

199. Negi S, Saini S, Tandel N, Sahu K, Mishra RPN, Tyagi RK. Translating treg therapy for inflammatory bowel disease in humanized mice. *Cells*. (2021) 10:1847. doi: 10.3390/cells10081847

200. Jin J, Liu X. Commentary: T cell metabolism: A new perspective on th17/treg cell imbalance in systemic lupus erythematosus. *Front Immunol*. (2023) 14:1164761. doi: 10.3389/fimmu.2023.1164761

201. Shao S, Yu X, Shen L. Autoimmune thyroid diseases and th17/treg lymphocytes. *Life Sci*. (2018) 192:160–5. doi: 10.1016/j.lfs.2017.11.026

202. Dall'Era M, Pauli ML, Remedios K, Taravati K, Sandova PM, Putnam AL, et al. Adoptive treg cell therapy in a patient with systemic lupus erythematosus. *Arthritis Rheumatol*. (2019) 71:431–40. doi: 10.1002/art.40737

203. Sun J, Yang Y, Huo X, Zhu B, Li Z, Jiang X, et al. Efficient therapeutic function and mechanisms of human polyclonal cd8(+)Cd103(+)Foxp3(+) regulatory T cells on collagen-induced arthritis in mice. *J Immunol Res*. (2019) 2019:8575407. doi: 10.1155/2019/8575407

204. Barsheshet Y, Wildbaum G, Levy E, Vitenshtein A, Akinseye C, Griggs J, et al. Ccr8(+)Foxp3(+) T(Reg) cells as master drivers of immune regulation. *Proc Natl Acad Sci U.S.A*. (2017) 114:6086–91. doi: 10.1073/pnas.1621280114

205. Aricha R, Reuveni D, Fuchs S, Souroujon MC. Suppression of experimental autoimmune myasthenia gravis by autologous T regulatory cells. *J Autoimmun*. (2016) 67:57–64. doi: 10.1016/j.jaut.2015.09.005

206. Haque M, Lei F, Xiong X, Das JK, Ren X, Fang D, et al. Stem cell-derived tissue-associated regulatory T cells suppress the activity of pathogenic cells in autoimmune diabetes. *JCI Insight*. (2019) 4:e126471. doi: 10.1172/jci.insight.126471

207. Liu D, Tu X, Huang C, Yuan Y, Wang Y, Liu X, et al. Adoptive transfers of cd4 (+) cd25(+) tregs partially alleviate mouse premature ovarian insufficiency. *Mol Reprod Dev*. (2020) 87:887–98. doi: 10.1002/mrd.23404

208. Huang H, Deng Z. Adoptive transfer of regulatory T cells stimulated by allogeneic hepatic stellate cells mitigates liver injury in mice with concanavalin a-induced autoimmune hepatitis. *Biochem Biophys Res Commun*. (2019) 512:14–21. doi: 10.1016/j.bbrc.2019.02.147

209. Wang K, Zhu T, Wang H, Yang J, Du S, Dong G, et al. Adoptive transfers of cd4 (+)Cd25(+) tregs raise foxp3 expression and alleviate mouse enteritis. *BioMed Res Int*. (2018) 2018:9064073. doi: 10.1155/2018/9064073

210. Jeon YW, Lim JY, Im KI, Kim N, Nam YS, Song YJ, et al. Enhancement of graft-versus-host disease control efficacy by adoptive transfer of type 1 regulatory T cells in bone marrow transplant model. *Stem Cells Dev*. (2019) 28:129–40. doi: 10.1089/scd.2018.0113

211. Roemhild A, Otto NM, Moll G, Abou-El-Enein M, Kaiser D, Bold G, et al. Regulatory T cells for minimising immune suppression in kidney transplantation: phase I/iia clinical trial. *BMJ*. (2020) 371:m3734. doi: 10.1136/bmj.m3734

212. Abbaszadeh S, Nosrati-Siahmazgi V, Musaie K, Rezaei S, Qahremani M, Xiao B, et al. Emerging strategies to bypass transplant rejection via biomaterial-assisted immunoengineering: insights from islets and beyond. *Adv Drug Delivery Rev*. (2023) 200:115050. doi: 10.1016/j.addr.2023.115050

213. Whitehill GD, Amarnath S, Muranski P, Keyvanfar K, Battiwalla M, Barrett AJ, et al. Adenosine selectively depletes alloreactive T cells to prevent gvhd while conserving immunity to viruses and leukemia. *Mol Ther*. (2016) 24:1655–64. doi: 10.1038/mt.2016.147

214. Handelsman S, Overbey J, Chen K, Lee J, Haj D, Li Y. Pd-L1's role in preventing alloreactive T cell responses following hematopoietic and organ transplant. *Cells*. (2023) 12:1609. doi: 10.3390/cells12121609

215. Cassady K, Martin PJ, Zeng D. Regulation of gvhd and gvl activity via pd-L1 interaction with pd-1 and cd80. *Front Immunol*. (2018) 9:3061. doi: 10.3389/fimmu.2018.03061

216. Huppert LA, Green MD, Kim L, Chow C, Leyfman Y, Daud AI, et al. Tissue-specific tregs in cancer metastasis: opportunities for precision immunotherapy. *Cell Mol Immunol*. (2022) 19:33–45. doi: 10.1038/s41423–021-00742–4

217. Beres AJ, Drobyski WR. The role of regulatory T cells in the biology of graft versus host disease. *Front Immunol*. (2013) 4:163. doi: 10.3389/fimmu.2013.00163

218. Arjomandnejad M, Kopec AL, Keeler AM. Car-T regulatory (Car-treg) cells: engineering and applications. *Biomedicines*. (2022) 10:287. doi: 10.3390/biomedicines10020287

219. Muller YD, Ferreira LMR, Ronin E, Ho P, Nguyen V, Faleo G, et al. Precision engineering of an anti-hla-A2 chimeric antigen receptor in regulatory T cells for transplant immune tolerance. *Front Immunol*. (2021) 12:686439. doi: 10.3389/fimmu.2021.686439

220. MacDonald KG, Hoeppli RE, Huang Q, Gillies J, Luciani DS, Orban PC, et al. Alloantigen-specific regulatory T cells generated with a chimeric antigen receptor. *J Clin Invest*. (2016) 126:1413–24. doi: 10.1172/JCI82771

221. Dabrowska A, Grubba M, Balihodzic A, Szot O, Sobocki BK, Perdyan A. The role of regulatory T cells in cancer treatment resistance. *Int J Mol Sci*. (2023) 24:14114. doi: 10.3390/ijms241814114

222. BaSudan AM. The role of immune checkpoint inhibitors in cancer therapy. *Clin Pract*. (2022) 13:22–40. doi: 10.3390/clinpract13010003

223. Marabelle A, Kohrt HE, Brody J, Torchia JA, Zhou G, Luong R, et al. Local treg immunomodulation cures metastatic lymphoma including cns sites. *Blood*. (2011) 118 (21):LBA–2. doi: 10.1182/blood.v118.21.lba-2.bld0076_p1_lba-2

224. Di Pilato M, Kim EY, Cadilha BL, Prussmann JN, Nasrallah MN, Seruggia D, et al. Targeting the cbm complex causes T(Reg) cells to prime tumours for immune checkpoint therapy. *Nature*. (2019) 570:112–6. doi: 10.1038/s41586–019-1215–2

225. Liu C, Chikina M, Deshpande R, Menk AV, Wang T, Tabib T, et al. Treg cells promote the srebp1-dependent metabolic fitness of tumor-promoting macrophages via repression of cd8(+) T cell-derived interferon-gamma. *Immunity*. (2019) 51:381–97 e6. doi: 10.1016/j.immuni.2019.06.017

226. Chow MT, Luster AD. Chemokines in cancer. *Cancer Immunol Res*. (2014) 2:1125–31. doi: 10.1158/2326–6066.CIR-14–0160

227. Li C, Jiang P, Wei S, Xu X, Wang J. Regulatory T cells in tumor microenvironment: new mechanisms, potential therapeutic strategies and future prospects. *Mol Cancer*. (2020) 19:116. doi: 10.1186/s12943–020-01234–1

228. Maeda S, Murakami K, Inoue A, Yonezawa T, Matsuki N. Ccr4 blockade depletes regulatory T cells and prolongs survival in a canine model of bladder cancer. *Cancer Immunol Res*. (2019) 7:1175–87. doi: 10.1158/2326–6066.CIR-18–0751

229. Wang H, Franco F, Tsui YC, Xie X, Trefny MP, Zappasodi R, et al. Cd36-mediated metabolic adaptation supports regulatory T cell survival and function in tumors. *Nat Immunol*. (2020) 21:298–308. doi: 10.1038/s41590–019-0589–5

230. Ward-Kavanagh LK, Lin WW, Sedy JR, Ware CF. The tnf receptor superfamily in co-stimulating and co-inhibitory responses. *Immunity*. (2016) 44:1005–19. doi: 10.1016/j.immuni.2016.04.019

231. Muller D. Targeting co-stimulatory receptors of the tnf superfamily for cancer immunotherapy. *BioDrugs*. (2023) 37:21–33. doi: 10.1007/s40259–022-00573–3

232. Kremer J, Henschel P, Simon D, Riet T, Falk C, Hardtke-Wolenski M, et al. Membrane-bound il-2 improves the expansion, survival, and phenotype of car tregs and confers resistance to calcineurin inhibitors. *Front Immunol*. (2022) 13:1005582. doi: 10.3389/fimmu.2022.1005582

frontiers | Frontiers in Immunology

TYPE Original Research
PUBLISHED 15 May 2024
DOI 10.3389/fimmu.2024.1379114

OPEN ACCESS

EDITED BY
Wai Po Chong,
Hong Kong Baptist University, China

REVIEWED BY
Luciana Cavalheiro Marti,
Albert Einstein Israelite Hospital, Brazil
Masaki Yasukawa,
Ehime Prefectural University of Health Sciences, Japan
Jun Li,
Nanjing Medical University, China

*CORRESPONDENCE
Zhihai Chen
chenzhihai0001@126.com
Ling Lin
linling4012@163.com

†These authors have contributed equally to this work and share first authorship

RECEIVED 30 January 2024
ACCEPTED 22 April 2024
PUBLISHED 15 May 2024

CITATION
Liu Z, Zhao C, Yu H, Zhang R, Xue X, Jiang Z, Ge Z, Xu Y, Zhang W, Lin L and Chen Z (2024) MCP-3 as a prognostic biomarker for severe fever with thrombocytopenia syndrome: a longitudinal cytokine profile study. *Front. Immunol.* 15:1379114. doi: 10.3389/fimmu.2024.1379114

MCP-3 as a prognostic biomarker for severe fever with thrombocytopenia syndrome: a longitudinal cytokine profile study

Zishuai Liu[1†], Chenxi Zhao[1†], Hong Yu[2†], Rongling Zhang[1], Xiaoyu Xue[1], Zhouling Jiang[1], Ziruo Ge[1], Yanli Xu[2], Wei Zhang[1], Ling Lin[2*] and Zhihai Chen[1*]

[1]National Key Laboratory of Intelligent Tracking and Forecasting for Infectious Diseases, Beijing Ditan Hospital, Capital Medical University, Beijing, China, [2]Department of Infectious Diseases, Yantai Qishan Hospital, Yantai, Shandong, China

Introduction: Severe fever with thrombocytopenia syndrome (SFTS) is characterized by a high mortality rate and is associated with immune dysregulation. Cytokine storms may play an important role in adverse disease regression, this study aimed to assess the validity of MCP-3 in predicting adverse outcomes in SFTS patients and to investigate the longitudinal cytokine profile in SFTS patients.

Methods: The prospective study was conducted at Yantai Qishan Hospital from May to November 2022. We collected clinical data and serial blood samples during hospitalization, patients with SFTS were divided into survival and non-survival groups based on the clinical prognosis.

Results: The levels of serum 48 cytokines were measured using Luminex assays. Compared to healthy controls, SFTS patients exhibited higher levels of most cytokines. The non-survival group had significantly higher levels of 32 cytokines compared to the survival group. Among these cytokines, MCP-3 was ranked as the most significant variable by the random forest (RF) model in predicting the poor prognosis of SFTS patients. Additionally, we validated the predictive effects of MCP-3 through receiver operating characteristic (ROC) curve analysis with an AUC of 0.882 (95% CI, 0.787-0.978, P <0.001), and the clinical applicability of MCP-3 was assessed favorably based on decision curve analysis (DCA). The Spearman correlation analysis indicated that the level of MCP-3 was positively correlated with ALT, AST, LDH, α-HBDH, APTT, D-dimer, and viral load (P<0.01).

Discussion: For the first time, our study identified and validated that MCP-3 could serve as a meaningful biomarker for predicting the fatal outcome of SFTS patients. The longitudinal cytokine profile analyzed that abnormally increased cytokines were associated with the poor prognosis of SFTS patients. Our study provides new insights into exploring the pathogenesis of cytokines with organ damage and leading to adverse effects.

KEYWORDS

severe fever with thrombocytopenia syndrome, longitudinal cytokine profile, MCP-3, biomarker, predictive

10.3389/fimmu.2024.1379114

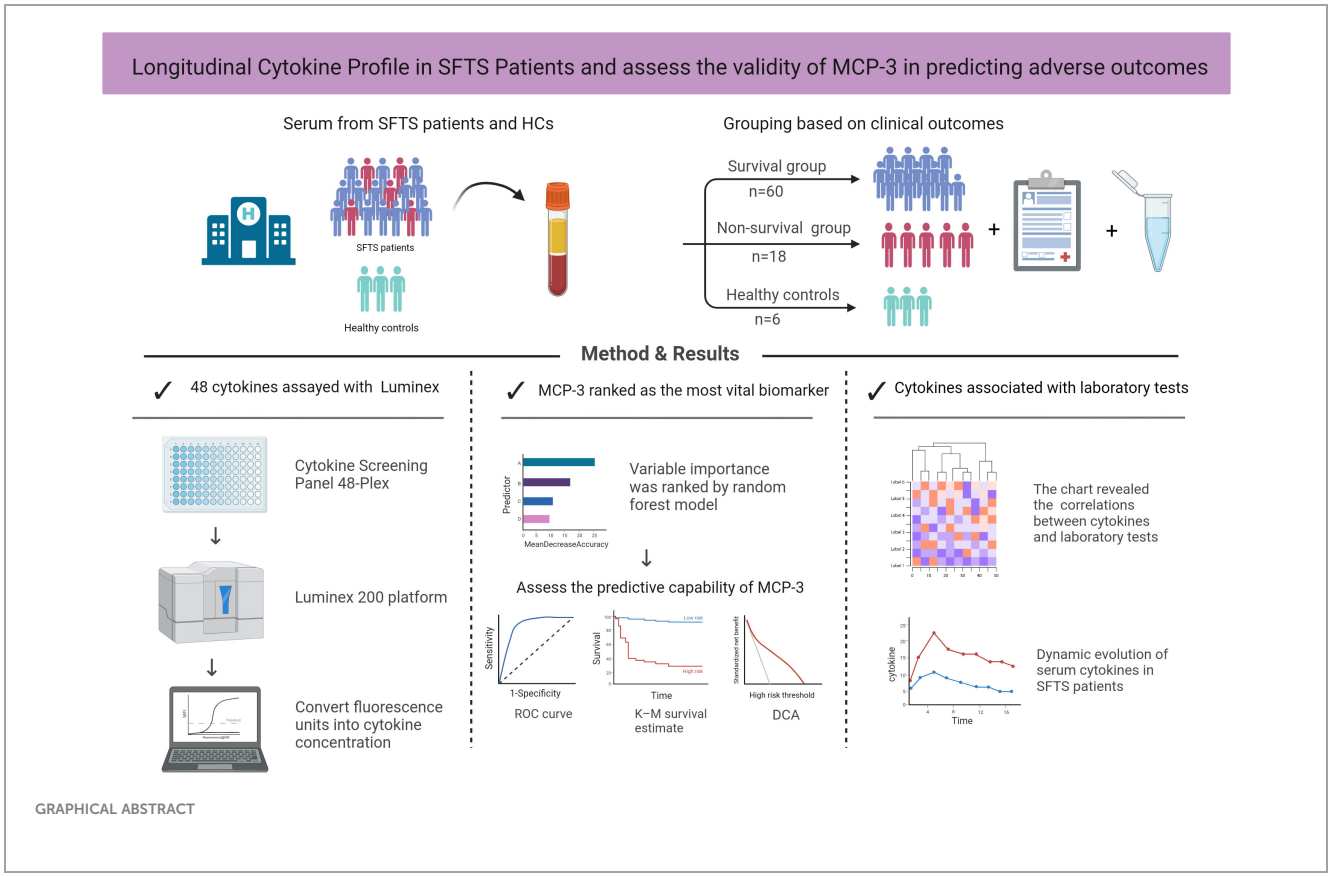

Introduction

Severe fever with thrombocytopenia syndrome (SFTS) is an acute tick-borne disease resulting from SFTS virus (SFTSV) infection (1). Reports indicate that SFTSV can also be transmitted among family members through close contact (2), involving exposure to blood and aerosols. Some patients were infected through close contact with sick domestic cats infected with SFTSV (3, 4). Since its first report in 2009, SFTSV has been spreading across several countries and regions, including Japan, South Korea, Taiwan, Vietnam, and Thailand (5–9). As of 2019, 13824 laboratory-confirmed cases have been reported across 25 provinces in China (10). Despite a decrease from 30% in the early stages due to improved understanding, the case fatality rate remains high at 6.1%-21.8% (11, 12), several studies showed the efficiency of favipiravir in treating SFTS patients (13, 14). Timely recognition and assessment of patients with severe conditions, providing sufficient and comprehensive supportive measures, are crucial for improving outcomes in individuals with SFTS. Therefore, accurately identifying critically ill patients at an early stage is of utmost importance in clinical practice.

Currently, the mechanism underlying the severity of SFTS is not well understood. Nevertheless, multiple studies have suggested a close association between the poor prognosis of SFTS patients and cytokine storm (15, 16). Numerous studies have explored the risk factors associated with adverse outcomes in SFTS patients, including clinical symptoms, signs, and laboratory parameters (17). However, only a limited number have delved into the role of cytokines in predicting a poor prognosis.

Monocyte chemoattractant protein-3 (MCP-3) is a chemokine encoded by the C-C motif chemokine ligand 7 (CCL7) gene (18). It is mainly expressed in monocytes, fibroblasts, and T cells. MCP-3 functions by attracting monocytes and eosinophils, but not neutrophils (19). Additionally, it enhances the anti-tumor activity of monocytes and binds to CC motif chemokine receptor (CCR) 1, CCR2, and CCR3, thereby influencing immune cell function (20). Previous studies have shown the robust performance of MCP-3 in identifying disease severity and predicting poor prognosis in various infectious and non-infectious diseases. For example, Sun L et al. successfully differentiated between mild and severe asthma patients using MCP-3 (21). Findings by Yang indicated a significant correlation between high serum MCP-3 concentrations and the severity of COVID-19 patients (22). Although the role of MCP-3 in predicting an unfavorable prognosis for SFTS patients remains unexplored, previous research on SFTS has indicated the crucial significance of MCP-3 in prognosticating a fatal outcome in SFTS patients. For instance, studies suggest that the MCP-3 binding protein CCR2 is the receptor for SFTSV to enter the host (23). Other studies have demonstrated that monocytes, one of the primary target cells of SFTSV, are closely associated with severe disease in patients (24). Additionally, eosinophils, one of the central chemotactic cells of MCP-3, have been identified as an independent risk factor for adverse outcomes in patients with

SFTS (25). Similarly, research has shown increased intrathecal expression of CCL7 in patients with tick-borne encephalitis (26).

It is reasonable to suspect that MCP-3 plays a significant role in the cytokine storm triggered by SFTSV infection. Furthermore, the concentration of MCP-3 closely correlates with the severity of SFTS disease, serving as a reliable indicator for predicting the prognosis of SFTS patients. To validate this hypothesis, we conducted a study using the Luminex technique to assess 48 cytokines in 78 SFTS patients with varying clinical outcomes. We also monitored the dynamic changes in these 48 factors as the disease progressed. Our study provides initial evidence of the valuable predictive and prognostic role of MCP-3 in SFTS disease.

Materials and methods

Study design and patients

This prospective study was performed from May to November 2022 at Yantai Qishan Hospital and included patients diagnosed with SFTS who were admitted to the hospital during this period and met the inclusion and exclusion criteria. The diagnostic criteria for SFTS were positive real-time fluorescent polymerase chain reaction (RT-PCR) for SFTS virus RNA during hospitalization. The exclusion criteria were: (1) Patients with other viral infections; (2) Previous leukemia, idiopathic thrombocytopenic purpura, and other blood system diseases; (3) Previous autoimmune diseases. In total, 78 patients meeting the enrollment criteria were included in the final analysis, of whom 18 had a fatal outcome. The endpoints observed in this study were defined as discharge or death (the complete study schematic chart is shown in Figure 1). The Ethics Committee of the lead center, Beijing Ditan Hospital, Capital Medical University, approved this study, which strictly adhered to the principles of the Declaration of Helsinki. Patients were informed and signed the informed consent.

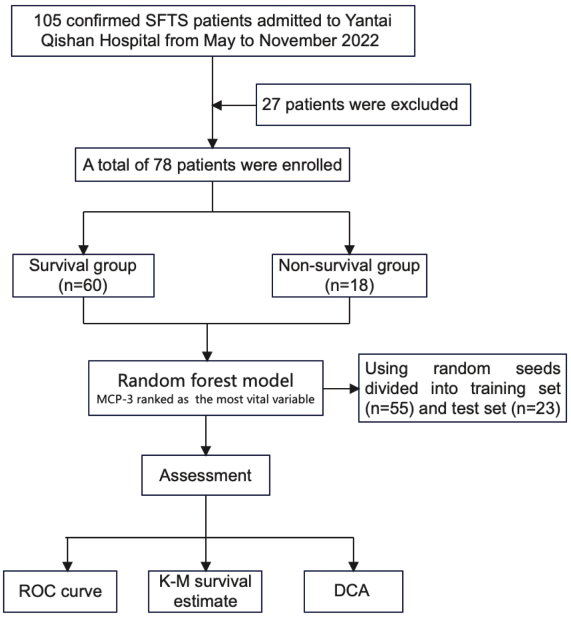

FIGURE 1
Workflow diagram of study design.

Data collection

Patient information, encompassing baseline demographics, clinical characteristics, and laboratory parameters, was extracted from medical records upon admission. Acute phase means within 7 days post-symptom onset (24, 27). We acquired serial peripheral blood samples from 78 SFTS patients 12 hours after admission and every other day during their hospitalization. These serum samples were promptly centrifuged and stored in a freezer at -80°C until further analysis. Besides, six volunteers were selected as healthy controls and matched for gender and age (Supplementary Table 1).

Cytokine assay

The subjects' serum levels of 48 cytokines were quantified with the Bio-Plex Pro Human Cytokine Screening Panel 48-Plex (Bio-Rad, Hercules, California, USA; 12007283) following the manufacturer protocol. Plate analysis was conducted using the Luminex 200 platform (Milliplex Analyst, version 5.1). We applied a standard curve with known recombinant human concentrations of cytokine to convert fluorescence units to cytokine concentration units (pg/mL). The assay examined the following cytokines: interleukin (IL)-1α, IL-1β, IL-1ra, IL-2, IL-2Rα, IL-3, IL-4, IL-5, IL-6, IL-7, IL-9, IL-10, IL-12(p40), IL-12 (p70), IL-13, IL-15, IL-16, IL-17, IL-18, leukemia inhibitory factor (LIF), granulocyte colony-stimulating factor (G-CSF), granulocyte macrophage colony-stimulating factor (GM-CSF), macrophage colony-stimulating factor (M-CSF), stem cell factor (SCF), stem cell growth factor (SCGF)-β, interferon (IFN)-γ, IFN-α2, tumor necrosis factor (TNF)-α, TNF-β, tumor necrosis factor-related apoptosis-inducing ligand (TRAIL), basic fibroblast growth factors (FGF), vascular endothelial growth factor (VEGF), platelet derived growth factor-BB (PDGF-BB), hepatocyte growth factor (HGF), β-nerve growth factor (NGF), CXCL1 (GRO-α), CXCL8 (IL-8), CXCL9 (MIG), CXCL10 (IP-10), CXCL12 (SDF-1α), CCL2 (MCP-1), CCL3 (MIP-1α), CCL4 (MIP-1β), CCL5 (RANTES), CCL7(MCP-3), CCL11 (Eotaxin), CCL27 (CTACK), macrophage migration Inhibitory Factor (MIF). In statistical analyses, cytokines were excluded if over 50% of values fell outside the upper or lower limits of detection, and if the concentration was below the lowest detection limit, 50% of the lowest detection value was used (28, 29).

Definition

Skin change is defined as at least one of the signs: skin color changes, skin eruption, or the development of nodules. Neurological abnormalities encompass changes in consciousness and signs such as involuntary movements, nerve reflexes, and muscle tension.

Statistical analyses

Normal distribution data were presented as mean ± standard deviation and compared between groups using the independent-samples t-test. Abnormally distributed data were presented as median with interquartile range (IQR) and compared between groups using the Mann-Whitney U test. Categorical variables were expressed as percentage and analyzed using the $\chi 2$ test. The RF algorithm was employed to screen for important variables, and the predictive accuracy of prognostics was assessed using a receiver operating characteristic (ROC) curve analysis. Correlations between variables were evaluated using the Spearman correlation test. Linear mixed models were utilized for continuous outcomes and estimated marginal means (EMMs) with a 95% confidence interval (CI) were calculated. Statistical analyses were conducted using SPSS software (version 26.0), and figures were generated using the R programming language (version 4.3.1). All tests were two-sided, and $P < 0.05$ was considered statistically significant.

Results

Baseline demographic, laboratory, and clinical characteristics

We enrolled 78 patients with confirmed SFTS in our study. Based on clinical outcomes, they were categorized into a survival group (n=60) and a non-survival group (n=18), resulting in a fatality rate of 23.1% (18/78). Table 1 presents the baseline demographics, clinical characteristics, and laboratory parameters at admission for both survival and non-survival groups. All SFTS patients had an average age of 65.89 ± 11.19 years. Among these patients, the survivors had an average age of 64.92 ± 11.76 years, while the non-survivors had higher average age of 69.11 ± 8.54 years. Out of the total 78 patients, 37 (47.4%) were male, including 27 (45.0%) in the survival group and 10 (55.6%) in the non-survival group. There was no significant difference in age or gender between the two groups ($P > 0.05$). In comparison to the survival group (925.5, 404.25-2773.25), the non-survival group (3858, 1746.5-4921) exhibited a higher viral load, demonstrating significant differences ($P < 0.05$). In terms of laboratory examination, we observed that alanine aminotransaminase (ALT), aspartate aminotransferase (AST), direct bilirubin (DBIL), blood urea nitrogen (BUN), creatinine (CREA), creatine kinase (CK), creatine kinase isoenzyme MB (CK-MB), α-hydroxybutyrate dehydrogenase (α-HBDH), lactate dehydrogenase (LDH), K^+, Na^+, procalcitonin (PCT), activated partial thromboplastin time (APTT), thrombin time (TT), and D-dimer levels were significantly higher in the non-survival group compared to the survival group ($P < 0.05$).All patients showed a decrease in white blood cell (WBC) counts, lymphocytes (LYM), and platelet (PLT) counts, while there was no significant difference between the two groups ($P > 0.05$).

Comparing cytokine levels during the acute phase between the two groups

Due to more than 50% of values being lower limits of detection, 8 cytokines, including IL-2, IL-3, IL-5, IL-7, IL-12 (p70), IL-15,

TABLE 1 Baseline demographics, clinical characteristics, and laboratory parameters of patients with SFTS.

Variables	All patients (N=78)	Survivors (N=60)	Non-Survivors (N=18)	*p*-value
Demographics				
Age(years)	65.89 ± 11.19	64.92 ± 11.76	69.11 ± 8.54	0.165
Male	37(47.4%)	27(45.0%)	10(55.6%)	0.432
Total disease duration (d)	13.00(11.00-17.25)	14.00(12.25-18.75)	10.50(8.75-13.25)	**0.003**
Time from onset to admission (d)	5.00(4.00-6.00)	5.00(4.00-6.00)	5.00(3.75-6.00)	0.991
Time of hospitalization(d)	9.00(6.75-13.00)	9.00(7.25-13.00)	6.00(3.75-8.25)	0.058
Highest temperature (°C)	38.71 ± 0.67	38.73 ± 0.71	38.63 ± 0.53	0.570
Viral load ($TCID_{50}$/ml)	1899.00(420.25-3780.50)	925.50(404.25-2773.25)	3858.00(1746.50-4921.00)	**0.005**
Bite by ticks	27(34.6%)	19(31.7%)	8(44.4%)	0.318
Symptoms				
Weak	56(71.8%)	43(71.7%)	13(72.2%)	0.963
Shiver	26(33.3%)	21(35.0%)	5(27.8%)	0.569
Inappetence	30(38.5%)	22(36.7%)	8(44.4%)	0.552
Nausea	26(33.3%)	18(30.0%)	8(44.4%)	0.254
Vomiting	17(21.8%)	10(16.7%)	7(38.9%)	0.093

(Continued)

TABLE 1 Continued

Variables	All patients (N=78)	Survivors (N=60)	Non-Survivors (N=18)	*p*-value
Symptoms				
Diarrhea	18(23.1%)	16(26.7%)	2(11.1%)	0.291
Abdominal pain	10(12.8%)	7(11.7%)	3(16.7%)	0.877
Muscular soreness	22(28.2%)	17(28.3%)	5(27.8%)	0.963
Signs				
Skin changes	5(6.4%)	2(3.3%)	3(16.7%)	0.140
Lymphadenectasis	19(24.4%)	17(28.3%)	2(11.1%)	0.238
Neurological system	12(15.4%)	8(13.3%)	4(22.2%)	0.586
Laboratory examination				
WBC (3.5-9.5*10^9/L)	2.90(1.76-4.18)	2.81(1.62-4.19)	3.06(2.25-4.41)	0.334
Neutrophils (1.8-6.3*10^9/L)	1.72(0.93-2.98)	1.63(0.87-2.88)	2.19(1.57-3.24)	0.148
Lymphocytes (1.1-3.2*10^9/L)	0.64(0.42-0.98)	0.64(0.43-1.00)	0.67(0.38-0.90)	0.695
Monocytes (0.1-0.6*10^9/L)	0.19(0.07-0.29)	0.18(0.07-0.26)	0.26(0.08-0.44)	0.196
HGB (130-175g/L)	140.05 ± 18.24	138.30 ± 17.44	145.89 ± 20.12	0.122
PLT (125-350*10^9/L)	59.00(46.75-78.25)	61.00(49.00-82.00)	51.00(42.00-64.75)	0.066
ALT (9-50U/L)	65.00(38.78-134.63)	52.70(38.30-111.78)	133.25(64.90-248.35)	**0.005**
AST (15-40U/L)	151.50(74.20-331.28)	120.25(61.55-205.28)	379.50(170.00-722.53)	**<0.001**
GGT (11-49U/L)	27.00(17.75-66.25)	25.50(17.00-63.50)	39.00(23.96-73.75)	0.245
ALP (40-150U/L)	59.65(51.38-90.78)	58.00(50.38-86.33)	65.30(54.08-108.98)	0.217
Albumin (35-53g/L)	30.92 ± 4.90	31.24 ± 4.85	29.86 ± 5.06	0.295
TBil (2.0-20.4μmol/L)	10.27(7.60-13.04)	9.38(7.50-12.49)	10.67(8.78-19.70)	0.081
DBil (0.1-3.4μmol/L)	3.39(2.36-5.14)	3.22(2.32-4.92)	4.61(2.94-8.26)	**0.030**
BUN (1.7-8.3mmol/L)	6.28(4.19-8.15)	5.34(3.87-6.86)	9.60(7.35-13.70)	**<0.001**
CREA (40-106μmol/L)	66.00(53.23-86.05)	62.60(51.65-71.50)	103.50(69.28-172.38)	**<0.001**
CK (0-190U/L)	497.00(213.25-1347.75)	366.00(183.25-961.75)	1345.00(475.25-2727.50)	**0.006**
CK-MB (0-5ng/mL)	4.02(2.32-10.50)	3.55(1.76-9.73)	7.50(3.50-22.47)	**0.012**
α-HBDH (72-182U/L)	481.51(263.52-584.00)	322.96(241.84-489.29)	609.02(507.60-936.73)	**<0.001**
LDH (80-285U/L)	611.00(370.00-980.25)	522.00(353.25-819.00)	1042.50(714.73-1829.75)	**<0.001**
K^+ (3.5-5.1mmol/L)	3.68(3.38-4.00)	3.61(3.31-3.87)	4.02(3.49-4.62)	**0.019**
Na^+(136-146mmol/L)	134.64 ± 4.69	133.97 ± 4.55	136.90 ± 4.55	**0.019**
Hs-CRP (0-5mg/L)	4.07(1.48-12.51)	3.48(1.27-9.46)	10.86(3.12-14.65)	0.081
PCT (0-0.05ng/ml)	0.16(0.10-0.46)	0.14(0.09-0.25)	0.51(0.30-1.04)	**<0.001**
PT (11-14.5s)	12.60(12.00-13.20)	12.60(11.90-13.20)	12.60(12.28-13.30)	0.316
APTT (28-43.5s)	49.85(43.90-58.65)	47.15(43.38-55.60)	58.70(51.23-66.00)	**0.002**
TT (14-21s)	23.85(21.48-27.90)	23.40(21.03-26.20)	29.15(23.38-42.18)	**0.006**
D-dimer (0-0.5μg/ml)	2.67(1.63-4.57)	2.45(1.38-3.42)	5.70(2.49-8.52)	**0.001**

The Categorical variables were presented by frequencies and percentages (n, %), and tested with the χ 2 test. Continuous variables were summarized as means and standard deviations (SD) or as medians and interquartile range (IQR) and tested with t-test or Mann–Whitney U test. P values comparing the group of survival and non-survival.
WBC, White blood cell; HGB, Hemoglobin; PLT, Platelet; ALT, Alanine aminotransferase; AST, Aspartate aminotransferase; GGT, γ-glutamyl transferase; ALP, Alkaline phosphatase; TBiL, Total bilirubin; DBil, Direct bilirubin; BUN, Blood urea nitrogen; CREA, Creatinine; CK, Creatine kinase; CK-MB, Creatine kinase isoenzyme MB; α-HBDH, α-hydroxybutyrate dehydrogenase; LDH, Lactate dehydrogenase; Hs-CRP, High-sensitivity C-reactive protein; PCT, Procalcitonin; PT, Prothrombin time; APTT, Activated partial thromboplastin time; TT, Thrombin time.
Bold values indicate p-values <0.05, statistically different.

VEGF, and β-NGF, were excluded from the analysis. The results revealed that in the acute phase of SFTS, non-survival group had significantly higher levels of 32 cytokines, such as IL-1α, IL-1β, IL-1ra, IL-2Rα, IL-4, IL-6, IL-10, IL-12(p40), IL-16, IL-17, L-18, LIF, G-CSF, M-CSF, SCF, IFN-γ, IFN-α2, TNF-α, TRAIL, basic FGF, HGF, MCP-1, MIP-1α, MCP-3, Eotaxin, CTACK, IL-8, MIG, IP-10, SDF-1α, and MIF compared to survival group, and these differences were statistically significant ($P < 0.05$). Simultaneously, these cytokine levels were elevated compared to healthy controls, except for MIF in survivors (Figure 2).

MCP-3 serves as a crucial biomarker in predicting the prognosis of SFTS patients

The 78 patients were randomly divided into a training set and a test set at a 7:3 ratio using random seeds with the RF algorithm model. Supplementary Figure 1A illustrates the relationship between error and the number of decision trees, with 500 trees chosen as the number of RF models, indicating a stable error. Subsequently, we employed ROC curves to evaluate the predictive ability of the model. The area under curve (AUC) of the ROC for the training set and test set was 1.000 (95% CI: 0.935-1.000) and 0.870 (95% CI: 0.664-0.972), respectively (Supplementary Figure 1B). We assessed the importance of 40 cytokines by analyzing the output results of MeanDecreaseAccuracy (Figure 3A) and MeanDecreaseGini (Figure 3B). The top 20 important variables were then presented, with MCP-3 identified as the most crucial predictive cytokine for the critical outcome of SFTS patients in acute phase.

Subsequently, ROC curve analysis was employed to assess the specificity and sensitivity of MCP-3 in predicting SFTS patients' fatal clinical outcomes. MCP-3 had an AUC of 0.882 (95% CI: 0.787-0.978, $P < 0.001$), with a cutoff value of 10.89 pg/ml (Figure 4A). Based on the cutoff value, all patients were categorized into low-risk groups, characterized by MCP-3 levels less than or equal to the cutoff value, and high-risk groups,

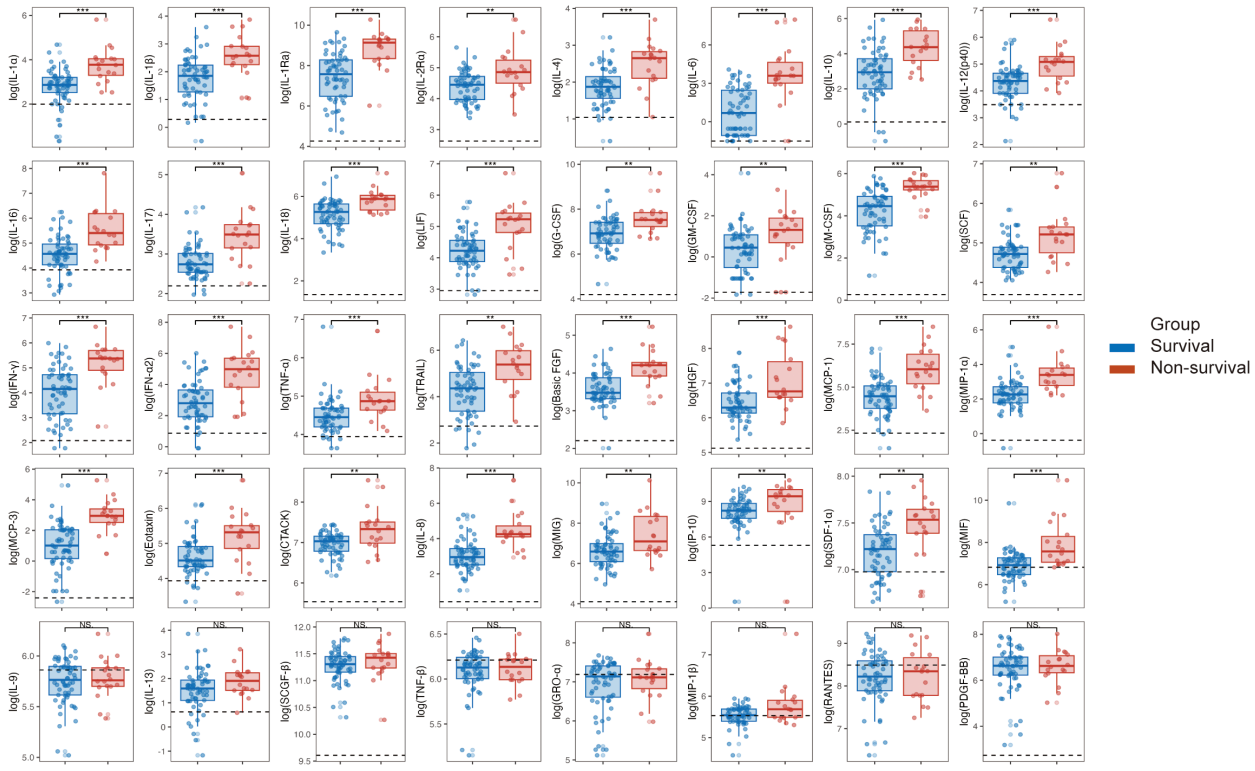

FIGURE 2
Comparison of cytokine levels between survival and non-survival groups in patients with SFTS in the acute phase. Following the logarithmic transformation of cytokine results, compare the acute-phase cytokine levels between the survival and non-survival groups in SFTS patients. *$P < 0.05$, **$P < 0.01$, ***$P < 0.001$. NS, not significant. IL, interleukin; IFN, interferon; TNF, tumor necrosis factor alpha; LIF, leukemia inhibitory factor; G-CSF, granulocyte colony stimulating factor; GM-CSF, granulocyte macrophage colony stimulating factor; M-CSF, macrophage colony stimulating factor; SCF, stem cell factor; SCGF-beta, stem cell growth factor beta; TRAIL, TNF related apoptosis-inducing ligand; Basic FGF, basic fibroblast growth factor; beta-NGF, nerve growth factor beta; HGF, hepatocyte growth factor; PDGF-BB, platelet derived growth factor-BB; VEGF, vascular endothelial growth factor; CTACK, cutaneous T cell attracting chemokine; Eotaxin, recombinant human eotaxin; GRO-alpha, growth-related oncogene alpha; IP-10, interferon inducible protein 10; MCP, monocyte chemoattractant protein; MIF, macrophage migration inhibitory factor; MIG, monokine induced by gamma interferon; MIP, macrophage inflammatory protein; RANTES, regulated upon activation normal T Cell expressed and presumably secreted; SDF-1alpha, stromal cell derived factor 1alpha.

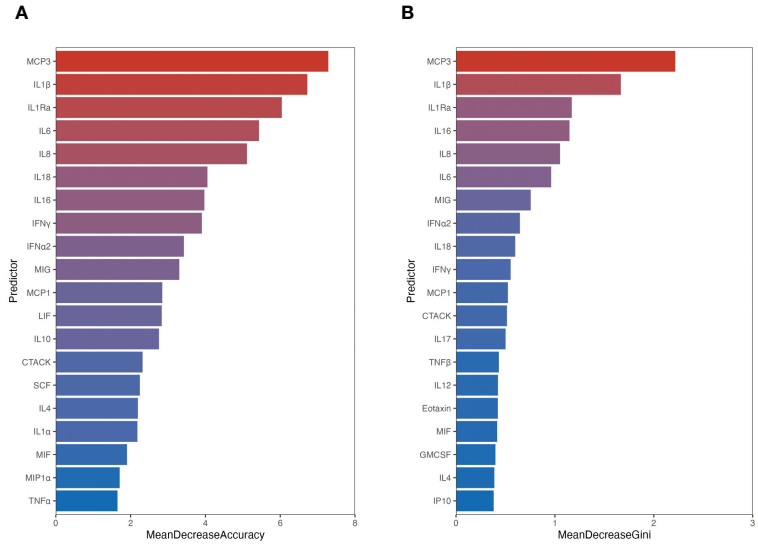

FIGURE 3
The importance of variables ranked by random forest. Variable importance was ranked according to calculating MeanDecreaseAccuracy **(A)** and MeanDecreaseGini **(B)**. The chart displays the top 20 important variables, with the color bar length indicating the contribution from each variable.

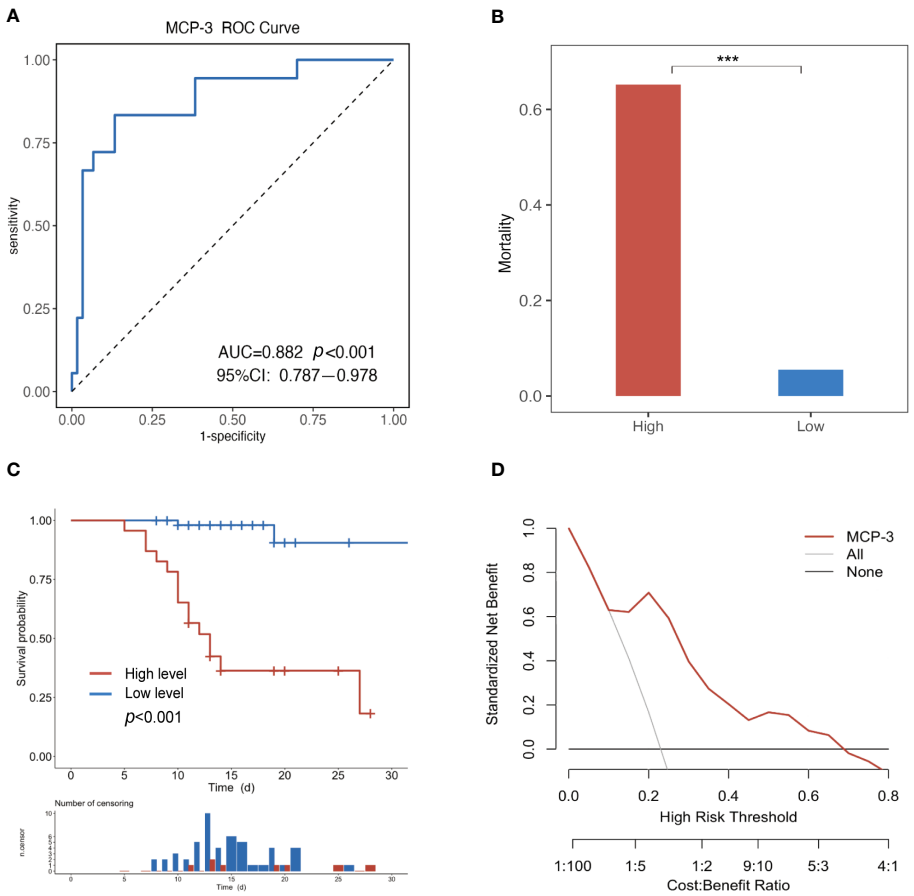

FIGURE 4
Evaluating the ability of MCP-3 to predict poor prognosis in SFTS patients. **(A)** The MCP-3 had an AUC of 0.882 ($P < 0.001$, 95%CI 0.787-0.978); **(B)** Comparing fatality across different MCP-3 levels. ***$P<0.001$. **(C)** Kaplan–Meier survival estimate based on the MCP-3 level cut-off; **(D)** Decision curve analysis for the MCP-3. The y-axis represents net benefit, and the x-axis represents the threshold probability (High Risk Threshold). MCP-3, monocyte chemoattractant protein-3; AUC, area under the receiver operating characteristic curve.

characterized by MCP-3 levels higher than the cutoff value. The fatality rate of the high-risk group (65.2%) was significantly higher than that of the low-risk group (5.5%) ($P < 0.001$) (Figure 4B). We further employed the Kaplan-Meier (KM) analysis method to estimate cumulative survival. The results revealed that SFTS patients in the high-risk group, also known as MCP-3 high group, exhibited lower cumulative survival than those in the low-risk group ($P < 0.001$) (Figure 4C). Furthermore, the clinical utility of MCP-3 in predicting adverse outcomes in patients with SFTS in the acute phase was evaluated through a decision curve analysis (DCA). As shown in Figure 4D, at threshold probabilities between 0.1 and 0.7, the clinical benefit of MCP-3 was markedly superior to that of complete intervention or no intervention at all.

Correlation analysis of cytokines with laboratory parameters

The correlation analysis of cytokines with laboratory parameters is presented in Figure 5. As depicted in the figure, MCP-3 exhibited positive correlations not only with various organ damage parameters, such as ALT, AST, LDH, α-HBDH, APTT, and D-dimer, but also with viral load. From Figure 5, it is evident that D-dimer exhibited significant positive correlations with various cytokines, particularly M-CSF, MCP-3, and IL-16. Moreover, LDH and α-HBDH, which are two markers of organ damage, showed positive correlations with various cytokines, especially with M-CSF, MCP-3, MIG, IL-16, IL-10, and HGF.

FIGURE 5
Bubble chart illustrating cytokines associated with laboratory tests. The chart depicts correlations between cytokines and laboratory tests using Spearman correlation analysis. Red bubbles indicate positive correlations, blue bubbles indicate negative correlations. The size of the bubbles represents significant differences, and all bubbles in the graphs indicate significant differences ($P < 0.01$). IL, interleukin; IFN, interferon; TNF, tumor necrosis factor alpha; LIF, leukemia Inhibitory factor; G-CSF, granulocyte colony stimulating factor; GM-CSF, granulocyte macrophage colony stimulating factor; M-CSF, macrophage colony stimulating factor; SCF, stem cell factor; SCGF-beta, stem cell growth factor beta; TRAIL, TNF related apoptosis-inducing ligand; Basic FGF, basic fibroblast growth factor; beta-NGF, nerve growth factor beta; HGF, hepatocyte growth factor; PDGF-BB, platelet derived growth factor-BB; VEGF, vascular endothelial growth factor; CTACK, cutaneous T cell attracting chemokine; Eotaxin, recombinant human eotaxin; GRO-alpha, growth-related oncogene alpha; IP-10, interferon inducible protein 10; MCP, monocyte chemoattractant protein; MIF, macrophage migration inhibitory factor; MIG, monokine induced by gamma interferon; MIP, macrophage inflammatory protein; RANTES, regulated upon activation normal T Cell expressed and presumably secreted; SDF-1alpha, stromal cell derived factor 1alpha; ALT, alanine aminotransaminase; AST, Aspartate aminotransferase; ALP, alkaline phosphatase; BUN, blood urea nitrogen; CREA, creatinine; CK, creatine phosphokinase; CK-MB, creatine kinase isoenzyme-MB; HGB, hemoglobin; PCT, procalcitonin; GGT, γ-glutamyl transferase; LDH, lactate dehydrogenase; PLT, platelet; PCT, procalcitonin; TBIL, total bilirubin; WBC, white blood cell; MONO, monocyte; α-HBDH, α-hydroxybutyrate dehydrogenase; TBIL, total bilirubin; APTT, activated partial thromboplastin time; ALB, albumin; TT, thrombin time; DBIL, direct bilirubin; HsCRP, hypersensitive C-reactive protein.

Longitudinal cytokine profiles of SFTS patients with different clinical outcomes

In this study, MCP-3 levels exhibited a rapid increase, reaching a maximum, followed by a decrease and stabilization at higher levels until death in non-survivors. These levels consistently surpassed those in survivors and healthy controls. A similar trend was observed for IL-1α, IL-1Ra, IL-4, IL-10, IL-17, LIF, IFN-γ, GM-CSF, M-CSF, SCGF-β, basic FGF, HGF, MCP-1, Eotaxin, MIG, and IP-10. The levels of IL-6, IL-16, IL-18, IFN-α2, HGF, MCP-1, MCP-3, Eotaxin, CTACK, MIG, and MIF were significantly elevated in non-survivors, whereas they remained relatively stable in survivors, comparable to healthy controls. Cytokines such as IL-6, IL-16, IFN-α2, HGF, MCP-1, MCP-3, Eotaxin, MIG, and MIF exhibited similar levels when comparing HCs and survivors. Additionally, we noted lower levels of IL-9, TNF-β, PDGF-BB, and RANTES in non-survivors compared to survivors during hospitalization. Unlike other cytokines, the concentrations of them tended to increase during the late course of the disease in survivors (Figure 6).

Discussion

SFTS is a newly emerging infectious disease with a high mortality rate. The World Health Organization has recognized SFTSV as one of the top-prioritized pathogens for research and development (30). Compared to healthy controls, the study observed that all SFTS patients showed increased levels of various cytokines, except for individual ones such as IL-9, TNF-β, GRO-α, and RANTES. Further analysis indicated that the non-survival group exhibited significantly higher levels of 32 cytokines than the survival group. This finding aligns with previous research, supporting the notion that the immune dysfunction-cytokine storm closely linked to the unfavorable prognosis of SFTS patients (31, 32).

According to the RF algorithm model, MCP-3 has identified as a crucial factor in predicting adverse clinical outcomes in SFTS patients. In non-survivors of SFTS, MCP-3 levels rapidly increased during the acute phase, reaching the highest level. As the disease progressed, MCP-3 concentrations decreased slightly but remained higher than in non-survivors until death. Moreover, compared to healthy controls, the MCP-3 concentration in the patients in the survival group showed a slight increase, but no significant difference observed.

MCP-3 is a member of the monocyte chemotactic proteins (MCP) subgroup of CC chemokines. It was produced by various cells, including monocytes, T lymphocytes, fibroblasts, and platelets (19). MCP-3 is a highly versatile chemokine, activating a broad spectrum of leukocytes, such as natural killer cells and T lymphocytes (33). It is a chemoattractant for monocytes, eosinophils, macrophages, basophils, lymphocytes, and dendritic cells (20). studies have demonstrated the pivotal role of MCP-3 in distinguishing between infectious and non-infectious diseases.

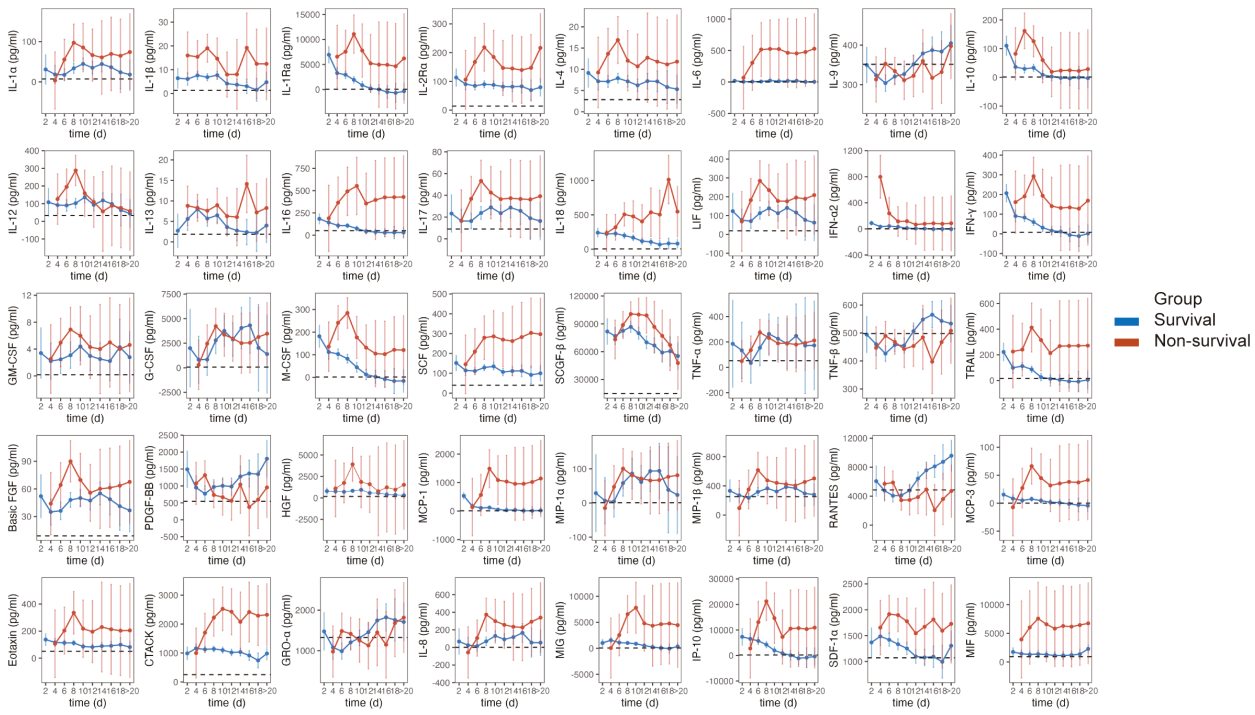

FIGURE 6
Dynamic evolution of serum cytokines in SFTS patients. Estimated marginal means (EMMs) and 95%CI with linear mixed-effects models for dynamic analysis of cytokines. Error bars indicate 95%CI. The dotted horizontal line within each cytokine panel represents the average value for healthy controls.

Research by Sun L's team indicates the potential utility of serum MCP-3 levels in distinguishing between patients with mild and severe asthma (21). Yang et al. examined 48 cytokines in the peripheral blood of COVID-19 patients, identifying IP-10, MCP-3, and IL-1ra as biomarkers associated with disease severity and fatal outcomes (34).

Although there is currently no relevant study on the mechanism by which MCP-3 mediates the severity of SFTS, we attempted to analyze it from two perspectives: viral infiltration and inflammatory damage. Our study found that the serum SFTSV level was significantly higher in the non-survival group than in the survival group, and the serum MCP-3 level positively correlated with the SFTSV. CCR2 is recognized as one of the primary receptors of MCP-3 (35). Recent studies have also identified CCR2 as the host receptor of SFTSV. Knocking out CCR2 has been shown to significantly reduce virus binding and infection, while increased expression of CCR2 leads to enhanced infection (23). Hence, it is plausible that MCP-3 assists CCR2 in mediating virus invasion into the host. Additionally, studies have demonstrated that in COVID-19 patients, the increase in viral load corresponds to the upregulation of critical chemokines, including CCL7, CCL2, CXCL8, and others (36, 37).

In terms of inflammation, MCP-3, as an inflammatory cytokine, plays a crucial role in maintaining a balanced level of circulating inflammatory monocytes. A deficiency in MCP-1 or MCP-3 results in approximately 40–50% decrease in monocyte recruitment during infection (38). A study by Girkin J's team demonstrated that CCL7 is the most significantly upregulated gene induced by rhinovirus infection, and inhibiting CCL7 reduces inflammation and airway hyperreactivity (AHR) (39). Additionally, children with naturally occurring viral infections release high concentrations of MCP-3 and MCP-4 into their nasal secretions (40). To examine the relationship between MCP-3 and organ damage, correlation analysis was conducted on laboratory indicators such as ALT, AST, LDH, α-HBDH, APTT, and D-dimer etc. Previous studies identified these indicators as independent risk factors for poor prognosis in SFTS patients. The findings revealed a significant positive correlation between MCP-3 and these indicators.

In this study, we found that the concentrations of TNF-β had increased in the late stage for survivors, and the related studies were rarely reported in SFTS. There was a study found that TNF-β was considerably increased in patients with COVID-19 (41). Previous studies have shown that the concentrations of RANTES in plasma tended to increase during the late course of the disease, which was consistent with our findings in the survival group (42, 43), similar finding was reported in the late stage of survivors with Middle East respiratory syndrome (MERS) that RANTES marked elevation (44). Our study also suggested that the PLT levels are closely correlated with the levels of RANTES. Another study manifested that RANTES had large fluctuations after onset, and the higher virus loads suppressed the production of RANTES to a large extent (15). RANTES can recruit and activate T cells and they may play a crucial role in recovery from SFTS.

This study has certain limitations. Firstly, the sample size is limited, and the source is singular. Secondly, although we observed the role of MCP-3 in the prognosis of SFTS patients, further experiments are needed to explore its mechanism of action. Lastly, in future research, we aim to expand the sample size and sources, employing sequencing technology to investigate the mechanisms underlying the elevated MCP-3 levels and their impact on patients with severe SFTS.

Conclusions

In summary, we observed a correlation between abnormally elevated MCP-3 levels and a poor prognosis in SFTS patients. This study is the first to reveal that MCP-3 levels could serve as a meaningful biomarker for predicting the severe and fatal outcome of SFTS patients. These findings contribute to the advancement of our understanding, exploration, and management of SFTS.

Data availability statement

The raw data supporting the conclusions of this article will be made available by the authors, without undue reservation.

Ethics statement

The studies involving humans were approved by the Ethics Committee of Beijing Ditan Hospital, Capital Medical University (NO. DTEC-KY2022-022-01) and conducted in accordance with the principles of the Helsinki Declaration. All participants provided written informed consent. The studies were conducted in accordance with the local legislation and institutional requirements. The participants provided their written informed consent to participate in this study.

Author contributions

ZL: Conceptualization, Formal Analysis, Methodology, Writing – original draft, Writing – review & editing. CZ: Conceptualization, Formal Analysis, Methodology, Visualization, Writing – original draft, Writing – review & editing. HY: Data curation, Methodology, Writing – original draft. RZ: Data curation, Formal Analysis, Writing – original draft. XX: Data curation, Formal Analysis, Writing – original draft. ZJ: Investigation, Resources, Writing – original draft. ZG: Data curation, Writing – original draft. YX: Investigation, Writing – original draft. WZ: Investigation, Writing – review & editing. LL: Supervision, Writing – review & editing. ZC: Conceptualization, Writing – review & editing.

Funding

The author(s) declare financial support was received for the research, authorship, and/or publication of this article. This work was supported by the National Natural Science Foundation of China (NO. 82072295).

Acknowledgments

We would like to express our gratitude to all the healthcare workers who contributed to this study. We extend our thanks to the Department of Infectious Diseases at Yantai Qishan Hospital for their valuable support. The graphical abstract was created with BioRender.com and has been obtained for use of copyrighted.

Conflict of interest

The authors declare that the research was conducted in the absence of any commercial or financial relationships that could be construed as a potential conflict of interest.

Publisher's note

Supplementary material

The Supplementary Material for this article can be found online at: https://www.frontiersin.org/articles/10.3389/fimmu.2024.1379114/full#supplementary-material

References

1. Yu XJ, Liang MF, Zhang SY, Liu Y, Li JD, Sun YL, et al. Fever with thrombocytopenia associated with a novel bunyavirus in China. *N Engl J Med*. (2011) 364:1523–32. doi: 10.1056/NEJMoa1010095

2. Liu T, Zhang N, Li H, Hou S, Liu X. Analysis of severe fever with thrombocytopenia syndrome cluster in east China. *Virol J*. (2023) 20:199. doi: 10.1186/s12985-023-02155-3

3. Yamanaka A, Kirino Y, Fujimoto S, Ueda N, Himeji D, Miura M, et al. Direct transmission of severe fever with thrombocytopenia syndrome virus from domestic cat to veterinary personnel. *Emerg Infect Dis*. (2020) 26:2994–8. doi: 10.3201/eid2612.191513

4. Park ES, Shimojima M, Nagata N, Ami Y, Yoshikawa T, Iwata-Yoshikawa N, et al. Severe Fever with Thrombocytopenia Syndrome Phlebovirus causes lethal viral hemorrhagic fever in cats. *Sci Rep*. (2019) 9:11990. doi: 10.1038/s41598-019-48317-8

5. Kobayashi Y, Kato H, Yamagishi T, Shimada T, Matsui T, Yoshikawa T, et al. Severe fever with thrombocytopenia syndrome, Japan, 2013-2017. *Emerg Infect Dis*. (2020) 26:692–9. doi: 10.3201/eid2604.191011

6. Yoo JR, Heo ST, Song SW, Bae SG, Lee S, Choi S, et al. Severe fever with thrombocytopenia syndrome virus in ticks and SFTS incidence in humans, South Korea. *Emerg Infect Dis*. (2020) 26:2292–4. doi: 10.3201/eid2609.200065

7. Lin TL, Ou SC, Maeda K, Shimoda H, Chan JP, Tu WC, et al. The first discovery of severe fever with thrombocytopenia syndrome virus in Taiwan. *Emerg Microbes Infect*. (2020) 9:148–51. doi: 10.1080/22221751.2019.1710436

8. Tran XC, Yun Y, Van An L, Kim SH, Thao NTP, Man PKC, et al. Endemic severe fever with thrombocytopenia syndrome, Vietnam. *Emerg Infect Dis*. (2019) 25:1029–31. doi: 10.3201/eid2505.181463

9. Rattanakomol P, Khongwichit S, Linsuwanon P, Lee KH, Vongpunsawad S, Poovorawan Y. Severe fever with thrombocytopenia syndrome virus infection, Thailand, 2019-2020. *Emerg Infect Dis*. (2022) 28:2572–4. doi: 10.3201/eid2812.221183

10. Huang X, Li J, Li A, Wang S, Li D. Epidemiological characteristics of severe fever with thrombocytopenia syndrome from 2010 to 2019 in mainland China. *Int J Environ Res Public Health*. (2021) 18:3092. doi: 10.3390/ijerph18063092

11. Wang Y, Song Z, Wei X, Yuan H, Xu X, Liang H, et al. Clinical laboratory parameters and fatality of Severe fever with thrombocytopenia syndrome patients: A systematic review and meta-analysis. *PloS Negl Trop Dis*. (2022) 16:e0010489. doi: 10.1371/journal.pntd.0010489

12. Liang S, Xie W, Li Z, Zhang N, Wang X, Qin Y, et al. Analysis of fatal cases of severe fever with thrombocytopenia syndrome in Jiangsu province, China, between 2011 and 2022: A retrospective study. *Front Public Health*. (2023) 11:1076226. doi: 10.3389/fpubh.2023.1076226

13. Suemori K, Saijo M, Yamanaka A, Himeji D, Kawamura M, Haku T, et al. A multicenter non-randomized, uncontrolled single arm trial for evaluation of the efficacy and the safety of the treatment with favipiravir for patients with severe fever with thrombocytopenia syndrome. *PloS Negl Trop Dis*. (2021) 15:e0009103. doi: 10.1371/journal.pntd.0009103

14. Yuan Y, Lu QB, Yao WS, Zhao J, Zhang XA, Cui N, et al. Clinical efficacy and safety evaluation of favipiravir in treating patients with severe fever with thrombocytopenia syndrome. *EBioMedicine*. (2021) 72:103591. doi: 10.1016/j.ebiom.2021.103591

15. He Z, Wang B, Li Y, Hu K, Yi Z, Ma H, et al. Changes in peripheral blood cytokines in patients with severe fever with thrombocytopenia syndrome. *J Med Virol*. (2021) 93:4704–13. doi: 10.1002/jmv.26877

16. Mendoza CA, Ebihara H, Yamaoka S. Immune modulation and immune-mediated pathogenesis of emerging tickborne banyangviruses. *Vaccines*. (2019) 7:125. doi: 10.3390/vaccines7040125

17. He Z, Wang B, Li Y, Du Y, Ma H, Li X, et al. Severe fever with thrombocytopenia syndrome: a systematic review and meta-analysis of epidemiology, clinical signs, routine laboratory diagnosis, risk factors, and outcomes. *BMC Infect Dis*. (2020) 20:575. doi: 10.1186/s12879-020-05303-0

18. Dahinden CA, Geiser T, Brunner T, von Tscharner V, Caput D, Ferrara P, et al. Monocyte chemotactic protein 3 is a most effective basophil- and eosinophil-activating chemokine. *J Exp Med*. (1994) 179:751–6. doi: 10.1084/jem.179.2.751

19. Rollins BJ. Chemokines. *Blood*. (1997) 90:909–28. doi: 10.1182/blood.V90.3.909

20. Power CA, Clemetson JM, Clemetson KJ, Wells TN. Chemokine and chemokine receptor mRNA expression in human platelets. *Cytokine*. (1995) 7:479–82. doi: 10.1006/cyto.1995.0065

21. Sun L, Peng B, Zhou J, Wang P, Mo Y, Xu G, et al. Difference of serum cytokine profile in allergic asthma patients according to disease severity. *J Asthma Allergy*. (2022) 15:315–26. doi: 10.2147/JAA.S345759

22. Yang Y, Shen C, Li J, Yuan J, Wei J, Huang F, et al. Plasma IP-10 and MCP-3 levels are highly associated with disease severity and predict the progression of COVID-19. *J Allergy Clin Immunol*. (2020) 146:119–127.e4. doi: 10.1016/j.jaci.2020.04.027

23. Zhang L, Peng X, Wang Q, Li J, Lv S, Han S, et al. CCR2 is a host entry receptor for severe fever with thrombocytopenia syndrome virus. *Sci Adv*. 9:eadg6856. doi: 10.1126/sciadv.adg6856

24. Li H, Li X, Lv S, Peng X, Cui N, Yang T, et al. Single-cell landscape of peripheral immune responses to fatal SFTS. *Cell Rep*. (2021) 37:110039. doi: 10.1016/j.celrep.2021.110039

25. Liu Z, Zhang R, Liu Y, Ma R, Zhang L, Zhao Z, et al. Eosinophils and basophils in severe fever with thrombocytopenia syndrome patients: Risk factors for predicting the prognosis on admission. *PloS Negl Trop Dis*. (2022) 16:e0010967. doi: 10.1371/journal.pntd.0010967

26. Grygorczuk S, Czupryna P, Pancewicz S, Świerzbińska R, Dunaj J, Siemieniako A, et al. The increased intrathecal expression of the monocyte-attracting chemokines CCL7 and CXCL12 in tick-borne encephalitis. *J Neurovirol*. (2021) 27:452–62. doi: 10.1007/s13365-021-00975-z

27. Liu Q, He B, Huang SY, Wei F, Zhu XQ. Severe fever with thrombocytopenia syndrome, an emerging tick-borne zoonosis. *Lancet Infect Dis*. (2014) 14:763–72. doi: 10.1016/S1473-3099(14)70718-2

28. Maher TM, Oballa E, Simpson JK, Porte J, Habgood A, Fahy WA, et al. An epithelial biomarker signature for idiopathic pulmonary fibrosis: an analysis from the multicentre PROFILE cohort study. *Lancet Respir Med*. (2017) 5:946–55. doi: 10.1016/S2213-2600(17)30430-7

29. Lubin JH, Colt JS, Camann D, Davis S, Cerhan JR, Severson RK, et al. Epidemiologic evaluation of measurement data in the presence of detection limits. *Environ Health Perspect*. (2004) 112:1691–6. doi: 10.1289/ehp.7199

30. Mehand MS, Millett P, Al-Shorbaji F, Roth C, Kieny MP, Murgue B. World health organization methodology to prioritize emerging infectious diseases in need of research and development. *Emerg Infect Dis*. (2018) 24:e171427. doi: 10.3201/eid2409.171427

31. Fajgenbaum DC, June CH. Cytokine storm. *N Engl J Med*. (2020) 383:2255–73. doi: 10.1056/NEJMra2026131

32. Kang SY, Yoo JR, Park Y, Kim SH, Heo ST, Park SH, et al. Fatal outcome of severe fever with thrombocytopenia syndrome (SFTS) and severe and critical COVID-

19 is associated with the hyperproduction of IL-10 and IL-6 and the low production of TGF-β. *J Med Virol*. (2023) 95:e28894. doi: 10.1002/jmv.28894

33. Menten P, Wuyts A, Van Damme J. Monocyte chemotactic protein-3. *Eur Cytokine Netw*. (2001) 12:554–60.

34. Yang Y, Shen C, Li J, Yuan J, Yang M, Wang F, et al. Exuberant elevation of IP-10, MCP-3 and IL-1ra during SARS-CoV-2 infection is associated with disease severity and fatal outcome. *medRxiv*. (2020). doi: 10.1101/2020.03.02.20029975

35. Huma ZE, Sanchez J, Lim HD, Bridgford JL, Huang C, Parker BJ, et al. Key determinants of selective binding and activation by the monocyte chemoattractant proteins at the chemokine receptor CCR2. *Sci Signal*. (2017) 10:eaai8529. doi: 10.1126/scisignal.aai8529

36. Lucas C, Wong P, Klein J, Castro TBR, Silva J, Sundaram M, et al. Longitudinal analyses reveal immunological misfiring in severe COVID-19. *Nature*. (2020) 584:463–9. doi: 10.1038/s41586-020-2588-y

37. Blanco-Melo D, Nilsson-Payant BE, Liu WC, Uhl S, Hoagland D, Møller R, et al. Imbalanced host response to SARS-coV-2 drives development of COVID-19. *Cell*. (2020) 181:1036–45. doi: 10.1016/j.cell.2020.04.026

38. Shi C, Pamer EG. Monocyte recruitment during infection and inflammation. *Nat Rev Immunol*. (2011) 11:762–74. doi: 10.1038/nri3070

39. Girkin J, Hatchwell L, Foster P, Johnston SL, Bartlett N, Collison A, et al. CCL7 and IRF7 mediate hallmark inflammatory and interferon responses following rhinovirus 1B infection. *J Immunol Baltim Md 1950*. (2015) 194:4924–30. doi: 10.4049/jimmunol.1401362

40. Santiago J, Hernández-Cruz JL, Manjarrez-Zavala ME, Montes-Vizuet R, Rosete-Olvera DP, Tapia-Díaz AM, et al. Role of monocyte chemotactic protein-3 and -4 in children with virus exacerbation of asthma. *Eur Respir J*. (2008) 32:1243–9. doi: 10.1183/09031936.00085107

41. Wang YC, Tsai CH, Wang YC, Yen LC, Chang YW, Sun JR, et al. SARS-CoV-2 nucleocapsid protein, rather than spike protein, triggers a cytokine storm originating from lung epithelial cells in patients with COVID-19. *Infection*. (2023). doi: 10.1007/s15010-023-02142-4

42. Xu DL, Zhang XM, Tian XY, Wang XJ, Zhao L, Gao MY, et al. Changes in cytokine levels in patients with severe fever with thrombocytopenia syndrome virus. *J Inflammation Res*. (2024) 17:211–22. doi: 10.2147/JIR.S444398

43. Hu LF, Wu T, Wang B, Wei YY, Kong QX, Ye Y, et al. The regulation of seventeen inflammatory mediators are associated with patient outcomes in severe fever with thrombocytopenia syndrome. *Sci Rep*. (2018) 8:159. doi: 10.1038/s41598-017-18616-z

44. Hong KH, Choi JP, Hong SH, Lee J, Kwon JS, Kim SM, et al. Predictors of mortality in Middle East respiratory syndrome (MERS). *Thorax*. (2018) 73(3):286–9. doi: 10.1136/thoraxjnl-2016-209313

frontiers | Frontiers in Immunology

TYPE Original Research
PUBLISHED 30 May 2024
DOI 10.3389/fimmu.2024.1388496

OPEN ACCESS

EDITED BY
Jian Zheng,
University of Louisville, United States

REVIEWED BY
Huihong Zeng,
Nanchang University, China
Shahan Mamoor,
Independent Researcher, East Islip, NY, United States

*CORRESPONDENCE
Alexei V. Tumanov
tumanov@uthscsa.edu
Ekaterina Koroleva
koroleva@uthscsa.edu

†PRESENT ADDRESS
Amanda R. Muñoz,
Department of Biology & Chemistry, Texas A&M International University, Laredo, TX, United States

‡These authors have contributed equally to this work

RECEIVED 19 February 2024
ACCEPTED 01 May 2024
PUBLISHED 30 May 2024

CITATION
Chen Q, Muñoz AR, Korchagina AA, Shou Y, Vallecer J, Todd AW, Shein SA, Tumanov AV and Koroleva E (2024) LTβR-RelB signaling in intestinal epithelial cells protects from chemotherapy-induced mucosal damage. *Front. Immunol.* 15:1388496. doi: 10.3389/fimmu.2024.1388496

LTβR-RelB signaling in intestinal epithelial cells protects from chemotherapy-induced mucosal damage

Qiangxing Chen[1,2], Amanda R. Muñoz[1†], Anna A. Korchagina[1], Yajun Shou[1,2], Jensine Vallecer[1], Austin W. Todd[1], Sergey A. Shein[1], Alexei V. Tumanov[1*‡] and Ekaterina Koroleva[1*‡]

[1]Department of Microbiology, Immunology and Molecular Genetics, University of Texas Health Science Center at San Antonio, San Antonio, TX, United States, [2]Department of Gastroenterology, Second Xiangya Hospital, and Research Center of Digestive Disease, Central South University, Changsha, Hunan, China

The intricate immune mechanisms governing mucosal healing following intestinal damage induced by cytotoxic drugs remain poorly understood. The goal of this study was to investigate the role of lymphotoxin beta receptor (LTβR) signaling in chemotherapy-induced intestinal damage. LTβR deficient mice exhibited heightened body weight loss, exacerbated intestinal pathology, increased proinflammatory cytokine expression, reduced IL-22 expression, and proliferation of intestinal epithelial cells following methotrexate (MTX) treatment. Furthermore, LTβR$^{-/-}$IL-22$^{-/-}$ mice succumbed to MTX treatment, suggesting that LTβR- and IL-22- dependent pathways jointly promote mucosal repair. Although both LTβR ligands LIGHT and LTβ were upregulated in the intestine early after MTX treatment, LIGHT$^{-/-}$ mice, but not LTβ$^{-/-}$ mice, displayed exacerbated disease. Further, we revealed the critical role of T cells in mucosal repair as T cell-deficient mice failed to upregulate intestinal LIGHT expression and exhibited increased body weight loss and intestinal pathology. Analysis of mice with conditional inactivation of LTβR revealed that LTβR signaling in intestinal epithelial cells, but not in Lgr5^{+} intestinal stem cells, macrophages or dendritic cells was critical for mucosal repair. Furthermore, inactivation of the non-canonical NF-kB pathway member RelB in intestinal epithelial cells promoted MTX-induced disease. Based on these results, we propose a model wherein LIGHT produced by T cells activates LTβR-RelB signaling in intestinal epithelial cells to facilitate mucosal repair following chemotherapy treatment.

KEYWORDS

LTβR, LIGHT, lymphotoxin, RelB, IL-22, methotrexate, intestinal damage

Abbreviations: LTβR, lymphotoxin beta receptor; LT, lymphotoxin; LIGHT, lymphotoxin-like inducible protein that competes with glycoprotein D for herpes virus entry on T cells, MTX, methotrexate; 5-FU, 5-Fluorouracil; SI, small intestine; WT, wild type; ISC, intestinal stem cells.

Introduction

Chemotherapy-induced intestinal damage poses a pervasive challenge, affecting up to 90% of patients undergoing chemotherapeutic treatments (1–3). The severity of this issue varies based on factors such as disease type, progression, drug type, and dosing regimen. The resultant gastrointestinal injury manifests in distressing symptoms like nausea, vomiting, diarrhea, and pain (2). Patient-specific risk factors, including age, ethnicity and gender also contribute to the varying susceptibility to intestinal damage during chemotherapy (4, 5). Beyond the immediate physical toll, chemotherapy-induced intestinal damage significantly impacts the quality of life for affected individuals (6). Moreover, it can compromise the effectiveness of treatments, leading to worse clinical outcomes, and potential economic repercussions due to the increased cost of care. Strikingly, reports indicate that 7.5% of deaths in chemotherapy patients result from nonselective toxicity rather than the disease itself (7). Therefore, therapeutic approaches such as combination of drug therapies and fecal microbiota transplantation are being developed to prevent or alleviate intestinal mucositis (8–12). However, despite these efforts, therapeutic targets remain limited, highlighting the need for a deeper understanding of the immune mechanisms governing mucosal repair following chemotherapy.

Due to rapid turnover of intestinal epithelial cells (IEC), the gastrointestinal (GI) tract is particularly sensitive to antineoplastic drugs such as methotrexate (MTX) and 5-Fluorouracil (5-FU) which inhibit cell growth and division (1, 13). MTX is a structural analog of folic acid which prevents folate metabolism via competitive inhibition of dihydrofolate reductase, resulting in the suppression of *de novo* synthesis of purines and pyrimidines (14). 5-FU mainly suppresses the action of thymidylate synthase but can also induce direct cytotoxicity through incorporation of its products into RNA and DNA (15). Animal models of chemotherapy-induced mucositis utilizing MTX and 5-FU treatments have been developed (2, 16, 17). Although the role of proinflammatory cytokines such as TNF, IL-6, IL-1 and reactive oxygen species (ROS) in pathogenesis of chemotherapy-induced mucositis is well recognized (1, 18), the immune mechanisms controlling the mucosal repair remain poorly understood.

IL-22 is an important cytokine of the interleukin-10 (IL-10) family of cytokines, produced by several hematopoietic cells, including helper T (Th) cells and innate lymphoid cells (ILCs) (19–22). IL-22 signals through the IL-22 receptor (IL-22R) paired with the IL-10Rβ subunit (23, 24). IL-10Rβ is ubiquitously expressed while IL-22R is selectively expressed by IECs and is involved in the regulation of epithelial repair and innate immunity (22, 25, 26). Furthermore, IL-22 can act on epithelial cells to induce secretion of antimicrobial proteins Reg3β and Reg3γ, which have been proposed to suppress inflammation and promote tissue recovery (27, 28). Additionally, IL-22 was shown to act directly on mouse and human intestinal stem cells (ISCs) to induce activation of the signal transducer and activator of transcription 3 (STAT3) to drive ISCs proliferation to increase organoid formation *in vitro* (26, 29). Moreover, a previous study revealed that group 3 ILCs (ILC3s) safeguard ISCs through production of IL-22 after MTX-induced acute small intestinal damage (30). However, a recent study suggested that ILC3-driven IEC proliferation in response to MTX-induced epithelial injury is independent of IL-22 (31). Furthermore, several studies demonstrated that IL-22 can exacerbate disease in psoriasis (32) and in several models of intestinal inflammation (33–36). Therefore, further understanding of IL-22-dependent and IL-22-independent pathways contributing to mucosal repair following chemotherapy-induced intestinal damage is critical for developing effective therapies.

Lymphotoxin beta receptor (LTβR), a core member of the tumor necrosis factor (TNF) receptor superfamily, exhibits wide expression across non-lymphocyte populations, including epithelial cells, dendritic cells (DCs), macrophages, mast cells, and stromal cells (37–39). LTβR interacts with two ligands: heterotrimeric lymphotoxin (LTα1β2, or LT) and homotrimeric LIGHT (TNFSF14), which are primarily expressed by lymphocytes and ILCs (37, 40). LTβR signaling serves pleiotropic functions, which include the control of lymphoid organ development and maintenance, as well as the regulation of inflammation and protective immunity to infections (38, 41). LTβR signaling activates canonical as well as non-canonical NF-κB signaling pathways to mediate both pro-inflammatory and anti-inflammatory responses (39, 42). Several studies have highlighted the protective role of LTβR signaling, which promotes mucosal healing in chemically-induced and infectious colitis models (43–47). Intriguingly, previous studies revealed the critical role of LTβR signaling in controlling IL-22 production by ILC3s in response to the mucosal bacterial pathogen *Citrobacter rodentium* (47) as well as in the DSS colitis model (45). Considering the role of ILC3s and IL-22 in MTX-induced mucosal repair (26, 30), we hypothesized that LTβR-dependent regulation of ILC3s and IL-22 mediates protection against chemotherapy-induced intestinal damage.

The goal of this study was to investigate the role of LTβR signaling in chemotherapy-induced intestinal damage using animal models of disease. Our data suggest that LIGHT-expressing T cells interact with LTβR on intestinal epithelial cells to induce non-canonical NF-κB signaling for protection against MTX-induced intestinal damage. Moreover, we show that LTβR and IL-22 pathways jointly protect from MTX-induced injury. Additionally, LTβR signaling also protects against 5-FU induced epithelial damage. These results support a novel role of LTβR signaling in mucosal repair following chemotherapy-induced intestinal injury by controlling cooperation of T cells and intestinal epithelial cells.

Materials and methods

Mice

All animal studies were conducted in accordance with the University of Texas Health Science Center at San Antonio Institutional Animal Care and Use Committee. 8–14 week old male and female mice were used for experiments. Age and sex matched littermate controls were used for all experiments. C57BL/6 (wild-type, WT) mice, RORγt$^{-/-}$ (48), TCRβδ$^{-/-}$ (49), IL-22$^{-/-}$ (50), RORγt-Cre

(48), Villin-Cre, Jax #021504 (51), LysM-Cre (52), CD11c-Cre (53), and Lgr5-EGFP-IRES-CreERT2 mice (54) (all on C57BL/6 background) were purchased from the Jackson Laboratory (Bar Harbor) and bred at the University of Texas Health Science Center at San Antonio. LTβR floxed (45), RelB floxed (55), LTβR$^{-/-}$ (45), LTβ$^{-/-}$ (56) and LIGHT$^{-/-}$ (TNFSF14$^{-/-}$) (57) mice were described previously. RORγt-LTβ$^{-/-}$ mice were generated by crossing LTβ floxed mice (58) with RORγt-Cre transgenic mice (48). Vil-LTβR$^{-/-}$, CD11c-LTβR$^{-/-}$, LysM-LTβR$^{-/-}$ and Lgr5-LTβR$^{-/-}$ mice were generated by crossing LTβR floxed mice with CD11c-Cre (53), LysM-Cre (52), and Lgr5-EGFP-IRES-CreERT2 mice (54), respectively. Lgr5-EGFP-IRES-CreERT2 (54) mice were intercrossed with LTβR$^{-/-}$ mice to generate Lgr5-reporter mice on LTβR-deficient background. To induce Cre-recombination, these mice were treated with 5 mg of tamoxifen for 4 consecutive days by oral gavage. Efficiency of *ltb*, *ltbr*, *relb* targeted gene deletion was validated in previous publications (43, 45, 47, 55, 59). All mice used in this research were housed under specific-pathogen-free conditions in line with National Institutes of Health guidelines.

Intestinal damage models

For MTX-induced intestinal damage, 8–14 week old mice were treated *i.p.* with 120 mg/kg of Methotrexate (MTX, RPI) on day 0 and 60 mg/kg on day 1. Mice were euthanized and tissues collected on day 2 or 5. For survival studies, mice were weighed daily and euthanized on day 14 or if body weight loss reached 20%. For 5-FU induced colitis, 8–12 week old mice were treated *i.p.* with 50 mg/kg of 5-fluorouracil (5-FU, Sigma-Aldrich) on days 0, 1, 2, 3. Mice were euthanized on day 5 and small intestine, cecum and colon were removed for analysis.

Assessment of 5-FU-induced colitis

The disease score was determined as an average of body weight loss (0 points, no weight loss; 1 point, weight loss of 1 to 5%; 2 points, weight loss of 5 to 10%; 3 points, weight loss of 10 to 20%; 4 points, weight loss >20%), signs of rectal bleeding (0 points, no blood in feces; 1point, positive hemoccult test; 2 points, dark feces; 3 points, visible blood in feces or traces of blood near anus; 4 points, gross bleeding from anus) and stool consistency (0 points, well-formed pellet; 1 point, soft pellet; 2 points, loose stool; 3 points, diarrhea; 4 points, no stool with dehydration). The scores were added to obtain a disease score ranging from 0 (healthy) to 16 (maximal activity of the disease). If the cecum was included, the cecum appearance score was determined as 0 points (normal), 1 point (slightly abnormal size), 2 points (significantly abnormal size) and 3 points (abnormal size with blood).

Histology

Small intestines, cecums and colons were dissected from mice and fixed in 10% neutral buffered formalin. Paraffin-embedded tissue sections were stained with hematoxylin and eosin (H&E) for tissue pathology evaluation. Images were taken with the Keyence BZ-X800 microscope. Small intestine pathology was scored as previously described (60). Villus, epithelium, inflammation, infiltration, crypt length and abscess, and bleeding, were evaluated on the scale from 0 to 3 and scores were summarized: villus length (0 = normal, 1 = short, 2 = extremely short), villus tops (0 = normal, 1 = damaged, 2 = severely damaged), epithelium (0 = normal, 1 = flattened, 2 = damaged, 3 = severely damaged), inflammation (0 = no infiltration, 1 = mild infiltration, 2 = severe infiltration), crypts (0 = normal, 1 = mild crypt loss, 2 = severe crypt loss), crypt abscesses (0 = none, 1 = present) and bleeding (0 = none, 1 = present). For cecum and colon histopathology score, we used a previously described scoring system (61).

Immunohistochemistry

5-Bromo-2′-deoxyuridine (BrdU, BD Biosciences, 100 mg/kg) was injected *i.p.* to mice two hours prior to analysis. Small intestines were fixed in 10% neutral buffered formalin and paraffin embedded. Sections were deparaffinized, rehydrated, and treated with 2 M HCl for 30 min at 37°C, and washed 3 times with PBS for 5 minutes, followed by 0.5% Triton X-100 for 30 minutes at room temperature. Tissue sections were blocked with goat serum at 37°C for 30 minutes and incubated with anti-BrdU antibody (Biolegend, clone 3D4) at 1:50 dilution at 4°C overnight. Sections were then incubated with HRP-conjugated goat anti-mouse IgG antibody (Biolegend) at 1:200 dilution at 37°C for 1h. Tissue sections were developed using DAB (Biolegend) and counterstained with hematoxylin. BrdU-positive cells were counted in 4 to 8 crypts per section. For Alcian Blue and Nuclear Fast Red staining slides were deparaffinized using Xylene and hydrated to distilled water. Slides were then incubated in 3% acetic acid for 3 min, stained in Alcian Blue solution pH 2.5 (American MasterTech) for 45 min, washed in running tap water, counter stained in nuclear fast red solution (American MasterTech) for 5 min, washed in running tap water, dehydrated to 100% ethanol, cleared in xylene, and mounted with Cytoseal 60 (Thermo Scientific) mounting medium. Images were taken with the Keyence BZ-X800 microscope.

RNA isolation and real-time reverse transcription PCR analysis

RNA from tissue or cultured cells was extracted using E.Z.N.A. Total RNA Kit I (Omega Bio-tek). RNA from lamina propria and intraepithelial fraction was isolated using RNeasy Micro Kit (QIAGEN). cDNA synthesis and real-time PCR were performed as described previously (43) using Power SYBR Green master mix (Applied Biosystems). Relative mRNA expression of target genes was determined using the comparative 2-$^{\Delta\Delta Ct}$ method and normalized to HPRT. Primers used are listed in Supplementary Table 1.

Epithelial cell line CMT-93

CMT-93 cells (mouse rectal carcinoma cell line, ATCC) were cultured in DMEM (Corning) containing 10% FBS. Cells were

treated with medium containing 5 μM MTX, or 0.5 μg/ml of agonistic αLTβR antibody (ACH6 clone, provided by Biogen Idec). Cells were incubated for 24 h before being harvested for RNA isolation.

Preparation of epithelial cells, intraepithelial lymphocytes, and lamina propria cells

To isolate epithelial cells, intestines were opened longitudinally, washed, cut, and incubated in DMEM supplemented with 5% FBS, antibiotics and 1mM DTT at 37°C with rotation (170 rpm) for 20 minutes and vortexed for 30 sec. Pieces were then incubated for additional 20 minutes with rotation (37°C) in PBS/15mM EDTA. Crypts were further digested with serum free DMEM with 2 mg/ml of Collagenase D (Roche) for 30 minutes with rotation (37°C). EC suspensions were passed through 70 μm cell strainer, resuspended in complete media and overlaid on the top of a 20%:40% Percoll (GE Healthcare) gradient. Epithelial cells were collected at the interphase of the 20%:40% Percoll gradient, washed and resuspended in DMEM. Intraepithelial lymphocytes (IELs) and lamina propria (LP) lymphocytes were isolated as described previously (62). Briefly, the small intestines were removed, opened longitudinally, and washed in cold PBS to remove fecal material. The whole small intestine or the ileum were cut in 1 cm pieces and incubated in RPMI 1640 media supplemented with 3% FBS, 15mM HEPES, 1 mM penicillin-streptomycin, and 2 mM EDTA with shaking at 150 rpm for 20 min at 37°C to remove epithelium and IEL. IELs were collected in the supernatants and passed through a mesh screen and separated by 40%:80% Percoll gradient. For LP isolation, the remaining tissues were digested in serum-free RPMI media containing 200 μg/ml Liberase TM (Roche) and 0.05% DNAse I (Sigma) on a shaker for 40 min at 37°C. The digested tissue was passed through a mesh strainer, washed with RPMI media containing 3% FBS and separated by a 40%:80% Percoll gradient.

Flow cytometry

For flow cytometry analysis, IELs and LP were preincubated for 20 min with anti-CD16/32 Fc-blocking mAb (2.4G2) and Zombie NIR™ Fixable viability dye (Biolegend) prior to surface staining. For cell surface staining single cell suspensions were incubated on ice with conjugated antibodies in PBS containing 2% of FBS. The following antibodies were used for surface staining: anti-MHCII (M5/114.15.2), anti-CCR2 (475301), anti-CD45 (30-F11), anti-CD8a (53–6.7), anti-NK1.1 (PK136), anti-CD11b (M1/70), anti-CD11c (N418), anti-TCRβ (H57–597), anti-Ly6G (1A8), anti-CD64 (X54–5/7.1), anti-Siglec-F (S17007L), anti-B220 (RA3–6B2), anti-CD4 (GK1.5), anti-CD3 (17A2), anti-CD8b (YTS156.7.7), anti-CD25 (PC61). For the transcriptional factors staining the following antibodies were used: anti-Foxp3 (MF-14) and anti-RORγt (Q31–378). For intracellular staining, cells were fixed and permeabilized with True-Nuclear™ transcriptional factor buffer set (Biolegend) according to the manufacturer's protocol. For Lgr5-GFP reporter staining, the following antibodies were used: anti-EpCAM (G8.8), anti-TER-119 (TER-119), anti-CD117 (c-Kit) (2B8), anti-CD31 (MEC13.3). All antibodies were purchased from BD Biosciences or Biolegend. Samples were acquired using an FACSCelesta or Cytek Aurora (Cytek Biosciences), and data were analyzed using FlowJo 10 software.

Statistical analysis

All statistics were determined using GraphPad Prism software (v9). Statistical significance was determined using one-way ANOVA or two-way ANOVA with Tukey's multiple comparison test, Mann-Whitney test, Kruskal Wallis test with Dunn's correction, or unpaired Student's t-test, as appropriate. Survival was assessed using the Log-rank (Mantel-Cox) and Gehan-Breslow-Wilcoxon tests. Not significant, $p > 0.05$ (ns); $p< 0.05$ (*); $p< 0.01$ (**); $p< 0.001$ (***); $p< 0.0001$ (****).

Results

LTβR signaling protects from chemotherapy-induced intestinal damage

LTβR signaling is a known regulator of intestinal inflammation (43–45, 63, 64). To investigate the role of LTβR signaling in chemotherapy-induced intestinal damage, we employed an acute epithelial injury model induced by MTX (1, 2) (Figure 1A). Compared to WT mice, LTβR$^{-/-}$ mice exhibited increased weight loss (Figures 1B, M) and increased mortality (Figure 1L) after MTX treatment. Macroscopic examination of small intestines on day 5 revealed severe pathology in LTβR$^{-/-}$ mice compared to control mice (Figure 1C) while the length and weight of the small intestines remained unchanged (Figure 1D). Histological analysis revealed severe destruction of the epithelial layer in LTβR$^{-/-}$ mice characterized by shortened villi, inflammatory cell infiltration, and increased loss of crypts (Figure 1E). Consistently, histopathology scores were significantly increased in the ileum and jejunum of LTβR$^{-/-}$ mice, with the duodenum exhibiting less pronounced damage (Figure 1E). Crypt regenerative capacity was reduced in both WT and LTβR$^{-/-}$ mice at day 2 after MTX administration (Figure 1F). While epithelial cell proliferation, measured by Ki-67 expression and BrdU incorporation, remained reduced in LTβR$^{-/-}$ mice, it was restored in WT mice by day 5 after MTX administration (Figures 1F, G).

Expression of key proinflammatory cytokines TNF, IL-1β and IFNγ, but not IL-6 was upregulated in the ileum of LTβR$^{-/-}$ mice at day 5 after MTX treatment (Figure 1H), as well as expression of chemokines CXCL1, CXCL2, CXCL9, CXCL10, CXCL13, and CCL2 (Figure 1I). Expression of IL-22 was significantly downregulated in the ileum of LTβR$^{-/-}$ mice compared to WT controls (Figure 1K). Expression of IL-22 dependent antimicrobial proteins Reg3β and Reg3γ in the ileum of LTβR$^{-/-}$ mice was also reduced compared to WT mice (Figure 1K). LTβR signaling is

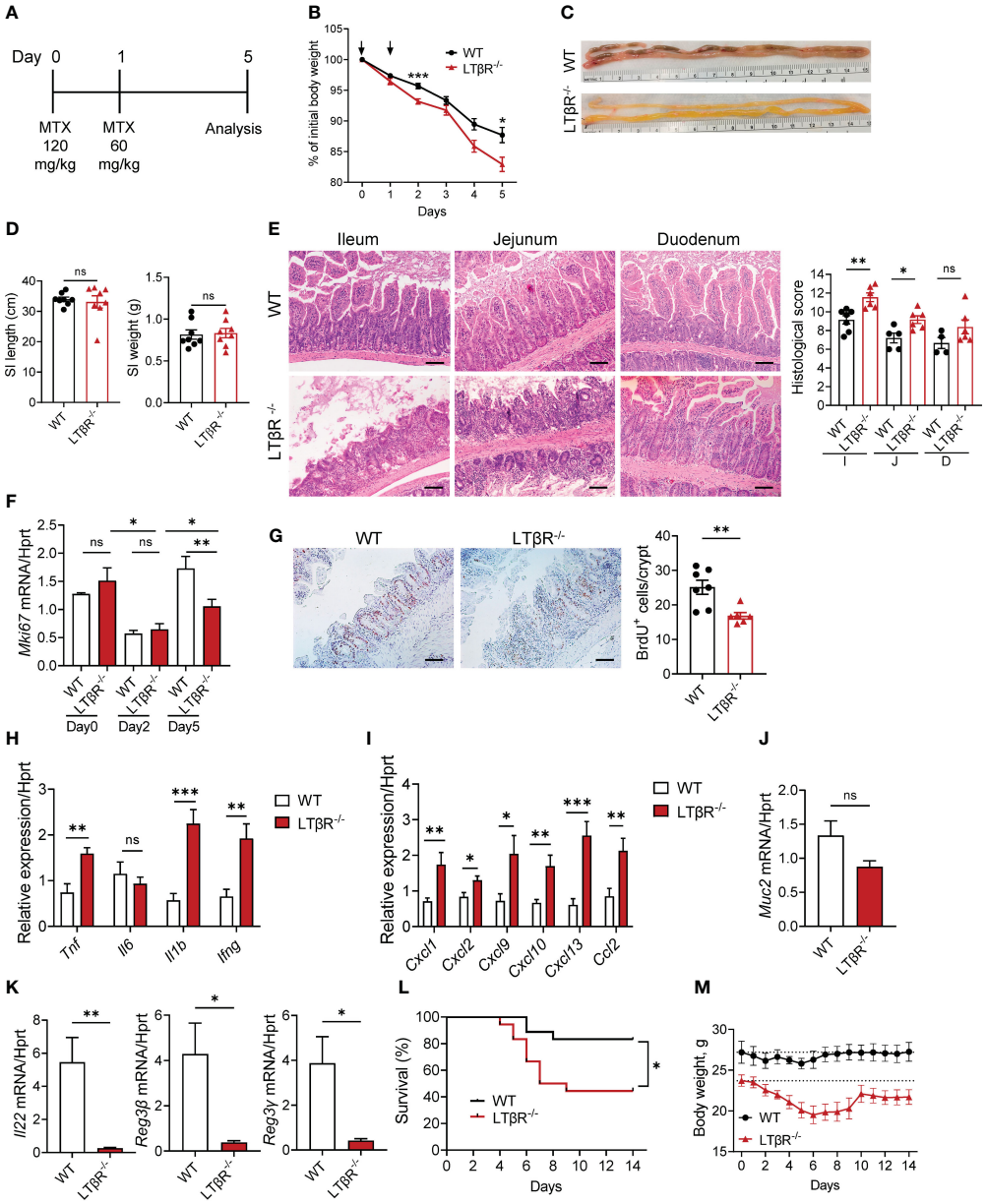

FIGURE 1
LTβR signaling protects against MTX-induced intestinal damage. **(A)** Schematic of the experiment. WT and LTβR$^{-/-}$ mice were injected i.p. with MTX on day 0 (120 mg/kg) and day 1 (60 mg/kg), and small intestine (SI) collected at day 5. **(B)** Body weight change. Black arrows: days of MTX treatment. n=25–28 mice per group. **(C)** Representative photographs of SI. **(D)** Measurements of SI. **(E)** Representative H&E images and histopathology scores. Scale bars, 100μm. I, Ileum; J, Jejunum; D, Duodenum. **(F)** Ki-67 mRNA expression in ileum at indicated time points. n=4–7 mice per group. **(G)** Representative images of BrdU^{+} cells/crypt in the ileum. Scale bars, 100μm. **(H–K)** Expression of cytokines **(H)**, chemokines **(I)**, Muc2 **(J)**, and IL-22 and antimicrobial proteins **(K)** in the ileum and quantification of BrdU^{+} cells measured by real-time PCR. n=7–8 mice per group. **(L, M)** Survival analysis (n=18 mice per group, **L**) and long-term body weight analysis (n=5 mice per group, dotted lines represent median starting body weight in each group, **M**). **(C–E)** Data represents 1 out of 6 independent experiments with similar results. (**B**, **F–L**) Data is combined from 2–6 independent experiments with similar results. Data shown as mean ± SEM. Statistics were determined using two-way ANOVA with Geisser-Greenhouse correction **(B, M)**, unpaired t test **(D–K)**, and Log-rank (Mantel-Cox) test **(L)**. ns, not significant; *p<0.05, **p<0.01, ***p<0.001.

known to promote goblet cell differentiation and production of mucins in the gut during *Listeria monocytogenes* infection or DSS-induced colitis (45, 59). Interestingly, we did not detect significant reduction of Muc2 expression in the gut of LTβR$^{-/-}$ mice (Figure 1J), suggesting that other LTβR-dependent factors contribute to mucosal repair after MTX-induced injury. Collectively, these data indicate that LTβR signaling is essential for the intestinal repair and control of inflammation after MTX-induced injury.

5-FU is another commonly used chemotherapeutic agent employed in the therapy of various cancers, which can cause damage to intestinal epithelial cells and result in intestinal mucositis (15, 65, 66). To test the role of LTβR signaling in a 5-FU model of chemotherapy-induced intestinal injury, we treated WT and LTβR$^{-/-}$ mice with 50 mg/kg 5-FU daily for 4 days (Supplementary Figure S1). 5-FU treated LTβR$^{-/-}$ mice exhibited aggravated body weight loss (Supplementary Figure S1A), increased

clinical disease score (Supplementary Figure S1B) and shortening of the colon (Supplementary Figure S1C). Histological analysis of colon and cecum sections of 5-FU treated LTβR$^{-/-}$ mice revealed severe mucosal damage characterized by loss of goblet cells and decreased crypt density which was accompanied by mass immune cell infiltration (Supplementary Figure S1D). Expression of proinflammatory cytokines TNF, IL-6, IL-1β and IFNγ was upregulated in the colon of 5-FU treated LTβR$^{-/-}$ mice compared to control mice, whereas IL-22 levels were similar (Supplementary Figure S1E). These data indicate that LTβR signaling also contributes to intestinal protection in 5-FU chemotherapy-induced intestinal inflammation.

LTβR signaling controls accumulation of B cells, neutrophils, CD8αα$^+$ and CD4$^+$ T cells in the small intestine early after MTX treatment

To define immune cell types in the small intestine early after MTX administration, we compared SI intraepithelial lymphocytes (IELs) and lamina propria (LP) immune cells in WT mice at steady state and at day 2 after MTX administration by flow cytometry. Gating strategy is shown on Supplementary Figure S2. We found an increased frequency of T cells (CD3$^+$) and non-conventional CD8αα$^+$ T cells in the IEL fraction after MTX administration (Supplementary Figure S3A). Interestingly, in the LP, frequency of Tregs was increased, although we did not find increased frequency of CD3$^+$ T cells (Supplementary Figure S3B). Analysis of myeloid cell populations revealed increased frequency of macrophages and neutrophils (Supplementary Figure S3C) after MTX administration. Gene expression analysis revealed rapid induction of proinflammatory cytokines TNF, IL-6, IL-1β and IFNγ, as well as IL-22 at day 2 (Supplementary Figure S3D). In contrast, by day 5 after MTX administration, expression of these cytokines returned to steady state levels (Supplementary Figure S3D). Expression of IFNγ-induced chemokines CXCL9, CXCL10 (67), neutrophil-recruiting chemokines CXCL1, CXCL2 (68), and CXCL13 and CCL2 chemokines was upregulated on day 2 after MTX administration and reduced to baseline by day 5 (Supplementary Figure S3E). These data indicate that MTX rapidly induces inflammation and promotes immune cell infiltration into the small intestine.

To define the impact of LTβR on the recruitment of immune cells after MTX treatment, we next analyzed immune cells in the SI of LTβR$^{-/-}$ mice at day 2 and compared them to control WT mice. We found an increased frequency of T cells and CD8αα$^+$ T cells in the SI IEL of LTβR$^{-/-}$ mice (Figure 2A). We did not observe a difference in total T cell frequency in the SI LP isolated from LTβR$^{-/-}$ mice; however, the frequency of CD4$^+$ T cells, B cells, DCs, and neutrophils was reduced (Figures 2B, C). Correspondingly, mRNA expression of the neutrophil-recruiting chemokine CXCL2 was reduced in the ileum of LTβR$^{-/-}$ mice on day 2 after MTX treatment (Figures 2C, E), in contrast to the increased levels of CXCL1, CXCL2 at day 5 post MTX treatment (Figure 1I). These results suggest that LTβR signaling controls early neutrophil recruitment after MTX-induced injury but is dispensable at later stages of the disease when inflammation is more pronounced. Similarly, we did not detect increased expression of proinflammatory cytokines TNF and IL-1β in the ileum of LTβR$^{-/-}$ mice at day 2 (Figure 2D) in contrast to day 5 after MTX administration (Figure 1H); however, expression of IFNγ and IFNγ-dependent chemokines CXCL9 and CXCL10 was elevated (Figures 2D, E). Interestingly, LTβR$^{-/-}$ mice failed to upregulate IL-22 expression early after MTX administration (Figure 2D), suggesting that LTβR signaling controls IL-22 production in this model of intestinal inflammation. Collectively, these results suggest that LTβR signaling inhibits inflammation during MTX-induced injury.

LTβR ligand LIGHT is necessary for protection from MTX-induced intestinal damage

LTβR signaling can be activated by two ligands, membrane-bound lymphotoxin (LTα1β2) and LIGHT (TNFSF14), both known regulators of intestinal inflammation (38, 40, 47, 64, 69). To test whether MTX treatment regulates expression of LTβR ligands, we analyzed expression of LIGHT and LTβ in the ileum, jejunum, and duodenum of WT mice during MTX treatment. Expression of both LIGHT and LTβ was significantly increased in the ileum on day 2 after MTX treatment and decreased at day 5 during resolution of MTX-induced injury (Figure 3A). Interestingly, expression of LIGHT was also increased in the LP and IEL fractions isolated from total small intestine on day 2 after MTX treatment, while we did not detect induction of LTβ expression (Figure 3B). Expression of LTα followed the same pattern as LTβ (Supplementary Figure S3F, G). To assess which LTβR ligand is essential for protection from MTX-induced injury, we treated WT, LTβ$^{-/-}$ and LIGHT$^{-/-}$ mice with MTX. While body weight loss in LTβ$^{-/-}$ mice followed the same pattern as in WT mice, LIGHT$^{-/-}$ mice lost significantly more body weight (Figure 3C), and all succumbed to the injury induced by MTX (Figure 3G). Consistently, histological analysis showed increased histopathology scores in the ileum of LIGHT$^{-/-}$ mice, but not in LTβ$^{-/-}$ mice, compared to WT controls (Figure 3D). Crypt regenerative capacity measured by expression of Ki-67 was markedly reduced in LIGHT$^{-/-}$ mice (Figure 3E). To further examine the role of LTβR ligands in MTX- induced inflammation, we next measured the expression of proinflammatory cytokines in the ileum of MTX-treated mice on day 5. Expression of TNF and IL-1β was increased in the ileum of LIGHT$^{-/-}$ but not LTβ$^{-/-}$ mice, while IFNγ levels were not changed (Figure 3F). IL-6 expression was not changed in LIGHT$^{-/-}$ mice but reduced in LTβ$^{-/-}$ mice (Figure 3F). We also found that production of IL-22 was reduced in the ileum of both LTβ$^{-/-}$ mice and LIGHT$^{-/-}$ mice (Figure 3F). Collectively, these data suggest that whereas both LIGHT and lymphotoxin are upregulated in the small intestine during MTX-induced injury and both LTβR ligands contribute to IL-22 production, LIGHT, but not LT reduces inflammation and promotes intestinal healing during MTX-induced injury.

Previous studies revealed that LT produced by RORγt$^+$ ILC in the intestine is critical for control of IL-22 production and

10.3389/fimmu.2024.1388496

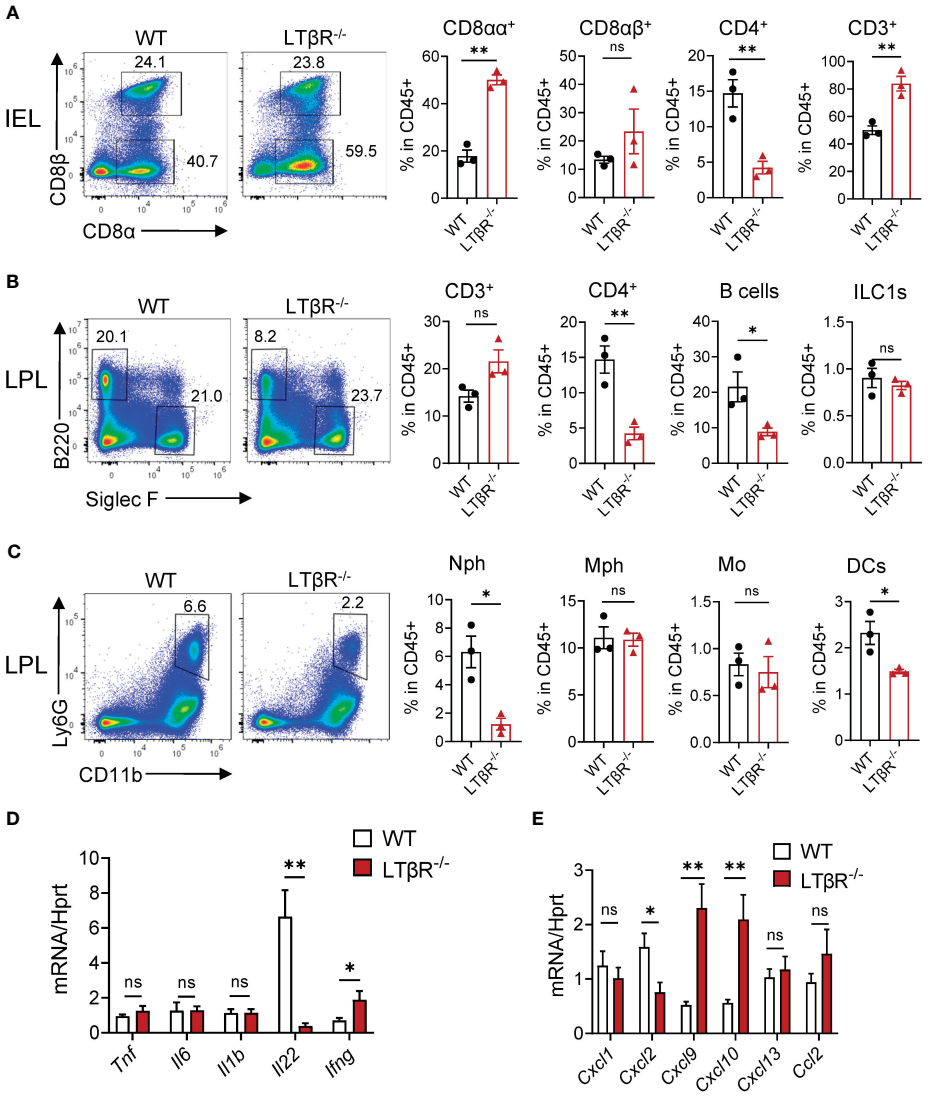

FIGURE 2
LTβR signaling controls accumulation of B cells, neutrophils and CD4$^+$ T cells in the small intestine early after MTX treatment. WT and LTβR$^{-/-}$ mice were treated as in Figure 1A. Small intestines were collected on day 2 for analysis. **(A)** Representative flow cytometry plots and frequency of T cell populations in SI IEL. Frequency is calculated in live CD45$^+$ gate. **(B, C)** Representative flow cytometry plots and frequency of cell populations in LP. B cells (CD45$^+$B220$^+$); CD4$^+$ T cells; CD3$^+$ T cells; ILC1s (CD45$^+$Ly6G$^-$B220$^-$SiglecF$^-$TCRβ$^-$CD64$^-$NK1.1$^+$); Neutrophils (Nph, Ly6G$^+$ CD11b$^+$); Macrophages (Mph, CD11c$^-$Ly6G$^-$SiglecF$^-$CD11b$^+$MHCII$^+$CD64$^+$); Monocytes (Mo, CD45$^+$Ly6G$^-$B220$^-$SiglecF$^-$TCRβ$^-$CD64$^+$MHCII$^-$CD11b$^+$CCR2$^+$); Dendritic cells (DCs, CD45$^+$Ly6G$^-$B220$^-$SiglecF$^-$TCRβ$^-$CD64$^-$MHCII$^+$CD11c$^+$). **(D)** Cytokine and **(E)** chemokine expression in the ileum on day 2 measured by real-time PCR. Data is representative from one of two independent experiments with similar results (n=3–6 per group). Data shown as mean ± SEM. ns, not significant, *p<0.05, **p<0.01. Statistics were determined using t test **(A, B)** or ANOVA with Sidak's multiple comparison test **(D, E)**. Gating strategy is shown in Supplementary Figure S2.

protection of mice against *Citrobacter rodentium* infection (43, 47). Moreover, depletion of ILCs in Rag1$^{-/-}$ mice resulted in reduced LTβ and IL-22 production in the ileum and diminished crypt proliferation during MTX treatment (30). To test whether LT produced by RORγt$^+$ cells is essential for protection against MTX-induced damage, we utilized mice with specific inactivation of LTβ in RORγt-expressing cells (RORγt-LTβ$^{-/-}$ mice) (47). Surprisingly, we did not find difference in body weight loss or histopathology score between RORγt-LTβ$^{-/-}$ mice and littermate control LTβ floxed mice (Figures 3H, I) despite reduced expression of IL-22 in the ileum of RORγt-LTβ$^{-/-}$ mice (Figure 3J). Thus, these results suggest that although LTβ produced by RORγt$^+$ cells is required for IL-22 production in the gut, it is dispensable for control of intestinal damage during MTX-induced disease.

T cell deficiency aggravates intestinal damage after MTX treatment

Recent studies implicated the role of RORγt$^+$ ILCs in the maintenance of ISCs and intestinal repair following MTX-induced intestinal damage (30, 31). Our data demonstrated that CD3$^+$ T cells are increased in the IEL after MTX treatment (Supplementary Figure S3A). To define the relative contribution

10.3389/fimmu.2024.1388496

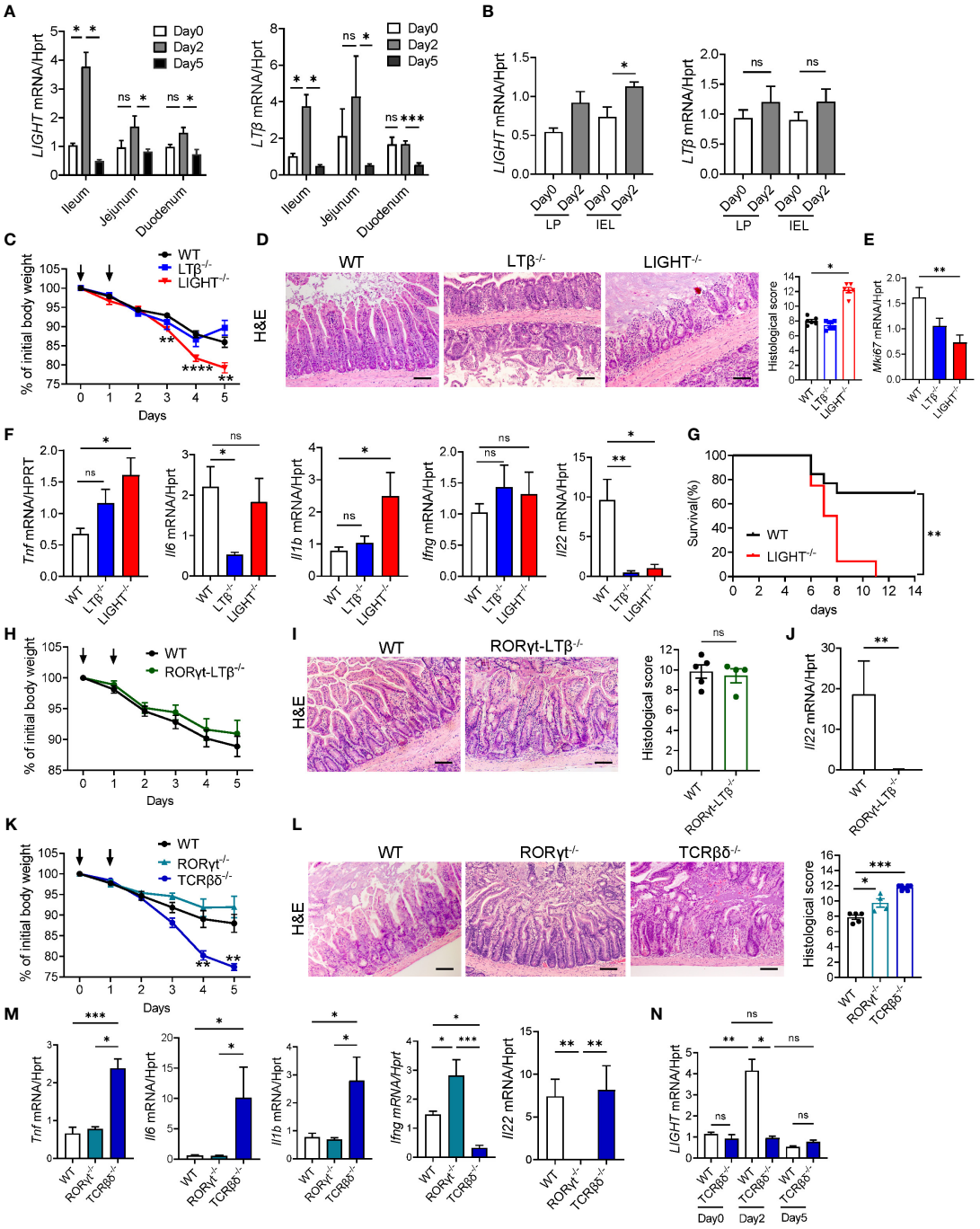

FIGURE 3
LIGHT and T cells protect against MTX-induced intestinal injury. **(A, B)** Kinetics of LIGHT and LTβ expression after MTX treatment in **(A)** ileum, jejunum and duodenum, and **(B)** LP and IEL from small intestine of WT mice. n=3–4 per group. **(C–F)** WT, LTβ$^{-/-}$ and LIGHT$^{-/-}$ mice were treated with MTX as in Figure 1A. **(C)** Body weight loss. Black arrows: days of MTX treatment. n=15–25 mice per group. **(D)** Representative H&E images (scale bars, 100μm) and histopathology scores; **(E)** Ki-67 and **(F)** cytokine expression in the ileum of WT, LTβ$^{-/-}$ and LIGHT$^{-/-}$ mice on day 5 after MTX treatment. n=6–8 mice per group. **(G)** Survival of LIGHT$^{-/-}$ mice after MTX treatment. n=8–13 mice per group. **(H–J)** WT and RORγt-LTβ$^{-/-}$ mice were treated with MTX as in Figure 1A. **(H)** Body weight loss; n=13–15 mice per group. **(I)** Representative H&E images (Scale bars, 100μm) and histopathology scores; and **(J)** IL-22 expression in the ileum on day 5 after MTX treatment. n=5 mice per group. **(K–M)** WT, RORγt$^{-/-}$ and TCRβδ$^{-/-}$ mice were treated with MTX as in Figure 1A. **(K)** Body weight loss; n=8–14 per group. **(L)** Representative H&E images (Scale bars, 100μm) and histopathology scores and **(M)** cytokine expression in the ileum on day 5 after MTX treatment. n= 7 mice per group. **(N)** LIGHT expression in the ileum of WT and TCRβδ$^{-/-}$ mice at indicated time points after MTX treatment analyzed by real-time PCR. n=4–7 mice per group. H&E images and histopathology scores are representative from 3–4 independent experiments with similar results. Data shown as mean ± SEM. Statistics were determined using two-way ANOVA with Geisser-Greenhouse correction **(A, C, K)**, Mann-Whitney test **(B, J)**, Kruskal-Wallis test **(D–F, L, M)** or Brown-Forsythe and Welch ANOVA tests **(N)**. ns, not significant, *p<0.05, **p<0.01, ***p<0.001, ****p<0.0001.

of T cells and ILC3s in MTX-induced pathology we treated mice which lack ILC3s (RORγt$^{-/-}$ mice) or T cells (TCRβδ$^{-/-}$ mice) with MTX. RORγt$^{-/-}$ mice displayed 5–10% of body weight loss similar to WT control mice, however histological analysis of the ileum demonstrated increased crypt loss and crypt flattening (Figures 3K, L). Unexpectedly, T cell-deficient mice lost more than 20% of body weight and had to be euthanized by day 5 of MTX treatment (Figure 3K). Histological analysis showed severe loss of crypts, increased inflammation, and bleeding (Figure 3L). Expression of proinflammatory cytokines TNF, IL-6 and IL-1β was increased in the ileum of TCRβδ$^{-/-}$ mice but not RORγt$^{-/-}$ mice (Figure 3M). These results suggest that T cells, but not ILC3s are critical for protection against MTX induced injury. Interestingly, IFNγ expression was very low in the ileum of TCRβδ$^{-/-}$ mice, indicating that T cells are the main producers of IFNγ in the ileum after MTX treatment. We did not find a defect in IL-22 expression in the ileum of TCRβδ$^{-/-}$ mice, however IL-22 transcript was almost undetectable in the ileum of RORγt$^{-/-}$ mice (Figure 3M), implying that RORγt^{+} ILCs but not T cells are the main source of IL-22 production after MTX-induced injury.

Since LIGHT is mainly produced by activated T cells (37, 40) and LIGHT$^{-/-}$ mice displayed increased intestinal pathology post MTX treatment (Figures 3C–G), we next analyzed kinetics of LIGHT expression in the ileum of TCRβδ$^{-/-}$ mice during MTX treatment. While we did not find difference in LIGHT levels between WT and TCRβδ$^{-/-}$ mice at steady-state, T cell-deficient mice failed to upregulate LIGHT in the ileum at day 2 post MTX treatment (Figure 3N). Thus, these data suggest that T cells are critical for protection from chemotherapy-induced intestinal injury and can serve as the primary source of LIGHT early after MTX-induced damage.

LTβR and IL-22 jointly protect from MTX-induced intestinal damage

IL-22 blockade during MTX-induced intestinal damage led to a significant loss of Lgr5^{+} stem cells, specifically in the duodenum (30), although crypt proliferation and crypt pathology in the small intestine of IL-22$^{-/-}$ mice after MTX treatment was indistinguishable from WT controls (31). We found that IL-22 expression is induced in the ileum on day 2 after MTX treatment (Supplementary Figure S3D) and that IL-22 is downregulated in LTβR$^{-/-}$ mice (Figures 1K, 2D), suggesting that LTβR signaling regulates production of IL-22 during MTX-induced injury. To determine whether LTβR plays a protective role independently of IL-22, we intercrossed LTβR$^{-/-}$ mice with IL-22$^{-/-}$ mice and compared intestinal pathology in IL-22$^{-/-}$ and LTβR$^{-/-}$ mice with double deficient LTβR$^{-/-}$IL-22$^{-/-}$ mice after MTX administration. We did not find difference in body weight loss, survival, or intestinal pathology between IL-22$^{-/-}$ and littermate heterozygous control WT mice (Figures 4A–D), consistent with previous studies (31). However, LTβR$^{-/-}$IL-22$^{-/-}$ mice displayed increased body weight loss, intestinal pathology and exacerbated mortality compared to IL-22$^{-/-}$ mice (Figures 4A–D) suggesting that loss of LTβR exacerbates MTX-induced intestinal pathology in IL-22$^{-/-}$ mice. Interestingly, body weight loss and mortality were exacerbated in LTβR$^{-/-}$IL-22$^{-/-}$ double deficient mice compared to LTβR$^{-/-}$ mice (Figures 4B, C), suggesting that complete loss of IL-22 exacerbates MTX-induced pathology in LTβR$^{-/-}$ mice. Consistently, LTβR$^{-/-}$IL-22$^{-/-}$ mice displayed increased levels of proinflammatory cytokines TNF, IL-1β, and IFNγ in the ileum compared to IL-22$^{-/-}$ and WT control mice (Figure 4E). These results imply that LTβR and IL-22 jointly protect from MTX-induced intestinal damage and that LTβR may control both IL-22 dependent and IL-22 independent pathways for mucosal protection.

LTβR signaling in epithelial cells is essential for mucosal repair following MTX-induced damage

Next, we sought to determine which LTβR-expressing cells are important for protection against MTX-induced epithelial injury. Since previous studies highlighted the role of LTβR signaling in intestinal epithelial cells for protection against epithelial injury caused by bacterial infection or by chemical agent (43, 45, 59), we tested whether LTβR signaling in epithelial cells is essential for mucosal repair during MTX-induced damage. Therefore, we generated mice with specific inactivation of LTβR in intestinal epithelial cells (Vil-LTβR$^{-/-}$ mice) by crossing LTβR floxed mice (45) with Villin-Cre (51). Vil-LTβR$^{-/-}$ mice demonstrated an accelerated body weight loss and increased mortality after MTX treatment, compared to littermate Cre-negative control mice (Figures 5A, F). Histological analysis and analysis of Ki-67 expression revealed increased tissue damage and reduced epithelial cell proliferation in the ileum of Vil-LTβR$^{-/-}$ mice compared to control mice (Figures 5B, C). Expression of proinflammatory cytokines TNF, IL-6, IL-1β and IFNγ was increased in the ileum of Vil-LTβR$^{-/-}$ mice on Day 5 (Figure 5D). Additionally, we found increased expression of CXCL1, CXCL2, CXCL9, CXCL10, CXCL13 and CCL2 chemokines in the ileum of Vil-LTβR$^{-/-}$ mice (Figure 5E). These results demonstrate that LTβR signaling in intestinal epithelial cells is essential for protection against MTX-induced injury.

Regeneration of intestinal epithelium after damage depends on continuous differentiation of epithelial cells from ISCs (70). Lgr5^{+} ISCs have the ability to give rise to all intestinal epithelial cells (71). The maintenance of ISCs after intestinal damage is dependent on IL-22 production by ILC3s (26, 30). Since LTβR signaling controls IL-22 production by ILC3s in several models of intestinal inflammation (45, 47), we sought to determine whether LTβR signaling in Lgr5^{+} ISCs directly contributes to epithelium regeneration after MTX-induced injury. Therefore, we generated Lgr5-LTβR$^{-/-}$ mice by crossing LTβR floxed mice (45) with Lgr5-EGFP-IRES-CreERT2 mice (54), and treated them with MTX. However, Lgr5-LTβR$^{-/-}$ mice did not show increased weight loss or aggravated intestinal pathology, compared to littermate Cre^{-} control mice (Figures 5G, H). Moreover, analysis of publicly available single-cell RNA-sequence survey of the small intestine epithelium in naïve WT mice (72) revealed that while LTβR was highly expressed in goblet cells and enterocytes, LTβR expression

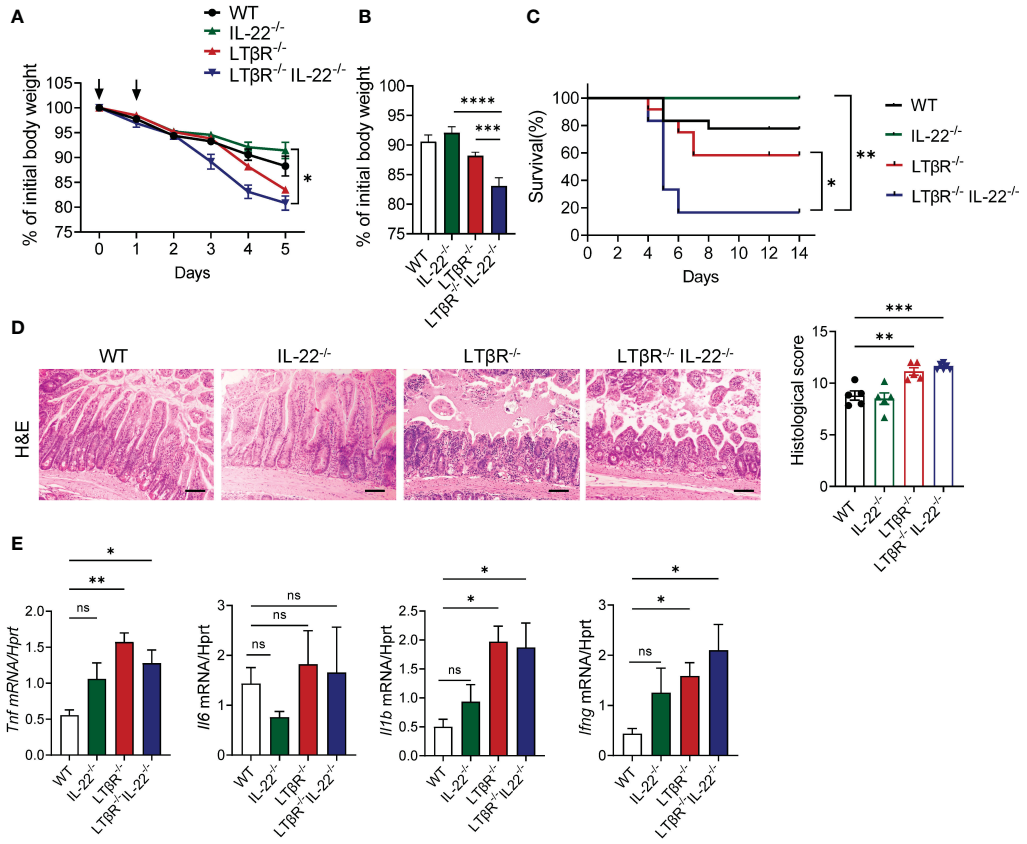

FIGURE 4
LTβR signaling cooperates with IL-22 for mucosal protection. LTβR$^{-/-}$ mice were intercrossed with IL-22$^{-/-}$ mice. Mice were treated with MTX as in Figure 1A. **(A)** Kinetics of body weight loss. n=8–18 mice per group. **(B)** Body weight loss at day 4 after MTX treatment. **(C)** Survival, n=6–18 mice per group. **(D)** Representative H&E images (scale bars, 100μm) and histopathology scores. **(E)** Expression of proinflammatory cytokines in the ileum on day 5. n=6–8 mice per group. Data was combined from 4–7 experiments with similar results. Statistics were determined using two-way ANOVA with Geisser-Greenhouse correction **(A)**, unpaired t test **(B)**, log-rank (Mantel-Cox) test **(C)**, ordinary one-way ANOVA **(D)**, Kruskal-Wallis test **(E)**. ns, not significant, *p<0.05, **p<0.01, ***p<0.001, ****p<0.0001.

was low-to moderate in Lgr5^{hi} ISC, TA.G2 or Paneth cells (Supplementary Figure S4A). Furthermore, to test whether global LTβR deficiency affects maintenance and/or proliferation of ISCs after mucosal damage, we intercrossed LTβR$^{-/-}$ mice with Lgr5-EGFP-IRES-CreERT2 reporter mice and analyzed epithelial cell populations in the ileum on day 5 after MTX treatment. We did not find significant difference in the ratio of Lgr5^{+} ISCs, Paneth cells, tuft cells, epithelial cells, goblet cells between control and LTβR$^{-/-}$ mice (Supplementary Figures S4B–G). Collectively, these data suggest that LTβR signaling is dispensable for ISC maintenance and proliferation after MTX-induced injury.

Previous studies have implicated the role of LTβR signaling in CD11c^{+} DCs for IL-22 production and mucosal protection against intestinal bacterial infection (47). In addition, LTβR expression in neutrophils contributes to mucosal repair in DSS-induced colitis (46). To define whether expression of LTβR in DCs and macrophages/monocytes contributes to protection from MTX-induced injury, we treated mice with CD11c^{+} DC-specific deficiency of LTβR (CD11c-LTβR$^{-/-}$mice) (45) and macrophage/neutrophil-specific LTβR deficiency (LysM-LTβR$^{-/-}$ mice) (43), as well as mice with combined deficiency (CD11c, LysM-LTβR$^{-/-}$) with MTX, and then analyzed body weight loss and pathology on day 5 after MTX administration. We did not find difference in body weight loss or intestinal pathology in any of these strains, compared to Cre^{-} littermate controls (Supplementary Figures S5A, B). Interestingly, IL-22 expression was decreased in the ileum of CD11c-LTβR$^{-/-}$ mice (Supplementary Figure S5C). This decrease suggests that while LTβR signaling in CD11c^{+} cells is not critical for control of intestinal injury after MTX treatment, it may contribute to the IL-22-dependent maintenance of ISCs. Collectively, our data suggest that LTβR signaling in epithelial cells, but not immune cells is essential for protection from MTX-induced intestinal damage.

Non-canonical NF-κB signaling in intestinal epithelial cells protects from MTX-induced intestinal damage

As our experiments with LTβR$^{-/-}$IL-22$^{-/-}$ mice (Figure 4) implied that LTβR-dependent IL-22- independent signaling could contribute to protection from MTX-induced damage, we next tested whether LTβR-dependent regulation of the NF-κB pathway is important for mucosal healing. LTβR signaling can activate both canonical and non-canonical NF-κB signaling pathways to produce

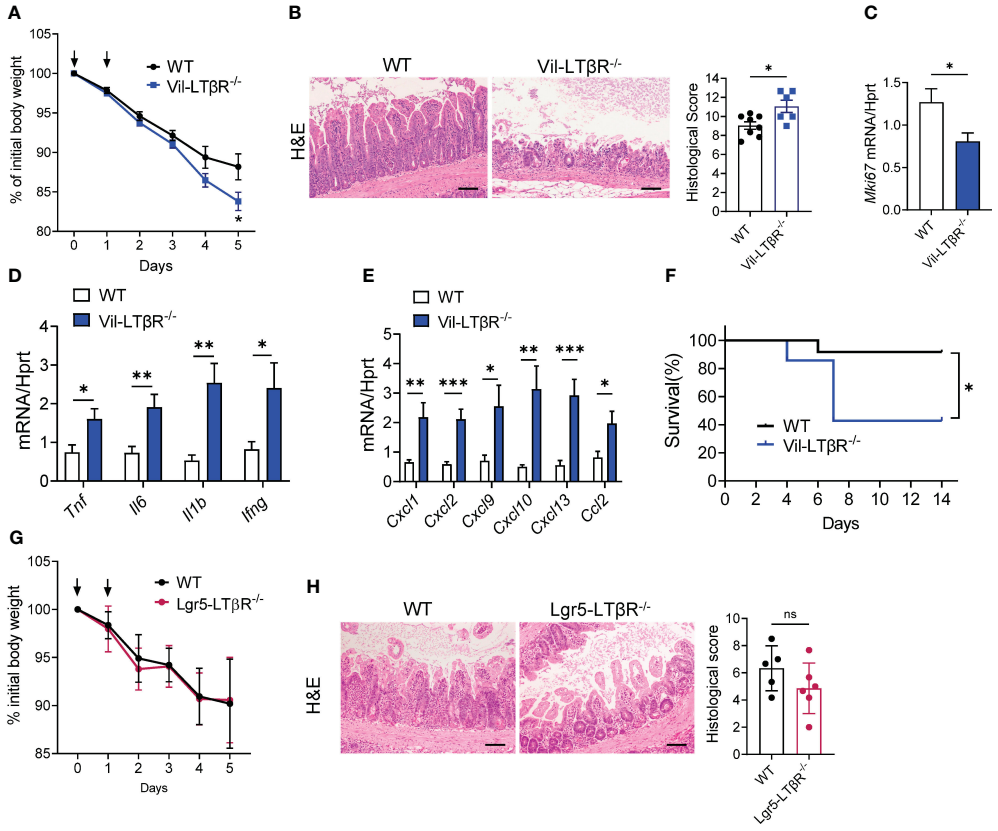

FIGURE 5
LTβR signaling in intestinal epithelial cells is required for protection against MTX-induced intestinal damage. **(A–F)** WT and Vil-LTβR$^{-/-}$ mice were treated with MTX, as in Figure 1A. **(A)** Body weight loss; n=19–22 mice per group. **(B)** Representative H&E images (scale bars, 100μm) and histopathology scores; Expression of **(C)** Ki-67, **(D)** cytokines and **(E)** chemokines in the ileum on day 5 after MTX treatment. n= 6–8 mice per group. **(F)** Survival; n=7–12 mice per group. **(G, H)** LTβR expression by Lgr5^{+} cells is dispensable for protection. WT and Lgr5-LTβR$^{-/-}$ mice were treated with MTX, as in Figure 1A, Lgr5-Cre expression was induced by tamoxifen administration. Mice were euthanized on day 5 for analysis. **(G)** Body weight change, n=11–14 mice per group **(H)** representative H&E images (scale bars, 100μm) and histopathology scores. Data combined from 2–5 independent experiments with similar results. Data shown as mean ± SEM. Statistics were determined using multiple unpaired t test **(A)**, Mann-Whitney test **(B)**, unpaired t test **(C–E, H)** or Log-rank (Mantel-Cox) test **(F)**. ns, not significant; *p<0.05, **p<0.01, ***p<0.001.

various proinflammatory cytokines and chemokines in response to the inflammatory stimuli (39, 42, 73). NF-κB signaling in intestinal epithelial cells can contribute to protection from intestinal inflammation in several animal models of disease (74). Recent studies demonstrated the important role of non-canonical NF-κB signaling in intestinal epithelial cells for protection from gut bacterial infections and intestinal inflammation (59, 75). We found that treatment of CMT-93 intestinal epithelial cells *in vitro* with MTX or with an agonistic αLTβR antibody induced expression of NF-κB2 (Figure 6A). Moreover, NF-κB2 was upregulated in the ileum after MTX treatment *in vivo* (Figure 6B). To test whether non-canonical NF-κB signaling in intestinal epithelial cells protects from intestinal inflammation caused by MTX treatment, we generated mice with specific inactivation of RelB in intestinal epithelial cells (Vil-RelB$^{-/-}$ mice) by crossing RelB floxed mice (55) with Villin-Cre mice (51). Vil-RelB$^{-/-}$ mice treated with MTX demonstrated aggravated weight loss and increased intestinal pathology, compared to littermate Cre^{-} control mice (Figures 6C, D). Whereas proliferation of intestinal epithelial cells in these mice was decreased (Figure 6E), expression of proinflammatory cytokines TNF and IL-1β was elevated (Figures 6F). In contrast to Vil-RelB$^{-/-}$, mice with inactivation of RelB in CD11c^{+} DCs (CD11c-RelB$^{-/-}$) did not display an increased body weight loss post MTX treatment (Supplementary Figure S5D), consistent with results in CD11c-LTβR$^{-/-}$ mice (Supplementary Figures S5A, B). Together, these results suggest that LTβR on intestinal epithelial cells activates non-canonical NF-κB signaling to promote recovery after MTX-induced injury (Figure 7).

Discussion

Accumulating evidence suggests that immune mechanisms may either exacerbate or ameliorate intestinal damage caused by chemotherapeutic drugs. Recent studies implicated the role of IL-22 and ILC3s in mucosal repair following MTX-induced intestinal damage (30, 31), however the role of other immune components and cytokines remains less defined. In this study we revealed the critical role of LTβR in protection from chemotherapy-induced intestinal damage. As previous studies demonstrated the role of LTβR in regulation of IL-22 production by ILC3s (45, 47), we hypothesized that LTβR-dependent regulation of ILC3s and IL-22

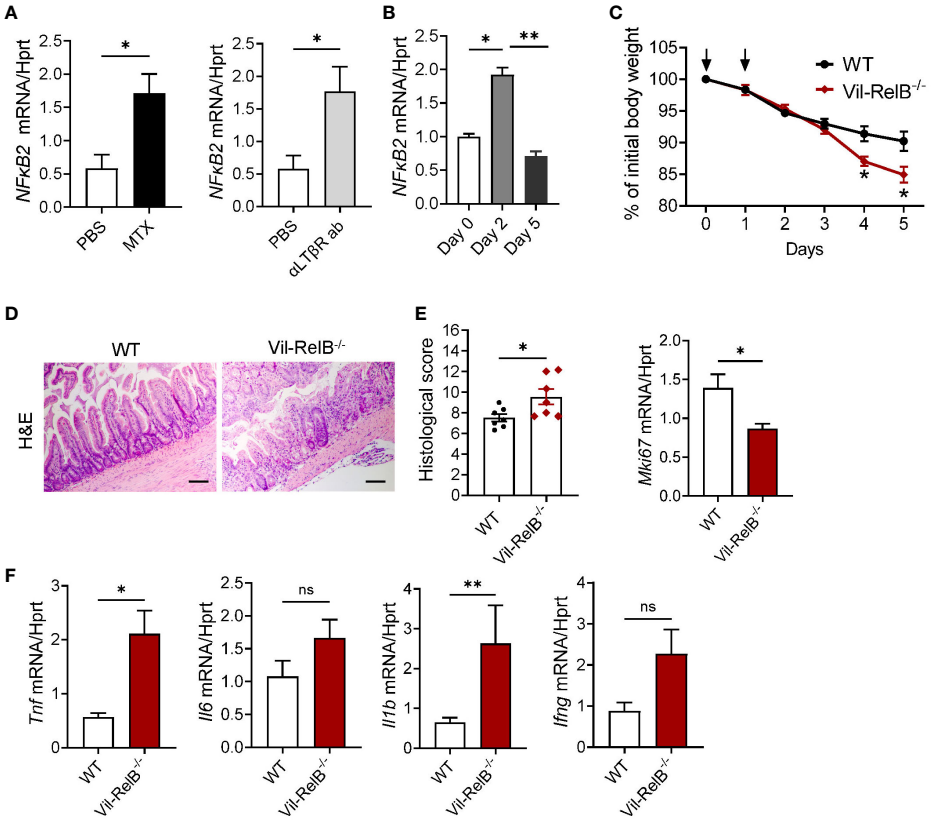

FIGURE 6
Non-canonical NF-κB signaling in intestinal epithelial cells protects from MTX-induced intestinal damage. **(A)** CMT-93 epithelial cells were treated with MTX (5 µmol/L) or agonistic αLTβR antibody (ACH6, 0.5µg/ml) for 24 hours. Nfκb2 expression was measured by real-time PCR. **(B)** Nfκb2 expression in the ileum of WT mice treated with MTX was measured by real-time PCR. n= 4–7 mice per group. **(C–F)** WT and Vil-RelB$^{-/-}$ mice were treated with MTX as on Figure 1A. **(C)** Body weight loss; n=14–30 per group. **(D)** representative H&E images (scale bars, 100µm) and histopathology scores; Expression of **(E)** Ki-67, and **(F)** proinflammatory cytokines in the ileum on day 5 after treatment. n= 5 mice per group. Data is combined from 3–4 independent experiments with similar results. Data shown as mean ± SEM. Statistics were determined using unpaired t test **(A, D)**, Mann-Whitney test **(A, B)**, two-way ANOVA with Geisser-Greenhouse correction **(C)**, or Kruskal-Wallis test **(E, F)**. ns, not significant; *p<0.05; **p<0.01.

mediates protection against chemotherapy-induced intestinal damage. However, our results suggest that although LT expression in ILC3s is critical for control of IL-22 production, it is dispensable for protection from MTX-induced injury. Instead, another LTβR ligand, LIGHT, produced by T cells was critical for protection. Moreover, LTβR and IL-22 pathways jointly participate in mucosal protection. Furthermore, we demonstrate that LTβR-dependent non-canonical NF-kB signaling in intestinal epithelial cells is required for mucosal repair.

Although the role of LTβR signaling in the development and maintenance of lymphoid tissues and inflammatory diseases is well established (41, 76–78), accumulating evidence suggests that LTβR regulates intestinal inflammation (43, 45–47, 64, 79, 80). However, the role of LTβR in chemotherapy-induced epithelial injury has not been investigated. Our data demonstrate that LTβR-deficient mice display increased body weight loss, severe pathology, reduced epithelial cell proliferation and increased mortality post MTX administration. This phenotype was associated with increased expression of proinflammatory cytokines TNF, IL-1β, IFNγ and chemokines CXCL1, CXC2, CXCL9, CXCL10, and CCL2 in the small intestine at day 5 post MTX administration, whereas IL-22 and IL-22 dependent expression of antibacterial proteins were reduced. These results are consistent with previous studies supporting the role of LTβR in regulation of colonic IL-22 production and protection against *C. rodentium* infection (44, 47). As increased expression of proinflammatory cytokines at day 5 can be a result of impaired epithelial cell proliferation, we next analyzed immune cell populations and cytokines at day 2 post MTX administration, during the disease induction phase. Our results show that expression of CXCL2 and IL-22 was reduced in the ileum of LTβR$^{-/-}$ mice, whereas IFNγ, CXCL9, CXCL10 were increased at day 2 post MTX treatment. This is consistent with LTβR function in controlling neutrophil recruiting chemokines in response to mucosal bacterial pathogen *C. rodentium* (43). Flow cytometry revealed an increased frequency of CD8αα^{+} IELs whereas proportion of CD4^{+} T cells was reduced in the IEL and LP of LTβR$^{-/-}$ mice. CD8αα^{+} IELs are known to play regulatory role in intestinal inflammation (81, 82). How LTβR signaling controls CD8αα^{+} IELs recruitment and the role of these cells in chemotherapy-induced epithelial damage remains to be determined.

Both LTβR ligands LT and LIGHT have been implicated in the regulation of inflammatory responses in the gut (43, 69, 79).

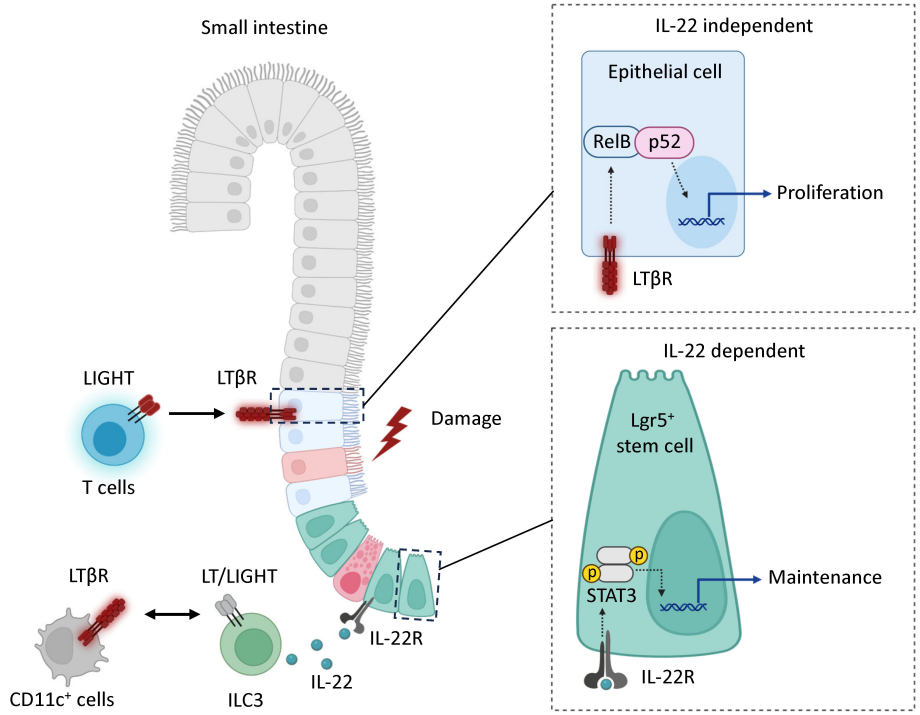

FIGURE 7
Model. LTβR signaling promotes mucosal healing following MTX-induced injury by controlling IL-22 dependent and IL-22 independent pathways. Mucosal damage promotes expression of LIGHT and LTβ in the intestine. In the IL-22 independent pathway, the interaction of LIGHT expressing T cells with LTβR in intestinal epithelial cells activates non-canonical RelB/p52 NF-kB signaling to promote proliferation of epithelial cells after injury. In the IL-22 dependent pathway, interaction of LIGHT/LT expressing ILC3s with CD11c$^+$ LTβR-expressing cells promotes secretion of IL-22 which interacts with IL-22R to support the maintenance of Lgr5$^+$ intestinal stem cells. LTβR expression in Lgr5$^+$ stem cells is dispensable for protection.

Surprisingly, LIGHT but not LTβ, was essential for protection from MTX-induced intestinal damage, as LIGHT$^{-/-}$ mice displayed increased intestinal pathology post MTX treatment whereas LTβ$^{-/-}$ mice did not exhibit an exacerbated pathology. Furthermore, inactivation of LTβ in ILC3s did not result in increased intestinal pathology, despite reduced IL-22 levels in the ileum of RORγt-LTβ$^{-/-}$ mice. These results highlight distinct roles of LIGHT and LT in different models of intestinal damage. Thus, LTβ expressed by RORγt$^+$ ILC3s is critical for protections against *C. rodentium*, while LIGHT is dispensable in this model (47). In contrast, LIGHT, rather than LTβ, was critical for protection against DSS-induced intestinal damage (69, 79). Interestingly, LIGHT$^{-/-}$ mice displayed reduced levels of IL-22 in the ileum post MTX treatment, suggesting that LIGHT signaling can also control IL-22 production in this model of intestinal damage. In contrast, in the *C. rodentium* colitis model, LTβ, but not LIGHT, was critical for IL-22 production (47). The distinct role of LIGHT and LTβ in these models of intestinal damage could be attributed to different LIGHT and LTβ producing cell types. Our data revealed that T cells are the major contributors to mucosal protection against MTX induced damage, because TCRβδ$^{-/-}$ mice displayed an exacerbated intestinal pathology compared to RORγt$^{-/-}$ mice. As LIGHT expression was rapidly increased in the intestine at day 2 post MTX treatment, but was ablated in TCRβδ$^{-/-}$ mice, this data suggest that LIGHT provided by T cells contribute to mucosal protection. It is also possible that LIGHT expression by other immune or stromal cells contribute to protection. Our results are in line with a previous study suggesting the role of LIGHT in regulation of intestinal stem cell gene signatures (83). The kinetics and level of LIGHT expression may explain protective versus pathogenic LIGHT-mediated responses in the gut. Consistent with this hypothesis, we detected only a transient induction of LIGHT expression in the MTX-induced injury model. In contrast, sustained overexpression of LIGHT on T cells can break down the immunosuppressive state mediated by Tregs and induce T cell- mediated intestinal inflammation (84, 85).

Previous studies demonstrated the critical role of IL-22 in promoting ISC proliferation after injury (19, 26, 29, 30). However, a recent study demonstrated that IL-22 deficient mice do not display increased intestinal pathology after MTX treatment, implicating IL-22 independent pathways, such as Hippo-Yap, in promoting intestinal epithelial cell proliferation after injury (31). Consistently, our study also did not detect an increased intestinal pathology in IL-22$^{-/-}$ mice post MTX treatment. Although IL-22 expression was impaired in the ileum of RORγt-LTβ$^{-/-}$ mice, these mice did not exhibit increased intestinal pathology. However, we revealed that genetic inactivation of IL-22 further exacerbated MTX-induced intestinal pathology in LTβR$^{-/-}$ mice. These results suggest that LTβR and IL-22 jointly promote mucosal repair after MTX-induced intestinal damage. Interestingly, LTβR stimulation may suppress YAP/TAZ activity in fibroblastic reticular cells in lymph nodes (86). However, the connection between LTβR

and Yap signaling in intestinal epithelial cells remains to be determined.

LTβR is expressed on a variety of epithelial, stromal, and myeloid cells in the gut, thereby participating in regulation of mucosal immune homeostasis (43, 45, 46, 59, 64, 87). Therefore, we wanted to determine which LTβR expressing cells are critical for protection against MTX-induced damage. Our results suggest that LTβR expression in intestinal epithelial cells is essential for protection, whereas LTβR expression on macrophages and dendritic cells is dispensable. The protective role of LTβR on intestinal epithelial cells was previously demonstrated in *C. rodentium* infection and DSS-induced colitis models (43, 45). However, genetic inactivation of LTβR in ISCs did not exacerbate intestinal disease, consistent with low expression of LTβR on $Lgr5^+$ stem cells (72). These results suggest that although LTβR on intestinal epithelial cells is critical for mucosal repair after MTX-induced damage, LTβR signaling in ISCs is dispensable for protection. The role of specific subsets of LTβR-expressing intestinal epithelial cells in mucosal repair after MTX-induced damage will be further defined in future studies.

LTβR stimulation leads to non-canonical NF-kB signaling, which involves NF-κB-inducing kinase (NIK) and IKKα, processing of p100 precursor and nuclear translocation of the non-canonical NF-κB complex p52/RelB (39, 42, 88). Additionally, LTβR stimulation can lead to activation of the canonical NF-κB pathway operating via NFκB1 (p50/RelA) transcription, which usually occurs within minutes and does not require novel gene expression, in contrast to the non-canonical pathway (73, 88). Non-canonical NF-kB signaling is thought to play a central role in induction of proinflammatory cytokines TNF, IL-6, IL-18, IL-1β early during chemotherapy-induced intestinal injury, thereby promoting inflammation (2, 3). In contrast, non-canonical NF-κB signaling in intestinal epithelial cells is important for protection from gut bacterial infections and intestinal inflammation (59, 74, 75). Our results are consistent with these studies and identify a previously unrecognized role for epithelial cell-intrinsic RelB expression in regulating mucosal repair after chemotherapy-induced intestinal damage.

Based on our results, we propose a model for a LTβR-dependent mechanism for mucosal healing after MTX-induced intestinal damage (Figure 7). MTX injury results in early upregulation of chemokines and increased recruitment of T cells to the epithelial layer. LIGHT, presumably produced by T cells interacts with LTβR on intestinal epithelial cells to activate non-canonical RelB signaling thereby promoting proliferation of epithelial cells after injury. Interactions between LIGHT/LT expressing $ROR\gamma t^+$ ILC3s and LTβR expressing $CD11c^+$ cells can also contribute to IL-22-dependent maintenance of ISCs after injury. Our data suggest that LTβR also promotes mucosal healing in 5-FU induced intestinal mucositis. The critical LTβR expressing cells and LTβR ligands in 5-FU induced intestinal injury remain to be determined.

Gaining insight into the immune regulation of mucosal healing post-cytotoxic drug exposure holds crucial implications for developing targeted therapeutic interventions. In summary, our study revealed a previously unrecognized role for the LTβR-RelB pathway in intestinal epithelial cells which promotes mucosal repair after chemotherapy-induced intestinal damage. These findings provide valuable insights into the immune mechanisms orchestrating mucosal healing after chemotherapy-induced intestinal injury, paving the way for potential therapeutic interventions.

Data availability statement

Publicly available datasets were analyzed in this study. This data can be found here: https://portals.broadinstitute.org/single_cell/study/small-intestinal-epithelium.

Ethics statement

The animal study was approved by The University of Texas Health Science Center at San Antonio Institutional Animal Care and Use Committee. The study was conducted in accordance with the local legislation and institutional requirements.

Author contributions

AVT: Conceptualization, Formal analysis, Funding acquisition, Investigation, Methodology, Project administration, Resources, Supervision, Visualization, Writing – original draft, Writing – review & editing. QC: Data curation, Formal analysis, Investigation, Methodology, Writing – original draft, Writing – review & editing. AM: Conceptualization, Formal analysis, Investigation, Supervision, Writing – review & editing. AK: Data curation, Formal analysis, Investigation, Visualization, Writing – review & editing. YS: Investigation, Writing – original draft. JV: Investigation, Writing – original draft. AWT: Investigation, Writing – review & editing. SS: Data curation, Formal analysis, Investigation, Writing – review & editing. EK: Conceptualization, Data curation, Formal analysis, Investigation, Methodology, Project administration, Resources, Supervision, Validation, Writing – original draft, Writing – review & editing.

Funding

The author(s) declare financial support was received for the research, authorship, and/or publication of this article. This research was supported by grants from the National Institutes of Health (NIH) NS112263, DE029187, the Cancer Prevention and Research Institute of Texas (CPRIT) RP210105, RP220470, and by the Max and Minnie Tomerlin Voelcker Fund. AM was supported by K12 GM111726 San Antonio Biomedical Education and Research-Institutional Research and Academic Career Development Award (SABER-IRACDA). The Flow Cytometry Shared Resource at UT Health San Antonio is supported by a grant from the National Cancer Institute (P30CA054174) to the Mays Cancer Center, a grant from the Cancer Prevention and Research Institute of Texas (CPRIT) (RP210126), a grant from the National Institutes of Health

(1S10OD030432), and support from the Office of the Vice President for Research at UT Health San Antonio.

Acknowledgments

We thank Dr. Michael Croft and Dr. Mitchell Kronenberg (La Jolla Institute for Immunology) for providing LIGHT$^{-/-}$ mice. We are grateful to Biogen Idec for providing anti-LTβR agonistic antibody. We thank Anna Tumanova for editing the manuscript. Figure 7 was created with BioRender.com.

Conflict of interest

The authors declare that the research was conducted in the absence of any commercial or financial relationships that could be construed as a potential conflict of interest.

The author(s) declared that they were an editorial board member of Frontiers, at the time of submission. This had no impact on the peer review process and the final decision

Publisher's note

All claims expressed in this article are solely those of the authors and do not necessarily represent those of their affiliated organizations, or those of the publisher, the editors and the reviewers. Any product that may be evaluated in this article, or claim that may be made by its manufacturer, is not guaranteed or endorsed by the publisher.

Supplementary material

The Supplementary Material for this article can be found online at: https://www.frontiersin.org/articles/10.3389/fimmu.2024.1388496/full#supplementary-material

SUPPLEMENTARY FIGURE 1
LTβR signaling protects against 5-FU induced intestinal inflammation. WT and LTβR$^{-/-}$ mice were treated with 5-Fluorouracil (5-FU, 50 mg/kg, i.p.) daily for 4 consecutive days, and analyzed at day 5. **(A)** Body weight change. Black arrows: days of 5-FU treatment. n=14–17 mice per group. **(B)** Disease score. **(C)** Representative photographs of colons and colon length. **(D)** Representative H&E images and histological scores. Scale bars, 100μm. **(E)** Cytokine expression in the colon. n= 7 mice per group. Data represents 1 of 3 independent experiments with similar results. Data shown as mean ± SEM. Statistics were determined using two-way ANOVA with Geisser-Greenhouse correction **(A)**, unpaired t test **(B–E)**. ns, not significant; * p<0.05, ** p<0.01, *** p<0.001, **** p<0.0001.

SUPPLEMENTARY FIGURE 2
Gating strategy of immune cell populations in SI. **(A)** Gating strategy of immune cell populations in IEL. Lin$^+$(Lineage$^+$): B220, Ly6G. Neutrophils were defined as CD45$^+$Lin$^+$MHCII-CD11b$^+$; B cells were defined as CD45$^+$Lin$^+$CD11b-MHCII$^+$; T cells were defined as CD45$^+$CD3$^+$ **(B)** Gating strategy of immune cell populations in LP. Neutrophils, CD45$^+$Ly6G$^+$CD11b$^+$; B cells, CD45$^+$Ly6G-B220$^+$; Eosinophils, CD45$^+$Ly6G$^-$B220$^-$CD11b$^+$Siglec F$^+$; T cells, CD45$^+$Ly6G$^-$B220$^-$SiglecF$^-$TCRβ$^+$; ILC1s, CD45$^+$Ly6G$^-$B220$^-$SiglecF$^-$TCRβ$^-$CD64$^-$NK1.1$^+$; Dendritic cells (DCs), CD45$^+$Ly6G$^-$B220$^-$SiglecF$^-$TCRβ$^-$CD64$^-$MHCII$^+$CD11c$^+$; Macrophages (Mph), CD45$^+$Ly6G$^-$B220$^-$SiglecF$^-$TCRβ$^-$CD64$^+$MHCII$^+$CD11b$^+$; Monocytes (Mo), CD45$^+$Ly6G$^-$B220$^-$SiglecF$^-$TCRβ$^-$CD64$^+$MHCII$^-$CD11b$^+$CCR2$^+$.

SUPPLEMENTARY FIGURE 3
Analysis of immune cell populations and cytokines in WT SI after MTX treatment. **(A–G)** WT mice were treated with MTX as in Figure 1A. Mice were euthanized on day 2 and small intestines were collected for analysis. **(A)** Representative flow cytometry plots and frequency of T cell populations in SI IEL. Frequency is calculated in live CD45$^+$ cells. **(B, C)** Representative flow cytometry plots and frequency of cell populations in LP. Tregs (B220$^-$CD3$^+$CD4$^+$CD25$^+$FoxP3$^+$); ILC1s (CD45$^+$Ly6G$^-$B220$^-$SiglecF$^-$TCRβ$^-$ CD64$^-$NK1.1$^+$); CD4$^+$ T cells; CD3$^+$ T cells; Macrophages (Mph, CD11c$^-$Ly6G$^-$SiglecF$^-$CD11b$^+$MHCII$^+$CD64$^+$); Neutrophils (Nph, Ly6G$^+$ CD11b$^+$); B cells (B220$^+$); DCs (CD45$^+$Ly6G$^-$B220$^-$SiglecF$^-$TCRβ$^-$ CD64$^-$MHCII$^+$CD11c$^+$). Expression of **(D)** cytokines and **(E)** chemokines in the ileum at day 0, 2 and 5 post MTX treatment. **(F, G)** LTα expression after MTX was measured by Real-Time PCR in WT **(F)** ileum, jejunum, and duodenum as well as **(G)** LP and IEL from small intestine. **(D–G)** Data are representative of two experiments (n=3–7 per group). Data shown as mean ± SEM. Statistics were determined using unpaired t test **(A–C, F, G)**, Mann-Whitney test **(D, E)**, Kruskal-Wallis test **(D–F)**. ns, not significant, * p<0.05, ** p<0.01, *** p<0.001, **** p<0.0001.

SUPPLEMENTARY FIGURE 4
Analysis of epithelial cell populations in the ileum of WT and LTβR$^{-/-}$ mice. **(A)** Expression of *Ltbr* and *Lgr5* in various small intestine derived cell types was determined by single-cell RNA-seq. Data was obtained from the study conducted by Haber et al. (72), using the Broad Institute Single-Cell Portal for data analysis (https://portals.broadinstitute.org/single_cell/study/small-intestinal-epithelium). **(B)** WT and LTβR$^{-/-}$ mice were crossed with Lgr5-GFP reporter mice. GFP expression was induced by tamoxifen administration and mice were treated with MTX as in Figure 1A. Mice were euthanized on day 5 and ileum epithelial cells analyzed by flow cytometry. Gating strategy. Tuft cells: EpCAM$^+$CD45$^+$; Lgr5$^+$ cells: EpCAM$^+$Lgr5$^+$CD31$^-$Ter119$^-$CD45$^-$; Paneth cells: EpCAM$^+$c-Kit$^+$CD31$^-$Ter119$^-$CD45$^-$; Epithelial cells: EpCAM$^+$CD31$^-$Ter119$^-$CD45$^-$. **(C–F)** Representative flow plot and frequency of cell populations. **(G)** Goblet cells analysis by Alcian Blue staining in small intestine. Scale bars, 100μm. Data show 1 of 2 independent experiments with similar results (n=3–5 per group). Data shown as mean ± SEM. Statistics were determined using unpaired t test. ns, not significant.

SUPPLEMENTARY FIGURE 5
LTβR signaling in macrophages and DCs is not essential for the protection from MTX induced intestinal injury. **(A–D)**. WT, LysM-LTβR$^{-/-}$, CD11c-LTβR$^{-/-}$, CD11c, LysM-LTβR$^{-/-}$ and CD11c-RelB$^{-/-}$ mice were treated with MTX as in Figure 1A. **(A, D)** Body weight loss (n=9–14 mice per group) and **(B)** Representative H&E images (scale bars, 100μm) with histopathology scores. **(C)** IL-22 expression in the ileum on day 5 after MTX treatment. n= 5–8 mice per group. Data are combined from 3–5 independent experiments with similar results. Data shown as mean ± SEM. Statistics were determined using two-way ANOVA with Geisser-Greenhouse correction **(A, D)**, Kruskal-Wallis test **(B)**, unpaired t test **(C)**. ns, not significant, * p<0.05.

References

1. Dahlgren D, Sjoblom M, Hellstrom PM, Lennernas H. Chemotherapeutics-induced intestinal mucositis: pathophysiology and potential treatment strategies. *Front Pharmacol.* (2021) 12:681417. doi: 10.3389/fphar.2021.681417

2. Sougiannis AT, VanderVeen BN, Davis JM, Fan D, Murphy EA. Understanding chemotherapy-induced intestinal mucositis and strategies to improve gut resilience. *Am J Physiol Gastrointest Liver Physiol.* (2021) 320:G712–G9. doi: 10.1152/ajpgi.00380.2020

3. Basile D, Di Nardo P, Corvaja C, Garattini SK, Pelizzari G, Lisanti C, et al. Mucosal injury during anti-cancer treatment: from pathobiology to bedside. *Cancers (Basel).* (2019) 11. doi: 10.3390/cancers11060857

4. Villa A, Sonis ST. Mucositis: pathobiology and management. *Curr Opin Oncol*. (2015) 27:159–64. doi: 10.1097/CCO.0000000000000180

5. Sonis ST. The pathobiology of mucositis. *Nat Rev Cancer*. (2004) 4:277–84. doi: 10.1038/nrc1318

6. Elting LS, Cooksley CD, Chambers MS, Garden AS. Risk, outcomes, and costs of radiation-induced oral mucositis among patients with head-and-neck Malignancies. *Int J Radiat Oncol Biol Phys*. (2007) 68:1110–20. doi: 10.1016/j.ijrobp.2007.01.053

7. O'Brien ME, Borthwick A, Rigg A, Leary A, Assersohn L, Last K, et al. Mortality within 30 days of chemotherapy: A clinical governance benchmarking issue for oncology patients. *Br J Cancer*. (2006) 95:1632–6. doi: 10.1038/sj.bjc.6603498

8. Iacovelli R, Pietrantonio F, Maggi C, de Braud F, Di Bartolomeo M. Combination or single-agent chemotherapy as adjuvant treatment of gastric cancer: A systematic review and meta-analysis of published trials. *Crit Rev Oncol Hematol*. (2016) 98:24–8. doi: 10.1016/j.critrevonc.2015.09.002

9. Heinemann V, von Weikersthal LF, Decker T, Kiani A, Vehling-Kaiser U, Al-Batran SE, et al. Folfiri plus cetuximab versus folfiri plus bevacizumab as first-line treatment for patients with metastatic colorectal cancer (Fire-3): A randomised, open-label, phase 3 trial. *Lancet Oncol*. (2014) 15:1065–75. doi: 10.1016/S1470–2045(14)70330–4

10. Becerra CR, Frenkel EP, Ashfaq R, Gaynor RB. Increased toxicity and lack of efficacy of rofecoxib in combination with chemotherapy for treatment of metastatic colorectal cancer: A phase II study. *Int J Cancer*. (2003) 105:868–72. doi: 10.1002/ijc.11164

11. Mego M, Chovanec J, Vochyanova-Andrezalova I, Konkolovsky P, Mikulova M, Reckova M, et al. Prevention of irinotecan induced diarrhea by probiotics: A randomized double blind, placebo controlled pilot study. *Complement Ther Med*. (2015) 23:356–62. doi: 10.1016/j.ctim.2015.03.008

12. Lee JY, Chu SH, Jeon JY, Lee MK, Park JH, Lee DC, et al. Effects of 12 weeks of probiotic supplementation on quality of life in colorectal cancer survivors: A double-blind, randomized, placebo-controlled trial. *Dig Liver Dis*. (2014) 46:1126–32. doi: 10.1016/j.dld.2014.09.004

13. Lu H, Liu H, Wang J, Shen J, Weng S, Han L, et al. The chemokine CXCL9 exacerbates chemotherapy-induced acute intestinal damage through inhibition of mucosal restitution. *J Cancer Res Clin Oncol*. (2015) 141:983–92. doi: 10.1007/s00432-014-1869-y

14. Zhou B, Xia X, Wang P, Chen S, Yu C, Huang R, et al. Induction and amelioration of methotrexate-induced gastrointestinal toxicity are related to immune response and gut microbiota. *EBioMedicine*. (2018) 33:122–33. doi: 10.1016/j.ebiom.2018.06.029

15. Sethy C, Kundu CN. 5-Fluorouracil (5-FU) resistance and the new strategy to enhance the sensitivity against cancer: implication of DNA repair inhibition. *BioMed Pharmacother*. (2021) 137:111285. doi: 10.1016/j.biopha.2021.111285

16. Sangild PT, Shen RL, Pontoppidan P, Rathe M. Animal models of chemotherapy-induced mucositis: translational relevance and challenges. *Am J Physiol Gastrointest Liver Physiol*. (2018) 314:G231–G46. doi: 10.1152/ajpgi.00204.2017

17. Sakai H, Sagara A, Matsumoto K, Hasegawa S, Sato K, Nishizaki M, et al. 5-fluorouracil induces diarrhea with changes in the expression of inflammatory cytokines and aquaporins in mouse intestines. *PloS One*. (2013) 8:e54788. doi: 10.1371/journal.pone.0054788

18. Sultani M, Stringer AM, Bowen JM, Gibson RJ. Anti-inflammatory cytokines: important immunoregulatory factors contributing to chemotherapy-induced gastrointestinal mucositis. *Chemother Res Pract*. (2012) 2012:490804. doi: 10.1155/2012/490804

19. Hanash AM, Dudakov JA, Hua G, O'Connor MH, Young LF, Singer NV, et al. Interleukin-22 protects intestinal stem cells from immune-mediated tissue damage and regulates sensitivity to graft versus host disease. *Immunity*. (2012) 37:339–50. doi: 10.1016/j.immuni.2012.05.028

20. Spits H, Di Santo JP. The expanding family of innate lymphoid cells: regulators and effectors of immunity and tissue remodeling. *Nat Immunol*. (2011) 12:21–7. doi: 10.1038/ni.1962

21. Dudakov JA, Hanash AM, van den Brink MR. Interleukin-22: immunobiology and pathology. *Annu Rev Immunol*. (2015) 33:747–85. doi: 10.1146/annurev-immunol-032414–112123

22. Keir M, Yi Y, Lu T, Ghilardi N. The role of il-22 in intestinal health and disease. *J Exp Med*. (2020) 217:e20192195. doi: 10.1084/jem.20192195

23. Renauld JC. Class ii cytokine receptors and their ligands: key antiviral and inflammatory modulators. *Nat Rev Immunol*. (2003) 3:667–76. doi: 10.1038/nri1153

24. Saxton RA, Henneberg LT, Calafiore M, Su L, Jude KM, Hanash AM, et al. The tissue protective functions of interleukin-22 can be decoupled from pro-inflammatory actions through structure-based design. *Immunity*. (2021) 54:660–72.e9. doi: 10.1016/j.immuni.2021.03.008

25. Wolk K, Kunz S, Witte E, Friedrich M, Asadullah K, Sabat R. IL-22 increases the innate immunity of tissues. *Immunity*. (2004) 21:241–54. doi: 10.1016/j.immuni.2004.07.007

26. Lindemans CA, Calafiore M, Mertelsmann AM, O'Connor MH, Dudakov JA, Jenq RR, et al. Interleukin-22 promotes intestinal-stem-cell-mediated epithelial regeneration. *Nature*. (2015) 528:560–4. doi: 10.1038/nature16460

27. Kinnebrew MA, Buffie CG, Diehl GE, Zenewicz LA, Leiner I, Hohl TM, et al. Interleukin 23 production by intestinal CD103(+)CD11b(+) dendritic cells in response to bacterial flagellin enhances mucosal innate immune defense. *Immunity*. (2012) 36:276–87. doi: 10.1016/j.immuni.2011.12.011

28. Lorchner H, Poling J, Gajawada P, Hou Y, Polyakova V, Kostin S, et al. Myocardial healing requires reg3beta-dependent accumulation of macrophages in the ischemic heart. *Nat Med*. (2015) 21:353–62. doi: 10.1038/nm.3816

29. Gronke K, Hernandez PP, Zimmermann J, Klose CSN, Kofoed-Branzk M, Guendel F, et al. Interleukin-22 protects intestinal stem cells against genotoxic stress. *Nature*. (2019) 566:249–53. doi: 10.1038/s41586–019-0899–7

30. Aparicio-Domingo P, Romera-Hernandez M, Karrich JJ, Cornelissen F, Papazian N, Lindenbergh-Kortleve DJ, et al. Type 3 innate lymphoid cells maintain intestinal epithelial stem cells after tissue damage. *J Exp Med*. (2015) 212:1783–91. doi: 10.1084/jem.20150318

31. Romera-Hernandez M, Aparicio-Domingo P, Papazian N, Karrich JJ, Cornelissen F, Hoogenboezem RM, et al. Yap1-driven intestinal repair is controlled by group 3 innate lymphoid cells. *Cell Rep*. (2020) 30:37–45.e3. doi: 10.1016/j.celrep.2019.11.115

32. Wolk K, Witte E, Wallace E, Docke WD, Kunz S, Asadullah K, et al. IL-22 regulates the expression of genes responsible for antimicrobial defense, cellular differentiation, and mobility in keratinocytes: A potential role in psoriasis. *Eur J Immunol*. (2006) 36:1309–23. doi: 10.1002/eji.200535503

33. Eken A, Singh AK, Treuting PM, Oukka M. IL-23R+ Innate lymphoid cells induce colitis via interleukin-22-dependent mechanism. *Mucosal Immunol*. (2014) 7:143–54. doi: 10.1038/mi.2013.33

34. Munoz M, Heimesaat MM, Danker K, Struck D, Lohmann U, Plickert R, et al. Interleukin (IL)-23 mediates toxoplasma gondii-induced immunopathology in the gut via matrixmetalloproteinase-2 and IL-22 but independent of IL-17. *J Exp Med*. (2009) 206:3047–59. doi: 10.1084/jem.20090900

35. Gunasekera DC, Ma J, Vacharathit V, Shah P, Ramakrishnan A, Uprety P, et al. The development of colitis in IL10(-/-) mice is dependent on IL-22. *Mucosal Immunol*. (2020) 13:493–506. doi: 10.1038/s41385–019-0252–3

36. Kamanaka M, Huber S, Zenewicz LA, Gagliani N, Rathinam C, O'Connor W Jr., et al. Memory/effector (Cd45rb(Lo)) cd4 T cells are controlled directly by IL-10 and cause IL-22-dependent intestinal pathology. *J Exp Med*. (2011) 208:1027–40. doi: 10.1084/jem.20102149

37. Ware CF. Network communications: lymphotoxins, LIGHT, and TNF. *Annu Rev Immunol*. (2005) 23:787–819. doi: 10.1146/annurev.immunol.23.021704.115719

38. Upadhyay V, Fu YX. Lymphotoxin signalling in immune homeostasis and the control of microorganisms. *Nat Rev Immunol*. (2013) 13:270–9. doi: 10.1038/nri3406

39. Albarbar B, Dunnill C, Georgopoulos NT. Regulation of cell fate by lymphotoxin (LT) receptor signalling: functional differences and similarities of the LT system to other TNF superfamily (TNFSF) members. *Cytokine Growth Factor Rev*. (2015) 26:659–71. doi: 10.1016/j.cytogfr.2015.05.001

40. Ware CF, Croft M, Neil GA. Realigning the light signaling network to control dysregulated inflammation. *J Exp Med*. (2022) 219. doi: 10.1084/jem.20220236

41. Koroleva EP, Fu YX, Tumanov AV. Lymphotoxin in physiology of lymphoid tissues - implication for antiviral defense. *Cytokine*. (2018) 101:39–47. doi: 10.1016/j.cyto.2016.08.018

42. Dejardin E, Droin NM, Delhase M, Haas E, Cao Y, Makris C, et al. The lymphotoxin-beta receptor induces different patterns of gene expression via two NF-kappaB pathways. *Immunity*. (2002) 17:525–35. doi: 10.1016/s1074–7613(02)00423–5

43. Wang Y, Koroleva EP, Kruglov AA, Kuprash DV, Nedospasov SA, Fu YX, et al. Lymphotoxin beta receptor signaling in intestinal epithelial cells orchestrates innate immune responses against mucosal bacterial infection. *Immunity*. (2010) 32:403–13. doi: 10.1016/j.immuni.2010.02.011

44. Ota N, Wong K, Valdez PA, Zheng Y, Crellin NK, Diehl L, et al. IL-22 bridges the lymphotoxin pathway with the maintenance of colonic lymphoid structures during infection with citrobacter rodentium. *Nat Immunol*. (2011) 12:941–8. doi: 10.1038/ni.2089

45. Macho-Fernandez E, Koroleva EP, Spencer CM, Tighe M, Torrado E, Cooper AM, et al. Lymphotoxin beta receptor signaling limits mucosal damage through driving IL-23 production by epithelial cells. *Mucosal Immunol*. (2015) 8:403–13. doi: 10.1038/mi.2014.78

46. Riffelmacher T, Giles DA, Zahner S, Dicker M, Andreyev AY, McArdle S, et al. Metabolic activation and colitis pathogenesis is prevented by lymphotoxin beta receptor expression in neutrophils. *Mucosal Immunol*. (2021) 14:679–90. doi: 10.1038/s41385–021-00378–7

47. Tumanov AV, Koroleva EP, Guo X, Wang Y, Kruglov A, Nedospasov S, et al. Lymphotoxin controls the IL-22 protection pathway in gut innate lymphoid cells during mucosal pathogen challenge. *Cell Host Microbe*. (2011) 10:44–53. doi: 10.1016/j.chom.2011.06.002

48. Eberl G, Marmon S, Sunshine MJ, Rennert PD, Choi Y, Littman DR. An essential function for the nuclear receptor rorgamma(T) in the generation of fetal lymphoid tissue inducer cells. *Nat Immunol*. (2004) 5:64–73. doi: 10.1038/ni1022

49. Mombaerts P, Clarke AR, Rudnicki MA, Iacomini J, Itohara S, Lafaille JJ, et al. Mutations in T-cell antigen receptor genes alpha and beta block thymocyte development at different stages. *Nature*. (1992) 360:225–31. doi: 10.1038/360225a0

50. Ahlfors H, Morrison PJ, Duarte JH, Li Y, Biro J, Tolaini M, et al. IL-22 fate reporter reveals origin and control of IL-22 production in homeostasis and infection. *J Immunol*. (2014) 193:4602–13. doi: 10.4049/jimmunol.1401244

51. Madison BB, Dunbar L, Qiao XT, Braunstein K, Braunstein E, Gumucio DL. Cis elements of the villin gene control expression in restricted domains of the vertical (Crypt) and horizontal (Duodenum, cecum) axes of the intestine. *J Biol Chem*. (2002) 277:33275–83. doi: 10.1074/jbc.M204935200

52. Clausen BE, Burkhardt C, Reith W, Renkawitz R, Forster I. Conditional gene targeting in macrophages and granulocytes using lysmcre mice. *Transgenic Res*. (1999) 8:265–77. doi: 10.1023/a:1008942828960

53. Stranges PB, Watson J, Cooper CJ, Choisy-Rossi CM, Stonebraker AC, Beighton RA, et al. Elimination of antigen-presenting cells and autoreactive T cells by fas contributes to prevention of autoimmunity. *Immunity*. (2007) 26:629–41. doi: 10.1016/j.immuni.2007.03.016

54. Barker N, van Es JH, Kuipers J, Kujala P, van den Born M, Cozijnsen M, et al. Identification of stem cells in small intestine and colon by marker gene Lgr5. *Nature*. (2007) 449:1003–7. doi: 10.1038/nature06196

55. Powolny-Budnicka I, Riemann M, Tanzer S, Schmid RM, Hehlgans T, Weih F. Rela and relb transcription factors in distinct thymocyte populations control lymphotoxin-dependent interleukin-17 production in gammadelta T cells. *Immunity*. (2011) 34:364–74. doi: 10.1016/j.immuni.2011.02.019

56. Alimzhanov MB, Kuprash DV, Kosco-Vilbois MH, Luz A, Turetskaya RL, Tarakhovsky A, et al. Abnormal development of secondary lymphoid tissues in lymphotoxin beta-deficient mice. *Proc Natl Acad Sci U.S.A*. (1997) 94:9302–7. doi: 10.1073/pnas.94.17.9302

57. Scheu S, Alferink J, Potzel T, Barchet W, Kalinke U, Pfeffer K. Targeted disruption of light causes defects in costimulatory T cell activation and reveals cooperation with lymphotoxin beta in mesenteric lymph node genesis. *J Exp Med*. (2002) 195:1613–24. doi: 10.1084/jem.20020215

58. Tumanov A, Kuprash D, Lagarkova M, Grivennikov S, Abe K, Shakhov A, et al. Distinct role of surface lymphotoxin expressed by B cells in the organization of secondary lymphoid tissues. *Immunity*. (2002) 17:239–50. doi: 10.1016/S1074-7613(02)00397-7

59. Pian Y, Chai Q, Ren B, Wang Y, Lv M, Qiu J, et al. Type 3 innate lymphoid cells direct goblet cell differentiation via the lt-ltbetar pathway during listeria infection. *J Immunol*. (2020) 205:853–63. doi: 10.4049/jimmunol.2000197

60. de Koning BA, van Dieren JM, Lindenbergh-Kortleve DJ, van der Sluis M, Matsumoto T, Yamaguchi K, et al. Contributions of mucosal immune cells to methotrexate-induced mucositis. *Int Immunol*. (2006) 18:941–9. doi: 10.1093/intimm/dxl030

61. Koelink PJ, Wildenberg ME, Stitt LW, Feagan BG, Koldijk M, van 't Wout AB, et al. Development of reliable, valid and responsive scoring systems for endoscopy and histology in animal models for inflammatory bowel disease. *J Crohns Colitis*. (2018) 12:794–803. doi: 10.1093/ecco-jcc/jjy035

62. Koroleva EP, Halperin S, Gubernatorova EO, Macho-Fernandez E, Spencer CM, Tumanov AV. Citrobacter rodentium-induced colitis: A robust model to study mucosal immune responses in the gut. *J Immunol Methods*. (2015) 421:61–72. doi: 10.1016/j.jim.2015.02.003

63. Mackay F, Browning JL, Lawton P, Shah SA, Comiskey M, Bhan AK, et al. Both the lymphotoxin and tumor necrosis factor pathways are involved in experimental murine models of colitis. *Gastroenterology*. (1998) 115:1464–75. doi: 10.1016/s0016–5085(98)70025–3

64. Gubernatorova EO, Tumanov AV. Tumor necrosis factor and lymphotoxin in regulation of intestinal inflammation. *Biochem (Mosc)*. (2016) 81:1309–25. doi: 10.1134/S0006297916110092

65. Li HL, Lu L, Wang XS, Qin LY, Wang P, Qiu SP, et al. Alteration of gut microbiota and inflammatory cytokine/chemokine profiles in 5-fluorouracil induced intestinal mucositis. *Front Cell Infect Microbiol*. (2017) 7:455. doi: 10.3389/fcimb.2017.00455

66. Badr AM, Alkharashi LA, Sherif IO, Alanteet AA, Alotaibi HN, Mahran YF. Il-17/notch1/stat3 pathway contributes to 5-fluorouracil-induced intestinal mucositis in rats: amelioration by thymol treatment. *Pharm (Basel)*. (2022) 15. doi: 10.3390/ph15111412

67. Metzemaekers M, Vanheule V, Janssens R, Struyf S, Proost P. Overview of the mechanisms that may contribute to the non-redundant activities of interferon-inducible cxc chemokine receptor 3 ligands. *Front Immunol*. (2017) 8:1970. doi: 10.3389/fimmu.2017.01970

68. Sawant KV, Sepuru KM, Lowry E, Penaranda B, Frevert CW, Garofalo RP, et al. Neutrophil recruitment by chemokines Cxcl1/KC and Cxcl2/MIP2: Role of Cxcr2 activation and glycosaminoglycan interactions. *J Leukoc Biol*. (2021) 109:777–91. doi: 10.1002/JLB.3A0820-207R

69. Krause P, Zahner SP, Kim G, Shaikh RB, Steinberg MW, Kronenberg M. The tumor necrosis factor family member TNFSF14 (LIGHT) is required for resolution of intestinal inflammation in mice. *Gastroenterology*. (2014) 146:1752–62.e4. doi: 10.1053/j.gastro.2014.02.010

70. Barker N. Adult intestinal stem cells: critical drivers of epithelial homeostasis and regeneration. *Nat Rev Mol Cell Biol*. (2014) 15:19–33. doi: 10.1038/nrm3721

71. Sato T, Vries RG, Snippert HJ, van de Wetering M, Barker N, Stange DE, et al. Single lgr5 stem cells build crypt-villus structures in vitro without a mesenchymal niche. *Nature*. (2009) 459:262–5. doi: 10.1038/nature07935

72. Haber AL, Biton M, Rogel N, Herbst RH, Shekhar K, Smillie C, et al. A single-cell survey of the small intestinal epithelium. *Nature*. (2017) 551:333–9. doi: 10.1038/nature24489

73. Piao W, Kasinath V, Saxena V, Lakhan R, Iyyathurai J, Bromberg JS. Ltbetar signaling controls lymphatic migration of immune cells. *Cells*. (2021) 10. doi: 10.3390/cells10040747

74. Wullaert A, Bonnet MC, Pasparakis M. Nf-kappab in the regulation of epithelial homeostasis and inflammation. *Cell Res*. (2011) 21:146–58. doi: 10.1038/cr.2010.175

75. Giacomin PR, Moy RH, Noti M, Osborne LC, Siracusa MC, Alenghat T, et al. Epithelial-intrinsic ikkalpha expression regulates group 3 innate lymphoid cell responses and antibacterial immunity. *J Exp Med*. (2015) 212:1513–28. doi: 10.1084/jem.20141831

76. Futterer A, Mink K, Luz A, Kosco-Vilbois MH, Pfeffer K. The lymphotoxin beta receptor controls organogenesis and affinity maturation in peripheral lymphoid tissues. *Immunity*. (1998) 9:59–70. doi: 10.1016/s1074-7613(00)80588-9

77. Browning JL. Inhibition of the lymphotoxin pathway as a therapy for autoimmune disease. *Immunol Rev*. (2008) 223:202–20. doi: 10.1111/j.1600-065X.2008.00633.x

78. Shou Y, Koroleva E, Spencer CM, Shein SA, Korchagina AA, Yusoof KA, et al. Redefining the role of lymphotoxin beta receptor in the maintenance of lymphoid organs and immune cell homeostasis in adulthood. *Front Immunol*. (2021) 12:712632. doi: 10.3389/fimmu.2021.712632

79. Giles DA, Zahner S, Krause P, van der Gracht E, Riffelmacher T, Morris V, et al. The tumor necrosis factor superfamily members TNFSF14 (LIGHT), lymphotoxin beta and lymphotoxin beta receptor interact to regulate intestinal inflammation. *Front Immunol*. (2018) 9:2585. doi: 10.3389/fimmu.2018.02585

80. Guendel F, Kofoed-Branzk M, Gronke K, Tizian C, Witkowski M, Cheng HW, et al. Group 3 innate lymphoid cells program a distinct subset of IL-22BP-producing dendritic cells demarcating solitary intestinal lymphoid tissues. *Immunity*. (2020) 53:1015–32.e8. doi: 10.1016/j.immuni.2020.10.012

81. Cheroutre H, Lambolez F, Mucida D. The light and dark sides of intestinal intraepithelial lymphocytes. *Nat Rev Immunol*. (2011) 11:445–56. doi: 10.1038/nri3007

82. Ma H, Qiu Y, Yang H. Intestinal intraepithelial lymphocytes: maintainers of intestinal immune tolerance and regulators of intestinal immunity. *J Leukoc Biol*. (2021) 109:339–47. doi: 10.1002/JLB.3RU0220–111

83. Kinchen J, Chen HH, Parikh K, Antanaviciute A, Jagielowicz M, Fawkner-Corbett D, et al. Structural remodeling of the human colonic mesenchyme in inflammatory bowel disease. *Cell*. (2018) 175:372–86.e17. doi: 10.1016/j.cell.2018.08.067

84. Wang J, Lo JC, Foster A, Yu P, Chen HM, Wang Y, et al. The regulation of T cell homeostasis and autoimmunity by T cell-derived light. *J Clin Invest*. (2001) 108:1771–80. doi: 10.1172/JCI13827

85. Shaikh RB, Santee S, Granger SW, Butrovich K, Cheung T, Kronenberg M, et al. Constitutive expression of light on T cells leads to lymphocyte activation, inflammation, and tissue destruction. *J Immunol*. (2001) 167:6330–7. doi: 10.4049/jimmunol.167.11.6330

86. Choi SY, Bae H, Jeong SH, Park I, Cho H, Hong SP, et al. YAP/TAZ direct commitment and maturation of lymph node fibroblastic reticular cells. *Nat Commun*. (2020) 11:519. doi: 10.1038/s41467–020-14293–1

87. Cheng HW, Morbe U, Lutge M, Engetschwiler C, Onder L, Novkovic M, et al. Intestinal fibroblastic reticular cell niches control innate lymphoid cell homeostasis and function. *Nat Commun*. (2022) 13:2027. doi: 10.1038/s41467–022-29734–2

88. Liu T, Zhang L, Joo D, Sun SC. Nf-kappab signaling in inflammation. *Signal Transduct Target Ther*. (2017) 2:17023–. doi: 10.1038/sigtrans.2017.23

frontiers | Frontiers in Immunology

TYPE Systematic Review
PUBLISHED 31 May 2024
DOI 10.3389/fimmu.2024.1413466

OPEN ACCESS

EDITED BY
Wai Po Chong,
Hong Kong Baptist University, China

REVIEWED BY
Weiwei Qian,
Sichuan University, China
Jiong Chen,
Ningbo University, China

*CORRESPONDENCE
Xinlian Liu
lxldly@cmc.edu.cn
Lushun Zhang
zhangls2012@cmc.edu.cn

†These authors have contributed equally to this work

RECEIVED 07 April 2024
ACCEPTED 15 May 2024
PUBLISHED 31 May 2024

CITATION
Liu W, Wang Q, Yeerlan J, Yan Y, Xu L, Jia C, Liu X and Zhang L (2024) Global research trends and hotspots for leukocyte cell-derived chemotaxin-2 from the past to 2023: a combined bibliometric review.
Front. Immunol. 15:1413466.
doi: 10.3389/fimmu.2024.1413466

Global research trends and hotspots for leukocyte cell-derived chemotaxin-2 from the past to 2023: a combined bibliometric review

Wei Liu[1†], Qin Wang[2†], Jianishaya Yeerlan[3], Yirui Yan[2], Luke Xu[2], Cui Jia[4], Xinlian Liu[4*] and Lushun Zhang[4*]

[1]Department of Neurology, Nanbu People's Hospital, Nanbu, China, [2]School of Laboratory Medicine, Chengdu Medical College, Chengdu, China, [3]School of Clinical Medicine, Chengdu Medical College, Chengdu, China, [4]Development and Regeneration Key Laboratory of Sichuan Province, Institute of Neuroscience, Department of Pathology and Pathophysiology, Chengdu Medical College, Chengdu, China

Leukocyte cell-derived chemotaxin-2 (LECT2) is an important cytokine synthesized by liver. Significant research interest is stimulated by its crucial involvement in inflammatory response, immune regulation, disease occurrence and development. However, bibliometric study on LECT2 is lacking. In order to comprehend the function and operation of LECT2 in human illnesses, we examined pertinent studies on LECT2 investigation in the Web of Science database, followed by utilizing CiteSpace, VOSview, and Scimago Graphica for assessing the yearly quantity of papers, countries/regions involved, establishments, authors, publications, citations, and key terms. Then we summarized the current research hotspots in this field. Our study found that the literature related to LECT2 has a fluctuating upward trend. "Angiogenesis", "ALECT2", "diagnosis", and "biliary atresia" are the current investigative frontiers. Our findings indicated that liver diseases (e.g. liver fibrosis and hepatic cell carcinoma), systemic inflammatory disease, and amyloidosis are the current research focus of LECT2. The current LECT2 research outcomes are not exceptional. We hope to promote the scientific research of LECT2 and exploit its potential for clinical diagnosis and treatment of related diseases through a comprehensive bibliometric review.

KEYWORDS

LECT2, bibliometrics, CiteSpace, VOSviewer, visualization

1 Introduction

Leukocyte-derived chemokines-2 (LECT2) is a 16 kDa chemokine that mediates neutrophil migration, and it belongs to the interleukin-8 family (1). The LECT2 gene is situated on chromosome 5q31.1-q32 (2). It is highly similar to the sequence of the chondromodulin repeat region of the chicken myb-induced myeloid 1 protein (3). This gene has the Val58Ile polymorphism regarding rheumatoid arthritis. Therefore, it is also called chondromodulin-II (ChM-II or CHM2) (4, 5). Human LECT2 protein contains three internal disulfide connections (Cys25-Cys60; Cys36-Cys41; Cys99-Cys142). Zinc binds to its disulfide bonds to inhibit the self-oligomerization of LECT2 *in vitro*, thereby stabilizing the LECT2 structure (6, 7).

LECT2 primarily produces by hepatocytes, released into the bloodstream (8). It is widely distributed in the liver, kidneys, intestines, skin, and brain (9–15). It is also expressed in many tissues, including muscle cells, endothelial cells, adipocytes, lymph nodes, spleen, bone marrow, and other immune tissues (16–19).

A series of research indicated that the LECT2 protein could play a role in the development and advancement of various conditions. Among immune system diseases like osteoarthritis (20) and rheumatoid arthritis (21), septicemia (22), atherosclerosis, osteoporosis (23), diabetes (18), atopic dermatitis (24), epithelial ovarian cancer (25), and obesity (26), LECT2 can activate and recruit immune cells to regulate inflammatory responses and immune responses (9). LECT2 regulates the bone microenvironment and promotes chondrocyte proliferation (20). New research has uncovered that in the pathogenesis of hepatocellular carcinoma (HCC), LECT2 can improve the tumor microenvironment (27, 28), and prevent vascular invasion and metastasis in HCC (29). Leukocyte chemotactic factor 2 amyloidosis (ALECT2) mainly expressed in the liver or kidney, and the overexpression of LECT2 is one of the important causes of ALECT2 amyloid deposition (30–32). Some researchers have found that LECT2 could promote the development of nerve cells in the brain (33, 34). Regarding obesity and insulin resistance, overexpression of LECT2 reduces insulin receptor substrate (IRS-1) levels (26, 35). The above studies have revealed the potential of LECT2 as a therapeutic target for related diseases. However, demand for more advanced research is critical because more complex mechanisms need to be further elucidated.

Currently, there is no bibliometric research on LECT2. Therefore, we utilize VOSviewer and CiteSpace bibliometric software for visual examination of the LECT2 literature from the Web of Science Core Collection (WoSCC). This method intertwines mathematical statistics, providing a systematic qualitative and quantitative evaluation. One of its benefits is the ability to assess the impact and contributions of various authors, countries, institutions, etc. general information. Additionally, it can illustrate the evolution of the field, identify research trends, and explore cutting-edge topics using the Scientific Knowledge Graph. This paper shows the macro development of LECT2 research, discusses the current research hotspots and frontiers, and provides a reference for follow-up related research.

2 Method

2.1 Search strategy and data collection

In order to guarantee the reliability and availability of the information, we conducted a search in the Web of Science Core Collection (WoSCC) database for articles on LECT2. The search term is " TS= ("LECT2" OR "Leukocyte cell-derived chemotaxin-2" OR "Chondromodulin-II" OR "ChM-II" OR "CHM2")". According to the purpose and content of this study, the disciplines of the Web of Science classified as fisheries, veterinary science, marine freshwater biology, zoology, oceanography, remote sensing, agriculture, dairy, and animal science were excluded. The publication period is limited from January 1, 2010 to December 31, 2023, reasonably. For one thing, the earliest publication relevant to the topic of this review was published in 2010. For another thing, the number of publications published in 2024 is too small to have a profound impact. Since the total number of papers on LECT2 is not large, there is no restriction on the type of publications. To avoid bias caused by the daily update of the database, we collected the search data on January 27, 2024, and obtained a total of 181 articles, including article (n=125), meeting abstract (n=33), review article (n=12), editorial material (n=6), letter (n=3), correction (n=1), retraction (n=1). The record format is all records and references. The data is in plain text, and then imported into CiteSpace. These 181 articles obtain 3928 different references, with 2857 citations, an average of 15.78 times per item, and 30 h-indexes.

2.2 Data analysis

This study used Microsoft Office Excel 2021, VOSviewer (v1.6.20), CiteSpace (v6.2.R7), Origin, Pajek, and Scimago Graphica to analyze 181 collected documents. Figure 1 is a flowchart of the data acquisition and visual analysis of this study. VOSviewer, a Java-based software created in 2009 by Van Eck and Waltman from the Center for Science and Technology Research (CWTS) at Leiden University in the Netherlands, is available for free. It has great features in displaying bibliometric maps, commonly used to build collaborative, co-quoting, and co-occurrence networks (36). The combination of VOSview with Scimago Graphica and Pajek makes images and data more diverse. CiteSpace, a program created by Professor Chaomei Chen from Drexel University in the US, is used for analyzing and visualizing bibliometric data. The advantage of this approach is that it shows the turning point of the scientific revolution through visually prominent nodes and connections to discover research hotspots and frontiers (37). According to the features and advantages of the above

tools, we make use of them to conduct corresponding Scientific Knowledge Graphs.

3 Results

3.1 The annual number of publications and trends

The annual number of publications can reflect the research process and trend in this field to a certain extent. In Figure 2, the increase in publications and citations is depicted. Between 2010 and 2021, there were notable fluctuations in the yearly numbers, with a general upward trend. The highest annual number of publications is 21 in 2020. The most significant increase is from 2013 to 2014, reaching 13 publications, suggesting a major advancement in LECT2 research during that period. The large number of publications in the past two years indicates that this field has attracted people's attention and has a good development trend. It is now garnering increasing interest from scholars.

3.2 Country/region and institutional analysis

There are 32 countries/regions and 237 institutions in total. The rankings, quantities, proportions, citation frequencies, and centralities of the top ten countries in terms of publications are displayed in Table 1. The top three countries/regions for publication are the United States (n = 66), mainland China (38), and Japan (39). The top three countries/regions in centrality are the United States (1.08), Germany (0.25), and mainland China (0.19), indicating that their research results have a greater impact on LECT2 research.

We employed VOSviewer and Scimago Graphica to generate a national geographic visualization atlas (Figure 3A). CiteSpace was used to generated a collaborative network analysis map amongst 32 countries, visualizing publications and partnerships. Labels denote nations with more than two publications (Figure 3B). Node sizes represent the number of publications; link width denotes partnership strength. As evident from Figures 3A, B, the USA leads in transnational cooperation, partnering with 21 nations including Italy, India, Poland, China, and so on. In Europe, Iceland, Netherlands, Switzerland, Portugal have carried out extensive and close cooperation on LECT2-related research.

Using publication volumes as an indicator, each institute's research output on LECT2 research is counted. The top 10 institutions on research of LECT2 are displayed in Table 2. Kanazawa University had the most publications with 19 articles, while the Mayo Clinic and the National Institute of Infectious Diseases followed with 15 and 10 articles respectively. The institutional collaboration map was created filtering institutions publishing less than ten times. As shown in Figure 4, institutional cooperation is relatively close. Mayo Clinic collaborated with 25 organizations such as Mayo Clinic Phoenix and Memorial Sloan Kettering Cancer Center. The National Institute of Health and Medical Research also maintains numerous collaborations with various institutions.

3.3 Analysis of authors partnerships

Table 3 lists the top 10 authors with the most posts. Of these authors, Satoshi Yamagoe has been cited the most. Toshinari Takamura has the highest number of articles with 14, followed by Hirofumi Misu with 13, and Shuichi Kaneko with 11. All of them are from Kanazawa University, and their research on LECT2 is biased toward the association of LECT2 with obesity and insulin resistance. The concept of co-citation is a research method to measure the degree of relationship between documents. Table 3 also displays the top ten authors who have the highest number of co-citations in academic works. The top three co-citations are

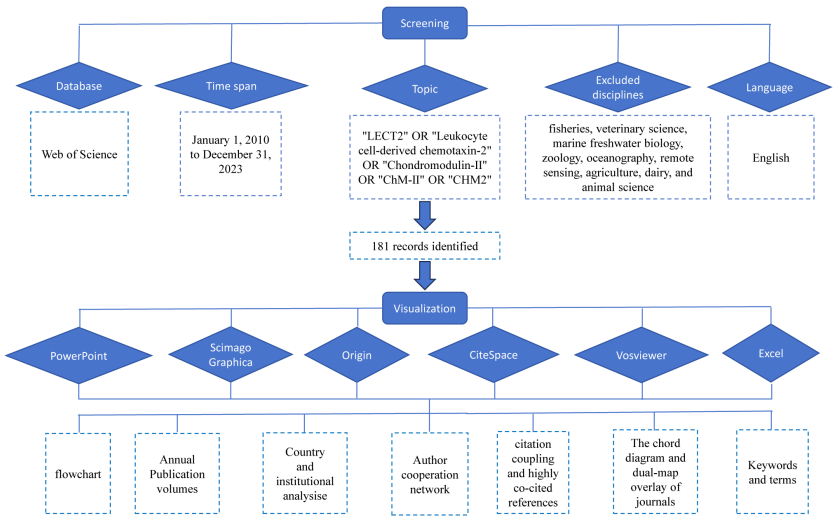

FIGURE 1
The flowchart illustrating the search strategy and selection process.

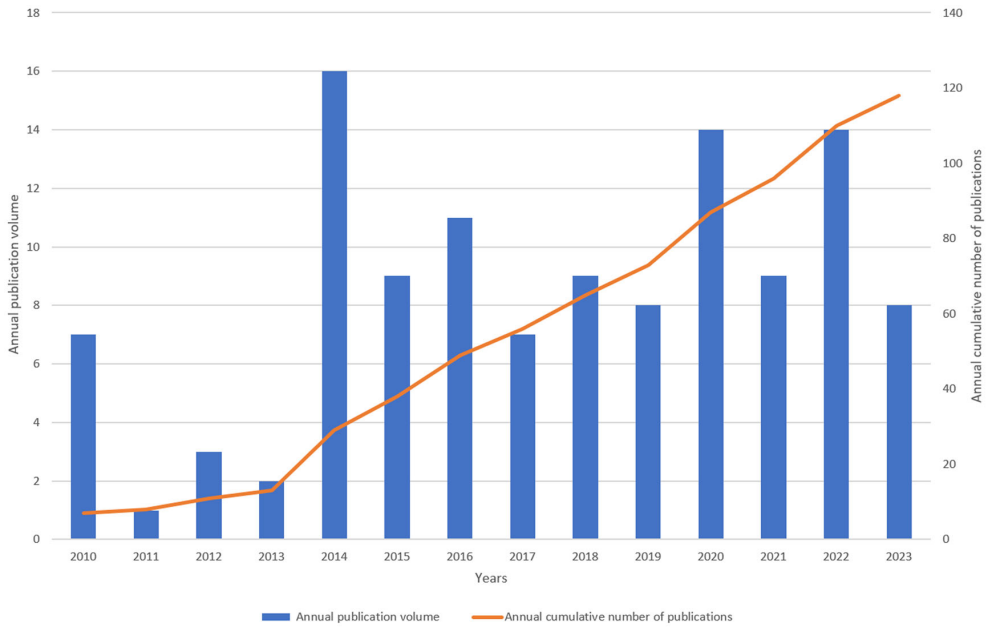

FIGURE 2
Annual output of research of leukocyte cel1-derived chemotaxin-2.

Yamagoe S (159 articles), Larsen CP (78 articles), and Okumura A (74 articles).

A total of 1005 authors were included in the literature data. The author cooperation network generated by CiteSpace was used to show the collaboration of 310 authors. The lines linking the nodes represent the cooperative relationships between authors, and the sizes of the nodes indicate the quantity of articles published on LECT2 by each author. Based on keywords, the authors' collaborative research was divided into 7 clusters, labeled #0- #6, and corresponding to the keywords shown in the color bars in Figure 5. Nodes of the same cluster are filled with the same color. In terms of Sigma, a metric that measures importance, it can be concluded that the top ranked author Aithal, Guruprasad P made a very important contribution to the research in this field. According to the lines in the diagram to analyze the collaboration between the authors, Takamura Toshinari and Shuichi Kaneko were the most active collaborators (Figure 5). Satoshi Yamagoe, Toshinari Takamura, and Shuichi Kaneko collaborated to uncover the therapeutic potential of LECT2 in treating infectious diseases and cancer (40). The cooperation between the authors promotes the breadth and depth of LECT2 research directions.

3.4 Analysis of journals and co-cited journals

A total of 118 journals published articles on LECT2. HEPATOLOGY had the highest number of publications with 17, while *PLOS ONE* came in second with 6. *KIDNEY INTERNATIONAL* ranks first in impact factor among the top 10 journals according to Table 4.

TABLE 1 Top 10 countries on research of LECT2.

Rank	Countries/Regions	Publications	Citations	Centrality
1	USA	66(36.5%)	1343	1.08
2	China Mainland	52(28.7%)	658	0.19
3	Japan	40(22.1%)	692	0.02
4	England	12(6.6%)	161	0.14
5	South Korea	9(5.0%)	204	0.02
6	Taiwan, China	7(3.9%)	96	0
7	Canada	6(3.3%)	81	0
8	France	5(2.8%)	307	0.01
9	Germany	5(2.8%)	167	0.25
10	Mexico	5(2.8%)	15	0

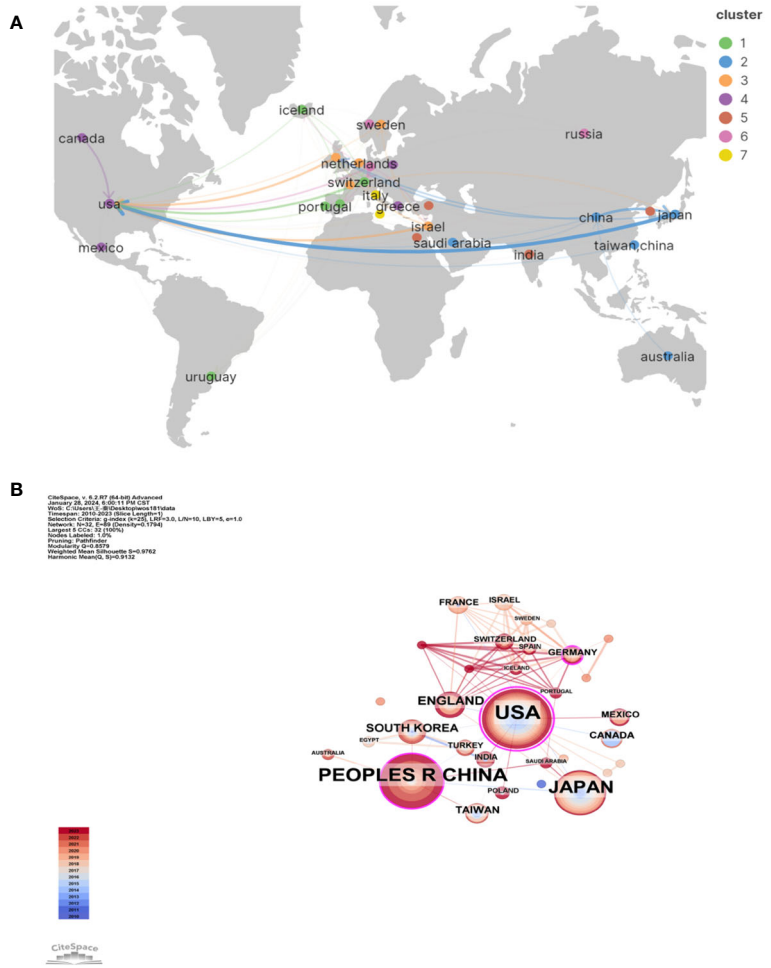

FIGURE 3
The geographical distribution **(A)** and visualization of countries **(B)** on research of leukocyte cell-derived chemotaxin-2.

We employed a chord diagram to illustrate journal citation connections (Figure 6A). Each colorful track signifies a journal, positioned radially. The string thickness visually quantifies the correlation strength. *KIDNEY INTERNATIONAL* boasts an extensive correlation with *AMERICAN JOURNAL OF KIDNEY DISEASES*, and a a relatively strong one with *CLINICAL*

TABLE 2 Top 10 institutions on research of LECT2.

Rank	Institution	Counts	Citations	Centrality
1	Kanazawa University	19(10.5%)	246	0.05
2	Mayo Clinic	15 (8.3%)	426	0.16
3	National Institute of Infectious Diseases (NIID)	10 (5.5%)	380	0.09
4	Zhejiang University	9 (5.0%)	187	0.05
5	Ningbo University	7 (3.9%)	143	0
6	Southern Medical University - China	6 (3.3%)	34	0
7	Institut National de la Sante et de la Recherche Medicale (Inserm)	5(2.8%)	307	0.15
8	Academia Sinica - Taiwan	4(2.2%)	83	0
9	Anhui Medical University	4(2.2%)	116	0
10	Loughborough University	4(2.2%)	90	0

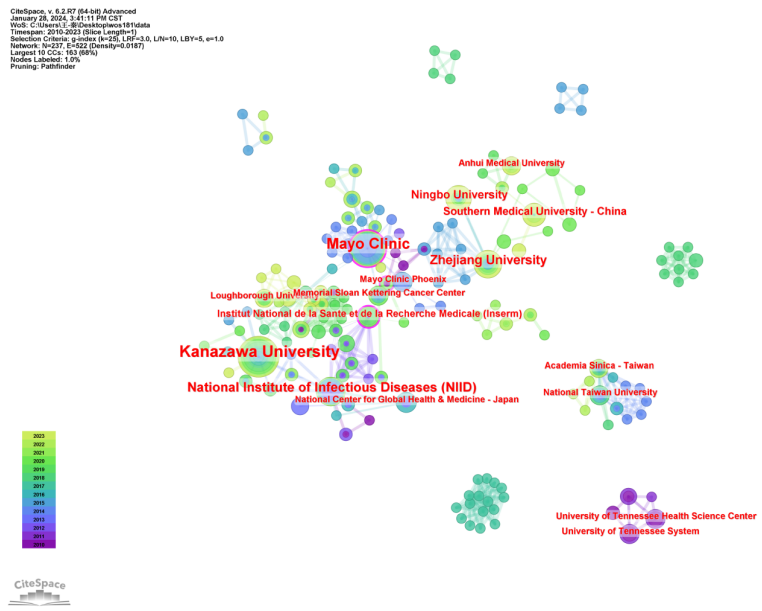

FIGURE 4
The visualization of institutions on research of leukocyte cell-derived chemotaxin-2.

NEPHROLOGY. It can be concluded that the citation connections between journals are highly active.

The dual-map overlay of journals illustrates the citation connections among the leading edge of knowledge and the knowledge base in the macrostructure. There are four macro structural development models: independence, divergence, convergence, and intersection. Understanding them can help researchers screen important references and grasp the historical development path of the topic. In Figure 6B, on the left is the distribution of journals where the original documents are located; on the right is the distribution of journals where the corresponding cited literature is located. The width of the link reflects how often it is referenced. The graph displays the top three significant pathways. The results of the double graph superposition show that hot journals (such as *HEPATOLOGY*) are mainly concentrated in the fields of molecular biology and immunology (see the center of the circle on the left). Hot cited journals are mainly concentrated in the fields of molecular biology, genetics (such as *HEPATOLOGY*, *BLOOD*) and health, nursing, medicine (such as *KIDNEY INT*) (see the center of the circle on the right).

The results also confirmed that the research hotspots of LECT2 have evolved from molecular biology and gene fields to immunology and medicine, medical, clinical respectively, while the research in the fields of health, nursing, and medicine has evolved to medicine, medical, and clinical.

3.5 Analysis of citation coupling and highly co-cited references

Citation coupling is a method to study the internal connection of scientific literature. If both papers cite the same article, then both

TABLE 3 Top 10 authors and co-cited authors on research of LECT2.

Rank	Authors	Documents	Citations	Co-Cited Authors	Citations
1	Toshinari Takamura	14	118	Satoshi Yamagoe	159
2	Hirofumi Misu	13	89	Christopher P Larsen	78
3	Shuichi Kaneko	11	55	Akihisa Okumura	74
4	Satoshi Yamagoe	10	308	Xin-Jiang Lu	66
5	Takayoshi Shirasaki	8	0	Merrill D Benson	65
6	Tetsuro Shimakami	8	0	Fei Lan	55
7	Kazuhisa Murai	8	0	Samar M Said	44
8	Masao Honda	8	0	Chi-Kuan Chen	40
9	Hiroaki Takayama	7	118	Takafumi Saito	39
10	Jiong Chen	7	143	Hwan-Jin Hwang	38

citations will be considered a citation pair. The degree of coupling reflects the degree of similarity to the literature research topic. In finding relevant literature and determining the direction of research, scholars are given better advice. VOSviewer was used to perform citation coupling analysis on the top 20 most cited articles (with a minimum of 33 citations). Nineteen of them form a total of 91 coupling relationships (Figure 7A). Each node represents a document, marked with the name of the first author and the year of publication. The four nodes marked as Nasr (2015), Dogan (2017), Said (2014), and Murphy (2010) are very tightly connected, indicating that the four articles are highly correlated with each other.

When multiple papers are referenced by another paper simultaneously, it forms a co-citation connection. Co-citation analysis is an evolving framework that can assist researchers in comprehending the latest advancements in the field of study. The Supplementary Materials show the top ten co-cites in the literature. The article titled "LECT2, a Ligand for Tie1, Plays a Crucial Role in Liver Fibrogenesis" is the most frequently cited. We use CiteSpace to generate a co-citation network of 413 nodes and 1523 connections, with a density of 0.0179 (Figure 7B). Overall, the co-occurrence relationship between pieces of literature is strong, and multiple nodes act as bridges between subgroups. The 12 purple outer ring nodes are the literatures with high intermediary centrality (Centrality greater than 0.1), which explains the significance. Further analysis of the main content of the literature, there are 5 articles related to liver diseases, 4 articles related to inflammatory immune mechanisms, and 3 articles related to obesity and amyloid lesions.

Through the above two analysis methods, representative documents can be screened by combining the frequencies of citations, the frequencies of co-citations, and the centrality of literature. In the article titled "LECT2 Controls Inflammatory Monocytes to Constrain Growth and Progression of Hepatocellular Carcinoma", the authors analyze how LECT2 influences the progression of HCC and suggest that LECT2 could be a beneficial immunotherapy choice for HCC. Another study revealed that LECT2 acts as a hepatokine connecting obesity with insulin resistance in skeletal muscle. It was discovered that the LECT2 protein hindered insulin signaling by phosphorylating Jun NH2-terminal kinase in C2C12 myocytes.

3.6 Analysis of keywords and burst terms

Keyword cooccurrence analysis reveals research hotspots by analyzing high-frequency keywords and their correlations. Table 5 lists the keywords, centrality, and first appearance for the top 20 cooccurrences. Intermediary centrality analysis reveals the mutation or transformation of research hotspots. CiteSpace was used, resulting in 294 keywords. Larger nodes correspond to more frequent cooccurrences. Purple outer ring node is an important keyword: expression, amino acid sequence, activation, beta-catenin, protein, obesity (Figure 8).

In the timeline (Supplementary Figure 1), each line is a cluster, numbered #0 #1 #2 #3, etc. and a total of 8 clusters are formed. The cluster reflects the temporal characteristics of the research field. The number of keywords in cluster #0 #1 #2 #3 #4 are the largest. The first group of human hepatocellular carcinoma (cluster #0) contains the keywords beta-catenin, gene expression, and diagnosis. etc. This indicates that hepatocellular carcinoma may be related to LECT2. The second group is systemic inflammation (cluster #1). Its keywords are expression, hepatocellular carcinoma, chondromodulin II. This group focused on the association of leukocyte-derived chemotaxin 2 expressions with systemic inflammation or immune regulation. The third group is chemotactic factor (cluster #2). The 4th group (cluster #3) is

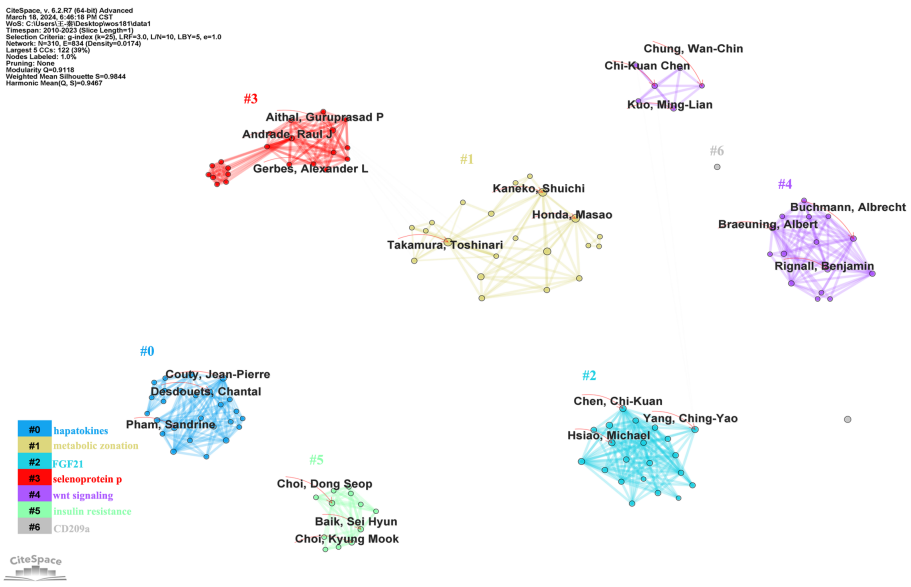

FIGURE 5
The author cooperation network on research of leukocyte cell-derived chemotaxin-2.

TABLE 4 Top 10 journals on research of LECT2.

Rank	Journal	Record Count	IF(2022)	JCR
1	HEPATOLOGY	17	3.6	Q2
2	PLOS ONE	6	3.7	Q2
3	AMYLOID-JOURNAL OF PROTEIN FOLDING DISORDERS	5	5.5	Q2
4	RONTIERS IN IMMUNOLOGY	5	7.3	Q1
5	KIDNEY INTERNATIONAL	5	19.6	Q1
6	AMERICAN JOURNAL OF KIDNEY DISEASES	4	13.2	Q1
7	APPLIED PHYSIOLOGY NUTRITION AND METABOLISM	3	3.4	Q2
8	FRONTIERS IN GENETICS	3	3.7	Q2
9	JOURNAL OF BIOL0GICAL CHEMISTRY	3	4.8	Q2
10	MODERN PATHOLOGY	3	7.5	Q1

JNK-dependent inhibition. The three most cited keywords are obesity, fatty liver disease, risk. This group of studies revealed the chemotactic effect of LECT2 on leukocytes. The 5th group (cluster #4) is selenoprotein p. Its research is linked to insulin resistance and green tea extracts. The keywords in the first five clusters indicate that LECT2 research has achieved more significant results in human hepatocellular carcinoma, systemic inflammation, chemotactic factor, selenoprotein p and JNK-dependent inhibition.

CiteSpace software can extract and detect burst terms to understand the research frontier, changes in research focus, and the latest research hotspot trends, and help predict future trends in the field. As shown in Supplementary Figure 2, 25 emergent words are

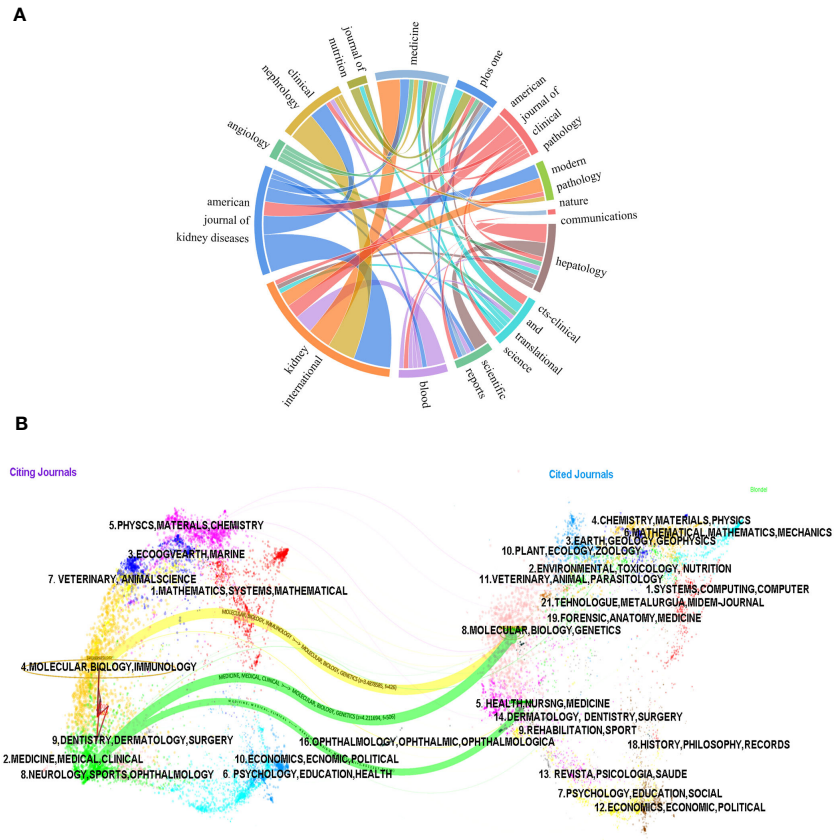

FIGURE 6
The chord diagram **(A)** and the dualmap overlay of journals **(B)** on research of leukocyte cell-derived chemotaxin-2 to illustrate journal citation connections.

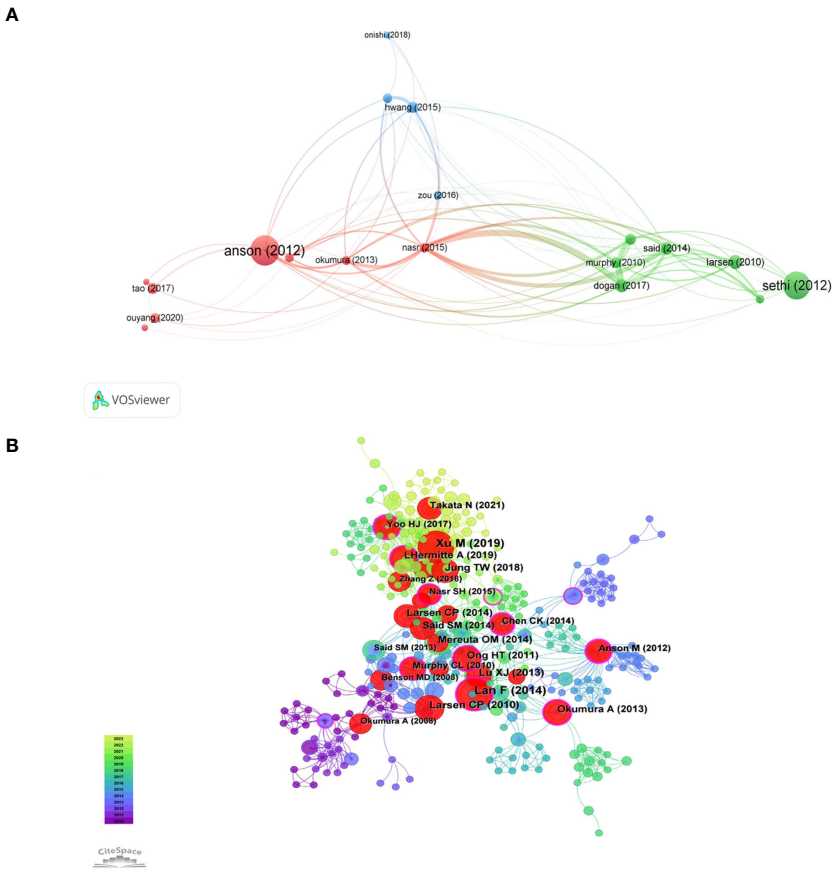

FIGURE 7
The visualization of f citation coupling **(A)** and and highly co-cited references **(B)** on research of leukocyte cell-derived chemotaxin-2.

obtained, showing the year of the initial appearance of the keyword, while Begin and End signify the beginning and conclusion of its relevance as a cutting-edge concept, with Strength denoting its emerging power. The red line indicates the particular period in history when the term gained popularity in academic research. Nodes that have not yet appeared are shown in a light blue color, while nodes that have started to appear are shown in a dark blue color. It is worth noting that insulin resistance (5.5) has the greatest emergent strength, followed by cell-derived chemotaxin 2 (2.7), selenoprotein p (2.67), and risk (2.56). From the time of appearance, diseases, and newly recognized proteins first appeared. Current research on LECT2 is focused on cell-derived chemotaxin 2, angiogenesis, leukocyte chemotactic factor 2 amyloidosis (ALECT2), diagnosis, and biliary atresia (BA), marking an emerging period of study.

4 Discussion

4.1 General information

Our bibliometric research assess the impact and contributions of various countries, institutions, authors, journals. The number of published articles exploded from 2013 to 2014, indicating a surge in interest among scholars. The countries with the most published papers are the United States, China, and Japan, demonstrating their maturity in this area. 118 journals have published research literature related to LECT, with *Hepatology* being the most prolific and *PLOS ONE* closely following. These journal data can be sued as a navigation for scholars aiming to publish in specific journals. Toshinari Takamura, Hirofumi Misu, and Shuichi Kaneko are the top three authors. The most cited author is Satoshi Yamagoe (n = 159) of the National Institute of Infectious Diseases (NIID). He and his research team firstly reported LECT2 protein in 1998, which is mainly produced by hepatocytes (2). Satoshi Yamagoe, Toshinari Takamura, and Shuichi Kaneko discovered that LECT2 interacts with MET (Mesenchymal to epithelial transition factor) to promote RIG-L-mediated innate immune responses. The findings hold promise for therapeutic applications in several infectious diseases and cancers (41).

4.2 Knowledge base

According to the result of co-citation network analysis in the literature, we can roughly determine the research basis of LECT2. In these 10 co-cited papers, the first, eighth, and tenth were on liver fibrosis and liver cancer; the second, sixth, and seventh were on

10.3389/fimmu.2024.1413466

TABLE 5 Top 20 keywords on research of LECT2.

Rank	keywords	Freq	Centrality	Year
1	expression	39	0.33	2010
2	protein	34	0.17	2010
3	beta catenin	15	0.21	2011
4	leukocyte cell-derived chemotaxin 2	14	0.14	2010
5	hepatocellular carcinoma	14	0.08	2013
6	activation	12	0.11	2012
7	amino acid sequence	12	0.17	2010
8	obesity	11	0.13	2015
9	insulin resistance	11	0.07	2017
10	purification	10	0.03	2010
11	diagnosis	10	0.07	2014
12	molecular cloning	9	0.09	2010
13	liver	9	0.04	2010
14	mass spectrometry	9	0.08	2013
15	renal amyloidosis	9	0.04	2015
16	chondromodulin ii	6	0.01	2013
17	disease	6	0.09	2010
18	selenoprotein p	5	0.01	2018
19	fatty liver disease	5	0.04	2010
20	biopsy	5	0.02	2015

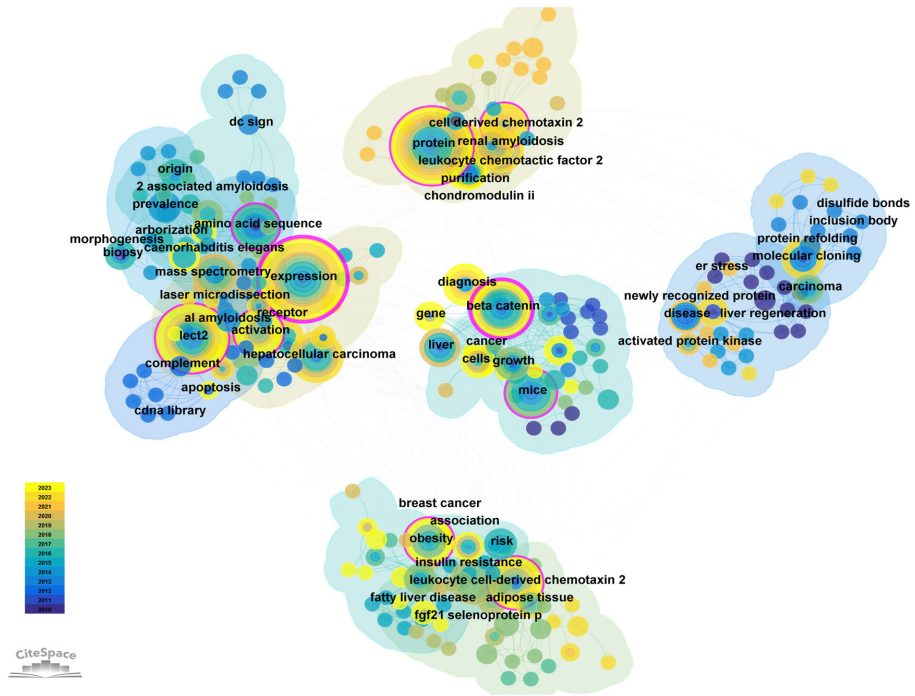

FIGURE 8
The cluster of keywords on research of LECT2.

obesity and insulin resistance; and the third, fifth, and ninth were on amyloidosis. Meng Xu et al. published the most co-cited study in *Cell* in 2019 (42). They found that LECT2 promoted the transformation of Tie1/Tie2 heterodimer to Tie2/Tie2. Tie1 and Tie2, two types of receptor tyrosine kinase (RTKs) on the surface of hepatic sinusoidal endothelial cells, are members of the TIE (Tyrosine kinase with immunoglobulin-like and EGF-like domains 1) receptor family that regulates angiogenesis. Overexpression of LECT2 leads to the deterioration of liver fibrosis by inhibiting portal vein angiogenesis and promoting sinus capillary formation (42). Additionally, Antoine L'Hermitte et al. and H T Ong all discovered the ability of LECT2 to inhibit the migration and growth of liver cancer cells (29, 39). Fei Lan, Okumura A and Tae Woo Jung proposed that LECT2 is a metabolism-related hepatokine, and predicted it as a therapeutic target for insulin resistance, respectively. It exerts a positive influence on Jun NH_2-terminal kinase (JNK) stavation-sensing kinase adenosine monophosphate-activated protein kinase negatively regulates its expression (26). Tae Woo Jung found that LECT2 enhanced inflammation by acting on downstream targets such as P38 and CD209a. It also promotes lipid synthesis by regulating sterol regulatory element-binding protein 1c (SREBP1c) (35). Christopher P Larsen published 2 papers in these 10 total cited papers. He first discovered an amyloid deposit composed of LECT2 (ALECT2). It is considered to be the third form of renal amyloidosis (31, 43). Based on that basis, Oana M Mereuta typed the liver amyloid deposits (44). Their findings lay the foundation for further research into the effects of LECT2 on amyloidosis. Researchers from the Laboratory of Biochemistry and Molecular Biology, Ningbo University found that LECT2 specifically binds to the CD209a receptor and activates macrophages (22).

4.3 Research hotspots and frontiers

Our methodological review focuses on the top 25 terms with the strongest citation bursts to identify the frontiers of LECT2, including Angiogenesis, ALECT2, cell-derived chemotaxin 2, diagnosis, and BA (Biliary Atresia). Angiogenesis affects the pathological stages of liver fibrosis and hepatocarcinogenesis, associated with RA, inflammation (45). Therefore, we can predict the pathway in which LECT2 affects these diseases. ALECT2 is an amyloidosis that occurs frequently in the kidney and liver. It is commonly seen in patients with nephrotic syndrome and azotemia triggered by overexpression of LECT2 (46). Cell-derived chemotaxin 2 is the third research hotspot, indicating that LECT2 mainly plays the biological function of chemotactic centrocytes in immune response. The diagnosis of diseases is also a hot research direction of LECT2, especially for tumors like HCC and breast cancer (13, 40, 47, 48). BA is the fifth research hotspot to study the mechanism of LECT2-induced liver fibrosis in patients with Biliary Atresia (49). We drew a mechanism diagram by Figdraw to illustrate how LECT2 affects the development of related diseases, including HCC, liver fibrogenesis, bacterial sepsis, inflammatory response (Figure 9). According to disease classification and the specific mechanism, the current research hotspots of LECT2 will be elucidated in each of the following sections.

4.3.1 Association of LECT2 with systemic inflammatory disease

Systemic inflammation is one of the research hotspots of LECT2. LECT2 has neutrophil chemotaxis and is involved in inflammatory and immune regulation processes. In general, LECT2 has immune

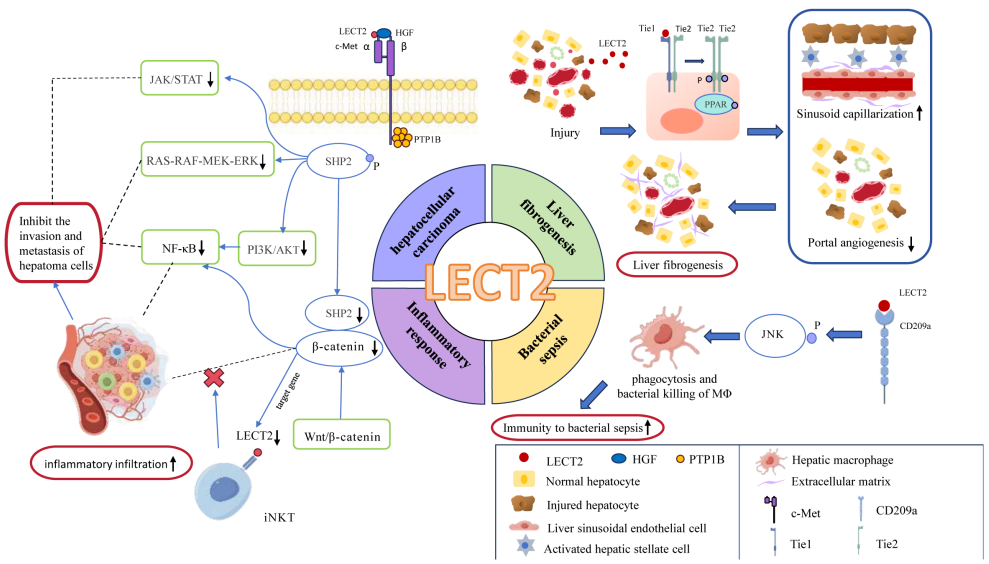

FIGURE 9
the mechanism diagram of LECT2's involvement in the regulation of related diseases, including hepatocellular carcinoma, liver fibrogenesis, bacterial sepsis, inflammatory response. In this figure, blue ovals represent enzymes or proteins; red rounded rectangles represent effects; green rounded rectangles represent the signaling pathways; Tie1, Tie2: as tyrosine kinase receptors, they are subtypes of Tie; PPAR, peroxisome proliferators-activated receptors; JNK, c-Jun N-terminal kinase; c-Met, cellular-mesenchymal epithelial transition factor; HGF, hepatocyte growth factor; PTP1B, Protein Tyrosine Phosphatase-1B; SHP2, Src homology 2 domain-containing protein tyrosine phosphatase.

cell activation, inflammatory mediator regulation, and anti-inflammatory effects (50, 51). Systemic inflammatory diseases related to LECT2 mainly include bacterial sepsis (22), atherosclerosis (52), osteoporosis (23), arthritis (38), and atopic dermatitis (24).

4.3.1.1 Anti-inflammatory effect of LECT2 in bacterial sepsis

LECT2 can chemotaxis immune cells and pathogenic phagocytose microorganisms, but the exact mechanism by which LECT2 exerts its anti-inflammatory effects is unclear. A large number of research results can provide some clues. LECT2 can directly interact with CD209a receptors to boost macrophages' capacity to phagocytose and eliminate bacteria through JNK phosphorylation (53). Then hepatic macrophages exert phagocytosis and bactericidal effects, thereby improving the body's immunity to bacterial sepsis (22). This finding provides a basis for LECT2 as a new targeted therapy for sepsis. Furthermore, LECT2 can also reduce tumor necrosis factor (TNF) expression via CD209a receptor and maintain HSC (hematopoietic stem cells) homeostasis (54). These findings may help in the treatment of various blood diseases.

4.3.1.2 Atherosclerosis

AS is a chronic immune inflammatory disease. The development of this condition involves various factors like dysfunctional endothelial cells, heightened levels of vascular adhesion molecules, elevated production of inflammatory cytokines, and accumulation of cholesterol in the walls of blood vessels. LECT2 may participate in these pathological processes, thus affecting the development of atherosclerotic lesions (52). Fatma Cavide Sonmez et al. proposed that LECT2 could be used as a new marker of AS (55). They found that LECT2 in atherosclerotic areas tended to be overexpressed through aortic wall perforation biopsy and immunohistochemical staining, which was confirmed in later studies (17, 56). Additional research has indicated that increased levels of LECT2 can impede the progression of AS. A genetically modified animal model containing the LECT2 gene is utilized to evaluate metabolic factors associated with the development of AS, including reduced levels of total cholesterol and low-density lipoprotein in the blood; lower levels of inflammatory cytokines and mRNA for monocyte chemoattractant protein-1 (MCP-1), matrix metallopeptidase 1 (MMP-1), tumor necrosis factor-α (TNF-α), interleukin-1β (IL-1β), and interleukin-8 (IL-8); higher quantities of smooth muscle cells and fewer CD68 macrophages, while CD31 endothelial cells remain unchanged (17). In contrast, another study found that the levels of intercellular adhesion molecule-1 and TNF-α, MCP-1, and IL-1β are elevated in LECT2-treated human umbilical vein endothelial cells and Tohoku Hospital Pediatrics-1 (THP-1 cells). These results indicated that LECT2 promotes the inflammatory response in AS. Therefore, the role of LECT2 in AS is controversial and needs to be confirmed by further researches (53).

4.3.1.3 Rheumatoid arthritis, osteoarthritis, and osteoporosis

As a chronic systemic disease, the key pathophysiological process of RA is the progressive destruction of articular cartilage and bone. This process also includes the imbalance of osteoclasts, mesenchymal stem cells, osteoblasts, and endothelial cells within the bone environment, as well as irregular chemotaxis and infiltration of inflammatory cells (20).

The occurrence of RA and osteoarthritis is connected to the G/A polymorphism at nucleotide 172 in exon 3 of the ChM-II gene (21). Research has analyzed the genetic code and X-ray injuries of individuals with RA and discovered that having the 172A gene variant notably raises the risk of developing RA and the severity of joint deterioration (38). In line with this finding, the arthritis severity was notably higher in LECT2-deficient mice compared to the wild-type control group in the collagen antibody-induced arthritis (CAIA model) induced by anti-type II collagen antibody. The distinct signs included damage to cartilage and bone, increased inflammation, and elevated levels of proinflammatory cytokines like IL-1β and IL-6 (57). In subsequent studies, the exogenous expression of LECT2 reduced the RA phenotype of LECT2 (-/-) mice (20).

Collectively, the aforementioned researches suggested that LECT2 acts as a suppressor in regulating RA. The precise molecular mechanism by which LECT2 regulates RA remains unknown. Further laboratory experiments are needed to investigate how LECT2 influences arthritis-related cytokines.

The development of osteoporosis could also be linked to LECT2. Recent research indicated that there was a notable increase in serum LECT2 levels in individuals with osteoporosis, which impacted the severity of osteopenia (23). Certain academics forecast that serum LECT2 could serve as a promising indicator for evaluating the likelihood of bone deterioration (58).

Research on RA, osteoarthritis, and osteoporosis suggests that LECT2 plays a role in controlling bone immune responses, making it crucial for bone health.

4.3.2 Association of LECT2 with liver disease

Numerous studies have demonstrated the involvement of LECT2 in various liver conditions, including hepatitis, acute liver failure (50), liver fibrosis (59), nonalcoholic fatty liver disease (60), cirrhosis, and HCC (29).

4.3.2.1 Liver injury and hepatitis

Previous research has shown that removing LECT2 during concanavalin A (ConA) -induced hepatitis can disturb the balance of Natural killer T cell (NKT cells) in the liver. In LECT2 (-/-) mice, NKT cells are significantly increased. Elevated levels of IL-4, Interferon-gamma (IFN-γ), and cytotoxicity towards syngeneic thymocytes are observed as well (61). Nevertheless, the quantity of traditional T cells, natural killer cells, and various other cell varieties stays constant according to a study (50). Additional research has uncovered how LECT2 controls the progression of hepatitis. LECT2 has the ability to trigger the signaling pathways of TGF-β-activated kinase 1 (TAK1), Mitogen-activated protein (MAP) kinase kinase 4 (MKK4), and JNK, converting remaining liver macrophages into an m1-like state and advancing liver inflammation (62).

Yuan Xie, Ke-Bo Zhong et al. found that the function of LECT2 in the process of acute liver damage and recovery (50). They

simulated liver damage caused by toxins and autoimmune reactions using carbon tetrachloride and concanavalin A (ConA) respectively. The degree of liver injury was evaluated by serum levels of Alanine Transaminase (ALT), Aspartate Aminotransferase (AST), and total bilirubin (Tbil). The results showed that LECT2 mRNA and serum LECT2 increased during the first to second days of exacerbation of liver injury. Compared with WT mice, LECT2-ko mice had less liver injury and less macrophage infiltration. These results confirmed the findings of Rachel J Church et al. (63).

Several research studies have indicated that LECT2 played a part in controlling acute liver damage and healing by managing the entry of various immune cells (64), and it could also serve as a potential biomarker for diagnosing liver injuries in clinical settings (10, 63, 65).

4.3.2.2 Liver fibrogenesis

LECT2 has the effect of promoting liver fibrosis. The use of ICG-001 and LF3 to block β-catenin/TCF4 transcriptional activity resulted in decreased levels of LECT2, pSer 675 β-catenin, and nuclear β-catenin. The results showed that LECT2 was regulated by β-catenin/TCF4 signaling, thereby regulating angiogenesis and participating in liver fibrosis (59). LECT2 can bind to Tie1 and activate peroxisome proliferators-activated receptors (PPAR) signaling to transform Tie1/Tie2 heterodimers into Tie2-Tie2 homodimers, thereby inhibiting endothelial cell invasion and metastasis. Knockdown of the LECT2 gene significantly promotes portal vein angiogenesis and sinusoidal capillary reduction, which alleviates the symptoms of liver fibrosis (42). Moreover, LECT2 is also considered a pivotal gene in BA liver fibrosis to boost fibrosis by triggering fibrous genes such as α-smooth muscle actin and collagen type I alpha 1 Chain (66). The above studies indicated that LECT2 could potentially be used as a biomarker to predict liver fibrogenesis. The use of AAV9-LECT2-shRNA combined with bevacizumab has shown promising outcomes in treating liver fibrosis during the development of new drugs (67).

4.3.2.3 Nonalcoholic fatty liver disease

NAFLD is not a typical systemic inflammatory disease (68). However, inflammation plays a pivotal role in its progression, from hepatic steatosis to nonalcoholic steatohepatitis and cirrhosis (69). LECT2 levels significantly increased in NAFLD (26, 35, 70). Studies have found two ways in which LECT2 promotes liver fat accumulation, including the STAT-1 pathway and transforming residual hepatic macrophages into an m1-like phenotype (71). Hwan-Jin Hwang and Tae Woo Jung have discovered that in the development of hepatic steatosis, adenosine 5'-monophosphate (AMP)-activated protein kinase (AMPK) and JNK mechanisms could play a role in regulating LECT2 expression and inducing liver inflammation (72). Meanwhile, LECT2 can stimulate LPS-triggered MKK4 and TGF-beta activated kinase 1 (MAP3K7) binding protein 2 (TAB2), activating JNK pathway (16). Therefore, LECT2 has the function of promotion on NAFLD progression.

4.3.2.4 Hepatocellular carcinoma

HCC is the first focus of LECT2 research at present. LECT2 affects the evolution of liver cancer by altering the tumor phenotype and tumor microenvironment (73). It effectively suppresses endothelial cell proliferation, migration, and angiogenesis (15, 74).

L'Hermitte A et al. found that the absence of LECT2 leads to an increase in immune infiltrations and promotes the epithelial-mesenchymal transformation of Ctnnb-1 mutant tumor hepatocytes (29). Other research findings indicate that LECT2 expression appears to contradict angiogenesis in HCC patients (39, 75). The growth and spread of HCC depend on angiogenesis (76). So individuals with elevated LECT2 levels tend to experience decreased vascular invasion and prolonged survival in cases of HCC (15). Prior research has revealed how LECT2 hinders the process of angiogenesis. LECT2 directly binds to vascular endothelial growth factor receptor 2 (VEGFR2), resulting in the inhibition of VEGF165-induced tyrosine phosphorylation of VEGFR2 and subsequent extracellular signal-regulated kinase and serine/threonine kinase AKT (also known as protein kinase B or PKB) phosphorylation (77). This provides insights into LECT2's anti-tumor activity.

LECT2 can also directly bind to the MET receptor on liver tumor cells at aa 159–175 of the α chain, preventing the interaction between the tyrosine kinase receptor MET and its ligand hepatocyte growth factor (HGF). Suppressing the downstream pathway of the HGF/MET axis, including phosphoinositide 3-kinase (PI3K)/AKT, RAS-RAF-MEK-ERK, and JAK/STAT, hinders the invasion and metastasis of hepatoma cells (74). Interaction between LECT2 and MET leads to the involvement of protein tyrosine phosphatase-1B (PTP1B) and the separation of adaptor proteins (such as Gab1, Grb2, Src, and PI3K), which inhibits MET dephosphorylation and enhances Src homology-2 domain-containing protein tyrosine phosphatase-2 (SHP2) phosphorylation (78). This shields RIG-I from degradation by SHP2/c-Cbl, enhancing IFN generation, and suppressing the replication of lymphocytic choriomeningitis virus (LCMV) (41), which implies that LECT2's impact on metabolism and tumors arises through affecting MET and PTP1B (79).

Furthermore, MET can regulate LECT2 expression by activating β-catenin in turn (80). In mouse liver, LECT2 is directly targeted by Wnt/β-catenin, triggering LECT2 expression exclusively during β-catenin-dependent hepatocyte proliferation (28). However, LECT2 expression is not up-regulated in some HCC specimens containing β-catenin-activating mutations, indicating that Wnt/β-catenin is not the only pathway that regulates LECT2 expression in liver cancer. LECT2 can also interconnect with iNKT cells, which blocks β-catenin-induced inflammation and influencing liver tumor invasion in turn (51). Other studies have shown that LECT2's tumor inhibition can also be achieved by inhibiting HCC glycolysis (81).

From the above studies, we can conclude that LECT2 may control HCC by three mechanisms: endothelial VEGF receptor signaling, MET signaling, and Wnt/β-catenin pathway. LECT2 may be a promising candidate for cancer therapy.

4.3.3 Association of LECT2 with amyloidosis

ALECT2, a form of renal amyloidosis, is ranked as the third most prevalent type and was initially described by Benson et al.in 2008 (30). LECT2, a subunit protein in amyloid fibrils, has been

identified as a protein capable of inducing systemic amyloidosis in cases of nephrotic syndrome and azotemia (31). This form of amyloidosis is common, accounting for 3 to 10 percent of amyloidosis reported abroad (82). Amyloidogenic LECT2 (ALECT2) forms clumps in various organs such as the lungs, spleen, adrenal glands, small intestine, gallbladder, ovaries, and uterus, but not in the heart or brain (83–86). Frequently diagnosed through clinical observation, chronic kidney failure is commonly accompanied by a mild presence of particles in the urine, with or without protein in the urine. Amyloid deposits in glomeruli, renal vessels, and stroma are common features in individuals suffering from nephrotic syndrome and renal failure (32, 87, 88).

LECT2-derived amyloidosis is ethnicity-related with a high prevalence in Hispanics (44, 89, 90). Excessive production of LECT2 leading to ALECT2 deposition is a prevalent factor in hepatic amyloidosis cases in the United States (44). Improved understanding and identification methods of this form of amyloidosis have led to a small amount of detection of ALECT2-induced amyloidosis in patients from Canadian Aboriginal northern British Columbia, Pakistan, Syria, and China who have chronic kidney disease (91–94). The implementation of laser microdissection and mass spectrometry (LMD/MS) has offered significant assistance in identifying and categorizing amyloidosis (87, 95). Analysis of LECT2 gene sequence in peripheral blood samples can serve as a predictive tool for LECT2 amyloidosis. In cases where all AL and AA markers yield negative results, further diagnostic measures should be taken to determine appropriate therapeutic interventions (96). The principle of non-maleficence should be prioritized, with cautious selection of potentially toxic treatments unless dealing with immunoglobulin light chain amyloidosis (46, 97–99). However, it is worth noting that ALECT2 remains inadequately investigated to date, leaving its pathogenesis still unclear.

4.4 Prospects for future treatments

There are no drugs on the market based on LECT2 as a therapeutic target. In the published study, there is only one drug development project for the LECT2 target by Alnylam Pharmaceuticals, Inc. The drug inhibits the expression of the LECT2 gene through RNA interference to treat amyloidosis. An existing patent provides a novel method for the treatment or prevention of tumors characterized by excessive activity of the Met receptor. Phosphorylation of MET in HCC cells is reduced by administration of agents that can increase the level or biological activity of the active fragment of the LECT2 protein in HCC cells. This method not only inhibits the proliferation, migration and invasiveness of HCC cells, but even includes human lung cancer cells, breast cancer cells, gastric cancer cells, ovarian cancer cells, hypopharyngeal cancer cells, colon cancer cells and glioma cells (100, 101). Gene therapy approaches targeting the LECT2 gene are also being explored. The DNA encoding the human LECT2 protein is transferred to cells for gene therapy by retroviral vectors or non-viral techniques such as receptor-mediated targeted DNA transfer, the use of ligand-DNA conjugates or adenovirus-ligand-DNA conjugates, lipid membrane fusion, or direct microinjection (102). LECT2 plays an important role in inflammation, immune response and tumor development, so it has the potential to be a target for future therapies. But more research is needed to verify its effectiveness and safety.

4.5 Advantages and shortcomings

There are multiple advantages to this research. The study utilized the Web of Science Core Collection Database, a comprehensive academic literature index database that includes reputable journals from multiple disciplines and is updated daily. As a literature search tool, it can ensure the credibility and high quality of bibliometric analysis data. Second, we used three bibliometric tools (Microsoft Office Excel 2021, VOSviewer, and CiteSpace) for visual analysis of bibliometrics. This method can reduce the distortion and bias caused by subjective information filtering. Finally, compared with the traditional review, the visual analysis and review of LECT2-related research in this study can more intuitively and comprehensively show the hot spots and frontiers in this field.

It's worth noting that some limitations do exist in this study. Firstly, publications in non-SCI journals or other databases may not be included in the statistics. In addition, our study solely reflected the citation frequency or publication count to gauge the importance of a paper, which might not fully account for other factors.

5 Conclusion

A thorough bibliometric analysis was carried out in this research, examining the current literature on LECT2, including an assessment of publication dates, countries, organizations, authors, and publications. An in-depth examination of trends, research hotspots, and frontiers was also performed. The analysis results show that the current research has made a breakthrough thanks to the cooperation between countries and institutions, and more scholars have participated in LECT2 research. Research has shown that LECT2 holds significant potential for the treatment of immune diseases, liver fibrosis, liver cancer, amyloidosis, and other illnesses. However, the findings are preliminary and need more exploration for a clearer understanding.

Data availability statement

Publicly available datasets were analyzed in this study. This data can be found here: Web of science.

Author contributions

WL: Writing – original draft, Visualization. QW: Writing – original draft, Visualization. JY: Writing – original draft. YY: Writing – original draft. LX: Writing – original draft. CJ: Writing – review & editing. XL: Writing – review & editing,

Funding acquisition. LZ: Writing – review & editing, Supervision, Project administration, Funding acquisition.

Funding

The author(s) declare financial support was received for the research, authorship, and/or publication of this article. This work was supported by the Sichuan Geriatrics Clinical Medical Research Center (23LHNBZZD05), the National College Student Innovation and Entrepreneurship Training Program Project (202213705036), and Sichuan Provincial College Student Innovation and Entrepreneurship Training Program Project (S202313705089, S202313705066).

Conflict of interest

The authors declare that the research was conducted in the absence of any commercial or financial relationships that could be construed as a potential conflict of interest.

Publisher's note

Supplementary material

The Supplementary Material for this article can be found online at: https://www.frontiersin.org/articles/10.3389/fimmu.2024.1413466/full#supplementary-material

SUPPLEMENTARY FILE 1
Contains a table (Word) of the top 10 references that are frequently cited together in studies on LECT2 research and two images (TIF). One of the images shows the top 25 keywords with the strongest citation bursts. Another image is timeline viewer related to LECT2.

References

1. Yamagoe S, Yamakawa Y, Matsuo Y, Minowada J, Mizuno S, Suzuki K. Purification and primary amino acid sequence of a novel neutrophil chemotactic factor lect2. *Immunol Lett*. (1996) 52:9–13. doi: 10.1016/0165–2478(96)02572–2

2. Yamagoe S, Kameoka Y, Hashimoto K, Mizuno S, Suzuki K. Molecular cloning, structural characterization, and chromosomal mapping of the human lect2 gene. *Genomics*. (1998) 48:324–9. doi: 10.1006/geno.1997.5198

3. Hiraki Y, Inoue H, Kondo J, Kamizono A, Yoshitake Y, Shukunami C, et al. A novel growth-promoting factor derived from fetal bovine cartilage, chondromodulin ii. Purification and amino acid sequence. *J Biol Chem*. (1996) 271:22657–62. doi: 10.1074/jbc.271.37.22657

4. Mori Y, Hiraki Y, Shukunami C, Kakudo S, Shiokawa M, Kagoshima M, et al. Stimulation of osteoblast proliferation by the cartilage-derived growth promoting factors chondromodulin-I and -ii. *FEBS Lett*. (1997) 406:310–4. doi: 10.1016/s0014–5793(97)00291–3

5. Yamagoe S, Watanabe T, Mizuno S, Suzuki K. The mouse lect2 gene: cloning of cdna and genomic DNA, structural characterization and chromosomal localization. *Gene*. (1998) 216:171–8. doi: 10.1016/s0378–1119(98)00294–7

6. Okumura A, Suzuki T, Dohmae N, Okabe T, Hashimoto Y, Nakazato K, et al. Identification and assignment of three disulfide bonds in mammalian leukocyte cell-derived chemotaxin 2 by matrix-assisted laser desorption/ionization time-of-flight mass spectrometry. *Biosci Trends*. (2009) 3:139–43.

7. Okumura A, Suzuki T, Miyatake H, Okabe T, Hashimoto Y, Miyakawa T, et al. Leukocyte cell-derived chemotaxin 2 is a zinc-binding protein. *FEBS Lett*. (2013) 587:404–9. doi: 10.1016/j.febslet.2013.01.025

8. Xie Y, Fan KW, Guan SX, Hu Y, Gao Y, Zhou WJ. Lect2: A pleiotropic and promising hepatokine, from bench to bedside. *J Cell Mol Med*. (2022) 26:3598–607. doi: 10.1111/jcmm.17407

9. Zhu MH, Liu YJ, Li CY, Tao F, Yang GJ, Chen J. The emerging roles of leukocyte cell-derived chemotaxin-2 in immune diseases: from mechanisms to therapeutic potential. *Front Immunol*. (2023) 14:1158083. doi: 10.3389/fimmu.2023.1158083

10. Sato Y, Watanabe H, Kameyama H, Kobayashi T, Yamamoto S, Takeishi T, et al. Serum lect2 level as a prognostic indicator in acute liver failure. *Transplant Proc*. (2004) 36:2359–61. doi: 10.1016/j.transproceed.2004.07.007

11. Ando K, Kato H, Kotani T, Ozaki M, Arimura Y, Yagi J. Plasma leukocyte cell-derived chemotaxin 2 is associated with the severity of systemic inflammation in patients with sepsis. *Microbiol Immunol*. (2012) 56:708–18. doi: 10.1111/j.1348-0421.2012.00488.x

12. Ikeda D, Ageta H, Tsuchida K, Yamada H. Itraq-based proteomics reveals novel biomarkers of osteoarthritis. *J Orthop Surg Res*. (2013) 18:565–72. doi: 10.3109/1354750x.2013.810667

13. Andres SA, Bickett KE, Alatoum MA, Kalbfleisch TS, Brock GN, Wittliff JL. Interaction between smoking history and gene expression levels impacts survival of breast cancer patients. *Breast Cancer Res Treat*. (2015) 152:545–56. doi: 10.1007/s10549-015-3507-z

14. MacDonald BT, Tamai K, He X. Wnt/beta-catenin signaling: components, mechanisms, and diseases. *Dev Cell*. (2009) 17:9–26. doi: 10.1016/j.devcel.2009.06.016

15. Chen CK, Yang CY, Hua KT, Ho MC, Johansson G, Jeng YM, et al. Leukocyte cell-derived chemotaxin 2 antagonizes met receptor activation to suppress hepatocellular carcinoma vascular invasion by protein tyrosine phosphatase 1b recruitment. *Hepatology*. (2014) 59:974–85. doi: 10.1002/hep.26738

16. Takata N, Ishii KA, Takayama H, Nagashimada M, Kamoshita K, Tanaka T, et al. Lect2 as a hepatokine links liver steatosis to inflammation *via* activating tissue macrophages in nash. *Sci Rep*. (2021) 11:555. doi: 10.1038/s41598–020-80689–0

17. He WM, Dai T, Chen J, Wang JA. Leukocyte cell-derived chemotaxin 2 inhibits development of atherosclerosis in mice. *Zool Res*. (2019) 40:317–23. doi: 10.24272/j.issn.2095–8137.2019.030

18. Kim J, Lee SK, Kim D, Lee E, Park CY, Choe H, et al. Adipose tissue lect2 expression is associated with obesity and insulin resistance in korean women. *Obes (Silver Spring)*. (2022) 30:1430–41. doi: 10.1002/oby.23445

19. Berthou F, Sobolewski C, Abegg D, Fournier M, Maeder C, Dolicka D, et al. Hepatic pten signaling regulates systemic metabolic homeostasis through hepatokines-mediated liver-to-peripheral organs crosstalk. *Int J Mol Sci*. (2022) 23(7): 3959. doi: 10.3390/ijms23073959

20. Zhu S, Bennett S, Li Y, Liu M, Xu J. The molecular structure and role of lect2 or chm-ii in arthritis, cancer, and other diseases. *J Cell Physiol*. (2022) 237:480–8. doi: 10.1002/jcp.30593

21. Graessler J, Verlohren M, Graessler A, Zeissig A, Kuhlisch E, Kopprasch S, et al. Association of chondromodulin-ii val58ile polymorphism with radiographic joint destruction in rheumatoid arthritis. *J Rheumatol*. (2005) 32:1654–61. doi: 0315162X-32-1654

22. Lu XJ, Chen J, Yu CH, Shi YH, He YQ, Zhang RC, et al. Lect2 protects mice against bacterial sepsis by activating macrophages *via* the cd209a receptor. *J Exp Med*. (2013) 210:5–13. doi: 10.1084/jem.20121466

23. Wang Q, Xu F, Chen J, Xie YQ, Xu SL, He WM. Serum leukocyte cell-derived chemotaxin 2 (Lect2) level is associated with osteoporosis. *Lab Med*. (2023) 54:106–11. doi: 10.1093/labmed/lmac080

24. Zhao K, Xu F, Jiang X, Chen J, Zhu X, Zhou Q, et al. Serum leukocyte cell-derived chemotaxin 2 level is associated with atopic dermatitis patients. *Ann Palliat Med*. (2021) 10:11006–12. doi: 10.21037/apm-21–2690

25. Wu C-J, Pan K-F, Chen J-Q, Tao YC, Liu Y-C, Chen B-R, et al. Loss of lect2 promotes ovarian cancer progression by inducing cancer invasiveness and facilitating an immunosuppressive environment. *Oncogene*. (2024) 43(7):511-23. doi: 10.1038/s41388-023-02918-w

26. Lan F, Misu H, Chikamoto K, Takayama H, Kikuchi A, Mohri K, et al. Lect2 functions as a hepatokine that links obesity to skeletal muscle insulin resistance. *Diabetes*. (2014) 63:1649–64. doi: 10.2337/db13–0728

27. Gajos-Michniewicz A, Czyz M. Wnt/beta-catenin signaling in hepatocellular carcinoma: the aberrant activation, pathogenic roles, and therapeutic opportunities. *Genes Dis*. (2024) 11:727–46. doi: 10.1016/j.gendis.2023.02.050

28. Ovejero C, Cavard C, Périanin A, Hakvoort T, Vermeulen J, Godard C, et al. Identification of the leukocyte cell-derived chemotaxin 2 as a direct target gene of beta-catenin in the liver. *Hepatology*. (2004) 40:167–76. doi: 10.1002/hep.20286

29. L'Hermitte A, Pham S, Cadoux M, Couchy G, Caruso S, Anson M, et al. Lect2 controls inflammatory monocytes to constrain the growth and progression of hepatocellular carcinoma. *Hepatology*. (2019) 69:160–78. doi: 10.1002/hep.30140

30. Benson MD, James S, Scott K, Liepnieks JJ, Kluve-Beckerman B. Leukocyte chemotactic factor 2: A novel renal amyloid protein. *Kidney Int*. (2008) 74:218–22. doi: 10.1038/ki.2008.152

31. Larsen CP, Walker PD, Weiss DT, Solomon A. Prevalence and morphology of leukocyte chemotactic factor 2-associated amyloid in renal biopsies. *Kidney Int*. (2010) 77:816–9. doi: 10.1038/ki.2010.9

32. Holanda DG, Acharya VK, Dogan A, Racusen LC, Atta MG. Atypical presentation of atypical amyloid. *Nephrol Dial Transplant*. (2011) 26:373–6. doi: 10.1093/ndt/gfq638

33. Koshimizu Y, Ohtomi M. Regulation of neurite extension by expression of lect2 and neurotrophins based on findings in lect2-knockout mice. *Brain Res*. (2010) 1311:1–11. doi: 10.1016/j.brainres.2009.11.010

34. Koshimizu Y, Ohtomi M. Regulation of katanin-P60 levels by lect2 adjusts microtubular morphology. *Neuroreport*. (2010) 21:646–50. doi: 10.1097/WNR.0b013e32833a7d6f

35. Jung TW, Chung YH, Kim HC, Abd El-Aty AM, Jeong JH. Lect2 promotes inflammation and insulin resistance in adipocytes *via* P38 pathways. *J Mol Endocrinol*. (2018) 61:37–45. doi: 10.1530/jme-17–0267

36. van Eck NJ, Waltman L. Software survey: vosviewer, a computer program for bibliometric mapping. *Scientometrics*. (2010) 84:523–38. doi: 10.1007/s11192–009-0146–3

37. Chen C. Searching for intellectual turning points: progressive knowledge domain visualization. *Proc Natl Acad Sci U.S.A*. (2004) 101 Suppl 1:5303–10. doi: 10.1073/pnas.0307513100

38. Kameoka Y, Yamagoe S, Hatano Y, Kasama T, Suzuki K. Val58ile polymorphism of the neutrophil chemoattractant lect2 and rheumatoid arthritis in the Japanese population. *Arthritis Rheum*. (2000) 43:1419–20. doi: 10.1002/1529–0131(200006)43:6<1419::Aid-anr28>3.0.Co;2-i

39. Ong HT, Tan PK, Wang SM, Hian Low DT, Ooi LL, Hui KM. The tumor suppressor function of lect2 in human hepatocellular carcinoma makes it a potential therapeutic target. *Cancer Gene Ther*. (2011) 18:399–406. doi: 10.1038/cgt.2011.5

40. Deacon CF. Dipeptidyl peptidase-4 inhibitors in the treatment of type 2 diabetes: A comparative review. *Diabetes Obes Metab*. (2011) 13:7–18. doi: 10.1111/dom.2011.13.issue-1

41. Shirasaki T, Yamagoe S, Shimakami T, Murai K, Imamura R, Ishii KA, et al. Leukocyte cell-derived chemotaxin 2 is an antiviral regulator acting through the proto-oncogene met. *Nat Commun*. (2022) 13(1):15. doi: 10.1038/s41467–022-30879–3

42. Xu M, Xu HH, Lin Y, Sun X, Wang LJ, Fang ZP, et al. Lect2, a ligand for tie1, plays a crucial role in liver fibrogenesis. *Cell*. (2019) 178:1478–92.e20. doi: 10.1016/j.cell.2019.07.021

43. Larsen CP, Kossmann RJ, Beggs ML, Solomon A, Walker PD. Clinical, morphologic, and genetic features of renal leukocyte chemotactic factor 2 amyloidosis. *Kidney Int*. (2014) 86:378–82. doi: 10.1038/ki.2014.11

44. Mereuta OM, Theis JD, Vrana JA, Law ME, Grogg KL, Dasari S, et al. Leukocyte cell-derived chemotaxin 2 (Lect2)-associated amyloidosis is a frequent cause of hepatic amyloidosis in the United States. *Blood*. (2014) 123:1479–82. doi: 10.1182/blood-2013–07-517938

45. Thomas H. Liver: delineating the role of angiogenesis in liver fibrosis. *Nat Rev Gastroenterol Hepatol*. (2018) 15:6. doi: 10.1038/nrgastro.2017.168

46. Mann BK, Bhandohal JS, Cobos E, Chitturi C, Eppanapally S. Lect-2 amyloidosis: what do we know? *J Investig Med*. (2022) 70:348–53. doi: 10.1136/jim-2021–002149

47. Slowik V, Apte U. Leukocyte cell-derived chemotaxin-2: it's role in pathophysiology and future in clinical medicine. *Clin Transl Sci*. (2017) 10:249–59. doi: 10.1111/cts.12469

48. Okabe H, Delgado E, Lee JM, Yang J, Kinoshita H, Hayashi H, et al. Role of leukocyte cell-derived chemotaxin 2 as a biomarker in hepatocellular carcinoma. *PloS One*. (2014) 9:11. doi: 10.1371/journal.pone.0098817

49. Zhao JF, Xu XD, Gou QY, Zheng QP, Ge L, Chen LZ, et al. Tgf-B1-mediated leukocyte cell-derived chemotaxin 2 is associated with liver fibrosis in biliary atresia. *Front Pediatr*. (2022) 10:901888. doi: 10.3389/fped.2022.901888

50. Xie Y, Zhong KB, Hu Y, Xi YL, Guan SX, Xu M, et al. Liver infiltration of multiple immune cells during the process of acute liver injury and repair. *World J Gastroenterol*. (2022) 28:6537–50. doi: 10.3748/wjg.v28.i46.6537

51. Anson M, Crain-Denoyelle AM, Baud V, Chereau F, Gougelet A, Terris B, et al. Oncogenic B-catenin triggers an inflammatory response that determines the aggressiveness of hepatocellular carcinoma in mice. *J Clin Invest*. (2012) 122:586–99. doi: 10.1172/jci43937

52. Wei M, Liu J, Pan H, Zhou Z, Guo K. Plasma leukocyte cell-derived chemotaxin 2 (Lect2) as a risk factor of coronary artery disease: A cross-sectional study. *Angiology*. (2022) 73:265–74. doi: 10.1177/00033197211028023

53. Hwang HJ, Jung TW, Hong HC, Seo JA, Kim SG, Kim NH, et al. Lect2 induces atherosclerotic inflammatory reaction *via* cd209 receptor-mediated jnk phosphorylation in human endothelial cells. *Metabolism*. (2015) 64:1175–82. doi: 10.1016/j.metabol.2015.06.001

54. Lu XJ, Chen Q, Rong YJ, Yang GJ, Li CH, Xu NY, et al. Lect2 drives haematopoietic stem cell expansion and mobilization *via* regulating the macrophages and osteolineage cells. *Nat Commun*. (2016) 7:13. doi: 10.1038/ncomms12719

55. Sonmez FC, Yildiz P, Akhtar MS, Aydin C, Sonmez O, Ay N, et al. New markers in atherosclerosis: thrombospondin-2 (Thbs-2) and leukocyte cell-derived chemotaxin-2 (Lect-2); an immunohistochemical study. *Med Sci Monit*. (2016) 22:5234–9. doi: 10.12659/msm.898889

56. Yoo HJ, Hwang SY, Choi JH, Lee HJ, Chung HS, Seo JA, et al. Association of leukocyte cell-derived chemotaxin 2 (Lect2) with nafld, metabolic syndrome, and atherosclerosis. *PloS One*. (2017) 12:e0174717. doi: 10.1371/journal.pone.0174717

57. Okumura A, Saito T, Otani I, Kojima K, Yamada Y, Ishida-Okawara A, et al. Suppressive role of leukocyte cell-derived chemotaxin 2 in mouse anti-type ii collagen antibody-induced arthritis. *Arthritis Rheum*. (2008) 58:413–21. doi: 10.1002/art.23215

58. Yeung AWK, Mozos I. The innovative and sustainable use of dental panoramic radiographs for the detection of osteoporosis. *Int J Environ Res Public Health*. (2020) 17(7):2449. doi: 10.3390/ijerph17072449

59. Gao Y, Fan SC, Zhao PF, Li HL, Cai CH, Li X, et al. 13-catenin/tcf4 inhibitors icg-001 and lf3 alleviate bdl-induced liver fibrosis by suppressing lect2 signaling. *Chem Biol Interact*. (2023) 371:10. doi: 10.1016/j.cbi.2023.110350

60. Park CY, Lee SK, Kim J, Kim D, Choe H, Jeong JH, et al. Endoplasmic reticulum stress increases lect2 expression *via* atf4. *Biochem Biophys Res Commun*. (2021) 585:169–76. doi: 10.1016/j.bbrc.2021.11.038

61. Segawa Y, Itokazu Y, Inoue N, Saito T, Suzuki K. Possible Changes in Expression of Chemotaxin Lect2 Mrna in Mouse Liver after Concanavalin a-Induced Hepatic Injury. *Biol Pharm Bull*. (2001) 24:425–8. doi: 10.1248/bpb.24.425

62. Maki K, Katsumi T, Hanatani T, Uchiyama F, Suzuki F, Hoshikawa K, et al. Elucidation of pericholangitis and periductal fibrosis in cholestatic liver diseases *via* extracellular vesicles released by polarized biliary epithelial cells. *Am J Physiol Cell Physiol*. (2024) 326:C1094-C1105. doi: 10.1152/ajpcell.00655.2023

63. Church RJ, Kullak-Ublick GA, Aubrecht J, Bonkovsky HL, Chalasani N, Fontana RJ, et al. Candidate biomarkers for the diagnosis and prognosis of drug-induced liver injury: an international collaborative effort. *Hepatology*. (2019) 69:760–73. doi: 10.1002/hep.29802

64. Dang MH, Kato H, Ueshiba H, Omori-Miyake M, Yamagoe S, Ando K, et al. Possible role of lect2 as an intrinsic regulatory factor in sea-induced toxicity in D-galactosamine-sensitized mice. *Clin Immunol*. (2010) 137:311–21. doi: 10.1016/j.clim.2010.08.002

65. Ravindra KC, Vaidya VS, Wang ZY, Federspiel JD, Virgen-Slane R, Everley RA, et al. Tandem mass tag-based quantitative proteomic profiling identifies candidate serum biomarkers of drug-induced liver injury in humans. *Nat Commun*. (2023) 14(1):1215. doi: 10.1038/s41467–023-36858–6

66. Kong M, Xiang B. Identifying biomarkers to predict the prognosis of biliary atresia by weighted gene co-expression network analysis. *Front Genet*. (2021) 12:760182. doi: 10.3389/fgene.2021.760182

67. Lin Y, Dong MQ, Liu ZM, Xu M, Huang ZH, Liu HJ, et al. A strategy of vascular-targeted therapy for liver fibrosis. *Hepatology*. (2022) 76:660–75. doi: 10.1002/hep.32299

68. Wang XJ, Malhi H. Nonalcoholic fatty liver disease. *Ann Intern Med*. (2018) 169:Itc65–itc80. doi: 10.7326/aitc201811060

69. Paternostro R, Trauner M. Current treatment of non-alcoholic fatty liver disease. *J Intern Med*. (2022) 292:190–204. doi: 10.1111/joim.13531

70. Okumura A, Unoki-Kubota H, Matsushita Y, Shiga T, Moriyoshi Y, Yamagoe S, et al. Increased serum leukocyte cell-derived chemotaxin 2 (Lect2) levels in obesity and fatty liver. *Biosci Trends*. (2013) 7:276–83. doi: 10.5582/bst.2013.v7.6.276

71. Wang J, Chen Y, Pan R, Wu C, Chen S, Li L, et al. Leukocyte cell-derived chemotaxin 2 promotes the development of nonalcoholic fatty liver disease through stat-1 pathway in mice. *Liver Int*. (2021) 41:777–87. doi: 10.1111/liv.14816

72. Hwang HJ, Jung TW, Kim BH, Hong HC, Seo JA, Kim SG, et al. A dipeptidyl peptidase-iv inhibitor improves hepatic steatosis and insulin resistance by ampk-dependent and jnk-dependent inhibition of lect2 expression. *Biochem Pharmacol*. (2015) 98:157–66. doi: 10.1016/j.bcp.2015.08.098

73. Qin J, Sun W, Zhang H, Wu Z, Shen J, Wang W, et al. Prognostic value of lect2 and relevance to immune infiltration in hepatocellular carcinoma. *Front Genet*. (2022) 13:951077. doi: 10.3389/fgene.2022.951077

74. Zhang Y, Xia M, Jin K, Wang S, Wei H, Fan C, et al. Function of the C-met receptor tyrosine kinase in carcinogenesis and associated therapeutic opportunities. *Mol Cancer*. (2018) 17:45. doi: 10.1186/s12943-018-0796-y

75. Chu TH, Ko CY, Tai PH, Chang YC, Huang CC, Wu TY, et al. Leukocyte cell-derived chemotaxin 2 regulates epithelial-mesenchymal transition and cancer stemness in hepatocellular carcinoma. *J Biol Chem*. (2022) 298(10):18. doi: 10.1016/j.jbc.2022.102442

76. Cheng K, Cai N, Zhu J, Yang X, Liang H, Zhang W. Tumor-associated macrophages in liver cancer: from mechanisms to therapy. *Cancer Commun (Lond)*. (2022) 42:1112–40. doi: 10.1002/cac2.12345

77. Chen CK, Yu WH, Cheng TY, Chen MW, Su CY, Yang YC, et al. Inhibition of vegf165/vegfr2-dependent signaling by lect2 suppresses hepatocellular carcinoma angiogenesis. *Sci Rep*. (2016) 6:31398. doi: 10.1038/srep31398

78. Liu R, Mathieu C, Berthelet J, Zhang W, Dupret JM, Rodrigues Lima F. Human protein tyrosine phosphatase 1b (Ptp1b): from structure to clinical inhibitor perspectives. *Int J Mol Sci*. (2022) 23(13):7027. doi: 10.3390/ijms23137027

79. Wiede F, Lu KH, Du X, Zeissig MN, Xu R, Goh PK, et al. Ptp1b is an intracellular checkpoint that limits T-cell and car T-cell antitumor immunity. *Cancer Discovery*. (2022) 12:752–73. doi: 10.1158/2159–8290.Cd-21–0694

80. Purcell R, Childs M, Maibach R, Miles C, Turner C, Zimmermann A, et al. Hgf/C-met related activation of B-catenin in hepatoblastoma. *J Exp Clin Cancer Res*. (2011) 30:96. doi: 10.1186/1756–9966-30–96

81. Lu CY, Fang SJ, Weng QY, Lv XL, Meng MM, Zhu JY, et al. Integrated analysis reveals critical glycolytic regulators in hepatocellular carcinoma. *Cell Commun Signal*. (2020) 18(1):14. doi: 10.1186/s12964–020-00539–4

82. Nasr SH, Dogan A, Larsen CP. Leukocyte cell-derived chemotaxin 2-associated amyloidosis: A recently recognized disease with distinct clinicopathologic characteristics. *Clin J Am Soc Nephrol*. (2015) 10:2084–93. doi: 10.2215/cjn.12551214

83. Mejia-Vilet JM, Cárdenas-Mastrascusa LR, Palacios-Cebreros EJ, Reyes-Macedo M, Portilla-Jiménez A, Morales-Buenrostro LE, et al. Lect2 amyloidosis in kidney transplantation: A report of 5 cases. *Am J Kidney Dis*. (2019) 74:563–6. doi: 10.1053/j.ajkd.2018.10.016

84. Khalighi MA, Yue A, Hwang MT, Wallace WD. Leukocyte chemotactic factor 2 (Lect2) amyloidosis presenting as pulmonary-renal syndrome: A case report and review of the literature. *Clin Kidney J*. (2013) 6:618–21. doi: 10.1093/ckj/sft126

85. Larsen CP, Beggs ML, Wilson JD, Lathrop SL. Prevalence and organ distribution of leukocyte chemotactic factor 2 amyloidosis (Alect2) among decedents in new Mexico. *Amyloid*. (2016) 23:119–23. doi: 10.3109/13506129.2016.1145110

86. Tariq H, Sharkey FE. Leukocyte cell-derived chemotaxin-2 amyloidosis (Alect2) in a patient with lung adenocarcinoma: an autopsy report and literature review. *Int J Surg Pathol*. (2018) 26:271–5. doi: 10.1177/1066896917735893

87. Said SM, Sethi S, Valeri AM, Leung N, Cornell LD, Fidler ME, et al. Renal amyloidosis: origin and clinicopathologic correlations of 474 recent cases. *Clin J Am Soc Nephrol*. (2013) 8:1515–23. doi: 10.2215/cjn.10491012

88. Said SM, Sethi S, Valeri AM, Chang A, Nast CC, Krahl L, et al. Characterization and outcomes of renal leukocyte chemotactic factor 2-associated amyloidosis. *Clin J Am Soc Nephrol*. (2014) 86:370–7. doi: 10.1038/ki.2013.558

89. de la Cruz Jasso MA, Mejía-Vilet JM, Del Toro-Cisneros N, Aguilar-León DE, Morales-Buenrostro LE, Herrera G, et al. Leukocyte chemotactic factor 2 amyloidosis (Alect2) distribution in a Mexican population. *Am J Clin Pathol*. (2023) 159:89–97. doi: 10.1093/ajcp/aqac138

90. Murphy CL, Wang S, Kestler D, Larsen C, Benson D, Weiss DT, et al. Leukocyte chemotactic factor 2 (Lect2)-associated renal amyloidosis: A case series. *Am J Kidney Dis*. (2010) 56:1100–7. doi: 10.1053/j.ajkd.2010.08.013

91. Li DY, Liu D, Wang SX, Yu XJ, Cui Z, Zhou FD, et al. Renal leukocyte chemotactic factor 2 (Alect2)-associated amyloidosis in chinese patients. *Amyloid*. (2020) 27:134–41. doi: 10.1080/13506129.2020.1722097

92. Hutton HL, DeMarco ML, Magil AB, Taylor P. Renal leukocyte chemotactic factor 2 (Lect2) amyloidosis in first nations people in northern British Columbia, Canada: A report of 4 cases. *Am J Kidney Dis*. (2014) 64:790–2. doi: 10.1053/j.ajkd.2014.06.017

93. Law S, Gillmore J, Gilbertson JA, Bass P, Salama AD. Karyomegalic interstitial nephritis with a novel fan1 gene mutation and concurrent alect2 amyloidosis. *BMC Nephrol*. (2020) 21(1):74. doi: 10.1186/s12882–020-01733–9

94. Gibier JB, Gilbertson JA, Perbet R, Leriche W, Truant S, Leteurtre E, et al. Incidental finding of leukocyte cell-derived chemotaxin 2-associated amyloidosis in a liver. *Ann Pathol*. (2020) 40:472–7. doi: 10.1016/j.annpat.2020.04.007

95. Dogan A. Amyloidosis: Insights from Proteomics. *Annu Rev Pathol*. (2017) 12:277-304. doi: 10.1146/annurev-pathol-052016-100200

96. Paueksakon P, Fogo AB, Sethi S. Leukocyte chemotactic factor 2 amyloidosis cannot be reliably diagnosed by immunohistochemical staining. *Hum Pathol*. (2014) 45:1445–50. doi: 10.1016/j.humpath.2014.02.020

97. Nasr SH, Said SM, Valeri AM, Sethi S, Fidler ME, Cornell LD, et al. The diagnosis and characteristics of renal heavy-chain and heavy/light-chain amyloidosis and their comparison with renal light-chain amyloidosis. *Kidney Int*. (2013) 83:463–70. doi: 10.1038/ki.2012.414

98. Chandan VS, Shah SS, Lam-Himlin DM, De Petris G, Mereuta OM, Dogan A, et al. Globular hepatic amyloid is highly sensitive and specific for lect2 amyloidosis. *Am J Surg Pathol*. (2015) 39:558–64. doi: 10.1097/pas.0000000000000373

99. Kowalski A, Cabrera J, Nasr S, Lerma E. Renal lect2 amyloidosis: A newly described disorder gaining greater recognition. *Clin Nephrol*. (2015) 84:236–40. doi: 10.5414/cn108549

100. Kuo ML WY. Methods and compositions related to reduced met phosphorylation by leukocyte cell-derived chemotaxin 2 in tumor cells. (2010). WO 2011076095A1.

101. Yin ZJ, Yan XM, Wang QM, Deng ZL, Tang KL, Cao ZW, et al. Detecting prognosis risk biomarkers for colon cancer through multi-omics-based prognostic analysis and target regulation simulation modeling. *Front Genet*. (2020) 11:16. doi: 10.3389/fgene.2020.00524

102. Dunlop MG. Gene therapy protocols. Totowa, NJ: Humana Press (1997). 339-348 p.

frontiers | Frontiers in Immunology

TYPE Original Research
PUBLISHED 24 June 2024
DOI 10.3389/fimmu.2024.1380889

OPEN ACCESS

EDITED BY
Wai Po Chong,
Hong Kong Baptist University, China

REVIEWED BY
Yi Long,
Sun Yat-sen University, China
Yiyong Tang,
Sun Yat-sen University, China

*CORRESPONDENCE
Miaomiao Dai
dmm772665671@163.com

RECEIVED 02 February 2024
ACCEPTED 10 June 2024
PUBLISHED 24 June 2024

CITATION
Ouyang Y and Dai M (2024) Causal relationships between systemic inflammatory cytokines and adhesive capsulitis: a bidirectional Mendelian randomization study. *Front. Immunol.* 15:1380889. doi: 10.3389/fimmu.2024.1380889

Causal relationships between systemic inflammatory cytokines and adhesive capsulitis: a bidirectional Mendelian randomization study

Yi Ouyang[1] and Miaomiao Dai[2]*

[1]Department of Joint Surgery, Shunde Hospital, Southern Medical University (The First People's Hospital of Shunde, Foshan), Foshan, Guangdong, China, [2]Department of Ophthalmology, Shunde Hospital, Southern Medical University (The First People's Hospital of Shunde, Foshan), Foshan, Guangdong, China

Background: Mounting evidence suggests a connection between inflammatory cytokines and adhesive capsulitis (AC). However, the specific systemic inflammatory cytokines contributing to AC have not been clearly identified. This study employed Mendelian randomization (MR) to explore the causal relationships between 41 inflammatory cytokines and AC.

Methods: In this bidirectional, two-sample MR analysis, genetic variations associated with AC were derived from a comprehensive genome-wide association study (GWAS). The inflammatory cytokines data were sourced from a GWAS summary involving 8,293 healthy participants. The primary MR method employed was inverse variance weighting, supplemented by MR-Egger, weighted median, and MR-pleiotropy residual sum and outlier for sensitivity analysis. Heterogeneity was assessed using Cochran's Q test, and the MR results were validated using the leave-one-out method.

Results: Elevated levels of interferon gamma-induced protein 10 (IP-10) (odds ratio (OR) = 1.086, 95% confidence interval (CI) = 1.002–1.178) and regulated on activation, normal T cell expressed and secreted (RANTES) (OR = 1.107, 95% CI = 1.026–1.195) were linked to an increased risk of AC. Increased levels of stromal cell-derived factor-1 alpha (SDF-1α) (OR = 0.879, 95% CI = 0.793–0.974) and tumor necrosis factor-alpha (TNF-α) (OR = 0.911, 95% CI = 0.831–0.999) were associated with a reduced AC risk. Moreover, genetically predicted AC exhibited associations with elevated cutaneous T cell attracting (CTACK) levels (OR = 1.202, 95% CI = 1.007–1.435) and diminished levels of interleukin-17 (IL-17) (OR = 0.678, 95% CI = 0.518–0.888) and interleukin-5 (IL-5) (OR = 0.786, 95% CI = 0.654–0.944), as confirmed through inverse-variance weighted (IVW) methods.

Conclusion: The present study successfully establishes a causal association between genetically proxied circulating levels of IP-10, RANTES, SDF-1α, and

TNF-α and the risk of AC. Additionally, AC contributes to an increase in CTACK and a decrease in IL-17 and IL-5. This significant finding not only enhances the understanding of the pathogenesis of AC but also holds promise for the development of effective clinical management strategies.

KEYWORDS

systemic inflammatory cytokines, inflammation, adhesive capsulitis, frozen shoulder, Mendelian randomization, causality

1 Introduction

Adhesive capsulitis (AC), commonly referred to as "frozen shoulder," is a prevalent ailment, impacting an estimated 2–5% of the general population (1). The actual incidence may be higher due to the condition being typically mild and self-limited, resulting in numerous cases going unreported and untreated (1). Characterized by a pathological progression involving gradual fibrosis of the glenohumeral joint, AC manifests with constrained active and passive range of motion, joint capsule contracture, and shoulder discomfort (2). Codman's work in 1934 marked a seminal depiction of AC as a painful constriction of shoulder mobility. Subsequently, the subject area was refined by Neviaser in 1945, who delineated AC as a pain-constrained restriction in glenohumeral range of motion (ROM) lacking structural deficits, thereby coining the term "adhesive capsulitis" (3). Primarily afflicting women aged 40 to 60, initial patient complaints regarding AC include pain during extreme ROM, persisting for at least a month, followed by the onset of joint limitation, notably in flexion, abduction (both at average and extreme angles), and external rotation (particularly between 45 and 90 degrees of abduction), significantly impeding daily activities (4). Though AC is conventionally perceived as self-resolving within 1 to 3 years, lingering symptoms persist in 20–50% of patients (5, 6).

The pathophysiological underpinnings of AC remain unclear, with proposed mechanisms encompassing inflammatory changes, fibrosis, and capsular contracture (7). Associations with diabetes mellitus, hypothyroidism, Dupuytren's contracture, and breast cancer treatment underscore its correlation with immune system perturbation and heightened inflammatory response (8). Notably, elevated levels of pro-inflammatory cytokines, including interleukin (IL)-1α, IL-1β, IL-6, IL-8, IL-17, and tumor necrosis factor-alpha (TNF-α), is a feature prominent in individuals with AC that fosters a pro-inflammatory milieu (9–11). Nevertheless, there exists debate regarding whether inflammatory cytokines are causative agents or consequential to disease progression and medication use following AC onset. Observational studies addressing this conundrum may be confounded by unforeseen variables or reverse causation, precluding definitive causal correlations.

Mendelian randomization (MR) is an analytical paradigm for discerning causal relationships between exposure and outcome through genetic variations in non-experimental data (12). Accounting for the random allele assignment during meiosis, MR effectively mitigates conventional confounding variables and reverse causation, thereby bolstering the evidentiary basis for causal inference (13). Leveraging two-sample MR analysis, researchers can scrutinize instrument–exposure and instrument–outcome relationships across distinct population samples, augmenting the versatility and efficacy of the analytical approach (14). This study utilized valid genetic variants from published genome-wide association study (GWAS) summary data encompassing 41 inflammatory cytokines to scrutinize their associations with AC, subsequently probing the direction of causation through the inversion of exposure and outcome variables.

2 Materials and methods

2.1 Study design

The bidirectional MR analysis, depicted in Figure 1, forms the crux of this study's investigative framework. This analytical approach relies on three pivotal assumptions: 1) the instrumental variable (IV), chosen as the genetic variation, must genuinely correlate with the targeted exposure; 2) the selected genetic variation should remain unrelated to any confounding factors; and 3) the genetic variation must solely influence the outcome through the designated exposure (15).

The study utilized two distinct sets of GWAS databases encompassing 41 systemic inflammatory cytokines and AC and unfolds in two phases. Firstly, the causal interplay between inflammatory cytokines and AC was ascertained by employing genetic variations associated with each inflammatory factor. Subsequently, the genetic variations linked to AC were explored to delineate the reciprocal causal relationship with inflammatory cytokines. Notably, the exclusive derivation of all GWAS data from individuals of European ancestry constituted a secondary analysis of previously published data, eliminating the need for additional ethical approvals.

2.2 Data sources

This study utilized the extensive GWAS meta-analysis of circulating concentrations of 41 cytokines, comprising data from

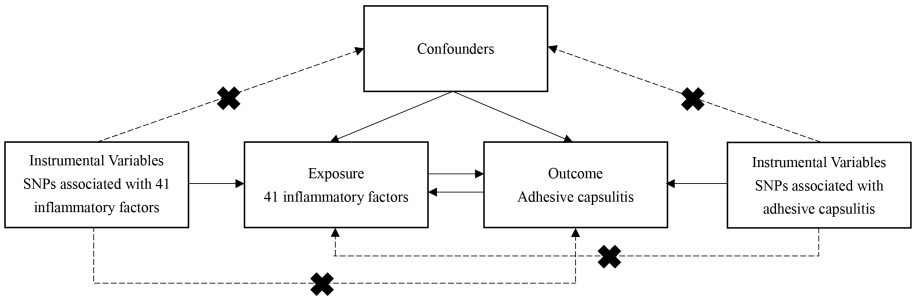

FIGURE 1
Flowchart of the study. The three assumptions of the MR study. Assumption 1: The instrumental variable, chosen as the genetic variation, must genuinely correlate with the targeted exposure. Assumption 2: The selected genetic variation should remain unrelated to any confounding factors. Assumption 3: The genetic variation must solely influence the outcome through the designated exposure.

8,293 Finnish individuals across three independent population cohorts: the Cardiovascular Risk in Young Finns Study, FINRISK1997, and FINRISK2002 (16). AC data, sourced from a combined GWAS analysis of FinnGen and the UK Biobank, integrates information from 10,104 cases identified through inpatient, surgical, and primary care codes, thereby constituting the most comprehensive GWAS data on AC involving individuals of European ancestry (Supplementary Table S1) (17).

2.3 Selection of IVs

To align with the stringent MR assumptions illustrated in Figure 1, the study considered all single nucleotide polymorphisms (SNPs) predicting exposures at genome-wide significance ($P < 5 \times 10^{-8}$) to exhibit strong and independent prediction ($r^2 < 0.001$ within 10 Mb). As only eight systemic inflammatory cytokines had three or more independent SNPs reaching genome-wide significance, the study adopted a less stringent threshold of 5×10^{-6} to enhance SNP availability for inflammatory cytokines. The thresholds were used to select genetic independent variables, as described before (18). Following these steps, a total of 41 distinct types of inflammatory cytokines were identified. SNPs with F-statistics less than 10, indicating weak IVs, were excluded. In adherence to MR principles, target SNPs were screened to eliminate those associated with the results. The effect alleles of the genetic variants were meticulously coordinated in both the exposure and outcome GWAS, Supplementary Tables S2 and S3.

2.4 Data analysis

The inverse-variance weighted (IVW) method was employed as the primary approach to estimate the causal effect of exposure on the outcome, adhering to the fundamental principles of an MR study for precise causal estimation. Additional complementary methods, such as the weighted median (WM) method and MR-Egger regression, were also utilized in diverse scenarios (19). The WM method, which utilizes the median MR estimate as the causal estimate, offers benefits over MR-Egger regression by reducing type I error and enhancing the power of causal estimation. MR-Egger regression incorporates the reciprocal of resultant variances as weights for the analysis and differs from the IVW method by considering the presence of an intercept term in the regression analysis. The intercept in the MR-Egger regression model enables detecting horizontal pleiotropy, whereby a P-value < 0.05 is considered statistically significant (20). Horizontal pleiotropy indicates that genetic IVs independently influence outcomes, which contradicts the definition of IVs. Sensitivity analyses, as presented in Table 1, further ensured the robustness of the findings. The Cochran's Q test, also detailed in Table 1, was employed to assess heterogeneity between SNPs. In instances where heterogeneity was present ($P < 0.05$), certain SNPs with small P-values were omitted, or a random-effects model was directly utilized to evaluate the MR effect. Finally, a leave-one-out analysis, depicted in Supplementary Figures S1-S7, was conducted to assess the stability of the results. The TwoSample package (21) and MR-PRESSO (22) in R (version 4.3.1) were employed for the analysis.

3 Results

The study selected 362 SNPs as IVs for 41 systemic inflammatory regulators, adhering to predefined guidelines to guarantee the suitability of the chosen SNPs. Notably, the F-statistics for each SNP utilized in the analysis surpassed 10, underscoring the robust nature of the IVs. As a result, no weak biases were observed in the outcomes, solidifying the reliability of the conclusions drawn from this study.

The primary outcomes from the principal MR analyses of the 41 cytokines are visually depicted in Figure 2, with detailed findings available in Supplementary Table S2. The genetically predicted systemic inflammatory cytokines exhibited evident associations with AC, as corroborated by the subsequent outcomes. Elevated levels of interferon gamma-induced protein 10 (IP-10) (odds ratio (OR) = 1.086, 95% confidence interval (CI) = 1.002–1.178, $P = 0.045$) and regulated on activation, normal T cell expressed and secreted (RANTES) (OR = 1.107, 95% CI = 1.026–1.195, $P = 0.009$) were linked to an increased risk of AC, as ascertained through the IVW methods (Table 2). The MR-Egger intercept failed to identify potential horizontal pleiotropy (P-value > 0.05).

TABLE 1 Heterogeneity test of the IVW and MR egger analyses and pleiotropy test (egger intercept).

Exposure	Outcome	Methods	Cochran's Q	Q-value	*P*-value (Pleiotropy test)
interferon gamma-induced protein 10 (IP10)	adhesive capsulitis	MR egger	4.386	0.495	0.683
		Inverse variance weighted	4.574	0.600	
regulated on activation, normal T cell expressed and secreted (RANTES)	adhesive capsulitis	MR egger	1.781	0.939	0.474
		Inverse variance weighted	2.363	0.937	
stromal cell-derived factor-1 alpha (SDF1α)	adhesive capsulitis	MR egger	1.775	0.777	0.729
		Inverse variance weighted	1.913	0.861	
tumor necrosis factor-alpha (TNF-α)	adhesive capsulitis	MR egger	1.394	0.498	0.474
		Inverse variance weighted	2.159	0.540	
adhesive capsulitis	Cutaneous T-cell attracting (CTACK)	MR egger	15.014	0.594	0.783
		Inverse variance weighted	15.092	0.656	
adhesive capsulitis	interleukin-17 (IL-17)	MR egger	0.060	0.970	0.338
		Inverse variance weighted	1.617	0.656	
adhesive capsulitis	IL-5	MR egger	13.480	0.704	0.880
		Inverse variance weighted	13.503	0.761	

Additionally, MR-Egger and IVW heterogeneity tests revealed an absence of conspicuous heterogeneity (P-value > 0.05). Sensitivity analyses via leave-one-out investigations revealed negligible influence (Supplementary Figures S1, S2). Notably, the inverse relationship, where higher levels of stromal cell-derived factor-1 alpha (SDF-1α) (OR = 0.879, 95% CI = 0.793–0.974, P = 0.014) and TNF-α (OR = 0.911, 95% CI = 0.831–0.999, P = 0.048) were associated with a reduced AC risk, as determined via IVW methods, with no indications of heterogeneity or horizontal pleiotropy in the results (P-value > 0.05). Comprehensive details are tabulated in Tables 1 and 2 and Supplementary Figures S3 and S4.

This study observed an inherent association between genetically predicted AC and cytokine levels. Significant results from the main MR analyses for AC are depicted in Figure 3, with detailed findings in Supplementary Table S3. Genetically predicted AC has been found to exhibit associations with elevated levels of cutaneous T cell attracting (CTACK) (OR = 1.202, 95% CI = 1.007–1.435, P = 0.042) and diminished levels of IL-17 (OR = 0.678, 95% CI = 0.518–0.888, P = 0.005) and IL-5 (OR = 0.786, 95% CI = 0.654–0.944, P = 0.010), as confirmed through IVW methods. These outcomes exhibit no evidence of pleiotropy or heterogeneity. Comprehensive details are presented in Tables 1 and 2 and Supplementary Figures S5-S7. Diagrammatic representations, including leave-one-out analysis, scatter plot, funnel plot, and forest plot, are available in Supplementary Figures S1-S7.

4 Discussion

The present study is a pioneering and expansive MR inquiry, representing the foremost exploration into the genetic causal interplay between systemic inflammatory cytokines and AC, and vice versa. Previous studies predominantly delved into localized inflammation within the capsule or synovium tissues, neglecting the systemic inflammatory response of the shoulder. Observational studies in clinical settings, often marred by confounding factors and reverse causation bias, inherently lead to distorted causal relationships. This study's findings revealed a positive association between genetically predicted levels of IP-10 and RANTES and the risk of AC, whereas the levels of SDF-1α and TNF-α exhibited a negative association. Additionally, genetic predisposition to AC suggests an increase in CTACK levels and a decrease in IL-17 and IL-5 levels. These robust findings have been validated by sensitivity analyses, underscoring the genetic regulatory nexus between systemic inflammatory cytokines and AC.

Systemic inflammatory cytokines constitute a group of molecules orchestrating diverse roles in inflammation regulation throughout the body. Maintaining equilibrium between pro-inflammatory and anti-inflammatory processes, these regulators ensure effective immune system functioning during infections, injuries, or diseases while preventing excessive tissue damage. Systemic inflammatory cytokines, including cytokines, chemokines, and various growth factors, collectively coordinate

Exposues	nSNPs	OR (95%CI)	pval
Chemokines			
CTACK	11	0.972 (0.898, 1.051)	0.473
Eotaxin	15	1.028 (0.952, 1.112)	0.479
GROα	9	1.063 (0.963, 1.174)	0.223
IP-10	7	1.086 (1.002, 1.178)	0.045
MCP1	14	1.086 (0.984, 1.198)	0.101
MCP3	5	1.024 (0.953, 1.100)	0.522
MIG	11	0.965 (0.887, 1.049)	0.400
MIP1α	3	1.026 (0.904, 1.164)	0.696
MIP1β	17	0.992 (0.916, 1.075)	0.852
RANTES	8	1.107 (1.026, 1.195)	0.009
SDF1α	6	0.879 (0.793, 0.974)	0.014
Growth factors			
βNGF	4	1.021 (0.920, 1.132)	0.700
bFGF	7	0.977 (0.806, 1.185)	0.812
GCSF	8	1.009 (0.913, 1.116)	0.859
HGF	8	0.947 (0.860, 1.042)	0.264
MCSF	11	1.005 (0.958, 1.054)	0.845
PDGFbb	11	0.949 (0.865, 1.041)	0.266
SCF	7	0.956 (0.861, 1.061)	0.397
SCGFβ	19	1.027 (0.973, 1.085)	0.334
VEGF	11	1.010 (0.934, 1.094)	0.796
Interleukins			
IL-10	14	1.007 (0.935, 1.085)	0.856
IL-12p70	13	1.014 (0.933, 1.101)	0.750
IL-13	10	1.031 (0.958, 1.108)	0.416
IL-16	7	0.962 (0.911, 1.015)	0.159
IL-17	6	0.956 (0.862, 1.059)	0.386
IL-18	10	0.987 (0.925, 1.053)	0.688
IL-1β	4	1.015 (0.919, 1.121)	0.773
IL-1ra	5	1.036 (0.937, 1.144)	0.492
IL-2	7	0.984 (0.904, 1.070)	0.707
IL-2ra	7	1.030 (0.963, 1.103)	0.388
IL-4	13	0.974 (0.902, 1.052)	0.497
IL-5	8	0.949 (0.879, 1.024)	0.174
IL-6	9	1.022 (0.920, 1.136)	0.681
IL-7	9	1.012 (0.950, 1.078)	0.712
IL-8	7	1.033 (0.916, 1.165)	0.596
IL-9	4	1.012 (0.915, 1.119)	0.817
Others			
IFN-γ	10	1.010 (0.919, 1.109)	0.839
MIF	7	1.057 (0.977, 1.143)	0.169
TNFα	4	0.911 (0.831, 0.999)	0.048
TNFβ	4	1.048 (0.954, 1.152)	0.327
TRAIL	12	0.996 (0.938, 1.057)	0.888

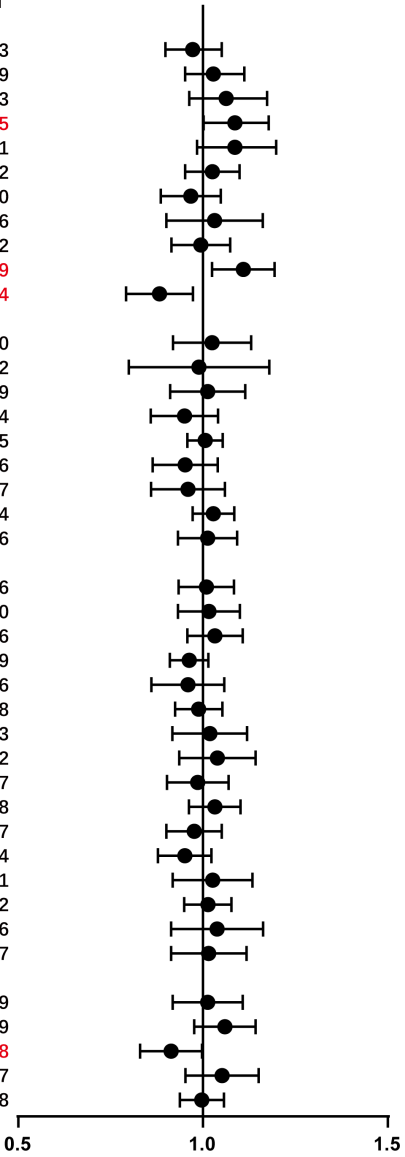

FIGURE 2
Causal correlations of 41 inflammatory cytokines on adhesive capsulitis (AC). The change in the odds ratio (OR) of AC per one standard deviation (SD) rise in the cytokine level is shown by OR and 95% confidence interval. The results from the inverse variance weighted method are shown for all cytokines. bNGF, beta nerve growth factor; CTACK, cutaneous T cell-attracting chemokine; FGFBasic, basic fibroblast growth factor; GCSF, granulocyte colony-stimulating factor; GROa, growth-regulated oncogene-a; HGF, hepatocyte growth factor; IFNg, interferon gamma; IL, interleukin; IP-10, interferon gamma-induced protein 10; MCP1, monocyte chemotactic protein 1; MCP3, monocyte-specific chemokine 3; MCSF, macrophage colony-stimulating factor; MIF, macrophage migration inhibitory factor; MIG, monokine induced by interferon gamma; MIP1a, macrophage inflammatory protein-1a; MIP1b, macrophage inflammatory protein-1b; PDGFbb, platelet-derived growth factor bb; RANTES, regulated upon activation normal T cell expressed and secreted factor; SCF, stem cell factor; SCGFb, stem cell growth factor beta; SDF-1a, stromal cell-derived factor-1 alpha; SNPs, single-nucleotide polymorphisms; TNF-a, tumor necrosis factor alpha; TNF-b, tumor necrosis factor beta; TRAIL, TNF-related apoptosis-inducing ligand; VEGF, vascular endothelial growth factor.

immune response processes (23). AC, an intricate and multifactor disorder linked to inflammatory changes, fibrosis, and capsular contracture, involves systemic inflammatory cytokines in its onset and development.

IP-10, also known as chemokine (C-X-C motif) ligand (CXCL) 10, is a 10 kDa secreted polypeptide categorized within the CXC chemokine family (24). This chemokine can activate integrin and orchestrate directed migration in various cell types, including activated T cells, monocytes, and natural killer cells. As a result, IP-10 plays a pivotal role in regulating inflammation at multiple levels (25). Beyond its fundamental functions, IP-10 exhibits additional pro-inflammatory properties, such as inducing molecules like IL-8 and CXCL-5, as well as the up-regulating costimulatory cell surface molecules (CD54, CD80, CD86, etc.) on monocytes (26). Notably, elevated levels of IP-10 have been observed in knee diseases such as osteoarthritis (OA) and rheumatoid arthritis (RA), suggesting a potential association with the influx of inflammatory cells in synovial tissue (27–29). This

TABLE 2 Bidirectional Mendelian randomization estimates of cytokines and meningiomas (IVW, MR-egger, weighted median, MR-PRESSO).

Exposure	Outcome	Number of SNPs	Methods	OR (95% CI)	*P*-value
interferon gamma-induced protein 10 (IP10)	adhesive capsulitis	7	MR egger	1.058 (0.915, 1.223)	0.482
			Weighted median	1.077 (0.969, 1.198)	0.169
			Inverse variance weighted	1.086 (1.002, 1.178)	0.045
regulated on activation, normal T cell expressed and secreted (RANTES)	adhesive capsulitis	8	MR egger	1.188 (0.976, 1.447)	0.137
			Weighted median	1.154 (1.043, 1.277)	0.006
			Inverse variance weighted	1.107 (1.026, 1.195)	0.009
stromal cell-derived factor-1 alpha (SDF1α)	adhesive capsulitis	6	MR egger	0.858 (0.729, 1.010)	0.139
			Weighted median	0.860 (0.755, 0.979)	0.023
			Inverse variance weighted	0.879 (0.793, 0.974)	0.014
tumor necrosis factor-alpha (TNF-α)	adhesive capsulitis	4	MR egger	0.848 (0.704, 1.021)	0.224
			Weighted median	0.896 (0.802, 1.000)	0.050
			Inverse variance weighted	0.911 (0.831, 0.999)	0.048
adhesive capsulitis	Cutaneous T-cell attracting (CTACK)	19	MR egger	1.298 (0.735, 2.295)	0.381
			Weighted median	1.162 (0.912, 1.480)	0.223
			Inverse variance weighted	1.202 (1.007, 1.435)	0.042
adhesive capsulitis	interleukin-17 (IL-17)	4	MR egger	4.935 (0.216, 112.719)	0.423
			Weighted median	0.719 (0.514, 1.006)	0.054
			Inverse variance weighted	0.678 (0.518, 0.888)	0.005
adhesive capsulitis	IL-5	19	MR egger	0.752 (0.417, 1.356)	0.356
			Weighted median	0.898 (0.699, 1.154)	0.401
			Inverse variance weighted	0.786 (0.654, 0.944)	0.010

raises the intriguing possibility that IP-10 may contribute to the onset of AC, an inflammatory shoulder condition related to synovial tissues. However, despite these possible associations, a paucity of relevant studies persists, highlighting the need for further research to explore this potential relationship comprehensively.

RANTES, a member of the cysteine-cysteine (CC) chemokine family that is also referred to as CC ligand 5 (CCL5), exhibits chemotactic properties on inflammatory cells and various other cell types by activating chemokine receptors (30). Similar to IP-10, the levels of RANTES increase in knee diseases like OA and RA, contributing to a pro-inflammatory milieu in these conditions (29, 31, 32). Notably, Norman et al. investigated the relationship between inflammation biomarkers and musculoskeletal pain, revealing no significant association between RANTES and shoulder pain (33). Despite this, direct studies on the relationship between RANTES and AC are limited, warranting further investigation. Additional research is imperative to delineate the precise role of RANTES in the pathophysiology of AC, exploring its potential as an early predictive indicator, preventive target, and therapeutic focus.

SDF-1, also identified as CXCL12, belongs to the CXC chemokine family (34). The upregulated expression of SDF-1 in OA and RA positions it as a potential therapeutic target for degenerative joint diseases (35). Kim et al. reported an elevation of SDF-1 levels in subacromial bursitis, a component of the pathological process in AC, sharing similar histological features and cell types with AC (36, 37). Contrary to prior studies, this study revealed a negative association between SDF-1α levels and the risk of AC. Interestingly, Wang et al. demonstrated that SDF-1 mitigates the nucleotide-binding oligomerization domain, leucine-rich repeat-containing pyrin domain 3 (NLRP3) inflammasome and pyroptosis in OA synoviocytes by activating the adenosine monophosphate-activated protein kinase (AMPK) signaling pathway, suggesting a potential anti-inflammatory role in OA (38). The intricate role of SDF-1 in joint inflammation necessitates further exploration in the context of AC.

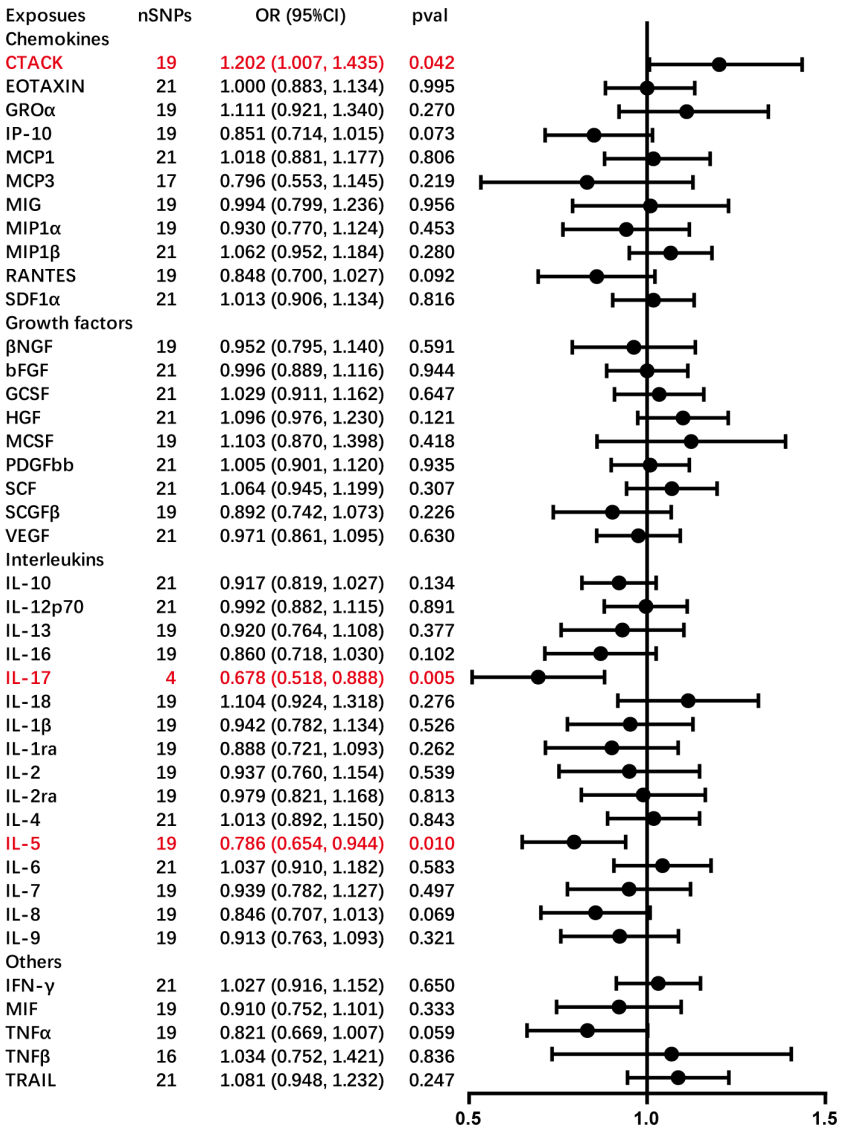

FIGURE 3
Causal correlations of adhesive capsulitis (AC) on 41 inflammatory cytokines. The change in the standard deviation (SD) of inflammatory cytokines per log odds increase in AC is represented by beta and the 95% confidence interval. The results from the inverse variance weighted method are shown for all cytokines. bNGF, beta nerve growth factor; CTACK, cutaneous T cell-attracting chemokine; FGFBasic, basic fibroblast growth factor; GCSF, granulocyte colony-stimulating factor; GROa; growth-regulated oncogene-a; HGF, hepatocyte growth factor; IFNg, interferon gamma; IL, interleukin; IP-10; interferon gamma-induced protein 10; MCP1, monocyte chemotactic protein 1; MCP3, monocyte-specific chemokine 3; MCSF, macrophage colony-stimulating factor; MIF, macrophage migration inhibitory factor; MIG, monokine induced by interferon gamma; MIP1a, macrophage inflammatory protein-1a; MIP1b, macrophage inflammatory protein-1b; PDGFbb, platelet-derived growth factor bb; RANTES, regulated upon activation normal T cell expressed and secreted factor; SCF, stem cell factor; SCGFb, stem cell growth factor beta; SDF-1a, stromal cell-derived factor-1 alpha; SNPs, single-nucleotide polymorphisms; TNF-a, tumor necrosis factor alpha; TNF-b, tumor necrosis factor beta; TRAIL, TNF-related apoptosis-inducing ligand; VEGF, vascular endothelial growth factor.

TNF-α is a well-recognized pro-inflammatory cytokine and plays a major role in the pathogenesis of immune-mediated inflammation of the joint (9). Lho et al. observed significantly elevated levels of TNF-α in the joint capsules and subacromial bursae of patients with AC (9). However, Nishimoto et al. noted higher TNF-α expression only in the subacromial bursa of patients with AC compared to those with shoulder instability, with no significant differences in the rotator interval and axillary recess (39). Bunker et al. reported only a slight elevation in TNF-α messenger ribonucleic acid (mRNA) expression in patients with AC, lacking statistical significance (40). The study by Schydlowsky et al. demonstrated no effect of subcutaneous TNF-α blockade injections on AC symptoms (41). Despite these disparate findings, this study revealed a negative association between TNF-α levels and AC risk, emphasizing the need for further exploration into the precise role of TNF-α in AC.

CTACK, also called CC chemokine ligand 27, is the cutaneous T cell attracting chemokine, consistently expressed by epidermal keratinocytes. This chemokine binds to chemokine receptor 10 on skin-homing T cells, suggesting a pivotal role in T cell-mediated inflammation. Despite its well-established presence in the skin, limited research has explored the implications of CTACK in joint

biology (42). Endres et al. proposed that CTACK expression is elevated in the synovial fluid of patients with RA compared to normal donors. This heightened expression significantly inhibited the migration of progenitors, indicating a potential regulatory role in the inflammatory processes associated with RA (43). Given the shared microenvironment between AC and RA (36), this study revealed an increase in CTACK levels in the context of AC. This novel finding contributes to the ongoing characterization of CTACK's potential role in AC and underscores the need for further investigation to elucidate its specific involvement in joint-related inflammation.

The IL family represents a group of lymphatic factors pivotal in activating and differentiating immune cells, as well as influencing processes such as proliferation, maturation, migration, and adhesion. These cytokines exhibit both pro-inflammatory and anti-inflammatory properties, with their primary role being the modulation of growth, differentiation, and activation during inflammatory and immune responses (44). Earlier studies have reported elevated expressions of IL-1α, IL-1β, IL-6, and IL-8 in patients with AC (9, 10, 45). However, the present study did not establish a causal relationship between these ILs and AC. IL-5, a homodimer cytokine, is involved in eosinophil differentiation, recruitment, maturation, activation, and degranulation. Its involvement in allergic and inflammatory immune responses is established in various diseases such as asthma, atopic dermatitis, chronic obstructive pulmonary disease, and eosinophilic gastrointestinal diseases (46). Although previous studies have reported higher IL-5 expression in OA and RA (47, 48), conflicting reports have indicated its absence in some patients with OA and RA (49, 50). Interestingly, this study identified a lower level of IL-5 associated with AC, emphasizing the need for further exploration into the role of IL-5 in the context of AC.

IL-17, a cytokine known for mediating inflammation, fibrosis, and pain signaling, serves as the signature cytokine of the Th17 T-helper cell population (51–54). Akbar et al. demonstrated that IL-17A exhibited significantly greater expression in AC tissue compared to control (11). However, this study found an association between AC and a lower level of IL-17. The limited literature on the role of IL-17 in AC underscores the necessity for additional studies to comprehensively understand its involvement in this condition.

The present study exhibits several strengths. Firstly, it marks the pioneering application of MR to assess the causal relationship between systemic inflammatory cytokines and AC using the latest summary-level data. Many previous investigations into the association between systemic inflammatory cytokines and AC relied on cross-sectional studies and animal models, limiting the ability to establish causality. This bidirectional MR study successfully circumvented reverse causality and mitigated residual confounding. Secondly, this analysis leveraged summary data from the most extensive GWAS meta-analysis on systemic inflammatory cytokines, combined with phenome-wide association study summary data from FinnGen, ensuring the robustness of the instruments for the MR analysis. MR-PRESSO and MR-Egger tests were employed to detect and address horizontal pleiotropy. Thirdly, from a clinical perspective, the study focused on serum, one of the most accessible and easily obtained biofluids, allowing for straightforward sample collection from both patients with AC and healthy controls. This offers an alternative to the highly invasive procedures required for collecting capsule and synovium samples from patients with AC. Furthermore, this study differs from previous research by examining both upstream and downstream circulating biomarkers, offering insights into prediction or treatment strategies for AC.

Nevertheless, it is crucial to acknowledge certain limitations in this study. Firstly, the genetic data predominantly originated from individuals of European descent, potentially limiting the applicability of the findings to other ethnic groups. Caution should be exercised when generalizing the results to diverse populations. Secondly, despite rigorous efforts to exclude SNPs associated with potential confounders and conducting various sensitivity analyses under different assumptions, there still exists a possibility of complex and multidirectional effects not being fully captured. Lastly, though MR analysis is a robust method for estimating causality, it should not replace randomized controlled trials (RCTs). Therefore, the causality inferred from this study may not necessarily align with the results observed in RCTs. It is imperative to conduct individual-based genetic observations and potentially incorporate RCTs in future research to further validate the causal relationships identified here.

5 Conclusion

The present study successfully establishes a causal association between genetically proxied circulating levels of IP-10, RANTES, SDF-1α, and TNF-α and the risk of AC. Additionally, AC was found to increase the levels of CTACK and decrease the levels of IL-17 and IL-5. This significant finding not only enhances the understanding of the pathogenesis of AC but also holds promise for developing effective clinical management strategies. Consequently, IP-10, RANTES, SDF-1α, and TNF-α emerge as potential therapeutic targets for the prevention and treatment of AC.

Data availability statement

The original contributions presented in the study are included in the article/Supplementary Material. Further inquiries can be directed to the corresponding author.

Author contributions

YO: Writing – original draft, Visualization, Validation, Software, Methodology, Investigation, Formal analysis, Data curation, Conceptualization. MD: Writing – review & editing, Supervision, Resources, Project administration.

Funding

The author(s) declare that no financial support was received for the research, authorship, and/or publication of this article.

Acknowledgments

We express our profound gratitude to all the contributors who generously shared the data used in this study. We extend our deepest appreciation to the participants and investigators of the FinnGen study, the systemic inflammatory cytokines study, and the GWAS data. We thank Bullet Edits Limited for the linguistic editing and proofreading of the manuscript.

Conflict of interest

The authors declare that the research was conducted in the absence of any commercial or financial relationships that could be construed as a potential conflict of interest.

Publisher's note

Supplementary material

The Supplementary Material for this article can be found online at: https://www.frontiersin.org/articles/10.3389/fimmu.2024.1380889/full#supplementary-material

References

1. Leafblad N, Mizels J, Tashjian R, Chalmers P. Adhesive capsulitis. *Phys Med Rehabil Clin N Am*. (2023) 34:453–68. doi: 10.1016/j.pmr.2022.12.009

2. Hsu JE, Anakwenze OA, Warrender WJ, Abboud JA. Current review of adhesive capsulitis. *J Shoulder Elbow Surg*. (2011) 20:502–14. doi: 10.1016/j.jse.2010.08.023

3. Al Khayyat SG, Falsetti P, Conticini E, Frediani B, Galletti S, Stella SM. Adhesive capsulitis and ultrasound diagnosis, an inseparable pair: a novel review. *J Ultrasound*. (2023) 26:369–84. doi: 10.1007/s40477–022-00725–9

4. de Sire A, Agostini F, Bernetti A, Mangone M, Ruggiero M, Dinatale S, et al. Non-surgical and rehabilitative interventions in patients with frozen shoulder: umbrella review of systematic reviews. *J Pain Res*. (2022) 15:2449–64. doi: 10.2147/jpr.S371513

5. Hand C, Clipsham K, Rees JL, Carr AJ. Long-term outcome of frozen shoulder. *J Shoulder Elbow Surg*. (2008) 17:231–6. doi: 10.1016/j.jse.2007.05.009

6. Binder AI, Bulgen DY, Hazleman BL, Roberts S. Frozen shoulder: a long-term prospective study. *Ann Rheum Dis*. (1984) 43:361–4. doi: 10.1136/ard.43.3.361

7. Koh KH. Corticosteroid injection for adhesive capsulitis in primary care: a systematic review of randomised clinical trials. *Singapore Med J*. (2016) 57:646–57. doi: 10.11622/smedj.2016146

8. Alghamdi A, Alyami AH, Althaqafi RMM, Alzeyadi A, Alrubaei FS, Alyami AA, et al. Cytokines' Role in the pathogenesis and their targeting for the prevention of frozen shoulder: A narrative review. *Cureus*. (2023) 15:e36070. doi: 10.7759/cureus.36070

9. Lho YM, Ha E, Cho CH, Song KS, Min BW, Bae KC, et al. Inflammatory cytokines are overexpressed in the subacromial bursa of frozen shoulder. *J Shoulder Elbow Surg*. (2013) 22:666–72. doi: 10.1016/j.jse.2012.06.014

10. Akbar M, McLean M, Garcia-Melchor E, Crowe LA, McMillan P, Fazzi UG, et al. Fibroblast activation and inflammation in frozen shoulder. *PloS One*. (2019) 14: e0215301. doi: 10.1371/journal.pone.0215301

11. Akbar M, Crowe LAN, McLean M, Garcia-Melchor E, MacDonald L, Carter K, et al. Translational targeting of inflammation and fibrosis in frozen shoulder: Molecular dissection of the T cell/IL-17A axis. *Proc Natl Acad Sci United States America*. (2021) 118:e2102715118. doi: 10.1073/pnas.2102715118

12. Xiang M, Wang Y, Gao Z, Wang J, Chen Q, Sun Z, et al. Exploring causal correlations between inflammatory cytokines and systemic lupus erythematosus: A Mendelian randomization. *Front Immunol*. (2022) 13:985729. doi: 10.3389/fimmu.2022.985729

13. Burgess S, Scott RA, Timpson NJ, Davey Smith G, Thompson SG. Using published data in Mendelian randomization: a blueprint for efficient identification of causal risk factors. *Eur J Epidemiol*. (2015) 30:543–52. doi: 10.1007/s10654-015-0011-z

14. Hartwig FP, Davies NM, Hemani G, Davey Smith G. Two-sample Mendelian randomization: avoiding the downsides of a powerful, widely applicable but potentially fallible technique. *Int J Epidemiol*. (2016) 45:1717–26. doi: 10.1093/ije/dyx028

15. Lawlor DA, Harbord RM, Sterne JA, Timpson N, Davey Smith G. Mendelian randomization: using genes as instruments for making causal inferences in epidemiology. *Stat Med*. (2008) 27:1133–63. doi: 10.1002/sim.3034

16. Ahola-Olli AV, Würtz P, Havulinna AS, Aalto K, Pitkänen N, Lehtimäki T, et al. Genome-wide association study identifies 27 loci influencing concentrations of circulating cytokines and growth factors. *Am J Hum Genet*. (2017) 100:40–50. doi: 10.1016/j.ajhg.2016.11.007

17. Green HD, Jones A, Evans JP, Wood AR, Beaumont RN, Tyrrell J, et al. A genome-wide association study identifies 5 loci associated with frozen shoulder and implicates diabetes as a causal risk factor. *PloS Genet*. (2021) 17:e1009577. doi: 10.1371/journal.pgen.1009577

18. Zhang Z, Wang S, Ren F, Yang L, Xie H, Pan L, et al. Inflammatory factors and risk of meningiomas: a bidirectional mendelian-randomization study. *Front Neurosci*. (2023) 17:1186312. doi: 10.3389/fnins.2023.1186312

19. Bowden J, Davey Smith G, Haycock PC, Burgess S. Consistent estimation in mendelian randomization with some invalid instruments using a weighted median estimator. *Genet Epidemiol*. (2016) 40:304–14. doi: 10.1002/gepi.21965

20. Burgess S, Thompson SG. Avoiding bias from weak instruments in Mendelian randomization studies. *Int J Epidemiol*. (2011) 40:755–64. doi: 10.1093/ije/dyr036

21. Hemani G, Zheng J, Elsworth B, Wade KH, Haberland V, Baird D, et al. The MR-Base platform supports systematic causal inference across the human phenome. *eLife*. (2018) 7:e34408. doi: 10.7554/eLife.34408

22. Verbanck M, Chen CY, Neale B, Do R. Detection of widespread horizontal pleiotropy in causal relationships inferred from Mendelian randomization between complex traits and diseases. *Nat Genet*. (2018) 50:693–8. doi: 10.1038/s41588–018-0099–7

23. Wang J, Zhao X, Luo R, Xia D, Liu Y, Shen T, et al. The causal association between systemic inflammatory regulators and primary ovarian insufficiency: a bidirectional mendelian randomization study. *J Ovarian Res*. (2023) 16:191. doi: 10.1186/s13048–023-01272–5

24. Lei J, Yin X, Shang H, Jiang Y. IP-10 is highly involved in HIV infection. *Cytokine*. (2019) 115:97–103. doi: 10.1016/j.cyto.2018.11.018

25. Lee EY, Lee ZH, Song YW. CXCL10 and autoimmune diseases. *Autoimmun Rev*. (2009) 8:379–83. doi: 10.1016/j.autrev.2008.12.002

26. Ragusa F, Fallahi P. IP-10 in occupational asthma: review of the literature and case-control study. *Clin Ter*. (2017) 168:e151–7. doi: 10.7417/CT.2017.1998

27. Alonso B, Bravo B, Mediavilla L, Gortazar AR, Forriol F, Vaquero J, et al. Osteoarthritis-related biomarkers profile in chronic anterior cruciate ligament injured knee. *Knee*. (2020) 27:51–60. doi: 10.1016/j.knee.2019.12.007

28. Maloley PM, England BR, Sayles HR, Thiele GM, Duryee MJ, Hunter CD, et al. Performance of a commercially available multiplex platform in the assessment of circulating cytokines and chemokines in patients with rheumatoid arthritis and osteoarthritis. *J Immunol Methods*. (2021) 495:113048. doi: 10.1016/j.jim.2021.113048

29. Beekhuizen M, Gierman LM, van Spil WE, Van Osch GJ, Huizinga TW, Saris DB, et al. An explorative study comparing levels of soluble mediators in control and osteoarthritic synovial fluid. *Osteoarthritis Cartilage*. (2013) 21:918–22. doi: 10.1016/j.joca.2013.04.002

30. Wen D, Du X, Qiao Y, Dong JZ, Ma CS. RANTES gene polymorphisms are not associated with rheumatoid arthritis and atopic dermatitis: a meta-analysis. *Int Rev Immunol*. (2015) 34:500–8. doi: 10.3109/08830185.2014.994815

31. Hampel U, Sesselmann S, Iserovich P, Sel S, Paulsen F, Sack R. Chemokine and cytokine levels in osteoarthritis and rheumatoid arthritis synovial fluid. *J Immunol Methods*. (2013) 396:134–9. doi: 10.1016/j.jim.2013.08.007

32. Toncheva A, Remichkova M, Ikonomova K, Dimitrova P, Ivanovska N. Inflammatory response in patients with active and inactive osteoarthritis. *Rheumatol Int*. (2009) 29:1197–203. doi: 10.1007/s00296–009-0864–0

33. Norman KS, Goode AP, Alvarez C, Hu D, George SZ, Schwartz TA, et al. Association of biomarkers with individual and multiple body sites of pain: the

johnston county osteoarthritis project. *J Pain Res*. (2022) 15:2393–404. doi: 10.2147/JPR.S365187

34. Li J, Chen H, Zhang D, Xie J, Zhou X. The role of stromal cell-derived factor 1 on cartilage development and disease. *Osteoarthritis Cartilage*. (2021) 29:313–22. doi: 10.1016/j.joca.2020.10.010

35. Bragg R, Gilbert W, Elmansi AM, Isales CM, Hamrick MW, Hill WD, et al. Stromal cell-derived factor-1 as a potential therapeutic target for osteoarthritis and rheumatoid arthritis. *Ther Adv Chronic Dis*. (2019) 10:2040622319882531. doi: 10.1177/2040622319882531

36. Kim YS, Bigliani LU, Fujisawa M, Murakami K, Chang SS, Lee HJ, et al. Stromal cell-derived factor 1 (SDF-1, CXCL12) is increased in subacromial bursitis and downregulated by steroid and nonsteroidal anti-inflammatory agents. *J Orthop Res*. (2006) 24:1756–64. doi: 10.1002/jor.20197

37. Nobuhara K, Sugiyama D, Ikeda H, Makiura M. Contracture of the shoulder. *Clin Orthopaedics Related Res*. (1990) 254):105–10. doi: 10.1097/00003086-199005000-00016

38. Wang S, Mobasheri A, Zhang Y, Wang Y, Dai T, Zhang Z. Exogenous stromal cell-derived factor-1 (SDF-1) suppresses the NLRP3 inflammasome and inhibits pyroptosis in synoviocytes from osteoarthritic joints via activation of the AMPK signaling pathway. *Inflammopharmacology*. (2021) 29:695–704. doi: 10.1007/s10787-021-00814-x

39. Nishimoto H, Fukuta S, Fukui N, Sairyo K, Yamaguchi T. Characteristics of gene expression in frozen shoulder. *BMC Musculoskelet Disord*. (2022) 23:811. doi: 10.1186/s12891–022-05762–3

40. Bunker TD, Reilly J, Baird KS, Hamblen DL. Expression of growth factors, cytokines and matrix metalloproteinases in frozen shoulder. *J Bone Joint Surg Br*. (2000) 82:768–73. doi: 10.1302/0301–620x.82b5.9888

41. Schydlowsky P, Szkudlarek M, Madsen OR. Treatment of frozen shoulder with subcutaneous TNF-alpha blockade compared with local glucocorticoid injection: a randomised pilot study. *Clin Rheumatol*. (2012) 31:1247–51. doi: 10.1007/s10067–012-1993–5

42. Rump L, Mattey DL, Kehoe O, Middleton J. An initial investigation into endothelial CC chemokine expression in the human rheumatoid synovium. *Cytokine*. (2017) 97:133–40. doi: 10.1016/j.cyto.2017.05.023

43. Endres M, Andreas K, Kalwitz G, Freymann U, Neumann K, Ringe J, et al. Chemokine profile of synovial fluid from normal, osteoarthritis and rheumatoid arthritis patients: CCL25, CXCL10 and XCL1 recruit human subchondral mesenchymal progenitor cells. *Osteoarthritis Cartilage*. (2010) 18:1458–66. doi: 10.1016/j.joca.2010.08.003

44. Ye L, Gao L, Cheng H. Inflammatory profiles of the interleukin family and network in cerebral hemorrhage. *Cell Mol Neurobiol*. (2018) 38:1321–33. doi: 10.1007/s10571-018-0601-x

45. Kabbabe B, Ramkumar S, Richardson M. Cytogenetic analysis of the pathology of frozen shoulder. *Int J Shoulder Surgery*. (2010) 4:75–8. doi: 10.4103/0973–6042.76966

46. Narendra DK, Hanania NA. Targeting IL-5 in COPD. *Int J Chron Obstruct Pulmon Dis*. (2019) 14:1045–51. doi: 10.2147/copd.S155306

47. Bahlas S, Damiati L, Dandachi N, Sait H, Alsefri M, Pushparaj PN. Rapid immunoprofiling of cytokines, chemokines and growth factors in patients with active rheumatoid arthritis using Luminex Multiple Analyte Profiling technology for precision medicine. *Clin Exp Rheumatol*. (2019) 37:112–9.

48. Barker T, Rogers VE, Henriksen VT, Aguirre D, Trawick RH, Rasmussen GL, et al. Serum cytokines are increased and circulating micronutrients are not altered in subjects with early compared to advanced knee osteoarthritis. *Cytokine*. (2014) 68:133–6. doi: 10.1016/j.cyto.2014.04.004

49. Wagner S, Fritz P, Einsele H, Sell S, Saal JG. Evaluation of synovial cytokine patterns in rheumatoid arthritis and osteoarthritis by quantitative reverse transcription polymerase chain reaction. *Rheumatol Int*. (1997) 16:191–6. doi: 10.1007/bf01330295

50. Sakkas LI, Scanzello C, Johanson N, Burkholder J, Mitra A, Salgame P, et al. T cells and T-cell cytokine transcripts in the synovial membrane in patients with osteoarthritis. *Clin Diagn Lab Immunol*. (1998) 5:430–7. doi: 10.1128/cdli.5.4.430–437.1998

51. Fang S, Huang Y, Wang S, Zhang Y, Luo X, Liu L, et al. IL-17A exacerbates fibrosis by promoting the proinflammatory and profibrotic function of orbital fibroblasts in TAO. *J Clin Endocrinol Metab*. (2016) 101:2955–65. doi: 10.1210/jc.2016–1882

52. Tan Z, Qian X, Jiang R, Liu Q, Wang Y, Chen C, et al. IL-17A plays a critical role in the pathogenesis of liver fibrosis through hepatic stellate cell activation. *J Immunol (Baltimore Md: 1950)*. (2013) 191:1835–44. doi: 10.4049/jimmunol.1203013

53. Sun C, Zhang J, Chen L, Liu T, Xu G, Li C, et al. IL-17 contributed to the neuropathic pain following peripheral nerve injury by promoting astrocyte proliferation and secretion of proinflammatory cytokines. *Mol Med Rep*. (2017) 15:89–96. doi: 10.3892/mmr.2016.6018

54. Kolls JK, Lindén A. Interleukin-17 family members and inflammation. *Immunity*. (2004) 21:467–76. doi: 10.1016/j.immuni.2004.08.018

frontiers | Frontiers in Immunology

TYPE Review
PUBLISHED 28 June 2024
DOI 10.3389/fimmu.2024.1391355

OPEN ACCESS

EDITED BY
Wai Po Chong,
Hong Kong Baptist University,
Hong Kong SAR, China

REVIEWED BY
Paco Herson,
The Ohio State University, United States
Pengyu Zong,
UCONN Health, United States

*CORRESPONDENCE
Jiexiu Zhao
zhaojiexiu@ciss.cn

RECEIVED 25 February 2024
ACCEPTED 17 June 2024
PUBLISHED 28 June 2024

CITATION
Huang P, Qu C, Rao Z, Wu D and Zhao J (2024) Bidirectional regulation mechanism of TRPM2 channel: role in oxidative stress, inflammation and ischemia-reperfusion injury. *Front. Immunol.* 15:1391355. doi: 10.3389/fimmu.2024.1391355

Bidirectional regulation mechanism of TRPM2 channel: role in oxidative stress, inflammation and ischemia-reperfusion injury

Peng Huang[1,2], Chaoyi Qu[3], Zhijian Rao[2,4], Dongzhe Wu[2,5] and Jiexiu Zhao[1,2*]

[1]School of Kinesiology, Shanghai University of Sport, Shanghai, China, [2]Exercise Biological Center, China Institute of Sport Science, Beijing, China, [3]Physical Education College, Hebei Normal University, Shijiazhuang, China, [4]College of Physical Education, Shanghai Normal University, Shanghai, China, [5]Department of Exercise Physiology, Beijing Sport University, Beijing, China

Transient receptor potential melastatin 2 (TRPM2) is a non-selective cation channel that exhibits Ca^{2+} permeability. The TRPM2 channel is expressed in various tissues and cells and can be activated by multiple factors, including endogenous ligands, Ca^{2+}, reactive oxygen species (ROS) and temperature. This article reviews the multiple roles of the TRPM2 channel in physiological and pathological processes, particularly on oxidative stress, inflammation and ischemia–reperfusion (I/R) injury. In oxidative stress, the excessive influx of Ca^{2+} caused by the activation of the TRPM2 channel may exacerbate cellular damage. However, under specific conditions, activating the TRPM2 channel can have a protective effect on cells. In inflammation, the activation of the TRPM2 channel may not only promote inflammatory response but also inhibit inflammation by regulating ROS production and bactericidal ability of macrophages and neutrophils. In I/R, the activation of the TRPM2 channel may worsen I/R injury to various organs, including the brain, heart, kidney and liver. However, activating the TRPM2 channel may protect the myocardium from I/R injury by regulating calcium influx and phosphorylating proline-rich tyrosine kinase 2 (Pyk2). A thorough investigation of the bidirectional role and regulatory mechanism of the TRPM2 channel in these physiological and pathological processes will aid in identifying new targets and strategies for treatment of related diseases.

KEYWORDS

TRPM2 channels, calcium signal, oxidative stress, inflammation, ischemia-reperfusion

1 Introduction

Transient receptor potential (TRP) channels are a class of ion channels that contain TRP protein homologous sequences (1). They are widely distributed throughout the animal kingdom. In mammals, approximately 28 types of TRP channels have been identified, the majority of which are non-selective cation channels, with the exception of TRPV5 and TRPV6 (2, 3). Most TRP family ion channels are permeable to Ca^{2+} and can be activated by physical and chemical factors (4, 5). Some channels can also act as temperature receptors, which help the body sense changes in ambient temperature (6, 7), or as oxidative stress receptors, which mediate the body's physiological activities (8–10). This multi-modal activation mechanism, which can be triggered by chemical, physical, and biological stimuli, enables the TRP family to play crucial roles in various physiological and pathological processes (4, 5). Transient receptor potential channel melastatin 2 (TRPM2) is a non-selective cation channel that has Ca^{2+} permeability. It was first discovered in 1998 and officially named as such in 2002 (11). The TRPM2 channel is widely expressed endogenously in tissues and cells, including the brain, heart, liver, skeletal muscle, lung, stomach, intestine, kidney, and pancreas (12–14). It is abundant in the brain, particularly in the hippocampus, substantia nigra (15, 16), hypothalamus (6, 7), striatum, and cerebral cortex, and expressed in various cell types, including microglia (17), astrocytes, neurons (18), endothelial cells, immune cells (19, 20), and cardiomyocytes (3, 15, 16, 21, 22).

Research has shown a strong correlation between the TRPM2 channel and oxidative stress, inflammation and ischemia–reperfusion (I/R). Activating the channel could increase intracellular Ca^{2+} levels, exacerbate oxidative stress and lead to cell death (23, 24). In certain circumstances, the entry of Ca^{2+} through TRPM2 channels can have a protective effect on tissues. In inflammation and I/R injury, the TRPM2 channel exhibits dual effects, that is, it can exacerbate tissue damage and protects tissues (25–29). However, the multifaceted role of TRPM2 in physiological and pathological processes have not been elucidated yet. This article provides a comprehensive review of the structure, regulatory mechanisms and diverse roles of the TRPM2 channel in physiological and pathological processes such as oxidative stress, inflammation and I/R. This work aims to gain a deep understanding of the physiological and pathological characteristics of the TRPM2 channel and offer new targets and strategies for treatment of relevant diseases.

2 Structure and biological characteristics of TRPM2 channel

The human TRPM2 gene is located on chromosome 21q22.3 and consists of 32 exons. Its gene size is approximately 90 kB, and the molecular weight of mammalian TRPM2 is 170 kd (30). The TRP family has a similar overall structure. TRPM2 consists of six transmembrane segments (TMS) (S1–S6) and intracellular N- and C-termini, The N-terminus contains TRPM homology regions (MHR1-4) (31), while the C-terminus includes a coiled-coil tetramerization domain (CCR) and a NUDT9-H domain (32, 33). A pore-forming loop between the S5 and S6 TMS allows for the permeability of various ions. Upon activation of the TRPM2 channel, cations such as Zn^{2+}, K^{+}, Ca^{2+} and Na^{+} can be transported across the membrane through this channel (3). TRPM2 differs from other members of the TRP family because of the presence of a unique NUDT9-H domain in its C-terminus, which is similar to that of the mitochondrial NUDT9 enzyme. Additionally, cryo-electron microscopy (cryo-EM) studies have reported a TRPM homology region 1/2 (MHR1/2 domain) located at the N-terminus of the channel. Research has demonstrated that this domain also serves as a binding site for adenosine diphosphate ribose (ADPR). These two domains render TRPM2 sensitive to ADPR, and upon ADPR binding, the channel opens and thus allows cations to enter the cell (34–37) (Figure 1). In addition to the full-length TRPM2 (TRPM2-L), several different physiological splice variants have been identified, including TRPM2-S, TRPM2-AS, TRPM2-ΔN, TRPM2-ΔC, TRPM2-SSF and TRPM2-TE. These variants exhibit varying levels of activity and may potentially co-regulate the functional activity of the full-length TRPM2. However, the current understanding of the physiological functions and interactions among these splice variants is limited (38, 39).

3 TRPM2 regulation

The TRPM2 channel can be activated by endogenous ligands, Ca^{2+} and cluster of reactive oxygen species (ROS) (40, 41). These factors not only have the capability to independently activate the TRPM2 channel but also act synergistically. Endogenous activators of TRPM2 include ADPR, cyclic adenosine diphosphate ribose (cADPR), nicotinamide adenine dinucleotide (NAD^{+}) and their metabolic derivatives (42, 43). ADPR is considered the most effective endogenous activator of TRPM2 due to its unique NUDT9-H domain (44). In mitochondria, NUDT9-ADPRase can convert NAD^{+} into ADPR (42). Besides mitochondrial sources, ADPR can also be generated in the nucleus through the poly (ADP–ribose) polymerase (PARP)/poly (ADP–ribose) glycohydrolase) (PARP/PARG) pathway when ROS accumulation leads to DNA damage, catalyzing the conversion of NAD^{+} to ADPR (45–47). The activation of TRPM2 is highly dependent on the levels of intracellular and extracellular Ca^{2+}. In the absence of Ca^{2+}, ADPR loses its activating effect on TRPM2 (48). This phenomenon may be due to an increased sensitivity of the TRPM2 channel to ADPR when Ca^{2+} is present (48). Recent cryo-EM studies have identified Ca^{2+} binding sites within the second and third TMS (S2-S3) of human TRPM2 (49), with similar highly conserved Ca^{2+} binding sites also found in other species including humans, zebrafish and Nematostella vectensis (49–51). Additionally, phosphatidylinositol 4,5-bisphosphate (PIP2) may also be involved in TRPM2 activation in the presence of ADPR and Ca^{2+}. Research has shown that PIP2 plays a crucial role in the activation of TRPM2 orthologues in humans, zebrafish, and sea anemones (51–53). In addition to facilitating the activating effect of ADPR, Ca^{2+} can independently

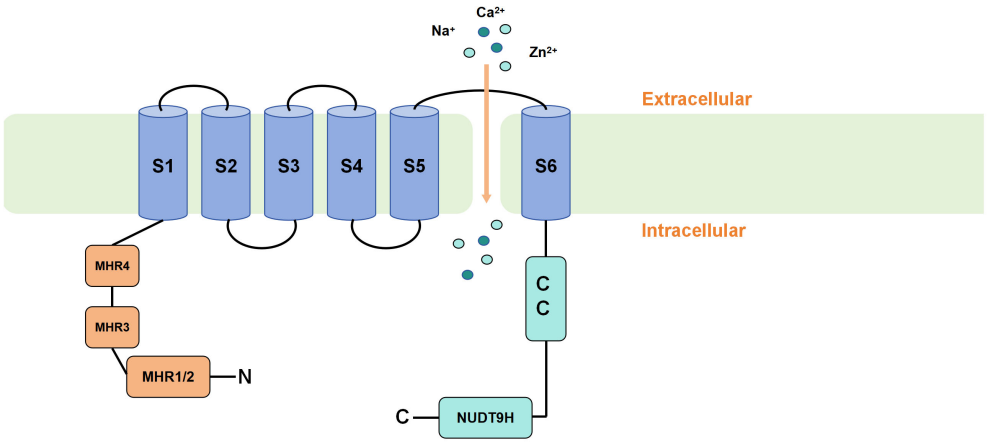

FIGURE 1
Schematic representation of TRPM2 membrane topology. TRPM2 consists of six transmembrane segments (TMS) (S1-S6) and intracellular N- and C-termini. The N-terminus contains TRPM homology regions (MHR1-4), while the C-terminus includes a coiled-coil tetramerization domain (CCR) and a unique NUDT9-H domain. Upon binding of ADPR to the MHR1/2 and NUDT9-H domains, TRPM2 is activated, causing the pore-forming loop between the S5 and S6 TMS to open and allow the influx of cations into the cell.

activate TRPM2 in the absence of ADPR (albeit with lower efficiency compared with ADPR) (54). Furthermore, Ca^{2+} is the only known agonist for certain TRPM2 splice variants (54), thereby emphasizing the importance of Ca^{2+} in TRPM2 activation. Apart from ADPR and NAD^+, another cyclic metabolite of NAD^+, cADPR, has also garnered significant attention. However, considerable debate exists regarding whether cADPR can bind to and gate TRPM2 channels, due to differences in experimental conditions and methodologies among different laboratories, leading to disparate results (43, 55–57). In addition to the aforementioned common endogenous agonists of TRPM2, recent studies have identified bilirubin as a new endogenous agonist of TRPM2, capable of directly binding and activating TRPM2 channels via a specific binding cavity in the transmembrane domain (58). Furthermore, certain analogs of ADPR have been identified as endogenous agonists of TRPM2. These encompass ADP-ribose-2'-phosphate (ADPRP) and 2'-Deoxyadenosine 5'-diphosphoribose (2dADPR), both demonstrating enhanced TRPM2 activation efficiency and evoking larger whole-cell currents relative to ADPR (59, 60). This discovery suggests a potentially fruitful avenue for future investigations into TRPM2 agonists.

The TRPM2 channel is activated by ROS and serves as a crucial oxidative stress sensor in the body (8–10). Although ROS are generally considered harmful, mitochondria release physiological levels of ROS under normal oxygen supply. These ROS function as signaling molecules, regulate numerous protein functions and play a vital role in maintaining normal physiological functions in the organism (61). Hydrogen peroxide (H_2O_2) is a crucial molecule involved in intracellular redox signaling. Micromolar levels of H_2O_2 as well as agents capable of generating ROS can activate TRPM2. However, controversy persists regarding whether H_2O_2 directly activates TRPM2 or operates through the PARP/PARG pathway in the nucleus or mitochondria to generate ADPR, which indirectly activates TRPM2. In addition, research has shown that ROS can induce the activation of protein kinase C and the phosphorylation of the Ser39 site on TRPM2-S. This event leads to the uncoupling of TRPM2-S from TRPM2, thereby relieving the inhibitory effect of TRPM2-S on TRPM2 and opening the TRPM2 channel (62).

TRPM2 channels act as thermosensors, regulating body temperature (6, 7). As early as 2008, studies observed that room temperature could influence H_2O_2-mediated opening of the TRPM2 channel (63). Temperatures exceeding 35°C can activate TRPM2 channel opening or facilitate its activation by ADPR and cADPR in rat insulinoma cells (41). TRPM2 serves as a thermosensor in the neural circuitry of the preoptic area involved in body temperature regulation and is activated when the body temperature exceeds 37°C (6). The activation and inhibition of TRPM2-positive neurons can respectively lead to a decrease and increase in body temperature, and downstream effects are associated with the release of oxytocin (64). TRPM2 channels in the brain respond to prolonged heat stimulation. The expression of TRPM2 mRNA in the embryonic mouse brain gradually increases under prolonged heat stimulation and affects embryonic development and neurogenesis (65). However, specific mechanisms governing the temperature activation of TRPM2 channels remain incompletely understood. The capacity of TRPM2 channels to respond to temperature renders them as sensors, which contribute to an organism's perception of environmental temperature and regulation of body temperature processes.

Certain metal cations, such as Zn^{2+} and Cu^{2+}, exert inhibitory effects on TRPM2 activation and serve as extracellular antagonists (66). Various drugs, including 12-deacetylscalaradial (DSD), clotrimazole (CTZ), anthranilic acid (ACA), flufenamic acid (FFA) and 2-aminoethoxydiphenyl borate (2-APB), can inhibit TRPM2 channel activity (67). However, these antagonists lack specificity for TRPM2. The activity of the TRPM2 channel is negatively regulated by cellular acidification (68). Exposure of

intracellular and extracellular environments to acidic conditions (pH of 5 to 6) suppresses the activity of TRPM2 (69).

4 Bidirectional regulation of TRPM2 in oxidative stress

Oxidative stress refers to the disruption of the balance between oxidation and antioxidation in the body and leads to excessive generation or reduced scavenging of ROS or reactive nitrogen species and even cell and tissue damage when severe (70). Under normal physiological conditions, ROS are generated naturally by the mitochondrial electron transport chain during respiration. ROS act as signaling molecules and regulate various physiological functions in the human body, such as promoting cell survival, proliferation and differentiation (71). Under pathological conditions, ROS are produced by neutrophils and phagocytes involved in inflammation and infection. The decrease in the activity of the mitochondrial electron transport chain is induced by various factors and can contribute to increased ROS production (72). Continuous exposure to high levels of ROS damages nuclear DNA. Due to the involvement of the PARP/PARG pathway in DNA damage repair in the nucleus, this process is accompanied by the production of ADPR. Studies have demonstrated that the sensitivity of TRPM2 channels to activation under pathological levels of ROS is significantly increased, which is directly related to the activation of PARP/PARG (39, 73, 74).

4.1 TRPM2-mediated cell death induced by oxidative stress

The TRPM2 channel serves as a crucial oxidative stress sensor in the body and plays a significant role in various physiological and pathological processes (8–10). Upon activating TRPM2, oxidative stress leads to a sustained increase in cytoplasmic Ca^{2+} concentration, triggers inflammation and exacerbate cellular damage, ultimately resulting in cell death (23, 24). For example, the excessive use of acetaminophen may lead to hepatocyte death and may be associated with the pronounced increase in reactive ROS induced by acetaminophen and the substantial influx of Ca^{2+} into cells through TRPM2 (14, 75, 76). Acetaminophen induces a rapid increase in intracellular Ca^{2+} concentration and cation current in cultured rat and mouse hepatocytes. This response is inhibited by treatment with CTZ, ACA, and TRPM2-specific small interfering RNA (TRPM2-siRNA) (14). Consistent with *in vitro* experiments, injection of acetaminophen into wild-type (WT) mice leads to extensive liver necrosis and lymphocytic infiltration, accompanied by increased concentrations of hepatic enzymes alanine transaminase and aspartate transaminase in the blood. However, these damages are significantly reduced in TRPM2 knockout (KO) mice (14). This study provides evidence supporting that acetaminophen induces acute liver injury through the generation of ROS, which increases PARP-mediated ADPR production, subsequently activating TRPM2 and inducing Ca^{2+} signaling. The massive influx of Ca^{2+} into the cell upon TRPM2 activation mediates the acute liver damage caused by acetaminophen through downstream pathways. Further research has elucidated the molecular and signaling mechanisms by which TRPM2 mediates acetaminophen-induced cell death. It is proposed that the entry of Ca^{2+} through TRPM2 activates the calcium/calmodulin-dependent protein kinase II (CaMKII), which subsequently phosphorylates Beclin-1. This phosphorylation reduces the interaction between Beclin-1 and PIK3C3, thereby inhibiting autophagy while promoting apoptosis. Consequently, this enhances hepatocyte sensitivity to cell death (76). Yang et al. (77) revealed that TRPM2 expressed on the membrane of myocardial cells is involved in ROS-mediated myocardial cell death. Excessive ROS can induce the production of ADPR by increasing PARP levels and subsequently activate TRPM2. This activation leads to the excessive uptake of Ca^{2+} and Na^{+} by the mitochondria, causing mitochondrial membrane dysfunction, release of cytochrome C and activation of caspase-3. Endothelial cells covering the vascular wall are particularly susceptible to oxidative stress. *In vitro* experiments have shown that exposure to H_2O_2 or tumor necrosis factor-alpha (TNF-α-induced) ROS generation leads to the activation of TRPM2 channels in endothelial cells, subsequently inducing caspase-dependent apoptosis (increased activity of caspase3, caspase8, and caspase9), thereby reducing endothelial cell survival rates. However, these effects are mitigated or abolished following intervention with TRPM2 inhibitors or TRPM2-siRNA (19, 78, 79). These findings support the pivotal role of TRPM2 activation and TRPM2-mediated Ca^{2+} signaling in oxidative stress-induced endothelial cell death and endothelial barrier dysfunction, potentially implicating certain vascular diseases. Neurons in the brain are highly susceptible to oxidative stress damage, and ROS-induced neuronal death is closely associated with cognitive impairment and the pathogenesis of various brain diseases. TRPM2 is widely and abundantly expressed in the brain, and previous studies have found that TRPM2 mediates the process of ROS-induced neuronal death (80–82). Fonfria et al. (80) demonstrated the involvement of the TRPM2 channel in H_2O_2-induced neuronal death using rat striatal neurons. They found that the induction of TRPM2-siRNA or transient transfection of striatal neurons with a plasmid expressing TRPM2-S resulted in a reduction of H_2O_2-induced cell death. Additionally, treatment with the PARP inhibitor SB-750139 attenuated this cell death (80). These findings suggest that PARP-dependent activation of the TRPM2 channel mediates the process of H_2O_2-induced neuronal death. In cortical neurons of rats treated with H_2O_2, similar results were observed, and the study further revealed the crucial role of TRPM2-mediated Ca^{2+} influx in H_2O_2-induced neuronal death (82). Additionally, researchers utilized hippocampal neuron cultures from WT and TRPM2 KO mice and found that hippocampal neurons from WT mice exhibited concentration-dependent and duration-dependent cell death upon H_2O_2 intervention, whereas this cell death was significantly reduced in TRPM2 KO neurons. H_2O_2 also induces significant Zn^{2+} influx, lysosomal Zn^{2+} release, and lysosomal dysfunction, leading to mitochondrial dysfunction, ROS accumulation, and ultimately cell death (81). These consistent findings collectively suggest that the

TRPM2 channel and its mediated excessive Ca^{2+} influx play a critical role in H_2O_2-induced neuronal death.

4.2 Protective effects of TRPM2 channel in oxidative stress

Contrary to the previous research findings, recent studies have revealed that under certain conditions, the entry of Ca^{2+} through the TRPM2 channel plays a significant physiological role in protecting various tissues from oxidative stress damage. When subjected to intraperitoneal injection of endotoxin, TRPM2 KO mice exhibit significantly lower survival rates than WT mice. These mice underwent severe oxidative stress and inflammatory reactions in their lungs (26). Further *in vitro* experiments showed that this phenomenon is caused by the entry of Ca^{2+} through TRPM2, which depolarizes the phagocyte cytoplasmic membrane and reduces ROS generation mediated by nicotinamide adenine dinucleotide phosphate (NADPH) oxidase (26). In cone neurons subjected to exogenous H_2O_2 intervention, inhibiting TRPM2 exacerbates oxidative stress damage to cells; this finding provides evidence that TRPM2 can protect neurons from oxidative stress injury (25). Moreover, TRPM2 mutations (P1018L) were identified in the brain tissues of patients with Guamanian amyotrophic lateral sclerosis and Parkinsonian dementia. Unlike the non-inactivating TRPM2, the P1018L mutant deactivates upon ADPR-induced channel opening, thereby restricting Ca^{2+} entry (63). This observation suggests that sustained Ca^{2+} influx triggered by activated TRPM2 channels is essential to maintain normal neuronal function. In the acute kidney injury model induced by chemotherapeutic drug cisplatin, the knockout of the TRPM2 gene exacerbates renal dysfunction and tissue damage. In TRPM2 KO mice and primary renal cells, the generation of mitochondrial cytochrome C and ROS increased, leading to intensified oxidative stress damage. However, the use of mitochondrial ROS scavenger Mito-tembo alleviates this damage. Hence, TRPM2 may mediate autophagy through a Ca^{2+}/AKT/mTOR-dependent mechanism to maintain mitochondrial dynamics and protect the kidneys from oxidative stress injury (83). In contrast to the previous studies on TRPM2-mediated endothelial dysfunction induced by oxidative stress, recent research has revealed that TRPM2 exerts vasodilatory effects upon activation by H_2O_2. Experimental approaches involved the use of hypertensive mouse models with either WT or NOX4-knockout (NOX4 KO) genotypes, as well as a rat aortic endothelial cell model. Mechanistic pathways were validated through inhibition of PARP, NOX4, and TRPM2, as well as TRPM2-siRNA. It was demonstrated that NOX4-induced H_2O_2 production, via the PARP/PARG pathway, generated ADPR, which subsequently activated TRPM2-mediated Ca^{2+} influx, leading to activation of endothelial nitric oxide synthase (eNOS) and nitric oxide (NO) release, thereby exerting vasodilatory effects. These experiments elucidated the molecular mechanism underlying the blood pressure-lowering and vascular protective effects induced by NOX4 activation, while also suggesting that TRPM2 may hold significant implications in ameliorating diseases associated with endothelial dysfunction, such as hypertension (84).

In summary, under physiological and pathological conditions, the activation of TRPM2 may exacerbate or alleviate oxidative stress damage (Figure 2), which may depend on the following factors: from a cellular and tissue-specific perspective, TRPM2 activation exacerbates oxidative stress-induced hepatocyte and cardiomyocyte damage, with mechanistic similarities involving ROS/PARP pathway-mediated ADPR production leading to TRPM2 activation, subsequent massive Ca^{2+} influx, and downstream effects resulting in cell apoptosis; In mouse renal tissue and phagocytic cells, TRPM2 activation appears to reduce ROS production. However, it is important to acknowledge the limitations of this conclusion. Firstly, it is uncertain whether this effect is specific to oxidative stress induced by endotoxin and cisplatin. Secondly, there is limited research on the role of TRPM2 in mediating oxidative stress-induced damage in renal tissue and phagocytic cells, necessitating further investigation to elucidate the relationship between TRPM2 and oxidative stress in these contexts; In neuronal cells, there is controversy surrounding the research findings, but the majority support that TRPM2 activation exacerbates cellular oxidative stress damage. However, differences between experimental results may be attributed to variations in extracellular environments and the use of nonspecific inhibitors. In endothelial cells, ROS-triggered TRPM2 activation may manifest dual effects, either promoting endothelial cell apoptosis or inducing vasodilation through NO release. However, whether both effects are simultaneously activated remains unclear, further highlighting the complexity of TRPM2 downstream pathways. Additionally, variations in the genetic background of mice used in different experiments may lead to disparate outcomes within the same tissue or cell types. Lastly, the lack of specific inhibitors for TRPM2 could potentially introduce bias into experimental results. Therefore, further comprehensive research is warranted to assess the specific role of TRPM2 in oxidative stress.

4.3 TRPM2 in diseases associated with oxidative stress

The Ca^{2+} influx induced by ROS activation of the TRPM2 channel significantly alters intracellular Ca^{2+} concentration, thereby affecting downstream effects including cell signaling, proliferation, apoptosis, and even cell death. TRPM2 occupies a pivotal position in the ROS and Ca^{2+} systems, and its activation-mediated cell death effects may link oxidative stress-induced pathological factors to related diseases. Research indicates that dysfunctional or dysregulated TRPM2 function has been associated with a range of pathological conditions, including neurodegenerative diseases and diabetes. Oxidative stress is associated with neurodegenerative diseases and a characteristic feature of physiological aging in the brain (85–87). Glutathione (GSH) is a crucial endogenous antioxidant in the body, and a decrease in its levels results in reduced cellular antioxidant defense and oxidative stress (88). Intraneuronal GSH levels decrease during aging, which may be linked to the expression of TRPM2. *In vitro* experiments demonstrated that inhibiting GSH synthesis results in reduced

expression and significantly increases TRPM2 activity. TRPM2 may have a significant role in age-related neurodegenerative diseases (89). Alzheimer's disease (AD) is a common age-related neurodegenerative disease characterized by progressive cognitive decline (90), deposition of brain neuronal β-amyloid (Aβ) plaques, increased reactive ROS, and intracellular Ca^{2+} overload (91). Oxidative stress alters Ca^{2+} homeostasis in AD patients and animal models (92, 93), leading to an increased concentration of intracellular free Ca^{2+}, which subsequently induces mitochondrial membrane depolarization and cell death (94). In AD mouse models, TRPM2 KO significantly ameliorates age-related memory impairments, synaptic loss, and activation of microglial cells (18). *In vitro* experiments also demonstrate that prolonged exposure of hippocampal neuronal cells to pathological concentrations of Aβ42 results in lysosomal Zn^{2+} release, mitochondrial Zn^{2+} accumulation, mitochondrial fragmentation, and substantial production of mitochondrial ROS, accompanied by extensive neuronal cell death. However, these aberrant changes induced by Aβ42 are abolished following intervention with 2-APB or TRPM2 KO. These experimental findings suggest a crucial role of TRPM2 in mediating Aβ-induced AD pathology (95). Furthermore, it is hypothesized that Aβ42 activates protein kinase C (PKC) and NADPH oxidase (NOX) to generate ROS, inducing ADPR production via the PARP/PARG pathway, thereby activating the TRPM2 channel. Subsequently, this leads to lysosomal dysfunction and increased lysosomal Zn^{2+} release, mitochondrial Zn^{2+} accumulation resulting in mitochondrial fragmentation, dysfunction, release of cytochrome C and mitochondrial ROS, ultimately leading to cell death through the apoptotic (95). The substantial Ca^{2+} influx induced by TRPM2 activation also mediates Aβ-induced cerebrovascular dysfunction. This mechanism is likely triggered by Aβ-induced oxidative-nitrosative stress in cerebral endothelial cells, causing DNA damage and excessive ADPR production via the PARP/PARG pathway. The activation of TRPM2 on endothelial cells leads to Ca^{2+} overload, ultimately impairing cerebral blood flow (96). Studies have found that patients with Type I bipolar disorder exhibit elevated baseline intracellular Ca^{2+} levels, and a susceptibility locus on chromosome 21q22.3, which includes the TRPM2 gene region, has been identified, suggesting a potential link between TRPM2 and bipolar disorder (97, 98). Additionally, excessive activation of TRPM2 in neurons may also be associated with the development of long-term depression (LTD) and Parkinson's disease (PD) (99, 100). In addition to neurons, TRPM2 has also been found to be expressed in pancreatic β-cells. Pancreatic β-cells have relatively weak antioxidant capabilities and are susceptible to oxidative stress damage, and a reduction in their number and dysfunction can lead to hypoinsulinemia, hyperglycemia, or diabetes (99). *In vitro*

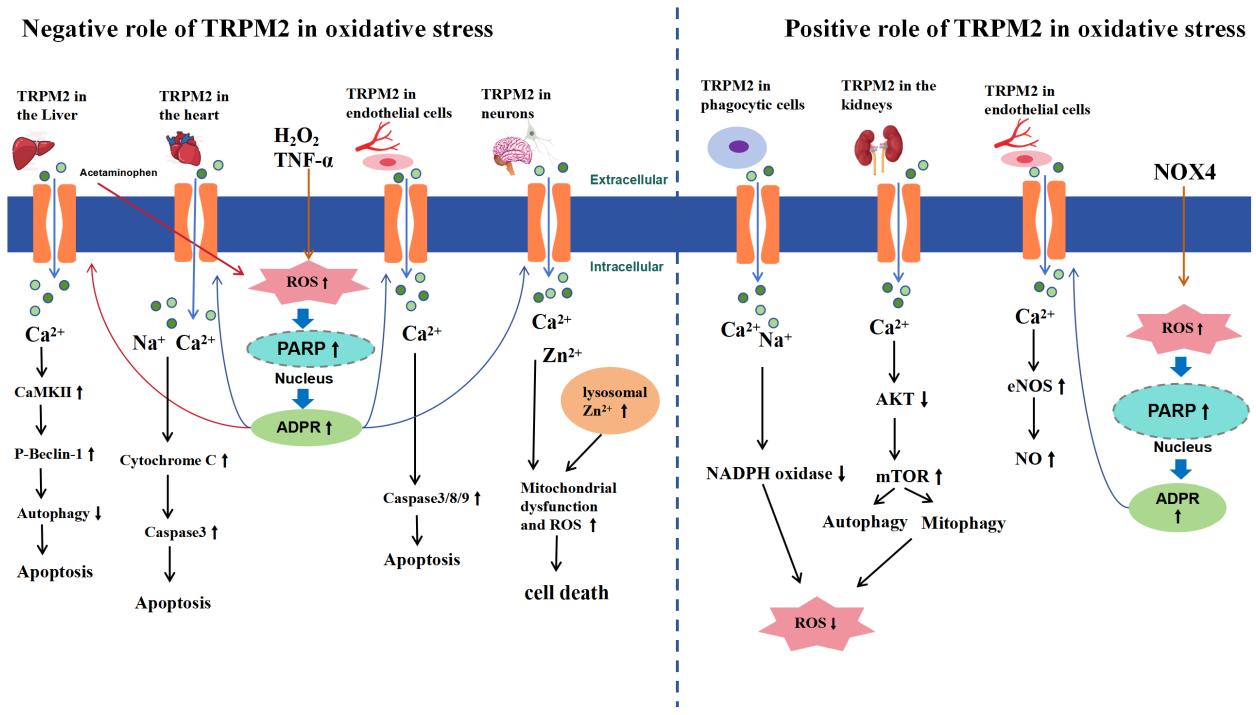

FIGURE 2
Schematic Representation of TRPM2-Mediated Signaling Pathways in Oxidative Stress. The left side of the diagram illustrates the negative effects of TRPM2 activation under oxidative stress, while the right side highlights the positive effects. In the liver, heart, endothelial cells, and brain neurons, extracellular H_2O_2 or TNF-α leads to intracellular ROS accumulation (acetaminophen-induced ROS accumulation is specific to liver conditions), inducing activation of PARP and PARG enzymes in the nucleus, which convert NAD^+ to ADPR, thereby activating TRPM2. Subsequently, a large influx of Ca^{2+}, Zn^{2+}, and Na^+ occurs, which, depending on the tissue, triggers apoptosis or cell death through activation of signaling pathways such as CaMKII and caspase (left side). In the kidney and phagocytic cells, TRPM2 activation-mediated Ca^{2+} and Na^+ influx promotes autophagy through the AKT-mTOR signaling pathway or inhibits NADPH to reduce ROS production. In endothelial cells, NOX4 generates ADPR via the ROS/PARP pathway to activate TRPM2, which can activate the eNOS/NO signaling pathway, leading to vasodilation (right side).

experiments using insulin-secreting cell lines (RIN-5F and INS-1 cells) have demonstrated that the activation of PARP-dependent TRPM2 channels mediates H_2O_2-induced apoptosis, accompanied by excessive Ca^{2+} release from intracellular lysosomes, ultimately leading to cell death. TRPM2 KO or the use of TRPM2 inhibitors can mitigate this cell death (101, 102). In streptozotocin (STZ)-induced rodent models of diabetes have confirmed this phenomenon, showing extensive loss of pancreatic β-cells and significantly elevated fasting blood glucose levels in mice, which are ameliorated in TRPM2 KO mice. PARP-dependent TRPM2 activation mediates Ca^{2+} influx and substantial lysosomal Zn^{2+} release, disrupting ionic homeostasis in pancreatic β-cells and triggering apoptosis through downstream effects (101). This indicates that TRPM2 may play a critical role in the pathogenesis of (type 1 diabetes) T1D and (type 2 diabetes) T2D by mediating oxidative stress-induced pancreatic β-cell death. Current research findings suggest that TRPM2 activation could be a significant factor in the onset and progression of neurodegenerative diseases or diabetes. Thus, TRPM2 may represent a promising new target for the treatment of certain ROS-related diseases.

4.4 Activation of TRPM2 promotes cancer cell survival

SH-SY5Y cells are a human neuroblastoma cell line initially derived from a neuroblastoma. They are commonly used *in vitro* to study various aspects of neuronal cell growth, differentiation, apoptosis, and mechanisms of neurodegenerative diseases. In SH-SY5Y cells, the activation of TRPM2 appears to play a critical role in promoting cell proliferation and survival. In SH-SY5Y cells subjected to low-dose H_2O_2 intervention, the expression of the splicing variant TRPM2-S, which can inhibit TRPM2 channel activity, results in decreased intracellular Ca^{2+} influx and elevated levels of ROS, leading to a reduction in cell survival rates (103). Chen et al. (103)study further elucidated that SH-SY5Y cells expressing TRPM2-S exhibited increased cell death upon exposure to H_2O_2, whereas cells expressing TRPM2-L were able to mitigate moderate oxidative stress-induced damage and reduce cell death by upregulating levels of forkhead box o3a (FOXO3a) and superoxide dismutase 2 (SOD2). Moreover, TRPM2 enhanced the growth capacity of SH-SY5Y cells. Besides its role in reducing cellular oxidative stress and enhancing antioxidant defenses to protect against cell death, TRPM2 was found to promote the growth and survival of SH-SY5Y cells through modulating autophagy (103). Autophagy is a lysosome-mediated degradation process and serves as a crucial mechanism for promoting cell survival (104). Additionally, autophagy plays a pivotal role in tumor growth by clearing damaged cellular components such as DNA and mitochondria, controlling ROS levels, enhancing cellular antioxidant capacity, and promoting tumor growth and survival (105–107). The absence of TRPM2 influences cellular autophagy (10, 83, 108, 109). Research that used CRISPR/Cas9 technology to knock out TRPM2 in SH-SY5Y neuroblastoma cells revealed inhibited cell growth. After doxorubicin intervention, oxygen consumption and ATP generation decrease, causing cellular bioenergetic impairment. Moreover, mitochondrial ROS production significantly increases. Pre-treatment with the antioxidant Mito-tembo reduces ROS levels and protects cellular viability (108). TRPM2 plays a crucial role in regulating the expression of hypoxia-inducible factor-1α/2α(HIF-1α/HIF-2α) and their downstream signaling pathways. The underlying mechanisms may involve factors, such as FOXO3a-SOD2, cytochrome c oxidase subunit 4.1/4.2 (COX4.1/4.2), BCL2/adenovirus E1B 19 kDa interacting protein 3 (BNIP3) and NADH:ubiquinone oxidoreductase subunit a4 like 2 (NDUFA4L2). SOD2 is an antioxidant enzyme located within the mitochondria. BNIP3 is a crucial factor in mitochondrial autophagy, and its reduction can lead to decreased mitophagy, resulting in the accumulation of dysfunctional mitochondria and an increase in ROS. The expression of NDUFA4L2 can reduce ROS production by affecting the activity of respiratory chain complex I. These downstream factors contribute to the reduction in intracellular ROS levels and protect cells from damages caused by oxidative stress (72). The above studies indicate that TRPM2 plays a crucial role in the proliferation and survival of SH-SY5Y cells by modulating intracellular ROS levels, antioxidant capacity, mitochondrial function, and autophagic capability.

In addition to neuroblastoma cells, recent studies have confirmed similar regulatory mechanisms of TRPM2 in acute myeloid leukemia cells and gastric cancer cells. Chen et al. (10) revealed that the knockout of TRPM2 in U937 cells suppressed cell proliferation and increased the sensitivity to atorvastatin intervention. In TRPM2 KO cells, mitochondrial membrane potential (ψm) and mitochondrial calcium uptake capacity significantly decreased. Mitochondrial function, including oxygen consumption rate and ATP production, were impaired, and the level of ROS significantly increased. Furthermore, the levels of nuclear factor erythroid 2-related factor 2 and transcription factors including HIF-1α/2α and FOXO3a decreased. Overall, the cellular antioxidant capacity was diminished. In TRPM2-deficient cells, there is a reduction in the key transcription factors ATF4 and cAMP response element-binding protein (CREB), which are essential for autophagosome biogenesis, and he levels of autophagy-related proteins such as unc-51-Like autophagy activating kinase 1, autophagy-related 7 and autophagy-related 5 decreased, leading to autophagy suppression. The restoration or enhancement of TRPM2 expression elevated cell viability as well as cellular proliferation and autophagic capability. Moreover, increased TRPM2 expression mitigated the increase in ROS level (10). Knockout of the TRPM2 gene in AGS and MKN-45 cells resulted in autophagy inhibition, impeded cell proliferation, promoted apoptosis and induced mitochondrial dysfunction characterized by reduced mitochondrial basal and maximal oxygen consumption rates as well as decreased ATP production. TRPM2, through the c-Jun N-terminal kinase (JNK) signaling pathway, modulates autophagy and the expression of autophagy-related proteins, including autophagy-related genes, microtubule-associated protein 1A/1B-light chain 3A/BII (LC3A/BII) and BNIP3. This regulation maintains mitochondrial energy metabolism, reduces cell sensitivity to doxorubicin and mitigates ROS generation (109). These data indicate that TRPM2 plays a

crucial role in the proliferation and survival of the aforementioned cells by modulating key transcription factors and target genes involved in mitochondrial function, bioenergetics, antioxidant capacity and autophagy.

High TRPM2 expression in various cancers suggests that TRPM2 promotes tumor cell survival (Figure 3). Studies using multiple tumor cell models have shown that inhibiting TRPM2 increases cell death and sensitivity to doxorubicin. TRPM2 supports tumor cell survival by enhancing mitochondrial function, increasing ATP production, promoting autophagy, reducing ROS levels, and boosting antioxidant capacity. This mechanism ensures tumor cell survival under high ROS conditions while maintaining mitochondrial bioenergetics to meet energy demands. However, whether this effect is exclusive to tumor cells remains unclear and requires further experimental investigation. Although the activation of TRPM2 by ROS in tumor cells is not desirable due to its cell survival-promoting effects, it suggests that pharmacological inhibition of TRPM2 in cancer could be a novel and highly promising therapeutic approach.

5 Bidirectional regulation of TRPM2 in inflammation

ROS-induced Ca^{2+} influx plays a crucial role in the immune system (110–112), being associated with the activation of many inflammasomes and inflammatory factors, as well as the expression of their downstream signaling pathways (113–116). TRPM2 serves as a critical link between ROS and Ca^{2+} influx and is expressed in various inflammatory cells, including monocytes, neutrophils, and macrophages (117, 118). Therefore, TRPM2 may significantly influence inflammation by modulating immune cell functions.

5.1 Negative role of TRPM2 in inflammation

Ca^{2+} entry through the TRPM2 channel can regulate the production of ROS-induced monocyte chemotactic factors (113, 117). In human U937 monocytes, H_2O_2 causes ADPR-mediated opening of TRPM2 channels, leading to Ca^{2+} influx. This activates Pyk2 and Ras-GTPase, amplifying extracellular signal-regulated kinase (Erk) signaling and promoting nuclear translocation of nuclear factor-kappa B (NF-κB), which results in CXCL8 production. In a dextran sodium sulfate (DSS)-induced ulcerative colitis model, TRPM2 KO mice showed reduced CXCL2 expression, decreased neutrophil infiltration, and attenuated colonic inflammation (113). Thus, inhibiting TRPM2 channel function may represent a novel strategy for treating inflammatory diseases. Chen et al. (119)revealed that the genetic ablation of TRPM2 in microglial cells mitigated kainic acid-induced activation of microglia and generated inflammatory factors, which are common neuroinflammatory manifestations in epilepsy. This phenomenon was not observed in TRPM2-depleted astrocytes. Experimental evidence further demonstrated that the knockout of TRPM2 operates through the AMPK/mTOR pathway to modulate autophagy, thereby suppressing the activation of microglial cells. Chronic inflammation in the brain constitutes a mechanistic and characteristic feature in the pathogenesis of epilepsy and multiple sclerosis. In rodent models of pilocarpine-induced epilepsy and cuprizone-induced multiple sclerosis, the deletion of TRPM2 reduced cytokine levels and attenuated inflammasome

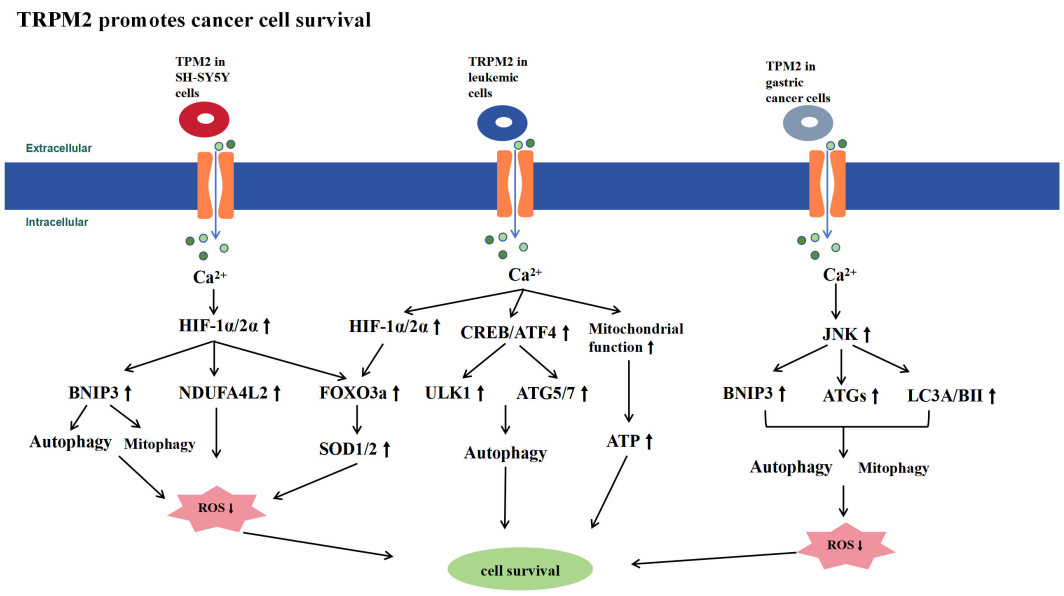

FIGURE 3
Schematic Representation of Signaling Pathways Promoting Tumor Cell Survival by TRPM2. TRPM2 is highly expressed in tumor cells and promotes their survival by controlling Ca^{2+} influx, which activates signaling pathways such as HIF-1α/2α, ATF4, CREB, and JNK. This activation enhances mitochondrial function, increases ATP production, promotes autophagy, reduces ROS levels, and boosts antioxidant capacity, thereby supporting tumor cell survival.

engagement within murine brain tissue. This reduction was associated with diminished levels of activation in neuroglial cells, consequently ameliorating the severity of neuroinflammation (120). Additionally, the knockout of TRPM2 confers protection against hepatic cell damage induced by I/R and oxygen-glucose deprivation/reoxygenation (OGD/R). This protective effect is possibly likely associated with the activation of autophagy and the suppression of the NLR family pyrin domain containing 3 (NLRP3) inflammasome pathway (121). Analysis of ovarian cancer-associated transcriptomic and clinical data obtained from The Cancer Genome Atlas, Genotype-tissue Expression (GTEx) and Gene Expression Omnibus (GEO) databases reveal a robust positive correlation in the expression of TRPM2 with the NLRP3, NLR family CARD domain containing 4, nucleotide-binding oligomerization domain 1, nucleotide-binding oligomerization domain 2 interleukin 1 beta and gasdermin D. The increase in the expression of TRPM2 may be strongly associated with adverse prognosis in ovarian cancer, suggesting its potential utility as a novel immunotherapeutic target to enhance the overall survival of patients with ovarian cancer (122). The aforementioned studies suggest that the activation of the TRPM2 channel leads to sustained Ca^{2+} influx, induces inflammasome activation and produces inflammatory and chemotactic factors. This process emerges as a crucial factor in exacerbating inflammatory responses and tissue damage. The inhibition of TRPM2 channel functionality emerges as a potential target for ameliorating cellular inflammation.

5.2 Positive role of TRPM2 in inflammation

A substantial body of current research indicates that activating the TRPM2 channel inhibits inflammatory responses (23, 26, 29, 123–125). Research indicates that the survival rate of TRPM2 KO mice significantly decreases compared with WT mice following intraperitoneal injection of endotoxin (LPS). The deletion of TRPM2 enhances the expression levels of chemokine ligand 2, IL-6 and TNF-α in the lungs of mice, thereby exacerbating the inflammatory response. In the response of phagocytic cells to infection, the production of NADPH oxidase-dependent ROS plays a crucial role in inflammatory mechanisms (126, 127). Activation of TRPM2 may inhibit this ROS production, thereby mitigating LPS-induced pulmonary inflammatory damage (26). The knockout of TRPM2 enhances neutrophil-mediated vascular inflammatory responses. TRPM2-/- mice exhibited a significant increase in neutrophil accumulation at the site of intraperitoneal LPS injection. This study suggests that TRPM2 can sense ROS generated by neutrophils and inhibit neutrophil migration. In this process, the oxidation of the N-terminal Cys549 residue of TRPM2 induces its binding to formyl peptide receptor 1 (FPR1), thereby inhibiting FPR1 internalization and signaling. This inhibition impedes neutrophil migration and alleviates neutrophil-induced inflammatory damage (123).

TRPM2 can also suppress inflammatory response induced by bacterial infections. In a murine model of sepsis induced by cecal ligation and puncture (CLP), compared with WT mice, TRPM2 KO mice exhibited a significantly increase in mortality rate. This finding was characterized by elevated bacterial burden in the blood, lungs, liver and spleen. The mortality rate was associated with bacterial burden, organ injury and systemic inflammation. Overall, TRPM2 enhances the antimicrobial capability of immune cells to bolster the host's anti-inflammatory capacity. Furthermore, TRPM2 potentially regulates the expression of heme oxygenase-1 by controlling Ca^{2+} influx, consequently promoting macrophage autophagy to enhance bacterial clearance (124, 125). In a murine sepsis model induced by intraperitoneal injection of Escherichia coli, TRPM2-/- mice exhibited a significantly increase in mortality rate and bacterial burden compared with WT mice, thereby exacerbating inflammatory responses. The absence of TRPM2 impaired the maturation of phagolysosomes, impeded their fusion with lysosomes in peritoneal macrophages and reduced the bactericidal capacity of macrophages. Increasing the intracellular Ca^{2+} concentration restored the bactericidal activity of macrophages, indicating that TRPM2 regulates the maturation of phagolysosomes in macrophages by controlling intracellular Ca^{2+} concentration and plays a crucial role in host defense against bacterial infections (128). Qian et al. (129) utilized TRPM2 KO neutrophils and TRPM2 KO mice in their study; they reported that TRPM2 induced the phosphorylation of p38 mitogen-activated protein kinase (MAPK) in neutrophils by mediating Ca^{2+} influx and regulated the release of elastase. This process enhances the bactericidal capacity of neutrophils. Research also revealed that TRPM2-/- mice are highly susceptible to infection with Listeria monocytogenes (Lm); post-infection decreased the levels of interleukin-12 and interferon-γ (23). In the same Lm model, TRPM2-/- mice presented with septic shock during infection and increased serum levels of TNF-α, IL-6 and IL-10. This study suggests that the activation of TRPM2 in neutrophils is beneficial in suppressing Lm dissemination and preventing neutrophil-mediated tissue damage, thereby contributing to the alleviation of local and systemic inflammatory levels (130). Furthermore, research has investigated the role of TRPM2 in macrophages by using Helicobacter pylori infection as a model of chronic inflammation. In comparison with WT mice, macrophages from TRPM2-/- mice exhibited an inability to regulate intracellular Ca^{2+} levels when stimulated with H. pylori. This phenomenon resulted in Ca^{2+} overload, wherein excessive intracellular Ca^{2+} enhanced the activities of MAPK and NADPH oxidase. The heightened activities of these components triggered macrophages to produce increased levels of ROS and inflammatory mediators, thereby exacerbating gastric inflammation in the mice. Hence, TRPM2 plays a regulatory and anti-inflammatory role in gastric inflammatory response (29).

Thus, TRPM2 exhibits a dual role in the immune system, acting both pro-inflammatory and anti-inflammatory (Figure 4), with various factors contributing to this outcome. In intestinal inflammation such as ulcerative colitis and chronic brain inflammation like epilepsy, TRPM2 activation may exacerbate the inflammatory response and tissue damage by causing excessive Ca^{2+} influx, leading to increased production of inflammatory cytokines and inflammasomes, or by inducing glial cell activation. Conversely, in LPS-induced inflammation, TRPM2 activation can mitigate the inflammatory response by inhibiting NADPH oxidase-dependent

10.3389/fimmu.2024.1391355

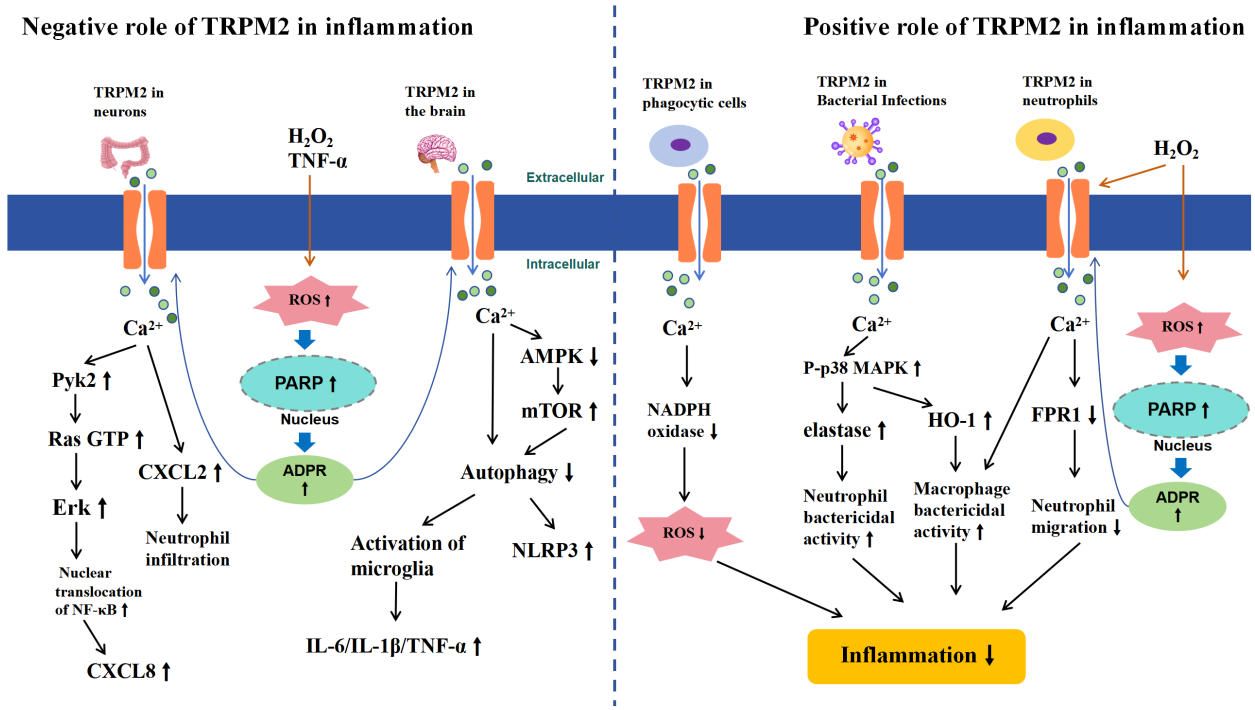

FIGURE 4
Schematic Representation of TRPM2-Mediated Signaling Pathways in Inflammation. The left half illustrates the negative role of TRPM2 activation in inflammation. In chronic inflammation of the gut and brain, extracellular H_2O_2 or TNF-α leads to intracellular ROS accumulation, inducing the activation of PARP and PARG enzymes in the nucleus, which convert NAD^+ to ADPR, thereby activating TRPM2. Subsequently, Ca^{2+} influxes into the cells, triggering CXCL secretion in the gut through the activation of Pyk2-Erk signaling pathways and increasing inflammatory cytokines and inflammasomes in the brain by inhibiting the AMPK/mTOR signaling pathway, which suppresses autophagy (left half). The right half illustrates the positive role of TRPM2 activation in inflammation. In inflammatory responses caused by macrophages, neutrophils, or bacterial infections, TRPM2-mediated Ca^{2+} influx reduces ROS production by inhibiting NADPH, decreases neutrophil migration by inhibiting FPR1, or enhances the bacterial clearance ability of immune surveillance cells by activating the p38MAPK signaling pathway, thereby reducing inflammation (right half).

ROS production and suppressing neutrophil aggregation and migration. Additionally, in the CLP model or inflammation caused by bacterial infections such as Lm, E. coli, and H. pylori, TRPM2 channel activation was found to suppress the inflammatory response, likely due to enhanced bacterial clearance by macrophages and neutrophils. This anti-inflammatory effect is not only effective in local tissues but also in reducing systemic inflammation levels. Therefore, the different roles of TRPM2 in inflammation are determined by the varying factors that trigger the inflammatory response, which may be related to the complex downstream signaling pathways of TRPM2. It remains unclear whether the anti-inflammatory effects of TRPM2 activation are limited to LPS and bacterial infection-induced inflammation. Future research is needed to further investigate the effects of TRPM2 activation in different inflammatory responses to fully understand the relationship between TRPM2 and inflammation.

6 Bidirectional regulation of TRPM2 in I/R

I/R is a complex process where tissue or organ blood flow is restricted and subsequently restored. Factors such as ischemia and hypoxia can lead to tissue damage and functional impairment. This phenomenon results in events, such as Ca^{2+} overload, oxidative stress and inflammatory responses, leading to cell death (131). I/R events may occur during myocardial infarction, stroke, acute kidney injury and organ transplantation. Oxidative stress and increased ROS production during cerebral I/R may activate non-selective cation channels, such as TRPM2, contributing to neuronal damage post I/R (131–133). ROS and intracellular Ca^{2+} overload are significant contributors to myocardial I/R injury, implicating the potential pivotal role of TRPM2 channels in these physiological and pathological processes.

6.1 Negative role of TRPM2 in I/R

In the heart, physiologically released ROS from the mitochondria may activate TRPM2 channels and provide sustained Ca^{2+} influx that is essential for normal cellular physiological functions (134). However, under pathological conditions such as I/R, an extensive influx of Ca^{2+} can lead to Ca^{2+} overload. The concomitant surge in ROS triggers oxidative stress, resulting in the opening of the mitochondrial permeability transition pore and caspase cascade activation, leading to cell death (77). TNF-α is a crucial pro-inflammatory factor involved in I/R injury and exacerbates cardiomyocyte death (135). Roberge et al.

(136) reported that TNF-α induces a nonspecific cation current in isolated adult mouse ventricular myocytes, which can be inhibited by TRPM2 inhibitors, namely, CTZ and FFA. TNF-α activation of PARP-1 and TRPM2 results in a significant influx of intracellular Ca^{2+}, potentially leading to mitochondrial Ca^{2+} overload, an increase in mitochondrial ROS, activation of caspase-8 and ultimately cardiomyocyte cell death (136). Conversely, inhibiting TRPM2 expression markedly reduces TNF-α-induced intracellular Ca^{2+} elevation and attenuates cardiomyocyte cell death. *In vivo* experiments revealed that, compared to WT mice, TRPM2-KO mice exhibited a significantly reduced myocardial infarct size and improved myocardial contractile function after left anterior descending coronary artery ligation and reperfusion. Additionally, the number of neutrophils and the activity of myeloperoxidase (MPO) in the I/R region were decreased. Neutrophils are a major source of pro-inflammatory mediators such as TNF-α and ROS, which exacerbate I/R-induced myocardial injury (137). These *in vivo* and *in vitro* findings indicate that TRPM2 plays a crucial role in mediating myocardial injury induced by I/R.

Depending on the severity and duration of ischemia, cerebral I/R can lead to varying degrees of neuronal dysfunction and death. Neuronal death during reperfusion, known as delayed neuronal death, is a major cause of ischemic brain injury (138). Studies have shown that TRPM2 activation plays a critical role in delayed neuronal death induced by I/R. During OGD/R, interventions with TRPM2 inhibitors ACA, CTZ, FFA, and 2-APB, as well as TRPM2-shRNA, significantly reduce cortical and hippocampal neuronal death and enhance cell viability (139–141). Studies have also demonstrated that genetic deletion of TRPM2 can alleviate hypoxic-ischemic brain injury in neonatal mice, characterized by reduced post-I/R cerebral infarct size and improved sensorimotor deficits (142). Of note, the efficacy of TRPM2 inhibition in ameliorating I/R brain injury appears to exhibit pronounced sex differences. Treatment with TRPM2 inhibitors, TRPM2-shRNA, or genetic ablation of TRPM2 expression did not significantly diminish delayed neuronal death in female mice following cardiac arrest-resuscitation (CA-R), reduce cerebral infarction in female mice subjected to middle cerebral artery occlusion-reperfusion (MCAO-R), or decrease delayed neuronal death in female mouse cortical and hippocampal neurons induced by OGD/R *in vitro* (139–141). The mechanistic basis for these gender-dependent disparities in treatment efficacy remains unclear, possibly related to differential hormone levels, higher male sensitivity to ADPR (143), or activation of distinct downstream signaling pathways following I/R.

Ischemic stroke manifests as focal cerebral ischemia, characterized by excessive release of the neurotransmitter glutamate, leading to overactivation of NMDA receptors and subsequent neuronal intracellular Ca^{2+} overload along with excessive ROS production (144). Studies have demonstrated the pivotal role of NMDA receptor expression and downstream signaling in TRPM2-mediated cerebral ischemic stroke (144, 145). In the hippocampal neurons of TRPM2-deficient mice, the expression of the N-methyl-D-aspartate receptor (NMDAR) subunit GluN2A is significantly upregulated, while the expression of GluN2B decreases. The activation of TRPM2 has dual effects on neuronal survival following brain I/R. On the one hand, TRPM2 activation inhibits GluN2A activity, leading to a reduction in Ca^{2+} influx through GluN2A and suppressing downstream pro-survival signaling pathways, including the PI3K-Akt pathway and MAPKK-ERK1/2 pathway. This inhibition results in an increased expression of the pro-apoptotic factor GSK-3β downstream of protein kinase B (Akt). On the other hand, TRPM2 activation promotes an increase in the postsynaptic density protein 95 expression, consequently activating the GluN2B subunit. This activation, in turn, induces cell death by inhibiting the phosphorylation of ERK1/2. The combined action of these mechanisms mediated by TRPM2 contributes to neuronal death following brain I/R (146, 147). Recent studies have found that TRPM2 can directly interact with GluN2A, selectively increasing the activity and the surface expression of NMDAR subunits by recruiting PKCγ (148). TRPM2 enhances NMDAR-induced excitotoxicity through its physical and functional coupling with extrasynaptic NMDARs. Interventions targeting the uncoupling of TRPM2-NMDAR can effectively mitigate ischemic stroke damage (149). Additionally, uncoupling TRPM2 from PKCγ has been shown to reduce excitotoxicity and neuronal death in both *in vitro* and *in vivo* experiments. Thus, the TRPM2-PKCγ uncoupling may also represent an effective therapeutic strategy for reducing NMDAR-mediated excitotoxicity in ischemic stroke (150). Research has found that TRPM2 in brain endothelial cells exacerbates neuronal death during ischemic stroke by promoting Ca^{2+} influx and interacting with CD36, thereby disrupting the blood-brain barrier (BBB). Specific knockout or inhibition of TRPM2 expression in endothelial cells results in reduced infarct size, decreased immune cell infiltration, and suppressed oxidative stress. Thus, TRPM2 in endothelial cells may represent a safer and more effective therapeutic target for ischemic stroke (151). Additionally, the highly neurotoxic Zn^{2+} may also play a role in TRPM2-mediated I/R brain injury. Furthermore, the significantly neurotoxic Zn^{2+} may also contribute to TRPM2-mediated I/R brain injury. Ye et al. (152) demonstrated using both *in vivo* and ex vivo brain I/R models that elevated intracellular levels of ROS and Zn^{2+} following brain I/R are critical contributors to the death of pyramidal neurons in the hippocampal CA1 region. TRPM2 KO significantly inhibited the increase in intracellular Zn^{2+}, reduced ROS levels, decreased the number of damaged or dead hippocampal pyramidal neurons, and markedly improved the 72-hour survival rate in mice, suggesting that TRPM2 activation leads to excessive intracellular Zn^{2+}, which targets mitochondria, causing mitochondrial dysfunction and increased ROS production, ultimately resulting in neuronal death (152). Further studies have identified a positive correlation between infarct volume and bilirubin levels in both stroke patients and mouse stroke models. Bilirubin has been found to act as an endogenous agonist of TRPM2, specifically binding to and activating the channel, thereby exacerbating brain damage during ischemic stroke. Targeting the blockade of TRPM2 channels from binding with bilirubin may represent an effective therapeutic strategy to mitigate and prevent stroke-related brain injury (58).

Murat et al. (153) research found that renal I/R induces damage to both glomeruli and renal tubules in rats, leading to elevated levels of malondialdehyde, caspase-3 and oxidative stress index (OSI)

within renal tissues. Concurrently, the activity of the antioxidant enzyme catalase (CAT) and the total antioxidant capacity decreased. Intraperitoneal administration of the TRPM2 inhibitor ACA resulted in a reduction of oxidative stress levels and an enhancement of antioxidant capacity in renal tissues, thereby improving the aforementioned renal I/R injuries. Research indicates that bilateral renal I/R induces tissue damage, functional impairment, inflammatory cell infiltration, and apoptosis in the kidneys of WT mice (154). However, in TRPM2-KO mice and those injected with 2-APB, there is an increased expression of anti-apoptotic proteins Bcl-2 and Bcl-xL, leading to significant mitigation of the aforementioned tissue damage. The study reveals a novel mechanism of TRPM2-mediated renal I/R injury, suggesting that I/R promotes an increase in Ras-related C3 botulinum toxin substrate 1(RAC1) levels and NOX activation in renal cells. RAC1 physically interacts with TRPM2, enhancing its expression, while also increasing NADPH oxidase activity. This cascade activates TRPM2 via the PARP/ADPR pathway, leading to apoptosis through the activation of caspase-3 and caspase-9, ultimately resulting in renal cell death and kidney injury (154).

Scholars have also investigated the role of TRPM2 in Hepatic I/R. TRPM2-mediated Ca^{2+} influx induces mitochondrial Ca^{2+} overload through the mitochondrial calcium uniporter (MCU), leading to an increase in the expression of arachidonate 12-lipoxygenase and the occurrence of mitochondrial lipid peroxidation and ferroptosis. Inhibition of TRPM2 by using a TRPM2 inhibitor alleviates such I/R-induced damage (155). Using TRPM2-deficient mice or siRNA-mediated TRPM2 knockdown mitigates hepatic I/R injuries (121, 156). These studies indicate that inhibiting the expression of TRPM2 may serve as an effective therapeutic strategy for diseases related to hepatic I/R injury, such as during liver transplantation.

6.2 The positive role of TRPM2 in cardiac I/R

However, other research suggests that the absence of TRPM2 exacerbates cardiac I/R injury. TRPM2 may protect the heart from I/R injury by improving mitochondrial dysfunction, maintaining cellular bioenergetics and reducing ROS levels (27, 28, 157, 158). Compared with healthy hearts, the expression of TRPM2 is significantly reduced in the cardiac tissues of patients with heart failure, indirectly supporting the hypothesis that TRPM2 has a cardioprotective effect (22). The expression of TRPM2 can also ameliorate doxorubicin-induced cardiac dysfunction and prolong the survival time of animals following doxorubicin intervention (158). Miller et al. (27)revealed that TRPM2 KO myocytes exhibited increased production of ROS when subjected to I/R. Simultaneously, antioxidant capacity significantly decreased, characterized by reduced expression of SOD and its upstream regulatory factors such as HIF-1α and FoxO3a; meanwhile, NADPH oxidase, which is involved in ROS generation, increased. These findings indicate that TRPM2 can protect myocytes from I/R and oxidative stress damage. This protective effect is associated with the reduction of ROS generation and enhanced antioxidant capacity in myocytes lacking TRPM2. Researchers employed proteomic techniques to explore the mechanisms by which the TRPM2 channel protects cardiomyocytes from I/R and oxidative stress damage. The most pronounced variances observed in canonical pathways between the hearts of mice with or without TRPM2 KO post I/R are associated with mitochondrial dysfunction and alterations in the tricarboxylic acid cycle. In TRPM2 KO mice, mitochondrial respiratory chain complexes I, III, and IV are downregulated, and the expression of complexes II and V is upregulated. The immunoblotting results confirmed the decreased expression of NDUFA4L2 and BNIP3. The myocardium of TRPM2 KO mice not only exhibited reduced ATP levels and oxygen consumption but also decreased ψm and a significant increase in ROS levels. The study suggests that the TRPM2 channel protects the heart from I/R injury by improving mitochondrial dysfunction and reducing ROS levels (157). Miller et al. (28) further investigated post I/R and WT mice hearts; the myocardium of TRPM2 KO mice exhibited a significant reduction in the expression of Pyk2 and its downstream pro-survival signaling molecules, pERK1/2, and pAkt. Following I/R in TRPM2 KO myocardial cells, ψm significantly decreased; patch clamp experiments revealed decreased activity of MCU, indicating a decline in mitochondrial Ca^{2+} uptake capacity. Simultaneously, ATP levels decreased, and ROS levels significantly increased. The activation of TRPM2-induced Ca^{2+} influx ameliorated these adverse reactions. Hence, TRPM2-mediated Ca^{2+} influx phosphorylates Pyk2, thereby enhancing mitochondrial calcium uptake and ATP generation capabilities after Pyk2 translocates to the mitochondria. Furthermore, Pyk2 protects the heart from I/R and oxidative stress injury by activating downstream pro-survival signaling pathways such as Akt and ERK1/2 (28).

In summary, the TRPM2 channel plays a crucial role in I/R, that is, it exacerbates and mitigates effects on I/R injury (Figure 5). In brain I/R, as typified by ischemic stroke, TRPM2 activation has been found to mediate brain injury through multiple mechanisms. These include increasing neurotoxicity via direct and indirect interactions with NMDA receptors, disrupting the BBB through interactions with CD36, and causing intracellular Ca^{2+} and Zn^{2+} overload, leading to oxidative stress. In renal I/R, TRPM2 disrupts redox balance and activates the caspase cascade, resulting in apoptosis and renal cell death. In hepatic I/R, TRPM2 activation mediates Ca^{2+} overload, which is associated with lipid peroxidation and ferroptosis. Thus, inhibiting TRPM2 expression may be a potential therapeutic target for treating these I/R-related diseases, offering new directions and strategies for clinical treatment. In myocardial I/R, TRPM2 appears to have dual and opposing effects. Some researchers posit that TRPM2 is crucial for mediating I/R-induced myocardial injury. Conversely, other studies suggest that TRPM2 may protect tissues from I/R injury by regulating Ca^{2+} influx, improving mitochondrial function, maintaining bioenergetics, and reducing ROS levels. The role of TRPM2 in myocardial I/R remains a contentious issue. Current research suggests that discrepancies in experimental results may be attributed to several factors: differences in mouse I/R models, with longer I/R times potentially causing more severe myocardial damage; variations in assessment methods; and differing experimental conditions, such as the use of different anesthetics (pentobarbital and isoflurane) and surgical techniques (open vs. closed chest surgery

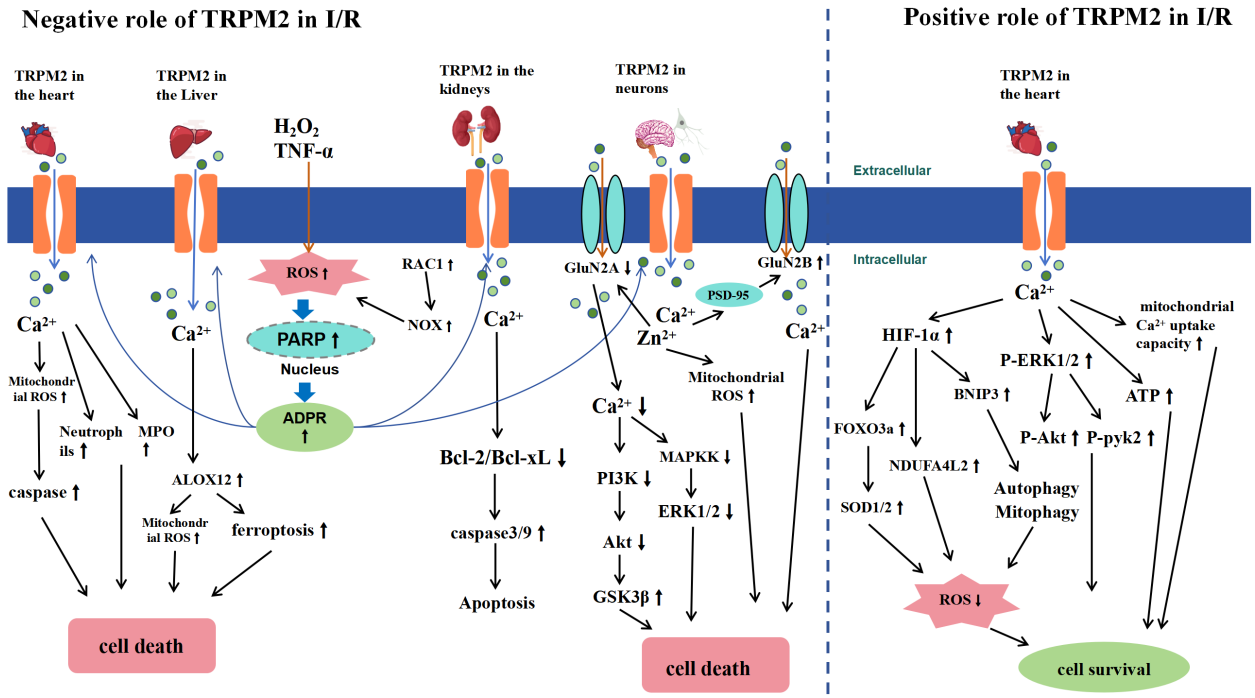

FIGURE 5
Schematic Representation of TRPM2-Mediated Signaling Pathways in Ischemia-Reperfusion (I/R) Injury. The left half of the diagram illustrates the negative effects of TRPM2 activation during I/R. I/R induces extracellular H2O2 or TNF-α, leading to intracellular ROS accumulation (RAC1-induced ROS accumulation occurs only in renal I/R). This accumulation activates nuclear PARP and PARG enzymes, converting NAD^+ to ADPR, subsequently activating TRPM2. The activation of TRPM2 results in a significant influx of Ca^{2+} and Zn^{2+}, which leads to cell death by increasing neutrophils, myeloperoxidase (MPO), and caspase in cardiomyocytes, inducing arachidonate 12-lipoxygenase (ALOX12) expression in the liver, increasing Bcl-2 and Bcl-xL expression in the kidney, and causing mitochondrial ROS accumulation and NMDA receptor activation in neurons, thereby inhibiting the downstream pro-survival signals of the Akt and ERK1/2 pathways. The right half of the diagram illustrates the positive effects of TRPM2 activation during I/R. TRPM2-mediated Ca^{2+} influx improves mitochondrial function, enhances ATP production, and reduces ROS levels by activating HIF-1α/-2α and ERK1/2 signaling pathways, thus protecting cardiomyocytes from I/R injury.

in mice). Future research should aim to standardize experimental design and conditions to clarify the specific role of TRPM2 in myocardial I/R. Overall, TRPM2 channels exhibit diverse biological effects in I/R injury, making them a focal point in the development of therapeutic strategies for related diseases.

7 Conclusion and future perspectives

The role of TRPM2 in physiological and pathological processes such as oxidative stress, inflammation and I/R is complex and multifaceted. The activation of TRPM2 leads to cation influx and exerts a dual effect by modulating downstream pathways; that is, it exerts protective and deleterious effects during cellular injury. The observed differences, and even contradictory results, in the experiments are speculated to be associated with several factors. Firstly, cell types, animal models and experimental conditions varied across different studies. Secondly, the diverse functional roles and outcomes of the TRPM2 channel may exhibit tissue-specific differences. Additionally, the intricate biological networks and signaling pathways involved in processes such as oxidative stress, inflammation and I/R could contribute to the diverse effects of TRPM2 channel activation. Finally, discrepancies in research outcomes may be attributed to differences in research methodologies and experimental techniques, including distinct knockout methods and the use of various pharmacological agents for interventions. Achieving a comprehensive understanding of the physiological and pathological roles of TRPM2 requires consistent experimental designs and further in-depth investigations.

Future investigations into the bidirectional role of TRPM2 in oxidative stress, inflammation, and I/R are essential for understanding its specific mechanistic contributions to neurodegenerative diseases characterized by chronic oxidative stress and inflammation, inflammatory bowel diseases, and I/R-related conditions such as myocardial infarction and stroke. To better utilize TRPM2 channels for therapeutic interventions in relevant diseases, the development of specific TRPM2 channel inhibitors is imperative. For instance, the non-specific inhibitor 2-APB, commonly used in many experiments, also affects other TRP channels, either inhibiting (e.g., TRPV6) (159) or activating (e.g., TRPV2) (160) them, thus potentially compromising the accuracy and consistency of experimental outcomes. Recent studies have shown promising outcomes in experimental settings with newly synthesized TRPM2-specific inhibitors, as well as interfering peptides designed to disrupt TRPM2 interactions with specific proteins. These research findings are exciting as they provide

powerful tools for further investigating the functional mechanisms of the TRPM2 pathway in future studies. Given the widespread expression of TRPM2 across various tissues and cells, including neurons, liver cells, cardiac myocytes, and immune cells, alongside the complex downstream signaling pathways associated with TRPM2, achieving a balance in the activation or inhibition of TRPM2 among different tissue cells to modulate physiological and pathological processes poses a challenging issue. Future research focusing on developing therapeutic strategies targeting specific intracellular signaling pathways in certain tissue cells holds great promise. Considering the bidirectional regulatory nature of TRPM2 channels, caution must be exercised in formulating treatment plans targeting TRPM2 as a therapeutic target until the precise effects of its activation or inhibition in different disease states are fully understood. In conclusion, research on TRPM2 channels is still in its exploratory phase, and future endeavors will further advance our understanding of this channel, providing new promising targets for the treatment of related diseases.

Author contributions

PH: Writing – original draft, Writing – review & editing. CQ: Writing – review & editing. ZR: Writing – review & editing. DW: Writing – review & editing. JZ: Conceptualization, Funding acquisition, Supervision, Writing – review & editing.

Funding

The author(s) declare financial support was received for the research, authorship, and/or publication of this article. This work was supported by Project 24-28 Supported by the Fundamental Research Funds for the China Institute of Sport Science, the National Natural Science Foundation of China (Nos.31371195 and 11775059), the National Key Technology R&D Program of China (Nos.2019YFF0301600), and the Doctoral Research Initiation Fund Project of Hebei Normal University (L2024B35).

Conflict of interest

The authors declare that the research was conducted in the absence of any commercial or financial relationships that could be construed as a potential conflict of interest.

Publisher's note

References

1. Hardie RC, Raghu P, Moore S, Juusola M, Baines RA, Sweeney ST. Calcium influx via TRP channels is required to maintain PIP2 levels in Drosophila photoreceptors. *Neuron*. (2001) 30:149–59. doi: 10.1016/S0896-6273(01)00269-0

2. Owsianik G, Talavera K, Voets T, Nilius B. Permeation and selectivity of TRP channels. *Annu Rev Physiol*. (2006) 68:685–717. doi: 10.1146/annurev.physiol.68.040204.101406

3. Jiang LH, Yang W, Zou J, Beech DJ. TRPM2 channel properties, functions and therapeutic potentials. *Expert Opin Ther Targets*. (2010) 14:973–88. doi: 10.1517/14728222.2010.510135

4. Clapham DE. TRP channels as cellular sensors. *Nature*. (2003) 426:517–24. doi: 10.1038/nature02196

5. Venkatachalam K, Montell C. TRP channels. *Annu Rev Biochem*. (2007) 76:387–417. doi: 10.1146/annurev.biochem.75.103004.142819

6. Song K, Wang H, Kamm GB, Pohle J, Reis FC, Heppenstall P, et al. The TRPM2 channel is a hypothalamic heat sensor that limits fever and can drive hypothermia. *Science*. (2016) 353:1393–98. doi: 10.1126/science.aaf7537

7. Kamm GB, Boffi JC, Zuza K, Nencini S, Campos J, Schrenk-Siemens K, et al. A synaptic temperature sensor for body cooling. *Neuron*. (2021) 109:3283–97.e11. doi: 10.1016/j.neuron.2021.10.001

8. Ying Y, Gong L, Tao X, Ding J, Chen N, Yao Y, et al. Genetic knockout of TRPM2 increases neuronal excitability of hippocampal neurons by inhibiting Kv7 channel in epilepsy. *Mol Neurobiol*. (2022) 59:6918–33. doi: 10.1007/s12035-022-02993-2

9. Miller BA, Cheung JY. TRPM2 protects against tissue damage following oxidative stress and ischaemia-reperfusion. *J Physiol*. (2016) 594:4181–91. doi: 10.1113/JP270934

10. Chen SJ, Bao L, Keefer K, Shanmughapriya S, Chen L, Lee J, et al. Transient receptor potential ion channel TRPM2 promotes AML proliferation and survival through modulation of mitochondrial function, ROS, and autophagy. *Cell Death Dis*. (2020) 11:247. doi: 10.1038/s41419-020-2454-8

11. Montell C, Birnbaumer L, Flockerzi V, Bindels RJ, Bruford EA, Caterina MJ, et al. A unified nomenclature for the superfamily of TRP cation channels. *Mol Cell*. (2002) 9:229–31. doi: 10.1016/S1097-2765(02)00448-3

12. Fonfria E, Murdock PR, Cusdin FS, Benham CD, Kelsell RE, Mcnulty S. Tissue distribution profiles of the human TRPM cation channel family. *J Recept Signal Transduct Res*. (2006) 26:159–78. doi: 10.1080/10799890600637506

13. Yue Z, Xie J, Yu AS, Stock J, Du J, Yue L. Role of TRP channels in the cardiovascular system. *Am J Physiol Heart Circ Physiol*. (2015) 308:H157–82. doi: 10.1152/ajpheart.00457.2014

14. Kheradpezhouh E, Ma L, Morphett A, Barritt GJ, Rychkov GY. TRPM2 channels mediate acetaminophen-induced liver damage. *Proc Natl Acad Sci U.S.A*. (2014) 111:3176–81. doi: 10.1073/pnas.1322657111

15. Sawamura S, Shirakawa H, Nakagawa T, Mori Y, Kaneko S. TRP channels in the brain: what are they there for? In: TIn: Emir TLR, editor. *Neurobiology of TRP Channels*. CRC Press/Taylor & Francis, Boca Raton (FL (2017). p. Chapter 16.

16. Turlova E, Feng ZP, Sun HS. The role of TRPM2 channels in neurons, glial cells and the blood-brain barrier in cerebral ischemia and hypoxia. *Acta Pharmacol Sin*. (2018) 39:713–21. doi: 10.1038/aps.2017.194

17. Haraguchi K, Kawamoto A, Isami K, Maeda S, Kusano A, Asakura K, et al. TRPM2 contributes to inflammatory and neuropathic pain through the aggravation of pronociceptive inflammatory responses in mice. *J Neurosci*. (2012) 32:3931–41. doi: 10.1523/JNEUROSCI.4703-11.2012

18. Ostapchenko VG, Chen M, Guzman MS, Xie YF, Lavine N, Fan J, et al. The transient receptor potential melastatin 2 (TRPM2) channel contributes to β-amyloid oligomer-related neurotoxicity and memory impairment. *J Neurosci*. (2015) 35:15157–69. doi: 10.1523/JNEUROSCI.4081-14.2015

19. Hecquet CM, Ahmmed GU, Vogel SM, Malik AB. Role of TRPM2 channel in mediating H2O2-induced Ca2+ entry and endothelial hyperpermeability. *Circ Res*. (2008) 102:347–55. doi: 10.1161/CIRCRESAHA.107.160176

20. Zou J, Ainscough JF, Yang W, Sedo A, Yu SP, Mei ZZ, et al. A differential role of macrophage TRPM2 channels in Ca^{2+} signaling and cell death in early responses to H_2O_2. *Am J Physiol Cell Physiol*. (2013) 305:C61–9. doi: 10.1152/ajpcell.00390.2012

21. Faouzi M, Penner R. TRPM2. *Handb Exp Pharmacol*. (2014) 222:403–26. doi: 10.1007/978-3-642-54215-2_16

22. Morine KJ, Paruchuri V, Qiao X, Aronovitz M, Huggins GS, Denofrio D, et al. Endoglin selectively modulates transient receptor potential channel expression in left and right heart failure. *Cardiovasc Pathol*. (2016) 25:478–82. doi: 10.1016/j.carpath.2016.08.004

23. Knowles H, Heizer JW, Li Y, Chapman K, Ogden CA, Andreasen K, et al. Transient Receptor Potential Melastatin 2 (TRPM2) ion channel is required for innate immunity against Listeria monocytogenes. *Proc Natl Acad Sci U.S.A*. (2011) 108:11578–83. doi: 10.1073/pnas.1010678108

24. Knowles H, Li Y, Perraud AL. The TRPM2 ion channel, an oxidative stress and metabolic sensor regulating innate immunity and inflammation. *Immunol Res*. (2013) 55:241–8. doi: 10.1007/s12026-012-8373-8

25. Bai JZ, Lipski J. Differential expression of TRPM2 and TRPV4 channels and their potential role in oxidative stress-induced cell death in organotypic hippocampal culture. *Neurotoxicology*. (2010) 31:204–14. doi: 10.1016/j.neuro.2010.01.001

26. Di A, Gao XP, Qian F, Kawamura T, Han J, Hecquet C, et al. The redox-sensitive cation channel TRPM2 modulates phagocyte ROS production and inflammation. *Nat Immunol*. (2011) 13:29–34. doi: 10.1038/ni.2171

27. Miller BA, Wang J, Hirschler-Laszkiewicz I, Gao E, Song J, Zhang XQ, et al. The second member of transient receptor potential-melastatin channel family protects hearts from ischemia-reperfusion injury. *Am J Physiol Heart Circ Physiol*. (2013) 304:H1010–22. doi: 10.1152/ajpheart.00906.2012

28. Miller BA, Wang J, Song J, Zhang XQ, Hirschler-Laszkiewicz I, Shanmughapriya S, et al. Trpm2 enhances physiological bioenergetics and protects against pathological oxidative cardiac injury: Role of Pyk2 phosphorylation. *J Cell Physiol*. (2019) 234:15048–60. doi: 10.1002/jcp.28146

29. Beceiro S, Radin JN, Chatuvedi R, Piazuelo MB, Horvarth DJ, Cortado H, et al. TRPM2 ion channels regulate macrophage polarization and gastric inflammation during Helicobacter pylori infection. *Mucosal Immunol*. (2017) 10:493–507. doi: 10.1038/mi.2016.60

30. Nagamine K, Kudoh J, Minoshima S, Kawasaki K, Asakawa S, Ito F, et al. Molecular cloning of a novel putative Ca2+ channel protein (TRPC7) highly expressed in brain. *Genomics*. (1998) 54:124–31. doi: 10.1006/geno.1998.5551

31. Perraud AL, Schmitz C, Scharenberg AM. TRPM2 Ca2+ permeable cation channels: from gene to biological function. *Cell Calcium*. (2003) 33:519–31. doi: 10.1016/S0143-4160(03)00057-5

32. Mei ZZ, Xia R, Beech DJ, Jiang LH. Intracellular coiled-coil domain engaged in subunit interaction and assembly of melastatin-related transient receptor potential channel 2. *J Biol Chem*. (2006) 281:38748–56. doi: 10.1074/jbc.M607591200

33. Fujiwara Y, Minor DL Jr. X-ray crystal structure of a TRPM assembly domain reveals an antiparallel four-stranded coiled-coil. *J Mol Biol*. (2008) 383:854–70. doi: 10.1016/j.jmb.2008.08.059

34. Yu P, Xue X, Zhang J, Hu X, Wu Y, Jiang LH, et al. Identification of the ADPR binding pocket in the NUDT9 homology domain of TRPM2. *J Gen Physiol*. (2017) 149:219–35. doi: 10.1085/jgp.201611675

35. Perraud AL, Fleig A, Dunn CA, Bagley LA, Launay P, Schmitz C, et al. ADP-ribose gating of the calcium-permeable LTRPC2 channel revealed by Nudix motif homology. *Nature*. (2001) 411:595–9. doi: 10.1038/35079100

36. Sano Y, Inamura K, Miyake A, Mochizuki S, Yokoi H, Matsushime H, et al. Immunocyte Ca2+ influx system mediated by LTRPC2. *Science*. (2001) 293:1327–30. doi: 10.1126/science.1062473

37. Huang Y, Winkler PA, Sun W, Lü W, Du J. Architecture of the TRPM2 channel and its activation mechanism by ADP-ribose and calcium. *Nature*. (2018) 562:145–49. doi: 10.1038/s41586-018-0558-4

38. Jiang LH. Subunit interaction in channel assembly and functional regulation of transient receptor potential melastatin (TRPM) channels. *Biochem Soc Trans*. (2007) 35:86–8. doi: 10.1042/BST0350086

39. Hara Y, Wakamori M, Ishii M, Maeno E, Nishida M, Yoshida T, et al. LTRPC2 Ca2+-permeable channel activated by changes in redox status confers susceptibility to cell death. *Mol Cell*. (2002) 9:163–73. doi: 10.1016/S1097-2765(01)00438-5

40. Kashio M, Sokabe T, Shintaku K, Uematsu T, Fukuta N, Kobayashi N, et al. Redox signal-mediated sensitization of transient receptor potential melastatin 2 (TRPM2) to temperature affects macrophage functions. *Proc Natl Acad Sci U.S.A*. (2012) 109:6745–50. doi: 10.1073/pnas.1114193109

41. Togashi K, Hara Y, Tominaga T, Higashi T, Konishi Y, Mori Y, et al. TRPM2 activation by cyclic ADP-ribose at body temperature is involved in insulin secretion. *EMBO J*. (2006) 25:1804–15. doi: 10.1038/sj.emboj.7601083

42. Perraud AL, Takanishi CL, Shen B, Kang S, Smith MK, Schmitz C, et al. Accumulation of free ADP-ribose from mitochondria mediates oxidative stress-induced gating of TRPM2 cation channels. *J Biol Chem*. (2005) 280:6138–48. doi: 10.1074/jbc.M411446200

43. Tóth B, Csanády L. Identification of direct and indirect effectors of the transient receptor potential melastatin 2 (TRPM2) cation channel. *J Biol Chem*. (2010) 285:30091–102. doi: 10.1074/jbc.M109.066464

44. Shen BW, Perraud AL, Scharenberg A, Stoddard BL. The crystal structure and mutational analysis of human NUDT9. *J Mol Biol*. (2003) 332:385–98. doi: 10.1016/S0022-2836(03)00954-9

45. Esposito E, Cuzzocrea S. Superoxide NO. peroxynitrite and PARP in circulatory shock and inflammation. *Front Biosci (Landmark Ed)*. (2009) 14:263–96. doi: 10.2741/3244

46. Fauzee NJ, Pan J, Wang YL. PARP and PARG inhibitors–new therapeutic targets in cancer treatment. *Pathol Oncol Res*. (2010) 16:469–78. doi: 10.1007/s12253-010-9266-6

47. Miller BA. Inhibition of TRPM2 function by PARP inhibitors protects cells from oxidative stress-induced death. *Br J Pharmacol*. (2004) 143:515–6. doi: 10.1038/sj.bjp.0705923

48. Starkus J, Beck A, Fleig A, Penner R. Regulation of TRPM2 by extra- and intracellular calcium. *J Gen Physiol*. (2007) 130:427–40. doi: 10.1085/jgp.200709836

49. Wang L, Fu TM, Zhou Y, Xia S, Greka A, Wu H. Structures and gating mechanism of human TRPM2. *Science*. (2018) 362(6421):eaav4809. doi: 10.1126/science.aav4809

50. Huang Y, Roth B, Lü W, Du J. Ligand recognition and gating mechanism through three ligand-binding sites of human TRPM2 channel. *Elife*. (2019) 8:e50175. doi: 10.7554/eLife.50175

51. Zhang Z, Tóth B, Szollosi A, Chen J, Csanády L. Structure of a TRPM2 channel in complex with Ca(2+) explains unique gating regulation. *Elife*. (2018) 7:e36409. doi: 10.7554/eLife.36409

52. Tóth B, Csanády L. Pore collapse underlies irreversible inactivation of TRPM2 cation channel currents. *Proc Natl Acad Sci U.S.A*. (2012) 109:13440–5. doi: 10.1073/pnas.1204702109

53. Barth D, Lückhoff A, Kühn FJP. Species-specific regulation of TRPM2 by PI(4,5)P(2) via the membrane interfacial cavity. *Int J Mol Sci*. (2021) 22(9):4637. doi: 10.3390/ijms22094637

54. Du J, Xie J, Yue L. Intracellular calcium activates TRPM2 and its alternative spliced isoforms. *Proc Natl Acad Sci U.S.A*. (2009) 106:7239–44. doi: 10.1073/pnas.0811725106

55. Heiner I, Eisfeld J, Warnstedt M, Radukina N, Jüngling E, Lückhoff A. Endogenous ADP-ribose enables calcium-regulated cation currents through TRPM2 channels in neutrophil granulocytes. *Biochem J*. (2006) 398:225–32. doi: 10.1042/BJ20060183

56. Yu P, Liu Z, Yu X, Ye P, Liu H, Xue X, et al. Direct Gating of the TRPM2 Channel by cADPR via Specific Interactions with the ADPR Binding Pocket. *Cell Rep*. (2019) 27:3684–95.e4. doi: 10.1016/j.celrep.2019.05.067

57. Riekehr WM, Sander S, Pick J, Tidow H, Bauche A, Guse AH, et al. cADPR does not activate TRPM2. *Int J Mol Sci*. (2022) 23(6):3163. doi: 10.3390/ijms23063163

58. Liu HW, Gong LN, Lai K, Yu XF, Liu ZQ, Li MX, et al. Bilirubin gates the TRPM2 channel as a direct agonist to exacerbate ischemic brain damage. *Neuron*. (2023) 111:1609–25.e6. doi: 10.1016/j.neuron.2023.02.022

59. Tóth B, Iordanov I, Csanády L. Ruling out pyridine dinucleotides as true TRPM2 channel activators reveals novel direct agonist ADP-ribose-2'-phosphate. *J Gen Physiol*. (2015) 145:419–30. doi: 10.1085/jgp.201511377

60. Fliegert R, Bauche A, Wolf Pérez AM, Watt JM, Rozewitz MD, Winzer R, et al. 2'-Deoxyadenosine 5'-diphosphoribose is an endogenous TRPM2 superagonist. *Nat Chem Biol*. (2017) 13:1036–44. doi: 10.1038/nchembio.2415

61. Dröge W. Free radicals in the physiological control of cell function. *Physiol Rev*. (2002) 82:47–95. doi: 10.1152/physrev.00018.2001

62. Hecquet CM, Zhang M, Mittal M, Vogel SM, Di A, Gao X, et al. Cooperative interaction of trp melastatin channel transient receptor potential (TRPM2) with its splice variant TRPM2 short variant is essential for endothelial cell apoptosis. *Circ Res*. (2014) 114:469–79. doi: 10.1161/CIRCRESAHA.114.302414

63. Hermosura MC, Cui AM, Go RC, Davenport B, Shetler CM, Heizer JW, et al. Altered functional properties of a TRPM2 variant in Guamanian ALS and PD. *Proc Natl Acad Sci U.S.A*. (2008) 105:18029–34. doi: 10.1073/pnas.0808218105

64. Zhong J, Amina S, Liang M, Akther S, Yuhi T, Nishimura T, et al. Cyclic ADP-Ribose and Heat Regulate Oxytocin Release via CD38 and TRPM2 in the Hypothalamus during Social or Psychological Stress in Mice. *Front Neurosci*. (2016) 10:304. doi: 10.3389/fnins.2016.00304

65. Li Y, Jiao J. Deficiency of TRPM2 leads to embryonic neurogenesis defects in hyperthermia. *Sci Adv*. (2020) 6:eaay6350. doi: 10.1126/sciadv.aay6350

66. Yang W, Manna PT, Zou J, Luo J, Beech DJ, Sivaprasadarao A, et al. Zinc inactivates melastatin transient receptor potential 2 channels via the outer pore. *J Biol Chem*. (2011) 286:23789–98. doi: 10.1074/jbc.M111.247478

67. Cheung JY, Miller BA. Transient receptor potential-melastatin channel family member 2: friend or foe. *Trans Am Clin Climatol Assoc*. (2017) 128:308–29.

68. Starkus JG, Fleig A, Penner R. The calcium-permeable non-selective cation channel TRPM2 is modulated by cellular acidification. *J Physiol*. (2010) 588:1227–40. doi: 10.1113/jphysiol.2010.187476

69. Du J, Xie J, Yue L. Modulation of TRPM2 by acidic pH and the underlying mechanisms for pH sensitivity. *J Gen Physiol*. (2009) 134:471–88. doi: 10.1085/jgp.200910254

70. Georgiou CD, Margaritis LH. Oxidative stress and NADPH oxidase: connecting electromagnetic fields, cation channels and biological effects. *Int J Mol Sci*. (2021) 22(18):10041. doi: 10.3390/ijms221810041

71. Averill-Bates D. Reactive oxygen species and cell signaling. Review. *Biochim Biophys Acta Mol Cell Res*. (2024) 1871:119573. doi: 10.1016/j.bbamcr.2023.119573

72. Tello D, Balsa E, Acosta-Iborra B, Fuertes-Yebra E, Elorza A, Ordóñez Á, et al. Induction of the mitochondrial NDUFA4L2 protein by HIF-1α decreases oxygen consumption by inhibiting Complex I activity. *Cell Metab*. (2011) 14:768–79. doi: 10.1016/j.cmet.2011.10.008

73. Wehage E, Eisfeld J, Heiner I, Jüngling E, Zitt C, Lückhoff A. Activation of the cation channel long transient receptor potential channel 2 (LTRPC2) by hydrogen peroxide. A splice variant reveals a mode of activation independent of ADP-ribose. *J Biol Chem*. (2002) 277:23150–6. doi: 10.1074/jbc.M112096200

74. Zhang W, Chu X, Tong Q, Cheung JY, Conrad K, Masker K, et al. A novel TRPM2 isoform inhibits calcium influx and susceptibility to cell death. *J Biol Chem*. (2003) 278:16222–9. doi: 10.1074/jbc.M300298200

75. Badr H, Kozai D, Sakaguchi R, Numata T, Mori Y. Different contribution of redox-sensitive transient receptor potential channels to acetaminophen-induced death of human hepatoma cell line. *Front Pharmacol*. (2016) 7:19. doi: 10.3389/fphar.2016.00019

76. Wang Q, Guo W, Hao B, Shi X, Lu Y, Wong CW, et al. Mechanistic study of TRPM2-Ca(2+)-CAMK2-BECN1 signaling in oxidative stress-induced autophagy inhibition. *Autophagy*. (2016) 12:1340–54. doi: 10.1080/15548627.2016.1187365

77. Yang KT, Chang WL, Yang PC, Chien CL, Lai MS, Su MJ, et al. Activation of the transient receptor potential M2 channel and poly(ADP-ribose) polymerase is involved in oxidative stress-induced cardiomyocyte death. *Cell Death Differ*. (2006) 13:1815–26. doi: 10.1038/sj.cdd.4401813

78. Sun L, Yau HY, Wong WY, Li RA, Huang Y, Yao X. Role of TRPM2 in H(2)O (2)-induced cell apoptosis in endothelial cells. *PloS One*. (2012) 7:e43186. doi: 10.1371/journal.pone.0043186

79. Deshpande SS, Angkeow P, Huang J, Ozaki M, Irani K. Rac1 inhibits TNF-alpha-induced endothelial cell apoptosis: dual regulation by reactive oxygen species. *FASEB J*. (2000) 14:1705–14. doi: 10.1096/fj.99-0910com

80. Fonfria E, Marshall IC, Boyfield I, Skaper SD, Hughes JP, Owen DE, et al. Amyloid beta-peptide(1-42) and hydrogen peroxide-induced toxicity are mediated by TRPM2 in rat primary striatal cultures. *J Neurochem*. (2005) 95:715–23. doi: 10.1111/j.1471-4159.2005.03396.x

81. Li X, Yang W, Jiang LH. Alteration in intracellular Zn(2+) homeostasis as a result of TRPM2 channel activation contributes to ROS-induced hippocampal neuronal death. *Front Mol Neurosci*. (2017) 10:414. doi: 10.3389/fnmol.2017.00414

82. Kaneko S, Kawakami S, Hara Y, Wakamori M, Itoh E, Minami T, et al. A critical role of TRPM2 in neuronal cell death by hydrogen peroxide. *J Pharmacol Sci*. (2006) 101:66–76. doi: 10.1254/jphs.FP0060128

83. Yu B, Jin L, Yao X, Zhang Y, Zhang G, Wang F, et al. TRPM2 protects against cisplatin-induced acute kidney injury and mitochondrial dysfunction via modulating autophagy. *Theranostics*. (2023) 13:4356–75. doi: 10.7150/thno.84655

84. Alves-Lopes R, Lacchini S, Neves KB, Harvey A, Montezano AC, Touyz RM. Vasoprotective effects of NOX4 are mediated via polymerase and transient receptor potential melastatin 2 cation channels in endothelial cells. *J Hypertens*. (2023) 41:1389–400. doi: 10.1097/HJH.0000000000003478

85. Chung WS, Welsh CA, Barres BA, Stevens B. Do glia drive synaptic and cognitive impairment in disease? *Nat Neurosci*. (2015) 18:1539–45. doi: 10.1038/nn.4142

86. Urrutia PJ, Hirsch EC, González-Billault C, Núñez MT. Hepcidin attenuates amyloid beta-induced inflammatory and pro-oxidant responses in astrocytes and microglia. *J Neurochem*. (2017) 142:140–52. doi: 10.1111/jnc.14005

87. Daulatzai MA. Fundamental role of pan-inflammation and oxidative-nitrosative pathways in neuropathogenesis of Alzheimer's disease in focal cerebral ischemic rats. *Am J Neurodegener Dis*. (2016) 5:102–30.

88. Cooper AJ, Kristal BS. Multiple roles of glutathione in the central nervous system. *Biol Chem*. (1997) 378:793–802.

89. Belrose JC, Xie YF, Gierszewski LJ, Macdonald JF, Jackson MF. Loss of glutathione homeostasis associated with neuronal senescence facilitates TRPM2 channel activation in cultured hippocampal pyramidal neurons. *Mol Brain*. (2012) 5:11. doi: 10.1186/1756-6606-5-11

90. Butterfield DA, Drake J, Pocernich C, Castegna A. Evidence of oxidative damage in Alzheimer's disease brain: central role for amyloid beta-peptide. *Trends Mol Med*. (2001) 7:548–54. doi: 10.1016/S1471-4914(01)02173-6

91. Balaban H, Nazıroğlu M, Demirci K, Övey İS. The protective role of selenium on scopolamine-induced memory impairment, oxidative stress, and apoptosis in aged rats: the involvement of TRPM2 and TRPV1 channels. *Mol Neurobiol*. (2017) 54:2852–68. doi: 10.1007/s12035-016-9835-0

92. Kurz AF. Uncommon neurodegenerative causes of dementia. *Int Psychogeriatr*. (2005) 17 Suppl 1:S35–49. doi: 10.1017/S1041610205001936

93. Nishimura I, Takazaki R, Kuwako K, Enokido Y, Yoshikawa K. Upregulation and antiapoptotic role of endogenous Alzheimer amyloid precursor protein in dorsal root ganglion neurons. *Exp Cell Res*. (2003) 286:241–51. doi: 10.1016/S0014-4827(03)00066-1

94. Nazıroğlu M. TRPM2 cation channels, oxidative stress and neurological diseases: where are we now? *Neurochem Res*. (2011) 36:355–66. doi: 10.1007/s11064-010-0347-4

95. Li X, Jiang LH. Multiple molecular mechanisms form a positive feedback loop driving amyloid β42 peptide-induced neurotoxicity via activation of the TRPM2 channel in hippocampal neurons. *Cell Death Dis*. (2018) 9:195. doi: 10.1038/s41419-018-0270-1

96. Park L, Wang G, Moore J, Girouard H, Zhou P, Anrather J, et al. The key role of transient receptor potential melastatin-2 channels in amyloid-β-induced neurovascular dysfunction. *Nat Commun*. (2014) 5:5318. doi: 10.1038/ncomms6318

97. Xu C, Macciardi F, Li PP, Yoon IS, Cooke RG, Hughes B, et al. Association of the putative susceptibility gene, transient receptor potential protein melastatin type 2, with bipolar disorder. *Am J Med Genet B Neuropsychiatr Genet*. (2006) 141b:36–43. doi: 10.1002/ajmg.b.30239

98. Mcquillin A, Bass NJ, Kalsi G, Lawrence J, Puri V, Choudhury K, et al. Fine mapping of a susceptibility locus for bipolar and genetically related unipolar affective disorders, to a region containing the C21ORF29 and TRPM2 genes on chromosome 21q22.3. *Mol Psychiatry*. (2006) 11:134–42. doi: 10.1038/sj.mp.4001759

99. Xie YF, Belrose JC, Lei G, Tymianski M, Mori Y, Macdonald JF, et al. Dependence of NMDA/GSK-3β mediated metaplasticity on TRPM2 channels at hippocampal CA3-CA1 synapses. *Mol Brain*. (2011) 4:44. doi: 10.1186/1756-6606-4-44

100. Sun Y, Sukumaran P, Selvaraj S, Cilz NI, Schaar A, Lei S, et al. TRPM2 promotes neurotoxin MPP(+)/MPTP-induced cell death. *Mol Neurobiol*. (2018) 55:409–20. doi: 10.1007/s12035-016-0338-9

101. Manna PT, Munsey TS, Abuarab N, Li F, Asipu A, Howell G, et al. TRPM2-mediated intracellular Zn2+ release triggers pancreatic β-cell death. *Biochem J*. (2015) 466:537–46. doi: 10.1042/BJ20140747

102. Ishii M, Hagiwara T, Mori Y, Shimizu S. Involvement of TRPM2 and L-type Ca^{2+} channels in Ca^{2+} entry and cell death induced by hydrogen peroxide in rat β-cell line RIN-5F. *J Toxicol Sci*. (2014) 39:199–209. doi: 10.2131/jts.39.199

103. Chen SJ, Zhang W, Tong Q, Conrad K, Hirschler-Laszkiewicz I, Bayerl M, et al. Role of TRPM2 in cell proliferation and susceptibility to oxidative stress. *Am J Physiol Cell Physiol*. (2013) 304:C548–60. doi: 10.1152/ajpcell.00069.2012

104. Chang H, Zou Z. Targeting autophagy to overcome drug resistance: further developments. *J Hematol Oncol*. (2020) 13:159. doi: 10.1186/s13045-020-01000-2

105. Auberger P, Puissant A. Autophagy, a key mechanism of oncogenesis and resistance in leukemia. *Blood*. (2017) 129:547–52. doi: 10.1182/blood-2016-07-692707

106. Piya S, Andreeff M, Borthakur G. Targeting autophagy to overcome chemoresistance in acute myleogenous leukemia. *Autophagy*. (2017) 13:214–15. doi: 10.1080/15548627.2016.1245263

107. Kania E, Pająk B, Orzechowski A. Calcium homeostasis and ER stress in control of autophagy in cancer cells. *BioMed Res Int*. (2015) 2015:352794. doi: 10.1155/2015/352794

108. Bao L, Chen SJ, Conrad K, Keefer K, Abraham T, Lee JP, et al. Depletion of the human ion channel TRPM2 in neuroblastoma demonstrates its key role in cell survival through modulation of mitochondrial reactive oxygen species and bioenergetics. *J Biol Chem*. (2016) 291:24449–64. doi: 10.1074/jbc.M116.747147

109. Almasi S, Kennedy BE, El-Aghil M, Sterea AM, Gujar S, Partida-Sánchez S, et al. TRPM2 channel-mediated regulation of autophagy maintains mitochondrial function and promotes gastric cancer cell survival via the JNK-signaling pathway. *J Biol Chem*. (2018) 293:3637–50. doi: 10.1074/jbc.M117.817635

110. Nathan C, Cunningham-Bussel A. Beyond oxidative stress: an immunologist's guide to reactive oxygen species. *Nat Rev Immunol*. (2013) 13:349–61. doi: 10.1038/nri3423

111. Yang Y, Bazhin AV, Werner J, Karakhanova S. Reactive oxygen species in the immune system. *Int Rev Immunol*. (2013) 32:249–70. doi: 10.3109/08830185.2012.755176

112. Morris G, Gevezova M, Sarafian V, Maes M. Redox regulation of the immune response. *Cell Mol Immunol*. (2022) 19:1079–101. doi: 10.1038/s41423-022-00902-0

113. Yamamoto S, Shimizu S, Kiyonaka S, Takahashi N, Wajima T, Hara Y, et al. TRPM2-mediated Ca2+influx induces chemokine production in monocytes that aggravates inflammatory neutrophil infiltration. *Nat Med*. (2008) 14:738–47. doi: 10.1038/nm1758

114. Zhou R, Yazdi AS, Menu P, Tschopp J. A role for mitochondria in NLRP3 inflammasome activation. *Nature*. (2011) 469:221–5. doi: 10.1038/nature09663

115. Wang L, Negro R, Wu H. TRPM2, linking oxidative stress and Ca(2+) permeation to NLRP3 inflammasome activation. *Curr Opin Immunol*. (2020) 62:131–35. doi: 10.1016/j.coi.2020.01.005

116. Tseng HH, Vong CT, Kwan YW, Lee SM, Hoi MP. TRPM2 regulates TXNIP-mediated NLRP3 inflammasome activation via interaction with p47 phox under high glucose in human monocytic cells. *Sci Rep*. (2016) 6:35016. doi: 10.1038/srep35016

117. Maliougina M, El Hiani Y. TRPM2: bridging calcium and ROS signaling pathways-implications for human diseases. *Front Physiol*. (2023) 14:1217828. doi: 10.3389/fphys.2023.1217828

118. Massullo P, Sumoza-Toledo A, Bhagat H, Partida-Sánchez S. TRPM channels, calcium and redox sensors during innate immune responses. *Semin Cell Dev Biol*. (2006) 17:654–66. doi: 10.1016/j.semcdb.2006.11.006

119. Chen C, Zhu T, Gong L, Hu Z, Wei H, Fan J, et al. Trpm2 deficiency in microglia attenuates neuroinflammation during epileptogenesis by upregulating autophagy via the AMPK/mTOR pathway. *Neurobiol Dis*. (2023) 186:106273. doi: 10.1016/j.nbd.2023.106273

120. Shao Y, Chen C, Zhu T, Sun Z, Li S, Gong L, et al. TRPM2 contributes to neuroinflammation and cognitive deficits in a cuprizone-induced multiple sclerosis model via NLRP3 inflammasome. *Neurobiol Dis*. (2021) 160:105534. doi: 10.1016/j.nbd.2021.105534

121. Zhang T, Huang W, Ma Y. Down-regulation of TRPM2 attenuates hepatic ischemia/reperfusion injury through activation of autophagy and inhibition of NLRP3 inflammasome pathway. *Int Immunopharmacol*. (2022) 104:108443. doi: 10.1016/j.intimp.2021.108443

122. Huang W, Wu Y, Luo N, Shuai X, Guo J, Wang C, et al. Identification of TRPM2 as a prognostic factor correlated with immune infiltration in ovarian cancer. *J Ovarian Res*. (2023) 16:169. doi: 10.1186/s13048-023-01225-y

123. Wang G, Cao L, Liu X, Sieracki NA, Di A, Wen X, et al. Oxidant sensing by TRPM2 inhibits neutrophil migration and mitigates inflammation. *Dev Cell*. (2016) 38:453–62. doi: 10.1016/j.devcel.2016.07.014

124. Qian X, Numata T, Zhang K, Li C, Hou J, Mori Y, et al. Transient receptor potential melastatin 2 protects mice against polymicrobial sepsis by enhancing bacterial clearance. *Anesthesiology*. (2014) 121:336–51. doi: 10.1097/ALN.0000000000000275

125. Qian X, Cheng H, Chen X. Transient receptor potential melastatin 2-mediated heme oxygenase-1 has a role for bacterial clearance by regulating autophagy in peritoneal macrophages during polymicrobial sepsis. *Innate Immun*. (2019) 25:530–38. doi: 10.1177/1753425919875796

126. Iles KE, Forman HJ. Macrophage signaling and respiratory burst. *Immunol Res*. (2002) 26:95–105. doi: 10.1385/IR:26:1-3

127. Gwinn MR, Vallyathan V. Respiratory burst: role in signal transduction in alveolar macrophages. *J Toxicol Environ Health B Crit Rev*. (2006) 9:27–39. doi: 10.1080/15287390500196081

128. Zhang Z, Cui P, Zhang K, Chen Q, Fang X. Transient receptor potential melastatin 2 regulates phagosome maturation and is required for bacterial clearance in Escherichia coli sepsis. *Anesthesiology*. (2017) 126:128–39. doi: 10.1097/ALN.0000000000001430

129. Qian X, Zhao H, Chen X, Li J. Disruption of transient receptor potential melastatin 2 decreases elastase release and bacterial clearance in neutrophils. *Innate Immun*. (2018) 24:122–30. doi: 10.1177/1753425918759181

130. Robledo-Avila FH, Ruiz-Rosado JD, Brockman KL, Partida-Sánchez S. The TRPM2 ion channel regulates inflammatory functions of neutrophils during listeria monocytogenes infection. *Front Immunol*. (2020) 11:97. doi: 10.3389/fimmu.2020.00097

131. Eltzschig HK, Eckle T. Ischemia and reperfusion–from mechanism to translation. *Nat Med*. (2011) 17:1391–401. doi: 10.1038/nm.2507

132. Przykaza Ł. Understanding the connection between common stroke comorbidities, their associated inflammation, and the course of the cerebral ischemia/reperfusion cascade. *Front Immunol*. (2021) 12:782569. doi: 10.3389/fimmu.2021.782569

133. Jiménez-Castro MB, Cornide-Petronio ME, Gracia-Sancho J, Peralta C. Inflammasome-mediated inflammation in liver ischemia-reperfusion injury. *Cells*. (2019) 8(10):1131. doi: 10.3390/cells8101131

134. Stanley BA, Sivakumaran V, Shi S, Mcdonald I, Lloyd D, Watson WH, et al. Thioredoxin reductase-2 is essential for keeping low levels of H(2)O(2) emission from isolated heart mitochondria. *J Biol Chem*. (2011) 286:33669–77. doi: 10.1074/jbc.M111.284612

135. Kleinbongard P, Schulz R, Heusch G. TNFα in myocardial ischemia/reperfusion, remodeling and heart failure. *Heart Fail Rev*. (2011) 16:49–69. doi: 10.1007/s10741-010-9180-8

136. Roberge S, Roussel J, Andersson DC, Meli AC, Vidal B, Blandel F, et al. TNF-α-mediated caspase-8 activation induces ROS production and TRPM2 activation in adult ventricular myocytes. *Cardiovasc Res*. (2014) 103:90–9. doi: 10.1093/cvr/cvu112

137. Hiroi T, Wajima T, Negoro T, Ishii M, Nakano Y, Kiuchi Y, et al. Neutrophil TRPM2 channels are implicated in the exacerbation of myocardial ischaemia/reperfusion injury. *Cardiovasc Res*. (2013) 97:271–81. doi: 10.1093/cvr/cvs332

138. Lipton P. Ischemic cell death in brain neurons. *Physiol Rev*. (1999) 79:1431–568. doi: 10.1152/physrev.1999.79.4.1431

139. Jia J, Verma S, Nakayama S, Quillinan N, Grafe MR, Hurn PD, et al. Sex differences in neuroprotection provided by inhibition of TRPM2 channels following experimental stroke. *J Cereb Blood Flow Metab*. (2011) 31:2160–8. doi: 10.1038/jcbfm.2011.77

140. Verma S, Quillinan N, Yang YF, Nakayama S, Cheng J, Kelley MH, et al. TRPM2 channel activation following in *vitro* ischemia contributes to male hippocampal cell death. *Neurosci Lett*. (2012) 530:41–6. doi: 10.1016/j.neulet.2012.09.044

141. Shimizu T, Macey TA, Quillinan N, Klawitter J, Perraud AL, Traystman RJ, et al. Androgen and PARP-1 regulation of TRPM2 channels after ischemic injury. *J Cereb Blood Flow Metab*. (2013) 33:1549–55. doi: 10.1038/jcbfm.2013.105

142. Huang S, Turlova E, Li F, Bao MH, Szeto V, Wong R, et al. Transient receptor potential melastatin 2 channels (TRPM2) mediate neonatal hypoxic-ischemic brain injury in mice. *Exp Neurol*. (2017) 296:32–40. doi: 10.1016/j.expneurol.2017.06.023

143. Lang JT, Mccullough LD. Pathways to ischemic neuronal cell death: are sex differences relevant? *J Transl Med*. (2008) 6:33. doi: 10.1186/1479-5876-6-33

144. Ge Y, Chen W, Axerio-Cilies P, Wang YT. NMDARs in cell survival and death: implications in stroke pathogenesis and treatment. *Trends Mol Med*. (2020) 26:533–51. doi: 10.1016/j.molmed.2020.03.001

145. Xu J, Zhang W, Dong J, Cao L, Huang Z. A new potential strategy for treatment of ischemic stroke: targeting TRPM2-NMDAR association. *Neurosci Bull*. (2023) 39:703–06. doi: 10.1007/s12264-022-00971-1

146. Alim I, Teves L, Li R, Mori Y, Tymianski M. Modulation of NMDAR subunit expression by TRPM2 channels regulates neuronal vulnerability to ischemic cell death. *J Neurosci*. (2013) 33:17264–77. doi: 10.1523/JNEUROSCI.1729-13.2013

147. Lai TW, Zhang S, Wang YT. Excitotoxicity and stroke: identifying novel targets for neuroprotection. *Prog Neurobiol*. (2014) 115:157–88. doi: 10.1016/j.pneurobio.2013.11.006

148. Tymianski M. Emerging mechanisms of disrupted cellular signaling in brain ischemia. *Nat Neurosci*. (2011) 14:1369–73. doi: 10.1038/nn.2951

149. Zong P, Feng J, Yue Z, Li Y, Wu G, Sun B, et al. Functional coupling of TRPM2 and extrasynaptic NMDARs exacerbates excitotoxicity in ischemic brain injury. *Neuron*. (2022) 110:1944–58.e8. doi: 10.1016/j.neuron.2022.03.021

150. Zong P, Feng J, Legere N, Li Y, Yue Z, Li CX, et al. TRPM2 enhances ischemic excitotoxicity by associating with PKCγ. *Cell Rep*. (2024) 43:113722. doi: 10.1016/j.celrep.2024.113722

151. Zong P, Feng J, Li CX, Jellison ER, Yue Z, Miller B, et al. Activation of endothelial TRPM2 exacerbates blood-brain barrier degradation in ischemic stroke. *Cardiovasc Res*. (2024) 120:188–202. doi: 10.1093/cvr/cvad126

152. Ye M, Yang W, Ainscough JF, Hu XP, Li X, Sedo A, et al. TRPM2 channel deficiency prevents delayed cytosolic Zn2+ accumulation and CA1 pyramidal neuronal death after transient global ischemia. *Cell Death Dis*. (2014) 5:e1541. doi: 10.1038/cddis.2014.494

153. Çakır M, Tekin S, Taşlıdere A, Çakan P, Düzova H, Gül CC. Protective effect of N-(p-amylcinnamoyl) anthranilic acid, phospholipase A(2) enzyme inhibitor, and transient receptor potential melastatin-2 channel blocker against renal ischemia-reperfusion injury. *J Cell Biochem*. (2019) 120:3822–32. doi: 10.1002/jcb.27664

154. Gao G, Wang W, Tadagavadi RK, Briley NE, Love MI, Miller BA, et al. TRPM2 mediates ischemic kidney injury and oxidant stress through RAC1. *J Clin Invest*. (2014) 124:4989–5001. doi: 10.1172/JCI76042

155. Zhong C, Yang J, Zhang Y, Fan X, Fan Y, Hua N, et al. TRPM2 Mediates Hepatic Ischemia-Reperfusion Injury via Ca(2+)-Induced Mitochondrial Lipid Peroxidation through Increasing ALOX12 Expression. *Res (Wash D C)*. (2023) 6:159. doi: 10.34133/research.0159

156. Li Y, Ren Z, Xu Y, Wu S. Role of transient receptor potential cation channel subfamily M member 2 in hepatic ischemia-reperfusion injury in the mouse and the underlying mechanisms. *Zhong Nan Da Xue Xue Bao Yi Xue Ban*. (2020) 45:766–73. doi: 10.11817/j.issn.1672-7347.2020.190064

157. Miller BA, Hoffman NE, Merali S, Zhang XQ, Wang J, Rajan S, et al. TRPM2 channels protect against cardiac ischemia-reperfusion injury: role of mitochondria. *J Biol Chem*. (2014) 289:7615–29. doi: 10.1074/jbc.M113.533851

158. Hoffman NE, Miller BA, Wang J, Elrod JW, Rajan S, Gao E, et al. Ca^{2+} entry via Trpm2 is essential for cardiac myocyte bioenergetics maintenance. *Am J Physiol Heart Circ Physiol*. (2015) 308:H637–50. doi: 10.1152/ajpheart.00720.2014

159. Singh AK, Saotome K, Mcgoldrick LL, Sobolevsky AI. Structural bases of TRP channel TRPV6 allosteric modulation by 2-APB. *Nat Commun*. (2018) 9:2465. doi: 10.1038/s41467-018-04828-y

160. Gochman A, Tan XF, Bae C, Chen H, Swartz KJ, Jara-Oseguera A. Cannabidiol sensitizes TRPV2 channels to activation by 2-APB. *Elife*. (2023) 12:e86166. doi: 10.7554/eLife.86166

frontiers | Frontiers in Immunology

TYPE Review
PUBLISHED 19 September 2024
DOI 10.3389/fimmu.2024.1449126

OPEN ACCESS

EDITED BY
Wai Po Chong,
Hong Kong Baptist University, China

REVIEWED BY
Rayees Sheikh,
Indian Institute of Integrative Medicine (CSIR), India
Ron Piran,
Bar-Ilan University, Israel

*CORRESPONDENCE
Lin Wang
lkzwl@126.com
Mao Lin
linmao@wchscu.edu.cn

RECEIVED 14 June 2024
ACCEPTED 03 September 2024
PUBLISHED 19 September 2024

CITATION
Xu K, Wang L, Lin M and He G (2024) Update on protease-activated receptor 2 in inflammatory and autoimmune dermatological diseases.
Front. Immunol. 15:1449126.
doi: 10.3389/fimmu.2024.1449126

Update on protease-activated receptor 2 in inflammatory and autoimmune dermatological diseases

Kejia Xu[1,2], Lin Wang[1,2*], Mao Lin[1*] and Gu He[1,2]

[1]Department of Dermatology, West China Hospital, Sichuan University, Chengdu, China, [2]Laboratory of Dermatology, Clinical Institute of Inflammation and Immunology, Frontiers Science Center for Disease Related Molecular Network and State Key Laboratory of Biotherapy, West China Hospital, Sichuan University, Chengdu, China

Protease-activated receptor 2 (PAR2) is a cell-surface receptor expressed in various cell types, including keratinocytes, neurons, immune and inflammatory cells. Activation of PAR2, whether via its canonical or biased pathways, triggers a series of signaling cascades that mediate numerous functions. This review aims to highlight the emerging roles and interactions of PAR2 in different skin cells. It specifically summarizes the latest insights into the roles of PAR2 in skin conditions such as atopic dermatitis (AD), psoriasis, vitiligo and melasma. It also considers these roles from the perspective of the cutaneous microenvironment in relation to other inflammatory and autoimmune dermatological disorders. Additionally, the review explores PAR2's involvement in associated comorbidities from both cutaneous and extracutaneous diseases. Therefore, PAR2 may serve as a key target for interactions among various cells within the local skin environment.

KEYWORDS

protease-activated receptor 2, signaling, immunity, inflammatory dermatological disease, comorbidity

1 Introduction

Protease-activated receptor 2 (PAR2), first described in 1994 (1), is a versatile transmembrane receptor that senses and responds to active proteases in the cellular microenvironment. As a member of protease-activated receptor and a subfamily of G protein-coupled receptors (GPCRs), PAR2 shares several common structural features including an extracellular NH2-terminal domain, seven transmembrane helices, three extracellular loops, three intracellular loops, and an intracellular COOH terminus (2). Uniquely, PAR2 can be activated by various proteases from both endogenous sources (e.g.trypsin, mast cell-derived tryptase, kallikrein-related peptidases (KLKs), and coagulation proteases (3) such as thrombin, Factor Xa (FXa), FVIIa, FIXa), as well as

membrane-type serine protease-1, human airway trypsin-like protease) and exogenous sources (e.g. bacteria, house dust mite (HDM), cockroaches, pollens, and molds), leading to a multitude of biological effects across various tissues and organ systems (4). To date, PAR2 has been widely expressed on epithelial cells, immune cells, neurons and so on, playing a critical role in homeostasis and in various disease processes, including asthma, lung injury, inflammatory bowel diseases, irritable bowel syndrome, neurogenic inflammation and cancer. In the skin and its microenvironment, functional PAR2 is primarily expressed in epidermal keratinocytes (KCs), and neighboring cells such as mast cells, eosinophils, neutrophils, dendritic cells, T cells and neurons, also exhibit PAR2 expression. Proteases like Der p3 and Der p9 from HDM (5), Per a7 from cockroaches allergens (6), KLK5, KLK14, trypsin are notable for proteolyzing PAR2, thereby mediating epidermal barrier homeostasis, innate and adaptive immunity, leukocyte recruitment, pigmentation, tumorigenesis and cutaneous paresthesia (7). Indeed, PAR2 appears to have a significant role in atopic dermatitis (AD), psoriasis, vitiligo, melasma, non-histaminergic pruritic skin disorders, syringoma and squamous cell carcinoma (4). Given the growing attention on inflammatory and autoimmune dermatological illnesses and their various cutaneous and extracutaneous comorbidities, PAR2 is considered a key target for facilitating cross-communication among different cells and tissues.

Previous reviews have examined the impacts of PAR2 on skin physiology and pathology (8, 9), however, to our knowledge, the detailed roles of PAR2 in inflammatory and autoimmune dermatological diseases have not yet been thoroughly investigated considering novel developments and emerging discoveries. Understanding the intricate connections, such as those involving resident skin cells and neurons expressing PAR2, could clarify the pathogenesis of diseases like AD, psoriasis, and vitiligo. Therefore, this review focuses on the latest updates on PAR2 and its potential effects in various cutaneous diseases from the perspective of the local cutaneous microenvironment. The dysregulation and abnormal expression of PAR2 in the cutaneous milieu may promote disease progression through cell-surface interactions, integration of extracellular signals, and induction of intracellular signaling pathways.

2 Activation, signaling and trafficking of PAR2

2.1 Protease-stimulated PAR2 activation

PAR2, a cell-surface receptor, primarily undergoes activation through proteolytic cleavage, which exposes a tethered ligand at specific extracellular N-terminal sites. The residues exposed from this cleavage bind to an extracellular docking domain, inducing a conformational change that triggers intracellular signaling. This proteolytic process, extensively studied and known as "canonical activation" was initially shown to involve trypsin cleaving mouse PAR2 at Arg^{38}/Ser^{39} and human PAR2 at Arg^{36}/Ser^{37}, thereby exposing the tethered ligands SLIGRL and SLIGKV, respectively (10). Subsequent research have identified other serine proteases, including tryptase, KLK4, KLK5, KLK14, Thrombin (11), FVIIa, FIXa and FXa, which also hydrolyze PAR2 at canonical sites with slight variations (12) (Figure 1A). "Noncanonical activation" describes the selective activation of specific intracellular signaling pathways by distinct ligands that cleave at biased sites or cause a conformational change in the receptor sufficient for activation (Figure 1B). These cleavage sites are either proximal or distal to the canonical sites (13). For instance, cysteine proteases Legumain and Cathepsin S cleave PAR2 at Asn^{30}/Arg^{31} (proximity) and Glu^{56}/Thr^{57} (distality), thus exposing distinct tethered ligands RSSKGR and TVFSVDEFSA, respectively (14, 15). Elastase similarly activates PAR2 by cleaving the receptor at Ser^{67}/Val^{68} in the extracellular N-terminal region (15). Additionally, the serine protease chymase disrupts intestinal epithelial barrier via a biased mechanism by cleaving PAR2 at Gly^{35}/Arg^{36} (16). In a previous study by Dulon et al (17), Pseudomonas aeruginosa cleaved PAR2 at Ser^{37}/Leu^{38}, thereby revealing LIGKV and disrupting the canonical tethered ligand. Similarly, Rayees et al. discovered later that pseudomonas aeruginosa interacted with alveolar macrophages, activating PAR2 and thereby affecting the macrophages' ability to phagocytize the bacteria (18) (Figure 1C). Synthetic peptides, known as activating peptides, can activate PAR2 directly without proteolysis, mimicking the activation pathways mentioned above. They have been designed to mimic the effects of proteases, facilitate the investigation of PAR2 functions and develop selective ligands (agonists or antagonists). Given the varying effects of different ligands on PAR2, biased signaling is likely to be preferred for developing targeted drugs (19). Therefore, multiple natural and corresponding synthetic ligands can activate PAR2 at biased sites.

2.2 Signaling

Upon activation, PAR2 initiates multiple signaling cascades essential for maintaining homeostasis in physiological and pathological processes (Figure 2A). These cascades regulate cytokine production, stimulate angiogenesis, and promote inflammatory and immune responses (20). The downstream signaling pathways are complex and varied based on factors including specific hydrolytic positions, types, kinetics, potency, and post-translational modifications of PAR2. For example, at a concentration of 1 nM, tryptase efficiently cleaved the PAR2 at Arg^{36}/Ser^{37}. However, at 100 nM, while tryptase still cleaved at this site, it could target additional sites, potentially inhibiting the efficiency of PAR2 activation (21). The glycosylation of PAR2 may impact its susceptibility to tryptase activation. Key phosphorylation sites ($Ser^{383\text{-}385}$, Ser^{387}-Thr^{392}) on the C-tail and the palmitoylation site (Cys^{361}) on helix-8 of PAR2 also influence subsequent intracellular signaling cascades (22). Proteolytic disarming of PAR2 at biased sites, achieved by permanently removing canonical proteolysis and destroying the tethered ligand sequence, further enhances signaling complexity due to alteration in the typical signaling response (17).

Activated PAR2 engages multiple G protein-dependent and β-arrestin-associated pathways. The Gα subunit and Gβγ dimers separate from heterotrimeric G proteins. Different Gα subtypes include $G\alpha_s$-regulated or Gαi-mediated AMP, $G\alpha_{12/13}$-dependent Rho-Kinase activity, and $G\alpha_q$-mediated Ca^{2+} release from the endoplasmic reticulum (23). In particular, once PAR2 is activated, rapid and transient $G\alpha_q$-regulated Ca^{2+} release occurs, leading to the phosphorylation of mitogen-activated protein kinases, such as ERK1/2, and PI3K/Akt signaling (24). Mutated versions of PAR2 can stimulate intracellular MAPK pathways without $G\alpha_q$ activation by cleaving other tethered ligands and corresponding soluble agonist peptides (25). The β-arrestin-associated signaling will be narrated in the next paragraph. Activation of PAR2 by trypsin results in Ca^{2+} mobilization, cAMP formation, and Rho-Kinase activity regulation by initiating $G\alpha_q$, $G\alpha_s$, $G\alpha_{12/13}$, and recruiting β-arrestin, therefore rendering PAR2 internalization and degradation. In contrast, Cathepsin S only stimulates $G\alpha_s$-mediated AMP formation, without $G\alpha_q$-dependent Ca^{2+} signaling or β-arrestin recruitment (26). Cathepsin S also interacts with PAR2 to trigger additional Ca^{2+}-dependent release through transient receptor potential (TRP) ion channels, bypassing the Gαq-mediated Ca^{2+} pathway in Xenopus laevis oocytes and mouse Dorsal Root Ganglion (DRG) neurons (15). Here, the Ca^{2+} released from intracellular stores, particularly from the Golgi apparatus upon PAR2 activation via trypsin, cathepsin-S, and neutrophil elastase, travels to the plasma membrane, where it plays a vital role in maintaining cellular signaling and ensuring the cell's responsiveness to extracellular cues. Elastase, cathepsin-G, and proteinase-3 fail to activate Gαq-coupled PAR2 calcium signaling, while Legumain and its activating peptide lack β-arrestin recruitment but still participate in other cellular signaling mechanisms (14). Therefore, the activation modes and distribution of PAR2 in different tissues and cell types further influence intracellular signaling pathways.

Furthermore, downstream signaling cascades of PAR2 include the interactions with other receptor tyrosine kinases (e.g. epidermal growth factor receptor, platelet-derived growth factor receptors, vascular endothelial growth factor), TRP ion channels (e.g. transient receptor potential vanilloid 1 (TRPV1), TRPV4, and transient

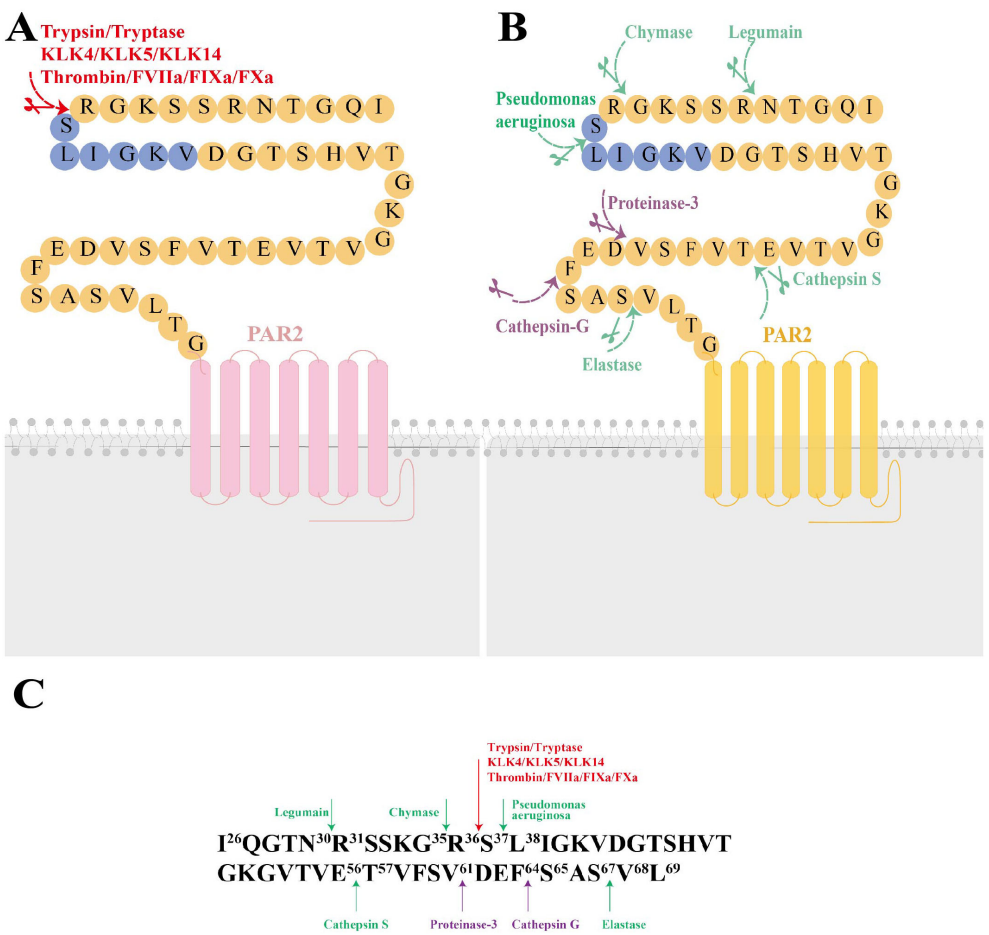

FIGURE 1
The molecular structure of Protease-Activated Receptor 2 (PAR2), its canonical and noncanonical activation mechanisms, and the responding proteases at the cleavage sites. **(A)** The molecular structure of PAR2 and its canonical activation by trypsin, tryptase, KLK4, KLK5, KLK14, FXa, FIXa, FVIIa, thrombin is illustrated. Canonical activation of PAR2 involves a proteolytic process that reveals the tethered ligand sequence at the Arg^{36}/Ser^{37} site (highlighted in red). **(B)** Noncanonical activation of PAR2 includes cleavage at biased sites (highlighted in green) or generates disarming changes (highlighted in purple). **(C)** major activating proteases and cleavage sites of PAR2. KLK4, kallikrein-related peptidase 4; KLK5, kallikrein-related peptidase 5; KLK14, kallikrein-related peptidase 14; FXα, Factor Xα; FIXa, Factor IXa; FVIIa, Factor VIIa.

10.3389/fimmu.2024.1449126

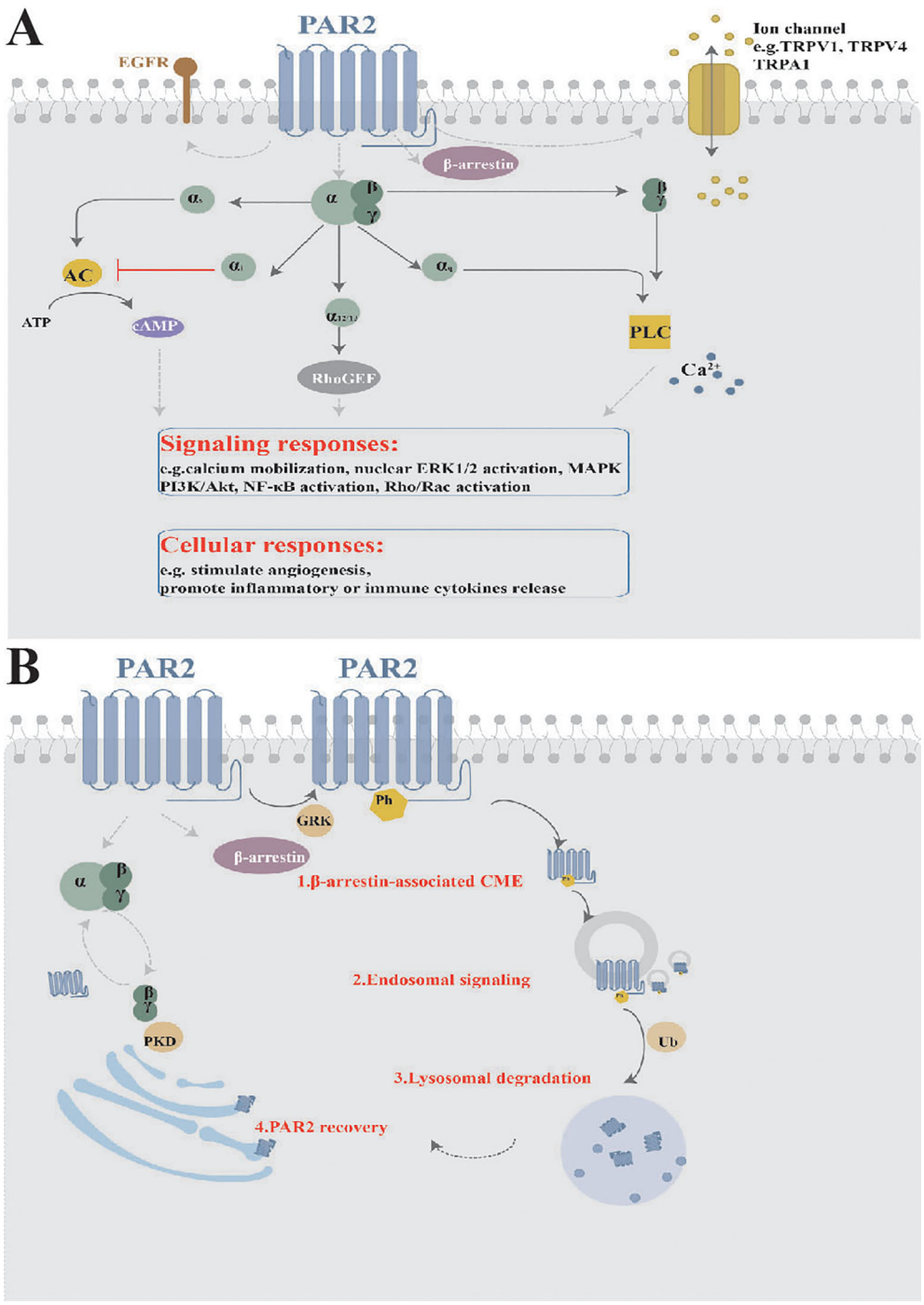

FIGURE 2
Signaling and Trafficking of PAR2. **(A)** Once activated, PAR2 initiates multiple downstream signaling cascades, including various intracellular signaling pathways, interactions with other receptor tyrosine kinases, and ion channel activation or releases, resulting in diverse cellular responses. **(B)** PAR2 trafficking involves processes such as endocytosis, degradation, and receptor recovery. MAPK, mitogen-activated protein kinases; EGFR, epidermal growth factor receptor; TRPV1, transient receptor potential vanilloid 1; TRPV4, transient receptor potential vanilloid 4; TRPA1, transient receptor potential ankyrin 1; NF-κB, nuclear factor kappa-B; PKD, Protein kinase D; GRK, G protein-coupled receptor (GPCR)-regulated kinase; CME, clathrin-mediated endocytosis; Ph, phosphorylation; Ub, ubiquitination.

receptor potential ankyrin 1 (TRPA1)), and alternative gene expression (e.g. NF-κB, Toll-like receptor 4 (TLR4)) (27–30). Numerous studies have shown that active PAR2 sensitizes TRPV1, TRPV4, and TRPA1 channels, which are responsible for neuro-inflammation and pain (31, 32). The interaction between PAR2 activation and TRP ion channels results in sustained Ca^{2+} influx from both the extracellular region and endoplasmic reticulum, elevating intracellular Ca^{2+} levels and exacerbating physiological and pathological effects. Moreover, microarray analysis has identified hundreds of genes downstream of PAR2

signaling related to cellular metabolism, cell cycle, MAPK pathway, inflammatory cytokines, and anti-complement function (33).

2.3 Trafficking

Upon interaction with pericellular proteases, PAR2 becomes rapidly desensitized and irreversibly hydrolyzed, rendering it unresponsive to similar proteases or their activating peptides. For example, treating neurons with PAR2 agonists results in desensitization of the receptor, abolishing its interaction with trypsin or tryptase (34). Additionally, PAR2 is predominantly phosphorylated at multiple COOH-terminal domains (e.g. Ser/Thr residues) by GPCR kinases, crucial for β-arrestin recruitment and receptor endocytosis (35). β-arrestin recruitment occurs within minutes of PAR2 activation (36). PAR2 then undergoes uncoupling and clathrin-mediated endocytosis (37), internalizing into early endosomes through Rab5a, causing sustained endosomal signaling (38). Finally, PAR2 is ubiquitinated and targeted to lysosomes for degradation (39). However, PAR2 can recover at the cell surface from the Golgi in Rab11-dependent, Gβγ and PKD dependent manner (40). The trafficking patterns are typical (Figure 2B), but biased activation proteases do not involve β-arrestin recruitment, indicating that PAR2 signaling transport is not fully elucidated.

In summary, the activation of PAR2 at different sites by endogenous and exogenous proteases results in various intracellular and extracellular signaling cascades. These processes enable the adjustment of cellular responses to microenvironmental variations. Interestingly, some reports have revealed that activating PAR2 also suppresses inflammation. Two studies clarified that PAR2 activated by thrombin inhibited calcium ion signaling thereby reducing TLR4-induced inflammatory signaling (11) and Pseudomonas aeruginosa bound to PAR2 enhanced the clearance of bacteria therefore preventing fatal outcomes in bacterial pneumonia separately (18). Both studies were particularly related to innate immunity. In addition, Dr. Ruf and his team developed PAR2 mutant mice, including PAR2-deficient (PAR2−/−) models, to study PAR2's specific roles in breast cancer progression, angiogenesis, diet-induced obesity and related metabolic disorders. Their studies are crucial for investigating biased PAR2 signaling and PAR2-dependent β-arrestin pathways, providing insight into PAR2's unique functions (41–43). From the above elaboration, We infer that PAR2 activation, whether through canonical or non-canonical pathways, can result in similar or opposing effects, depending on the activation mechanism, receptor cleavage sites, and downstream signaling. Thus, A deeper understanding these mechanisms could offer opportunities for developing targeted therapies, potentially improving treatment efficacy for diseases characterized by dysregulated PAR2 signaling.

3 Function of PAR2 in skin

PAR2 expression has been detected in a diverse set of cell types within the cutaneous microenvironment, such as keratinocytes in the epidermis, and mast cells, eosinophils together with neurons in the dermis and subcutaneous tissue (Figure 3A). These cells interact and collectively influence skin inflammation, immune response and itching sensations. In the following sections, we will delve into the different types of cells expressing PAR2 and their respective functions.

3.1 PAR2 in keratinocytes

Keratinocytes make up approximately 95% of the epidermis and play a major role in maintaining the epidermal permeability barrier, mediating inflammation and immune responses, and regulating pigmentation. In human keratinocytes, PAR2 expression is significantly higher in the granular layer and is further enhanced in inflamed skin (10). Importantly, PAR2 localizes to lipid rafts in both human and murine keratinocytes (44). Studies in mice have shown that strong PAR2 expression in the epidermis during embryonic development, starting as early as embryonic day 17 (45). Here, the role of PAR2 in keratinocytes and the possible effects PAR2 on them are summarized:1. Cutaneous Barrier Function: PAR2 expressed in KCs regulates the epidermal barrier by initiating cytoskeletal rearrangements, modifying plasma membrane dynamics in response to barrier disruptions. Moreover, application of SLIGRL (an exogenous PAR2 agonist) protects and rapidly repairs the skin barrier (46). 2. Inflammation and Immune Responses: PAR2 could activate a wide variety of inflammatory cytokines and chemokines following the disruption of the epidermal permeability barrier. Moniaga et al. (47) found that when disrupted epidermal barrier occurred, activation of PAR2 led to the production of thymic stromal lymphopoietin (TSLP), a Th2-skewing skin inflammation and basophil accumulation were subsequently observed. These processes were suppressed by a PAR2 antagonist. Similarly, epidermal KLK5 (a serine protease for PAR2) directly activated PAR2, leading to a Th2 environment because of a series of cytokines and chemokines production (e.g. IL-1, TNF-α, GM-CSF, TSLP) (48). Hou et al. also revealed that both trypsin and SLIGKV could stimulate the chemokines like IL-8 secretion (49). 3. Pigmentation Regulation: In the absence of PAR2 expression in melanocytes, the effects on pigmentation are therefore attributed to melanosome transfer and paracrine melanogenesis, which are mediated by keratinocyte-melanocyte interactions. Darker skin exhibits higher levels of epidermal PAR2 compared to lighter skin due to more remarkable melanocore and melanosomes uptake by keratinocyte phagocytosis (50, 51). Kim et al. discovered that PAR2 also induced melanogenesis by stimulating stem cell factor from keratinocytes (52). 4. Cell Proliferation and Differentiation: Activated PAR2 inhibits keratinocyte growth with growth factor-supplemented or growth factor-free conditions (53). However, the involvement of PAR2 in keratinocyte differentiation is equivocal. Some research suggests that PAR2 activation promotes differentiation, while others indicate opposite outcomes. As the same study by Derian et al., both SLIGRL (a PAR2 selective agonist) and SFLLRN (a PAR2 stimulator) decreased differentiation by low expression of involucrin and transglutaminase type I (differentiation markers of keratinocytes) (53). Another study demonstrated that in primary human keratinocytes, decreased markers of differentiation were observed

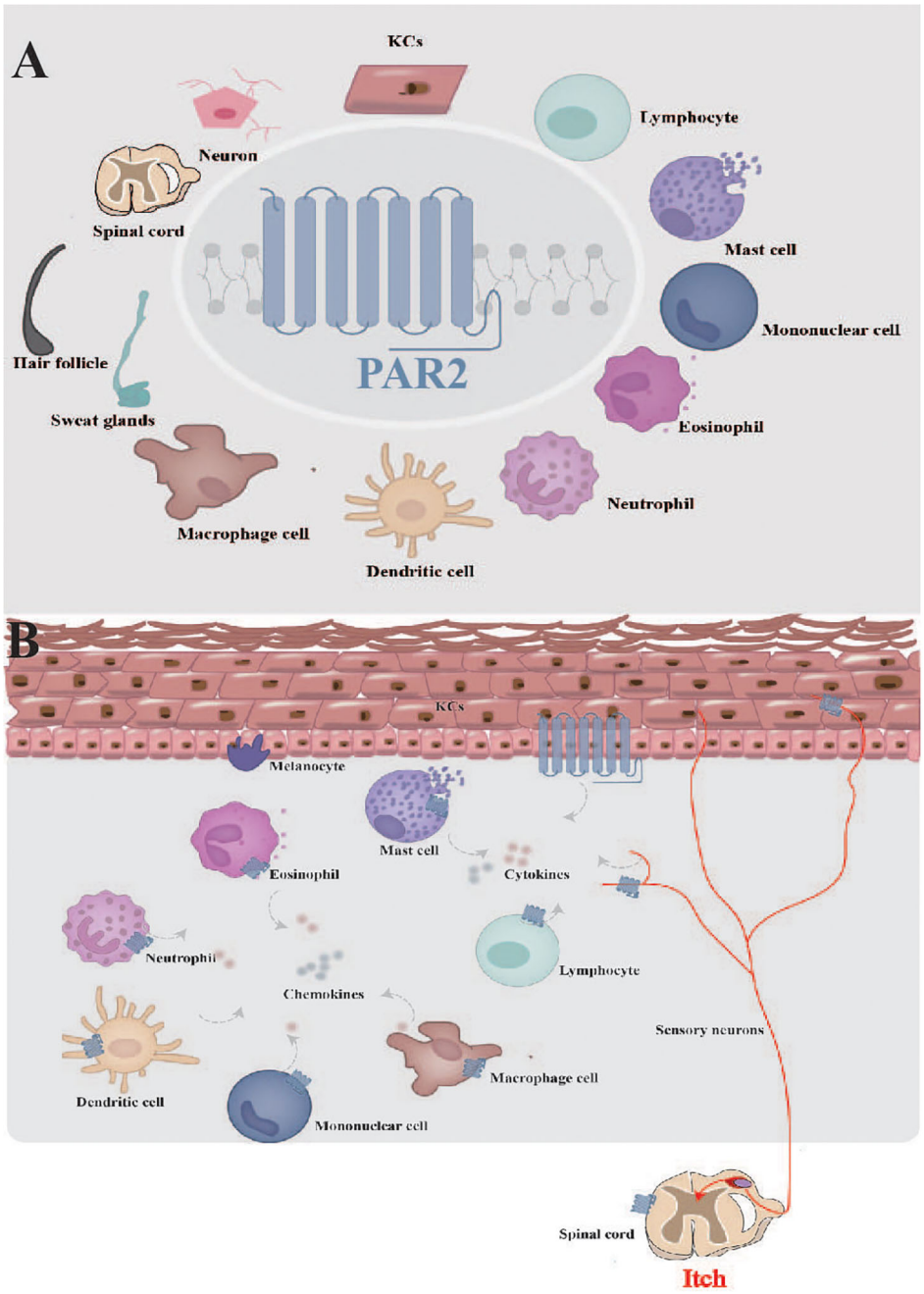

FIGURE 3
Function of PAR2 in skin. **(A)** PAR2 is widely expressed in the cutaneous microenvironment. **(B)** PAR2, expressed by various cells within cutaneous microenvironment, serves as a complex target for interactions among sensory neurons, resident skin cells, and transiently infiltrating cells. KCs, keratinocytes.

after PAR2 activation (54). Conversely, PAR2 promoted differentiation of keratinocytes when the epidermal barrier was compromised (55). The cause of the discrepancy remains unclear. Considering PAR2's known ability to trigger intracellular calcium release, earlier researchers speculated that the lower differentiation mediated by PAR2 might be because the epidermis is a stratified epithelium, unlike other tissues (53). Recent findings from professor Piran's team suggest that PAR2's dual functions, depending on the activation site, could explain this contradiction (56). They propose that initial activation of PAR2 in the immune system exacerbates injury and inflammation, while if PAR2 is activated later within affected tissues, it promotes healing and regeneration. In their studies on liver regeneration models, they found that PAR2's effects depend on the type of injury: it exacerbated immune-mediated damage but aided in regeneration following direct tissue injury (57). This dual role was confirmed in autoimmune diabetes

and appeared to be consistent across various tissues (58). Although keratinocyte differentiation involves limited tissue regeneration, the conflicting roles of PAR2 in this process underscore its complex functions and suggest that PAR2 may have different effects within the same tissue type. Interestingly, we found that PAR2 promotes keratinocyte differentiation when the skin barrier is compromised. We speculate that broader inflammatory and immune responses, exacerbated by PAR2-mediated disruption of the skin barrier, may account for its varying effects on keratinocytes. Further research is needed to validate this.

In summary, PAR2 expressed in keratinocytes induces various and interactive functions: it negatively impacts the barrier function and cell proliferation, positively influences pro-inflammatory cytokine release and pigmentation, but has contradictory effects on cell differentiation.

3.2 PAR2 in immune and inflammatory cells

Activation of PAR2 expressed in keratinocytes, can significantly impact various immune and inflammatory cells (e.g. mast cells, eosinophils, lymphocytes, mononuclear cells, neutrophils, macrophages and dendritic cells), leading to complex immune and inflammatory responses. Interestingly, these cells also express PAR2, potentially amplifying and complicating these reactions. Mast cells (MCs), which contain tryptase, express PAR2 on the plasma membrane and intracellular granule membranes (59). Upon activation, it induces histamine or IL-8, thereby exacerbating inflammation and immune responses (60). In the latest research, the tryptase/PAR-2 axis has been identified as a critical component of the crosstalk between MCs and keratinocytes in skin inflammation (61). Analogously, the tryptase/PAR2 axis contributes to the hyperpigmentation of cutaneous lesions in mastocytosis without enhancing melanocyte activity (62). PAR2 is strongly expressed in human peripheral blood eosinophils, and tryptase from MCs could activate eosinophils to generate IL-6, IL-8 and leukotrienes. The release of IL-6 and IL-8 can be prevented by a PAR2 antagonist in a concentration-dependent manner (63). PAR2 also promotes neutrophils recruitment and upregulates IL-17 receptor signaling, along with promoting chemokines and cytokines (e.g. IL-23 and CXCL2) (64, 65). Similarly, PAR2 induces dendritic cells (DCs) maturation and may play a role in DCs trafficking to lymphnodes, thereby enhancing immune response (66). The influences of PAR2 on T lymphocytes are complicated. PAR2 is located on human $CD4^+$ T cells and natural killer cells but not on $CD8^+$ or γδT cells (67). However, activation of PAR2 in lymphocytes leads to the release of reactive oxygen species (ROS) (68). Thus, PAR2 is expressed by most immune cells in both the innate and adaptive immune systems, contributing to allergic inflammation and immunity. The co-expression and co-regulation of PAR2 among different cells may influence the intensity, duration, and the outcome of immune-inflammatory responses. Importantly, PAR2 is proposed as a potential target for the treatment of related diseases due to its significant role in modulating immune and inflammatory responses.

3.3 PAR2 in neurons

The dermis and subcutaneous tissue contain a complex network of nerves intertwined with various cell types responsible for sensory perception and the regulation of inflammatory cytokines. PAR2 is expressed by peripheral nerve endings, trigeminal ganglia, and primary spinal afferent neurons in the dorsal root ganglia, implicating it in neurogenic inflammation and sensation perception (69). Activation of PAR2 can induce edema and neutrophil infiltration by releasing calcitonin gene-related peptide and substance P (70). Additionally, PAR2 can sensitize TRPV1 by phosphorylation, amplifying intracellular processes (71). Gu et al. found that HDM allergens significantly enhanced TRPV1 in mouse pulmonary sensory neurons (72). Various studies suggest that PAR2 directly evokes pain, though evidence regarding its role in pruritus and thermal hyperalgesia is controversial. Initially, Vergnolle et al. discovered that PAR2 agonists induced both thermal and mechanical hyperalgesia (73). Nevertheless, Hassler et al. illustrated that in mice with PAR2 deleted in all sensory neurons, PAR2 expression in sensory neurons is merely responsible for pain-related behaviors, but not for thermal hyperalgesia or itch. The pain-relevant effects may be attributed to the mediation of the ERK signaling pathway activity (74). Furthermore, intradermal injection of PAR2 agonists can induce scratching behavior and activate neurons in the superficial dorsal horn of mice, indicating a role for PAR2 in the perception and signaling of itch at the neuronal level (75). These differences may be due to the peripheral and central innervation targets of PAR2-expressing neurons, as well as the sufficient proportion of these neurons to elicit different sensations. Furthermore, based on the study by Piran et al. (56–58), we infer that the debate over whether PAR2 triggers pruritus and thermal hyperalgesia, might hinge on if PAR2 is first activated within the immune system or not.

3.4 PAR2 in other cells

Besides, it has been found that skin appendages, such as hair follicles and myoepithelial cells of sweat glands, express PAR2 to varying extents (16). In addition, both trypsin and synthesized PAR2 agonists significantly enhanced the migration, adhesion, and proliferation of fibroblasts and macrophages, underscoring its crucial role in wound healing (76).

Together, the roles of PAR2 in the skin are complex and interrelated, given its varied distributions within the cutaneous microenvironment (Figure 3B). Elucidating the mechanisms involving PAR2 may provide important insights into the general understanding of this class of receptors in the skin.

4 PAR2 in inflammatory and autoimmune dermatological diseases

To date, numerous reports have demonstrated the dysregulation of PAR2 in inflammatory and autoimmune

dermatological diseases, suggesting it as a potential marker. This discussion predominantly focuses on the impacts of PAR2 in atopic dermatitis, psoriasis, vitiligo, melasma, and other conditions such as rosacea, acne, and dermatomyositis, as summarized in Table 1. Therefore, potent PAR2 agonists and antagonists have emerged as enticing therapeutic agents although they are currently still in the experimental stage, primarily tested in genetically engineered mouse models.

4.1 Atopic dermatitis

Atopic dermatitis, also known as atopic eczema, is the most common inflammatory skin disorder, characterized by genetic barrier defects, allergic inflammation and intractable pruritus (77). Recent consensus illustrates that it may be a systemic disease involving multiple allergic and respiratory comorbidities (78). The mechanisms are not well understood, but they are believed to influence neuro-immune and neuro-epidermal communications in the local microenvironment (79). Several genes related to epidermal barrier homeostasis, including SPINK5, and filaggrin, have been identified as abnormal in AD, resulting in elevated skin pH and increased penetration of allergens through the defective skin barrier. SPINK5 encodes lympho-epithelial Kazal-type-related inhibitor (LEKTI) (80), a major inhibitor of KLKs. Studies suggest that single nucleotide polymorphisms E420K and D386N of SPINK5 reduce LEKTI function, thus up-regulating KLKs expression in AD patients. Accordingly, endogenous serine proteases of PAR2 (e.g. KLK5 and KLK14) are active, facilitating easier allergen penetration through the skin barrier in AD (81). Many reports have revealed elevated expression and activation of PAR2 in the lesional skin of AD patients (82).Upon stimulation, PAR2 in epidermal keratinocytes and peripheral nerves leads to releasing Th2 cytokines, intensifying inflammation by attracting immune cells, and initiating neurogenic inflammation associated with itching sensation (55, 83, 84). Owing to active KLKs in AD, PAR2 also indirectly correlates with the regulation of antimicrobial peptides, which are key for innate immunity (83). Moreover, a transgenic mouse model overexpressing epidermal PAR2 presents AD-like appearance, with enhanced PAR2 in nerve fibers contributing to itching behavior due to direct neuro-epidermal communication (85). Another study indicated that elevated PAR2 expression on nerve fibers prompted itching following the application of PAR2 agonists (86). Briefly, current data focus primarily on keratinocytes and slightly on neurons, without exploration of the role of PAR2 on immune and inflammatory cells. In a study by Smith, after treatment with HDM, model mice with epidermal overexpression of PAR2, particularly cell-specific, exhibited typical AD symptoms and significant infiltration of mast cells and eosinophils, though there was no deeper investigation into PAR2's role in these cells (87). Thus, we infer that PAR2 is implicated in inflammation, pruritus, and barrier regulation in AD, but also affects relevant comorbidities caused by overactive mast cells.

These findings illustrate that PAR2 could be a promising therapeutic target in AD. Studies on PAR2 antagonists, including ENMD-1198 (88) and NPS-1577 (89), have demonstrated varying degrees of alleviation in AD symptoms. In 2019, Barr et al. demonstrated that PZ-235 could be a promising option for AD by targeting neuro-immune interactions *in vivo*, thereby reducing scratching behavior, attenuating the production of inflammatory-immune factors, and decreasing lesion severity (90). Furthermore, latest data reveal that topical doxycycline monohydrate hydrogel, which downregulates PAR2 activity, exhibits significant clinical efficacy in AD patients (91).

4.2 Psoriasis

Psoriasis is a prevalent chronic inflammatory dermatological condition, characterized by a multifactorial etiology involving both immune dysregulation and genetic predispositions. In genetically susceptible individuals, various external and internal stimuli activate the immune system, triggering a series of cellular responses that include the participation of plasmacytoid dendritic cells, macrophages, mast cells and T cells. The immune activation results in the hyperproliferation and aberrant differentiation of keratinocytes, as well as severe pruritus (92). Current research has predominantly focused on the role of PAR2 in plaque psoriasis, revealing differential expression levels of PAR2 across various cell types within psoriatic lesions. In previous studies, patients with psoriasis vulgaris have exhibited lower levels of PAR2 in keratinocytes. This reduction may be attributed to a process of PAR2 internalization, where excessive stimulation promotes PAR2-mediated IL-8 production, leading to an accumulation of inflammatory cells in the epidermis without sufficient PAR2 replenishment (93). In the context of mast cells, Carvalho et al. demonstrated a significant increase in PAR2 levels in the lesional skin of psoriasis patients compared to healthy skin. This could result from the persistent activation of mast cells, which is a characteristic feature of psoriasis. Moreover, interaction of PAR2-activating peptides with mast cells results in elevated secretion of IL-8 rather than histamine release (94). Notably, Nattkemper et al. recently discovered that epidermal expression of PAR2 was significantly increased in scalp psoriasis accompanied by severe itch. The difference may be due to the distinct distribution of PAR2 across different body areas, as it is present on sensory nerve endings, epidermal keratinocytes, and the inner root sheath (IRS) in scalp hair follicles (95). Furthermore, a study measuring PAR2 levels over time in psoriasis patients treated with a combination of ultraviolet rays and methotrexate reported a significant decrease in PAR2 levels. This decrease may result from alterations in antigen-presenting cells, intracellular signaling pathways, and anti-inflammatory processes induced by this combined therapy. However, the study did not clarify which specific cell types had varying PAR2 levels (96). These pieces of evidence indicate that PAR2 in psoriasis exhibits diverse effects depending on its location in different cell types-lower expression in keratinocytes versus higher expression in mast cells and enhanced epidermal expression of PAR2 in scalp-indicating a closely correlated pathophysiology involving multiple cell variants in the cutaneous microenvironment. In this context, immune and inflammatory cells

TABLE 1 Summary of effects of PAR2 on inflammatory and autoimmune dermatological diseases.

Relevant diseases	Hypothesized effect		PAR2 perplexing effects		location	Potential mechanism	Role	Indication
	Promotes	Inhibits	aggravator-activated primarily in the immune system	alleviator-activated primarily in the affected tissue				
Atopic dermatitis(AD)	√				epidermal keratinocytes and peripheral nerves	promotion of Th2 cytokines (e.g. IL-4, IL-13 and TSLP) and GM-CSF	Th2 inflammatory response; induction of immunity; initiating neurogenic inflammation; disrupting epidermal barrier function;	(82–84)
Atopic dermatitis(AD)	√				epidermal keratinocytes	exaggerating neuro-epidermal communication	disrupting epidermal barrier function; initiating neurogenic inflammation	(85)
Atopic dermatitis(AD)	√				nerve fibers	increasing CGRP, substance P and releasing ion channels	neurogenic pruritus (histamine-independence)	(86)
Atopic dermatitis(AD)	√		√		epidermal keratinocytes and mast cells	promoting chemokines and cytokines	promoting barrier defects, allergic inflammation and pruritus	(87)
Psoriasis		√			epidermal keratinocytes	promoting cytokines (e.g. IL-8), accumulating epidermal inflammatory cells	inducting immunity and inflammation	(93)
Psoriasis	√		√		mast cells	promotion cytokines (e.g. IL-8)	inducing immunity and inflammation	(94)
Psoriasis	√				epidermal keratinocytes	promoting cytokines and chemokines	inducing immunity, inflammation and pruritus	(95)
Vitiligo		√			epidermal keratinocytes	antioxidant responses (e.g.Nrf2, MDA level)	transferring melanosomes	(100–102)
melasma	√				epidermal keratinocytes	formation of telangiectatic erythema	inducing inflammation	(104)
melasma	√				epidermal keratinocytes	stimulating keratinocyte differentiation and influencing redox leveling	effects on melanosome transfer and melanogenesis	(105)
Rosacea	√				epidermal keratinocytes	influencing Cathelicidin and VEGF	induction of inflammation	(109)
Rosacea	√				epidermal keratinocytes and neurons	influencing TRPV1 on vasoregulation and nociception	neurogenic inflammation	(110)

(Continued)

10.3389/fimmu.2024.1449126

TABLE 1 Continued

Relevant diseases	Hypothesized effect		PAR2 perplexing effects		location	Potential mechanism	Role	Indication
	Promotes	Inhibits	aggravator-activated primarily in the immune system	alleviator-activated primarily in the affected tissue				
Acne	√				sebaceous glands	/	sebum secretion and induction of immunity;	(111)
Allergic contact dermatitis	√		√		epidermal keratinocytes and myeloid cells	promoting the development of T cell	inducing immunity	(113)
Dermatomyositis	√		√		peripheral blood mononuclear cells (PBMCs) and muscle tissues	altering the cytoskeleton of dermal microvascular endothelial cells	inducing immunity, inflammation	(115)
Skin photoaging	√				epidermal keratinocytes	promoting inflammatory responses through Akt-mediated phosphorylation of NF-κB along with FoxO6 (Ser184), and suppressing the antioxidant enzyme MnSOD,	inducing inflammation and ROS	(117)
Other chronic pruritic conditions(e.g., cowhage, spicules-induced, dermatophyte-associated and scabies itch)	√				epidermal keratinocytes and neurons	releasing ion channels (e.g.TRPV3) and promotion of Th2 cytokines	induction of neurogenic pruritus and inflammation	(120)
	√		√		epidermal keratinocytes and mast cells	amplification of neuro-epidermal communication and inflamatory responses	induction of immunity inflammation and itch	(121, 122)

10.3389/fimmu.2024.1449126

closely interact with basal keratinocytes or adjacent blood vessels in the dermis. Consequently, PAR2 antagonists may present a potential therapeutic strategy for managing inflammation and itch associated with psoriasis.

4.3 Vitiligo

Vitiligo is an autoimmune skin disorder characterized by the loss of functional melanocytes, resulting in white patches on the skin and mucous membranes, as well as white hair (97). It is increasingly recognized as a systemic disease with various comorbidities, such as AD, alopecia areata, and systemic lupus erythematosus (98). Currently, the essential pathogenesis involves persistent oxidative stress resulting from dysfunction in the nuclear factor erythroid 2-related factor 2 pathway, along with autoimmunity stemming from hyperactive innate and adaptive immune responses. Consequently, treatments have primarily targeted antioxidants and immunosuppressants (99). In recent years, PAR2 has been identified as a key player in the pathogenesis of vitiligo, despite not being present in melanocytes. In 2009, Moretti and colleagues (100) first discovered that PAR2 levels were significantly reduced in the lesions of white patches compared to non-lesional skin in vitiligo. Interestingly, this phenomenon was not observed in other non-vitiligo depigmentation conditions, such as pityriasis versicolor and lichen simplex chronicus. This implies that PAR2 downregulation is specific to vitiligo-related depigmentation. The reduced PAR2 may impair the function of keratinocytes in white patches, including the inhibition of melanosome transfer to neighboring cells. Kim et al. later illustrated that PAR2 can enhance Nrf2-mediated antioxidant responses, protecting the skin from excessive oxidative damage and thus maintaining pigmentation through interactions between keratinocytes and melanocytes (101). Their study may explain the lower levels of PAR2 in vitiligo. Additionally, Tang found that phototherapy such as narrow band, may regulate pigmentation in vitiligo by affecting PAR2 on keratinocytes, influencing melanosome uptake and malondialdehyde level (102). Collectively, the decrease in PAR2 plays a critical role in the pathogenesis of vitiligo. Further research is necessary to understand whether PAR2 influences immunity and whether other cells, such as mast cells and T cells, undergo similar PAR2 changes in vitiligo. Understanding the exact mechanism of PAR2 may enhance our knowledge of the crosstalk between melanocytes and their surrounding cells, inform the potential for comorbidities, and aid in the development of effective therapeutic strategies for vitiligo.

4.4 Melasma

Melasma is a common chronic acquired hyperpigmentation disorder that usually affects photoexposed areas in predisposed individuals, with ultraviolet (UV) radiation being the primary risk factor. Although the exact pathogenesis remains unclear, it is acknowledged that melasma originates from alterations in several cell types, including melanocytes, keratinocytes and mast cells. These changes lead to the production and transfer of mature melanosomes throughout the epidermis (103). PAR2 has been increasingly recognized as a significant contributor to the pathogenesis of melasma, especially in melanosome transfer and melanogenesis through a specific paracrine mechanism. For instance, Lee et al. discovered that the PAR2 expression was increased in melasma patients and positively correlated with clinical telangiectatic erythema. Upregulation of PAR2 by VEGF stimulation was clearly evident, suggesting that abnormal PAR2 activity may facilitate inflammatory erythema (104). A recent study by Kim et al. indicated that PAR2 might be involved in a series of reactions involving the NRF2 pathway, which subsequently inhibits primary cilia formation and the Hedgehog signaling pathway, while also stimulating keratinocyte differentiation. These processes ultimately lead to increased melanin synthesis and excessive transfer of melanosomes to keratinocytes in melasma (105). Moreover, UV radiation was found to upregulate epidermal PAR2 expression and proteolysis, with notable variations among different skin phototypes (106). Given that mast cells degranulate under UV radiation, it is inferred that PAR2 present in mast cells may also influence the associated pathogenesis of melasma. Therefore, promising PAR2 antagonists may offer a novel therapeutic approach for the treatment of melasma. Further research is needed to fully elucidate the role of PAR2 in melasma.

4.5 Others

Rosacea is a chronic inflammatory dermatosis characterized by facial flushing, telangiectasia, inflammatory papules and pustules, primarily affecting the central face. Neurovascular and neuroimmune dysregulation are significant contributors to the mechanisms underlying rosacea (107). External stimuli such as heat or alcohol can exacerbate the condition due to heightened skin sensitivity. Among the factors involved, the cathelicidin LL-37 (an antimicrobial peptide) activation pathway is the best understood and most classical pathway in rosacea pathogenesis (108). In 2014, a positive correlation between PAR2 and cathelicidin was observed in rosacea patients. Additionally, treatment with PAR2-activating peptides *in vitro* led to increased levels of cathelicidin and VEGF (109). Moreover, TRPV1, found on neurons and keratinocytes, was activated via upregulated PAR2 in rosacea (110). PAR2 also appears to influence the development of acne. A study by Lee et al. found greater PAR2 expression in sebaceous glands, rather than the epidermis, in inflammatory acne lesions (111). Allergic contact dermatitis (ACD), a type IV hypersensitivity reaction, often requires treatment to reduce inflammation induced by re-exposure to allergens (112). Remarkably, a latest study revealed that myeloid cells expressed increased PAR2 in human ACD, promoting the development of T cell-mediated inflammation (113). Dermatomyositis, a rare autoimmune disease characterized by skin rash and muscle weakness, was found to involve increased levels of Cathepsin G in peripheral blood mononuclear cells and

muscle tissues. This increase correlated with disease severity and was found to induce PAR2 secretion, suggesting an indirect role for PAR2 (14–115). Skin photoaging arises from long-term exposure to UV irradiation, leading to ROS production and inflammatory responses (116). A 2021 report illustrated that active PAR2 in keratinocytes promoted inflammatory responses through Akt-mediated phosphorylation of NF-κB and FoxO6, while also suppressing the antioxidant enzyme MnSOD, thereby progressively increasing ROS levels (117). Drawing from the research by Piran et al (56–58), We speculate that active PAR2 here was related to both T-lymphocyte-mediated immune inflammation and PAR2 activation within the affected keratinocytes themselves. PAR2 could eventually aggravate inflammation, suggesting that the two processes above may have a synergistic effect in skin photoaging, where tissue regeneration is not involved. PAR2 is also implicated in various chronic pruritic conditions, particularly in histamine-independent pruritus caused by cowhage spicules, dermatophytes, and scabies (118). The pathogenesis of pruritus involves a complex network of interactions among keratinocytes, sensory neurons, mast cells and transiently infiltrating immune cells (119). Emerging reports suggest that keratinocytes act as the initial sensor for itch signaling, and that interaction with various cells excessively exacerbates inflammation and itching. Activation of epidermal PAR2 triggers intracellular PLC-Ca^{2+} signaling, leading to TSLP-relevant scratching behavior. TSLP then promotes the generation of type 2 cytokines and stimulates PAR2, TRPV1, and TRPA1 in sensory neurons, exacerbating itch responses. Additionally, PAR2 activation in dorsal root ganglia enhances the function of epidermal TRPV3, perpetuating the itch-scratch cycle (120). In a study by Park et al (121), the PAR2-TRPV3-TSLP pathway was identified as critical in the pruritus experienced by burn scar patients. Another study by Kristen et al. found that PAR2 expression was significantly increased in the epidermis and mast cells near the dermal-epidermal junction in scabies-infested tissues, explaining why conventional antihistamines are often ineffective against scabies itch (122). Collectively, these findings highlight the potential of PAR2 agonists and antagonists for developing new therapeutic strategies that could not only address the limitations of classical antipruritics but also circumvent the side effects associated with topical corticosteroids.

5 Conclusion

In summary, our comprehension of the role of PAR2 in cutaneous immune and inflammatory processes is advancing swiftly, uncovering novel insights and potential therapeutic targets. This review underscores several critical aspects: (a). The proteolytic activation of PAR2 at different sites initiates intricate signaling cascades, emphasizing the importance of biased activation for a deeper understanding of its roles in specific diseases. (b). PAR2, present in various cells within the cutaneous microenvironment, acts as a multifaceted target for interactions among sensory neurons, resident skin cells, and transiently infiltrating cells. Accordingly, potent PAR2 agonists and antagonists hold promise for addressing the complexities of inflammatory and autoimmune dermatological diseases. (c). PAR2 plays a crucial role in elucidating neuro-immune and immune-inflammatory interactions in these conditions, thereby offering valuable insights into the mechanisms underlying their diverse cutaneous and extracutaneous comorbidities.

Author contributions

KJX: Conceptualization, Visualization, Writing – original draft, Writing – review & editing. LW: Investigation, Writing – review & editing, Funding acquisition. ML: Funding acquisition, Writing – original draft, Writing – review & editing. GH: Investigation, Writing – original draft, Writing – review & editing.

Funding

The author(s) declare financial support was received for the research, authorship, and/or publication of this article. This study was supported by grants from the Postdoctor Research Fund of West China Hospital, Sichuan University (2024HXBH155), Chongqing medical scientific research project (Joint project of Chongqing Health Commission and Science and Technology Bureau) (2022DBXM007), National Natural Science Foundation of China (81402601, 22177084), “Youth Qi Huang Scholar” project by State Administration of Traditional Chinese Medicine of China.

Conflict of interest

The authors declare that the research was conducted in the absence of any commercial or financial relationships that could be construed as a potential conflict of interest.

Publisher’s note

References

1. Nystedt S, Emilsson K, Wahlestedt C, Sundelin J. Molecular cloning of a potential proteinase activated receptor. *Proc Natl Acad Sci USA*. (1994) 91:9208–12. doi: 10.1073/pnas.91.20.9208

2. Jin M, Yang HW, Tao AL, Wei JF. Evolution of the protease-activated receptor family in vertebrates. *Int J Mol Med*. (2016) 37:593–602. doi: 10.3892/ijmm.2016.2464

3. Borensztajn K, Stiekema J, Nijmeijer S, Reitsma PH, Peppelenbosch MP, Spek CA. Factor Xa stimulates proinflammatory and profibrotic responses in fibroblasts via protease-activated receptor-2 activation. *Am J Pathol*. (2008) 172:309–20. doi: 10.2353/ajpath.2008.070347

4. Pawar NR, Buzza MS, Antalis TM. Membrane-anchored serine proteases and protease-activated receptor-2-mediated signaling: co-conspirators in cancer progression. *Cancer Res*. (2019) 79:301–10. doi: 10.1158/0008-5472.CAN-18-1745

5. Sun G, Stacey MA, Schmidt M, Mori L, Mattoli S. Interaction of mite allergens Der p3 and Der p9 with protease-activated receptor-2 expressed by lung epithelial cells. *J Immunol*. (2001) 167:1014–21. doi: 10.4049/jimmunol.167.2.1014

6. Do DC, Zhao Y, Gao P. Cockroach allergen exposure and risk of asthma. *Allergy*. (2016) 71:463–74. doi: 10.1111/all.12827

7. Peach CJ, Edgington-Mitchell LE, Bunnett NW, Schmidt BL. Protease-activated receptors in health and disease. *Physiol Rev*. (2023) 103:717–85. doi: 10.1152/physrev.00044.2021

8. Rattenholl A, Steinhoff M. Proteinase-activated receptor-2 in the skin: receptor expression, activation and function during health and disease. *Drug News Perspect*. (2008) 21:369–81. doi: 10.1358/dnp.2008.21.7.1255294

9. Henehan M, De Benedetto A. Update on protease-activated receptor 2 in cutaneous barrier, differentiation, tumorigenesis and pigmentation, and its role in related dermatologic diseases. *Exp Dermatol*. (2019) 28:877–85. doi: 10.1111/exd.13936

10. Steinhoff M, Corvera CU, Thoma MS, Kong W, McAlpine BE, Caughey GH, et al. Proteinase-activated receptor-2 in human skin: tissue distribution and activation of keratinocytes by mast cell tryptase. *Exp Dermatol*. (1999) 8:282–94. doi: 10.1111/j.1600-0625.1999.tb00383.x

11. Rayees S, Joshi JC, Tauseef M, Anwar M, Baweja S, Rochford I, et al. PAR2-mediated cAMP generation suppresses TRPV4-dependent ca^{2+} Signaling in alveolar macrophages to resolve TLR4-induced inflammation. *Cell Rep*. (2019) 27:793–805.e4. doi: 10.1016/j.celrep.2019.03.053

12. Andersen HH. Protease-activated receptor-2: A multifaceted molecular transducer in the human skin. *Ann Dermatol*. (2016) 28:771–2. doi: 10.5021/ad.2016.28.6.771

13. Zhao P, Metcalf M, Bunnett NW. Biased signaling of protease-activated receptors. *Front Endocrinol (Lausanne)*. (2014) 5:67. doi: 10.3389/fendo.2014.00067

14. Tu NH, Jensen DD, Anderson BM, Chen E, Jimenez-Vargas NN, Scheff NN, et al. Legumain induces oral cancer pain by biased agonism of protease-activated receptor-2. *J Neurosci*. (2021) 41:193–210. doi: 10.1523/JNEUROSCI.1211-20.2020

15. Zhao P, Pattison LA, Jensen DD, Jimenez-Vargas NN, Latorre R, Lieu T, et al. Protein kinase D and Gβγ mediate sustained nociceptive signaling by biased agonists of protease-activated receptor-2. *J Biol Chem*. (2019) 294:10649–62. doi: 10.1074/jbc.RA118.006935

16. Hollenberg MD, Mihara K, Polley D, Suen JY, Han A, Fairlie DP, et al. Biased signalling and proteinase-activated receptors (PARs): targeting inflammatory disease. *Br J Pharmacol*. (2014) 171:1180–94. doi: 10.1111/bph.12544

17. Dulon S, Leduc D, Cottrell GS, D'Alayer J, Hansen KK, Bunnett NW, et al. Pseudomonas aeruginosa elastase disables proteinase-activated receptor 2 in respiratory epithelial cells. *Am J Respir Cell Mol Biol*. (2005) 32:411–19. doi: 10.1165/rcmb.2004-0274OC

18. Rayees S, Joshi JC, Joshi B, Vellingiri V, Banerjee S, Mehta D. Protease-activated receptor 2 promotes clearance of *Pseudomonas aeruginosa* infection by inducing cAMP-Rac1 signaling in alveolar macrophages. *Front Pharmacol*. (2022) 13:874197. doi: 10.3389/fphar.2022.874197

19. Cheng RKY, Fiez-Vandal C, Schlenker O, Edman K, Aggeler B, Brown DG, et al. Structural insight into allosteric modulation of protease-activated receptor 2. *Nature*. (2017) 545:112–5. doi: 10.1038/nature22309

20. Piran R, Lee SH, Kuss P, Hao E, Newlin R, Millán JL, et al. PAR2 regulates regeneration, transdifferentiation, and death. *Cell Death Dis*. (2016) 7:e2452. doi: 10.1038/cddis.2016.357

21. Molino M, Barnathan ES, Numerof R, Clark J, Dreyer M, Cumashi A, et al. Interactions of mast cell tryptase with thrombin receptors and PAR-2. *J Biol Chem*. (1997) 272:4043–49. doi: 10.1074/jbc.272.7.4043

22. Compton SJ, Renaux B, Wijesuriya SJ, Hollenberg MD. Glycosylation and the activation of proteinase-activated receptor 2 (PAR(2)) by human mast cell tryptase. *Br J Pharmacol*. (2001) 134:705–18. doi: 10.1038/sj.bjp.070

23. Al-Ani B, Saifeddine M, Kawabata A, Hollenberg MD. Proteinase activated receptor 2: Role of extracellular loop 2 for ligand-mediated activation. *Br J Pharmacol*. (1999) 128:1105–13. doi: 10.1038/sj.bjp.0702834

24. Ramachandran R, Mihara K, Mathur M, Rochdi MD, Bouvier M, Defea K, et al. Agonist-biased signaling via proteinase activated receptor-2: differential activation of calcium and mitogen-activated protein kinase pathways. *Mol Pharmacol*. (2009) 76:791–801. doi: 10.1124/mol.109.055509PMC2769049

25. Tanaka Y, Sekiguchi F, Hong H, Kawabata A. PAR2 triggers IL-8 release via MEK/ERK and PI3-kinase/Akt pathways in GI epithelial cells. *Biochem Biophys Res Commun*. (2008) 377:622–6. doi: 10.1016/j.bbrc.2008.10.018

26. Jimenez-Vargas NN, Pattison LA, Zhao P, Lieu T, Latorre R, Jensen DD, et al. Protease-activated receptor-2 in endosomes signals persistent pain of irritable bowel syndrome. *Proc Natl Acad Sci USA*. (2018) 115:E7438–47. doi: 10.1073/pnas.1721891115

27. Kawao N, Nagataki M, Nagasawa K, Kubo S, Cushing K, Wada T, et al. Signal transduction for proteinase-activated receptor-2-triggered prostaglandin E2 formation in human lung epithelial cells. *J Pharmacol Exp Ther*. (2005) 315:576–89. doi: 10.1124/jpet.105.089490

28. Jiang Y, Zhuo X, Fu X, Wu Y, Mao C. Targeting PAR2 overcomes gefitinib resistance in non-small-cell lung cancer cells through inhibition of EGFR transactivation. *Front Pharmacol*. (2021) 12:625289. doi: 10.3389/fphar.2021.625289

29. Kaufmann R, Oettel C, Horn A, Halbhuber KJ, Eitner A, Krieg R, et al. Met receptor tyrosine kinase transactivation is involved in proteinase-activated receptor-2-mediated hepatocellular carcinoma cell invasion. *Carcinogenesis*. (2009) 30:1487–96. doi: 10.1093/carcin/bgp153

30. Amadesi S, Cottrell GS, Divino L, Chapman K, Grady EF, Bautista F, et al. Protease-activated receptor 2 sensitizes TRPV1 by protein kinase Cepsilon and A-dependent mechanisms in rats and mice. *J Physiol*. (2006) 575:555–71. doi: 10.1113/jphysiol.2006.111534

31. Grace MS, Lieu T, Darby B, Abogadie FC, Veldhuis N, Bunnett NW, et al. The tyrosine kinase inhibitor bafetinib inhibits PAR2-induced activation of TRPV4 channels in *vitro* and pain in vivo. *Br J Pharmacol*. (2014) 171:3881–94. doi: 10.1111/bph.12750

32. Wu J, Liu TT, Zhou YM, Qiu CY, Ren P, Jiao M, et al. Sensitization of ASIC3 by proteinase-activated receptor 2 signaling contributes to acidosis-induced nociception. *J Neuroinflamm*. (2017) 14:150. doi: 10.1186/s12974-017-0916-4

33. Johnson JJ, Miller DL, Jiang R, Liu Y, Shi Z, Tarwater L, et al. Protease-activated receptor-2 (PAR-2)-mediated NF-κB activation suppresses inflammation-associated tumor suppressor microRNAs in oral squamous cell carcinoma. *J Biol Chem*. (2016) 291:6936–45. doi: 10.1074/jbc.M115.692640

34. Steinhoff M, Vergnolle N, Young SH, Tognetto M, Amadesi S, Ennes HS, et al. Agonists of proteinase-activated receptor 2 induce inflammation by a neurogenic mechanism. *Nat Med*. (2000) 6:151–8. doi: 10.1038/72247

35. Ricks TK, Trejo J. Phosphorylation of protease-activated receptor-2 differentially regulates desensitization and internalization. *J Biol Chem*. (2009) 284:34444–57. doi: 10.1074/jbc.M109.048942

36. Ayoub MA, Pin JP. Interaction of protease-activated receptor 2 with G proteins and β-arrestin 1 studied by bioluminescence resonance energy transfer. *Front Endocrinol*. (2013) 4:196. doi: 10.3389/fendo.2013.00196

37. Dery O, Thoma MS, Wong H, Grady EF, Bunnett NW. Trafficking of proteinase-activated receptor-2 and β-arrestin-1 tagged with green fluorescent protein. *J Biol Chem*. (1999) 274:18524–35. doi: 10.1074/jbc.274.26.18524

38. Latorre RA, Hegron A, Peach CJ, Teng SA, Tonello RA, Retamal JA, et al. Mice expressing fluorescent PAR(2) reveal that endocytosis mediates colonic inflammation and pain. *Proc Natl Acad Sci USA*. (2022) 119:e2112059119. doi: 10.1073/pnas.2112059119

39. Hasdemir B, Bunnett N, Cottrell GS. Hepatocyte growth factor-regulated tyrosine kinase substrate (HRS) mediates post-endocytic trafficking of protease-activated receptor 2 and calcitonin receptor-like receptor. *J Biol Chem*. (2007) 282:29646–57. doi: 10.1074/jbc.M702974200

40. Jensen DD, Zhao P, Jimenez-Vargas NN, Lieu T, Gerges M, Yeatman HR, et al. Protein kinase D and Gβγ subunits mediate agonist-evoked translocation of protease-activated receptor-2 from the golgi apparatus to the plasma membrane. *J Biol Chem*. (2016) 291:11285–99. doi: 10.1074/jbc.M115.710681

41. Rothmeier AS, Liu E, Chakrabarty S, Disse J, Mueller BM, Østergaard H, et al. Identification of the integrin-binding site on coagulation factor VIIa required for proangiogenic PAR2 signaling. *Blood*. (2018) 131:674–85. doi: 10.1182/blood-2017-02-768218

42. Badeanlou L, Furlan-Freguia C, Yang G, Ruf W, Samad F. Tissue factor-protease-activated receptor 2 signaling promotes diet-induced obesity and adipose inflammation. *Nat Med*. (2011) 17:1490–97. doi: 10.1038/nm.2461

43. Versteeg HH, Schaffner F, Kerver M, Ellies LG, Andrade-Gordon P, Mueller BM, et al. Protease-activated receptor (PAR) 2, but not PAR1, signaling promotes the development of mammary adenocarcinoma in polyoma middle T mice. *Cancer Res*. (2008) 68:7219–27. doi: 10.1158/0008-5472

44. Hachem JP, Houben E, Crumrine D, Man MQ, Schurer N, Roelandt T, et al. Serine protease signaling of epidermal permeability barrier homeostasis. *J Invest Dermatol*. (2006) 126:2074–86. doi: 10.1038/sj.jid.5700351

45. Jenkins AL, Chinni C, De Niese MR, Blackhart B, Mackie EJ. Expression of protease-activated receptor-2 during embryonic development. *Dev Dyn*. (2000) 218:465–71. doi: 10.1002/1097-0177(200007)218:3<465::AID-DVDY1013>3.0.CO;2-5

46. Roelandt T, Heughebaert C, Verween G, Giddelo C, Verbeken G, Pirnay JP, et al. Actin dynamics regulate immediate PAR-2-dependent responses to acute epidermal permeability barrier abrogation. *J Dermatol Sci*. (2011) 61:101–09. doi: 10.1016/j.jdermsci.2010.11.016

47. Moniaga CS, Jeong SK, Egawa G, Nakajima S, Hara-Chikuma M, Jeon JE, et al. Protease activity enhances production of thymic stromal lymphopoietin and basophil accumulation in flaky tail mice. *Am J Pathol*. (2013) 182:841–51. doi: 10.1016/j.ajpath.2013.01.003

48. Briot A, Deraison C, Lacroix M, Bonnart C, Robin A, Besson C, et al. Kallikrein 5 induces atopic dermatitis-like lesions through PAR2-mediated thymic stromal lymphopoietin expression in Netherton syndrome. *J Exp Med*. (2009) 206:1135–47. doi: 10.1084/jem.20082242

49. Hou L, Kapas S, Cruchley AT, Macey MG, Harriott P, Chinni C, et al. Immunolocalization of protease-activated receptor-2 in skin: receptor activation stimulates interleukin-8 secretion by keratinocytes in vitro. *Immunology*. (1998) 94:356–62. doi: 10.1046/j.1365-2567.1998.00528.x

50. Babiarz-Magee L, Chen N, Seiberg M, Lin CB. The expression and activation of protease-activated receptor-2 correlate with skin color. *Pigment Cell Res*. (2004) 17:241–51. doi: 10.1111/j.1600-0749.2004.00133.x

51. Moreiras H, Bento-Lopes L, Neto MV, Escrevente C, Cabaço LC, Hall MJ, et al. Melanocore uptake by keratinocytes occurs through phagocytosis and involves protease-activated receptor-2 internalization. *Traffic*. (2022) 23:331–45. doi: 10.1111/tra.12843

52. Kim JY, Kim DS, Sohn H, Lee EJ, Oh SH. PAR-2 is involved in melanogenesis by mediating stem cell factor production in keratinocytes. *Exp Dermatol*. (2016) 25:487–89. doi: 10.1111/exd.12982

53. Derian CK, Eckardt AJ, Andrade-Gordon P. Differential regulation of human keratinocyte growth and differentiation by a novel family of protease-activated receptors. *Cell Growth Differ*. (1997) 8:743–49.

54. Nadeau P, Henehan M, De Benedetto A. Activation of protease-activated receptor 2 leads to impairment of keratinocyte tight junction integrity. *J Allergy Clin Immunol*. (2018) 142:281–284.e7. doi: 10.1016/j.jaci.2018.01.007

55. Roelandt T, Heughebaert C, Hachem JP. Proteolytically active allergens cause barrier breakdown. *J Invest Dermatol*. (2008) 128:1878–80. doi: 10.1038/jid.2008.168

56. Reches G, Piran R. Par2-mediated responses in inflammation and regeneration: choosing between repair and damage. *Inflammation Regener*. (2024) 44:26. doi: 10.1186/s41232-024-00338-1

57. Reches G, Blondheim Shraga NR, Carrette F, Malka A, Saleev N, Gubbay Y, et al. Resolving the conflicts around Par2 opposing roles in regeneration by comparing immune-mediated and toxic-induced injuries. *Inflammation Regener*. (2022) 42:52. doi: 10.1186/s41232-022-00238-2

58. Reches G, Khoon L, Ghanayiem N, Malka A, Piran R. Controlling autoimmune diabetes onset by targeting Protease-Activated Receptor 2. *BioMed Pharmacother*. (2024) 175:116622. doi: 10.1016/j.biopha.2024.116622

59. D'Andrea MR, Rogahn CJ, Andrade-Gordon P. Localization of protease-activated receptors-1 and -2 in human mast cells: indications for an amplified mast cell degranulation cascade. *Biotech Histochem*. (2000) 75:85–90. doi: 10.3109/10520290009064152

60. Moormann C, Artuc M, Pohl E, Varga G, Buddenkotte J, Vergnolle N, et al. Functional characterization and expression analysis of the proteinase-activated receptor-2 in human cutaneous mast cells. *J Invest Dermatol*. (2006) 126:746–55. doi: 10.1038/sj.jid.5700169

61. Redhu D, Franke K, Aparicio-Soto M, Kumari V, Pazur K, Illerhaus A, et al. Mast cells instruct keratinocytes to produce thymic stromal lymphopoietin: Relevance of the tryptase/protease-activated receptor 2 axis. *J Allergy Clin Immunol*. (2022) 149:2053–61. doi: 10.1016/j.jaci.2022.01.029

62. Hashimoto T, Okuzawa M, Okuno S, Satoh T. Mast cell protease/protease-activated receptor-2 axis: Another mechanism of pigmentation in cutaneous lesions of mastocytosis. *J Eur Acad Dermatol Venereol*. (2023) 37:e529–31. doi: 10.1111/jdv.18823

63. Bolton SJ, McNulty CA, Thomas RJ, Hewitt CR, Wardlaw AJ. Expression of and functional responses to protease-activated receptors on human eosinophils. *J Leukoc Biol*. (2003) 74:60–8. doi: 10.1189/jlb.0702351

64. Silva IS, Almeida AD, Lima Filho ACM, Fernandes-Braga W, Barra A, Oliveira HMC, et al. Platelet-activating factor and protease-activated receptor 2 cooperate to promote neutrophil recruitment and lung inflammation through nuclear factor-kappa B transactivation. *Sci Rep*. (2023) 13:21637. doi: 10.1038/s41598-023-48365-1

65. Nadeem A, Al-Harbi NO, Ahmad SF, Ibrahim KE, Alotaibi MR, Siddiqui N, et al. Protease activated receptor-2 mediated upregulation of IL-17 receptor signaling on airway epithelial cells is responsible for neutrophilic infiltration during acute exposure of house dust mite allergens in mice. *Chem Biol Interact*. (2019) 304:52–60. doi: 10.1016/j.cbi.2019.03.001

66. Shpacovitch V, Feld M, Hollenberg MD, Luger TA, Steinhoff M. Role of protease-activated receptors in inflammatory responses, innate and adaptive immunity. *J Leukoc Biol*. (2008) 83:1309–22. doi: 10.1189/jlb.0108001

67. Bushell TJ, Cunningham MR, McIntosh KA, Moudio S, Plevin R. Protease-activated receptor 2: are common functions in glial and immune cells linked to inflammation-related CNS disorders? *Curr Drug Targets*. (2016) 17:1861–70. doi: 10.2174/1389450117666151209115232

68. Lim SY, Tennant GM, Kennedy S, Wainwright CL, Kane KA. Activation of mouse protease-activated receptor-2 induces lymphocyte adhesion and generation of reactive oxygen species. *Br J Pharmacol*. (2006) 149:591–9. doi: 10.1038/sj.bjp.0706905

69. Dinh QT, Cryer A, Dinh S, Trevisani M, Georgiewa P, Chung F, et al. Protease-activated receptor 2 expression in trigeminal neurons innervating the rat nasal mucosa. *Neuropeptides*. (2005) 39:461–66. doi: 10.1016/j.npep.2005.07.003

70. Weidner C, Klede M, Rukwied R, Lischetzki G, Neisius U, Skov PS, et al. Acute effects of substance P and calcitonin gene-related peptide in human skin–a microdialysis study. *J Invest Dermatol*. (2000) 115:1015–20. doi: 10.1046/j.1523-1747.2000.00142.x

71. Amadesi S, Nie J, Vergnolle N, Cottrell GS, Grady EF, Trevisani M, et al. Protease-activated receptor 2 sensitizes the capsaicin receptor transient receptor potential vanilloid receptor 1 to induce hyperalgesia. *J Neurosci*. (2004) 24:4300–12. doi: 10.1523/JNEUROSCI.5679-03.2004

72. Gu Q, Lee LY. House dust mite potentiates capsaicin-evoked Ca^{2+} transients in mouse pulmonary sensory neurons via activation of protease-activated receptor-2. *Exp Physiol*. (2012) 97:534–43. doi: 10.1113/expphysiol.2011.060764

73. Vergnolle N, Bunnett NW, Sharkey KA, Brussee V, Compton SJ, Grady EF, et al. Proteinase-activated receptor-2 and hyperalgesia: A novel pain pathway. *Nat Med*. (2001) 7:821–6. doi: 10.1038/89945

74. Hassler SN, Kume M, Mwirigi JM, Ahmad A, Shiers S, Wangzhou A, et al. The cellular basis of protease-activated receptor 2-evoked mechanical and affective pain. *JCI Insight*. (2020) 5:e137393. doi: 10.1172/jci.insight.137393

75. Akiyama T, Merrill AW, Zanotto K, Carstens MI, Carstens E. Scratching behavior and Fos expression in superficial dorsal horn elicited by protease-activated receptor agonists and other itch mediators in mice. *J Pharmacol Exp Ther*. (2009) 329:945–51. doi: 10.1124/jpet.109.152256

76. Xiang Y, Jiang Y, Lu L. Low-dose trypsin accelerates wound healing via protease-activated receptor 2. *ACS Pharmacol Transl Sci*. (2024) 7:274–84. doi: 10.1021/acsptsci.3c00263

77. Ständer S. Atopic dermatiti. *N Engl J Med*. (2021) 384:1136–43. doi: 10.1056/NEJMra2023911

78. Piontek K, Ittermann T, Arnold A, Völzke H, Baumeister SE, Apfelbacher C. Prevalence, atopic and psychological comorbidity of physician-diagnosed atopic dermatitis in an adult general population sample: A cross-sectional study. *Allergy*. (2022) 77:1915–7. doi: 10.1111/all.15288

79. Liu AW, Gillis JE, Sumpter TL, Kaplan DH. Neuroimmune interactions in atopic and allergic contact dermatitis. *J Allergy Clin Immunol*. (2023) 151:1169–77. doi: 10.1016/j.jaci.2023.03.013

80. Morizane S, Sunagawa K, Nomura H, Ouchida M. Aberrant serine protease activities in atopic dermatitis. *J Dermatol Sci*. (2022) 107:2–7. doi: 10.1016/j.jdermsci.2022.06.004

81. Fortugno P, Furio L, Teson M, Berretti M, El Hachem M, Zambruno G, et al. The 420K LEKTI variant alters LEKTI proteolytic activation and results in protease deregulation: implications for atopic dermatitis. *Hum Mol Genet*. (2012) 21:4187–200. doi: 10.1093/hmg/dds243

82. Ramesh K, Matta SA, Chew FT, Mok YK. Exonic t lympho-epithelial Kazal-type related inhibitor action and enhance its degradation. *Allergy*. (2020) 75:403–11. doi: 10.1111/all.14018

83. Lee SE, Jeong SK, Lee SH. Protease and protease-activated receptor-2 signaling in the pathogenesis of atopic dermatitis. *Yonsei Med J*. (2010) 51:808–22. doi: 10.3349/ymj.2010.51.6.80

84. Redhu D, Franke K, Kumari V, Francuzik W, Babina M, Worm M. Thymic stromal lymphopoietin production induced by skin irritation results from concomitant activation of protease-activated receptor 2 and interleukin 1 pathways. *Br J Dermatol*. (2020) 182:119–29. doi: 10.1111/bjd.17940

85. Buhl T, Ikoma A, Kempkes C, Cevikbas F, Sulk M, Buddenkotte J, et al. Protease-activated receptor-2 regulates neuro-epidermal communication in atopic dermatitis. *Front Immunol*. (2020) 11:1740. doi: 10.3389/fimmu.2020.01740

86. Steinhoff M, Neisius U, Ikoma A, Fartasch M, Heyer G, PS S, et al. Proteinase-activated receptor-2 mediates itch: a novel pathway for pruritus in human skin. *J Neurosci*. (2003) 23:6176–80. doi: 10.1523/JNEUROSCI.23-15-06176.2003

87. Smith L, Gatault S, Casals-Diaz L, Kelly PA, Camerer E, Métais C, et al. House dust mite-treated PAR2 over-expressor mouse: A novel model of atopic dermatitis. *Exp Dermatol*. (2019) 28:1298–308. doi: 10.1111/exd.14030

88. Jeong SK, Kim HJ, Youm JK, Ahn SK, Choi EH, Sohn MH, et al. Mite and cockroach allergens activate protease-activated receptor 2 and delay epidermal permeability barrier recovery. *J Invest Dermatol*. (2008) 128:1930–39. doi: 10.1038/jid.2008.13

89. Sakai T, Hatano Y, Matsuda-Hirose H, Zhang W, Takahashi D, Jeong SK, et al. Combined benefits of a PAR2 inhibitor and stratum corneum acidification for murine atopic dermatitis. *J Invest Dermatol*. (2016) 136:538–41. doi: 10.1016/j.jid.2015.11.011

90. Barr TP, Garzia C, Guha S, Fletcher EK, Nguyen N, Wieschhaus AJ, et al. PAR2 pepducin-based suppression of inflammation and itch in atopic dermatitis models. *J Invest Dermatol*. (2019) 139:412–21. doi: 10.1016/j.jid.2018.08.019

91. Bohannon M, Liu M, Nadeau P, Talton J, Gibson D, Datta S, et al. Topical doxycycline monohydrate hydrogel 1% targeting proteases/PAR2 pathway is a novel

therapeutic for atopic dermatitis. *Exp Dermatol*. (2020) 29:1171–75. doi: 10.1111/exd.14201

92. Wang ZH, Shi DM. Research progress on the neutrophil components and their interactions with immune cells in the development of psoriasis. *Skin Res Technol*. (2023) 29:e13404. doi: 10.1111/srt.13404

93. Iwakiri K, Ghazizadeh M, Jin E, Fujiwara M, Takemura T, Takezaki S, et al. Human airway trypsin-like protease induces PAR-2-mediated IL-8 release in psoriasis vulgaris. *J Invest Dermatol*. (2004) 122:937–44. doi: 10.1111/j.0022-202X.2004.22415.x

94. Carvalho RF, Nilsson G, Harvima IT. Increased mast cell expression of PAR-2 in skin inflammatory diseases and release of IL-8 upon PAR-2 activation. *Exp Dermatol*. (2010) 19:117–22. doi: 10.1111/j.1600-0625.2009.00998.x

95. Nattkemper LA, Lipman ZM, Ingrasci G, Maldonado C, Garces JC, Loayza E, et al. Neuroimmune mediators of pruritus in hispanic scalp psoriatic itch. *Acta Derm Venereol*. (2023) 103:adv4463. doi: 10.2340/actadv.v103.4463

96. Abdel Raheem HM, Shehata HA, Rashed LA, Saleh MA. Decreased level of PAR2 in Psoriasis and MF patients receiving Phototherapy. *Photodermatol Photoimmunol Photomed*. (2019) 35:282–83. doi: 10.1111/phpp.12464

97. Rau A, Grant-Kels JM. The ethics of depigmentation for vitiligo. *J Am Acad Dermatol*. (2024) 29:S0190-9622(24)00131-2. doi: 10.1016/j.jaad.2024.01.031

98. Hu Z, Wang T. Beyond skin white spots: Vitiligo and associated comorbidities. *Front Med (Lausanne)*. (2023) 10:1072837. doi: 10.3389/fmed.2023.1072837

99. Chang WL, Ko CH. The role of oxidative stress in vitiligo: an update on its pathogenesis and therapeutic implications. *Cells*. (2023) 12:936. doi: 10.3390/cells12060936

100. Moretti S, Nassini R, Prignano F, Pacini A, Materazzi S, Naldini A, et al. Protease-activated receptor-2 downregulation is associated to vitiligo lesions. *Pigment Cell Melanoma Res*. (2009) 22:335–8. doi: 10.1111/j.1755-148X.2009.00562.x

101. Kim JY, Kim DY, Son H, Kim YJ, Oh SH. Protease-activated receptor-2 activates NQO-1 via Nrf2 stabilization in keratinocytes. *J Dermatol Sci*. (2014) 74:48–55. doi: 10.1016/j.jdermsci.2013.11.010

102. Tang L, Wu W, Fu W, Hu Y. The effects of phototherapy and melanocytes on keratinocytes. *Exp Ther Med*. (2018) 15:3459–66. doi: 10.3892/etm.2018.5807

103. Espósito ACC, Cassiano DP, da Silva CN, Lima PB, Dias JAF, Hassun K, et al. Update on melasma-part I: pathogenesis. *Dermatol Ther (Heidelb)*. (2022) 12:1967–88. doi: 10.1007/s13555-022-00779-x

104. Lee SH, Kim JM, Lee SE, Jeong SK, Lee SH. Upregulation of protease-activated receptor-2 in keratinocytes by epidermal vascular endothelial growth factor in *vitro* and in vivo. *Exp Dermatol*. (2017) 26:286–8. doi: 10.1111/exd.13183

105. Kim NH, Lee AY. Oxidative stress induces skin pigmentation in melasma by inhibiting hedgehog signaling. *Antioxid (Basel)*. (2023) 12:1969. doi: 10.3390/antiox12111969

106. Scott G, Deng A, Rodriguez-Burford C, Seiberg M, Han R, Babiarz L, et al. Protease-activated receptor 2, a receptor involved in melanosome transfer, is upregulated in human skin by ultraviolet irradiation. *J Invest Dermatol*. (2001) 117:1412–20. doi: 10.1046/j.0022-202x.2001.01575.x

107. Deng Z, Chen M, Zhao Z, Xiao W, Liu T, Peng Q, et al. Whole genome sequencing identifies genetic variants associated with neurogenic inflammation in rosacea. *Nat Commun*. (2023) 14:3958. doi: 10.1038/s41467-023-39761-2

108. Croitoru DO, Piguet V. Cathelicidin LL-37 ignites primed NLRP3 inflammasomes in rosacea. *J Invest Dermatol*. (2021) 141:2780–2. doi: 10.1016/j.jid.2021.04.024

109. Kim JY, Kim YJ, Lim BJ, Sohn HJ, Shin D, Oh SH. Increased expression of cathelicidin by direct activation of protease-activated receptor 2: possible implications on the pathogenesis of rosacea. *Yonsei Med J*. (2014) 55:1648–55. doi: 10.3349/ymj.2014.55.6.1648

110. Kim HB, Na EY, Yun SJ, Lee JB. The effect of capsaicin on neuroinflammatory mediators of rosacea. *Ann Dermatol*. (2022) 34:261–69. doi: 10.5021/ad.21.223

111. Lee SE, Kim JM, Jeong SK, Choi EH, Zouboulis CC, Lee SH. Expression of protease-activated receptor-2 in SZ95 sebocytes and its role in sebaceous lipogenesis, inflammation, and innate immunity. *J Invest Dermatol*. (2015) 135:2219–27. doi: 10.1038/jid.2015.151

112. Adler BL, DeLeo VA. Allergic contact dermatitis. *JAMA Dermatol*. (2021) 157:364. doi: 10.1001/jamadermatol.2020.5639

113. Fleischer MI, Röhrig N, Raker VK, Springer J, Becker D, Ritz S, et al. Protease- and cell type-specific activation of protease-activated receptor 2 in cutaneous inflammation. *J Thromb Haemost*. (2022) 20:2823–36. doi: 10.1111/jth.15894

114. O'Connell KA, LaChance AH. Dermatomyositis. *N Engl J Med*. (2021) 384:2437. doi: 10.1056/NEJMicm2033425

115. Gao S, Zhu H, Yang H, Zhang H, Li Q, Luo H. The role and mechanism of cathepsin G in dermatomyositis. *BioMed Pharmacother*. (2017) 94:697–704. doi: 10.1016/j.biopha.2017.07.088

116. Hajialiasgary Najafabadi A, Soheilifar MH, Masoudi-Khoram N. Exosomes in skin photoaging: biological functions and therapeutic opportunity. *Cell Commun Signal*. (2024) 22:32. doi: 10.1186/s12964-023-01451-3

117. Bang E, Kim DH, Chung HY. Protease-activated receptor 2 induces ROS-mediated inflammation through Akt-mediated NF-κB and FoxO6 modulation during skin photoaging. *Redox Biol*. (2021) 44:102022. doi: 10.1016/j.redox.2021.102022

118. Kim HS, Hashimoto T, Fischer K, Bernigaud C, Chosidow O, Yosipovitch G. Scabies itch: an update on neuroimmune interactions and novel targets. *J Eur Acad Dermatol Venereol*. (2021) 35:1765–76. doi: 10.1111/jdv.17334

119. Yang H, Chen W, Zhu R, Wang J, Meng J. Critical players and therapeutic targets in chronic itch. *Int J Mol Sci*. (2022) 23:9935. doi: 10.3390/ijms23179935

120. Zhao J, Munanairi A, Liu XY, Zhang J, Hu L, Hu M, et al. PAR2 mediates itch via TRPV3 signaling in keratinocytes. *J Invest Dermatol*. (2020) 140:1524–32. doi: 10.1016/j.jid.2020.01.012

121. Park CW, Kim HJ, Choi YW, Chung BY, Woo SY, Song DK, et al. TRPV3 channel in keratinocytes in scars with post-burn pruritus. *Int J Mol Sci*. (2017) 18:2425. doi: 10.3390/ijms18112425

122. Sanders KM, Nattkemper LA, Rosen JD, Andersen HH, Hsiang J, Romanelli P, et al. Non-histaminergic itch mediators elevated in the skin of a porcine model of scabies and of human scabies patients. *J Invest Dermatol*. (2019) 139:971–73. doi: 10.1016/j.jid.2018.09.032

frontiers | Frontiers in Immunology

TYPE Original Research
PUBLISHED 27 September 2024
DOI 10.3389/fimmu.2024.1415350

OPEN ACCESS

EDITED BY
Wai Po Chong,
Hong Kong Baptist University, Hong Kong SAR, China

REVIEWED BY
Makoto Makishima,
Nihon University, Japan
Thomas Haarmann-Stemmann,
Leibniz-Institut für Umweltmedizinische Forschung (IUF), Germany

*CORRESPONDENCE
Dong Hun Lee
ivymed27@snu.ac.kr
Soyun Cho
sycho@snu.ac.kr

†These authors have contributed equally to this work and share first authorship

‡These authors have contributed equally to this work

RECEIVED 10 April 2024
ACCEPTED 23 August 2024
PUBLISHED 27 September 2024

CITATION
Lee JS, Lee Y, Jang S, Oh J-H, Lee DH and Cho S (2024) Pregnane X receptor reduces particulate matter-induced type 17 inflammation in atopic dermatitis. *Front. Immunol.* 15:1415350. doi: 10.3389/fimmu.2024.1415350

Pregnane X receptor reduces particulate matter-induced type 17 inflammation in atopic dermatitis

Ji Su Lee[1,2†], Youngae Lee[2,3,4†], Sunhyae Jang[2,4,5], Jang-Hee Oh[1,3,4], Dong Hun Lee[1,2,3,4*‡] and Soyun Cho[1,4,6*‡]

[1]Department of Dermatology, Seoul National University College of Medicine, Seoul, Republic of Korea, [2]Department of Dermatology, Seoul National University Hospital, Seoul, Republic of Korea, [3]Laboratory of Cutaneous Aging Research, Biomedical Research Institute, Seoul National University Hospital, Seoul, Republic of Korea, [4]Institute of Human-Environment Interface Biology, Medical Research Center, Seoul National University, Seoul, Republic of Korea, [5]Laboratory of Cutaneous Aging and Hair Research, Clinical Research Institute, Seoul National University Hospital, Seoul, Republic of Korea, [6]Department of Dermatology, Seoul Metropolitan Government – Seoul National University (SMG-SNU) Boramae Medical Center, Seoul, Republic of Korea

Background: Epidemiological evidence suggests that particulate matter (PM) exposure can trigger or worsen atopic dermatitis (AD); however, the underlying mechanisms remain unclear. Recently, pregnane X receptor (PXR), a xenobiotic receptor, was reported to be related to skin inflammation in AD.

Objectives: This study aimed to explore the effects of PM on AD and investigate the role of PXR in PM-exposed AD.

Methods: *In vivo* and *in vitro* AD-like models were employed, using BALB/c mice, immortalized human keratinocytes (HaCaT), and mouse $CD4^+$ T cells.

Results: Topical application of PM significantly increased dermatitis score and skin thickness in AD-like mice. PM treatment increased the mRNA and protein levels of type 17 inflammatory mediators, including interleukin (IL)-17A, IL-23A, IL-1β, and IL-6, in AD-like mice and human keratinocytes. PM also activated PXR signaling, and PXR knockdown exacerbated PM-induced type 17 inflammation in human keratinocytes and mouse $CD4^+$ T cells. In contrast, PXR activation by rifampicin (a human PXR agonist) reduced PM-induced type 17 inflammation. Mechanistically, PXR activation led to a pronounced inhibition of the nuclear factor kappa B (NF-κB) pathway.

Conclusion: In summary, PM exposure induces type 17 inflammation and PXR activation in AD. PXR activation reduces PM-induced type 17 inflammation by suppressing the NF-κB signaling pathway. Thus, PXR represents a promising therapeutic target for controlling the PM-induced AD aggravation.

KEYWORDS

particulate matter, air pollution, pregnane X receptor, atopic dermatitis, type 17 inflammation

1 Introduction

Particulate matter (PM) from ambient air is a key component of air pollutants and is a complex mixture of solid and liquid particles, including nitrates, sulfates, elemental and organic carbon, organic compounds (e.g., polycyclic aromatic hydrocarbons (PAHs)), biological compounds (e.g., endotoxins and cell fragments), and metals (e.g., iron, copper, nickel, and zinc) (1). PM can be classified according to particle diameter as follows: PM_{10} (coarse particles, ≤10 μm), $PM_{2.5}$ (fine particles, ≤2.5 μm), and $PM_{0.1}$ (ultrafine particles, ≤0.1 μm) (1, 2). Most studies on the effects of PM on health have focused on cardiovascular and respiratory diseases (3); however, increasing evidence demonstrates that PM also detrimentally affects the skin (2, 4–7).

Atopic dermatitis (AD) is a chronic, relapsing, inflammatory skin disease that places a significant burden on healthcare resources and patients' quality of life (8). AD is a multifactorial disease resulting from complex interactions among genetic predisposition, environmental factors, immune dysregulation, and skin barrier dysfunction. The prevalence of AD is continuously increasing, particularly in countries with rapidly developing urban areas, which emphasizes the role of the environment in AD pathogenesis (8–10). Several epidemiological studies have indicated that PM exposure contributes to the aggravation and development of AD (2, 6, 11–14). However, these studies were primarily focused on epidemiological perspectives and did not investigate the mechanisms underlying the effects of PM on AD, which remain unclear.

One of the putative mechanisms involved is xenobiotic metabolism, which is the process of detoxifying exogenous (e.g., pollutants) and endogenous (e.g., bilirubin) chemicals (15–17). This process is regulated by xenobiotic receptors, including pregnane X receptor (PXR), aryl hydrocarbon receptor (AHR), and constitutive androstane receptor (CAR). Xenobiotic receptors function beyond xenobiotic metabolism and are additionally involved in various cellular processes, including inflammation, oxidative stress, cell proliferation and death, lipid metabolism, tissue injury and repair, and cancer development (15). As the first barrier of the human body, the skin is exposed to numerous factors, such as pollutants, that can serve as ligands and activate xenobiotic receptors (18) which are expressed in epidermal keratinocytes, dermal fibroblasts, and immune cells (15). Some studies have shown that xenobiotic metabolism is triggered in the skin of patients with AD (15–18). However, most studies have focused on AHR, and little is known about the role of PXR in PM-exposed AD skin. Interestingly, PXR has demonstrated both anti-inflammatory (19–22) and pro-inflammatory effects (18, 23), suggesting context- and ligand-dependent dual roles (15). Therefore, additional studies are needed to determine the specific function of PXR in PM-exposed AD.

In the present study, we aimed to elucidate PM-induced effects on AD and the role of PXR in PM-exposed AD *in vivo* in mice skin and *in vitro* in human cell lines. We observed that PM induces type 17 inflammation and PXR activation. Activated PXR reduces PM-induced type 17 inflammatory mediators through suppression of the nuclear factor kappa B (NF-κB) signaling pathway in AD. Thus, targeting PXR is a promising strategy to attenuate the PM-induced flare-up or progression of AD. Our results provide novel insights into protecting skin health against air pollution.

2 Materials and methods

Detailed experimental methods are presented in the Supplementary Methods.

2.1 PM preparation

Standard reference material (SRM) 2786 (PM) was purchased from the National Institute of Standards and Technology (NIST, Gaithersburg, MD, USA). This material, with a mean particle diameter of 2.8 μm, was collected from ambient air in Prague, Czechia and represents atmospheric $PM_{2.5}$ obtained from the urban environment containing PAH, metals, biological combustion products, and other substances (Supplementary Table 1) (24). SRM 2786 was resuspended in phosphate-buffered saline (PBS) at a concentration of 50 mg/ml and stored at 4°C until use. SRM stock solution was vortexed for 5 min at maximum speed and sonicated for 5 min using a Bandelin sonicator (Bandelin, Berlin, Germany) immediately before treatment.

2.2 Animals, induction of AD, and PM treatment

We used the 2,4-dinitrochlorobenzene (DNCB)-induced AD-like mouse model, as previously described (25–30). Six-week-old female BALB/c mice were purchased from Orient Bio Inc. (Seongnam, Gyeonggi, Republic of Korea) and housed under semi-specific pathogen-free conditions with individually ventilated cages (24 ± 2 °C with a 12-h light-dark cycle). They were fed standard laboratory chow and water *ad libitum*. The experimental schedule is summarized in Figure 1A. After 1 week of acclimation, the dorsal area of the mice was shaved and depilated (1.5 × 2 cm^2). On Day 7 and Day 5, after shaving and depilation, 100 μL of 1% DNCB dissolved in an acetone: olive oil mixture (3:1 vol/vol) was applied to the dorsal skin of the mice (DNCB sensitization). The cutaneous DNCB-sensitized mice were divided into four groups: (1) Control, (2) AD, (3) AD + Low PM, and (4) AD + High PM. From Day 0 to Day 16, the vehicle (acetone and olive oil mixture) was applied to the dorsum three times a week in the control group. In AD, AD + low PM, and AD + high PM, 200 μL of 0.3% DNCB was applied to the dorsum three times a week (DNCB challenge). From Day 5, 20 μg/cm^2 and 100 μg/cm^2 of PM (SRM 2786) in PBS (31, 32) was additionally applied 1 h after DNCB application in the AD + low PM and AD + high PM group, respectively.

Abbreviations: AD, atopic dermatitis; AHR, aryl hydrocarbon receptor; DNCB, 2,4-dinitrochlorobenzene; IFN-γ, interferon gamma; IgE, immunoglobulin E; IL, interleukin; NF-kB, nuclear factor kappa B; PAH, polycyclic aromatic hydrocarbon; PM, particulate matter; PXR, pregnane X receptor; Th, T helper; TNF-α, tumor necrosis factor alpha; UGT, uridine-5'-diphospho-glucuronosyltransferase.

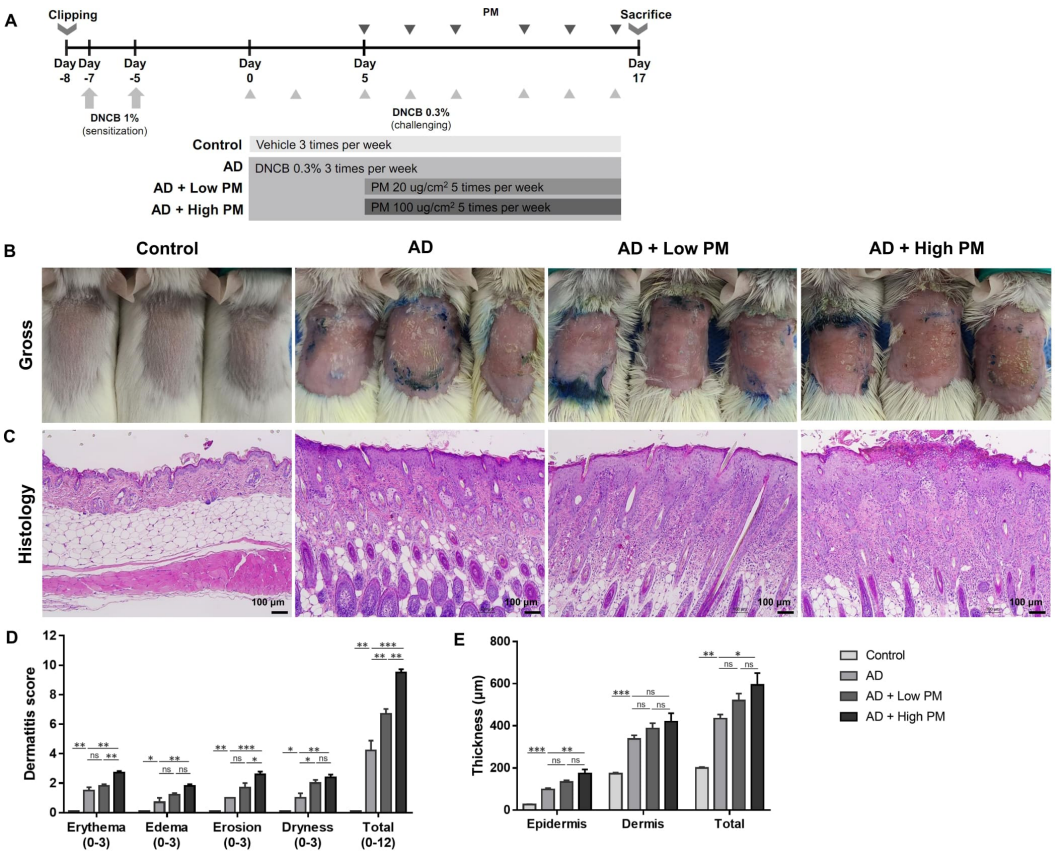

FIGURE 1
Particulate matter (PM) exposure aggravates atopic dermatitis (AD)-like features in AD-like mice in clinical and histopathological examinations. **(A)** Mouse experimental schedule. We generated a 2,4-dinitrochlorobenzene (DNCB)-induced AD-like model using BALB/c mice. AD-like mice were additionally treated with either low (20 μg/cm^2) or high (100 μg/cm^2) concentration of PM. **(B, D)** DNCB-treated mice showed AD-like skin lesions with erythema, edema, erosion, and dryness/scales. Dermatitis score increased in the AD group and further increased in the AD + PM groups in a dose-dependent manner. **(C, E)** Histology of the PM-exposed AD-like mice stained with hematoxylin and eosin. DNCB-treated mice showed AD-like features such as hyperkeratosis, acanthosis, spongiosis, and inflammatory cell infiltration. PM further increased the skin thickness. Data are representative of two independent experiments and are shown as the mean ± SEM (n = 5 mice in each group). ns, nonsignificant; *P <.05; **P <.01; ***P <.001. P-values were obtained by the unpaired Student's *t* test and one-way ANOVA.

2.3 Cell culture, induction of AD, and PM treatment

HaCaT cells (immortalized human keratinocytes) were cultured in Dulbecco's modified Eagle's medium (DMEM, Welgene, Daegu, Republic of Korea) supplemented with 10% fetal bovine serum (FBS, Thermo Fisher Scientific, Waltham, MA, USA) and 1% penicillin-streptomycin at 37°C in a humidified atmosphere of 5% CO_2. Cells were first seeded (1.5×10^5 cells/dish in a 35 mm dish) and grown for 2–3 days and then starved with 0% FBS-DMEM for 1 day at >80% confluence. Subsequently, cells were co-stimulated with tumor necrosis factor alpha (TNF-α) (2 ng/mL) and interferon gamma (IFN-γ) (10 ng/mL) to induce AD-like keratinocytes as previously described (33–37). TNF-α and IFN-γ-treated AD-like keratinocytes are known to produce type 2 inflammation-mediated chemokines like thymus and activation-regulated chemokine (TARC) and macrophage-derived chemokine (MDC) and decrease the expression of barrier-related proteins including filaggrin and loricrin (33–37). Recombinant TNF-α and IFN-γ were purchased from R&D Systems (Minneapolis, MN, USA). After 1 h, cells were additionally treated with PM (100 μg/ml). Thereafter, the cells were harvested for mRNA or protein analysis at 4 h after treatment, and supernatants were harvested for protein analysis at 24 h after treatment.

2.4 Isolation and activation of mouse CD4$^+$ T cells

Mouse CD4$^+$ T cells from the spleen were isolated using magnetic activated cell sorting (MACS) LS columns, adhering to the manufacturer's guidelines (Miltenyi Biotec, Bergisch Gladbach, North Rhine-Westphalia, Germany). For the activation of mouse T cells, purified CD4$^+$ T cells (2×10^5) were stimulated with plate-bound anti-CD3ε (5 μg/ml) and soluble anti-CD28 (2 μg/ml) antibodies for 72 h, either in the presence of a vehicle or PM. CD4$^+$ T cells were cultured in RPMI 1640 (Welgene) supplemented with HEPES, non-essential amino acids, sodium pyruvate, glutamine, penicillin-streptomycin, and 10% FBS. Antibodies against CD3ε (clone 145-2C11) and CD28 (clone 37.51) were purchased from eBioscience (San Diego, CA, USA). Mouse CD4 MicroBeads (clone L3T4) were purchased from Miltenyi Biotec. All culture reagents for mouse CD4$^+$ T cells were purchased from Sigma-Aldrich (St. Louis, MO, USA). Mouse interleukin (IL)-4

and IL-17A production levels in the culture supernatants were measured using ELISA, following the manufacturer's protocol from BioLegend (San Diego, CA, USA).

2.5 Statistics

All statistical analyses were performed using SPSS 19.0 software (IBM, Armonk, NY, USA). The results are expressed as the mean ± standard error of means (SEM). Comparisons between two groups were performed using unpaired Student's *t*-test. Comparisons between three or more groups were performed using one-way analysis of variance (ANOVA) with Tukey's *post hoc* test. Data are representative of two to three independent experiments (n = 3–5 per group). P-values <.05 indicated significance.

2.6 Study approval

The animal experimental protocol was approved by the Seoul National University Hospital Institutional Animal Care and Use Committee (No.19-0090-S1A0). All experiments were performed in accordance with the approved experimental protocol.

3 Results

3.1 PM exposure aggravates AD-like inflammation

We employed the DNCB-induced AD-like mouse model, which is a well-established AD-like *in vivo* model (25–30). DNCB-treated mice showed AD-like skin lesions characterized by erythema, edema, erosion, and dryness/scales (Figure 1B). Histological examination revealed hyperkeratosis, acanthosis, spongiosis, and extensive infiltration of inflammatory cells in the epidermis and dermis (Figure 1C). Topical application of low (20 μg/cm^2) or high (100 μg/cm^2) concentrations of $PM_{2.5}$ (SRM 2786) further aggravated the AD-like skin lesions (Figures 1B, C). In addition to individual scores reflecting erythema, edema, erosion, and dryness, the overall dermatitis score was significantly increased in the AD group compared to that in the control group and further increased in the PM groups in a dose-dependent manner (AD, 4.20 ± 0.68; AD + low PM, 6.70 ± 0.34; AD + high PM, 9.5 ± 0.22) (Figure 1D). Similarly, epidermal thickness and skin thickness (sum of epidermal and dermal thicknesses) were significantly increased in the AD group and further increased in the high-PM groups (Figure 1E).

3.2 PM exposure increases type 17 inflammation in AD-like inflammation

Next, we analyzed key pathogenic cytokines associated with AD in skin tissues. As expected, the mRNA (Figures 2A, B) and protein (Figures 2C, D) levels of type 2 cytokines, including IL-4 and IL-13, were increased after AD induction. Serum immunoglobulin E (IgE) levels were also significantly increased in AD-like mice skin lesions (Figure 2E). However, IL-4, IL-13, and serum IgE levels did not show a further significant increase by additional PM treatment (Figures 2A–E).

Previous studies have suggested that in addition to the type 2 immune response, type 17 immune response also contributes to AD pathogenesis (38–41) and is associated with PM exposure (17, 42–48). We observed a modest increase in the levels of major type 17 inflammatory mediators, IL-17A and IL-23A, after AD induction (Figures 2F–I). Notably, IL-17A mRNA and protein were significantly increased with both low and high PM exposure (Figures 2F, H), and those of IL-23A were significantly increased after high PM treatment (Figures 2G, I). Other type 17 inflammation-related cytokines including IL-1β and IL-6 were increased after AD induction and showed a further incremental tendency after additional PM treatment (Supplementary Figure 1).

3.3 PM exposure activates PXR in AD-like inflammation

To investigate the role of PXR in PM-exposed AD, we examined the expression of PXR and its downstream genes in the skin. Indeed, the levels of PXR mRNA and protein were significantly increased in the AD group and were further increased with additional PM treatment, particularly for high PM exposure (Figures 2J, K). Consistently, high PM exposure significantly induced downstream PXR genes in mice such as *CYP3A11* (Figure 2L), indicating that PM exposure activated the PXR signaling pathway.

3.4 PM exposure increases type 17 inflammation-related cytokine production and activates PXR in AD-like keratinocytes

We employed a TNF-α- and IFN-γ-stimulated *in vitro* AD-like HaCaT cell model, which produces type 2 inflammation-mediated chemokines and decreases the expression of barrier-related proteins, as previously reported (33–37). We further administered 100 μg/ml of PM to these cells, which was the highest concentration that did not induce cytotoxicity (Figures 3A, B). Similar to AD-like inflammation in mice, AD-like keratinocytes showed an increase in type 17 inflammation-related cytokines (IL-17A, IL-23A, IL-1β, and IL-6), which was further significantly increased after additional PM treatment, except for IL-23A (Figures 3C–I), whose protein was undetectable. Specifically, IL-17A mRNA and protein levels were considerably increased after PM treatment (Figures 3C, G), consistent with *in vivo* findings (Figures 2F, H). Moreover, PM treatment in keratinocytes significantly increased PXR mRNA levels and its downstream gene in humans, *UGT1A1* (Figures 3J, L). Luciferase activity of PXR increased in the PM-treated AD-like keratinocytes (Supplementary Figure 2A). PXR protein levels were also increased in PM-exposed AD-like keratinocytes (Figure 3K). Collectively, the PM-treated AD-like keratinocytes recapitulated the characteristic features of PM-treated AD-like mice, such as type 17 inflammation and PXR activation.

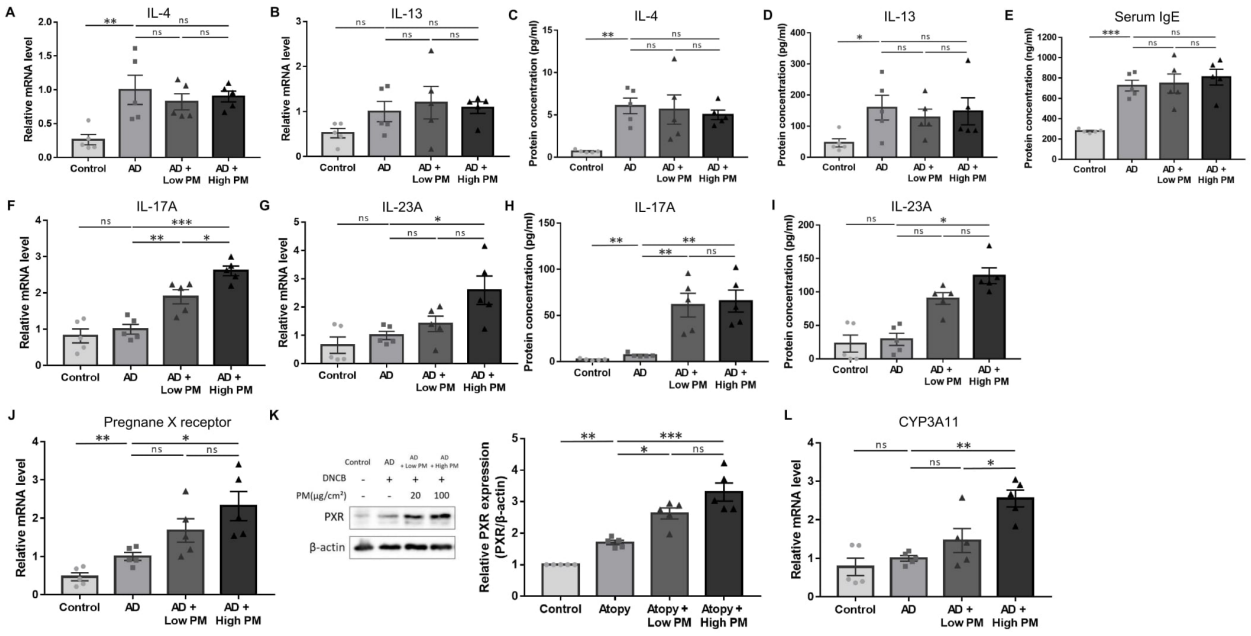

FIGURE 2
Change in the expression of type 2 and type 17 cytokines, pregnane X receptor (PXR), and downstream genes after atopic dermatitis (AD) induction and additional particulate matter (PM) treatment in mice. **(A, B)** mRNA and **(C, D)** protein levels of type 2 cytokines (interleukin (IL)-4 and IL-13) and **(E)** serum immunoglobulin E levels increased after AD induction but did not further increase after PM treatment. **(F, G)** mRNA and **(H, I)** protein levels of type 17 cytokines (IL-17A and IL-23A) increased slightly after AD induction and further increased after PM treatment. **(J)** mRNA and **(K)** protein levels of PXR increased after additional PM treatment. **(L)** Downstream gene of PXR in mice (*CYP3A11*) increased after additional PM treatment. Data are representative of two independent experiments and are shown as the mean ± SEM (n = 5 mice in each group). The mRNA data were normalized to the AD group. ns, nonsignificant; *P <.05; **P <.01; ***P <.001. P-values were obtained using the unpaired Student's t test and one-way ANOVA.

3.5 PXR activation reduces PM-induced type 17 inflammation

Previous studies have demonstrated that PXR suppresses inflammation and regulates tissue damage (19–22). However, other reports suggest that PXR activation triggers inflammatory responses in a context-specific manner (15, 18, 23). We knocked down PXR in keratinocytes using PXR siRNA prior to AD induction and PM treatment to clarify the specific role of PXR in PM-induced type 17 inflammation in AD. The mRNA and protein levels of PXR were decreased after PXR siRNA transfection (Figures 3J, K), along with its downstream gene, *UGT1A1* (Figure 3L). Compared to control siRNA-transfected cells, PXR siRNA-transfected keratinocytes showed a significant increase in the mRNA levels of type 17 inflammation-related cytokines (IL-17A, IL-23A, IL-1β, and IL-6) after PM treatment (Figures 3C–F). Furthermore, the increase in IL-17A, IL-1β, and IL-6 was confirmed at the protein level (Figures 3G–I). Consistently, SPA70, a human PXR antagonist, increased the mRNA levels of IL-1β, IL-6, and IL-23A in PM-treated AD-like keratinocytes (Supplementary Figures 3A–C). In the meanwhile, CH223191, an AHR antagonist, increased the mRNA levels of IL-1β, IL-6, and IL-23A in PM-treated AD-like keratinocytes (Supplementary Figures 4A–C). Our findings suggest that PXR activation induced by PM exposure limits the PM-induced type 17 inflammation in AD, aside from AHR. To confirm these assumptions, we treated keratinocytes with rifampicin, a potent human PXR agonist (15) before AD induction and PM treatment. Rifampicin increased the luciferase activity of PXR (Supplementary Figure 2B). Rifampicin increased the mRNA level of *UGT1A1* in a dose-dependent manner (Figure 4A) and accelerated the PM-induced increase in *UGT1A1* in AD-like keratinocytes (Figure 4B), indicating the activation of the PXR signaling pathway. Indeed, rifampicin treatment reduced PM-induced type 17 inflammation in AD-like keratinocytes, with decreased mRNA (IL-17A, IL-23A, IL-1β, and IL-6) and protein (IL-17A, IL-1β, and IL-6) levels of type 17 cytokines after PM treatment in rifampicin-treated keratinocytes (Figures 4C–I). When comparing the effect of rifampicin treatment, the expressions of IL-1β and IL-6 were higher in PXR siRNA-transfected AD-like keratinocytes compared to control siRNA-transfected AD-like keratinocytes (Supplementary Figures 5A, B). This finding suggests that the effect of rifampicin was partially canceled by PXR knockdown.

3.6 Exposure to PM amplifies IL-17A production in mouse CD4$^+$ T cells, with a more pronounced increase observed in PXR knockdown conditions

To assess the direct impact of PM on IL-17A production in activated CD4$^+$ T cells *in vitro*, we utilized CD4$^+$ T cells from mouse splenocytes and subjected them to stimulation with varying concentrations of PM to establish an optimal concentration. After a 24-hour stimulation with 25, 50, or 100 μm/ml of PM, there were no observed cytotoxic effects on mouse CD4$^+$ T cells compared to control cells; however, exposure to 200 or 400 μg/ml of PM exhibited cytotoxic

10.3389/fimmu.2024.1415350

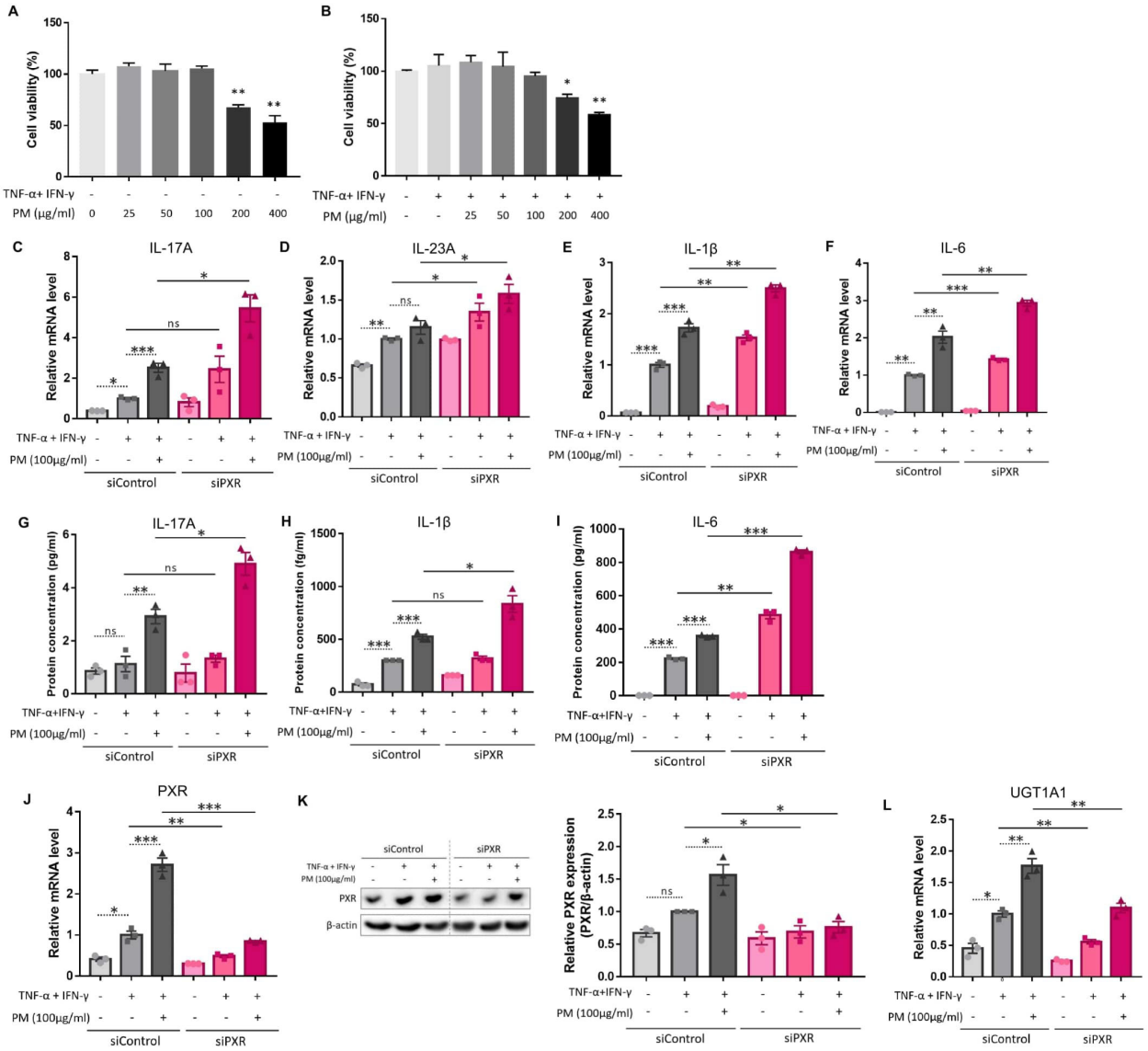

FIGURE 3
Comparison of the expression of type 17 inflammation-related cytokines, pregnane X receptor (PXR), and its downstream gene after atopic dermatitis (AD) induction and additional particulate matter (PM) treatment between control and PXR siRNA-transfected keratinocytes. The cell viability of **(A)** normal keratinocytes and **(B)** AD-like keratinocytes (TNF-α/IFN-γ-treated keratinocytes) was sustained with PM concentration increment until 100 μg/ml, after which it started to decrease. **(C–F)** mRNA and **(G–I)** protein levels of type 17 inflammatory cytokines (IL-17A, IL-23A, IL-1β, and IL-6) increased after AD induction, and further increased after PM treatment. IL-23A protein was undetectable. **(C–I)** Increased type 17 inflammation was exaggerated after PXR gene silencing using siRNA transfection. **(J)** mRNA and **(K)** protein levels of PXR increased after additional PM treatment. **(L)** Downstream gene of PXR in humans (*UGT1A1*) increased after additional PM treatment. **(J–L)** PM-induced PXR activation was suppressed after PXR siRNA transfection. Data are representative of three independent experiments and are shown as the mean ± SEM (n = 3 in each group). The mRNA data were normalized to the AD-like keratinocytes transfected with control siRNA without PM treatment. ns, nonsignificant; *P <.05; **P <.01; ***P <.001. P-values were obtained using the unpaired Student's t test and one-way ANOVA.

effects on the cells relative to control (Figure 5A). ELISA analysis revealed a significant enhancement in IL-17A production, but not IL-4, in anti-CD3/CD28-stimulated $CD4^+$ T cells when exposed to 25, 50, or 100 μm/ml of PM (Figures 5B, C). Furthermore, the knockdown of PXR significantly enhances the production of IL-17A of anti-CD3/CD28-stimulated CD4+ T cells in response to PM exposure. After 100 μg/ml PM treatment in anti-CD3/CD28-stimulated CD4+ T cells, IL-17A production increased by 55.7% in PXR siRNA-transfected group, compared to 32.6% in control siRNA-transfected group (Figures 5D, E). These findings suggest that exposure to PM enhances IL-17A production in activated $CD4^+$ T cells, and PXR suppresses PM-induced IL-17A production in these cells.

3.7 PM-induced PXR activation suppresses the NF-κB signaling pathway

Next, we sought to identify the signaling pathway mediated by PXR activation. PXR and NF-κB pathways are known to exert reciprocal repression (15, 49). PM has been shown to activate the

10.3389/fimmu.2024.1415350

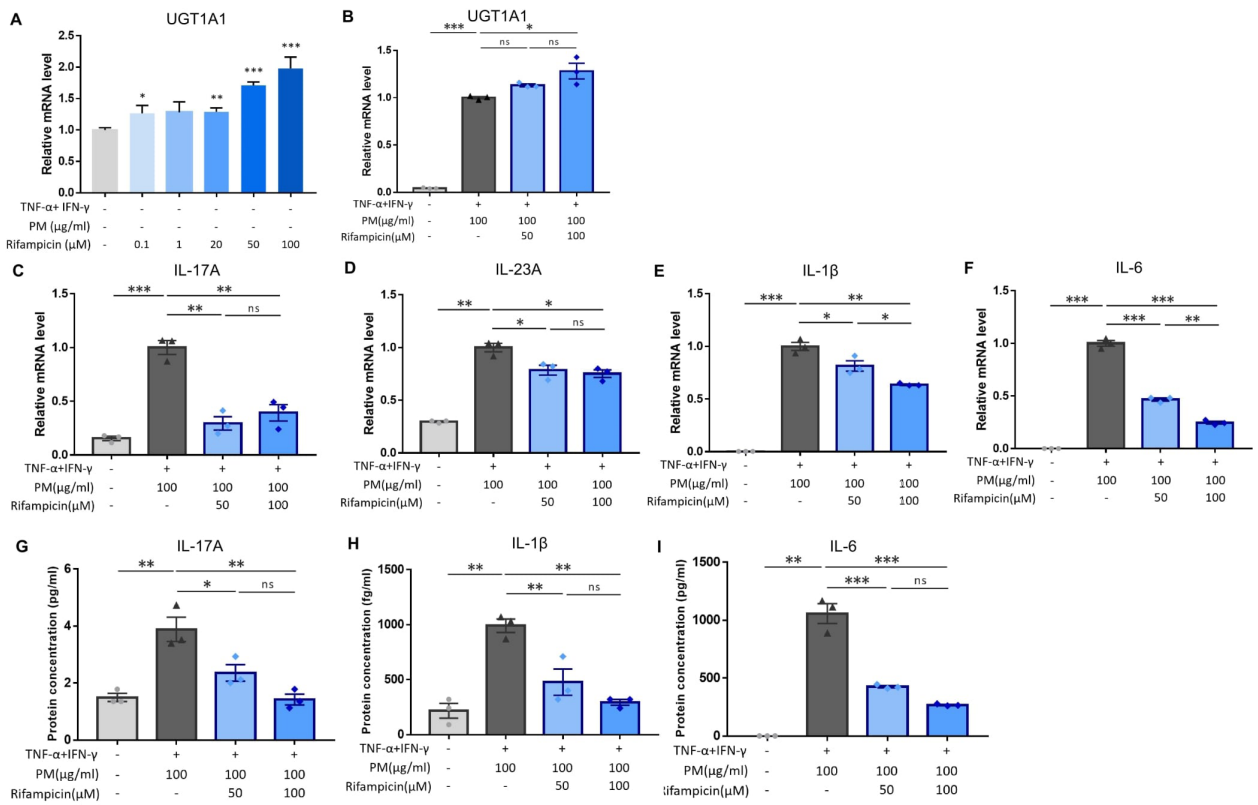

FIGURE 4
Influence of rifampicin (human pregnane X receptor (PXR) agonist) treatment in particulate matter (PM)-induced type 17 inflammation in atopic dermatitis (AD). **(A)** *UGT1A1*, a downstream gene of human PXR, increased by rifampicin treatment in a dose-dependent manner. **(B)** Rifampicin further increased the mRNA level of *UGT1A1* after PM treatment. **(C–F)** mRNA and **(G–I)** protein levels of type 17 inflammation-related cytokines (IL-17A, IL-23A, IL-1β, and IL-6) increased by PM treatment in AD-like keratinocytes, and rifampicin reduced the effects of PM in a dose-dependent manner. Data are representative of three independent experiments and are shown as the mean ± SEM (n = 3 in each group). For **(A, B)**, the mRNA data were normalized to the untreated keratinocytes, while for **(C–I)**, the mRNA data were normalized to the PM-treated AD-like keratinocytes without rifampicin treatment. ns, nonsignificant; *P <.05; **P <.01; ***P <.001. P-values were obtained using the unpaired Student's t test and one-way ANOVA.

NF-kB signaling pathway (2, 6, 17, 32, 50) which promotes Th17 differentiation and IL-17 and IL-23 production (50, 51). We investigated whether the antagonistic relationship between PXR and NF-κB was involved in PM-exposed AD by comparing the activation of NF-κB signaling pathway between control and PXR siRNA-transfected AD-like keratinocytes after PM treatment (Figure 6). In control siRNA-transfected keratinocytes, PM gradually increased PXR protein levels up to 30 min, which remained at a similar level at 60 min (Figures 6A, B). Additionally, these keratinocytes exhibited an increase in phosphorylated p65 levels up to 30 min, followed by a decrease at 60 min (Figures 6A, C). In contrast, in PXR siRNA-transfected keratinocytes, PM induced an earlier and more substantial increase in phosphorylated p65 levels, reaching their peak at 15 min and maintaining slightly lower levels until 60 min (Figures 6A, C). In control siRNA-transfected keratinocytes, phosphorylated IκBα reached its maximum level at 60 min, whereas in the PXR siRNA-transfected keratinocytes, its peak level occurred earlier, at 15 and 60 min (Figures 6A, D). Phosphorylated p65 levels increased following SPA70 treatment (Supplementary Figure 6), which was consistent with the increased phosphorylated p65 levels observed in PXR knockdown keratinocytes. These findings indicate that PM exposure in the context of PXR knockdown resulted in an earlier activation of IκBα, followed by a more potent and earlier activation of p65 in AD-like keratinocytes (Figure 7). Conversely, the PM-induced activation of PXR might constrain NF-κB signaling, potentially contributing to the reduction of type 17 inflammation caused by PM (Figure 7).

4 Discussion

PM can penetrate intact and barrier-disrupted skin through hair follicles and intercellularly in barrier-disrupted skin (52). We previously showed that repeated topical application of PM resulted in neutrophil-dominant dermal inflammation in barrier-disrupted skin (52). Epidemiological studies showed that PM contributes to the aggravation and development of AD (2, 6, 11–14). The underlying mechanisms have been suggested to involve skin barrier impairment, dysfunctional inflammation, microbiome alteration, and oxidative damage (6).

PM induces type 17 inflammation in epithelial and immune cells in the lung (42, 43, 45). In ovalbumin-treated mouse skin and keratinocytes, PM exposure increased transcripts related to Th17

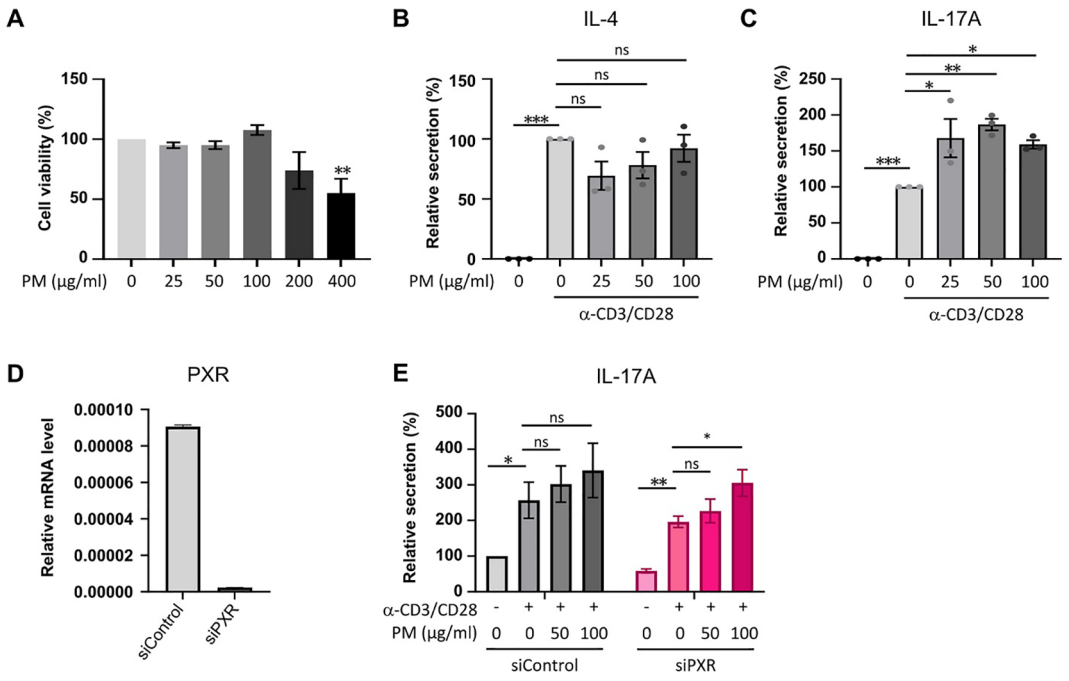

FIGURE 5
The exposure to PM amplifies IL-17A production in activated CD4+ T cells, with a more pronounced effect observed in PXR knockdown CD4+ T cells. **(A)** Assessment of cell viability in mouse CD4+ T cells exposed to varying concentrations of PM. **(B, C)** Quantification of IL-4 **(B)** and IL-17A **(C)** protein levels in mouse CD4+ T cells following stimulation with anti-CD3/CD28 in the presence of varying concentrations of PM. **(D)** Expression mRNA levels of PXR in control or PXR siRNA transfected mouse CD4+ T cells. **(E)** Evaluation of IL-17A production in mouse CD4+ T cells transfected with control or PXR siRNA, stimulated with anti-CD3/CD28 in the presence of PM (n=5). The relative secretions of IL-17A were normalized to those of the untreated control siRNA-transfected group. Data are representative of two independent experiments and are shown as the mean ± SEM (n = 3-5 mice). ns, nonsignificant; *P <.05; **P <.01; ***P <.001. P-values were obtained employing the unpaired Student's t-test and one-way ANOVA.

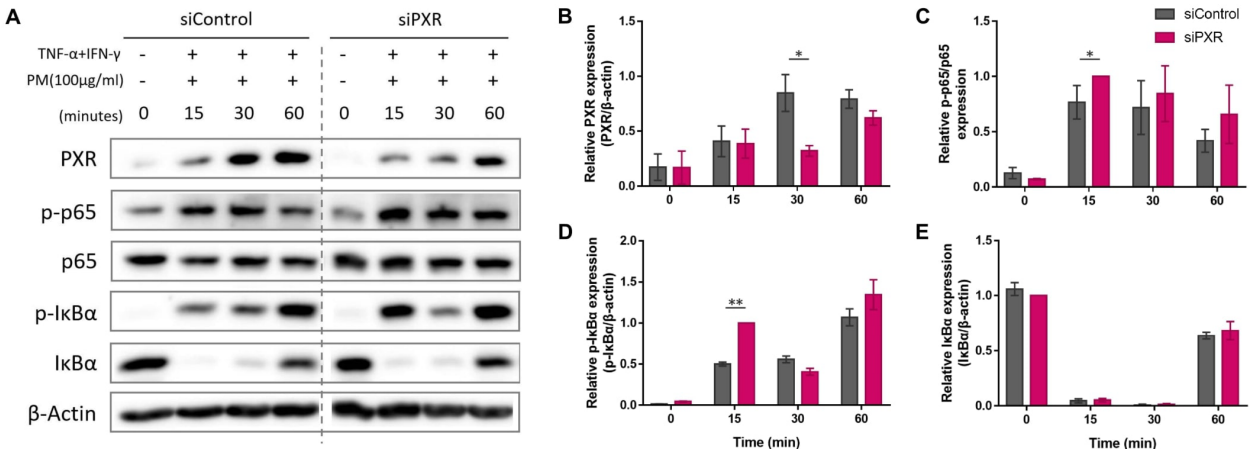

FIGURE 6
Comparison of the expression of the nuclear factor kappa B (NF-κB) signaling pathway components after particulate matter (PM) treatment between control and pregnane X receptor (PXR) siRNA-transfected atopic dermatitis (AD)-like keratinocytes. **(A, B)** In control siRNA-transfected keratinocytes, PM gradually increased PXR protein levels up to 30 min and remained at a similar level at 60 min. **(A, C)** Control siRNA-transfected keratinocytes exhibited an increase in phosphorylated p65 levels up to 30 min, followed by a decrease at 60 min. In PXR siRNA-transfected keratinocytes, PM induced an earlier and more substantial increase in phosphorylated p65 levels, reaching their peak at 15 min and maintaining slightly lower levels until 60 min. **(A, D)** In control siRNA-transfected keratinocytes, phosphorylated IκBα reached its maximum level at 60 min, whereas in the PXR siRNA-transfected keratinocytes, its peak level occurred earlier, at 15 and 60 min. **(A, E)** IκBα degraded at first and then recovered in both groups. Collectively, the PM-induced activation of PXR might constrain NF-κB signaling, potentially contributing to the reduction of type 17 inflammation caused by PM. Three independent experiments were performed. **(A)** shows representative immunoblot images from these experiments. In **(B–E)**, data from all three experiments are presented as mean ± SEM (n = 3 per group). For panels **(B, D, E)**, the expressions of PXR, phosphorylated IκBα, and IκBα were normalized to β-actin. **(C)** shows the expression ratio of phosphorylated p65 to total p65. *P <.05; **P <.01. P-values were obtained using the unpaired Student's t test.

cell differentiation and the IL-17 signaling pathway (17, 48). In the present study, we showed that PM exposure induces robust type 17 inflammation in both *in vivo* and *in vitro* AD-like inflammation models. In addition to type 2 immune responses, type 17 immune response is essential in AD pathogenesis (38). IL-17, the main cytokine in type 17 immune response, regulates type 2 immune response, stimulates epithelial cells and fibroblasts to secrete pro-inflammatory cytokines such as IL-8 and IL-6, and promotes tissue fibrosis (38, 53). IL-17 contributes to the progression of AD to chronic disease (38, 39). We previously showed that the IL-17A/IL-33 circuit amplifies and sustains chronic AD (40). Collectively, our results suggest that PM can accelerate the progression to the chronic phase of AD via the activation of type 17 inflammation. Notably, AD in the Asian population had greater Th17 polarization and psoriasiform features such as parakeratosis and increased neutrophils compared to AD in European-Americans (54–56), and PM exposure may aggravate the psoriasiform features of AD in Asian people. Coincidently, according to the World Air Quality Report 2021, 16 out of the 20 most polluted countries in the world are located in Asia. This implies that severe air pollution in Asia may affect the unique phenotype of AD in the Asian population.

Recent studies have shown that PXR signaling was activated in the skin of patients with AD (18) and downstream genes of human PXR encoding uridine-5'-diphospho-glucuronosyltransferases (UGTs) were increased in AD and PM-exposed AD (16, 17), but the role of PXR remained unclear. We observed that PM activated PXR in AD-like inflammation models both *in vivo* and *in vitro*. The transcriptional regulatory mechanisms that govern PXR gene expression are complex and not fully understood. Ets-1 and peroxisome proliferator-activated receptor alpha (PPARα) have been identified as key regulators, binding to proximal promoter sites of PXR and modulating its expression (57, 58). Interestingly both Ets-1 and PPARα appear to be implicated in AD pathogenesis. Mice deficient in either factor exhibit AD-like features, and their expression is diminished in the skin of AD patients compared to healthy controls (59, 60). These findings suggest a potential link between PXR regulation and AD development, warranting further investigation. In our study, PXR knockdown exacerbated PM-

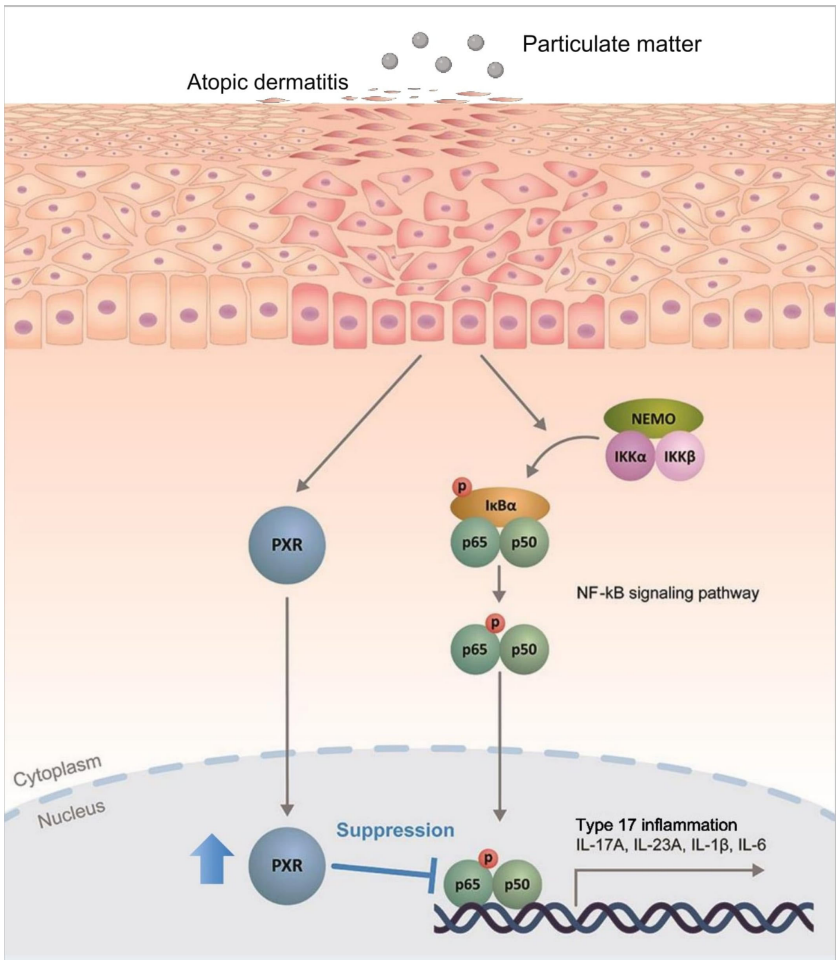

FIGURE 7
Schematic illustration demonstrating the protective role of pregnane X receptor (PXR) in particulate matter (PM)-exposed atopic dermatitis. PM induces type 17 inflammation through nuclear factor kappa B (NF-κB) signaling pathway in AD. Simultaneously, PM activates PXR and activated PXR suppresses NF-κB signaling pathway, mitigating the PM-induced type 17 inflammation in AD.

induced type 17 inflammation in AD-like keratinocytes, as well as IL-17A production in $CD4^+$ T cells. Furthermore, the use of a PXR agonist, rifampicin, reduced this inflammation, indicating that PXR activation in PM-exposed AD can protect against PM-induced type 17 inflammation. In contrast, overexpression of PXR may induce pro-inflammatory effects and produce AD-like inflammation as transgenic mice constitutively expressing human PXR in basal keratinocytes (K14-VPPXR mice) exhibited AD-like features such as skin barrier impairment, increased serum IgE, and increased Th2/Th17 skin immune responses (18). This contrasting role of PXR might be context- and ligand-dependent (15). It is possible that the persistent and basal state where PXR activation occurs may affect its pro- or anti-inflammatory role. Similarly, the activation of AHR by pollutants induces inflammation in exposed skin, but therapeutic AHR-modulating agents such as tapinarof show anti-inflammatory effects in inflammatory disorders such as AD and psoriasis (15, 61–63).

The NF-κB signaling pathway, implicated in the progression and maintenance of AD, is an important molecular target in the treatment of AD (64). NF-κB promotes the production of IL-17 and other pro-inflammatory cytokines such as IL-6 and IL-1. Meanwhile, IL-17 activates NF-κB in a feed-forward manner and stimulates the production of inflammatory mediators and keratinocyte proliferation (50, 51). PXR and NF-κB pathways are known to reciprocally suppress each other, in a context-dependent manner (15, 49). Consistently, our results suggest that PXR activation, induced by PM exposure, mediates the inhibition of NF-kB signaling pathway in AD, which might contribute to reducing type 17 inflammation and the associated exacerbation of AD.

This study has several limitations. First, our PM treatment may not fully mimic real-life exposure. Quantifying PM accumulation on the skin is challenging due to heterogeneous nature of PM, varying concentrations depending on geographical and meteorological factors, and differences in individual skin conditions. In the present study, we selected PM concentrations based on previous experimental studies, aiming to reflect realistic exposures. We employed PBS as the vehicle for PM suspension to minimize potential cytotoxicity and mouse skin irritation. Although many PM components exhibit limited water solubility, we tried to achieve uniform dispersion of PM in PBS through vigorous sonication, to ensure consistent exposure conditions while maintaining cellular and tissue viability. However, further research is needed to validate these conditions and ensure they accurately represent real-world exposure. Additionally, future studies may include comparative analyses using different vehicles, including organic solvents, to evaluate their effects on PM activity and cellular responses. Second, the manipulation of PXR expression and activation was performed only *in vitro*, necessitating further confirmation through *in vivo* experiments. To further validate and extend our results, future studies should employ PXR knockout mouse models and administer PXR agonist treatments in mice with AD-like conditions.

This study provides evidence that PM intensifies type 17 inflammation in AD, both *in vivo* and *in vitro*. Furthermore, it uncovers a previously unappreciated role of PXR, which is activated by PM and plays a crucial role in reducing PM-induced type 17 inflammation through suppressing the NF-kB signaling pathway. Consequently, targeting PXR may represent a potential therapeutic approach to mitigate the progression toward chronic or psoriasiform AD triggered by PM exposure. Given the complexity of the immune responses of AD, further investigations in varied *in vivo* and *in vitro* models is necessary to confirm the role of PXR in PM-exposed AD. Moreover, delving into the potential protective effect of PXR agonists such as rifampicin against air pollution in human subjects warrants further investigation.

Data availability statement

The original contributions presented in the study are included in the article/Supplementary Material. Further inquiries can be directed to the corresponding authors.

Ethics statement

Ethical approval was not required for the studies on humans in accordance with the local legislation and institutional requirements because only commercially available established cell lines were used. The animal study was approved by Seoul National University Hospital Institutional Animal Care and Use Committee. The study was conducted in accordance with the local legislation and institutional requirements.

Author contributions

JSL: Conceptualization, Data curation, Formal analysis, Investigation, Methodology, Project administration, Validation, Visualization, Writing – original draft, Writing – review & editing. YL: Conceptualization, Data curation, Formal analysis, Methodology, Writing – original draft, Writing – review & editing. SJ: Conceptualization, Methodology, Project administration, Writing – original draft, Writing – review & editing. JO: Conceptualization, Investigation, Methodology, Writing – original draft, Writing – review & editing. DHL: Conceptualization, Funding acquisition, Investigation, Project administration, Resources, Supervision, Writing – original draft, Writing – review & editing. SC: Conceptualization, Funding acquisition, Investigation, Project administration, Resources, Supervision, Writing – original draft, Writing – review & editing.

Funding

The author(s) declare financial support was received for the research, authorship, and/or publication of this article. This study was funded in part by the Basic Science Research Program through the National Research Foundation (NRF) of the Republic of Korea funded by the Ministry of Education, Science and Technology (2018R1D1A1A09082209). The funding source was not involved in the collection, analysis, and interpretation of data, in the writing of the article, and in the decision to submit the article to publication.

Conflict of interest

The authors declare that the research was conducted in the absence of any commercial or financial relationships that could be construed as a potential conflict of interest.

Publisher's note

All claims expressed in this article are solely those of the authors and do not necessarily represent those of their affiliated organizations, or those of the publisher, the editors and the reviewers. Any product that may be evaluated in this article, or claim that may be made by its manufacturer, is not guaranteed or endorsed by the publisher.

Supplementary material

The Supplementary Material for this article can be found online at: https://www.frontiersin.org/articles/10.3389/fimmu.2024.1415350/full#supplementary-material

References

1. Kim K-H, Kabir E, Kabir S. A review on the human health impact of airborne particulate matter. *Environ Int.* (2015) 74:136–43. doi: 10.1016/j.envint.2014.10.005

2. Dijkhoff IM, Drasler B, Karakocak BB, Petri-Fink A, Valacchi G, Eeman M, et al. Impact of airborne particulate matter on skin: A systematic review from epidemiology to in vitro studies. *Particle fibre Toxicol.* (2020) 17:35. doi: 10.1186/s12989-020-00366-y

3. Anderson JO, Thundiyil JG, Stolbach A. Clearing the air: A review of the effects of particulate matter air pollution on human health. *J Med Toxicol.* (2012) 8:166–75. doi: 10.1007/s13181-011-0203-1

4. Kim KE, Cho D, Park HJ. Air pollution and skin diseases: adverse effects of airborne particulate matter on various skin diseases. *Life Sci.* (2016) 152:126–34. doi: 10.1016/j.lfs.2016.03.039

5. Araviiskaia E, Berardesca E, Bieber T, Gontijo G, Sanchez Viera M, Marrot L, et al. The impact of airborne pollution on skin. *J Eur Acad Dermatol Venereology.* (2019) 33:1496–505. doi: 10.1111/jdv.15583

6. Hendricks AJ, Eichenfield LF, Shi VY. The impact of airborne pollution on atopic dermatitis: A literature review. *Br J Dermatol.* (2020) 183:16–23. doi: 10.1111/bjd.18781

7. Mancebo SE, Wang SQ. Recognizing the impact of ambient air pollution on skin health. *J Eur Acad Dermatol Venereology.* (2015) 29:2326–32. doi: 10.1111/jdv.13250

8. Nutten S. Atopic dermatitis: global epidemiology and risk factors. *Ann Nutr Metab.* (2015) 66 Suppl 1:8–16. doi: 10.1159/000370220

9. Kantor R, Silverberg JI. Environmental risk factors and their role in the management of atopic dermatitis. *Expert Rev Clin Immunol.* (2017) 13:15–26. doi: 10.1080/1744666x.2016.1212660

10. Weidinger S, Novak N. Atopic dermatitis. *Lancet (London England).* (2016) 387:1109–22. doi: 10.1016/s0140-6736(15)00149-x

11. Ahn K. The role of air pollutants in atopic dermatitis. *J Allergy Clin Immunol.* (2014) 134:993–9. doi: 10.1016/j.jaci.2014.09.023

12. Tang KT, Ku KC, Chen DY, Lin CH, Tsuang BJ, Chen YH. Adult atopic dermatitis and exposure to air pollutants-a nationwide population-based study. *Ann allergy Asthma Immunol.* (2017) 118:351–5. doi: 10.1016/j.anai.2016.12.005

13. Hassoun Y, James C, Bernstein DI. The effects or air pollution on the development of atopic disease. *Clin Rev Allergy Immunol.* (2019) 57:403–14. doi: 10.1007/s12016-019-08730-3

14. Kim J, Kim EH, Oh I, Jung K, Han Y, Cheong HK, et al. Symptoms of atopic dermatitis are influenced by outdoor air pollution. *J Allergy Clin Immunol.* (2013) 132:495–8.e1. doi: 10.1016/j.jaci.2013.04.019

15. Minzaghi D, Pavel P, Dubrac S. Xenobiotic receptors and their mates in atopic dermatitis. *Int J Mol Sci.* (2019) 20:4234. doi: 10.3390/ijms20174234

16. Blunder S, Kõks S, Kõks G, Reimann E, Hackl H, Gruber R, et al. Enhanced expression of genes related to xenobiotic metabolism in the skin of patients with atopic dermatitis but not with ichthyosis vulgaris. *J Invest Dermatol.* (2018) 138:98–108. doi: 10.1016/j.jid.2017.08.036

17. Woo YR, Park SY, Choi K, Hong ES, Kim S, Kim HS. Air pollution and atopic dermatitis (Ad): the impact of particulate matter (Pm10) on an ad mouse-model. *Int J Mol Sci.* (2020) 21:6079. doi: 10.3390/ijms21176079

18. Elentner A, Schmuth M, Yannoutsos N, Eichmann TO, Gruber R, Radner FPW, et al. Epidermal overexpression of xenobiotic receptor pxr impairs the epidermal barrier and triggers th2 immune response. *J Invest Dermatol.* (2018) 138:109–20. doi: 10.1016/j.jid.2017.07.846

19. Oladimeji PO, Chen T. Pxr: more than just a master xenobiotic receptor. *Mol Pharmacol.* (2018) 93:119–27. doi: 10.1124/mol.117.110155

20. Rogers RS, Parker A, Vainer PD, Elliott E, Sudbeck D, Parimi K, et al. The interface between cell signaling pathways and pregnane X receptor. *Cells.* (2021) 10:3262. doi: 10.3390/cells10113262

21. Erickson SL, Alston L, Nieves K, Chang TKH, Mani S, Flannigan KL, et al. The xenobiotic sensing pregnane X receptor regulates tissue damage and inflammation triggered by C difficile toxins. *FASEB J.* (2020) 34:2198–212. doi: 10.1096/fj.201902083RR

22. Tanaka Y, Uchi H, Ito T, Furue M. Indirubin-pregnane X receptor-jnk axis accelerates skin wound healing. *Sci Rep.* (2019) 9:18174. doi: 10.1038/s41598-019-54754-2

23. Elentner A, Ortner D, Clausen B, Gonzalez FJ, Fernández-Salguero PM, Schmuth M, et al. Skin response to a carcinogen involves the xenobiotic receptor pregnane X receptor. *Exp Dermatol.* (2015) 24:835–40. doi: 10.1111/exd.12766

24. Schantz MM, Cleveland D, Heckert NA, Kucklick JR, Leigh SD, Long SE, et al. Development of two fine particulate matter standard reference materials (<4 µm and <10 µm) for the determination of organic and inorganic constituents. *Analytical bioanalytical Chem.* (2016) 408:4257–66. doi: 10.1007/s00216-016-9519-7

25. Martel BC, Lovato P, Bäumer W, Olivry T. Translational animal models of atopic dermatitis for preclinical studies. *Yale J Biol Med.* (2017) 90:389–402.

26. Gilhar A, Reich K, Keren A, Kabashima K, Steinhoff M, Paus R. Mouse models of atopic dermatitis: A critical reappraisal. *Exp Dermatol.* (2021) 30:319–36. doi: 10.1111/exd.14270

27. Li L, Mu Z, Liu P, Wang Y, Yang F, Han X. Mdivi-1 alleviates atopic dermatitis through the inhibition of nlrp3 inflammasome. *Exp Dermatol.* (2021) 30:1734–44. doi: 10.1111/exd.14412

28. Yang L, Fu J, Han X, Zhang C, Xia L, Zhu R, et al. Hsa_Circ_0004287 inhibits macrophage-mediated inflammation in an N(6)-methyladenosine-dependent manner in atopic dermatitis and psoriasis. *J Allergy Clin Immunol.* (2022) 149:2021–33. doi: 10.1016/j.jaci.2021.11.024

29. Kim S, Han SY, Lee J, Kim NR, Lee BR, Kim H, et al. Bifidobacterium longum and galactooligosaccharide improve skin barrier dysfunction and atopic dermatitis-like skin. *Allergy Asthma Immunol Res.* (2022) 14:549–64. doi: 10.4168/aair.2022.14.5.549

30. Lee HS, Kim J, Choi HG, Kim EK, Jun CD. Licoricidin abrogates T-cell activation by modulating ptpn1 activity and attenuates atopic dermatitis *in vivo*. *J Invest Dermatol.* (2021) 141:2490–8.e6. doi: 10.1016/j.jid.2021.02.759

31. Pan TL, Wang PW, Aljuffali IA, Huang CT, Lee CW, Fang JY. The impact of urban particulate pollution on skin barrier function and the subsequent drug absorption. *J Dermatol Sci.* (2015) 78:51–60. doi: 10.1016/j.jdermsci.2015.01.011

32. Lee C-W, Lin Z-C, Hu SC-S, Chiang Y-C, Hsu L-F, Lin Y-C, et al. Urban particulate matter down-regulates filaggrin via cox2 expression/pge2 production leading to skin barrier dysfunction. *Sci Rep.* (2016) 6:27995. doi: 10.1038/srep27995

33. Ahn SS, Yeo H, Jung E, Lim Y, Lee YH, Shin SY. Fra1:C-jun: hdac1 complex down-regulates filaggrin expression upon tnfα and ifnγ Stimulation in keratinocytes. *Proc Natl Acad Sci United States America.* (2022) 119:e2123451119. doi: 10.1073/pnas.2123451119

34. Kim HJ, Baek J, Lee JR, Roh JY, Jung Y. Optimization of cytokine milieu to reproduce atopic dermatitis-related gene expression in hacat keratinocyte cell line. *Immune network.* (2018) 18:e9. doi: 10.4110/in.2018.18.e9

35. Lee H, Lee DH, Oh J-H, Chung JH. Skullcapflavone ii suppresses tnf-A/ifn-Γ-induced tarc, mdc, and ctss production in hacat cells. *Int J Mol Sci.* (2021) 22:6428. doi: 10.3390/ijms22126428

36. Kim SM, Ha SE, Vetrivel P, Kim HH, Bhosale PB, Park JE, et al. Cellular function of annexin A1 protein mimetic peptide ac2-26 in human skin keratinocyte hacat and fibroblast detroit 551 cells. *Nutrients.* (2020) 12:3261. doi: 10.3390/nu12113261

37. Jia J, Mo X, Yan F, Liu J, Ye S, Zhang Y, et al. Role of yap-related T cell imbalance and epidermal keratinocyte dysfunction in the pathogenesis of atopic dermatitis. *J Dermatol Sci.* (2021) 101:164–73. doi: 10.1016/j.jdermsci.2020.12.004

38. Klonowska J, Gleń J, Nowicki RJ, Trzeciak M. New cytokines in the pathogenesis of atopic dermatitis - new therapeutic targets. *Int J Mol Sci*. (2018) 19:3086. doi: 10.3390/ijms19103086

39. Dhingra N, Suárez-Fariñas M, Fuentes-Duculan J, Gittler JK, Shemer A, Raz A, et al. Attenuated neutrophil axis in atopic dermatitis compared to psoriasis reflects th17 pathway differences between these diseases. *J Allergy Clin Immunol*. (2013) 132:498–501.e3. doi: 10.1016/j.jaci.2013.04.043

40. Kim MH, Jin SP, Jang S, Choi JY, Chung DH, Lee DH, et al. Il-17a-producting innate lymphoid cells promote skin inflammation by inducing il-33-driven type 2 immune responses. *J Invest Dermatol*. (2020) 140:827–37.e9. doi: 10.1016/j.jid.2019.08.447

41. Furue M. Regulation of filaggrin, loricrin, and involucrin by il-4, il-13, il-17a, il-22, ahr, and nrf2: pathogenic implications in atopic dermatitis. *Int J Mol Sci*. (2020) 21:5382. doi: 10.3390/ijms21155382

42. Zhang R, Chen S, Chen L, Ye L, Jiang Y, Peng H, et al. Single-cell transcriptomics reveals immune dysregulation mediated by il-17a in initiation of chronic lung injuries upon real-ambient particulate matter exposure. *Particle fibre Toxicol*. (2022) 19:42. doi: 10.1186/s12989-022-00483-w

43. Cong LH, Li T, Wang H, Wu YN, Wang SP, Zhao YY, et al. Il-17a-producing T cells exacerbate fine particulate matter-induced lung inflammation and fibrosis by inhibiting pi3k/akt/mtor-mediated autophagy. *J Cell Mol Med*. (2020) 24:8532–44. doi: 10.1111/jcmm.15475

44. Sun L, Fu J, Lin SH, Sun JL, Xia L, Lin CH, et al. Particulate matter of 2.5 Mm or less in diameter disturbs the balance of th17/regulatory T cells by targeting glutamate oxaloacetate transaminase 1 and hypoxia-inducible factor 1α in an asthma model. *J Allergy Clin Immunol*. (2020) 145:402–14. doi: 10.1016/j.jaci.2019.10.008

45. Zhang J, Fulgar CC, Mar T, Young DE, Zhang Q, Bein KJ, et al. Th17-induced neutrophils enhance the pulmonary allergic response following balb/C exposure to hous dust mite allergen and fine particulate matter from california and China. *Toxicological Sci*. (2018) 164:627–43. doi: 10.1093/toxsci/kfy127

46. Castañeda AR, Pinkerton KE, Bein KJ, Magaña-Méndez A, Yang HT, Ashwood P, et al. Ambient particulate matter activates the aryl hydrocarbon receptor in dendritic cells and enhances th17 polarization. *Toxicol Lett*. (2018) 292:85–96. doi: 10.1016/j.toxlet.2018.04.020

47. van Voorhis M, Knopp S, Julliard W, Fechner JH, Zhang X, Schauer JJ, et al. Exposure to atmospheric particulate matter enhances th17 polarization through the aryl hydrocarbon receptor. *PloS One*. (2013) 8:e82545. doi: 10.1371/journal.pone.0082545

48. Kim H-J, Bae I-H, Son ED, Park J, Cha N, Na H-W, et al. Transcriptome analysis of airborne pm2.5-induced detrimental effects on human keratinocytes. *Toxicol Lett*. (2017) 273:26–35. doi: 10.1016/j.toxlet.2017.03.010

49. Zhou C, Tabb MM, Nelson EL, Grün F, Verma S, Sadatrafiei A, et al. Mutual repression between steroid and xenobiotic receptor and nf-kappab signaling pathways links xenobiotic metabolism and inflammation. *J Clin Invest*. (2006) 116:2280–9. doi: 10.1172/jci26283

50. Ryu YS, Kang KA, Piao MJ, Ahn MJ, Yi JM, Hyun YM, et al. Particulate matter induces inflammatory cytokine production via activation of nfκb by tlr5-nox4-ros signaling in human skin keratinocyte and mouse skin. *Redox Biol*. (2019) 21:101080. doi: 10.1016/j.redox.2018.101080

51. Liu T, Zhang L, Joo D, Sun SC. Nf-Kb signaling in inflammation. *Signal transduction targeted Ther*. (2017) 2:17023. doi: 10.1038/sigtrans.2017.23

52. Jin SP, Li Z, Choi EK, Lee S, Kim YK, Seo EY, et al. Urban particulate matter in air pollution penetrates into the barrier-disrupted skin and produces ros-dependent cutaneous inflammatory response in vivo. *J Dermatol Sci*. (2018) 91:175–83. doi: 10.1016/j.jdermsci.2018.04.015

53. Cesare AD, Meglio PD, Nestle FO. A role for th17 cells in the immunopathogenesis of atopic dermatitis? *J Invest Dermatol*. (2008) 128:2569–71. doi: 10.1038/jid.2008.283

54. Chan TC, Sanyal RD, Pavel AB, Glickman J, Zheng X, Xu H, et al. Atopic dermatitis in chinese patients shows th2/th17 skewing with psoriasiform features. *J Allergy Clin Immunol*. (2018) 142:1013–7. doi: 10.1016/j.jaci.2018.06.016

55. Noda S, Suárez-Fariñas M, Ungar B, Kim SJ, de Guzman Strong C, Xu H, et al. The asian atopic dermatitis phenotype combines features of atopic dermatitis and psoriasis with increased th17 polarization. *J Allergy Clin Immunol*. (2015) 136:1254–64. doi: 10.1016/j.jaci.2015.08.015

56. Czarnowicki T, He H, Krueger JG, Guttman-Yassky E. Atopic dermatitis endotypes and implications for targeted therapeutics. *J Allergy Clin Immunol*. (2019) 143:1–11. doi: 10.1016/j.jaci.2018.10.032

57. Kumari S, Mukhopadhyay G, Tyagi RK. Transcriptional regulation of mouse pxr gene: an interplay of transregulatory factors. *PloS One*. (2012) 7:e44126. doi: 10.1371/journal.pone.0044126

58. Aouabdi S, Gibson G, Plant N. Transcriptional regulation of the pxr gene: identification and characterization of a functional peroxisome proliferator-activated receptor alpha binding site within the proximal promoter of pxr. *Drug Metab disposition*. (2006) 34:138–44. doi: 10.1124/dmd.105.006064

59. Lee CG, Kwon HK, Kang H, Kim Y, Nam JH, Won YH, et al. Ets1 suppresses atopic dermatitis by suppressing pathogenic T cell responses. *JCI Insight*. (2019) 4:e124202. doi: 10.1172/jci.insight.124202

60. Staumont-Sallé D, Abboud G, Brénuchon C, Kanda A, Roumier T, Lavogiez C, et al. Peroxisome proliferator-activated receptor alpha regulates skin inflammation and humoral response in atopic dermatitis. *J Allergy Clin Immunol*. (2008) 121:962–8.e6. doi: 10.1016/j.jaci.2007.12.1165

61. Lebwohl MG, Stein Gold L, Strober B, Papp KA, Armstrong AW, Bagel J, et al. Phase 3 trials of tapinarof cream for plaque psoriasis. *New Engl J Med*. (2021) 385:2219–29. doi: 10.1056/NEJMoa2103629

62. Paller AS, Stein Gold L, Soung J, Tallman AM, Rubenstein DS, Gooderham M. Efficacy and patient-reported outcomes from a phase 2b, randomized clinical trial of tapinarof cream for the treatment of adolescents and adults with atopic dermatitis. *J Am Acad Dermatol*. (2021) 84:632–8. doi: 10.1016/j.jaad.2020.05.135

63. Haarmann-Stemmann T, Esser C, Krutmann J. The janus-faced role of aryl hydrocarbon receptor signaling in the skin: consequences for prevention and treatment of skin disorders. *J Invest Dermatol*. (2015) 135:2572–6. doi: 10.1038/jid.2015.285

64. Dajee M, Muchamuel T, Schryver B, Oo A, Alleman-Sposeto J, De Vry CG, et al. Blockade of experimental atopic dermatitis via topical nf-kappab decoy oligonucleotide. *J Invest Dermatol*. (2006) 126:1792–803. doi: 10.1038/sj.jid.5700307

frontiers | Frontiers in Immunology

TYPE Review
PUBLISHED 08 October 2024
DOI 10.3389/fimmu.2024.1478624

OPEN ACCESS

EDITED BY
Jian Zheng,
University of Louisville, United States

REVIEWED BY
Gandhi Fernando Pavon,
National Institute of Respiratory Diseases (INER), Mexico
Xin Sun,
Air Force Medical University, China

*CORRESPONDENCE
Huijuan Gao
gaohuijuan@mail.tsinghua.edu.cn
Qingli Luo
qingqingluo2010@163.com

†These authors have contributed equally to this work and share first authorship

RECEIVED 10 August 2024
ACCEPTED 18 September 2024
PUBLISHED 08 October 2024

CITATION
Xie C, Yang J, Gul A, Li Y, Zhang R, Yalikun M, Lv X, Lin Y, Luo Q and Gao H (2024) Immunologic aspects of asthma: from molecular mechanisms to disease pathophysiology and clinical translation. *Front. Immunol.* 15:1478624. doi: 10.3389/fimmu.2024.1478624

Immunologic aspects of asthma: from molecular mechanisms to disease pathophysiology and clinical translation

Cong Xie[1,2†], Jingyan Yang[3†], Aman Gul[2,4,5†], Yifan Li[2], Rui Zhang[6], Maimaititusun Yalikun[2], Xiaotong Lv[7], Yuhan Lin[1,8], Qingli Luo[2*] and Huijuan Gao[1*]

[1]Department of Endocrinology and Clinical Immunology, Yuquan Hospital, School of Clinical Medicine, Tsinghua University, Beijing, China, [2]Department of Integrative Medicine, Huashan Hospital Affiliated to Fudan University, Fudan Institutes of Integrative Medicine, Fudan University Shanghai Medical College, Shanghai, China, [3]The Third Affiliated Hospital, Beijing University of Chinese Medicine, Beijing, China, [4]Department of Respiratory Medicine, Uyghur Medicines Hospital of Xinjiang Uyghur Autonomous Region, Urumqi, China, [5]College of Life Science and Technology, Xinjiang University, Urumqi, China, [6]Department of Pulmonary and Critical Care Medicine, Shenzhen Hospital of Guangzhou University of Chinese Medicine (Futian), Shenzhen, China, [7]Department of Cardiology, The Second Affiliated Hospital of Tianjin University of Traditional Chinese Medicine, Tianjin, China, [8]Dongzhimen Hospital, Beijing University of Chinese Medicine, Beijing, China

In the present review, we focused on recent translational and clinical discoveries in asthma immunology, facilitating phenotyping and stratified or personalized interventions for patients with this condition. The immune processes behind chronic inflammation in asthma exhibit marked heterogeneity, with diverse phenotypes defining discernible features and endotypes illuminating the underlying molecular mechanisms. In particular, two primary endotypes of asthma have been identified: "type 2-high," characterized by increased eosinophil levels in the airways and sputum of patients, and "type 2-low," distinguished by increased neutrophils or a pauci-granulocytic profile. Our review encompasses significant advances in both innate and adaptive immunities, with emphasis on the key cellular and molecular mediators, and delves into innovative biological and targeted therapies for all the asthma endotypes. Recognizing that the immunopathology of asthma is dynamic and continuous, exhibiting spatial and temporal variabilities, is the central theme of this review. This complexity is underscored through the innumerable interactions involved, rather than being driven by a single predominant factor. Integrated efforts to improve our understanding of the pathophysiological characteristics of asthma indicate a trend toward an approach based on disease biology, encompassing the combined examination of the clinical, cellular, and molecular dimensions of the disease to more accurately correlate clinical traits with specific disease mechanisms.

KEYWORDS

lung, asthma, immunity, inflammation, allergy, T_H2 cytokines, immunotherapy

1 Introduction

Asthma is a familiar, chronic, noncommunicable lung disease affecting approximately 300 million people worldwide (1), including 45.7 million adults in China (2). The prevalence of asthma considerably varies across different countries and regions; the prevalence is higher in urban areas and individuals with some risk factors, including allergies, smoking, and air pollution exposure. Although asthma incidence appears to be stabilizing after decades of rapid growth in many developed countries, its prevalence is increasing rapidly in low- and middle-income countries. This increase in prevalence may be owing to the worsening of fossil fuel pollution and the adoption of Westernized lifestyles. Furthermore, the absence of accurate diagnosis and standardized treatments in these developing countries increases the asthma burden on patients, their families, and society as a whole (3).

An expiratory airflow limitation is the primary feature of asthma; however, this limitation is generally reversible but related to airway lumen diameter narrowing. The narrowing occurs because of chronic inflammation in the walls of the airway, which is marked by the infiltration and activation of different immune cells, including eosinophils, neutrophils, lymphocytes, dendritic cells (DCs), innate lymphoid cells (ILCs), and mast cells, inducing processes such as bronchial hyperresponsiveness, mucus hypersecretion, and airway remodeling.

The clinical traits of asthma, i.e., dyspnea, coughing, wheezing, chest tightness, loss of lung function, exacerbation tendency, and asthma severity, suggest that the disease encompasses distinct underlying mechanisms, in which structural and immune cells interact to manifest the pathogenetic features of asthma. However, the relative contribution of these features may differ among patients with asthma, coupled with remarkable differences in genetic variations and environmental exposure; this results in significant heterogeneity in clinical manifestations and inflammatory biomarker expression.

Asthma has different clinical characteristics ("phenotypes") and underlying causative mechanisms ("endotypes") (4). Historically, clinicians have categorized asthma into two phenotypes: intrinsic (nonallergic) and extrinsic (allergic) (5). The primary difference between these two phenotypes is that allergic asthma generally occurs during childhood, whereas nonallergic asthma usually begins in adulthood. Allergic asthma typically manifests as acute episodes with increased airway responsiveness after allergen stimulation; it is more responsive to inhaled corticosteroids (ICSs) compared with nonallergic asthma (6). More recently, various clinical parameters, including onset age, condition severity and duration, frequency of acute exacerbation, impairment in respiratory function, level of symptom control, biomarkers, and treatment response, including potential hormone resistance, have been utilized to classify the phenotypes of asthma.

Some of the most common phenotypes, including allergic asthma, nonallergic asthma, adult-onset (late-onset) asthma, asthma with persistent airflow limitation, and obesity-associated asthma, have been listed in the updated 2023 and 2024 Global Initiative for Asthma (GINA) guidelines (7). Simultaneously, researchers in the field of basic medical sciences, particularly immunologists using murine models of allergic asthma and/or inflammation, have confirmed the pivotal role of the elements of the T helper (T_H2) immune pathway in exacerbating inflammation and airway hyperreactivity (8, 9). T_H2 cells are involved in the generation of cytokines that induce the different essential characteristics of asthma, including tissue eosinophilia (interleukin [IL]-5), bronchial hyperresponsiveness (IL-13), and goblet cell metaplasia (IL-4 and IL-13) (10). Recent studies have extended this understanding and suggested that apart from T_H2 cells, other innate immune cells, including mast cells, basophils, group 2 ILCs, IL-4- and/or IL-13-activated macrophages ("M2"), and a small portion of IL-4-secreting natural killer (NK)/NKT cells, also contribute to T_H2 cell induced cytokine production in asthma; as a result, the terminology has gradually shifted from "T_H2 cell-high" to "type 2-high" asthma (11). However, this "type 2-high" profile, primarily characterized by eosinophilia, is only observed in roughly 50% of patients with asthma (12). The remaining patients, categorized as "type 2-low" asthma, without eosinophilia, exhibit distinct immune features, including airway neutrophilia, obesity-associated systemic inflammation, or minimal immune activation signs in some cases (13).

In patients with asthma, there is specific chronic inflammation in the lower airway mucosa. Although the major cellular components associated with this inflammation type have been ascertained, the interplay between the inflammatory cells in different spatial and temporal dimensions remains unclear (14); furthermore, it is not known how this inflammation translates into asthma symptoms. Similar to other atopic diseases, asthma pathogenesis involves several factors, including genetic predisposition, the airway initiation of specific IgE (sIgE) to respiratory allergens, and an overactive immune system that produces excessive amounts of inflammatory mediators. To date, the acute inflammatory changes observed in asthma have garnered considerable attention; in this chronic condition, inflammation persists for many years in most patients. Superimposed on this chronic inflammatory state are acute inflammatory episodes, which correspond to exacerbations of asthma.

Moving from patients to animal or cellular models and back represents an iterative process by which we can elucidate the intricate pathophysiology of asthma. Herein, we focus on the underlying immunological aspects of asthma in the context of recent insights into its extraordinary heterogeneity by summarizing the findings from human studies on particular pathways along with rigorous basic experimentation that has collected a surplus of molecular details.

2 Pro-inflammatory and anti-inflammatory arms of the immune landscape in asthma

Under the guidance of locally released chemokines, many inflammatory cells are recruited to the lungs from the

bloodstream; these cells exert functional properties for asthma development. Furthermore, airway structural cells, including epithelial cells, fibroblasts, and airway smooth muscle cells (SMCs), are essential inflammatory mediator sources that actively participate in the inflammatory process. In individuals with asthma, both innate (mast cells, DCs, eosinophils, neutrophils, basophils, ILCs, monocytes, and macrophages) and adaptive (T and B lymphocytes) immunities are involved in the inflammatory cell profile (15).

A landmark study conducted in the mid-1980s reported the classical $CD4^+$T lymphocyte subsets (T_H1 and T_H2 cells) (16); since then, it is well-known that T_H2 cells orchestrate eosinophilic airway inflammation by producing abundant amounts of IL-4, IL-5, and IL-13 (17). IL-4 is required for allergic sensitization and IgE class switching, IL-5 is warranted for eosinophil survival, IL-13 exerts multifunctional effects in the lungs, including a vital role in controlling mucus production, goblet cell metaplasia, bronchial hyperresponsiveness, and airway remodeling (18). In contrast, T_H1 cells release IL-2, interferon (IFN)-γ, and tumor necrosis factor (TNF)-α, possibly conferring a protective role in asthma because they can directly antagonize pathologic T_H2 responses to control eosinophilic inflammation (19). To support this, IL-12, a pro-T_H1 cell cytokine, administration in mice suppresses antigen-induced airway hyperresponsiveness and inflammation by producing IFN-γ via T_H1 cells (20, 21). However, recent studies on the phenotype of type 2-low asthma have demonstrated the dominance of IFN-γ^+T_H1 cells in severe disease forms, which is potentially associated with corticosteroid refractoriness (22, 23).

In addition to T_H2 cells, T_H17 cells and their produced cytokine IL-17A are prominent and extensively studied in the context of asthma, particularly in severe, steroid-resistant cases (24). These T_H17-derived cytokines, including IL-17 and IL-22, are related to increased neutrophil recruitment in the airways (25). To this end, neutrophil extracellular traps and cytoplasts further promote T_H17 polarization and neutrophilic inflammation in severe asthma (26). However, the precise roles of T_H17 cells and IL-17 in mouse asthma models remain unknown primarily because IL-17 may play dual regulatory roles: it plays a protective role in the challenge stage but worsens asthma under other conditions (27, 28). In chronic asthma models, IL-17A induces the proliferation of fibroblasts (29), inhibits the anti-inflammatory effects of regulatory T cells (Tregs) (30), and directly contracts bronchial SMCs (31).

Increasing evidence in animals indicates that a major hallmark of several autoimmune disorders, including asthma, is functional defects in Tregs (32). In a broader perspective, as a diverse population, Tregs comprise $CD4^+CD25^+$ forkhead box (Fox)$p3^+$ natural and inducible Tregs, IL-10-producing Tr1 cells, transforming growth factor (TGF)-β-producing T_H3 cells, and other minor subsets with suppressive functions, including $CD4^-CD8^-$ T and γδT cells (33). In children with asthma, both $CD4^+CD25^{hi}$ Tregs and Foxp3 mRNA expression decrease in the peripheral blood and bronchoalveolar lavage fluid (BALF); this phenomenon can be reversed following treatment with inhaled glucocorticoids (34). Recently, a study has revealed that numerical and functional deficiencies in Tregs may increase the asthma risk in children and young adults; however, the association between Tregs and the risk or severity of asthma in the elderly may be weaker (35).

The discovery of a distinct cohort of IL-9-secreting $CD4^+$T cells, called T_H9 cells, has enhanced the intricacies of T cell subsets. These cells are produced in response to IL-4 and TGF-β (36). These T_H9 cells facilitate the binding of the transcription factors PU.1 and interferon-regulatory factor (IRF)-4 to the *Il9* promoter (37). Furthermore, IL-25 (i.e., IL-17E) enhances IL-9 secretion from T_H9 cells (38). IL-9 promotes allergic responses, including IgE production and eosinophilia (39). In allergic inflammation experimental models, mast cell accumulation is IL-9-dependent (40); however, lung-infiltrating mast cells and protease expression in mast cells were significantly decreased in mice with PU.1 deficiency (41). Subsequent studies have demonstrated that the deletion of a regulatory region in the *Il9* locus, which is vital for initiating the IL-9 expression and T_H9 cell maturation, effectively alleviates allergic lung inflammation (42, 43). Several clinical trials involving a humanized anti-IL-9 monoclonal antibody (mAb), MEDI-528, have been successfully completed in individuals with asthma, demonstrating some degree of efficacy (44, 45).

At present, studies suggest that alveolar macrophages possess comprehensive immunoregulatory capabilities in asthma, beyond those of a pathogenic barrier to lung tissues (46). Based on the stimulation type, surface markers, pattern of secreted cytokines, and functional characteristics, two main polarized macrophage subpopulations have been identified: "M1" macrophages, which are classically activated, and "M2" macrophages, which are alternatively activated (47). Although controversial, some studies have demonstrated that M2 macrophages express T_H2-associated cytokines (IL-4 and IL-13) and TGF-β, which participate in type 2 inflammation and airway remodeling in allergic asthma (48). However, M2 macrophages release high levels of IL-10 and TGF-β, playing roles in inflammation resolution, wound repair, and homeostasis maintenance, further complicating the precise function of M2 macrophages (49).

Despite the well-known heterogeneity of asthma, an imbalanced immune microenvironment is a prerequisite for its development. This imbalance encompasses the dynamic interplay of T cells and macrophages, beginning from the initial stages and continuing until disease progression. Instead of attributing the disease solely to specific subsets, alterations in the interactions and functions between different subgroups may play significant roles (50). Such interactions and functions may be referred to as "pro-inflammatory/anti-inflammatory balance regulatory networks" (Figure 1). Notably, the classical paradigm of T_H2-skewed immune responses remains relevant; however, emerging evidence suggests that it is considerably more sophisticated *in vivo* than previously envisaged, involving extremely uneven cell subpopulations and different cytokine expression patterns that dynamically fine-tune themselves based on different spatiotemporal cues.

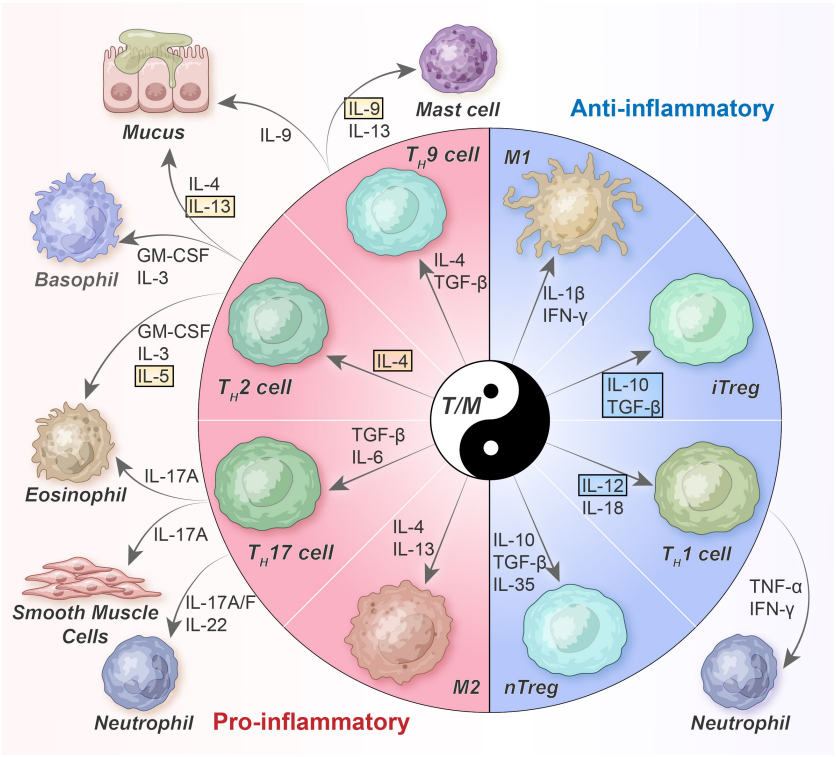

FIGURE 1
Balanced T-cell/macrophage networks and their cytokine milieu in asthma. T_H2 cells orchestrate allergic inflammation by secreting T_H2 cytokines such as IL-4, IL-5, IL-9, and IL-13. However, T_H1 cells, which are differentiated because of IL-12 and IL-18, inhibit T_H2 cells by producing IFN-γ. T_H17 cells, affected by IL-6 and TGF-β, follow a distinct differentiation pathway. In general, Tregs mitigate the activity of other T_H cells by secreting TGF-β and IL-10; however, their functionality may be compromised under asthma conditions. nTreg, naturally occurring Tregs; iTreg, inducible Tregs; GM-CSF, granulocyte-macrophage colony stimulating factor; TGF, transforming growth factor; TNF, tumor necrosis factor; IFN, interferon.

3 Mechanisms leading to asthma

3.1 Step 1. Dysregulated epithelial barrier and early innate immune response

3.1.1 Epithelial injury, activation, and derived signals

Bronchial epithelial cells, which are strategically positioned at the host and environment interface, play vital roles in preserving respiratory mucosal integrity and stability because of mechanical-physical barriers, ciliary clearance, and immunoregulatory functions; they serve as the first line of defense against pathogens and airborne allergens (51). Early investigation of airway asthma pathology has revealed that epithelial cells are damaged, disintegrated, and dysfunctional. As a result, the "epithelial barrier hypothesis" has been established, suggesting that various allergic and autoimmune diseases have similar triggering mechanisms (52).

Different asthma phenotypes exhibit airway epithelial abnormalities, primarily manifesting as increased epithelial leakage, decreased inflammatory thresholds, ciliated cell shedding, detached columnar cells (Creola bodies), and impaired intercellular adhesion (53). Under homeostatic conditions, an impermeable epithelial barrier is formed; this barrier is maintained primarily by tight junctions (TJs) at the apical end of columnar cells. This barrier is further reinforced via different adhesion mechanisms in the basal and basolateral surfaces of epithelial cells, including adherens junctions (AJs) and (hemi)desmosomes (54). The bronchial biopsies of patients with asthma have revealed that zonula occludens-1 (ZO-1) and occludin, which are TJ proteins, are irregular stained, suggesting functional defects in epithelial connections (55). Compared with control subjects, the cultured airway epithelial cells of patients with asthma also suggest TJ protein degradations (55); in contrast, E-cadherin and α-catenin, AJ proteins, expression is decreased (56).

The vulnerability of the airway epithelium to environmental irritants and the dysfunctional repair mechanisms after such injuries are vital for asthma development (57). Aeroallergens such as house dust mites (HDMs), pollens, and fungi, microbes such as viruses and bacteria, and environmental pollutants such as cigarette smoke, particulate matter $(PM)_{2.5}$, and diesel exhaust, directly impede the integrity of TJ barriers of the airway epithelium (58). Furthermore, insufficient antioxidant and antiviral mechanisms in asthmatic airways may increase the susceptibility of epithelial cells to oxidative and virus-induced damage.

Genome-wide association studies (GWAS) have confirmed that the genetic predisposition for asthma development is partially associated with barrier dysfunction; single-nucleotide polymorphisms (SNPs) have been identified in multiple genes, including protocadherin-1 (*PCDH1*), cadherin-related family

member-3 (*CDHR3*), and orosomucoid-like protein isoform-3 (*ORMDL3*) (53). Furthermore, experimental mouse models that simulate three asthma phenotypes, i.e., type 2^{high}-eosinophilic, type 2^{low}-neutrophilic, and mixed granulocytic, were employed to differentiate the effects of phenotypes on the disruption of the epithelial barrier by focusing on TJ proteins and mucins. Many TJ proteins, including ZO-1 and claudin-18, were decreased in the asthma phenotypes; however, the degree of reduction was different. In contrast, claudin-4 is only overexpressed in neutrophilic asthma. Moreover, phenotype-specific discrepancies are found in mucins: MUC5AC and MUC5B are overexpressed in the asthma phenotypes; however, it is more pronounced in neutrophilic and mixed asthma (59).

In addition to its essential role as a physical barrier, the airway epithelium also modulates the initial innate immune response (Figure 2). Epithelial cells express several pattern recognition receptors (PRRs), rapidly detecting and responding to pathogen-associated molecular patterns (PAMPs) found in microorganisms as well as damage-associated molecular patterns (DAMPs) released due to tissue injury, cellular stress and cell death (60).

Because of PRR activation on epithelial cells, large amounts of cytokines, chemokines, and antimicrobial peptides are secreted, attracting and activating innate and adaptive immune cells. During bacterial pathogen invasion, bacterial cell wall components can be sensed via various PRRs on airway epithelial cells, including toll-like receptor (TLR)-2, which recognizes elements such as lipoteichoic acid in gram-positive bacteria, TLR4, which recognizes lipopolysaccharide (LPS) in gram-negative bacteria, and NOD1 and NOD2, which recognize peptidoglycans. As a result, nuclear factor kappa B (NF-κB) is activated, initiating immune responses and eventually regulating bacterial clearance (61).

During viral infection, TLR3, TLR7/8, retinoic acid-inducible gene I (RIG-I), melanoma differentiation-associated protein-5 (MDA5), and laboratory of genetic and physiology-2 (LGP2) can recognize nucleic acid patterns (62). Furthermore, the activation of PRR-dependent epithelial cells results in the

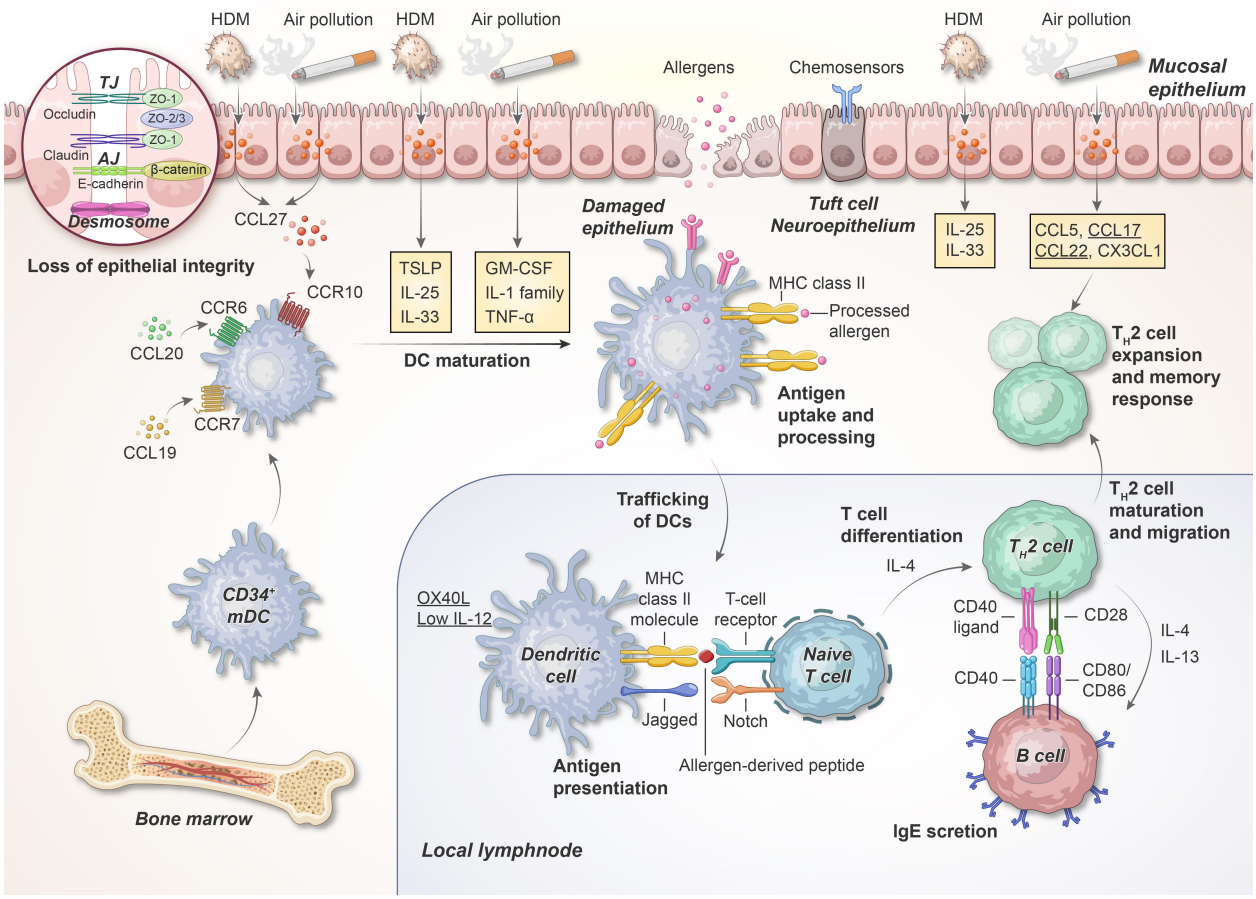

FIGURE 2
Early phase of allergen sensitizations in the airway. Inhaled allergens and air pollutants with protease activity can cleave epithelial TJs and trigger the PRRs on the epithelial cells; this results in the production of cytokines, including IL-1, IL-25, IL-33, TSLP, GM-CSF, and TNF-α. When these cytokines are released, DCs migrate toward the T cell region of the adjacent lymph nodes. Here, DCs interact with naive T cells via the TCR, MHC class II molecules, and co-stimulatory molecules, thereby facilitating T_H cell differentiation. HDM, house dust mite; TJ, tight junction; AJ, adherens junction; ZO, zonula occludens; TSLP, thymic stromal lymphopoietin; mDC, myeloid DCs, MHC, major histocompatibility complex. This illustration was adapted from Holgate, 2012 (75).

production of endogenous danger signals (i.e., DAMPs), including free adenosine triphosphate (ATP), uric acid, and high-motility group box 1 (HMGB1) protein, and activation of DCs with granulocyte-macrophage colony-stimulating factor (GM-CSF), IL-1α, and IL-33 (63).

The contemporary viewpoint suggests that tissue disturbances are the primary factor responsible for type 2 immunity rather than direct antigen recognition. In genetically susceptible individuals, with impaired epithelial barrier function, airways are vulnerable to viral infections and inhaled allergens in early life. This triggers immature DCs, guiding T_H2 cell responses and sensitization to local allergens (64). Airway exposure to allergens, pollutants, or pathogens results in the release of epithelial-derived cytokines such as IL-33 and IL-25 and thymic stromal lymphopoietin (TSLP), a member of the IL-2 cytokine family. These cytokines, commonly called "alarmins," exert pleiotropic properties; however, they synergistically activate DCs, ILC2s, memory T_H2 cells, eosinophils, and mast cells, acting upstream in a sustained type 2 immune response cascade (65).

In mice, IL-33 and IL-25 activate OX40-ligand (OX40L, or CD252) expression on ILC2s, thereby activating ILC2 proliferation and cytokine production (66); in contrast, TSLP can prime DCs to improve type 2 immunity by activating T and B cells. If either one or a combination of these "alarmins" are neutralized, the development of the salient characteristics of asthma, including eosinophilia, airway hyperactivity, and peribronchial collagen deposition, may be inhibited, contingent upon the model allergen used (67–70). Moreover, clinical research suggests that after allergen inhalation for 24 h, the expression level of IL-33, IL-25, and TSLP is increased in the airway epithelium of patients with allergic asthma, correlating with the degree of airway obstruction (71). Large-scale GWAS have confirmed that SNPs in *IL33* (located at 9p24.1), *IL1RL1* (encoding the IL-33 receptor; also called suppression of tumorigenicity 2 [ST2], located at the 2q12.1 locus), and *TSLP* (5q22.1 locus) are positively associated with the risk of developing asthma; furthermore, epigenome analysis has revealed that they frequently exhibit an active chromatin state (72). Therefore, epithelial-derived alarmins may function as "early signals" in patients with different asthma phenotypes and can serve as potential therapeutic targets for allergic airway inflammation. At present, a mAb directed against TSLP (tezepelumab), has been approved for treating severe asthma in step 5 of the GINA guidelines (73). Biologic agents targeting IL-33 such as itepekimab are undergoing clinical trials (74) (Table 1).

3.1.2 DCs deliver immunogenic messages to naive T cells

The interaction between specialized antigen-presenting airway DCs and T cells facilitates allergen sensitization. Allergen processing into small peptides and selectively presenting these processed peptides to the T cell receptors (TCRs) of naive T cells via major histocompatibility complex (MHC) class II molecules (i.e., the "first signal" or antigen-specific signal) are the underlying mechanisms (75).

Effective allergen signaling warrants co-stimulatory interplay between DCs and T cells that occurs in local lymphoid collections; this results in the differentiation of T cells into T_H2-type T cells (i.e., the "second signal" or co-stimulatory signal) (76). Specifically, the activation of epithelial cells can result in the release of chemoattractants (C-C motif chemokine ligand [CCL]-20, CCL19 and CCL27, the ligands for CCR6, CCR7, and CCR10, respectively) that attract immature DCs that then differentiate and activate inflammation and adaptive immunity. A subset of conventional DCs (cDC2s) that depend on IRF4 for their development is responsible for initiating T_H2 responses in mouse lungs and other organs (77). Several epithelial-derived cytokines, including IL-1α (78), GM-CSF (78), IL-33 (79), TSLP (80), and CSF1 (81), can directly target $CD11b^+CD172a\ (SIRP\alpha)^+$ cDC2s, involved in the differentiation of T_H2 cells. However, T_H2 responses are not induced by lung-resident $CD103^+XCR1^+$ cDC1s (IRF8 and the basic leucine zipper transcriptional factor ATF-like 3 [Batf3]-dependent) and monocyte-derived DCs (moDCs). In fact, they may confer protection against asthma development by producing IL-12, a T_H1-associated cytokine, thereby inhibiting T_H2 responses (82). Moreover, plasmacytoid DCs (pDCs) play a tolerogenic role in allergic lung inflammation, inducing $Foxp3^+$ Tregs in response to inhaled antigens, at least partially by upregulating programmed death-ligand 1 (PD-L1, or CD274), a T cell inhibitory ligand (83).

T cell differentiation is driven by the migration of allergen-loaded cDC2s to the regional lymph nodes from the lung tissues; this may be regulated by ILC2-derived IL-13 and type I IFNs (84, 85). Furthermore, epithelial cell-derived cytokines and chemokines, including IL-25, IL-33, CCL17 (thymus- and activation-regulated chemokine, TARC), and CCL22 (macrophage-derived chemokine, MDC), affect the activation of DCs, maturation of T_H2 cells, and their mucosal migration. In asthma models challenged with allergen, $CD11b^+$ DCs may be an important source of CCL17 and CCL22 (by activating their CCR4 receptors), T_H2 cell-attracting inflammatory chemokines, and eosinophil-selective chemokines (i.e., the "third signal" or DC-secreted cytokines) (86). In clinical settings, activated DCs considerably increase in the airways of individuals suffering from asthma and ongoing inflammation (87); the high-affinity receptor FcεRI is expressed in their lung cDC2s express (88, 89), with increased levels of CD86 and OX40L (90).

Indeed, because DCs can perceive danger signals, process antigens, and migrate to draining lymph nodes, they occupy the intersection between innate and adaptive immunities in the lungs.

3.2 Step 2. Adaptive immune reaction: features of type 2-high and type 2-low inflammation

Because tolerance or immune regulation fails in step 1, adaptive immune inflammation develops in the lung; this comprises $CD4^+$ T_H2, T_H1, T_H17, ILC2, and IgE-producing B cells (Figure 3). T_H2 cytokines such as IL-4, IL-5, and IL-13 primarily drive allergic inflammation. However, pro-inflammatory cytokines, including TNF-α and IL-1β, augment inflammatory responses and play a role in more severe diseases. Some cytokines, including IL-10 and

TABLE 1 Classic and novel treatments developed for asthma.

Pharmacotherapies	Mechanism of action	Drugs
Traditional drugs		
Glucocorticoids	Inhibit a variety of inflammatory genes, including cytokines, inflammatory enzymes, adhesion molecules and inflammatory mediator receptors	Beclomethasone, budesonide (BUD), triamcinolone (TAA), fluticasone propionate, flunisolide (FNS)
Short/long-acting β_2-adrenoceptor agonists (SABA/LABA)	Relax bronchial smooth muscles	Salbutamol [1968], terbutaline, formoterol, salmeterol, indacaterol
Short/long-acting muscarinic antagonists (SAMA/LAMA)	Relax bronchial smooth muscles	Ipratropium, oxitropium
Theophylline	Suppresses phosphodiesterase (PDE) and increase the concentration of cyclic adenosine monophosphate (cAMP) in smooth muscle cells	Aminophylline, diprophylline, cholinophylline, doxofylline
H_1-antihistamine	Serves as neutral receptor antagonists or inverse agonists of the histamine H_1 receptor, can block the action of histamine	Chlorpheniramine, loratadine, cetirizine, ketotifen
Mast cell stabilizer	Inhibits the degranulation of allergic mediators	Disodium cromoglycate, tranilast
Leukotriene (LT) receptor antagonists	Block the cysteinyl LT (cysLT) receptor type I	Zafirlukast, montelukast [1998], pranlukast
PDE4 inhibitors	Inhibit the activity of PDE4, a specific cAMP hydrolase, thus increasing the level of cAMP in cells	Roflumilast
Biologics		
Anti-IgE antibody	Binds free IgE	**Omalizumab** (FDA[2003]-, EMA[2005]-, and NMPA [2017]-approved)
Anti-IL-4R antibody	Fully humanized IgG4 monoclonal antibody (mAb) that targets IL-4Rα subunits	**Dupilumab** (EMA[2017]-, FDA[2018]-, and NMPA [2023]-approved)
Anti-IL-5 antibody	IgG1 antibody against IL-5	**Mepolizumab** (FDA[2015]-, EMA[2015]-, and NMPA [2024]- approved)
Anti-IL-5 antibody	IgG4 antibody against IL-5	**Reslizumab** (FDA[2016]- and EMA[2016]-approved)
Anti-IL-5R antibody	Inhibits binding of IL-5 to IL-5Rα	**Benralizumab** (FDA[2017]-, EMA[2018]-, and NMPA [2024]-approved)
Anti-IL-9 antibody	Blocks IL-9	MEDI-528
Anti-IL-13 antibody	Inhibits the dimerization of IL-13Rα1 and IL-4Rα	Lebrikizumab
Anti-IL-13 antibody	IgG4 mAb targeting IL-13	Tralokinumab
Anti-IL-17 antibody	Blocks IL-17	Secukinumab
Anti-IL-17R antibody	Anti-IL-17RA mAb, which blocks IL-17A, IL-17F, and IL-17E (IL-25)	Brodalumab (AMG 827)
Anti-TSLP antibody	Human IgG2 mAb against TSLP	**Tezepelumab** (FDA[2021]-approved)
Anti-IL-33 antibody	Humanized IgG4 mAb with anti-alarmin activity against IL-33	Itepekimab
Anti-ST2 antibody	Fully human IgG2 mAb that binds to ST2 and inhibits IL-33 signaling	Astegolimab
Anti-DP2 antagonist	Highly selective prostaglandin D_2 (PGD_2) receptor 2 (DP2) antagonists	Fevipiprant
Anti-IL-6 antibody	Humanized IL-6 receptor blocker	Tocilizumab

FDA, U. S. Food and Drug Administration; EMA, European Medicines Agency; NMPA, National Medical Products Administration of P. R. China.

IL-12, exert anti-inflammatory properties and appear to be insufficient among individuals with asthma.

Diverse asthma phenotypes are primarily driven by the complex interaction between type 1 and type 2 immune pathways (Table 2). In the early 1990s, some years after studies on the immune system in mice helped develop the T_H1/T_H2 T-lymphocyte-focused paradigm, the concept that airway inflammation in atopic asthma is associated with activated T_H2 cells was first recognized (91). In another study, GATA3 was identified as a master transcription factor for T_H2 cell development and cytokine production (92).

10.3389/fimmu.2024.1478624

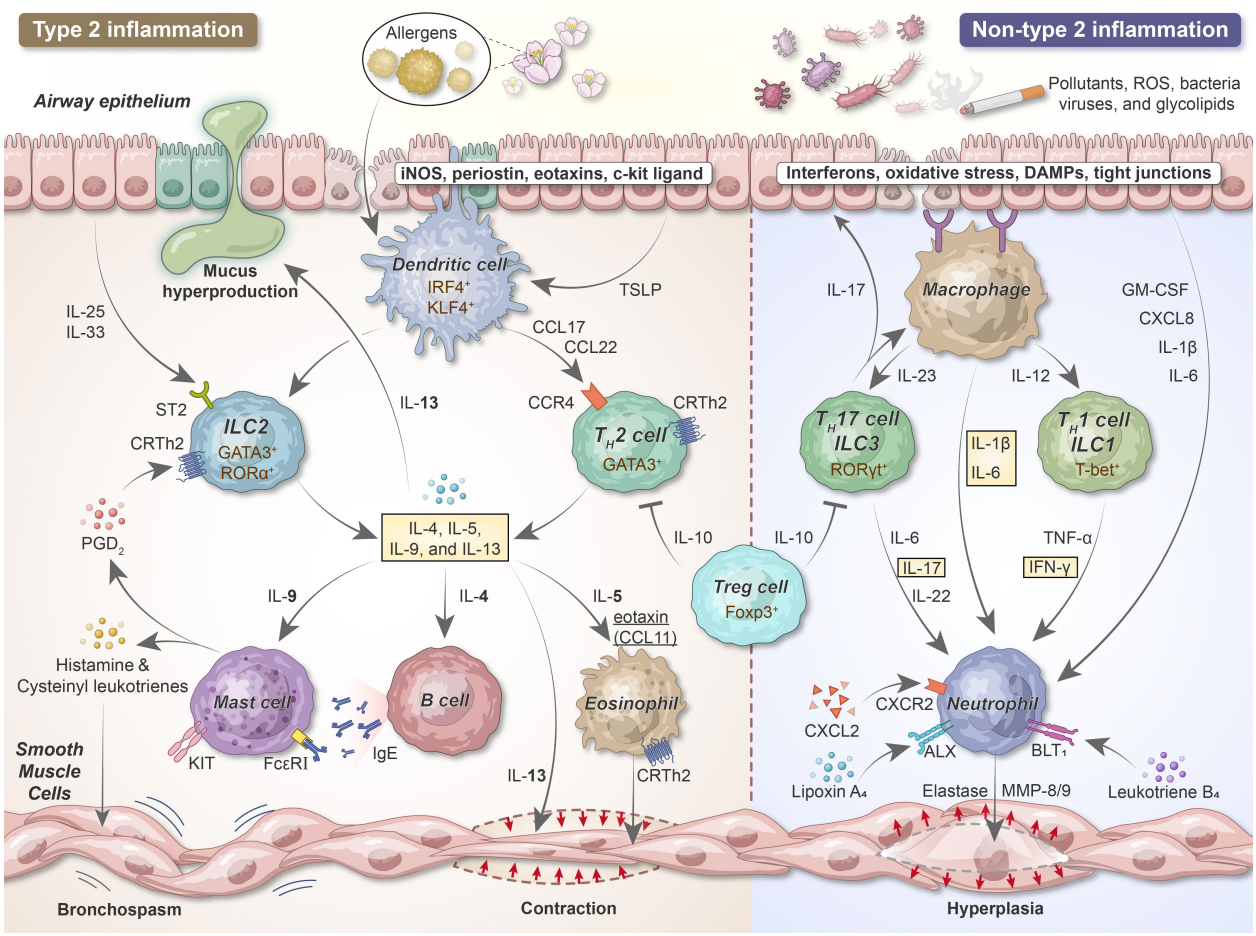

FIGURE 3
The development of airway inflammation and bronchial hyperresponsiveness in acute asthma. After sensitization, epithelial cells release alarmins (TSLP, IL-25, and IL-33) that activate DCs and ILCs. Upon the uptake, processing, and presentation of antigens to naive T cells, DCs promote naive T cell differentiation into T_H2 lymphocytes. ILC2s and T_H2 secrete IL-4, IL-5, IL-9, and IL-13, exerting vital roles in type 2 inflammation. Pollutants, cigarette smoke, viruses, and bacteria can damage and stimulate the airway epithelium, thereby releasing IL-1β, IL-6, and chemokines such as IL-8 acting as neutrophil chemoattractants. DCs and macrophages recruit neutrophils and release pro-inflammatory cytokines via T_H1/ILC1 and T_H17/ILC3 cells. iNOS, inducible nitric oxide synthase; IRF4, interferon regulatory factor 4; KLF4, Kruppel-like factor 4; ST2, suppressor of tumorigenicity 2; GATA, GATA-binding protein; ROR, RAR-related orphan receptor; Foxp3, forkhead box protein 3; T-bet, T-box expressed in T cells; PGD_2, prostaglandin D_2; MMP, matrix metalloproteinase.

Likewise, T-bet (93) and retinoic acid-related orphan receptor γt (RORγt) (94) are vital for differentiating T_H1 and T_H17 cells, respectively. In the last decade, solid data regarding the mechanisms underlying lineage development and the molecules associated with ILC subset functions have been obtained, wherein ILC1s, ILC2s, and ILC3s share and mirror the characteristics of $CD4^+$ T_H1, T_H2, and T_H17 cells (95). ILC1s, similar to T_H1 and NK cells, generate IFN-γ upon IL-12 and IL-15 stimulation and depend on T-bet for their development. ILC2s depend on GATA3 and RORα and generate type 2 cytokines such as IL-5, IL-13, and IL-9, but little IL-4. ILC3 development requires RORγt; they respond to IL-23 and IL-1β, thereby producing IL-17 and IL-22.

The ability of both $CD4^+$ T cells and ILCs to rapidly release various cytokines in response to environmental stimuli such as tissue damage, pathogen invasion, or cellular stress is a fundamental characteristic. Accumulating evidence indicates that the plasticity and maintenance of the subsets of T_H cells and ILCs are regulated by a delicate balance between their transcription factors, which are activated by differentiation-oriented cytokines; furthermore, they are affected by epigenetic modifications due to tissue microenvironment alterations (96). With an in-depth understanding of these cell types, we can gain invaluable insight into the mechanisms underlying the development of type 2-high and type 2-low asthma phenotypes (97).

3.2.1 Type 2 inflammation

Immunologists use mice to set up an ovalbumin (OVA)-induced allergic asthma model; this provides a window for elucidating the pathophysiology of the type 2-high asthma endotype and developing novel therapeutics (98). This is a pure T_H2 response in which sensitization is achieved by intraperitoneally injecting the model antigen alum (adjuvant)-emulsified OVA and challenging with aerosolized OVA; this promotes IL-4, IL-5, IL-9, and IL-13 production and OVA-specific IgE and IgG1 synthesis.

10.3389/fimmu.2024.1478624

TABLE 2 Asthma phenotypes and cellular mechanism of type 2-high and type 2-low inflammation.

Features		T2-"high"	T2-"low"
Clinical	Age	Early-onset, children	Late-onset, adult
	Clinical behavior	Often associated with allergic rhinitis, positive skin prick test to aeroallergens or presence of allergen-specific Ig E	Corticosteroid resistant, absent of eosinophilia
	Diagnostic criteria	Blood eosinophils **≥150/μl**, and/or FeNO ≥20 ppb, and/or sputum eosinophils ≥2%, and/or asthma is clinically allergen-driven [GINA 2024]	—
	Obesity/metabolic dysfunction	May be present	Often present
	Exacerbations	Allergen induced exacerbate	Cigarette smoke, pollution and viral induced exacerbate
	Medication sensitivity	More responsive to corticosteroids and bronchodilators	Less responsive to corticosteroids and bronchodilators
Inflammatory response	Epithelial cells	Secrete TSLP, IL-33, and IL-25	Secrete IL-1β and IL-23
	DCs	DC2 express IL-4, OX-40L, CCL17, and PGE2	DCs secreted IL-6, IL-23, and TGF-β
	NKT cells	NKT cells secreted type 2 cytokines	Monocyte and NKT cells secreted IL-8
	T_H cells	T_H2 secreted IL-4, IL-5, and IL-13	T_H1 secreted IFN-γ and TNF-α
		T_H9 secreted IL-9	T_H17 secreted IL-17
	ILCs	ILC2s secreted type 2 cytokines	ILC3s secreted IL-17
	B cells	IgE class-switched B cells	—
	Mast cells	Mast cells secreted proteas and PGD2	—
	Effector cells	Eosinophils secreted IL-4, IL-5, IL-13, granule proteins (MBP, EPO, ECP, EDN) and cysteinyl leukotrienes	Neutrophilic or paucigranulocytic

Using this model, it was discovered that IL-4, via IL-4Rα, can promote IgE class switch recombination of B cells and plasma cell differentiation, worsen bronchial hyperreactivity, and induce the expression of adhesion molecules such as ICAM-1 (CD54) and VCAM-1 (CD106), priming the vascular endothelium for eosinophils extravasation (99). Uniquely, IL-4 is critically involved in the differentiation of naive T_H cells into T_H2 cells.

IL-5 is an essential cytokine for eosinophil development, maturation, activation, proliferation, and survival (100). However, it may not exert chemotactic effects on eosinophils. CCR3 is selectively activated by eotaxin-1 (CCL11), eotaxin-2 (CCL24), and eotaxin-3 (CCL26) (101), combined with the expression of some adhesion molecules, including VCAM-1 (which is upregulated by IL-4 and IL-13) (102), facilitating the recruitment of eosinophils from the bloodstream to the lung mucosa and interstitium.

IL-13 and IL-4 have similar biological properties because both cytokines can function via the IL-4Rα chain and phosphorylate STAT6, a downstream transcription factor (103). However, the key difference is that IL-13 majorly participates in the effector phase of type 2 immune responses, thereby affecting the development of several traditional pathophysiological characteristics of asthma owing to the effects it exerts on lung structural cells, including epithelial cells (mucus-secreting goblet cell differentiation and proliferation), SMCs (smooth muscle hypertrophy induction and enhanced contractility), fibroblasts (extracellular matrix [ECM] production), and endothelial cells (vascular remodeling) (8, 104). Unlike IL-4, IL-13 plays no role in the differentiation of T cells because IL-13R is not expressed in immature T cells. This disparity may be because canonical T_H2 cells produce high levels of IL-13 at the effector site of the lungs, whereas IL-4 is primarily produced by T follicular helper (T_{FH}) cells in the lymph nodes (105). Furthermore, in airway epithelial cells, IL-13 augments the expression of inducible nitric oxide synthase (iNOS); iNOS is primarily involved in generating fractional exhaled nitric oxide (FeNO), a diagnostic biomarker to examine type 2 inflammation in the respiratory tract (106).

IL-9 is released by a subset of $CD4^+$ T cells (T_H9 cells), potentially by classical T_H2 cells, as well as by ILC2s. IL-9 drives mast cell survival, bronchial hyperresponsiveness, mucus cell metaplasia, and airway wall remodeling in mouse models (107). Therefore, IL-4, IL-5, IL-9, and IL-13, serving as classical type 2 cytokines, share common characteristics; however, each cytokine exhibits an exclusive functional profile.

The discovery that eosinophil-rich responses could be induced in mice lacking T and B cells has piqued our interest over the past few years that ILC2s as an important player in the pathogenesis of asthma (108). ILC2s are significantly increased in the blood and in the bronchoalveolar of asthmatic patients (109). Both ILC2s and T_H2 cells belong to the lymphoid lineage and generate similar cytokine patterns. Their functions considerably overlap in asthma, although there are some detailed differences. In the presence of IL-

25 or IL-33, ILC2s can directly control the key features of type 2 asthma, including eosinophilia, bronchial hyperreactivity, and goblet cell hyperplasia, by producing IL-5, IL-9, and IL-13 (110). Furthermore, ILCs function as antigen-presenting cells that use MHC class II molecules to present antigenic epitopes and express OX40L to support $CD4^+$ T lymphocyte activity (111, 112). Moreover, in local tissue settings, ILC2s interact with both DCs and T_H2 cells in complex bidirectional crosstalk, modulating the intensity of type 2 responses to properly respond to perceived environmental threats (84, 113).

Cellular activation and inflammatory mediator release are representative characteristics of type 2-high asthma, which can be observed via mast cell degranulation and eosinophil vacuolation. The interplay between IgE and high-affinity FcεRI on granulocytes, including mast cells and basophils, results in the initiation of cell activation and degranulation, releasing multiple preformed and newly synthesized mediators, cytokines, chemokines, and growth factors. The ready-made mediators stored in cytoplasmic granules include biogenic amines (e.g., histamine and serotonin), neutral proteases (e.g., tryptase, chymase, and carboxypeptidase A), proteoglycans (e.g., heparin and chondroitin sulfate), and some cytokines (e.g., TNF-α) and growth factors (e.g., vascular endothelial growth factor A [VEGFA]) (114). T_H2-dependent trypsin-expression cell (MC_T) are the main type of mast cells that contribute to mild-to-moderate allergic asthma (115). However, in more severe asthma forms, mast cells containing both trypsin and chymase (MC_{TC}) become dominant; compared with MC_T, MC_{TC} relies more on stem-cell factors (SCF, i.e., the KIT ligand) for survival (116).

Lipid-derived mediators can be secreted by FcεRI aggregation-activated mast cells. They are responsible for arachidonic acid metabolism via the cyclooxygenase (COX) and lipoxygenase (LOX) pathways, releasing prostaglandins (PGs, particularly PGD_2), leukotriene B4 (LTB_4), and cysteinyl leukotrienes (CysLTs, including LTC_4, LTD_4, and LTE_4) (117). Histamines, PGs, and CysLTs as potent bronchoconstrictors and can lead to bronchospasm, vasodilation, plasma leakage, mucus production, and elevated cellular recruitment in the lungs. PGD_2 acts on type 1 PGD_2 receptor (DP1) to contract the airway smooth muscle and CRTH2, a T_H2 cell-expressed chemokine receptor, i.e., DP2, to chemoattract T_H2 cells, ILC2s, and eosinophils (118). Several anti-allergic drugs targeting the abovementioned mediators, including antihistamines, leukotriene modifiers, mast cell membrane stabilizers, and DP2-receptor antagonists, have been developed to decrease type 2 inflammation in the airways. These drugs are majorly used as adjunctive therapies for patients who inadequately respond to regular treatment strategies for allergic asthma, particularly those with allergic rhinitis and allergic skin diseases.

In recent years, non-steroidal anti-inflammatory-drug (NSAID)-exacerbated respiratory disease (NERD) has attracted increasing attention (119). As a prominent severe type 2-high asthma phenotype that appears in adulthood, it is characterized by increased production of CysLTs, high prevalence of coexisting chronic rhinosinusitis with nasal polyps (CRSwNP), and hypersensitivity to aspirin, emphasizing that dysregulation of arachidonic acid metabolism likely exacerbates the worsening of upper and lower airway symptoms of asthma.

3.2.2 Non-type 2 inflammation

Asthma is generally linked to increased eosinophils and T_H2 cytokines; however, some patients present with a predominantly neutrophilic disease, also called "non-type 2" or "type 2-low" asthma; this asthma phenotype lacks T_H2 cytokine signatures but may exhibit severe glucocorticoid resistance (13). Other features associated with severe neutrophilic asthma include advanced age, impaired lung function, decreased reversibility of bronchodilator responsiveness, microbial infections, tobacco consumption, and obesity (120). Although the molecular mechanism underlying airway neutrophilic inflammation remains unelucidated, it primarily involves the IFN-γ-mediated type 1 and IL-17-mediated type 3 immune pathways (121).

In general, PRRs (such as TLRs) activation in response to microbial infections leads to a type 1 immune response; it involves immune cells that can release IFN-γ, including $CD4^+$ T_H1 cells, type 1 ILCs (ILC1s), NK cells, and $CD8^+$ cytotoxic T (T_C1) cells (122). The development of naïve T cells in the T_H1 or T_C1 direction can be induced by intracellular microbes that interact with the TLRs on DCs in the presence of IL-12 and IL-18 derived from DCs and IFN-γ derived from NK cells or ILC1s. The BALF cells isolated from patients with severe type 2-low asthma and lung tissues obtained from corresponding mouse models showed increased levels of IFN-γ and decreased expression of secretory leukocyte protease inhibitor (SLPI), which correlated with high airway resistance and steroid insensitivity (123). At present, the pathogenic roles of type 1 immunity in asthma remain controversial. IFN-γ signaling may be absent in the airway epithelial cells of patients with asthma (124); this abnormality increases their vulnerability to viral infections and worsens asthma (125). In contrast, other studies have demonstrated that severe asthma episodes are associated with high IFN-γ and IL-17A expression in the airways (126, 127). Despite receiving high-dose corticosteroid treatment, $CD4^+$ T cells with IFN-γ^+ (T_H1 cells) were higher in the BALF of patients with severe asthma than in that of patients with mild or moderate asthma (123, 126).

IL-17 cytokine family members, including IL-17A and IL-17F, mediate the type 3 immune process. Extracellular bacteria and fungi induce IL-1β and IL-23 production by myeloid DCs (mDCs); as a result, primitive $CD161^+$ T cells differentiate into $CD4^+$ T_H17 or $CD8^+$ T_C17 cells and trigger ILC3s to generate cytokines (122). Furthermore, IL-17A, IL-17F, and IL-22 regulate neutrophilic influx into tissues by inducing airway epithelial and stromal cells to generate cytokines such as G-CSF, GM-CSF, and IL-6, as well as chemokines such as CXCL1, CXCL6, and CXCL8 (IL-8); this promotes neutrophil activation and migration (128). Other cells, including γδT cells, NKT cells, and granulocytes, are also known to secrete IL-17 cytokines (129). In some individuals with moderate-to-severe asthma, these cytokines are increased in the blood, sputum, and bronchial biopsies, correlating with increased disease severity (130). In mice and humans, T_H17-related cytokines play a role in airway remodeling by inducing mucous cell metaplasia, promoting

fibroblast and SMC proliferation, and directly contracting bronchial SMCs, thereby narrowing the airway (31, 131). Unfortunately, despite the relatively large amount of evidence via observational studies, a randomized clinical trial of brodalumab, an IL-17 receptor-neutralizing antibody, in patients with poorly controlled moderate-to-severe asthma failed to exhibit significant benefits in all-comers (132) (Table 1).

3.2.3 Phenotype overlap and systemic inflammation

Owing to a strong relationship between heterogeneity and asthma, the dichotomous viewpoint of asthma categorization may be oversimplified; it only appears at the extremes of the continuous spectrum (129). Based on asthma endotype complexity, two primary inflammatory signatures involving T_H2 or T_H17 cells and their respective cytokines have been categorized as discrete subpopulations; however, recent evidence suggests the simultaneous occurrence of type 2 and non-type 2 immune responses in some patients (133). Most T_H cells display a degree of plasticity that depends on environmental factors and may be redirected toward other effector $CD4^+$ cells. Interestingly, a study suggested that the T_H2 and T_H17 inflammatory pathways are mutually regulated in patients with asthma; the suppression of the T_H2 pathway promotes a T_H17 response; therefore, the dual blockade of T_H2 and T_H17 functionalities may be rewarding for asthma treatment (134).

Historically, IL-17 was considered to be derived from conventional T_H17 cells; however, a novel $CD4^+$ T_H2 memory or effector cell subset that collectively expresses GATA3 and RORγt and produces T_H2 and T_H17 cytokines has now been identified; this subset persists as the predominant IL-17-producing T cell population during the chronic phase of asthma (135). In individuals with severe and corticoid-resistant asthma, dual-positive T_H2/T_H17 cells (i.e., IL-17-producing T_H2 cells) were significantly increased in the peripheral blood and BALF (136, 137). These dual-positive T_H2/T_H17 cells are characterized by higher levels of IL-4 production and increased expression of MEK1 (mitogen-activated protein-extracellular signal-regulated kinase [ERK] kinase 1), mediating resistance to dexamethasone-induced cell death (136). This can partially explain why a $T_H2/T_H17^{predominant}$ endotype causes more severe asthma compared with the traditional $T_H2^{predominat}$ and T_H2^{low} endotype (136). Additional research has demonstrated that IL-1β, IL-6, anti-IFN-γ, and IL-21, which is a cytokine environment that stimulates T cells in asthma to differentiate into the same biphenotypic cells, promote dual-positive T_H2/T_H17 cell differentiation, worsening asthma (137). Similarly, under specific alterations in the inflammatory microenvironment, T_H17 cells repolarize toward the T_H2 profile, adjusting their cytokine expression to a T_H2-like pattern (138).

In a recent cross-sectional study in humans, phenotype distribution was examined in patients with mild-to-severe asthma (139). Phenotype overlap is extremely common in patients with asthma (73.4%), encompassing combinations of type 2-related, non-type 2-related, and mixed type 2/non-type 2 inflammation. The last group is particularly concerning; it accounts for approximately 50% of the total number of patients and exhibits the worst clinical outcomes. The average age or onset age is younger in the type 2 group, intermediate in the mixed one, and older in the non-type 2 group and might reflect immune inflammatory status evolution, beginning from a canonical type 2 signature and progressively transforming into a more complex mixed type 2/non-type 2 signature. As individuals age, those who develop pure type 2 asthma in the early years may encounter various environmental stimuli throughout their lives, possibly triggering different pathways and altering the original type 2 predominance (140).

Asthma is being increasingly acknowledged as a systemic disease, in which inflammation is not limited to the airways but remarkably cross-communicates with other distant organs by releasing inflammatory mediators (141). In patients with asthma, increased IL-6 and IL-1β levels are markers for systemic inflammation and are associated with reduced forced expiratory volume in 1 second (FEV_1) and elevated acute exacerbations (142, 143). The analysis of the clinical traits of patients with asthma suggested that an imbalanced diet with excessive calorie intake and the resulting metabolically related inflammation can affect both innate and adaptive defense mechanisms in the respiratory tract (144). The burden of obesity-associated inflammation may increase the risk of developing asthma. White adipose tissue secretes pro-inflammatory cytokines such as IL-1β, IL-6, TNF-α, and leptin, which may negatively impact lower airway function by increasing airway hyperreactivity (145). Interestingly, increased plasma IL-6 levels and systemic inflammation are observed in both type 2-high and type 2-low asthma; however, they are not associated with upstream type 2 inflammation, with no data for the increase in IL-6 expression in the sputum (143).

3.3 Step 3. Transition from airway inflammation to structural changes

3.3.1 Chronicity of inflammation

Inflammation persists when humans are continuously or repeatedly exposed to viruses, bacteria, allergens, air pollutants, tobacco smoke, and/or oxidative stress; furthermore, there are many innate immune cells in the bronchial mucosa epithelium, including eosinophils, neutrophils, basophils, and monocyte–macrophage lineage cells, as well as blood-derived adaptive immune cells, including T_H2 cells, other T cell types, and B cells. Chronic inflammation and airway remodeling simultaneously occur because of the continuous cycle of epithelial damage and repair; this results in disease chronicity, which is a characteristic of asthma. In general, the inflammatory process of asthma is primarily confined to the conducting airways. However, with disease progression to a more chronic state, inflammatory cells infiltrate the proximal of the trachea and larynx and distal of the smaller airways, periodically involving neighboring alveoli. The inflammatory responses in the small airways may primarily occur outside the airway smooth muscle, whereas submucosal inflammation is predominant in the large airways.

Microscopically, inflammation can affect all layers of the airwall in patients with chronic asthma. The epithelium does not exhibit the normal pseudostratified appearance and may be stripped, with

only the basal layer remaining. The basal cells are hyperplastic, with squamous metaplasia. Furthermore, goblet cell hyperplasia is observed. Characteristically, the basement membrane of the epithelium is thickened and hyalinized. Moreover, mucous glands in the bronchial submucosa are hyperplastic. In addition, the submucosa is edematous and contains a mixed inflammatory infiltrate, with different numbers of eosinophils. Bronchial smooth muscle hyperplasia and hypertrophy are the most typical features of status asthmaticus. In all bronchial tube wall layers, eosinophil, monocyte, lymphocyte, and plasma cell infiltration is observed. In some cases of fatal asthma, mucus plugs comprising mucin glycoproteins and plasma proteins may block the airways; furthermore, Charcot–Leyden crystals, the disintegrating product of eosinophils, are often observed in the tube walls and mucus plugs (146).

Of note, several reinforcing feedback loops promote the perpetuation of chronic airway inflammation among patients with asthma (Figure 4). For example, in type 2-high asthma, T_H2 cells and ILC2s are significant IL-4, IL-5, and IL-13 sources; furthermore, infiltrating mast cells, eosinophils, and basophils play vital roles in producing type 2 cytokines. Collectively, these cells maintain the environment needed for the survival of type 2 cytokines, thereby supporting chronic disease development. IL-4 neutralizes the suppressive function of Tregs and inhibits their generation, allowing the differentiation of IL-4-producing T_H2 cells or ILC2s (147, 148). The co-engagement of sIgE bound to FcεRI receptors on mast cells and basophils results in the massive release of IL-4, a major mediator of B cell class switching and IgE synthesis. IL-5 mediates eosinophil differentiation and function, whereas eosinophils, in turn, secrete large amounts of IL-5. Alarmins that activate T_H2 cells and ILC2s are released by damaged airway epithelial cells, leading to cytokine (IL-4 and IL-13) production; this significantly increase the expression of histone deacetylases (HDACs) and

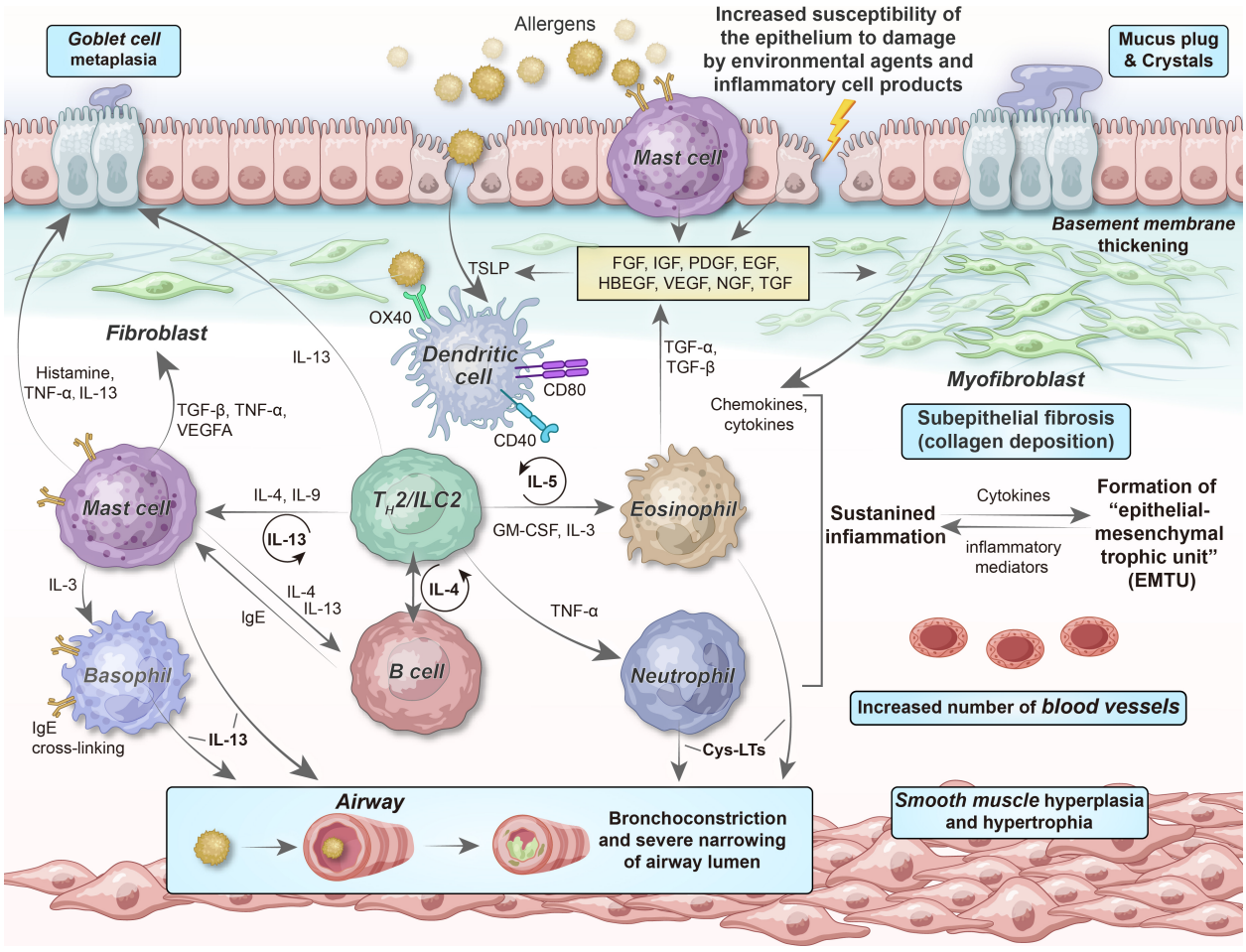

FIGURE 4
Relationship of epithelial–mesenchymal communication to airway inflammation and remodeling in chronic persistent asthma. The chronicity of inflammation is associated with repeated damage–repair responses that contribute to establishing the EMTU, which, in turn, provides a continuous tissue environment ("soil") for T_H2 cell/ILC2-related inflammation ("seed"). The interdependency among chronic inflammation, altered immunity, and structural changes, involving epithelial cells, (myo)fibroblasts, SMCs, and their secretory ECM, microvasculature, and neural networks, can describe why chronic airway inflammation persists even if obvious environmental stimuli are absent, as well as the reason for the failure to obtain complete therapeutic responses to anti-inflammatory drugs at the more severe and chronic end of the asthma spectrum. FGF, fibroblast growth factor; IGF, insulin-like growth factor; PDGF, platelet-derived growth factor; EGF, epidermal growth factor; HBEGF, heparin-binding EGF-like growth factor; VEGF, vascular endothelial growth factor; NGF, nerve growth factor; TGF, transforming growth factor; Cys-LTs, cysteinyl leukotrienes.

silent information regulator genes (SIRTs), whose activities are inversely correlated with the integrity of the epithelial barrier (149).

To break the abovementioned vicious cycle and inhibit continuous asthma progression, several anti-inflammatory drugs have been developed (Table 1). However, the redundancy of cytokine sources and overlapping effects of inflammatory mediators increases the robustness of the pro-inflammatory network, making treatment with a single targeted therapy (e.g., cytokine-specific monoclonal antibodies) challenging. To date, the inhaled administration of glucocorticoids remains the most effective treatment modality for asthma; they modulate (mostly downregulate) the expression of approximately 200 genes to exert anti-inflammatory effects.

Recently, the concept of "trained innate immunity" has garnered attention to explain the pathological mechanisms underlying chronic inflammation in asthma (150). Immunologic memory, long considered a specific feature of adaptive immunity, primarily depends on antigen receptor gene rearrangements and lymphocyte clone production. However, emerging literature suggests that the innate immune system can exhibit memory features (151). Abnormal innate immune memory frequently exacerbates the inflammatory responses observed in asthma. Furthermore, repeated exposure to different non-specific stimuli can result in conditionally trained immunity in innate immune cells, including airway epithelial cells, DCs, ILC2s, mast cells, monocytes, macrophages, and NK cells. Depending on the upregulation of pro-inflammatory factors such as IL-1, IL-6, TNF-α, and CCL17 or anti-inflammatory mediators such as IL-10, these cells develop into a pro-inflammatory or anti-inflammatory state. Signaling pathways impinging on transcription factors and an intricate interconnection between epigenetic modifications and metabolic reprogramming may help maintain this state, possibly favoring (pro-inflammatory state) or preventing (anti-inflammatory state) asthma development or progression (152).

3.3.2 Bronchial epithelial–mesenchymal transition and lung tissue remodeling

Airway remodeling, an outstanding feature of chronic asthma, is characterized by aberrant epithelial repair and fibroblast accumulation, contributing to ECM deposition, which results in fixed bronchial obstruction (153). EMT is a dynamic approach in which epithelial cells acquire mesenchymal characteristics and lose their epithelial phenotype; it plays a vital role in normal development, tissue remodeling, fibrosis, and cancer progression. Based on its functional significance, EMT can be classified into three types: type I EMT presents during embryonic development, type II EMT participates in wound healing and organ fibrosis, and type III EMT is related to the metastasis of malignant tumors and transformation of tumor phenotypes. Among these types, type II EMT participates in asthmatic airway remodeling (154).

In general, epithelial injury and ciliopathies; mucosal edema; goblet cell hyperplasia; basal membrane thickening; increased blood vessel supply; increased mass of subepithelial fibroblasts, myofibroblasts, and airway SMCs; and ECM protein deposition are the pathological changes that occur during airway remodeling. These events result in excessive airway reactivity, with mucus formation and plugging extending into the small airways, resulting in airway trapping and overinflation; this ultimately results in decreased lung function in patients with chronic asthma (155).

As a hallmark of airway remodeling, subepithelial fibrosis is proportional to disease severity and duration (156). Through EMT, airway epithelial cells lose apical–basal polarity, undergo cytoskeletal changes, and lose intercellular adhesion and TJs; furthermore, the expression level of epithelial markers, including E-cadherin, is decreased and that of interstitial markers, including α-smooth muscle actin (α-SMA) and vimentin, is increased (157, 158); this results in airway epithelial cell differentiation into myofibroblasts, thereby exacerbating the degree of subepithelial fibrosis (159). Among the signaling pathways involved in EMT, the TGF-β_1/Smad, Wnt/β-catenin, and Sonic Hedgehog signaling pathways have been extensively studied and occupy a central position (160).

The prevailing view is that inflammation is the primary driver and amplifier of most airway remodeling processes. Various cytokines, chemokines, and growth factors released from inflammatory and tissue cells in the airways form a complex signaling milieu, driving structural changes in the lung tissue. In type 2-high asthma, activated eosinophils release cytotoxic granular proteins, including eosinophil cationic protein (ECP), major binding protein (MBP), eosinophil peroxidase (EPO), and eosinophil-derived neurotoxin (EDN), LTC_4, and platelet-activating factor (PAF), leading to airway constriction, mucus secretion, and increased blood permeability (161). Furthermore, eosinophils are a major source of TGF-β, inducing subepithelial fibrosis, airway smooth muscle hypertrophy, and goblet cell proliferation (162). Epithelial damage and delayed repair stimulate the production of several growth factors, including epidermal growth factor (EGF), TGF-β, and VEGF, which driving airway fibrosis and SMC, neuronal, and capillary proliferation, resembling a chronic wound scenario (163). SMCs are the primary structural cells present in the bronchial airways. During asthmatic airway inflammation, airway SMCs undergo continuous proliferation and hypertrophy, along with deposition of ECM and differentiation of goblet cells (164). Based on these structural changes, SMCs also participate in inflammatory and remodeling processes via the expression of cell adhesion molecules (CAMs), cytokine receptors, chemokine receptors, and TLRs (165). Furthermore, by releasing cytokines such as IL-4, IL-9, and IL-13, T_H2 cells and ILC2s promote subepithelial fibrosis, epithelial goblet cell metaplasia, and SMC proliferation (166). In another striking animal study, the researchers reported that when airway inflammation levels were almost similar, mice without T_H17 cells had lesser airway remodeling than controls. Therefore, T_H17 cells induce airway remodeling in a T_H2 response-independent manner (30).

Although airway remodeling is frequently associated with inflammation, this perspective is being challenged and should not be assumed to occur downstream from a single (or central) mechanism. First, airway remodeling can occur in early disease

stages or preschool-aged children; however, modeling is less pronounced in adult-onset asthmatic airways (167), suggesting that it is simply not a consequence of inflammation. Second, more severe tissue remodeling, characterized by the excessive deposition of connective tissues with gradual lung function loss, is rare in moderate-to-severe asthma and only develops over time in patients receiving insufficient therapy (54). Lastly, anti-inflammatory treatment may partially reverse airway remodeling and airflow obstruction; however, it generally requires long-term rehabilitation (168).

A new hypothesis about persistent asthma has emerged in which epithelial damage in individuals with asthma triggers abnormal communication between the epithelium and basal myofibroblast sheaths, which is mediated via growth factors, thereby driving airway remodeling; this is called activation of the "epithelial–mesenchymal trophic unit (EMTU)" (169). In contrast, the cytokine milieu generated by the EMTU endows a favorable environment for sustained chronic inflammation. This leads to several functionally significant alterations in the architecture of the affected tissue, including considerable airway wall thickening (including the epithelium, lamina reticularis, submucosa, and smooth muscles), ECM protein deposition (including periostin (170), fibronectin (171), tenascin-C, osteopontin, and "repair-type" collagens I, III, V, and VI), and goblet cell hyperplasia; this is linked to increased mucus production. In individuals who have such airway wall thickening, bronchoconstriction severely narrows the airway lumen compared with that occurring in normal thickness airway walls.

Irrespective of the underlying mechanism, repeated bronchoconstriction, in and of itself, upregulates pro-fibrogenic cytokines and deposits subepithelial collagen (172). Therefore, in addition to chronic inflammation and tissue injury response, changes in mechanical stress may also lead to airway wall remodeling via the action of epithelial-inducible proteins such as YKL-40 (encoded by the gene *CHI3L1*; i.e., chitinase-3-like protein 1) (173), resistin-like molecule-β (RELMβ) (174), and members of the plasminogen activator system (175).

A groundbreaking endoscopic treatment has highlighted the importance of airway remodeling and mechanical transduction as drivers of asthma pathogenesis. Bronchial thermoplasty (BT) is a non-pharmacological intervention in which therapeutic radio-frequency energy is applied in a controlled manner to the bronchial walls to heat the tissues; BT can decrease the frequency and severity of asthmatic attacks (Evidence B) (176). This temperature-controlled radio-frequency energy is locally delivered to the proximal airways to produce clinical effects and alleviate patient symptoms by decreasing the mass of smooth muscles. However, the other effects of BT on airway remodeling and how it provides clinical benefits remain unclear, potentially involving the downregulation of cytokines such as TGF-β and RANTES (CCL5) (177), inhibition of RBM (reticular basement membrane) thickness and ECM deposition (178), modulation of innervation and vascularization, and improvement of the regenerative capacity of the airway epithelium (179). Nevertheless, evidence regarding its effectiveness and long-term safety is limited, and, at present, it can only be leveraged in research trials or within the scope of national registries as an additional treatment for some adult patients with moderate-to-severe asthma.

3.4 Step 4. Turning point: disease exacerbation or remission

3.4.1 Allergen-induced exacerbation of type 2-high asthma

As previously discussed, in stable type 2-high asthma, the airway epithelium releases TSLP, IL-25, and IL-33, differentiating DC-activated T_H2 cells. Therefore, IL-5 and GM-CSF are secreted by these T_H2 cells, which along with epithelial-derived eotaxins, monocyte chemotactic proteins (MCPs), and RANTES regulate eosinophil production, maturation, recruitment, and activation. Ultimately, the local degranulation of lung eosinophils damages the airway epithelium. Meanwhile, IL-9 and IL-13, as T_H2 cytokines, induce goblet cell metaplasia (62).

Several other factors, including indoor allergens such as dust mites, pet fur, and cockroaches; outdoor allergens such as catkins, pollen, fungi, and cold air; and dietary allergies such as aspirin and some high-protein fish, shrimp, crabs, and eggs, can aggravate inflammatory responses during the acute worsening of type 2-high asthma. The PRRs in the airway epithelium can detect allergens and other environmental stimuli. $PM_{2.5}$ extracts can acutely exacerbate allergic lung inflammation in an inflammasome-dependent manner via the TLR2/NF-κB/NLRP3 pathway (180). Overlaid on the general type 2-high inflammatory response, epithelial cells produce TARC (CCL17), a major chemokine for recruiting T_H17 cells; TARC enhances the pro-inflammatory effects of T_H2 cells by releasing IL-17 and secreting IL-8, leading to neutrophil recruitment (Figure 5). Evidence suggests that TARC levels are significantly elevated in the BALF of individuals with allergen-challenged asthma exacerbation. The combinations of IL-4, IL-13, and TNF-α elicit TARC release from airway SMCs, thereby promoting the force generation of smooth muscles and airway stenosis (181).

Abnormal contraction of the bronchial smooth muscle is a key pathological process that induces airway hyperresponsiveness in asthma. The inflammatory cytokines generated during asthma exacerbation, primarily IL-13, can not only directly act on IL-13 and IL-4 receptors on airway SMCs (182), thereby enhancing agonist-evoked excitatory effects by upregulating pro-inflammatory mediators such as IL-1β and TNF-α (183), but also modulate G protein-coupled receptor (GPCR, e.g., muscarinic receptor)-related signaling pathways and/or inhibit cAMP production, thereby altering calcium homeostasis in airway SMCs (184). Newly synthesized mediators released from airway SMCs promote immune cell recruitment and activation, thereby sharpening an ongoing inflammatory response. Persistent airway inflammation helps enhance the strength generated by airway smooth muscles, possibly increasing the number and size of airway SMCs. Understanding the regulation of airway smooth muscle function and combining this information with the underlying immunologic processes that drive asthma

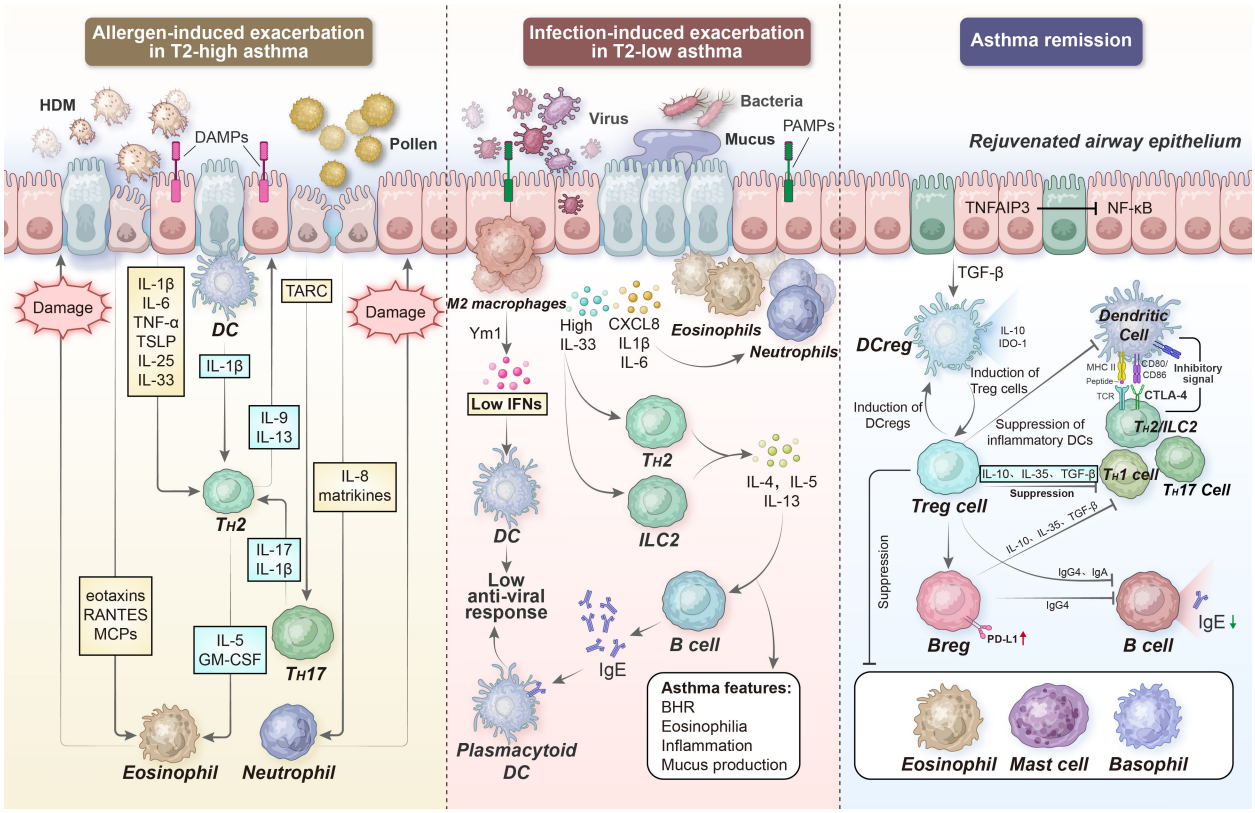

FIGURE 5
Acute exacerbation and remission of asthma. During allergen- and infection-induced asthma exacerbation, the PRRs in the airway epithelium can detect many other additional factors. Subsequently, epithelial cells in the airway release TSLP, IL-25, and IL-33 to support DC-activated T_H2 cell differentiation; on the other hand, they secrete TARC and IL-8 to recruit T_H17 cells and neutrophils, respectively. In turn, the local degranulation of lung eosinophils and neutrophils damages the airway epithelium, further impairing barrier integrity and enhancing ongoing inflammation. However, several regulatory immune cell types, including DCregs, Tregs, and Bregs can limit or resolve inflammation, partially via IL-10-, TGF-β-, and IL-35-dependent mechanisms. DAMPs, damage-associated molecular patterns; PAMPs, pathogen-associated molecular patterns; TARC, thymus activation regulated chemokine; RANTES, regulated upon activation normal T cell expressed and secreted; Ym1, chitinase-like protein 3; BHR, bronchial hyperresponsiveness; TNFAIP3, tumor necrosis factor alpha-induced protein 3; IDO-1, indoleamine 2,3-dioxygenase 1, CTLA-4, cytotoxic T-lymphocyte-associated protein 4.

pathogenesis may become an important breakthrough in addressing the treatment mysteries of asthma (185).

In a very recent study, using a human allergen-induced asthma exacerbation model, single-cell RNA sequencing (scRNA-seq) was utilized to compare the lower airway mucosa of patients with asthma and allergic controls without asthma (186). The airway epithelium of patients with asthma was highly dynamic, with the upregulation of the genes involved in mucus metaplasia, matrix remodeling, and glycolysis; however, antioxidant and growth factor pathways observed in controls were not induced. In particular, following allergen exposure, *IL9*-expressing pathogenic T_H2 cells were observed in the asthmatic airways, along with the enrichment of cDC2s and CCR2-expressing monocyte-derived cells, which upregulated the expression of inflammatory mediators and metalloproteinases. Moreover, a unique T_H2-mononuclear phagocyte-basal cell interactome was discovered in patients with asthma, characterized by type 2 programming of immune and structural cells and the involvement of additional signals, including the TNF family and cellular metabolism pathways.

3.4.2 Infection-induced exacerbation of type 2-low asthma

Across all age groups, respiratory tract infections are closely associated with wheezing illnesses, possibly affecting asthma development and severity. Airway infection caused by viruses, chlamydia, or mycoplasma may play a vital role in asthma pathogenesis: repeated respiratory infections during early childhood (particularly respiratory syncytial virus [RSV]) encompass the strongest predictors of future asthma risk (187); on the other hand, to date, viral infections (primarily rhinovirus [RV]) are the most common reason for the acute worsening of already established adult asthma; this results in the acute aggravation of disease symptoms, warranting increased medication use and emergency department visits and hospitalization and intensive care measures in some cases (188).

In most patients with asthma, relatively mild respiratory viruses such as RV, RSV, adenovirus, human metapneumovirus, influenza viruses, and parainfluenza viruses lead to acute exacerbation. After infection, host cells such as airway epithelial cells induce

inflammatory responses to counteract the viruses. This cellular response may facilitate the acute exacerbation of asthma.

Cellular responses to viruses are initiated by TLR-3, TLR-7, and TLR-8, RIG-I, and MDA5 detecting a single-stranded RNA (or else a double-stranded RNA during replication) (189). The activation of these receptors drives a vigorous innate immune response via the induction of primary interferons (e.g., IFN-β), which results in the activation of NKT cells and alternative activation of macrophages (M2), thereby maintaining airway pathology through the production of IL-13 (190). In the lungs, anti-viral immunity heavily depends on type I (IFN-α and IFN-β) and type III (IL-29 [IFN-λ1], IL-28A [IFN-λ2], IL-28B [IFN-λ3], and IFN-λ4) IFN production, cytokine (such as IL-1, IFN-γ, TNF, IL-6, IL-12, and IL-18) secretion, and chemokine (such as CCL3, CCL5, CXCL8, and CXCL10) release (191) (Figure 5).

Many studies have suggested that IFN production is either delayed (192) or deficient (124, 193) in patients with asthma, resulting in the absence of adequate clearance rates for their immune responses to viral infections (194). This defect is associated with epithelial barrier and TJ disruption. Recently, studies have demonstrated that the exogenous dosing of IFN-β decreases viral exacerbations in mild-to-moderate asthma by restoring impaired antiviral innate immunity (195, 196). Additional factors that affect viral infection severity and asthma exacerbation risk include the enhanced expression of viral receptors (such as ICAM-1, low density lipoprotein receptor [LDLR], and CDHR3) (197, 198), high body mass index of patients (199), excessive increase in blood eosinophils (patients with type 2-high asthma) (199), reproducible changes in the DNA methylome (200, 201), and disturbances in the airway microbiota (202, 203).

Compared with viral respiratory infections, bacterial infections have a smaller and less important effect. In patients with acute asthma exacerbation, only a small proportion have isolated bacteria from their sputum (204).Airway bacterial infections may occur secondary to viral-induced epithelial barrier disruption, resulting in increased inflammation and risk of asthma exacerbation (205). However, there is limited evidence linking bacterial infections to acute asthma exacerbation. In a large-scale study, the colonization levels of dominant bacterial pathogens were not statistically significantly different in children with recurring and acute wheezing and those without a wheezing history (206).

Notably, the long-term oral administration of low-dose azithromycin, a macrolide antibiotic, can significantly decrease the acute exacerbation of eosinophilic and non-eosinophilic asthma, improve the quality of life of patients with severe asthma, and decrease the risk of lower respiratory tract infections (207, 208). Azithromycin exerts antibacterial, anti-inflammatory, and immunomodulatory properties and is cost-effective. At present, guidelines recommend using this antibiotic for refractory asthma. Nevertheless, potential issues such as antimicrobial resistance and side effects such as cardiac toxicity and gastrointestinal adverse reactions may restrict the widespread use of this antibiotic (209, 210).

Infection-induced asthma is not always a type 2-low inflammation. Allergic bronchopulmonary aspergillosis (ABPA) is a type 2-high inflammatory lung disease caused by an allergy to Aspergillus fumigatus, commonly presenting with treatment-resistant asthma and recurrent pulmonary shadows, which may be accompanied by bronchiectasis (211). This disease is not rare, but it is often misdiagnosed or overlooked clinically. Classical immunology suggests that the usual response of the human host to fungal clearance is a T_H1 $CD4^+$ T-cell response, which mediates the phagocytic function of macrophages and neutrophils. In contrast, the immune reaction in ABPA is predominantly mediated by T_H2 cells, which not only cannot eradicate the fungi but also cause a massive influx and degranulation of mast cells and eosinophils, releasing various inflammatory mediators and cytokines, including IL-4, IL-5, IL-13, as well as total and *A.fumigatus*-specific IgE. Persistent inflammation will lead to airway mucus plugging, bronchiectasis, and pulmonary fibrosis. If not controlled, it can culminate in end-organ damage and clinical manifestations, which warrants our vigilance.

3.4.3 Suppression and resolution of airway inflammation

Although asthma cannot be completely cured, it is possible to further pursue more realistic and achievable goals. Remission is defined as the long-term absence of disease signs and symptoms, accompanied or not by the normalization of the underlying pathology. Clinically remitted asthma requires stable lung function and the endorsement of patients or clinicians, in addition to at least 12 months without significant asthma symptoms and exacerbations; on the other hand, complete remission (cure) warrants the normalization of the underlying pathology, including resolution of airway inflammation (212). Both remission types may be achieved with or without treatment. Based on the clinical settings and research populations, clinicians and researchers can flexibly adjust the achievable and measurable definitions of asthma remission.

The introduction of ICS in the 1980s revolutionized the treatment of asthma, and to this day it remains the cornerstone for gaining optimal asthma control. ICS is generally effective in mitigating symptoms of mild-to-moderate asthma, enhancing lung function, and preventing exacerbations. The emergence of combination therapy with ICS, long-acting β_2-agonists (LABA), and long-acting muscarinic antagonists (LAMA) has further improved asthma management. However, some studies have indicated that patients with inactive asthma, even when in complete remission, still exhibit some degree of persistent subclinical airway inflammation, hyperresponsiveness, and remodeling (213–215), possibly determining the future risk of recurrence (216, 217). Furthermore, many cross-sectional studies have examined the inflammatory markers associated with clinical and complete asthma remission in different samples such as blood, sputum, BALF, or endobronchial biopsies and eosinophils, neutrophils, mast cells, IgE, FeNO, iNOS, histamine, ECP, and EPO (214, 218–222). Most of these studies have confirmed that these markers are higher in subjects with asthma remission than in healthy controls and lower than in those with persistent asthma (223), although some studies have found no significant differences between the groups.

Further defining the clinical features and pathophysiology of asthma remission may be beneficial; however, future studies to

explore its phenotype and underlying mechanisms are vital (212). Here, we focus on the immunological aspects of the natural ablation of asthma inflammation, accentuating the role of allergen immunotolerance and regulatory immune cells.

In healthy individuals, an overt immune response is not provoked during exposure to innocuous environmental antigens, if not combined with tissue damage or danger signals. Mechanistically, the clonal anergy state of T cells can be induced by isolated TCR stimulation in the absence of co-stimulatory signals. When the antigen (allergen) dose is extremely low, lymphocytes cannot be effectively activated, resulting in the unresponsiveness of the immune system (low-zone tolerance); in contrast, if the antigen over occupied TCRs, it may lead to the apoptosis of effector T cells or the induction of Treg cells that suppress immune responses, thereby also presenting an unresponsive state (high-zone tolerance). This provides a theoretical basis for the later proposed "hygiene hypothesis" and "diet-microbiome hypothesis" (224). The former suggests that in the urbanized regions of highly industrialized countries, owing to improvements in sanitation and public health and decreased exposure to infectious sources during early life, the adaptive immune system of children may not be fully exercised and developed, increasing the risk of asthma, allergic diseases, and autoimmune conditions. In contrast, rural lifestyles and large families, combined with unhygienic contact with older siblings, livestock, and soil, confer some level of protection and tolerance against allergens (225). The latter offers another explanation, i.e., a decrease in dietary fiber intake and an increase in fat intake and changes in eating habits and dietary structures will modify the composition of gut microbiota, leading to a loss of symbiotic functions of non-pathogenic bacteria and an overall reduction in microbiome diversity, as well as an increase in allergic reactions (226).

Prior exposure to some environmental factors and microbial contents, including farm dust, butyrate, LPS, and N-glycolylneuraminic acid, can suppress the responses of the airway epithelium to allergens because they induce the expression of TNF-α induced protein-3 (TNFAIP3, also called A20), a negative regulator of NF-κB activation (227). This effect inhibits the production of IL-33, GM-CSF, and the DC chemokine CCL20 by epithelial cells in response to allergen inhalation, and promotes the production of tolerance-inducing cytokines such as TGF-β; this induces tolerogenic or regulatory DCs (DCregs) that promote Treg development. In particular, the dampening of immunologic responsiveness and maintenance of allergen tolerance contribute to regulatory immune cells, notably Tregs and regulatory B cells (Bregs) (228) (Figure 5). Tregs exert a broad suppressive effect on several immune cells; this effect is achieved by secreting cytokines such as IL-10 and TGF-β and other inhibitory factors such as indoleamine 2,3-dioxygenase (IDO-1), as well as by providing co-inhibitory molecules such as cytotoxic T-lymphocyte-associated protein 4 (CTLA-4), programmed cell death protein 1 (PD-1, or CD279), and PD-L1 (229). Tregs directly suppress mast cells, eosinophils, basophils, ILC2s, and inflammatory DCs involved in programming effector T cell subsets (T_H1, T_H2, and T_H17 cells). Furthermore, In Treg-derived cytokines, primarily IL-10, IL-35, and TGF-β, induce Bregs and produce IgG4 and IgA antibodies via B cells. In addition, Bregs produce anti-inflammatory cytokines, thereby suppressing effector T-cell responses (230).

A key event in generating normal immune responses to allergens is redirecting allergen-specific effector T cells toward a regulatory phenotype; this phenomenon accounts for some degree of the clinical efficacy of allergen-specific immunotherapy (AIT) (231). In instances where an immunologically proven allergen-driven mechanism of asthma, AIT represents the sole etiologic remedy for allergic manifestations (232, 233). It involves repeatedly administering high doses of causative allergens, generally via subcutaneous injection (SCIT) or sublingual application (SLIT), to induce a permanent state of tolerance and long-term benefits after discontinuing the treatment (234). AIT can be safely used to treat adolescents and adults with mild-to-moderate and well-controlled allergic asthma, not only significantly controlling symptoms and decreasing acute attacks but also decreasing the need for ICS dosage. Furthermore, AIT can prevent the further development of rhinitis into asthmatic symptoms in children (235). However, caution should be exercised when using AIT to treat uncontrolled and severe asthma (236).

4 Challenges ahead and future directions

Despite being in close contact with harmful chemicals and pathogenic microorganisms in the external environment, the human lungs can maintain efficient gas exchange. This relies on the protective role of the immune system of the lung mucosa against various harmful factors. The dynamic regulation of lung structure and immune cells is an essential guarantee for maintaining lung immune homeostasis. The disruption of this immune homeostasis may result in asthma development. As a heterogeneous condition, asthma presents with chronic airway inflammation, with the involvement of various cells and cellular components and association with airway hyperresponsiveness. If bronchial asthma is not promptly diagnosed and treated, it can lead to irreversible airway narrowing and tissue remodeling with disease progression.

In the last few years, a significant paradigm shift has been observed in our perception of asthma pathobiology, largely because of an improved understanding of its heterogeneity and different endotypes. Initially, asthma was considered a unique T_H2 cell-mediated disease, a dogma largely developed from mouse asthma models that drove the development of several type 2-oriented monoclonal antibodies. As present, these biologics are successfully used in clinical settings, primarily to decrease the frequency of exacerbations in patients receiving conventional therapy. However, this immune process is absent in 50% of patients; this condition is termed "type 2-low asthma," whose existence and definition remain uncertain, encompassing various asthma subtypes such as neutrophilic, mixed granulocytic, or paucigranulocytic forms and is characterized by normal eosinophils and low type 2 inflammation marker expression.

Various aspects of innate or adaptive immunity responses to allergens, environmental triggers, or viruses are involved in developing allergen sensitization, asthma symptoms, exacerbations,

and treatment responses. Extensive crosstalk exists between airway epithelial and immune cells during disease initiation and persistence, indicating that epithelial barrier restoration in asthma requires greater attention. With an increase in the complexity and severity of disease manifestations, the complexity of the accompanying immunopathology also increases, with the possible involvement of additional adaptive immunity elements and structural changes in the airways. While there has been significant advancement in the understanding of some of the current immunological advances in asthma, additional studies are warranted to ascribe the mechanisms underlying asthma inception and identify additional biomarkers that facilitate targeted interventions, by prioritizing the development of tools for the rapid, accurate, and low-cost diagnosis of the endotypes and sub-endotypes of asthma.

Clinicians have begun to realize that the one-size-fits-all "stepwise approach to therapy" cannot entirely meet the optimal diagnostic and therapeutic needs of all patients, particularly those with severe or refractory asthma. The concept of "treatable traits (TTs)" has been proposed as a way to address the diverse pathophysiological factors involved in severe asthma and overcome the limitations of existing treatment strategies (237). This notion of personalized medicine, which advocates multidisciplinary teamwork and is based on multidimensional assessment, represents a shift toward precision medicine. By offering greater flexibility and comprehensiveness in treatment, this concept can significantly improve health-related quality of life and asthma control while decreasing acute exacerbations (238, 239).

Immunological advances have always resonated with the progress of clinical asthma research, mutually complementing each other. However, new curative or even preventive treatments that can control symptoms in patients with asthma are warranted in the future, to alleviate the significant burden it places on society. For example, motivated by the marked success of an adoptive cellular immunotherapy based on the chimeric antigen receptor (CAR) for treating various malignant tumor types, a research group developed a cytokine-anchored CAR-T (CCAR-T) cell system using chimeric IL-5/CD28/CD3ζ receptors and revealed the targeted killing effect of IL-5-anchored CCAR-T cells on eosinophils *in vivo* and *in vitro*, as well as their protective effect on allergic airway inflammation, significantly surpassing the quintessential therapeutic window of current mAb-based treatments in clinical settings (240). This research group innovatively employed the CCAR-T cell system to treat severe eosinophilic asthma, which may be a milestone achievement in future research on various intractable allergic diseases.

A unified and innovative approach is required to address the challenges posed by asthma. Contemporary cutting-edge methods, including but not restricted to single-cell sequencing, phenomics, genetic lineage tracing, tissue imaging systems, and organoid technology, which can achieve obtain highly multiplexed information with subcellular spatial resolution, and their in-depth computational analysis may help better define asthma in the forthcoming years. It is imperative to underscore that the key to the successful development of personalized and phenotype-specific asthma treatments lies in continuously collaborating with clinical experts and immunologists and integrating bench and bedside approaches.

Author contributions

CX: Conceptualization, Visualization, Writing – original draft. JY: Writing – original draft. AG: Writing – original draft. YFL: Writing – original draft. RZ: Writing – original draft. MY: Writing – original draft. XL: Writing – original draft. YHL: Writing – original draft. QL: Funding acquisition, Supervision, Writing – review & editing. HG: Conceptualization, Funding acquisition, Supervision, Writing – review & editing.

Funding

The author(s) declare that financial support was received for the research, authorship, and/or publication of this article. This work was supported by the National Natural Science Foundation of China (NSFC, no. 82104812 to HG and no. 82004318 to QL), the Young Elite Scientists Sponsorship Program by China Association for Science and Technology (to HG), and the Capital's Funds for Health Improvement and Research (CFH, no. 2024-2-4131 to HG). The opinions, results, and conclusions reported in this paper are those of the authors and are independent from the funding sources, and all of the funders had no involvement in the writing, analysis, or interpretation of results, or the decision to submit for publication.

Acknowledgments

The authors express the gratitude to Dr. Huahua Zhong (National Center for Neurological Disorders, Huashan Hospital Affiliated to Fudan University, Shanghai, China), Dr. Jinrong Lin (Institute of Sports Medicine, Fudan University, Shanghai, China; Present address: Botnar Research Centre, Nuffield Department of Orthopaedics, Rheumatology, and Musculoskeletal Sciences, University of Oxford, Oxford, UK) and Dr. Yong Wu (Department of Nephrology, Hunan Provincial Key Laboratory of Kidney Disease and Blood Purification, the 2nd Xiangya Hospital of Central South University, Changsha, China) for their honest-to-goodness assistance with language editing and figure artwork.

Conflict of interest

The authors declare that the research was conducted in the absence of any commercial or financial relationships that could be construed as a potential conflict of interest.

Publisher's note

References

1. Porsbjerg C, Melen E, Lehtimaki L, Shaw D. Asthma. *Lancet*. (2023) 401:858–73. doi: 10.1016/S0140-6736(22)02125-0

2. Huang K, Yang T, Xu J, Yang L, Zhao J, Zhang X, et al. Prevalence, risk factors, and management of asthma in China: A national cross-sectional study. *Lancet*. (2019) 394:407–18. doi: 10.1016/S0140-6736(19)31147-X

3. Meghji J, Mortimer K, Agusti A, Allwood BW, Asher I, Bateman ED, et al. Improving lung health in low-income and middle-income countries: from challenges to solutions. *Lancet*. (2021) 397:928–40. doi: 10.1016/S0140-6736(21)00458-X

4. Wenzel SE. Asthma phenotypes: the evolution from clinical to molecular approaches. *Nat Med*. (2012) 18:716–25. doi: 10.1038/nm.2678

5. Walker C, Bode E, Boer L, Hansel TT, Blaser K, Virchow JC Jr. Allergic and nonallergic asthmatics have distinct patterns of T-cell activation and cytokine production in peripheral blood and bronchoalveolar lavage. *Am Rev Respir Dis*. (1992) 146:109–15. doi: 10.1164/ajrccm/146.1.109

6. Green RH, Brightling CE, Woltmann G, Parker D, Wardlaw AJ, Pavord ID. Analysis of induced sputum in adults with asthma: identification of subgroup with isolated sputum neutrophilia and poor response to inhaled corticosteroids. *Thorax*. (2002) 57:875–9. doi: 10.1136/thorax.57.10.875

7. Venkatesan P. 2023 Gina report for asthma. *Lancet Respir Med*. (2023) 11:589. doi: 10.1016/S2213-2600(23)00230-8

8. Wills-Karp M, Luyimbazi J, Xu X, Schofield B, Neben TY, Karp CL, et al. Interleukin-13: central mediator of allergic asthma. *Science*. (1998) 282:2258–61. doi: 10.1126/science.282.5397.2258

9. Grunig G, Warnock M, Wakil AE, Venkayya R, Brombacher F, Rennick DM, et al. Requirement for il-13 independently of il-4 in experimental asthma. *Science*. (1998) 282:2261–3. doi: 10.1126/science.282.5397.2261

10. Lambrecht BN, Hammad H, Fahy JV. The cytokines of asthma. *Immunity*. (2019) 50:975–91. doi: 10.1016/j.immuni.2019.03.018

11. Hammad H, Lambrecht BN. The basic immunology of asthma. *Cell*. (2021) 184:1469–85. doi: 10.1016/j.cell.2021.02.016

12. Fahy JV. Type 2 inflammation in asthma–present in most, absent in many. *Nat Rev Immunol*. (2015) 15:57–65. doi: 10.1038/nri3786

13. Sze E, Bhalla A, Nair P. Mechanisms and therapeutic strategies for non-T2 asthma. *Allergy*. (2020) 75:311–25. doi: 10.1111/all.13985

14. Luo W, Hu J, Xu W, Dong J. Distinct spatial and temporal roles for th1, th2, and th17 cells in asthma. *Front Immunol*. (2022) 13:974066. doi: 10.3389/fimmu.2022.974066

15. Barnes PJ. Cellular and molecular mechanisms of asthma and copd. *Clin Sci (Lond)*. (2017) 131:1541–58. doi: 10.1042/CS20160487

16. Mosmann TR, Cherwinski H, Bond MW, Giedlin MA, Coffman RL. Two types of murine helper T cell clone. I. Definition according to profiles of lymphokine activities and secreted proteins. *J Immunol*. (1986) 136:2348–57. doi: 10.4049/jimmunol.136.7.2348

17. Harker JA, Lloyd CM. T helper 2 cells in asthma. *J Exp Med*. (2023) 220: e20221094. doi: 10.1084/jem.20221094

18. Finkelman FD, Hogan SP, Hershey GK, Rothenberg ME, Wills-Karp M. Importance of cytokines in murine allergic airway disease and human asthma. *J Immunol*. (2010) 184:1663–74. doi: 10.4049/jimmunol.0902185

19. Szabo SJ, Sullivan BM, Peng SL, Glimcher LH. Molecular mechanisms regulating th1 immune responses. *Annu Rev Immunol*. (2003) 21:713–58. doi: 10.1146/annurev.immunol.21.120601.140942

20. Gavett SH, O'Hearn DJ, Li X, Huang SK, Finkelman FD, Wills-Karp M. Interleukin 12 inhibits antigen-induced airway hyperresponsiveness, inflammation, and th2 cytokine expression in mice. *J Exp Med*. (1995) 182:1527–36. doi: 10.1084/jem.182.5.1527

21. Cohn L, Homer RJ, Niu N, Bottomly K. T helper 1 cells and interferon gamma regulate allergic airway inflammation and mucus production. *J Exp Med*. (1999) 190:1309–18. doi: 10.1084/jem.190.9.1309

22. Wisniewski JA, Muehling LM, Eccles JD, Capaldo BJ, Agrawal R, Shirley DA, et al. T(H)1 signatures are present in the lower airways of children with severe asthma, regardless of allergic status. *J Allergy Clin Immunol*. (2018) 141:2048–60.e13. doi: 10.1016/j.jaci.2017.08.020

23. Britt RD Jr., Thompson MA, Sasse S, Pabelick CM, Gerber AN, Prakash YS. Th1 cytokines tnf-alpha and ifn-gamma promote corticosteroid resistance in developing human airway smooth muscle. *Am J Physiol Lung Cell Mol Physiol*. (2019) 316:L71–81. doi: 10.1152/ajplung.00547.2017

24. Newcomb DC, Peebles RS Jr. Th17-mediated inflammation in asthma. *Curr Opin Immunol*. (2013) 25:755–60. doi: 10.1016/j.coi.2013.08.002

25. Bullone M, Carriero V, Bertolini F, Folino A, Mannelli A, Di Stefano A, et al. Elevated serum ige, oral corticosteroid dependence and il-17/22 expression in highly neutrophilic asthma. *Eur Respir J*. (2019) 54:1900068. doi: 10.1183/13993003.00068-2019

26. Krishnamoorthy N, Douda DN, Bruggemann TR, Ricklefs I, Duvall MG, Abdulnour RE, et al. Neutrophil cytoplasts induce T(H)17 differentiation and skew inflammation toward neutrophilia in severe asthma. *Sci Immunol*. (2018) 3:eaao4747. doi: 10.1126/sciimmunol.aao4747

27. Schnyder-Candrian S, Togbe D, Couillin I, Mercier I, Brombacher F, Quesniaux V, et al. Interleukin-17 is a negative regulator of established allergic asthma. *J Exp Med*. (2006) 203:2715–25. doi: 10.1084/jem.20061401

28. Wakashin H, Hirose K, Maezawa Y, Kagami S, Suto A, Watanabe N, et al. Il-23 and th17 cells enhance th2-cell-mediated eosinophilic airway inflammation in mice. *Am J Respir Crit Care Med*. (2008) 178:1023–32. doi: 10.1164/rccm.200801-086OC

29. Bellini A, Marini MA, Bianchetti L, Barczyk M, Schmidt M, Mattoli S. Interleukin (Il)-4, il-13, and il-17a differentially affect the profibrotic and proinflammatory functions of fibrocytes from asthmatic patients. *Mucosal Immunol*. (2012) 5:140–9. doi: 10.1038/mi.2011.60

30. Zhao J, Lloyd CM, Noble A. Th17 responses in chronic allergic airway inflammation abrogate regulatory T-cell-mediated tolerance and contribute to airway remodeling. *Mucosal Immunol*. (2013) 6:335–46. doi: 10.1038/mi.2012.76

31. Kudo M, Melton AC, Chen C, Engler MB, Huang KE, Ren X, et al. Il-17a produced by alphabeta T cells drives airway hyper-responsiveness in mice and enhances mouse and human airway smooth muscle contraction. *Nat Med*. (2012) 18:547–54. doi: 10.1038/nm.2684

32. Lin W, Truong N, Grossman WJ, Haribhai D, Williams CB, Wang J, et al. Allergic dysregulation and hyperimmunoglobulinemia E in foxp3 mutant mice. *J Allergy Clin Immunol*. (2005) 116:1106–15. doi: 10.1016/j.jaci.2005.08.046

33. Tang Q, Bluestone JA. The foxp3+ Regulatory T cell: A jack of all trades, master of regulation. *Nat Immunol*. (2008) 9:239–44. doi: 10.1038/ni1572

34. Hartl D, Koller B, Mehlhorn AT, Reinhardt D, Nicolai T, Schendel DJ, et al. Quantitative and functional impairment of pulmonary cd4+Cd25hi regulatory T cells in pediatric asthma. *J Allergy Clin Immunol*. (2007) 119:1258–66. doi: 10.1016/j.jaci.2007.02.023

35. Birmingham JM, Chesnova B, Wisnivesky JP, Calatroni A, Federman J, Bunyavanich S, et al. The effect of age on T-regulatory cell number and function in patients with asthma. *Allergy Asthma Immunol Res*. (2021) 13:646–54. doi: 10.4168/aair.2021.13.4.646

36. Veldhoen M, Uyttenhove C, van Snick J, Helmby H, Westendorf A, Buer J, et al. Transforming growth factor-beta 'Reprograms' the differentiation of T helper 2 cells and promotes an interleukin 9-producing subset. *Nat Immunol*. (2008) 9:1341–6. doi: 10.1038/ni.1659

37. Kaplan MH. The transcription factor network in th9 cells. *Semin Immunopathol*. (2017) 39:11–20. doi: 10.1007/s00281-016-0600-2

38. Angkasekwinai P, Chang SH, Thapa M, Watarai H, Dong C. Regulation of il-9 expression by il-25 signaling. *Nat Immunol*. (2010) 11:250–6. doi: 10.1038/ni.1846

39. Koch S, Sopel N, Finotto S. Th9 and other il-9-producing cells in allergic asthma. *Semin Immunopathol*. (2017) 39:55–68. doi: 10.1007/s00281-016-0601-1

40. Pajulas A, Fu Y, Cheung CCL, Chu M, Cannon A, Alakhras N, et al. Interleukin-9 promotes mast cell progenitor proliferation and ccr2-dependent mast cell migration in allergic airway inflammation. *Mucosal Immunol*. (2023) 16:432–45. doi: 10.1016/j.mucimm.2023.05.002

41. Sehra S, Yao W, Nguyen ET, Glosson-Byers NL, Akhtar N, Zhou B, et al. Th9 cells are required for tissue mast cell accumulation during allergic inflammation. *J Allergy Clin Immunol*. (2015) 136:433–40.e1. doi: 10.1016/j.jaci.2015.01.021

42. Lloyd CM, Harker JA. Epigenetic control of interleukin-9 in asthma. *N Engl J Med*. (2018) 379:87–9. doi: 10.1056/NEJMcibr1803610

43. Schwartz DM, Farley TK, Richoz N, Yao C, Shih HY, Petermann F, et al. Retinoic acid receptor alpha represses a th9 transcriptional and epigenomic program to reduce allergic pathology. *Immunity*. (2019) 50:106–20.e10. doi: 10.1016/j.immuni.2018.12.014

44. Parker JM, Oh CK, LaForce C, Miller SD, Pearlman DS, Le C, et al. Safety profile and clinical activity of multiple subcutaneous doses of medi-528, a humanized anti-interleukin-9 monoclonal antibody, in two randomized phase 2a studies in subjects with asthma. *BMC Pulm Med*. (2011) 11:14. doi: 10.1186/1471-2466-11-14

45. Oh CK, Leigh R, McLaurin KK, Kim K, Hultquist M, Molfino NA. A randomized, controlled trial to evaluate the effect of an anti-interleukin-9 monoclonal antibody in adults with uncontrolled asthma. *Respir Res*. (2013) 14:93. doi: 10.1186/1465-9921-14-93

46. Britt RD Jr., Ruwanpathirana A, Ford ML, Lewis BW. Macrophages orchestrate airway inflammation, remodeling, and resolution in asthma. *Int J Mol Sci*. (2023) 24:10451. doi: 10.3390/ijms241310451

47. Murray PJ, Allen JE, Biswas SK, Fisher EA, Gilroy DW, Goerdt S, et al. Macrophage activation and polarization: nomenclature and experimental guidelines. *Immunity*. (2014) 41:14–20. doi: 10.1016/j.immuni.2014.06.008

48. Girodet PO, Nguyen D, Mancini JD, Hundal M, Zhou X, Israel E, et al. Alternative macrophage activation is increased in asthma. *Am J Respir Cell Mol Biol*. (2016) 55:467–75. doi: 10.1165/rcmb.2015-0295OC

49. Saradna A, Do DC, Kumar S, Fu QL, Gao P. Macrophage polarization and allergic asthma. *Transl Res*. (2018) 191:1–14. doi: 10.1016/j.trsl.2017.09.002

50. Liu X, Fang L, Guo TB, Mei H, Zhang JZ. Drug targets in the cytokine universe for autoimmune disease. *Trends Immunol*. (2013) 34:120–8. doi: 10.1016/j.it.2012.10.003

51. Hewitt RJ, Lloyd CM. Regulation of immune responses by the airway epithelial cell landscape. *Nat Rev Immunol*. (2021) 21:347–62. doi: 10.1038/s41577-020-00477-9

52. Akdis CA. Does the epithelial barrier hypothesis explain the increase in allergy, autoimmunity and other chronic conditions? *Nat Rev Immunol*. (2021) 21:739–51. doi: 10.1038/s41577-021-00538-7

53. Hellings PW, Steelant B. Epithelial barriers in allergy and asthma. *J Allergy Clin Immunol*. (2020) 145:1499–509. doi: 10.1016/j.jaci.2020.04.010

54. Komlosi ZI, van de Veen W, Kovacs N, Szucs G, Sokolowska M, O'Mahony L, et al. Cellular and molecular mechanisms of allergic asthma. *Mol Aspects Med*. (2022) 85:100995. doi: 10.1016/j.mam.2021.100995

55. Xiao C, Puddicombe SM, Field S, Haywood J, Broughton-Head V, Puxeddu I, et al. Defective epithelial barrier function in asthma. *J Allergy Clin Immunol*. (2011) 128:549–56.e1-12. doi: 10.1016/j.jaci.2011.05.038

56. de Boer WI, Sharma HS, Baelemans SM, Hoogsteden HC, Lambrecht BN, Braunstahl GJ. Altered expression of epithelial junctional proteins in atopic asthma: possible role in inflammation. *Can J Physiol Pharmacol*. (2008) 86:105–12. doi: 10.1139/y08-004

57. Raby KL, Michaeloudes C, Tonkin J, Chung KF, Bhavsar PK. Mechanisms of airway epithelial injury and abnormal repair in asthma and copd. *Front Immunol*. (2023) 14:1201658. doi: 10.3389/fimmu.2023.1201658

58. Celebi Sozener Z, Cevhertas L, Nadeau K, Akdis M, Akdis CA. Environmental factors in epithelial barrier dysfunction. *J Allergy Clin Immunol*. (2020) 145:1517–28. doi: 10.1016/j.jaci.2020.04.024

59. Tan HT, Hagner S, Ruchti F, Radzikowska U, Tan G, Altunbulakli C, et al. Tight junction, mucin, and inflammasome-related molecules are differentially expressed in eosinophilic, mixed, and neutrophilic experimental asthma in mice. *Allergy*. (2019) 74:294–307. doi: 10.1111/all.13619

60. Heijink IH, Kuchibhotla VNS, Roffel MP, Maes T, Knight DA, Sayers I, et al. Epithelial cell dysfunction, a major driver of asthma development. *Allergy*. (2020) 75:1902–17. doi: 10.1111/all.14421

61. Uehara A, Fujimoto Y, Fukase K, Takada H. Various human epithelial cells express functional toll-like receptors, nod1 and nod2 to produce anti-microbial peptides, but not proinflammatory cytokines. *Mol Immunol*. (2007) 44:3100–11. doi: 10.1016/j.molimm.2007.02.007

62. Frey A, Lunding LP, Ehlers JC, Weckmann M, Zissler UM, Wegmann M. More than just a barrier: the immune functions of the airway epithelium in asthma pathogenesis. *Front Immunol*. (2020) 11:761. doi: 10.3389/fimmu.2020.00761

63. Hammad H, Lambrecht BN. Barrier epithelial cells and the control of type 2 immunity. *Immunity*. (2015) 43:29–40. doi: 10.1016/j.immuni.2015.07.007

64. Hammad H, Lambrecht BN. Dendritic cells and epithelial cells: linking innate and adaptive immunity in asthma. *Nat Rev Immunol*. (2008) 8:193–204. doi: 10.1038/nri2275

65. Gauvreau GM, Bergeron C, Boulet LP, Cockcroft DW, Cote A, Davis BE, et al. Sounding the alarmins-the role of alarmin cytokines in asthma. *Allergy*. (2023) 78:402–17. doi: 10.1111/all.15609

66. Halim TYF, Rana BMJ, Walker JA, Kerscher B, Knolle MD, Jolin HE, et al. Tissue-restricted adaptive type 2 immunity is orchestrated by expression of the costimulatory molecule ox40l on group 2 innate lymphoid cells. *Immunity*. (2018) 48:1195–207.e6. doi: 10.1016/j.immuni.2018.05.003

67. Chu DK, Llop-Guevara A, Walker TD, Flader K, Goncharova S, Boudreau JE, et al. Il-33, but not thymic stromal lymphopoietin or il-25, is central to mite and peanut allergic sensitization. *J Allergy Clin Immunol*. (2013) 131:187–200.e1-8. doi: 10.1016/j.jaci.2012.08.002

68. Gregory LG, Jones CP, Walker SA, Sawant D, Gowers KH, Campbell GA, et al. Il-25 drives remodelling in allergic airways disease induced by house dust mite. *Thorax*. (2013) 68:82–90. doi: 10.1136/thoraxjnl-2012-202003

69. Iijima K, Kobayashi T, Hara K, Kephart GM, Ziegler SF, McKenzie AN, et al. Il-33 and thymic stromal lymphopoietin mediate immune pathology in response to chronic airborne allergen exposure. *J Immunol*. (2014) 193:1549–59. doi: 10.4049/jimmunol.1302984

70. Van Dyken SJ, Nussbaum JC, Lee J, Molofsky AB, Liang HE, Pollack JL, et al. A tissue checkpoint regulates type 2 immunity. *Nat Immunol*. (2016) 17:1381–7. doi: 10.1038/ni.3582

71. Wang W, Li Y, Lv Z, Chen Y, Li Y, Huang K, et al. Bronchial allergen challenge of patients with atopic asthma triggers an alarmin (Il-33, tslp, and il-25) response in the airways epithelium and submucosa. *J Immunol*. (2018) 201:2221–31. doi: 10.4049/jimmunol.1800709

72. Demenais F, Margaritte-Jeannin P, Barnes KC, Cookson WOC, Altmuller J, Ang W, et al. Multiancestry association study identifies new asthma risk loci that colocalize with immune-cell enhancer marks. *Nat Genet*. (2018) 50:42–53. doi: 10.1038/s41588-017-0014-7

73. Corren J, Menzies-Gow A, Chupp G, Israel E, Korn S, Cook B, et al. Efficacy of tezepelumab in severe, uncontrolled asthma: pooled analysis of the pathway and navigator clinical trials. *Am J Respir Crit Care Med*. (2023) 208:13–24. doi: 10.1164/rccm.202210-2005OC

74. Wechsler ME, Ruddy MK, Pavord ID, Israel E, Rabe KF, Ford LB, et al. Efficacy and safety of itepekimab in patients with moderate-to-severe asthma. *N Engl J Med*. (2021) 385:1656–68. doi: 10.1056/NEJMoa2024257

75. Holgate ST. Innate and adaptive immune responses in asthma. *Nat Med*. (2012) 18:673–83. doi: 10.1038/nm.2731

76. Edner NM, Carlesso G, Rush JS, Walker LSK. Targeting co-stimulatory molecules in autoimmune disease. *Nat Rev Drug Discovery*. (2020) 19:860–83. doi: 10.1038/s41573-020-0081-9

77. Deckers J, Sichien D, Plantinga M, Van Moorleghem J, Vanheerswynghels M, Hoste E, et al. Epicutaneous sensitization to house dust mite allergen requires interferon regulatory factor 4-dependent dermal dendritic cells. *J Allergy Clin Immunol*. (2017) 140:1364–77.e2. doi: 10.1016/j.jaci.2016.12.970

78. Willart MA, Deswarte K, Pouliot P, Braun H, Beyaert R, Lambrecht BN, et al. Interleukin-1alpha controls allergic sensitization to inhaled house dust mite via the epithelial release of gm-csf and il-33. *J Exp Med*. (2012) 209:1505–17. doi: 10.1084/jem.20112691

79. Rank MA, Kobayashi T, Kozaki H, Bartemes KR, Squillace DL, Kita H. Il-33-activated dendritic cells induce an atypical th2-type response. *J Allergy Clin Immunol*. (2009) 123:1047–54. doi: 10.1016/j.jaci.2009.02.026

80. Melum GR, Farkas L, Scheel C, Van Dieren B, Gran E, Liu YJ, et al. A thymic stromal lymphopoietin-responsive dendritic cell subset mediates allergic responses in the upper airway mucosa. *J Allergy Clin Immunol*. (2014) 134:613–21.e7. doi: 10.1016/j.jaci.2014.05.010

81. Moon HG, Kim SJ, Lee MK, Kang H, Choi HS, Harijith A, et al. Colony-stimulating factor 1 and its receptor are new potential therapeutic targets for allergic asthma. *Allergy*. (2020) 75:357–69. doi: 10.1111/all.14011

82. Conejero L, Khouili SC, Martinez-Cano S, Izquierdo HM, Brandi P, Sancho D. Lung cd103+ Dendritic cells restrain allergic airway inflammation through il-12 production. *JCI Insight*. (2017) 2:e90420. doi: 10.1172/jci.insight.90420

83. Kool M, van Nimwegen M, Willart MA, Muskens F, Boon L, Smit JJ, et al. An anti-inflammatory role for plasmacytoid dendritic cells in allergic airway inflammation. *J Immunol*. (2009) 183:1074–82. doi: 10.4049/jimmunol.0900471

84. Halim TY, Steer CA, Matha L, Gold MJ, Martinez-Gonzalez I, McNagny KM, et al. Group 2 innate lymphoid cells are critical for the initiation of adaptive T helper 2 cell-mediated allergic lung inflammation. *Immunity*. (2014) 40:425–35. doi: 10.1016/j.immuni.2014.01.011

85. Webb LM, Lundie RJ, Borger JG, Brown SL, Connor LM, Cartwright AN, et al. Type I interferon is required for T helper (Th) 2 induction by dendritic cells. *EMBO J*. (2017) 36:2404–18. doi: 10.15252/embj.201695345

86. Beaty SR, Rose CE Jr., Sung SS. Diverse and potent chemokine production by lung cd11bhigh dendritic cells in homeostasis and in allergic lung inflammation. *J Immunol*. (2007) 178:1882–95. doi: 10.4049/jimmunol.178.3.1882

87. El-Gammal A, Oliveria JP, Howie K, Watson R, Mitchell P, Chen R, et al. Allergen-induced changes in bone marrow and airway dendritic cells in subjects with asthma. *Am J Respir Crit Care Med*. (2016) 194:169–77. doi: 10.1164/rccm.201508-1623OC

88. Dutertre CA, Becht E, Irac SE, Khalilnezhad A, Narang V, Khalilnezhad S, et al. Single-cell analysis of human mononuclear phagocytes reveals subset-defining markers and identifies circulating inflammatory dendritic cells. *Immunity*. (2019) 51:573–89.e8. doi: 10.1016/j.immuni.2019.08.008

89. Naessens T, Morias Y, Hamrud E, Gehrmann U, Budida R, Mattsson J, et al. Human lung conventional dendritic cells orchestrate lymphoid neogenesis during chronic obstructive pulmonary disease. *Am J Respir Crit Care Med*. (2020) 202:535–48. doi: 10.1164/rccm.201906-1123OC

90. Vroman H, Tindemans I, Lukkes M, van Nimwegen M, de Boer GM, Tramper-Stranders GA, et al. Type ii conventional dendritic cells of asthmatic patients with frequent exacerbations have an altered phenotype and frequency. *Eur Respir J*. (2020) 55:1900859. doi: 10.1183/13993003.00859-2019

91. Robinson DS, Hamid Q, Ying S, Tsicopoulos A, Barkans J, Bentley AM, et al. Predominant th2-like bronchoalveolar T-lymphocyte population in atopic asthma. *N Engl J Med*. (1992) 326:298–304. doi: 10.1056/NEJM199201303260504

92. Zheng W, Flavell RA. The transcription factor gata-3 is necessary and sufficient for th2 cytokine gene expression in cd4 T cells. *Cell*. (1997) 89:587–96. doi: 10.1016/s0092-8674(00)80240-8

93. Szabo SJ, Kim ST, Costa GL, Zhang X, Fathman CG, Glimcher LH. A novel transcription factor, T-bet, directs th1 lineage commitment. *Cell*. (2000) 100:655–69. doi: 10.1016/s0092-8674(00)80702-3

94. Ivanov II, McKenzie BS, Zhou L, Tadokoro CE, Lepelley A, Lafaille JJ, et al. The orphan nuclear receptor rorgammat directs the differentiation program of proinflammatory il-17+ T helper cells. *Cell*. (2006) 126:1121–33. doi: 10.1016/j.cell.2006.07.035

95. Vivier E, Artis D, Colonna M, Diefenbach A, Di Santo JP, Eberl G, et al. Innate lymphoid cells: 10 years on. *Cell*. (2018) 174:1054–66. doi: 10.1016/j.cell.2018.07.017

96. Korchagina AA, Shein SA, Koroleva E, Tumanov AV. Transcriptional control of ilc identity. *Front Immunol*. (2023) 14:1146077. doi: 10.3389/fimmu.2023.1146077

97. ASamoah K, Chung KF, Zounemat Kermani N, Bodinier B, Dahlen SE, Djukanovic R, et al. Proteomic signatures of eosinophilic and neutrophilic asthma

from serum and sputum. *EBioMedicine*. (2023) 99:104936. doi: 10.1016/j.ebiom.2023.104936

98. Woodrow JS, Sheats MK, Cooper B, Bayless R. Asthma: the use of animal models and their translational utility. *Cells*. (2023) 12:1091. doi: 10.3390/cells12071091

99. Corry DB, Folkesson HG, Warnock ML, Erle DJ, Matthay MA, Wiener-Kronish JP, et al. Interleukin 4, but not interleukin 5 or eosinophils, is required in a murine model of acute airway hyperreactivity. *J Exp Med*. (1996) 183:109–17. doi: 10.1084/jem.183.1.109

100. Pelaia C, Paoletti G, Puggioni F, Racca F, Pelaia G, Canonica GW, et al. Interleukin-5 in the pathophysiology of severe asthma. *Front Physiol*. (2019) 10:1514. doi: 10.3389/fphys.2019.01514

101. Ying S, Robinson DS, Meng Q, Rottman J, Kennedy R, Ringler DJ, et al. Enhanced expression of eotaxin and ccr3 mrna and protein in atopic asthma. Association with airway hyperresponsiveness and predominant co-localization of eotaxin mrna to bronchial epithelial and endothelial cells. *Eur J Immunol*. (1997) 27:3507–16. doi: 10.1002/eji.1830271252

102. Nagata M, Sedgwick JB, Vrtis R, Busse WW. Endothelial cells upregulate eosinophil superoxide generation via vcam-1 expression. *Clin Exp Allergy*. (1999) 29:550–61. doi: 10.1046/j.1365-2222.1999.00506.x

103. Kuperman D, Schofield B, Wills-Karp M, Grusby MJ. Signal transducer and activator of transcription factor 6 (Stat6)-deficient mice are protected from antigen-induced airway hyperresponsiveness and mucus production. *J Exp Med*. (1998) 187:939–48. doi: 10.1084/jem.187.6.939

104. Zhu Z, Homer RJ, Wang Z, Chen Q, Geba GP, Wang J, et al. Pulmonary expression of interleukin-13 causes inflammation, mucus hypersecretion, subepithelial fibrosis, physiologic abnormalities, and eotaxin production. *J Clin Invest*. (1999) 103:779–88. doi: 10.1172/JCI5909

105. Dell'Aringa M, Reinhardt RL. Notch signaling represents an important checkpoint between follicular T-helper and canonical T-helper 2 cell fate. *Mucosal Immunol*. (2018) 11:1079–91. doi: 10.1038/s41385-018-0012-9

106. Chibana K, Trudeau JB, Mustovich AT, Hu H, Zhao J, Balzar S, et al. Il-13 induced increases in nitrite levels are primarily driven by increases in inducible nitric oxide synthase as compared with effects on arginases in human primary bronchial epithelial cells. *Clin Exp Allergy*. (2008) 38:936–46. doi: 10.1111/j.1365-2222.2008.02969.x

107. Kearley J, Erjefalt JS, Andersson C, Benjamin E, Jones CP, Robichaud A, et al. Il-9 governs allergen-induced mast cell numbers in the lung and chronic remodeling of the airways. *Am J Respir Crit Care Med*. (2011) 183:865–75. doi: 10.1164/rccm.200909-1462OC

108. Thio CL, Chang YJ. The modulation of pulmonary group 2 innate lymphoid cell function in asthma: from inflammatory mediators to environmental and metabolic factors. *Exp Mol Med*. (2023) 55:1872–84. doi: 10.1038/s12276-023-01021-0

109. Winkler C, Hochdorfer T, Israelsson E, Hasselberg A, Cavallin A, Thorn K, et al. Activation of group 2 innate lymphoid cells after allergen challenge in asthmatic patients. *J Allergy Clin Immunol*. (2019) 144:61–9.e7. doi: 10.1016/j.jaci.2019.01.027

110. Klein Wolterink RG, Kleinjan A, van Nimwegen M, Bergen I, de Bruijn M, Levani Y, et al. Pulmonary innate lymphoid cells are major producers of il-5 and il-13 in murine models of allergic asthma. *Eur J Immunol*. (2012) 42:1106–16. doi: 10.1002/eji.201142018

111. Oliphant CJ, Hwang YY, Walker JA, Salimi M, Wong SH, Brewer JM, et al. Mhcii-mediated dialog between group 2 innate lymphoid cells and cd4(+) T cells potentiates type 2 immunity and promotes parasitic helminth expulsion. *Immunity*. (2014) 41:283–95. doi: 10.1016/j.immuni.2014.06.016

112. Drake LY, Iijima K, Kita H. Group 2 innate lymphoid cells and cd4+ T cells cooperate to mediate type 2 immune response in mice. *Allergy*. (2014) 69:1300–7. doi: 10.1111/all.12446

113. Halim TY, Hwang YY, Scanlon ST, Zaghouani H, Garbi N, Fallon PG, et al. Group 2 innate lymphoid cells license dendritic cells to potentiate memory th2 cell responses. *Nat Immunol*. (2016) 17:57–64. doi: 10.1038/ni.3294

114. Galli SJ, Tsai M, Piliponsky AM. The development of allergic inflammation. *Nature*. (2008) 454:445–54. doi: 10.1038/nature07204

115. Fajt ML, Wenzel SE. Mast cells, their subtypes, and relation to asthma phenotypes. *Ann Am Thorac Soc*. (2013) 10 Suppl:S158–64. doi: 10.1513/AnnalsATS.201303-064AW

116. Balzar S, Fajt ML, Comhair SA, Erzurum SC, Bleecker E, Busse WW, et al. Mast cell phenotype, location, and activation in severe asthma. Data from the severe asthma research program. *Am J Respir Crit Care Med*. (2011) 183:299–309. doi: 10.1164/rccm.201002-0295OC

117. Elieh Ali Komi D, Bjermer L. Mast cell-mediated orchestration of the immune responses in human allergic asthma: current insights. *Clin Rev Allergy Immunol*. (2019) 56:234–47. doi: 10.1007/s12016-018-8720-1

118. Fajt ML, Gelhaus SL, Freeman B, Uvalle CE, Trudeau JB, Holguin F, et al. Prostaglandin D(2) pathway upregulation: relation to asthma severity, control, and th2 inflammation. *J Allergy Clin Immunol*. (2013) 131:1504–12. doi: 10.1016/j.jaci.2013.01.035

119. Woo SD, Luu QQ, Park HS. Nsaid-exacerbated respiratory disease (Nerd): from pathogenesis to improved care. *Front Pharmacol*. (2020) 11:1147. doi: 10.3389/fphar.2020.01147

120. Carr TF, Kraft M. Use of biomarkers to identify phenotypes and endotypes of severeasthma. *Ann Allergy Asthma Immunol*. (2018) 121:414–20. doi: 10.1016/j.anai.2018.07.029

121. Fitzpatrick AM, Chipps BE, Holguin F, Woodruff PG. T2-"Low" Asthma: overview and management strategies. *J Allergy Clin Immunol Pract*. (2020) 8:452–63. doi: 10.1016/j.jaip.2019.11.006

122. Annunziato F, Romagnani C, Romagnani S. The 3 major types of innate and adaptive cell-mediated effector immunity. *J Allergy Clin Immunol*. (2015) 135:626–35. doi: 10.1016/j.jaci.2014.11.001

123. Raundhal M, Morse C, Khare A, Oriss TB, Milosevic J, Trudeau J, et al. High ifn-gamma and low slpi mark severe asthma in mice and humans. *J Clin Invest*. (2015) 125:3037–50. doi: 10.1172/JCI80911

124. Wark PA, Johnston SL, Bucchieri F, Powell R, Puddicombe S, Laza-Stanca V, et al. Asthmatic bronchial epithelial cells have a deficient innate immune response to infection with rhinovirus. *J Exp Med*. (2005) 201:937–47. doi: 10.1084/jem.20041901

125. Edwards MR, Regamey N, Vareille M, Kieninger E, Gupta A, Shoemark A, et al. Impaired innate interferon induction in severe therapy resistant atopic asthmatic children. *Mucosal Immunol*. (2013) 6:797–806. doi: 10.1038/mi.2012.118

126. Oriss TB, Raundhal M, Morse C, Huff RE, Das S, Hannum R, et al. Irf5 distinguishes severe asthma in humans and drives th1 phenotype and airway hyperreactivity in mice. *JCI Insight*. (2017) 2:e91019. doi: 10.1172/jci.insight.91019

127. Bhakta NR, Christenson SA, Nerella S, Solberg OD, Nguyen CP, Choy DF, et al. Ifn-stimulated gene expression, type 2 inflammation, and endoplasmic reticulum stress in asthma. *Am J Respir Crit Care Med*. (2018) 197:313–24. doi: 10.1164/rccm.201706-1070OC

128. Veldhoen M. Interleukin 17 is a chief orchestrator of immunity. *Nat Immunol*. (2017) 18:612–21. doi: 10.1038/ni.3742

129. Lambrecht BN, Hammad H. The immunology of asthma. *Nat Immunol*. (2015) 16:45–56. doi: 10.1038/ni.3049

130. Al-Ramli W, Prefontaine D, Chouiali F, Martin JG, Olivenstein R, Lemiere C, et al. T(H)17-associated cytokines (Il-17a and il-17f) in severe asthma. *J Allergy Clin Immunol*. (2009) 123:1185–7. doi: 10.1016/j.jaci.2009.02.024

131. Chang Y, Al-Alwan L, Risse PA, Halayko AJ, Martin JG, Baglole CJ, et al. Th17-associated cytokines promote human airway smooth muscle cell proliferation. *FASEB J*. (2012) 26:5152–60. doi: 10.1096/fj.12-208033

132. Busse WW, Holgate S, Kerwin E, Chon Y, Feng J, Lin J, et al. Randomized, double-blind, placebo-controlled study of brodalumab, a human anti-il-17 receptor monoclonal antibody, in moderate to severe asthma. *Am J Respir Crit Care Med*. (2013) 188:1294–302. doi: 10.1164/rccm.201212-2318OC

133. Seys SF, Grabowski M, Adriaensen W, Decraene A, Dilissen E, Vanoirbeek JA, et al. Sputum cytokine mapping reveals an 'Il-5, il-17a, il-25-high' Pattern associated with poorly controlled asthma. *Clin Exp Allergy*. (2013) 43:1009–17. doi: 10.1111/cea.12125

134. Choy DF, Hart KM, Borthwick LA, Shikotra A, Nagarkar DR, Siddiqui S, et al. Th2 and th17 inflammatory pathways are reciprocally regulated in asthma. *Sci Transl Med*. (2015) 7:301ra129. doi: 10.1126/scitranslmed.aab3142

135. Wang YH, Voo KS, Liu B, Chen CY, Uygungil B, Spoede W, et al. A novel subset of cd4(+) T(H)2 memory/effector cells that produce inflammatory il-17 cytokine and promote the exacerbation of chronic allergic asthma. *J Exp Med*. (2010) 207:2479–91. doi: 10.1084/jem.20101376

136. Irvin C, Zafar I, Good J, Rollins D, Christianson C, Gorska MM, et al. Increased frequency of dual-positive th2/th17 cells in bronchoalveolar lavage fluid characterizes a population of patients with severe asthma. *J Allergy Clin Immunol*. (2014) 134:1175–86.e7. doi: 10.1016/j.jaci.2014.05.038

137. Sun W, Yuan Y, Qiu L, Zeng Q, Jia J, Xiang X, et al. Increased proportion of dual-positive th2-th17 cells promotes a more severe subtype of asthma. *Can Respir J*. (2021) 2021:9999122. doi: 10.1155/2021/9999122

138. Tortola L, Jacobs A, Pohlmeier L, Obermair FJ, Ampenberger F, Bodenmiller B, et al. High-dimensional T helper cell profiling reveals a broad diversity of stably committed effector states and uncovers interlineage relationships. *Immunity*. (2020) 53:597–613.e6. doi: 10.1016/j.immuni.2020.07.001

139. Han YY, Zhang X, Wang J, Wang G, Oliver BG, Zhang HP, et al. Multidimensional assessment of asthma identifies clinically relevant phenotype overlap: A cross-sectional study. *J Allergy Clin Immunol Pract*. (2021) 9:349–62.e18. doi: 10.1016/j.jaip.2020.07.048

140. Ricciardolo FLM, Guida G, Bertolini F, Di Stefano A, Carriero V. Phenotype overlap in the natural history of asthma. *Eur Respir Rev*. (2023) 32:220201. doi: 10.1183/16000617.0201-2022

141. Pite H, Aguiar L, Morello J, Monteiro EC, Alves AC, Bourbon M, et al. Metabolic dysfunction and asthma: current perspectives. *J Asthma Allergy*. (2020) 13:237–47. doi: 10.2147/JAA.S208823

142. Morjaria JB, Babu KS, Vijayanand P, Chauhan AJ, Davies DE, Holgate ST. Sputum il-6 concentrations in severe asthma and its relationship with fev1. *Thorax*. (2011) 66:537. doi: 10.1136/thx.2010.136523

143. Peters MC, McGrath KW, Hawkins GA, Hastie AT, Levy BD, Israel E, et al. Plasma interleukin-6 concentrations, metabolic dysfunction, and asthma severity: A cross-sectional analysis of two cohorts. *Lancet Respir Med*. (2016) 4:574–84. doi: 10.1016/S2213-2600(16)30048-0

144. Cottrell L, Neal WA, Ice C, Perez MK, Piedimonte G. Metabolic abnormalities in children with asthma. *Am J Respir Crit Care Med*. (2011) 183:441–8. doi: 10.1164/rccm.201004-0603OC

145. McGinley B, Punjabi NM. Obesity, metabolic abnormalities, and asthma: establishing causal links. *Am J Respir Crit Care Med*. (2011) 183:424–5. doi: 10.1164/rccm.201009-1525ED

146. Persson EK, Verstraete K, Heyndrickx I, Gevaert E, Aegerter H, Percier JM, et al. Protein crystallization promotes type 2 immunity and is reversible by antibody treatment. *Science*. (2019) 364:eaaw4295. doi: 10.1126/science.aaw4295

147. Mantel PY, Kuipers H, Boyman O, Rhyner C, Ouaked N, Ruckert B, et al. Gata3-driven th2 responses inhibit tgf-beta1-induced foxp3 expression and the formation of regulatory T cells. *PLoS Biol*. (2007) 5:e329. doi: 10.1371/journal.pbio.0050329

148. Noval Rivas M, Burton OT, Oettgen HC, Chatila T. Il-4 production by group 2 innate lymphoid cells promotes food allergy by blocking regulatory T-cell function. *J Allergy Clin Immunol*. (2016) 138:801–11.e9. doi: 10.1016/j.jaci.2016.02.030

149. Steelant B, Wawrzyniak P, Martens K, Jonckheere AC, Pugin B, Schrijvers R, et al. Blocking histone deacetylase activity as a novel target for epithelial barrier defects in patients with allergic rhinitis. *J Allergy Clin Immunol*. (2019) 144:1242–53.e7. doi: 10.1016/j.jaci.2019.04.027

150. Wegmann M. Trained immunity in allergic asthma. *J Allergy Clin Immunol*. (2023) 151:1471–3. doi: 10.1016/j.jaci.2023.02.023

151. Netea MG, Dominguez-Andres J, Barreiro LB, Chavakis T, Divangahi M, Fuchs E, et al. Defining trained immunity and its role in health and disease. *Nat Rev Immunol*. (2020) 20:375–88. doi: 10.1038/s41577-020-0285-6

152. Fanucchi S, Dominguez-Andres J, Joosten LAB, Netea MG, Mhlanga MM. The intersection of epigenetics and metabolism in trained immunity. *Immunity*. (2021) 54:32–43. doi: 10.1016/j.immuni.2020.10.011

153. Varricchi G, Brightling CE, Grainge C, Lambrecht BN, Chanez P. Airway remodelling in asthma and the epithelium: on the edge of a new era. *Eur Respir J*. (2024) 63:2301619. doi: 10.1183/13993003.01619-2023

154. Rout-Pitt N, Farrow N, Parsons D, Donnelley M. Epithelial mesenchymal transition (Emt): A universal process in lung diseases with implications for cystic fibrosis pathophysiology. *Respir Res*. (2018) 19:136. doi: 10.1186/s12931-018-0834-8

155. Hopp RJ, Wilson MC, Pasha MA. Small airway disease in pediatric asthma: the who, what, when, where, why, and how to remediate. A review and commentary. *Clin Rev Allergy Immunol*. (2022) 62:145–59. doi: 10.1007/s12016-020-08818-1

156. Sun Y, Shi Z, Liu B, Li X, Li G, Yang F, et al. Ykl-40 mediates airway remodeling in asthma via activating fak and mapk signaling pathway. *Cell Cycle*. (2020) 19:1378–90. doi: 10.1080/15384101.2020.1750811

157. Sun Z, Ji N, Ma Q, Zhu R, Chen Z, Wang Z, et al. Epithelial-mesenchymal transition in asthma airway remodeling is regulated by the il-33/cd146 axis. *Front Immunol*. (2020) 11:1598. doi: 10.3389/fimmu.2020.01598

158. Song Y, Wang Z, Jiang J, Piao Y, Li L, Xu C, et al. Dek-targeting aptamer dta-64 attenuates bronchial emt-mediated airway remodelling by suppressing tgf-beta1/smad, mapk and pi3k signalling pathway in asthma. *J Cell Mol Med*. (2020) 24:13739–50. doi: 10.1111/jcmm.15942

159. Yang N, Zhang H, Cai X, Shang Y. Epigallocatechin-3-gallate inhibits inflammation and epithelial–Mesenchymal transition through the pi3k/akt pathway via upregulation of pten in asthma. *Int J Mol Med*. (2018) 41:818–28. doi: 10.3892/ijmm.2017.3292

160. Pain M, Bermudez O, Lacoste P, Royer PJ, Botturi K, Tissot A, et al. Tissue remodelling in chronic bronchial diseases: from the epithelial to mesenchymal phenotype. *Eur Respir Rev*. (2014) 23:118–30. doi: 10.1183/09059180.00004413

161. Canas JA, Sastre B, Rodrigo-Munoz JM, Fernandez-Nieto M, Barranco P, Quirce S, et al. Eosinophil-derived exosomes contribute to asthma remodelling by activating structural lung cells. *Clin Exp Allergy*. (2018) 48:1173–85. doi: 10.1111/cea.13122

162. Kay AB, Phipps S, Robinson DS. A role for eosinophils in airway remodelling in asthma. *Trends Immunol*. (2004) 25:477–82. doi: 10.1016/j.it.2004.07.006

163. Lopez-Guisa JM, Powers C, File D, Cochrane E, Jimenez N, Debley JS. Airway epithelial cells from asthmatic children differentially express proremodeling factors. *J Allergy Clin Immunol*. (2012) 129:990–7.e6. doi: 10.1016/j.jaci.2011.11.035

164. Gosens R, Grainge C. Bronchoconstriction and airway biology: potential impact and therapeutic opportunities. *Chest*. (2015) 147:798–803. doi: 10.1378/chest.14-1142

165. Joubert P, Hamid Q. Role of airway smooth muscle in airway remodeling. *J Allergy Clin Immunol*. (2005) 116:713–6. doi: 10.1016/j.jaci.2005.05.042

166. Boucherat O, Boczkowski J, Jeannotte L, Delacourt C. Cellular and molecular mechanisms of goblet cell metaplasia in the respiratory airways. *Exp Lung Res*. (2013) 39:207–16. doi: 10.3109/01902148.2013.791733

167. Tan DJ, Walters EH, Perret JL, Lodge CJ, Lowe AJ, Matheson MC, et al. Age-of-asthma onset as a determinant of different asthma phenotypes in adults: A systematic review and meta-analysis of the literature. *Expert Rev Respir Med*. (2015) 9:109–23. doi: 10.1586/17476348.2015.1000311

168. Boulet LP. Airway remodeling in asthma: update on mechanisms and therapeutic approaches. *Curr Opin Pulm Med*. (2018) 24:56–62. doi: 10.1097/MCP.0000000000000441

169. Holgate ST, Holloway J, Wilson S, Bucchieri F, Puddicombe S, Davies DE. Epithelial-mesenchymal communication in the pathogenesis of chronic asthma. *Proc Am Thorac Soc*. (2004) 1:93–8. doi: 10.1513/pats.2306034

170. Baldo DC, Romaldini JG, Pizzichini MMM, Cancado JED, Dellavance A, Stirbulov R. Periostin as an important biomarker of inflammatory phenotype T2 in Brazilian asthma patients. *J Bras Pneumol*. (2023) 49:e20220040. doi: 10.36416/1806-3756/e20220040

171. Ge Q, Zeng Q, Tjin G, Lau E, Black JL, Oliver BG, et al. Differential deposition of fibronectin by asthmatic bronchial epithelial cells. *Am J Physiol Lung Cell Mol Physiol*. (2015) 309:L1093–102. doi: 10.1152/ajplung.00019.2015

172. Grainge CL, Lau LC, Ward JA, Dulay V, Lahiff G, Wilson S, et al. Effect of bronchoconstriction on airway remodeling in asthma. *N Engl J Med*. (2011) 364:2006–15. doi: 10.1056/NEJMoa1014350

173. Park JA, Drazen JM, Tschumperlin DJ. The chitinase-like protein ykl-40 is secreted by airway epithelial cells at base line and in response to compressive mechanical stress. *J Biol Chem*. (2010) 285:29817–25. doi: 10.1074/jbc.M110.103416

174. Grainge C, Dulay V, Ward J, Sammut D, Davies E, Green B, et al. Resistin-like molecule-beta is induced following bronchoconstriction of asthmatic airways. *Respirology*. (2012) 17:1094–100. doi: 10.1111/j.1440-1843.2012.02215.x

175. Chu EK, Cheng J, Foley JS, Mecham BH, Owen CA, Haley KJ, et al. Induction of the plasminogen activator system by mechanical stimulation of human bronchial epithelial cells. *Am J Respir Cell Mol Biol*. (2006) 35:628–38. doi: 10.1165/rcmb.2006-0040OC

176. Chaudhuri R, Rubin A, Sumino K, Lapa ESJR, Niven R, Siddiqui S, et al. Safety and effectiveness of bronchial thermoplasty after 10 years in patients with persistent asthma (Bt10+): A follow-up of three randomised controlled trials. *Lancet Respir Med*. (2021) 9:457–66. doi: 10.1016/S2213-2600(20)30408-2

177. Denner DR, Doeing DC, Hogarth DK, Dugan K, Naureckas ET, White SR. Airway inflammation after bronchial thermoplasty for severe asthma. *Ann Am Thorac Soc*. (2015) 12:1302–9. doi: 10.1513/AnnalsATS.201502-082OC

178. Wijsman PC, Goorsenberg AWM, Keijzer N, d'Hooghe JNS, Ten Hacken NHT, Shah PL, et al. Airway wall extracellular matrix changes induced by bronchial thermoplasty in severe asthma. *J Allergy Clin Immunol*. (2023) 153:435–46.e4. doi: 10.1016/j.jaci.2023.09.035

179. d'Hooghe JNS, Ten Hacken NHT, Weersink EJM, Sterk PJ, Annema JT, Bonta PI. Emerging understanding of the mechanism of action of bronchial thermoplasty in asthma. *Pharmacol Ther*. (2018) 181:101–7. doi: 10.1016/j.pharmthera.2017.07.015

180. Dai MY, Chen FF, Wang Y, Wang MZ, Lv YX. Liu RY. Particulate matters induce acute exacerbation of allergic airway inflammation via the tlr2/nf-kappab/nlrp3 signaling pathway. *Toxicol Lett*. (2020) 321:146–54. doi: 10.1016/j.toxlet.2019.12.013

181. Faffe DS, Whitehead T, Moore PE, Baraldo S, Flynt L, Bourgeois K, et al. Il-13 and il-4 promote tarc release in human airway smooth muscle cells: role of il-4 receptor genotype. *Am J Physiol Lung Cell Mol Physiol*. (2003) 285:L907–14. doi: 10.1152/ajplung.00120.2003

182. Kibe A, Inoue H, Fukuyama S, Machida K, Matsumoto K, Koto H, et al. Differential regulation by glucocorticoid of interleukin-13-induced eosinophilia, hyperresponsiveness, and goblet cell hyperplasia in mouse airways. *Am J Respir Crit Care Med*. (2003) 167:50–6. doi: 10.1164/rccm.2110084

183. Tliba O, Deshpande D, Chen H, Van Besien C, Kannan M, Panettieri RA Jr., et al. Il-13 enhances agonist-evoked calcium signals and contractile responses in airway smooth muscle. *Br J Pharmacol*. (2003) 140:1159–62. doi: 10.1038/sj.bjp.0705558

184. Amrani Y, Panettieri RA Jr. Modulation of calcium homeostasis as a mechanism for altering smooth muscle responsiveness in asthma. *Curr Opin Allergy Clin Immunol*. (2002) 2:39–45. doi: 10.1097/00130832-200202000-00007

185. Adams DC, Hariri LP, Miller AJ, Wang Y, Cho JL, Villiger M, et al. Birefringence microscopy platform for assessing airway smooth muscle structure and function *in vivo*. *Sci Transl Med*. (2016) 8:359ra131. doi: 10.1126/scitranslmed.aag1424

186. Alladina J, Smith NP, Kooistra T, Slowikowski K, Kernin IJ, Deguine J, et al. A human model of asthma exacerbation reveals transcriptional programs and cell circuits specific to allergic asthma. *Sci Immunol*. (2023) 8:eabq6352. doi: 10.1126/sciimmunol.abq6352

187. Rosas-Salazar C, Chirkova T, Gebretsadik T, Chappell JD, Peebles RS Jr., Dupont WD, et al. Respiratory Syncytial Virus Infection during Infancy and Asthma during Childhood in the USA (Inspire): A Population-Based, Prospective Birth Cohort Study. *Lancet*. (2023) 401:1669–80. doi: 10.1016/S0140-6736(23)00811-5

188. Jartti T, Gern JE. Role of viral infections in the development and exacerbation of asthma in children. *J Allergy Clin Immunol*. (2017) 140:895–906. doi: 10.1016/j.jaci.2017.08.003

189. Slater L, Bartlett NW, Haas JJ, Zhu J, Message SD, Walton RP, et al. Co-ordinated role of tlr3, rig-I and mda5 in the innate response to rhinovirus in bronchial epithelium. *PLoS Pathog*. (2010) 6:e1001178. doi: 10.1371/journal.ppat.1001178

190. Kim EY, Battaile JT, Patel AC, You Y, Agapov E, Grayson MH, et al. Persistent activation of an innate immune response translates respiratory viral infection into chronic lung disease. *Nat Med*. (2008) 14:633–40. doi: 10.1038/nm1770

191. Ortega H, Nickle D, Carter L. Rhinovirus and asthma: challenges and opportunities. *Rev Med Virol*. (2021) 31:e2193. doi: 10.1002/rmv.2193

192. Veerati PC, Troy NM, Reid AT, Li NF, Nichol KS, Kaur P, et al. Airway epithelial cell immunity is delayed during rhinovirus infection in asthma and copd. *Front Immunol*. (2020) 11:974. doi: 10.3389/fimmu.2020.00974

193. Zhu J, Message SD, Mallia P, Kebadze T, Contoli M, Ward CK, et al. Bronchial mucosal ifn-alpha/beta and pattern recognition receptor expression in patients with experimental rhinovirus-induced asthma exacerbations. *J Allergy Clin Immunol*. (2019) 143:114–25.e4. doi: 10.1016/j.jaci.2018.04.003

194. Holt PG, Mok D, Panda D, Renn L, Fabozzi G, deKlerk NH, et al. Developmental regulation of type 1 and type 3 interferon production and risk for infant infections and asthma development. *J Allergy Clin Immunol*. (2019) 143:1176–82.e5. doi: 10.1016/j.jaci.2018.08.035

195. Djukanovic R, Harrison T, Johnston SL, Gabbay F, Wark P, Thomson NC, et al. The effect of inhaled ifn-beta on worsening of asthma symptoms caused by viral infections. A randomized trial. *Am J Respir Crit Care Med*. (2014) 190:145–54. doi: 10.1164/rccm.201312-2235OC

196. Watson A, Spalluto CM, McCrae C, Cellura D, Burke H, Cunoosamy D, et al. Dynamics of ifn-beta responses during respiratory viral infection. Insights for therapeutic strategies. *Am J Respir Crit Care Med*. (2020) 201:83–94. doi: 10.1164/rccm.201901-0214OC

197. Basnet S, Palmenberg AC, Gern JE. Rhinoviruses and their receptors. *Chest*. (2019) 155:1018–25. doi: 10.1016/j.chest.2018.12.012

198. Bonnelykke K, Sleiman P, Nielsen K, Kreiner-Moller E, Mercader JM, Belgrave D, et al. A genome-wide association study identifies cdhr3 as a susceptibility locus for early childhood asthma with severe exacerbations. *Nat Genet*. (2014) 46:51–5. doi: 10.1038/ng.2830

199. Denlinger LC, Phillips BR, Ramratnam S, Ross K, Bhakta NR, Cardet JC, et al. Inflammatory and comorbid features of patients with severe asthma and frequent exacerbations. *Am J Respir Crit Care Med*. (2017) 195:302–13. doi: 10.1164/rccm.201602-0419OC

200. McErlean P, Favoreto S Jr., Costa FF, Shen J, Quraishi J, Biyasheva A, et al. Human rhinovirus infection causes different DNA methylation changes in nasal epithelial cells from healthy and asthmatic subjects. *BMC Med Genomics*. (2014) 7:37. doi: 10.1186/1755-8794-7-37

201. Lund RJ, Osmala M, Malonzo M, Lukkarinen M, Leino A, Salmi J, et al. Atopic asthma after rhinovirus-induced wheezing is associated with DNA methylation change in the smad3 gene promoter. *Allergy*. (2018) 73:1735–40. doi: 10.1111/all.13473

202. McCauley K, Durack J, Valladares R, Fadrosh DW, Lin DL, Calatroni A, et al. Distinct nasal airway bacterial microbiotas differentially relate to exacerbation in pediatric patients with asthma. *J Allergy Clin Immunol*. (2019) 144:1187–97. doi: 10.1016/j.jaci.2019.05.035

203. McCauley KE, Flynn K, Calatroni A, DiMassa V, LaMere B, Fadrosh DW, et al. Seasonal airway microbiome and transcriptome interactions promote childhood asthma exacerbations. *J Allergy Clin Immunol*. (2022) 150:204–13. doi: 10.1016/j.jaci.2022.01.020

204. Cazzola M, Matera MG, Rossi F. Bronchial hyperresponsiveness and bacterial respiratory infections. *Clin Ther*. (1991) 13:157–71.

205. Kim CK, Callaway Z, Gern JE. Viral infections and associated factors that promote acute exacerbations of asthma. *Allergy Asthma Immunol Res*. (2018) 10:12–7. doi: 10.4168/aair.2018.10.1.12

206. Nagayama Y, Tsubaki T, Nakayama S, Sawada K, Taguchi K, Toba T, et al. Bacterial colonization in respiratory secretions from acute and recurrent wheezing infants and children. *Pediatr Allergy Immunol*. (2007) 18:110–7. doi: 10.1111/j.1399-3038.2006.00492.x

207. Gibson PG, Yang IA, Upham JW, Reynolds PN, Hodge S, James AL, et al. Effect of azithromycin on asthma exacerbations and quality of life in adults with persistent uncontrolled asthma (Amazes): A randomised, double-blind, placebo-controlled trial. *Lancet*. (2017) 390:659–68. doi: 10.1016/S0140-6736(17)31281-3

208. Brusselle GG, Vanderstichele C, Jordens P, Deman R, Slabbynck H, Ringoet V, et al. Azithromycin for prevention of exacerbations in severe asthma (Azisast): A multicentre randomised double-blind placebo-controlled trial. *Thorax*. (2013) 68:322–9. doi: 10.1136/thoraxjnl-2012-202698

209. Taylor SL, Leong LEX, Mobegi FM, Choo JM, Wesselingh S, Yang IA, et al. Long-term azithromycin reduces haemophilus influenzae and increases antibiotic resistance in severe asthma. *Am J Respir Crit Care Med*. (2019) 200:309–17. doi: 10.1164/rccm.201809-1739OC

210. Undela K, Goldsmith L, Kew KM, Ferrara G. Macrolides versus placebo for chronic asthma. *Cochrane Database Syst Rev*. (2021) 11:CD002997. doi: 10.1002/14651858.CD002997.pub5

211. Agarwal R, Sehgal IS, Dhooria S, Muthu V, Prasad KT, Bal A, et al. Allergic bronchopulmonary aspergillosis. *Indian J Med Res*. (2020) 151:529–49. doi: 10.4103/ijmr.IJMR_1187_19

212. Carpaij OA, Burgess JK, Kerstjens HAM, Nawijn MC, van den Berge M. A review on the pathophysiology of asthma remission. *Pharmacol Ther*. (2019) 201:8–24. doi: 10.1016/j.pharmthera.2019.05.002

213. Broekema M, Volbeda F, Timens W, Dijkstra A, Lee NA, Lee JJ, et al. Airway eosinophilia in remission and progression of asthma: accumulation with a fast decline of fev(1). *Respir Med*. (2010) 104:1254–62. doi: 10.1016/j.rmed.2010.03.030

214. Broekema M, Timens W, Vonk JM, Volbeda F, Lodewijk ME, Hylkema MN, et al. Persisting remodeling and less airway wall eosinophil activation in complete remission of asthma. *Am J Respir Crit Care Med*. (2011) 183:310–6. doi: 10.1164/rccm.201003-0494OC

215. Mak JC, Ho SP, Ho AS, Law BK, Cheung AH, Ho JC, et al. Sustained elevation of systemic oxidative stress and inflammation in exacerbation and remission of asthma. *ISRN Allergy*. (2013) 2013:561831. doi: 10.1155/2013/561831

216. Boulet LP, Turcotte H, Brochu A. Persistence of airway obstruction and hyperresponsiveness in subjects with asthma remission. *Chest*. (1994) 105:1024–31. doi: 10.1378/chest.105.4.1024

217. van den Toorn LM, Overbeek SE, de Jongste JC, Leman K, Hoogsteden HC, Prins JB. Airway inflammation is present during clinical remission of atopic asthma. *Am J Respir Crit Care Med*. (2001) 164:2107–13. doi: 10.1164/ajrccm.164.11.2006165

218. Kim BS, Lee E, Lee MJ, Kang MJ, Yoon J, Cho HJ, et al. Different functional genes of upper airway microbiome associated with natural course of childhood asthma. *Allergy*. (2018) 73:644–52. doi: 10.1111/all.13331

219. Waserman S, Nair P, Snider D, Conway M, Jayaram L, McCleary LM, et al. Local and systemic immunological parameters associated with remission of asthma symptoms in children. *Allergy Asthma Clin Immunol*. (2012) 8:16. doi: 10.1186/1710-1492-8-16

220. van Den Toorn LM, Prins JB, Overbeek SE, Hoogsteden HC, de Jongste JC. Adolescents in clinical remission of atopic asthma have elevated exhaled nitric oxide levels and bronchial hyperresponsiveness. *Am J Respir Crit Care Med*. (2000) 162:953–7. doi: 10.1164/ajrccm.162.3.9909033

221. Warke TJ, Fitch PS, Brown V, Taylor R, Lyons JD, Ennis M, et al. Outgrown asthma does not mean no airways inflammation. *Eur Respir J*. (2002) 19:284–7. doi: 10.1183/09031936.02.00882002

222. Boulet LP, Turcott H, Plante S, Chakir J. Airway function, inflammation and regulatory T cell function in subjects in asthma remission. *Can Respir J*. (2012) 19:19–25. doi: 10.1155/2012/347989

223. Tomiita M, Campos-Alberto E, Shima M, Namiki M, Sugimoto K, Kojima H, et al. Interleukin-10 and interleukin-5 balance in patients with active asthma, those in remission, and healthy controls. *Asia Pac Allergy*. (2015) 5:210–5. doi: 10.5415/apallergy.2015.5.4.210

224. Wypych TP, Marsland BJ, Ubags NDJ. The impact of diet on immunity and respiratory diseases. *Ann Am Thorac Soc*. (2017) 14:S339–S47. doi: 10.1513/AnnalsATS.201703-255AW

225. Bach JF. Revisiting the hygiene hypothesis in the context of autoimmunity. *Front Immunol*. (2020) 11:615192. doi: 10.3389/fimmu.2020.615192

226. Haahtela T. A biodiversity hypothesis. *Allergy*. (2019) 74:1445–56. doi: 10.1111/all.13763

227. Schuijs MJ, Willart MA, Vergote K, Gras D, Deswarte K, Ege MJ, et al. Farm Dust and Endotoxin Protect against Allergy through A20 Induction in Lung Epithelial Cells. *Science*. (2015) 349:1106–10. doi: 10.1126/science.aac6623

228. Palomares O, Akdis M, Martin-Fontecha M, Akdis CA. Mechanisms of immune regulation in allergic diseases: the role of regulatory T and B cells. *Immunol Rev*. (2017) 278:219–36. doi: 10.1111/imr.12555

229. Martin-Orozco E, Norte-Munoz M, Martinez-Garcia J. Regulatory T cells in allergy and asthma. *Front Pediatr*. (2017) 5:117. doi: 10.3389/fped.2017.00117

230. Wang L, Fu Y, Chu Y. Regulatory B cells. *Adv Exp Med Biol*. (2020) 1254:87–103. doi: 10.1007/978-981-15-3532-1_8

231. Durham SR, Shamji MH. Allergen immunotherapy: past, present and future. *Nat Rev Immunol*. (2023) 23:317–28. doi: 10.1038/s41577-022-00786-1

232. Pfaar O, Lou H, Zhang Y, Klimek L, Zhang L. Recent developments and highlights in allergen immunotherapy. *Allergy*. (2018) 73:2274–89. doi: 10.1111/all.13652

233. Kappen JH, Agache I, Jutel M, Pillai P, Corrigan CJ. Allergen immunotherapy for asthma. *J Allergy Clin Immunol Pract*. (2024) 12:23–30. doi: 10.1016/j.jaip.2023.11.031

234. Durham SR, Penagos M. Sublingual or subcutaneous immunotherapy for allergic rhinitis? *J Allergy Clin Immunol*. (2016) 137:339–49.e10. doi: 10.1016/j.jaci.2015.12.1298

235. Farraia M, Paciencia I, Castro Mendes F, Cavaleiro Rufo J, Shamji M, Agache I, et al. Allergen immunotherapy for asthma prevention: A systematic review and meta-analysis of randomized and non-randomized controlled studies. *Allergy*. (2022) 77:1719–35. doi: 10.1111/all.15295

236. Caimmi D, Demoly P. A review of allergen immunotherapy in asthma. *Allergy Asthma Proc*. (2022) 43:310–3. doi: 10.2500/aap.2022.43.210113

237. Agusti A, Gibson PG, McDonald VM. Treatable traits in airway disease: from theory to practice. *J Allergy Clin Immunol Pract*. (2023) 11:713–23. doi: 10.1016/j.jaip.2023.01.011

238. McDonald VM, Clark VL, Cordova-Rivera L, Wark PAB, Baines KJ, Gibson PG. Targeting treatable traits in severe asthma: A randomised controlled trial. *Eur Respir J*. (2020) 55:1901509. doi: 10.1183/13993003.01509-2019

239. Janssen SMJ, van Helvoort HAC, Tjalma TA, Antons JC, Djamin RS, Simons SO, et al. Impact of treatable traits on asthma control and quality of life. *J Allergy Clin Immunol Pract*. (2023) 11:1823–33.e4. doi: 10.1016/j.jaip.2023.02.034

240. Chen S, Chen G, Xu F, Sun B, Chen X, Hu W, et al. Treatment of allergic eosinophilic asthma through engineered il-5-anchored chimeric antigen receptor T cells. *Cell Discovery*. (2022) 8:80. doi: 10.1038/s41421-022-00433-y

frontiers | Frontiers in Immunology

TYPE Original Research
PUBLISHED 18 October 2024
DOI 10.3389/fimmu.2024.1452788

OPEN ACCESS

EDITED BY
Jian Zheng,
University of Louisville, United States

REVIEWED BY
Ruangang Pan,
The University of Iowa, United States
Javier Mora,
University of Costa Rica, Costa Rica

*CORRESPONDENCE
Simon Rousseau
simon.rousseau@mcgill.ca

RECEIVED 21 June 2024
ACCEPTED 17 September 2024
PUBLISHED 18 October 2024

CITATION
Bédard-Matteau J, Soulé A, Liu KY, Fourcade L, Fraser DD, Emad A and Rousseau S (2024) Circulating IL-17F, but not IL-17A, is elevated in severe COVID-19 and leads to an ERK1/2 and p38 MAPK-dependent increase in ICAM-1 cell surface expression and neutrophil adhesion on endothelial cells. *Front. Immunol.* 15:1452788. doi: 10.3389/fimmu.2024.1452788

Circulating IL-17F, but not IL-17A, is elevated in severe COVID-19 and leads to an ERK1/2 and p38 MAPK-dependent increase in ICAM-1 cell surface expression and neutrophil adhesion on endothelial cells

Jérôme Bédard-Matteau[1,2,3], Antoine Soulé[4], Katelyn Yixiu Liu[1,2], Lyvia Fourcade[1,2], Douglas D. Fraser[5,6], Amin Emad[4,7] and Simon Rousseau[1,2,3]*

[1]The Meakins-Christie Laboratories, Research Institute of the McGill University Heath Centre, Montréal, QC, Canada, [2]Department of Medicine, Faculty of Medicine, McGill University, Montréal, QC, Canada, [3]Department of Pharmacology and Therapeutics, McGill University, Montréal, QC, Canada, [4]Department of Electrical and Computer Engineering, McGill University, Montréal, QC, Canada, [5]Children's Health Research Institute & Lawson Health Research Institute, London, ON, Canada, [6]Department of Pediatrics, Western University, London, ON, Canada, [7]Mila, Quebec AI Institute, Montréal, QC, Canada

Background: Severe COVID-19 is associated with neutrophilic inflammation and immunothrombosis. Several members of the IL-17 cytokine family have been associated with neutrophilic inflammation and activation of the endothelium. Therefore, we investigated whether these cytokines were associated with COVID-19.

Methods: We investigated the association between COVID-19 and circulating plasma levels of IL-17 cytokine family members in participants to the Biobanque québécoise de la COVID-19 (BQC19), a prospective observational cohort and an independent cohort from Western University (London, Ontario). We measured the in vitro impact of IL-17F on intercellular adhesion molecule 1 (ICAM-1) cell surface expression and neutrophil adhesion on endothelial cells in culture. The contribution of two Mitogen Activated Protein Kinase (MAPK) pathways was determined using small molecule inhibitors PD184352 (a MKK1/MKK2 inhibitor) and BIRB0796 (a p38 MAPK inhibitor).

Results: We found increased IL-17D and IL-17F plasma levels when comparing SARS-CoV-2-positive vs negative hospitalized participants. Moreover, increased plasma levels of IL-17D, IL-17E and IL-17F were noted when comparing severe versus mild COVID-19. IL-17F, but not IL-17A, was significantly elevated in people with COVID-19 compared to healthy controls and with more severe disease. In vitro work on endothelial cells treated with IL-17F for 24h showed an increase cell surface expression of ICAM-1 accompanied by neutrophil adhesion. The introduction of two MAPK inhibitors significantly reduced the binding of neutrophils while also reducing ICAM-1 expression at the surface level of endothelial cells, but not its intracellular expression.

Discussion: Overall, these results have identified an association between two cytokines of the IL-17 family (IL-17D and IL-17F) with COVID-19 and disease severity. Considering that IL-17F stimulation promotes neutrophil adhesion to the endothelium in a MAPK-dependent manner, it is attractive to speculate that this pathway may contribute to pathogenic immunothrombosis in concert with other molecular effectors.

KEYWORDS

cytokines, neutrophil binding, endothelial function, MAPK, ICAM-1, COVID-19

Introduction

COVID-19 is an infectious disease attributable to the SARS-CoV-2 virus. Worldwide, nearly 800 million people have been infected by the virus since 2020. The wide range of symptoms in COVID-19 cases makes the disease extremely heterogeneous as some individuals have asymptomatic to mild flu-like symptoms and others can be severely ill, necessitating hospitalization in intensive care units (1). In the most severe cases, some hallmarks of the disease are neutrophilia, immunothrombosis, endothelial dysfunction (2), and acute respiratory distress syndrome (ARDS) (3–12). These severe cases also show a dysfunctional activation of the immune system that ultimately leads to organ damage (3). Many cytokines are involved in the immune response associated with COVID-19. The notable increase in interleukin 6 (IL-6) and accompanying neutrophilia raises the possible involvement of the interleukin 17 (IL-17) cytokine family, known to be associated with neutrophilia and a potent activator of the endothelium (13). Accordingly, high saliva levels of IL-17A have been associated with COVID-19 severity (14).

On the whole, IL-17 is associated with host protection against infections, and when deregulated can lead to autoimmune and inflammatory diseases. The IL-17 cytokine family consists of six isoforms, IL-17 A through F, utilizing the five IL-17 receptors, IL-17RA to IL-17RE (15). IL-17A is the most studied isoform of the family. Although IL-17F and IL-17A are highly homologous and share many physiological functions, the biological role of IL-17F remains less understood. One distinction is that IL-17A is mainly produced by T helper cells (Th17), while IL-17F is, in addition to Th17 cells, produced by innate immune cells and epithelial cells (16). Both IL-17A and IL-17F bind the IL-17RA/RC heterodimer. It is reported that IL-17A activation of the receptor is 10 to 30 times more potent than IL-17F binding, which emphasizes the differences in affinity and the vital role that IL-17A plays in driving autoimmunity (17). The activation of the IL-17RA/RC heterodimer leads to the activation of the canonical nuclear factor (NF-κB) as well as the mitogen-activated protein kinase (MAPK) pathways (17). All these factors lead to the triggering of the activation of the transcription of IL-17 signature genes including cytokines and chemokines driving neutrophil recruitment (16, 17). The MAPK pathways include extracellular signal-regulated kinase (ERK), p38, and JUN N-terminal kinase (JNK) (18). A previous study showed how IL-17A promotes endothelial activation and neutrophil recruitment in a p38 MAPK-dependent matter (13).

Neutrophil adhesion is part of the five steps of the neutrophil recruitment cascade. It requires many adhesion molecules. Essentially, when endothelial cells are activated by proinflammatory cytokines, adhesion molecules such as selectins and intercellular adhesion molecule 1 (ICAM-1) have their expression increased within minutes (19). These molecules are essential for the initial steps of the recruitment cascade to capture circulating neutrophils. ICAM-1 molecules are present at the surface of endothelial cells and form a bond with a receptor at the surface of neutrophils and lymphocyte function-associated antigen 1 (LFA1). ICAM-1 binding to LFA1 is vital for firm neutrophil adhesion: the bound neutrophils are able to continue the recruitment cascade, ultimately leading to transmigration (19).

In this study, we have investigated the impact of IL-17F activation on endothelial cells and its impact on neutrophil recruitment and ICAM-1 expression at the surface level in the context of acute COVID-19.

Methods

Datasets

We obtained clinical data and information on circulating proteins from the Biobanque québécoise de la COVID-19 (BQC19; www.quebeccovidbiobank.ca) (20). Validation was carried out in data obtained from Western University (London, Ontario) as previously reported (21).

Cell culture

Primary human umbilical vein endothelial cells (HUVECs) were obtained from American Type Culture Collection (ATCC)

(PCS-100-013). These cells were derived from 10 individual donors, minimizing the variability associated with material derived from a single donor. The HUVECs were grown in 199 media (316-020-CL, Wisent Bio Product), supplemented with 20% FBS (080-450, Wisent Bio Product), 60 µg/ml endothelial cell growth supplement (Cedarlane, R&D system, CCM027), 2mM L-glutamine (609-065-EL, Wisent Bio Product), 50 µg/ml heparin (H4784-250MG, Sigma Aldrich), and a 1:100 dilution of penicillin-streptomycin 100X (450-201-EL, Wisent Bio Product). However, during treatments, the penicillin was removed from the growing media to avoid any interactions. The cells were cultured from passages 2-7 (13). HUVECs were plated on a gelatin-coated surface [100mm diameter Fisherbrand™ Petri Dishes (Catalog #FB085712), 6-well clear flat bottomed TC-treated plates (83,3920,005, SARSTEDT) and 24-well flat bottom with lid, TC-treated, and sterile (3526, Corning Incorporated) plates]. The sterile coating solution comprised gelatin powder 0.5% (G-1890-500G, Sigma Aldrich) in PBS (311-010-CL, Wisent Bio Product). A 2-hour minimum incubation was required for the coating at 37°C. The gelatin-coated plates could then be kept at 4°C for up to 4 weeks. The cell culture manipulations were done in a 1300 Series A2 biological safety cabinet (BSC) (ThermoFisher).

Endothelial cells stimulation

The recombinant human IL-17F was purchased from Cerdarlane/R&D (#1335-IL-025/CF). In total, 25 µg of IL-17F was reconstituted in 250 µL of HCl 4mM to give a 100 µg/ml stock solution. The working solution used in this study was 100 ng/ml of IL-17F. The negative control consisted of fully complemented 199 media, changed on the day of the experiment. PD184352 (PZ0181-5MG, Sigma Aldrich), a selective non-competitive inhibitor of MEK (MKK1: MAPK kinase), was used at a final concentration of 2µM in DMSO to prevent ERK1/2 activation. BIRB 796 (#5989, Bio-techne), an allosteric high-affinity p38 MAPK inhibitor, was used at a final concentration of 0.1 µM in DMSO to prevent p38a/b MAPK activation. HUVECs were pre-exposed for 1 h to the inhibitors, followed by a 24-h exposure to the 100 ng/ml IL-17F treatment.

Immunofluorescence

In the 24-well plates, 12 mm diameter round glass coverslips (Catalog# 170-C12MM, Ultident) were used. The reagents used for the cell fixation and permeabilization were PBS + paraformaldehyde (PFA) 4% (Catalog # J19943.K2, ThermoFisher), PBS + Bovine Serum Albumin 1% (BSA) (catalog #9048-46-8, Sigma Aldrich), and finally, PBS + triton 0.2% (Catalog #HFH10, ThermoFisher). Following permeabilization, a 30-min blocking step was performed using a solution of 3% BSA in PBS (catalog #A7906-50G, Sigma Aldrich). The fixed cells were then incubated for 1 h with the primary ICAM-1 antibody (catalog #MEM-111, ab2213, Abcam) at a concentration of 1:200 in the blocking solution, followed by extensive washing. They were then incubated for 30 min with DAPI (Catalog #62248, ThermoFisher) at a concentration of 1:1000 in PBS+BSA 3% to stain the DNA and visualize the nuclei. Phalloidin-TRITC (Catalog# 5783, Bio-Techne) was used to visualize the actin cytoskeleton at a concentration of 1:100 in PBS +BSA 3% and the secondary antibody that was used to stain for ICAM-1 was Alexa Fluor 488 goat anti-mouse (catalog # A11029, Invitrogen) at a 1:500 concentration. The coverslips were mounted using Fluoromount-G™ Mounting Medium (Catalog #00-4958-02, ThermoFisher). The slides were left to dry and conserved at 4°C for confocal imaging analysis.

Neutrophil binding assay

HUVECs were grown at 90% confluency on gelatin-coated coverslips in 24-well plates. IL-17F treatment was applied to the cell for 30 min. Human peripheral neutrophils were isolated from the blood of healthy donors following this protocol (22). Once the neutrophils were isolated, they were stained using calcein-AM 1 mM stock (catalog # C1430, Invitrogen) for 30 min in RPMI (Catalog # 350-000-CL, Wisent Bio Product) at 37°C. After washes, the neutrophils stained were added to the IL-17F-treated cells for 30 min. Fixation with PFA 4% and staining were as described for the immunofluorescence analysis.

Imaging analysis

The imaging was done using a Zeiss LMS700 confocal microscope and a Zeiss Axio Imager M2. A 20x objective was used to obtain the results. All of the analysis of the images was done using Fiji/ImageJ software for Microsoft Windows.

Flow cytometry

Acquisition of the flow cytometry samples was done using a BD FACSCanto II system. After 24 h of IL-17F treatment, cells were detached from the 6-well plates with trypsin (Catalog #325-045-EL, Wisent Bio Product). The cells were transferred into FACS tubes (catalog# 149595, Fisher Scientific) for flow staining. The viability marker was incubated for 20 min on ice (Catalog #423102, BioLegend). An Fc receptor-blocking solution was then applied for 10 min on ice (catalog #422302, Biolegend). Fixing/permeabilization of the samples was done using the BD Cytofix/CytoPerm and the BD Perm/Wash kits (catalog #554772/554723, BD). The primary antibody ICAM-1 1:1000 and secondary antibody Alexa Fluor 488 1:1000 were incubated for 30 min. The samples were fixed using 2% PFA and filtered before flow acquisition. The software FlowJo 10.2 was used to analyze the experiment.

Statistical analysis

The data were analyzed on the GraphPad software version 9.2. The Shapiro-Wilk normality test was done on all data to ensure normality and allowed us to use parametric tests such as one-way ANOVA followed by Tukey's multiple comparisons test.

Results

IL-17F, but not IL-17A, is elevated in severe COVID-19

As aforementioned, severe COVID-19 is associated with some hallmark conditions such as neutrophilia, immunothrombosis, and ARDS (3–12). Since the IL-17 cytokine family, and in particular, IL-17A and IL-17F, has been associated with neutrophilic inflammation (4, 8, 9, 23, 24), we investigated the abundance of IL-17 cytokines in the plasma of hospitalized participants of the BQC19, a prospective observational cohort (20), using data from a SomaScan 5K array, an aptamer-based multiplex technology (25). We first compared the plasma levels of the IL-17 cytokines between SARS-CoV-2-positive (n=758) and negative (n=291) participants. No differences were observed for IL-17E (IL-25), a cytokine associated with Th2 responses rather than Th17 (Table 1 and Figure 1A). We found decreased levels of IL-17A, IL-17B, and IL-17C and increased levels of IL-17D and IL-17F in the SARS-CoV-2 positive hospitalized participants compared with the negative hospitalized participants, with the most significant changes being for IL-17B and IL-17D (Table 1 and Figure 1A). We then investigated whether IL-17 cytokines were associated with disease severity using the WHO classification (1), comparing only SARS-CoV-2-positive hospitalized participants in the BQC19 cohort (mild: n= 262; severe: n= 673). No significant differences were observed for IL-17A, but we found decreased levels of IL-17B and IL-17C and increased levels of IL-17D, IL-17E, and IL-17F in patients with severe COVID-19 compared with patients with mild COVID-19, with the most significant changes being for IL-17D and IL-17F (Table 1 and Figure 1B). To confirm the findings obtained from participants in the BQC19, we validated the results in an independent cohort from Western University (London, Ontario) (21). Analysis of the circulating proteins in these samples was performed on a different platform, an Olink Explore 1196 panel (21). In accordance with the findings obtained in BQC19, IL-17F levels were significantly elevated in COVID-19-positive participants from the ward (p=0.05) or ICU (p=0.0022) compared to the healthy controls (Figure 1C). Moreover, the COVID-19-positive participants from the ICU had significantly greater levels than those from the ward (p=0.0035) (Figure 1C). In contrast, IL-17A levels were not significantly elevated in the COVID-19-positive participants from the ward or ICU compared to the healthy controls (Figure 1D). While IL-17A and IL-17F signal through the same receptor complex (IL-17RA/RC) and have been proposed to act redundantly (17), the results obtained from investigating these two cohorts show that IL-17F but not IL-17A was associated with SARS-CoV-2 infection in the hospitalized participants and that IL-17F but not IL-17A levels are associated with more severe disease. Due to the nature of the two proteomic analyses, we can only report the relative values of the cytokines, which is a limitation when assessing such a large number of proteins simultaneously.

IL-17F drives ERK1/2 and p38 MAPK-dependent neutrophil adhesion on HUVECs

We previously showed that an important target of IL-17A is the endothelium regulating neutrophil adhesion *in vivo* (13). Considering the results demonstrating that in severe COVID-19, IL-17F levels are increased, we investigated whether IL-17F alone

TABLE 1 IL-17 family target enrichment.

Cytokine	Analysis	Enriched or depleted	p-value	Corrected p value
IL-17 A	COVID+ vs COVID-	depleted	0.008126	0.012188832
IL-17 B	COVID+ vs COVID-	depleted	1.76E-18	1.05E-17
IL-17 C	COVID+ vs COVID-	depleted	0.018907	0.022688623
IL-17 D	COVID+ vs COVID-	enriched	3.88E-09	1.17E-08
IL-17 F	COVID+ vs COVID-	enriched	0.000387	0.00077347
IL-17 E	COVID+ vs COVID-	depleted	0.651637	0.651637108
IL-17 A	Mild vs Severe COVID	enriched	0.059217	0.059216624
IL-17 B	Mild vs Severe COVID	depleted	1.08E-15	2.16E-15
IL-17 C	Mild vs Severe COVID	depleted	6.18E-06	7.42E-06
IL-17 D	Mild vs Severe COVID	enriched	2.92E-32	1.75E-31
IL-17 F	Mild vs Severe COVID	enriched	4.80E-28	1.44E-27
IL-17 E	Mild vs Severe COVID	enriched	5.10E-10	7.65E-10

10.3389/fimmu.2024.1452788

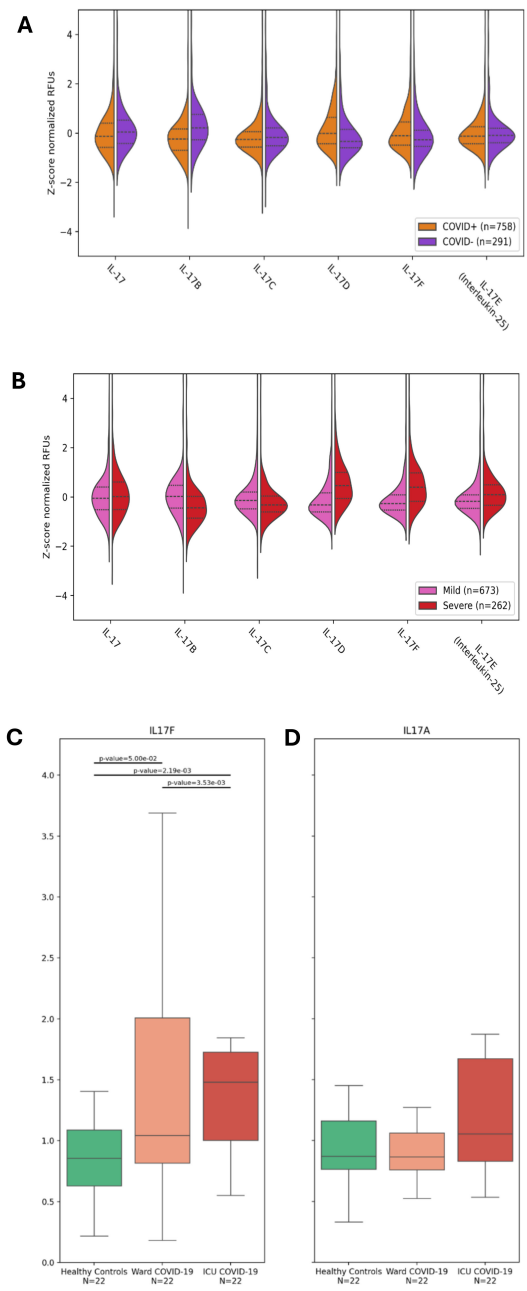

FIGURE 1
IL-17F is enriched in severe COVID-19 but not IL-17A. **(A, B)** Violin plots showing the enrichment or depletion of the IL-17 cytokine family. **(A)** Shows infected patients (n=758) vs uninfected patients (n=291). **(B)** Shows disease severity, comparing mild (n=673) and severe (n=262) conditions. The y-axis shows the z-score normalization of the relative fluorescence units (RFUs). These values were obtained from the plasma of BQC19 participants, seeking to measure circulating levels of the IL-17 family (on the x-axis). Data were analyzed using the two-tailed Wilcoxon rank-sum test. **(C, D)**. IL-17F **(C)** and IL-17A **(D)** levels were measured in the plasma of healthy controls (n=22) and COVID-19-participants from the ward (n=22) or the ICU (n=22) using an Olink Explore 1196 panel as described previously (21). The bar graphs represent the normalized values (NPX) for each of the two cytokines. Data were analyzed using the two-sided Mann-Whitney U test. The bars represent the compared groups, with the exact *p* values reported. The absence of bars means the comparison was not significant.

was sufficient to activate endothelial cells *in vitro* and mediate neutrophil adhesion. HUVECs, a well-established model, were exposed to IL-17F for 24 h and then incubated with freshly isolated calcein-labeled human neutrophils for 30 min before washing the unbound cells and enumerating the adhered neutrophils. The HUVECs were simultaneously stained for ICAM-1 to visualize its expression using immunofluorescence. We observed that ICAM-1 expression was low in the untreated HUVECs (Figure 2A). This was associated with very few neutrophils adhering to the surface of endothelial cells (4 ± 1.2) (Figures 2A, B). When treated with 100 ng/ml of IL-17F for 24 h, the expression of ICAM-1 was increased (Figure 2A) and >10 times more neutrophils were able to adhere (48 ± 4) (Figures 2A, B). We previously showed that p38 MAPK inhibition prevented ICAM-1 expression and neutrophil adhesion in response to IL-17A (13). Preincubating HUVECs with either BIRB0796 to block p38 MAPK activity or PD184352 to prevent ERK1/2 activation partially decreased the number of neutrophils adhering in response to IL17F (one-way ANOVA, F= 55, p<0001; followed by Tukey's multiple comparisons test: 21 ± 1.5 ***, p = 0.0003 and 19.5 ± 1.6 ****, p=0.0001). However, when combining the two MAPK pathway inhibitors, PD184352 and BIRB 796, the adhesion of neutrophils was reduced to levels comparable to untreated cells (3 ± 0.5 vs. 48 ± 4 ****, p= <0.0001) (Figure 2B). The results suggest that both p38 MAPK and ERK1/2 contribute to the adhesion of neutrophils to endothelial cells mediated by IL-17F.

Surprisingly, when examining ICAM-1 expression using immunofluorescence, the results revealed that the MAPK pathway inhibitors did not inhibit ICAM-1 protein expression (Figure 2A bottom panel). Closer examination revealed that while the intensity of the signals was not decreased, its localization may have been affected, with more pronounced perinuclear staining in the presence of BIRB0796 and PD184352. Indeed, as mentioned previously, ICAM-1 is one of the essential molecules for the interaction and the adhesion of neutrophils on the surface of endothelial cells. If ICAM-1 is still being expressed but not at the right place, the neutrophils may not be able to interact with the HUVECs, thereby reducing the number of adhered neutrophils as observed.

An ERK1/2 and p38 MAPK-dependent increase in ICAM-1 cell surface expression in IL-17F-treated HUVECs

We conducted flow cytometry analyses to compare the total expression of ICAM-1 with the surface-level expression. The goal was to determine whether the MAPK pathway inhibitors affected ICAM-1 protein expression at the surface of HUVECs following 24 h of IL-17F treatment. The cells were permeabilized to measure the total ICAM-1 expression or left unpermeabilized, allowing the ICAM-1 antibody to only bind to the ICAM-1 protein at the surface of the cells. The basal level of ICAM-1 expression was 13% ± 1.5% for both the permeabilized and not permeabilized conditions. In the not permeabilized group only (Figure 3A top panel) our one-

way ANOVA followed by Tukey's multiple comparisons test was able to show significance when comparing the IL-17F-only group with the group with both inhibitors (**p=0.0023). There was also significance between the basal level and the IL-17F group (p=0.04) and finally between the group with both inhibitors and the BIRB 796 group (p=0.04) The combination of both inhibitors showed a significant reduction in ICAM-1 expression at the surface level (Figure 3B) (23.0% ± 1.7% vs 10.0% ± 1.1%***, p = 0.0005). These findings are coherent with the neutrophil adhesion assay, where the presence of both the MAPK inhibitors restored a basal-level phenotype (i.e., no neutrophil adhesion and basal-level ICAM-1 surface expression). This suggests that to inhibit neutrophil adhesion to similar basal level, the inhibition of both the MAPK pathways (p38 MAPK and ERK1/2) is required. In agreement with our immunofluorescence findings, the presence of the MAPK pathway inhibitors did not significantly reduce the total expression of ICAM-1 in response to IL-17F (p= 0.2, ns) (Figure 3C). This suggests that the ICAM-1 protein is still being expressed but not, however, at the surface level for the interaction with the neutrophils, preventing their adhesion.

Discussion

Overall, our analysis of the plasma from participants to BQC19 revealed increased levels of IL-17F and IL-17D when comparing

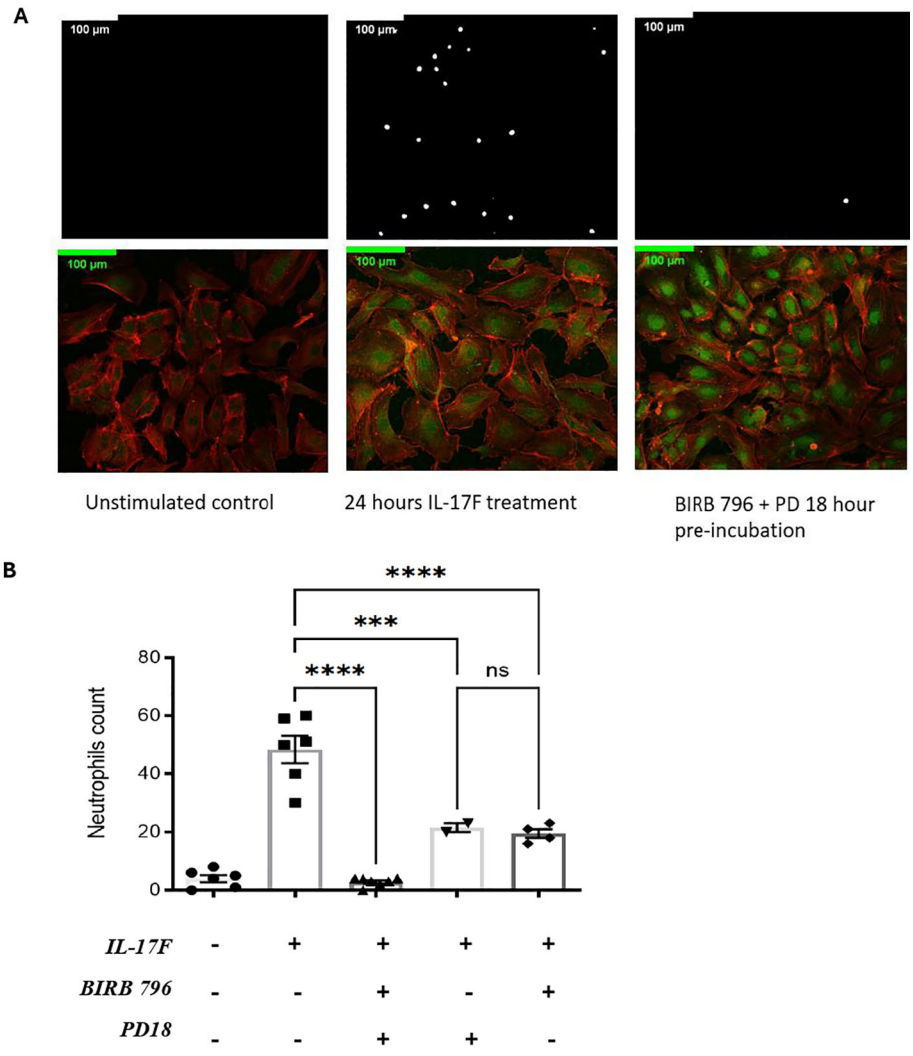

FIGURE 2
IL-17F drives ERK1/2 and p38 MAPK-dependent ICAM-1 cell surface expression and adhesion of neutrophils in HUVECs. **(A)** Neutrophils were incubated with calcein-AM for 24 h. After incubation, endothelial cells were treated with IL-17F for 24 h and BIRD 796 + PD18 for 1 h. The white point represents neutrophils binding to treated endothelial cells (top panels). Immunofluorescence of HUVECs under different conditions are shown (bottom panels). F-actin was stained with phalloidine 565 (red) and ICAM-1 with Alexa 488 indirect staining (green). Cells were visualized using a Zeiss LMS700 confocal microscope and a Zeiss Axio Imager M2. Fiji/Image J was used to analyze the images. Representative images are shown at ×20 magnification (n = 4). **(B)** Representative of the neutrophil counts under different conditions (n=2-). Data are presented as mean ± SEM and were compared with a one-way ANOVA followed by Tukey's multiple comparisons test with a pair-wise comparison between the positive control (Il-17F+/BIRB 796-/PD18-) and the three other groups. Significance levels are shown as ns (non-significant), ***(p<0.001), and **** (p<0.0001). HUVEC, human umbilical vein endothelial cell.

SARS-CoV-2-positive and SARS-CoV-2-negative hospitalized participants. Interestingly, IL-17A levels were decreased in this comparison, but it is important to note that the COVID-19-negative participants are not healthy controls, but participants who were hospitalized for suspected COVID-19 but were found to be negative for SARS-CoV-2. The underlying condition leading to their hospitalization may well have led to a significant increase in IL-17A that is greater than that elicited by SARS-CoV-2. Another notable finding was the cytokines associated with disease severity. The levels of IL-17F and IL-17D were found to be significantly elevated, while IL-17A showed no significant difference when comparing severe SARS-CoV-2 and mild SARS-CoV-2 hospitalized participants. Although Il-17A and IL-17F are known to signal through the same receptor IL-17RA/RC, the results obtained here from the analysis indicate that IL-17F and not IL-17A was significantly enriched in the plasma of patients with severe COVID-19. We confirmed this difference between IL-17F and IL-17A in an independent cohort from Western University (21), where similar observations were made (Figures 1C, D). Interestingly, not only is this cohort independent, but the study also used a different technology to assess the protein levels, further strengthening the conclusion that the observed changes reflect the cytokine levels and not the method of detection. This does not mean that IL-17A is absent in severe COVID-19 or that it does not play a role in the pathobiology of the disease. Previous studies showed an association of IL-17A salivary levels with COVID-19 severity (14), as well as an imbalance in the Th17/Treg axis (26), leading to the suggestion that an IL-17A blockade could constitute a viable therapeutic strategy (27, 28). However, the BISHOP study, which investigated the blockade of IL-17A with secukinumab in hospitalized COVID-19 patients, failed to show efficacy in treating COVID-19 (29). Our results show an association between IL-17F and COVID-19 severity in the large BQC19 cohort rather than IL-17A, which may provide an explanation for the lack of efficacy when targeting IL-17A alone. The results also suggest that either targeting IL-17F or abrogating the activity of both cytokines, targeting their common downstream receptor IL-17RC, could be another therapeutic avenue to attenuate the severe outcomes of COVID-19.

In the cell-based experiments, we focused initially on IL-17F given its close relationship with IL-17A in terms of downstream signaling. Following the activation of IL-17 receptors, the MAPK and NF-κB pathways are activated (30, 31), which regulates

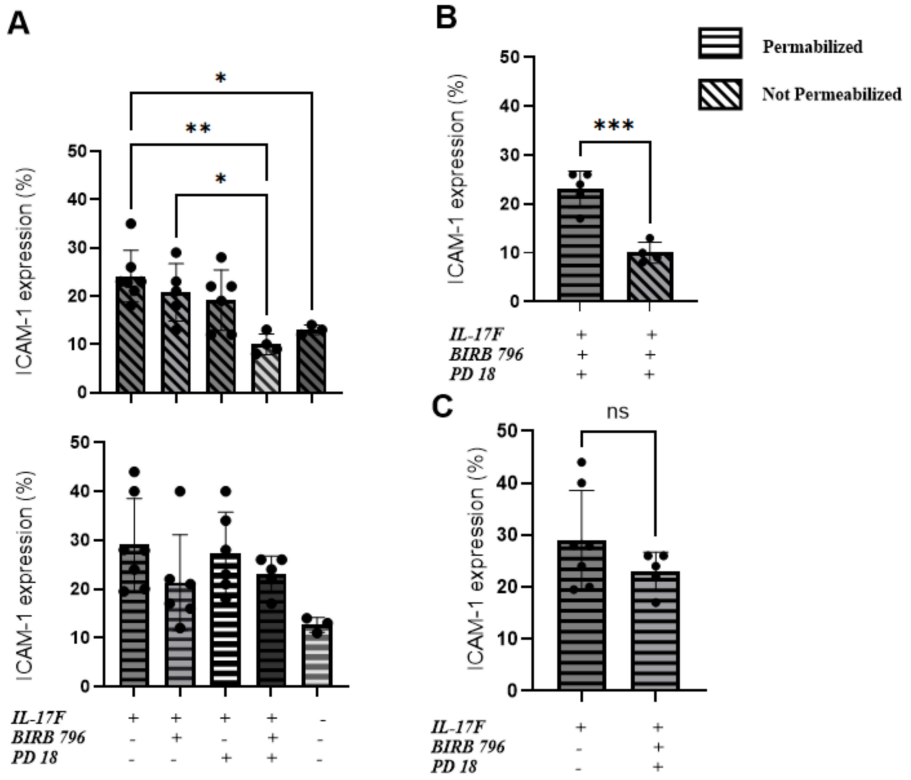

FIGURE 3
An ERK1/2 and p38 MAPK-dependent increase in ICAM-1 cell surface expression in IL-17F-treated HUVECs. Percentages of total ICAM-1 expression compared to cell surface expression (n=5). This represents the percentage of ICAM-1-positive cells based on our flow cytometry gating strategy accessible on page 9 of the raw data submission. Data are presented as mean ± SEM Statistical significance was shown using a one-way ANOVA followed by Tukey's multiple comparisons test. **(A)** The top panel is the not-permeabilized group in the experiment whereas the bottom panel is the permeabilized group in the experiment. **(B)** Comparison between the permeabilized and not permeabilized groups in the groups with the two inhibitors. **(C)** The IL-17F group vs the group with the two inhibitors, showing no statistically significant difference in ICAM-1=positive cells. The permeabilized group is represented by horizontal hatched lines and the not permeabilized group is represented by diagonal hatched lines. The x-axis shows the percentage of cells positive for ICAM-1 Significance levels are shown as ns (non-significant), *(p<0.05), **(p<0.01), and ***(p<0.001). HUVEC, human umbilical vein endothelial cell.

downstream effector function via the upregulation of proinflammatory molecules such as chemokines, cytokines, adhesion molecules, and matrix metalloproteinases (32). All these molecules play important roles in the proinflammatory state of endothelial cells and the recruitment of immune cells, such as neutrophils, to the site of infections (16). They can contribute to hallmark features of severe COVID-19 disease such as neutrophilia, immunothrombosis, endothelial dysfunction, and ARDS (2, 7–9, 11). In this study, we focused on ICAM-1, an important adhesion molecule expressed on endothelial cells that is essential for neutrophil adhesion. ICAM-1 is a 90 kDa glycoprotein located at the cell surface. It is a ligand for the integrins present at the surface level of neutrophils, i.e., LFA1. Its activity is vital for regulating leukocyte recruitment in circulation to the sites of inflammation (33). Its soluble form has been found to be elevated in COVID-19 and is associated with angiogenesis in post-COVID conditions (34). Our results demonstrate that IL-17F activates the endothelium, increasing ICAM-1 cell surface expression and, subsequently, neutrophil adhesion. The introduction of two inhibitors of the MAPK pathways, PD184352 (an MKK1/MKK2 inhibitor) and BIRB0796 (a p38 MAPK inhibitor), led to decreased neutrophil adhesion on the surface of HUVECs (Figure 4). This decreased neutrophil binding was seemingly due to a reduction in the expression of ICAM-1 molecules at the surface level. ICAM-1 expression is closely associated with the activation of NF-κB by cytokines such as TNFα, IL-6, IL-1β, and IL-17A (13, 33, 35). Upon joint inhibition of the p38 and ERK1/2 MAPK pathways, we observed neutrophil binding returning to the basal level but, intriguingly, ICAM-1 was still present but not expressed at the cell surface. This suggests that p38 and ERK1/2 MAPK are not required for IL-17F-driven ICAM-1 transcription in HUVECs, a role likely accomplished by NF-κB. They are, however, required for cell surface expression.

IL-17A and IL-17F are known to play a role in the development of inflammation and host defense following the activation of their IL-17RA/RC receptor, leading to the expression of proinflammatory molecules (36). However, IL-17D is a considerably less studied member of the IL-17 family. Still, we found it to be elevated in SARS-CoV-2-positive participants in the BQC19 cohort and it was also associated with disease severity to an even greater extent than IL-17F. Interestingly, our findings of elevated IL-17D in COVID-19 are in accordance with, and validate, the results reported in the Western University cohort (21). IL-17A and IL-17F have approximately 50% homology, while IL-17F and IL-17D are reported to have 25% homology (36). Unlike other IL-17 family members, IL-17D has an extended C-terminal domain capable of mediating its distinctive receptor interactions (36). Until a few years ago, the IL-17D receptor was still unknown. It was recently

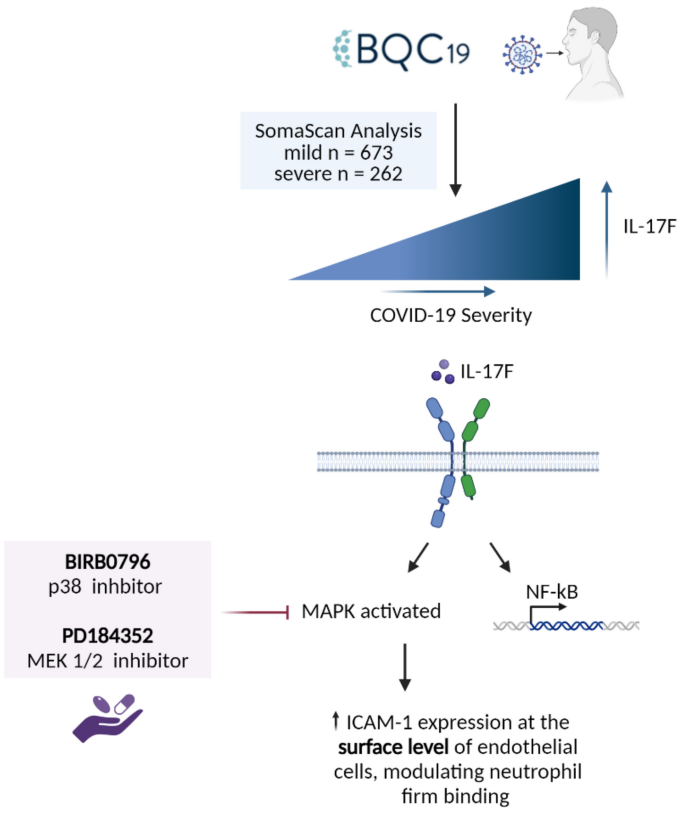

FIGURE 4
Summary of the findings. IL-17F was found to be significantly enriched in the patients with more severe forms of COVID-19. IL-17F activates the IL-17RA/RC receptor which leads to the activation of MAPK pathways as well as transcription factors such as NF-κB. The activation of the MAPK pathways (p38 and ERK) leads to the increase of ICAM-1 expression at the surface level of endothelial cells, thereby increasing neutrophil adhesion. When two MAPK inhibitors are introduced, neutrophil adhesion is significantly reduced as well as the expression of ICAM-1 at the surface level.

published that IL-17D does not bind to any IL-17 receptors but rather on CD93, a glycoprotein expressed on innate lymphoid cells type 3 (ILC3) that is implicated in the production of cytokines associated with T helper cells 17 (37). In that study, mice lacking CD93 receptors on ILC3 cells had impaired IL-22 production and severe colonic inflammation. In another study, IL-17D stimulation of HUVECs increased IL-8 production in an NF-κB dependent manner (38). These levels of IL-8 were physiologically relevant to inhibit hemopoiesis (36). Although knowledge of the role of IL-17D in humans is limited, IL-17D may play a role in regulating the hematopoietic response to inflammation through the production of proinflammatory cytokines derived from ILC3 (36). Another study found that IL-17D played a crucial role during intracellular bacteria and influenza A infection by suppressing the activity of CD8 T cells through the regulation of dendritic cells (39). Additional research is required to better understand the role of IL-17D in inflammation within the context of viral respiratory infections.

Conclusion

Circulating IL-17F is associated with more severe COVID-19. Furthermore, IL-17F promotes neutrophil adhesion to endothelial cells, an event associated with ICAM-1 cell surface expression in a MAPK-dependent manner.

Data availability statement

The datasets presented in this study can be found in online repositories. The names of the repository/repositories and accession number(s) can be found in the article/Supplementary Material.

Ethics statement

The studies involving humans were approved by Institutional Ethics Review Board of the McGill University Health Centre (protocol # 2022-8672/Long Covid and 2023-9261). The studies were conducted in accordance with the local legislation and institutional requirements. Written informed consent for participation in this study was provided by the participants' legal guardians/next of kin.

Author contributions

JB: Writing – review & editing, Writing – original draft, Visualization, Validation, Methodology, Investigation, Formal Analysis, Data curation, Conceptualization. AS: Writing – review & editing, Writing – original draft, Validation, Software, Methodology, Investigation, Formal Analysis. KL: Writing – review & editing, Writing – original draft, Visualization, Methodology, Formal Analysis. LF: Writing – review & editing, Writing – original draft, Visualization, Formal Analysis. AE: Writing – review & editing, Writing – original draft, Supervision, Software, Investigation, Funding acquisition, Formal Analysis, Conceptualization. SR: Writing – review & editing, Writing – original draft, Visualization, Validation, Supervision, Resources, Project administration, Methodology, Investigation, Funding acquisition, Formal Analysis, Data curation, Conceptualization. DDF: Writing – review & editing, Validation, Data curation, Resources.

Funding

The author(s) declare that financial support was received for the research, authorship, and/or publication of this article. This study was supported by the Fonds de recherche du Québec - Santé (FRQS)- Réseau en Santé Respiratoire du Québec- projets équipe, the Canadian Lung Association and the Canadian Institute of Health Research (SR). This work was also supported by Natural Sciences and Engineering Research Council of Canada (NSERC) grant RGPIN-2019-04460 (AE).

Acknowledgments

This work was made possible through open sharing of data and samples from the Biobanque québécoise de la COVID-19, funded by the Fonds de recherche du Québec - Santé, Génome Québec, the Public Health Agency of Canada, and, as of March 2022, the Ministère de la Santé et des Services Sociaux du Québec. We thank all the participants in BQC19 for their contribution and IJM for support with the figures.

Conflict of interest

The authors declare that the research was conducted in the absence of any commercial or financial relationships that could be construed as a potential conflict of interest.

The author(s) declared that they were an editorial board member of Frontiers, at the time of submission. This had no impact on the peer review process and the final decision.

Publisher's note

Supplementary material

The Supplementary Material for this article can be found online at: https://www.frontiersin.org/articles/10.3389/fimmu.2024.1452788/full#supplementary-material

References

1. COVID-19 Treatment Guidelines Panel. Coronavirus disease 2019 (COVID-19) treatment guidelines(2024). Available online at: https://www.covid19treatmentguidelines.nih.gov/overview/clinical-spectrum/ (accessed June 06, 2024).

2. Kitselman AK, Bédard-Matteau J, Rousseau S, Tabrizchi R, Daneshtalab N. Sex differences in vascular endothelial function related to acute and long COVID-19. *Vascul Pharmacol*. (2024) 154:107250. doi: 10.1016/j.vph.2023.107250

3. Bonaventura A, Vecchié A, Dagna L, Martinod K, Dixon DL, Van Tassell BW, et al. Endothelial dysfunction and immunothrombosis as key pathogenic mechanisms in COVID-19. *Nat Rev Immunol*. (2021) 21:319–29. doi: 10.1038/s41577-021-00536-9

4. Blasco A, Coronado MJ, Hernández-Terciado F, Martín P, Royuela A, Ramil E, et al. Assessment of neutrophil extracellular traps in coronary thrombus of a case series of patients with COVID-19 and myocardial infarction. *JAMA Cardiol*. (2020) 6:1–6. doi: 10.1001/jamacardio.2020.7308

5. Desilles JP, Solo Nomenjanahary M, Consoli A, Ollivier V, Faille D, Bourrienne MC, et al. Impact of COVID-19 on thrombus composition and response to thrombolysis: Insights from a monocentric cohort population of COVID-19 patients with acute ischemic stroke. *J Thromb Haemost*. (2022) 20:919–28. doi: 10.1111/jth.15646

6. Englert H, Rangaswamy C, Deppermann C, Sperhake JP, Krisp C, Schreier D, et al. Defective NET clearance contributes to sustained FXII activation in COVID-19-associated pulmonary thrombo-inflammation. *EBioMedicine*. (2021) 67:103382. doi: 10.1016/j.ebiom.2021.103382

7. Leppkes M, Knopf J, Naschberger E, Lindemann A, Singh J, Herrmann I, et al. Vascular occlusion by neutrophil extracellular traps in COVID-19. *EBioMedicine*. (2020) 58:102925. doi: 10.1016/j.ebiom.2020.102925

8. Middleton EA, He XY, Denorme F, Campbell RA, Ng D, Salvatore SP, et al. Neutrophil extracellular traps contribute to immunothrombosis in COVID-19 acute respiratory distress syndrome. *Blood*. (2020) 136:1169–79. doi: 10.1182/blood.2020007008

9. Obermayer A, Jakob LM, Haslbauer JD, Matter MS, Tzankov A, Stoiber W. Neutrophil extracellular traps in fatal COVID-19-associated lung injury. *Dis Markers*. (2021) 2021:5566826. doi: 10.1155/2021/5566826

10. Ouwendijk WJD, Raadsen MP, van Kampen JJA, Verdijk RM, von der Thusen JH, Guo L, et al. High levels of neutrophil extracellular traps persist in the lower respiratory tract of critically ill patients with coronavirus disease 2019. *J Infect Dis*. (2021) 223:1512–21. doi: 10.1093/infdis/jiab050

11. Petito E, Falcinelli E, Paliani U, Cesari E, Vaudo G, Sebastiano M, et al. Association of neutrophil activation, more than platelet activation, with thrombotic complications in coronavirus disease 2019. *J Infect Dis*. (2021) 223:933–44. doi: 10.1093/infdis/jiaa756

12. Skendros P, Mitsios A, Chrysanthopoulou A, Mastellos DC, Metallidis S, Rafailidis P, et al. Complement and tissue factor-enriched neutrophil extracellular traps are key drivers in COVID-19 immunothrombosis. *J Clin Invest*. (2020) 130:6151–7. doi: 10.1172/JCI141374

13. Roussel L, Houle F, Chan C, Yao Y, Bérubé J, Olivenstein R, et al. IL-17 promotes p38 MAPK-dependent endothelial activation enhancing neutrophil recruitment to sites of inflammation. *J Immunol*. (2010) 184:4531–7. doi: 10.4049/jimmunol.0903162

14. Sharif-Askari FS, Sharif-Askari NS, Hafezi S, Mdkhana B, Alsayed HAH, Ansari AW, et al. Interleukin-17, a salivary biomarker for COVID-19 severity. *PloS One*. (2022) 17:e0274841. doi: 10.1371/journal.pone.0274841

15. Mills KHG. IL-17 and IL-17-producing cells in protection versus pathology. *Nat Rev Immunol*. (2022) 23:38–54. doi: 10.1038/s41577-022-00746-9

16. Harumichi Ishigame SK, Nagai T, Kadoki M, Nambu A, Komiyama Y, Fujikado N, et al. Differential roles of interleukin-17A and -17F in host defense against mucoepithelial bacterial infection and allergic responses. *Immunity*. (2009) 30:108–19. doi: 10.1016/j.immuni.2008.11.009

17. Monin L, Gaffen SL. Interleukin 17 family cytokines: signaling mechanisms, biological activities, and therapeutic implications. *Cold Spring Harb Perspect Biol*. (2018) 10. doi: 10.1101/cshperspect.a028522

18. Amatya N, Garg AV, Gaffen SL. IL-17 signaling: the yin and the yang. *Trends Immunol*. (2017) 38:310–22. doi: 10.1016/j.it.2017.01.006

19. Kolaczkowska E, Kubes P. Neutrophil recruitment and function in health and inflammation. *Nat Rev Immunol*. (2013) 13:159–75. doi: 10.1038/nri3399

20. Tremblay K, Rousseau S, Zawati MH, Auld D, Chassé M, Coderre D, et al. The Biobanque québécoise de la COVID-19 (BQC19)-A cohort to prospectively study the clinical and biological determinants of COVID-19 clinical trajectories. *PloS One*. (2021) 16:e0245031. doi: 10.1371/journal.pone.0245031

21. Iosef C, Martin CM, Slessarev M, Gillio-Meina C, Cepinskas G, Han VKM, et al. COVID-19 plasma proteome reveals novel temporal and cell-specific signatures for disease severity and high-precision disease management. *J Cell Mol Med*. (2023) 27:141–57. doi: 10.1111/jcmm.17622

22. Najmeh S, Cools-Lartigue J, Giannias B, Spicer J, Ferri LE. Simplified human neutrophil extracellular traps (NETs) isolation and handling. *J Vis Exp*. (2015) 16 (98):52687. doi: 10.3791/52687

23. Avdeev SN, Trushenko NV, Tsareva NA, Yaroshetskiy AI, Merzhoeva ZM, Nuralieva GS, et al. Anti-IL-17 monoclonal antibodies in hospitalized patients with severe COVID-19: A pilot study. *Cytokine*. (2021) 146:155627. doi: 10.1016/j.cyto.2021.155627

24. Pacha O, Sallman MA, Evans SE. COVID-19: a case for inhibiting IL-17? *Nat Rev Immunol*. (2020) 20:345–6. doi: 10.1038/s41577-020-0328-z

25. Davies DR, Gelinas AD, Zhang C, Rohloff JC, Carter JD, O'Connell D, et al. Unique motifs and hydrophobic interactions shape the binding of modified DNA ligands to protein targets. *Proc Natl Acad Sci U S A*. (2012) 109:19971–6. doi: 10.1073/pnas.1213933109

26. Sadeghi A, Tahmasebi S, Mahmood A, Kuznetsova M, Valizadeh H, Taghizadieh A, et al. Th17 and Treg cells function in SARS-CoV2 patients compared with healthy controls. *J Cell Physiol*. (2021) 236:2829–39. doi: 10.1002/jcp.v236.4

27. Shibabaw T. Inflammatory cytokine: IL-17A signaling pathway in patients present with COVID-19 and current treatment strategy. *J Inflammation Res*. (2020) 13:673–80. doi: 10.2147/JIR.S278335

28. Montazersaheb S, Hosseiniyan Khatibi SM, Hejazi MS, Tarhriz V, Farjami A, Ghasemian Sorbeni F, et al. COVID-19 infection: an overview on cytokine storm and related interventions. *Virol J*. (2022) 19:92. doi: 10.1186/s12985-022-01814-1

29. Resende GG, da Cruz Lage R, Lobê SQ, Medeiros AF, Costa ESAD, Nogueira Sá AT, et al. Blockade of interleukin seventeen (IL-17A) with secukinumab in hospitalized COVID-19 patients - the BISHOP study. *Infect Dis (Lond)*. (2022) 54:591–9. doi: 10.1080/23744235.2022.2066171

30. Gaffen SL. Structure and signalling in the IL-17 receptor family. *Nat Rev Immunol*. (2009) 9:556–67. doi: 10.1038/nri2586

31. Dragoni S, Hudson N, Kenny BA, Burgoyne T, McKenzie JA, Gill Y, et al. Endothelial MAPKs direct ICAM-1 signaling to divergent inflammatory functions. *J Immunol*. (2017) 198:4074–85. doi: 10.4049/jimmunol.1600823

32. Onishi RM, Gaffen SL. Interleukin-17 and its target genes: mechanisms of interleukin-17 function in disease. *Immunology*. (2010) 129:311–21. doi: 10.1111/j.1365-2567.2009.03240.x

33. Bui TM, Wiesolek HL, Sumagin R. ICAM-1: A master regulator of cellular responses in inflammation, injury resolution, and tumorigenesis. *J Leukoc Biol*. (2020) 108:787–99. doi: 10.1002/JLB.2MR0220-549R

34. Patel MA, Knauer MJ, Nicholson M, Daley M, Van Nynatten LR, Martin C, et al. Elevated vascular transformation blood biomarkers in Long-COVID indicate angiogenesis as a key pathophysiological mechanism. *Mol Med*. (2022) 28:122. doi: 10.1186/s10020-022-00548-8

35. Xue J, Thippegowda PB, Hu G, Bachmaier K, Christman JW, Malik AB, et al. NF-kappaB regulates thrombin-induced ICAM-1 gene expression in cooperation with NFAT by binding to the intronic NF-kappaB site in the ICAM-1 gene. *Physiol Genomics*. (2009) 38:42–53. doi: 10.1152/physiolgenomics.00012.2009

36. Liu X, Sun S, Liu D. IL-17D: A less studied cytokine of IL-17 family. *Int Arch Allergy Immunol*. (2020) 181:618–23. doi: 10.1159/000508255

37. Huang J, Lee HY, Zhao X, Han J, Su Y, Sun Q, et al. Interleukin-17D regulates group 3 innate lymphoid cell function through its receptor CD93. *Immunity*. (2021) 54:673–86.e4. doi: 10.1016/j.immuni.2021.03.018

38. Starnes T, Broxmeyer HE, Robertson MJ, Hromas R. Cutting edge: IL-17D, a novel member of the IL-17 family, stimulates cytokine production and inhibits hemopoiesis. *J Immunol*. (2002) 169:642–6. doi: 10.4049/jimmunol.169.2.642

39. Lee Y, Clinton J, Yao C, Chang SH. Interleukin-17D promotes pathogenicity during infection by suppressing CD8 T cell activity. *Front Immunol*. (2019) 10:1172. doi: 10.3389/fimmu.2019.01172

frontiers | Frontiers in Immunology

TYPE Original Research
PUBLISHED 21 October 2024
DOI 10.3389/fimmu.2024.1465938

OPEN ACCESS

EDITED BY
Jian Zheng,
University of Louisville, United States

REVIEWED BY
Hima Dhakal,
University of Louisville, United States
Harim Tavares Dos Santos,
University of Missouri, United States

*CORRESPONDENCE
Chen Zhang
zhangchen710cool@qq.com
Liang Hu
huliang@mail.ccmu.edu.cn

†These authors have contributed equally to this work and share first authorship

RECEIVED 17 July 2024
ACCEPTED 26 September 2024
PUBLISHED 21 October 2024

CITATION
Yang Z, Liu M, Chang Z, Du C, Yang Y, Zhang C and Hu L (2024) Myeloid-derived growth factor promotes M2 macrophage polarization and attenuates Sjögren's syndrome via suppression of the CX3CL1/CX3CR1 axis.
Front. Immunol. 15:1465938.
doi: 10.3389/fimmu.2024.1465938

Myeloid-derived growth factor promotes M2 macrophage polarization and attenuates Sjögren's syndrome via suppression of the CX3CL1/CX3CR1 axis

Zi Yang[1,2†], Mangnan Liu[1†], Zhichao Chang[2], Conglin Du[2], Yang Yang[2,3], Chen Zhang[1*] and Liang Hu[2,4*]

[1]Department of Endodontics, School of Stomatology, Capital Medical University, Beijing, China, [2]Salivary Gland Disease Center and Beijing Key Laboratory of Tooth Regeneration and Function Reconstruction, School of Stomatology and Beijing Laboratory of Oral Health, Beijing, China, [3]Department of Oral and Maxillofacial & Head and Neck Oncology, School of Stomatology, Capital Medical University, Beijing, China, [4]Outpatient Department of Oral and Maxillofacial Surgery, School of Stomatology, Capital Medical University, Beijing, China

Introduction: Primary Sjögren syndrome (pSS) is a systemic autoimmune disease that is characterized by the infiltration of immune cells into the salivary glands. The re-establishment of salivary glands (SGs) function in pSS remains a clinical challenge. Myeloid-derived growth factor (MYDGF) has anti-inflammatory, immunomodulatory, and tissue-functional restorative abilities. However, its potential to restore SGs function during pSS has not yet been investigated.

Methods: Nonobese diabetic (NOD)/LtJ mice (pSS model) were intravenously administered with adeno-associated viruses carrying MYDGF at 11 weeks of age. Salivary flow rates were determined before and after treatment. Mice were killed 5 weeks after MYDGF treatment, and submandibular glands were collected for analyses of histological disease scores, inflammatory cell infiltration, PCR determination of genes, and Western blotting of functional proteins. Furthermore, mRNA sequencing and bioinformatics were used to predict the mechanism underlying the therapeutic effect of MYDGF.

Results: Treatment of NOD/LtJ mice with MYDGF alleviated pSS, as indicated by increased salivary flow rate, reduced lymphocyte infiltration, attenuated glandular inflammation, and enhanced AQP5 and NKCC1 expression. The gene expression levels of cytokines and chemokines, including *Ccl12, Ccl3, Il1r1*, *Ccr2*, *Cx3cr1*, *Il7*, *Mmp2*, *Mmp14*, *Il1b*, and *Il7*, significantly decreased after treatment with MYDGF, as determined by RNA sequencing. Meanwhile, MYDGF inhibits infiltration of macrophages (Mϕ) in SGs, induces polarization of M2ϕ, and suppresses C-X3C motif ligand 1 (CX3CL1)/C-X3C motif receptor 1 (CX3CR1) axis.

Conclusions: Our findings showed that MYDGF could revitalize the SGs function of pSS, inhibit infiltration of Mϕ, and promote M2ϕ polarization via suppression of the CX3CL1/CX3CR1 axis, which has implications for potential therapy for pSS.

KEYWORDS

Sjögren's syndrome, salivary glands, myeloid-derived growth factor, M2 macrophage polarization, CX3CL1, CX3CR1

1 Introduction

Primary Sjögren syndrome (pSS) is a systemic autoimmune disease that affects the salivary and lacrimal glands, resulting in xerostomia and xerophthalmia. The prognosis of the disease leads to systemic complications in approximately 20%–50% of patients with pSS (1). Immunosuppressive and anti-inflammatory therapy (2), regenerative therapy (3), and gene therapy (4) have been reported to alleviate xerostomia of pSS. There is no gold standard for xerostomia treatment currently, and effective clinical treatment for pSS is still in high demand.

The salivary glands (SGs) of pSS patients are characterized by infiltration of immune cells, especially T cells, B cells, dendritic cells (DCs), macrophages (Mϕ), and natural killer (NK) cells (5). Patients with pSS showed increased levels of several Mϕ- and lymphocyte-derived cytokines, such as IL-1b, IL-6, IL-17, MMP3, and TNF-α, indicating an immune activation state (5, 6). Several chemokines, such as CC motif ligand 2 (CCL2)/CC motif receptor 2 (CCR2) and C-X3C motif ligand 1 (CX3CL1)/C-X3C motif receptor 1 (CX3CR1) are associated with lymphocyte homing and vary from one tissue site to another (7, 8). These chemokines are reported to associate with the severity of pSS.

Bone marrow-derived cells (BMDCs), a pool of progenitor and pluripotent stem cells, secrete various cytokines, growth factors, and exosomes. Recent studies have shown that BMDCs can re-establish functions in pSS (9, 10). Given the tissue-specific responses of BMDCs, an increasing number of studies have focused on their paracrine effects as alternative cell-free treatments for various diseases (11, 12). Myeloid-derived growth factor (MYDGF) is a paracrine protein produced by BMDCs, particularly by bone marrow-derived monocytes and Mϕ. Our previous study showed that MYDGF relieves inflammation of inflammatory bowel disease (13). Moreover, MYDGF inhibits inflammation, blunts leukocyte homing, and protects endothelial injury via nuclear factor κB (NF-κB) signaling (14, 15). However, the effects of MYDGF on pSS and its possible underlying mechanisms remain unknown.

In the present study, we used nonobese diabetic (NOD)/LtJ female mice as an animal model of pSS. The function of SGs following MYDGF treatment was analyzed, and the underlying molecular mechanisms of MYDGF were investigated. The present study reveals the function and underlying mechanism of interactions between MYDGF and the host immune system in pSS, providing potential strategies for improving the therapeutic efficacy of pSS.

2 Materials and methods

2.1 Animal experiments

Female Institute of Cancer Research (ICR) and NOD/LtJ 6-week-old mice purchased from Beijing Vital River Laboratory Animal Technology (Beijing, China) were used as normal and the pSS model subjects. All mouse experiments were approved by the Ethics Review Commission of the Laboratory Animal Center of Capital Medical University (approval number: AEEI-2023-056). The mice had free access to soy-based food and water and were kept under a light/dark cycle for 12/12 h at a constant temperature.

2.2 Adeno-associated-virus -treated mice

The *Mydgf* gene sequence (GenBank accession number NM 080837.2) was directly synthesized into the CMV-betaGlobin-EGFP-T2A-MCS-3Flag-SV40 PolyA vector. The mice received a single injection of adeno-associated virus (AAV)-MYDGF or AAV-GFP at a dose of 1×10^{12} viral genomes through the tail vein for 11 weeks. The ICR mice were designated as the normal group and did not receive any treatment. NOD/LtJ mice were categorized into the following groups based on the material used for intravenous injection (n = 8 per group): (1) SS group, not administered anything; (2) AAV-GFP group, AAV-GFP administered; and (3) AAV-MYDGF group, AAV-MYDGF administered. Saliva secretion flow rates for all four groups were recorded at weeks 8, 11, 14, and 16. Mice were killed at week 16, and submandibular glands, spleen, and blood were collected for further experiments.

2.3 Measurement of stimulated saliva flow

The ICR and NOD/LtJ mice were anesthetized with pentobarbital sodium (50 mg/kg). After an intraperitoneal injection of pilocarpine (50 mg/mL) at a dose of 0.1 mL/kg body weight, stimulated saliva flow was measured 10 min later. A cotton

ball was placed under the tongue and held steadily during a 10-min period to collect saliva. The weight difference of the cotton ball before and after saliva collection was calculated.

2.4 Hematoxylin and eosin staining

At 16 weeks, all animals were killed, and the submandibular glands were harvested. Portions of the submandibular glands were fixed in 4% paraformaldehyde and then embedded in paraffin. Four-micrometer sections were obtained, deparaffinized, hydrated, and stained with hematoxylin and eosin (HE) and for immunofluorescence. The counts and areas of inflammatory foci containing > 50 lymphocytes per 4 mm^2 of tissue were calculated.

2.5 Immunofluorescence and immunohistochemistry (IHC) staining

The sections were dewaxed and rehydrated for immunohistochemistry with xylol and alcohol, respectively. Antigen retrieval was conducted by sodium citrate in microwave conditions. The slides were further blocked with 3% bovine serum albumin (BSA; Beyotime, Shanghai, China) for 1 h at 37°C. Primary antibodies, including anti-IL-6 (1:100, ab290735, Abcam, Waltham, MA, USA), anti-TNF-α (1:100, ab6671, Abcam), anti-AQP5 (1:1,000, ab305303, Abcam), anti-NKCC1 (1:200, 13884-1-AP, Proteintech, Wuhan, China), anti-F4/80 (GB113373, Servicebio, Wuhan, China), anti-CD86 (GB115630, Servicebio), anti-CD206 (GB113497, Servicebio), anti-CX3CL1 (60339-1-1g, Proteintech), anti-CX3CR1 (13885-1-AP, Proteintech), were incubated with the slides at 4°C overnight. Secondary antibodies (1: 1,000, A32723, A-11012, Thermo Fisher, Waltham, MA, USA) and Fluoroshield™ with 4',6-diamidino-2-phenylindole (DAPI) (Sigma-Aldrich Corp., St. Louis, MO, USA) were used for immunofluorescence (IF) staining. The secondary antibody (PV-9000, ZSGB-Bio, Beijing, China) and DAB kit (8059P, Cell Signaling Technology, Boston, USA) were used in immunohistochemistry (IHC) staining. Stained samples were evaluated using a fluorescence microscope (BX61, Olympus, Tokyo, Japan).

2.6 Western blot

Portions of the submandibular glands were ground and prepared with lysis buffer (C1053, Applygen, Beijing, China) according to the manufacturer's instructions. Protein concentrations were determined by Coomassie Brilliant Blue (1610435, Bio-Rad, Hercules, CA, USA). Equal amounts of cellular proteins (30 μg) were boiled for 10 min at 98°C. Equal amounts of protein extracts were loaded onto FuturePAGE™ 4%–20% polyacrylamide gels (ACE, Nanjing, China) for electrophoresis and transferred to nitrocellulose membranes. Bands were detected immunologically using polyclonal antibodies (1: 1,000) against AQP5 (ab305303, Abcam), MYDGF (11353-1-AP, Proteintech), and β- actin (AC026, Abclonal, Wuhan, China), which were used as a loading control. Immunoblot bands were visualized following the application of the ECL detection system (ChemiDoc™ MP Imaging System, Bio-Rad, CA, USA).

2.7 Flow cytometry

The spleens of the AAV-GFP and AAV-MYDGF group were ground and filtrated through a Falcon 70 μm filter (Corning Inc., Corning, NY, USA). R ed blood cell lysis buffer (R1010, Solarbio, Beijing, China) was then added, and the mixture was centrifuged at 500×*g*. A single-cell suspension was stained with the following antibodies: CD4 (100559, BV510, RM4-5, Biolegend San Diego, CA, USA), CD45 (147716, Alexa Fluor 700, I3/2.3, Biolegend), TCRβ (109220, APC-Cyanine7, H57-597, Biolegend), F4/80 (123131, BV421, BM8, Biolegend), CD80 (104705, FITC, 16-10A1, Biolegend), CD163 (155305, APC, S150491, Biolegend), IL-4 (504103, PE, 11B11, Biolegend), IL-17A (506922, PE-Cyanine7, TC11-18H10.1, Biolegend), FOXP3 (126409, Pacific Blue, MF-14, Biolegend), and IFN-γ (505817, Pacific Blue, XMG1.2, Biolegend). For intracellular cytokine staining, cells were stimulated with a cell stimulation cocktail (00-4970-93, Invitrogen, Waltham, MA, USA) and a protein transport inhibitor cocktail (00-4980-03, Invitrogen) at 37°C for 6 h, followed by fixation with the fixation/permeabilization buffer solution (554714, BD Bioscience, New jersey, USA). Foxp3/Transcription Factor Fixation/Permeabilization Concentrate and Diluent (00-5521, Invitrogen) were used for intranuclear staining. Stained cells were analyzed using an LSRFortessa (BD Biosciences), and the data were analyzed using FlowJo software (Tree Star, Ashland, OR, USA).

2.8 RNA sequencing

Samples of submandibular glands from the AAV-GFP and AAV-MYDGF groups were collected for RNA sequencing. The preparation of transcriptome libraries and sequencing were performed by OE Biotech Co. Ltd. (Shanghai, China). A comparison was conducted to identify genes that were differentially regulated between the AAV-GFP and AAV-MYDGF groups. A p-value < 0.05 and a fold change > 1.5 or < 0.75 were set as the thresholds for significant differential expression. The Gene Ontology (GO) enrichment analysis, Kyoto Encyclopedia of Genes and Genomes (KEGG) enrichment analysis, and Gene Set Enrichment Analysis (GSEA) were performed using R based on a hypergeometric distribution.

2.9 Quantitative real-time polymerase chain reaction

Portions of the submandibular glands were ground, and total RNA was collected using the RNAprep pure Tissue Kit (DP431, Tiangen Biotech, Beijing, China). The RNA was then reverse-transcribed into cDNA using the NovoScript® Plus All-in-one 1st Strand cDNA Synthesis SuperMix (E047-01A; Novoprotein,

Suzhou, China). Quantitative real-time polymerase chain reaction (qRT-PCR) was performed using an NovoStart®SYBR qPCR SuperMix Plus (E096-01B; Novoprotein). After normalizing target gene expression, the data were quantified using the $2^{-\Delta\Delta Ct}$ method. The genes and their corresponding primer sequences are listed in Supplementary Table S1.

2.10 Enzyme-linked immunosorbent assay

Blood samples were collected after the animals were anesthetized. Serum was obtained by centrifugation at 1,500 rpm for 30 min at room temperature and then stored at − 20°C. The concentrations of CX3CL1 and CX3CR1 in serum were detected by mouse CX3CL1 and CX3CR1 enzyme-linked immunosorbent assay (ELISA) Kit (SYP-M0090, SYP- M0768, UpingBio Technology, Shenzhen, China).

2.11 Terminal deoxynucleotidyl transferase dUTP nick end labeling assay

Terminal deoxynucleotidyl transferase dUTP nick end labeling (TUNEL) staining was performed using a One- step TUNEL Apoptosis Assay Kit (C1090; Beyotime, Shanghai, China). Images were captured under a confocal microscope, and the number of TUNEL-positive cells was calculated using Image J software (NIH, Bethesda, MD, U SA).

2.12 Statistical analysis

All results are presented as mean ± SDs. The one-way ANOVA test was used to determine significant differences among multiple groups, while the Kruskal–Wallis test was used to compare differences with non-normal distribution. Student's *t*-test was performed to compare differences between two groups with normal distribution. Statistical analysis was performed using SPSS 19.0 and by GraphPad Prism 8 software (San Diego, CA, USA). In the figures, asterisks denote statistical significance as follows: ^{ns} $p > 0.05$, * $p < 0.05$, ** $p < 0.01$, and *** $p < 0.001$.

3 Results

3.1 MYDGF treatment alleviates xerostomia and revitalizes SG function in NOD/LtJ mice

NOD/LtJ mice were used as a spontaneous pSS model, exhibiting characteristic lymphocyte infiltration in the exocrine glands and SG dysfunction. The animal experiments were conducted as illustrated in Figure 1A. A decrease in salivary secretion was observed between the fifth and eighth weeks, after which it was maintained at a low level (16). At the 11th week, the salivary flow rate in NOD/LtJ mice significantly decreased compared to that in ICR mice (Figure 1B, $p < 0.05$), indicating that the early stage of the pSS model had been established. To assess the effect of MYDGF during the early stages of pSS, AAV-GFP and AAV-MYDGF were injected in the 11th week. After 5 weeks of AAV-MYDGF treatment, salivary function and histologic examination were performed in the 16th week.

The saliva flow rate in the SS and AAV-GFP groups was reduced at 16 weeks compared to that at 8 weeks. However, MYDGF treatment significantly maintained the saliva flow rate compared to that of the SS and AAV-GFP groups (Figure 1B, $p < 0.01$). As indicated by HE staining, the number and area of lymphocyte infiltration foci in the submandibular glands were significantly reduced in the AAV-MYDGF group compared to those in the SS and AAV-GFP groups (Figure 1C, $p < 0.01$). Aquaporin-5 (AQP5) and the $Na^+/K^+/2Cl^-$ cotransporter (NKCC1) are two important transmembrane transporter proteins involved in salivary secretion in SG acinar cells. Both proteins were significantly reduced at the onset of SS, which correlated with decreased salivary secretion (17–19). Immunofluorescence (IF) staining showed that AQP5 and NKCC1 were widely expressed in the acinar cells of the submandibular glands of ICR mice, and their expression in the membrane of acinar cells was strongly enhanced in the AAV-MYDGF group compared to that in the SS and AAV-GFP groups (Figures 1D, E, $p < 0.001$). Western blotting showed similar protein expression levels of AQP5 and MYDGF in the AAV-MYDGF group, supporting our results (Figure 1F, $p < 0.05$ or $p < 0.01$). Overall, MYDGF treatment inhibited lymphocyte infiltration and restored salivary secretion during the early stages of pSS.

3.2 MYDGF ameliorates inflammation and chemokines of SGs in NOD/LtJ mice

Submandibular gland samples from the AAV-GFP and AAV-MYDGF groups were subjected to RNA sequencing to investigate the underlying mechanisms of MYDGF treatment in pSS. Principal component analysis (PCA) showed a distinct separation between the two groups, confirming the comparability of the samples (Figure 2A). Furthermore, a total of 2,047 differentially expressed genes (DGEs) were identified in the AAV-MYDGF group compared to the AAV-GFP group, with 1,189 upregulated and 858 downregulated. Notably, the expression levels of chemokines associated with the severity of pSS, such as *Ccl12*, *Ccl3*, *Il1r1*, *Ccr2*, *Cx3cr1*, *Il7*, *Mmp2*, *Mmp14*, *Il1b*, and *Il7*, were significantly lower in the AAV- MYDGF group than in the AAV-GFP group. Genes associated with the function of SGs, including *Aqp5*, *Sox2*, *Slc12a8*, *Lgr5*, and *Dusp2*, were significantly upregulated in the AAV-MYDGF group (Figure 2B, $p < 0.05$).

GO analysis revealed that MYDGF treatment upregulated biological processes, including neutral amino acid transport, vesicle-mediated transport, protein transport, and endoplasmic reticulum-to-Golgi vesicle-mediated transport (Supplementary Figures S1A, B). Additionally, KEGG analysis showed that metabolism-related signaling pathways were upregulated, while the PI3K-AKT and Hippo signaling pathways were downregulated following MYDGF treatment (Figures 2C, D, $p <$

10.3389/fimmu.2024.1465938

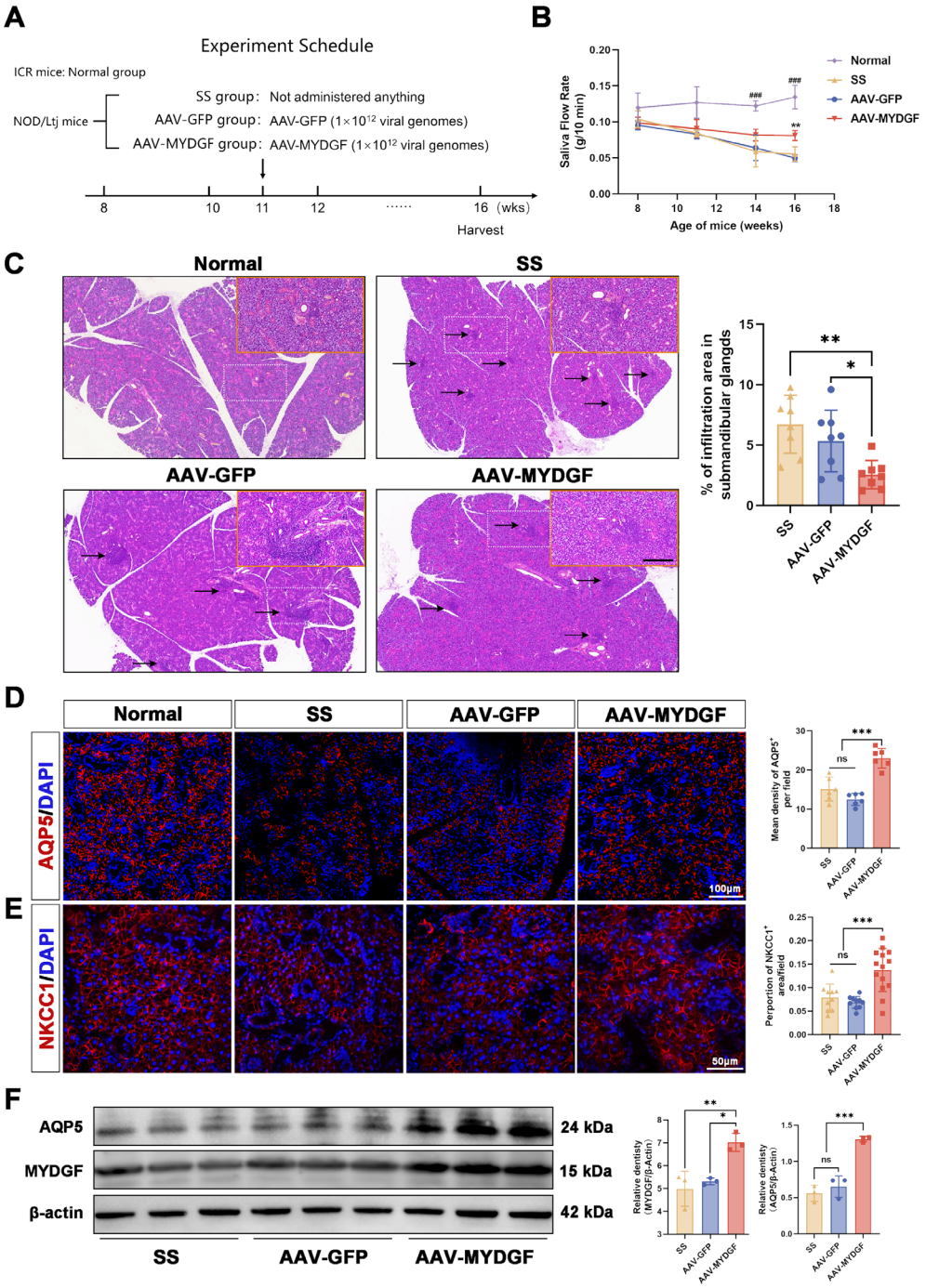

FIGURE 1
MYDGF alleviated the function of salivary glands in NOD/Ltj mice. **(A)** Schematic of the animal experiment and treatment. **(B)** Saliva flow rate (g/10 min) of four groups (** $p < 0.01$ vs. AAV-GFP and SS group; ### $p < 0.001$ vs. SS, AAV- GFP, and AAV-MYDFG groups). **(C)** HE-stained histological images of submandibular glands and quantitative analysis of infiltration area showed that the number and area of lymphocyte infiltration foci (black arrows) were considerably reduced in the AAV-MYDGF group than those in the SS and AAV-GFP groups (scale bars: 500 μm and 200 μm; ^{ns} no significant difference; *** $p < 0.001$). **(D)** Immunofluorescence staining of AQP5 (red) and quantitative analysis showed the expression of AQP5 was strongly increased in the AAV-MYDGF group compared with the SS and AAV-GFP groups (scale bar: 100 μm, *** $p < 0.001$). **(E)** Immunofluorescence staining of NKCC1 (red) and quantitative analysis showed the expression of NKCC1 was significantly increased in the AAV-MYDGF group (scale bar: 50 μm, *** $p < 0.001$). **(F)** Western blot analysis showed that the expression of AQP5 and MYDGF in theAAV-MYDGF group was significantly increased compared with the SS and AAV-GFP groups (* $p < 0.05$; ** $p < 0.01$; *** $p < 0.001$). One-way analysis of variance (ANOVA) was used to compare the differences among multiple groups, with the Bonferroni method applied to used to compare the intergroup variation.

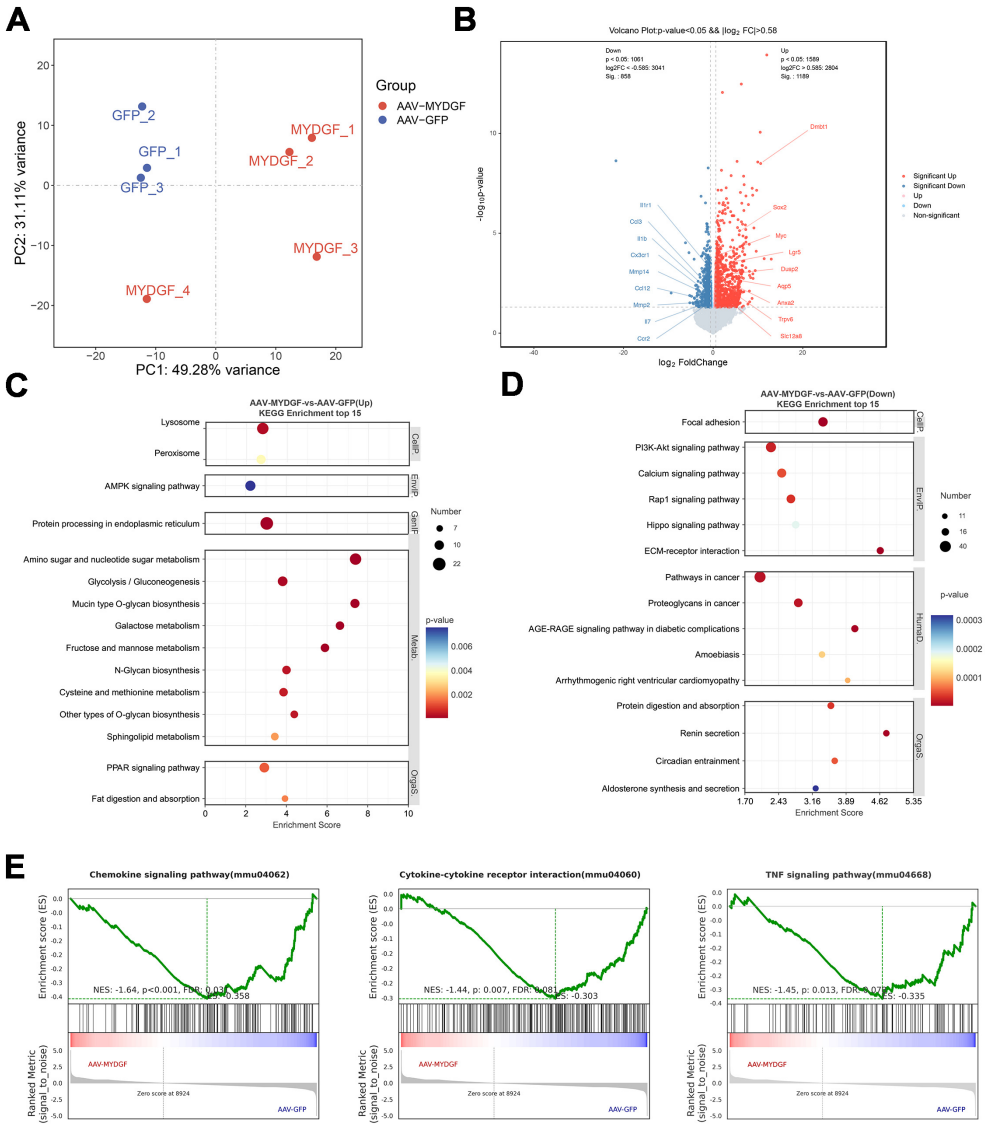

FIGURE 2
Transcriptome analysis of submandibular glands of NOD/Ltj mice treated with AAV-GFP and AAV-MYDGF. **(A)** The principal component analysis (PCA) showed the distinct separation between the AAV-GFP and AAV-MYDGF group. **(B)** Volcano plot of differentially expressed genes (DEGs) showed that the gene expression of chemokines, such as *Ccl12*, *Ccl3*, *Il1r1*, *Ccr2*, and *Cx3cr1* were significantly decreased in the AAV-MYDGF group ($p < 0.05$). **(C, D)** Top 15 KEGG enrichment. **(E)** GSEA showed that TNF signaling pathway, cytokine-cytokine receptor interaction and chemokine signaling pathway were significantly downregulated in the AAV-MYDGF group.

0.05). GSEA showed that TNF signaling pathway, cytokine-cytokine receptor interaction and chemokine signaling pathway were significantly downregulated in the AAV-MYDGF group (Figure 2E, $p < 0.05$). In addition, IHC staining showed that the expression levels of TNF- α and IL-6 were significantly decreased in the AAV-MYDGF group (Supplementary Figures S2A–D; $p < 0.001$), indicating that MYDGF inhibits inflammation and revitalizes SG function by modulating the secretion of cytokines and chemokines. TUNEL staining revealed a significant increase in the number of TUNEL$^+$ cells within the lymphocyte infiltration foci in the salivary glands of the AAV-MYDGF group compared to the AAV-GFP group (Figures 3A, B, $p < 0.05$). Overall, MYDGF alleviated inflammation, inhibited the expression of chemokines, and promoted the necrosis of lymphocytes infiltrating the submandibular glands.

3.3 MYDGF inhibits infiltration of Mϕ in SGs and induces polarization of M2ϕ

An imbalance in T helper cells contributes to the pathogenesis of pSS by producing proinflammatory cytokines (18, 20, 21). The ratio of T helper lymphocyte subsets in the spleen was determined using flow cytometry. The results showed that the ratios of Th1 (CD4$^+$/IFN-γ$^+$) or Th2 (CD4$^+$/IL4$^+$) cells, representing Th1 or Th2 cells, respectively, were not significantly different between the AAV-

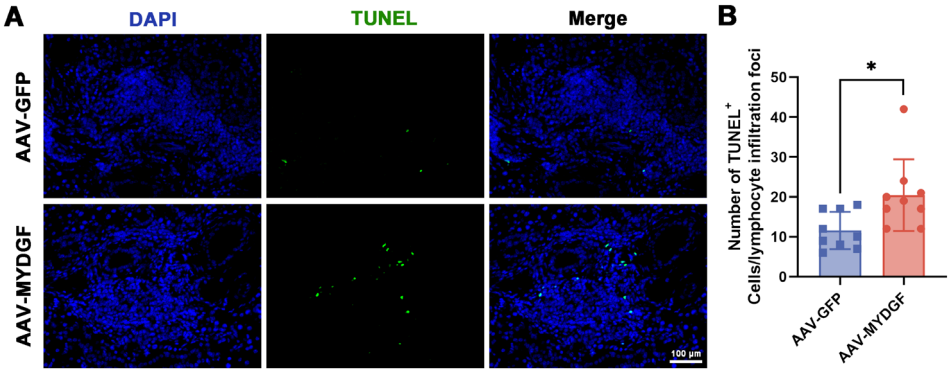

FIGURE 3
MYDGF promotes the apoptosis of immune cells of lymphocyte infiltration foci. **(A, B)** The TUNEL staining showed that the number of TUNEL$^+$ cells in lymphocyte infiltration foci of submandibular glands was significantly increased in the AAV-MYDGF group (scale bar: 100 μm, * $p < 0.05$). Student's *t*-test was performed to compare difference between two groups with normal distribution.

MYDGF and AAV-GFP groups (Supplementary Figures S3A, B, $p > 0.05$). Additionally, the ratio of Th17 (CD4$^+$/RORg$^+$) to Treg (CD4$^+$/CD25$^+$/FOXP3$^+$) cells was not significantly different between the AAV-MYDGF and AAV-GFP groups (Supplementary Figures S3C, D, $p > 0.05$).

Mϕ, a crucial component of the innate immune system, correlates with pSS severity (22). Flow cytometry analysis of the spleen revealed that treatment with MYDGF increased the ratio of M2ϕ (F4/80$^+$/CD163$^+$) and decreased the ratio of M1ϕ (F4/80$^+$/CD80$^+$) (Figures 4A, B, $p < 0.05$). Based on immunohistochemical staining of submandibular glands, the number of positive F4/80$^+$ cells was significantly decreased in the AAV-MYDGF group compared to the AAV-GPF group (Figures 4C–E, $p < 0.001$). Double immunofluorescence staining of F4/80 and CD206 indicated that MYDGF treatment significantly promoted the polarization of M2ϕ compared to the AAV-GPF group (Figures 4C, F, $p < 0.001$). Meanwhile, IF of F4/80 and CD86 showed that MYDGF treatment significantly decreased the polarization of M1ϕ (Figures 4D, G, $p < 0.001$). In summary, MYDGF suppresses the infiltration of Mϕ and promotes M2ϕ polarization in pSS.

3.4 MYDGF inhibits inflammation via suppression of the CX3CL1/CX3CR1 axis

Based on RNA sequencing, we found that the expression of *Cx3cr1* was significantly decreased in the AAV-MYDGF group (Figure 2B, $p < 0.05$). RT-PCR showed that after treatment with MYDGF, the expression of chemokine- or cytokine-related genes, including *Ccl2*, *Ccl3*, *Ccl12*, *Mmp2*, *Cx3cl1*, and *Cx3cr1*, was significantly decreased, with *Cx3cl1* and *Cx3cr1* showing the most pronounced reduction (Figure 5A; Supplementary Figure S4, $p < 0.01$). The serum concentrations of CX3CL1 and CX3CR1 significantly decreased after MYDGF treatment (Figure 5B, $p < 0.05$). IHC staining of submandibular glands showed that MYDGF decreased the expression of CX3CL1 and CX3CR1 in SGs (Figures 5C, D, $p < 0.05$). CX3CL1/CX3CR1 were the most significantly decreased chemokines in serum and submandibular glands after treatment of MYDGF.

3 Discussion

pSS is a chronic autoimmune disease that affects the exocrine glands and causes systemic autoimmune lesions (23). Characteristics of pSS include inflammatory cell infiltration and increased cytokine and chemokine production. However, the pathogenesis of pSS is not fully understood, and effective clinical therapies are still limited. MYDGF, a paracrine protein of BMDCs, inhibits inflammation and blunts immune cell homing and migration (13–15). Further research is required to determine whether MYDGF can be used as an alternative cell-free therapy to alleviate xerostomia in patients with pSS. In the present study, MYDGF demonstrated the ability to inhibit inflammation, reduce the migration of lymphocytes and Mϕ in SGs, and re-establish the impaired SG function of pSS. In addition, we found that MYDGF promote d the polarization of M2ϕ and suppressed the expression of CX3CL1 and CX3CR1 in both the spleen and SGs. Our results indicate the therapeutic potential and molecular mechanisms of MYDGF in pSS.

Previous studies have shown that pSS is triggered by a T-cell-mediated autoimmune response (24) and B-cell activation (25); however, other immune cells, including Mϕ, have also been observed in SGs and peripheral blood mononuclear cells (PBMCs), contributing to the onset or development of SS (26). However, the role of Mϕ in SS has not been widely investigated. Mϕ has been found to generate reactive oxygen species and communicate with other innate and adaptive immune cells in SGs (27). CD11b^{Hi} Mϕ promotes CCR4 expression in CD4$^+$ T cells, thereby improving the migratory capacity in pSS (23). Additionally, the transplantation of CD4$^+$ T cells also induces Mϕ infiltration, and the depletion of Mϕ is sufficient to ameliorate the dysfunction of the lacrimal glands and eyes (28). Therefore, targeting Mϕ infiltration is a promising treatment strategy for pSS.

Meanwhile, the polarization of M1ϕ may play a significant role in the development of pSS and could be associated with disease

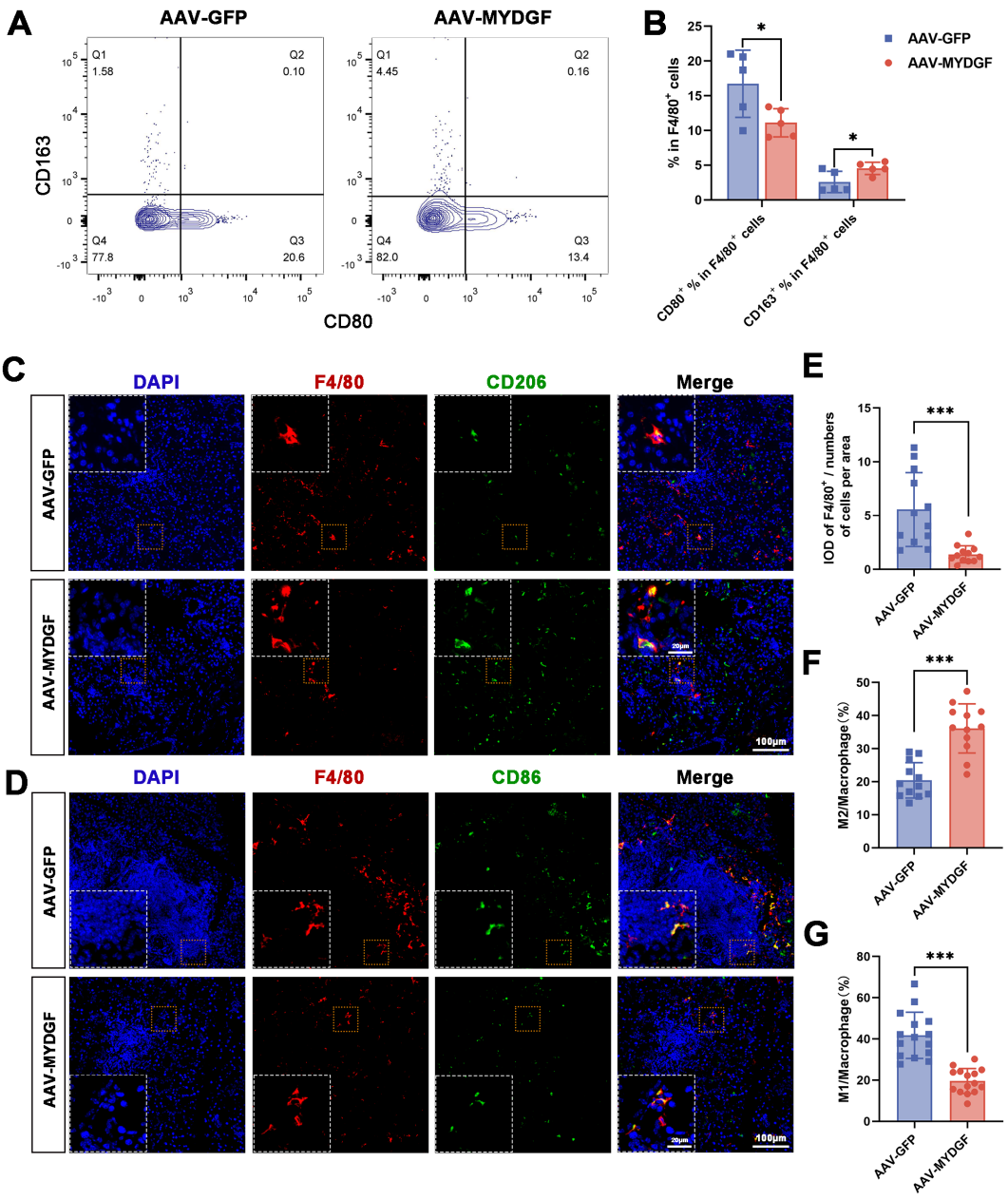

FIGURE 4
MYDGF inhibits the infiltration of Mϕ in the submandibular glands and induces polarization of M2ϕ. **(A, B)** Flow cytometry of the spleen showed that the ratio of M2ϕ ($F4/80^+/CD163^+$) was increased and the ratio of M1ϕ ($F4/80^+/CD80^+$) was decreased after treatment of MYDGF (* $p < 0.05$). **(C, E, F)** Double immunofluorescence of the submandibular glands with DAPI (blue), F4/80 (red), and CD206 (green) revealed that the numbers of positive of $F4/80^+$ cells was significantly decreased, and the ration of M2ϕ was significantly increased in the AAV-MYDGF group compared with the AAV-GPF group (scale bar: 100 and 20 μm, *** $p < 0.001$). **(D, G)** Double immunofluorescence of the submandibular glands with DAPI (blue), F4/80 (red), and CD86 (green) revealed that the ratio of M1ϕ was significantly decreased in the AAV-MYDGF group compared with the AAV-GPF group (scale bar: 100 and 20 μm, *** $p < 0.001$). Student's *t*-test was performed to compare difference between two groups with normal distribution.

activity. The expression of $CD86^+$ M1ϕ is significantly higher, while that of $CD206^+$ M2ϕ is significantly lower in the SGs and PBMCs of pSS patients compared to non-pSS controls (22). In the PBMCs of pSS patients, the high abundance of proinflammatory M1ϕ is accompanied by an increased presence of other immune cells, including T cells, B cells, and DCs (26). The portions of $CXCR3^+CD163^+$ M2ϕ decreased as disease severity increased, indicating that M2ϕ may contribute to the progression of pSS (29). Therefore, modulating the imbalance of Mϕ polarization could potentially serve as a promising therapeutic method to ameliorate pSS.

BMDCs release a broad range of soluble factors in a paracrine manner that may promote tissue protection and repair (30). MYDGF, also known as C19orf10, is abundantly found in various cellular microenvironments, including the calcium-rich endoplasmic reticulum and Golgi apparatus (31). It can be secreted and released from BMDCs as a potential paracrine active factor in response to stress (32). Recent studies have shown that

10.3389/fimmu.2024.1465938

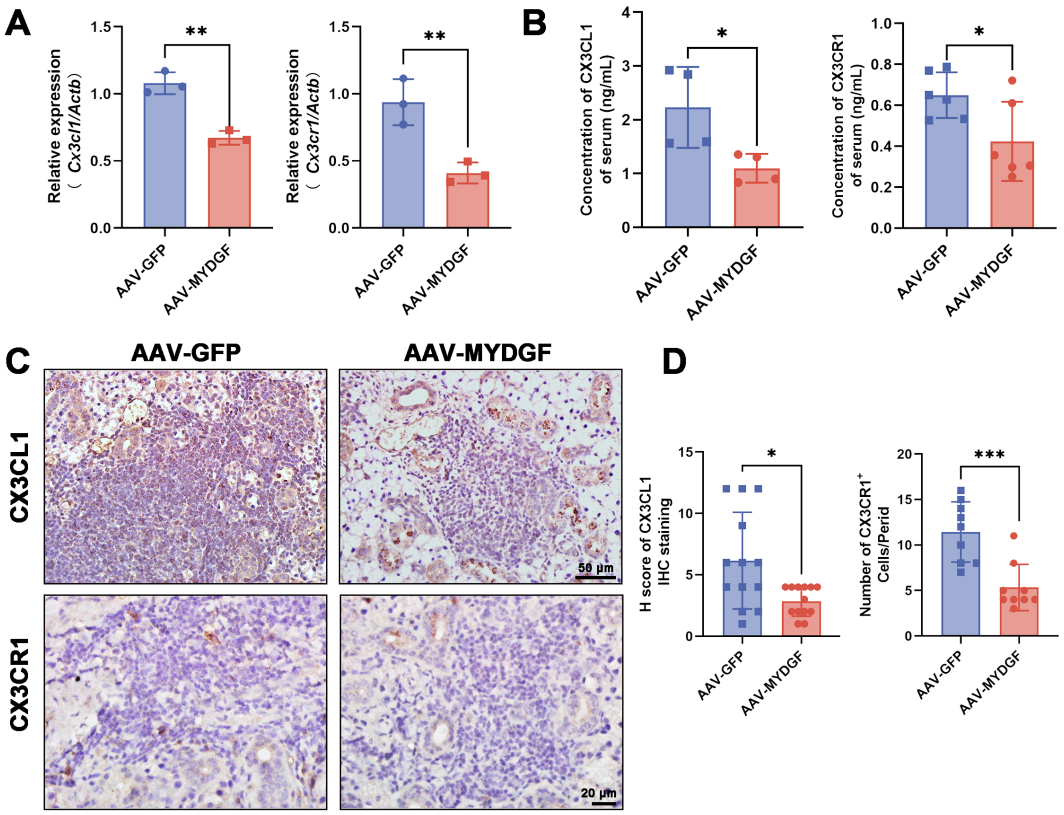

FIGURE 5
MYDGF inhibits inflammation via suppression of the CX3CL1/CX3CR1 axis. **(A)** RT-PCR showed that the mRNA expression of *Cx3cl1* and *Cx3cr1* of SGs was significantly decreased after treatment of MYDGF (** $p < 0.01$). **(B)** The concentration of CX3CL1 and CX3CR1 of serum measured by ELISA was significantly decreased after treatment of MYDGF (* $p < 0.05$). **(C, D)** Immunohistochemistry staining and quantitative analysis showed that MYDGF could decrease the expression of CX3CL1 and CX3CR1 of SGs (* $p < 0.05$; *** $p < 0.001$). Student's *t*-test was performed to compare differences between two groups with a normal distribution. The Kruskal–Wallis test was employed to compare differences with non-normal distribution.

MYDGF has potent cardiac myocyte-protective and angiogenic activities, offering protection against cardiovascular and metabolic diseases (14, 32–34). MYDGF reduces inflammation (TNF-a, IL-1β, and IL-6) and leukocyte homing, as well as Mϕ accumulation within aortic plaques (14). The present study confirmed that MYDGF alleviated the inflammatory response (IL-6 and TNF-α) in SGs, downregulated the TNF signaling pathway, and promoted immune cell apoptosis of the lymphocyte infiltration foci, thereby re-establishing the function of SGs. Our results demonstrated that MYDGF significantly reduces the infiltration of Mϕ. Consistent with this finding, MYDGF has a direct effect on Mϕ, as it has been reported to reduce their inflammation and migration (14). In addition, MYDGF enhance s the numbers and proportions of M2ϕ in a dextran sodium sulfate (DSS)–induced colitis model (13), and it decreases M1ϕ polarization while increasing M2ϕ polarization in primary Kupffer cells and in nonalcoholic fatty liver disease mouse model (15). Consistent with previous studies, our results demonstrate that MYDGF promote s the polarization of M2ϕ in SGs.

Furthermore, several cytokines and chemokines secreted by Mϕ contribute to the development of pSS (7). CX3CL1, the only member of the CX3C chemokine family, and its sole receptor, CX3CR1, are involved in the recruitment of monocytes/Mϕ and lymphocytes, playing crucial roles in various autoimmune diseases (35). The expression of fractalkine, the soluble chemokine CX3CL1 cleaved from membrane-bound CX3CL1, CX3CR1-expressed T cells, and Mϕ, was significantly elevated in the lacrimal glands of NOD/LtJ mice (36). CX3CL1 expression levels are higher in the serum of patients with SS compared to healthy controls, and $CX3CR1^+$ cells are found in close proximity to the inflammatory foci (8). Therefore, CX3CL1/CX3CR1 may serve as a novel tool for evaluating pSS. The present study found that treatment with MYDGF inhibited the expression of cytokines and chemokines, and the expression of CX3CL1 and CX3CR1 in the serum and SGs was significantly downregulated by MYDGF, indicating that MYDGF may reduce infiltration of the immune system by modulating the production of chemokines such as the CX3CL1/CX3CR1 axis.

The results of the present study imply that MYDGF significantly alleviates pSS by reducing inflammation and re-establishing SG function. MYDGF demonstrated the potential to inhibit Mϕ infiltration, suppress M1ϕ polarization, and promote M2ϕ polarization. In addition, MYDGF inhibited the expression of genes related to chemokines and inflammatory factors in the submandibular glands, particularly by significantly suppressing the CX3CL1/CX3CR1 axis, and promoted the apoptosis of immune cells within lymphatic infiltrates. However, the complex

signaling mechanisms by which MYDGF inhibits Mϕ migration and promotes M2ϕ polarization remain unclear, and the crucial role of the CX3CL1/CX3CR1 axis or other chemokines in migration and polarization requires further investigation in future research.

Data availability statement

The raw and processed data from RNA-Seq sequencing in this study have been deposited with the national center for biotechnology infromation (NCBI) under accession number PRJNA1169323 (https://www.ncbi.nlm.nih.gov/bioproject/PRJNA1169323).

Ethics statement

The animal study was approved by Ethics Review Commission of the Laboratory Animal Center of Capital Medical University. The study was conducted in accordance with the local legislation and institutional requirements.

Author contributions

ZY: Writing – review & editing, Writing – original draft. ML: Writing – original draft. ZC: Writing – original draft. CD: Writing – review & editing. YY: Writing – review & editing. CZ: Writing – review & editing. LH: Writing – review & editing.

Funding

The author(s) declare that financial support was received for the research, authorship, and/or publication of this article. This work was supported by the Beijing Stomatological Hospital, Capital Medical University Young Scientist Program (YSP202204, YSP202008); the Beijing Municipal Natural Science Foundation (7232070), National Natural Science Foundation of China (82370940, 82001065); the Beijing Hospitals Authority Youth Programme (QML20211502); and the Beijing Talents Fund (2018000021469G284).

Conflict of interest

The authors declare that the research was conducted in the absence of any commercial or financial relationships that could be construed as a potential conflict of interest.

Publisher's note

Supplementary material

The Supplementary Material for this article can be found online at: https://www.frontiersin.org/articles/10.3389/fimmu.2024.1465938/full#supplementary-material

SUPPLEMENTARY FIGURE 1
Transcriptome analysis of salivary glands of NOD/Ltj mice treated with AAV-GFP and AAV-MYDGF. **(A, B)** GO analysis.

SUPPLEMENTARY FIGURE 2
MYDGF ameliorates inflammation of SGs in NOD/Ltj mice. **(A, B)** Immunohistochemistry (IHC) staining and quantitative analysis showed that MYDGF could decrease the expression of TNF-a of SGs, *** $P < 0.001$; **(C, D)** IHC staining and quantitative analysis showed that MYDGF could decrease the expression of IL-6 of submandibular glands, *** $P < 0.001$. Scale bars: 100 and 50 μm. Student's t-test was performed to compare difference between two groups with normal distribution.

SUPPLEMENTARY FIGURE 3
The ratio of T helper lymphocyte subsets did not differ in the AAV-MYDGF and AAV-GFP groups. Flow cytometry showed the ratio of **(A)** Th1, **(B)** Th2, **(C)** Th17, **(D)** Treg were no significantly difference in the AAV-MYDGF and AAV-GFP group, ^{ns} no significant difference. Student's t-test was performed to compare difference between two groups with normal distribution.

SUPPLEMENTARY FIGURE 4
Chemokine- and cytokine-related gene of AAV-GFP and AAV-MYDGF group by qRT-PCR.

References

1. Tan Z, Wang L, Li X. Composition and regulation of the immune microenvironment of salivary gland in Sjögren's syndrome. *Front Immunol.* (2022) 13:967304. doi: 10.3389/fimmu.2022.967304

2. Felten R, Devauchelle-Pensec V, Seror R, Duffau P, Saadoun D, Hachulla E, et al. Interleukin 6 receptor inhibition in primary Sjögren syndrome: a multicentre double-blind randomised placebo-controlled trial. *Ann Rheum Dis.* (2021) 80:329–38. doi: 10.1136/annrheumdis-2020-218467

3. Xu J, Wang D, Liu D, Fan Z, Zhang H, Liu O, et al. Allogeneic mesenchymal stem cell treatment alleviates experimental and clinical Sjögren syndrome. *Blood.* (2012) 120:3142–51. doi: 10.1182/blood-2011-11-391144

4. Lai Z, Yin H, Cabrera-Pérez J, Guimaro MC, Afione S, Michael DG, et al. Aquaporin gene therapy corrects Sjögren's syndrome phenotype in mice. *Proc Natl Acad Sci U S A.* (2016) 113:5694–9. doi: 10.1073/pnas.1601992113

5. Zhan Q, Zhang J, Lin Y, Chen W, Fan X, Zhang D. Pathogenesis and treatment of Sjogren's syndrome: Review and update. *Front Immunol.* (2023) 14:1127417. doi: 10.3389/fimmu.2023.1127417

6. Baturone R, Soto MJ, Márquez M, Macías I, de Oca MM, Medina F, et al. Health-related quality of life in patients with primary Sjögren's syndrome: relationship with serum levels of proinflammatory cytokines. *Scand J Rheumatol.* (2009) 38:386–9. doi: 10.1080/03009740902973821

7. Liao J, Yu X, Huang Z, He Q, Yang J, Zhang Y, et al. Chemokines and lymphocyte homing in Sjögren's syndrome. *Front Immunol.* (2024) 15:1345381. doi: 10.3389/fimmu.2024.1345381

8. Astorri E, Scrivo R, Bombardieri M, Picarelli G, Pecorella I, Porzia A, et al. CX3CL1 and CX3CR1 expression in tertiary lymphoid structures in salivary gland infiltrates: fractalkine contribution to lymphoid neogenesis in Sjogren's syndrome. *Rheumatol (Oxford).* (2014) 53:611–20. doi: 10.1093/rheumatology/ket401

9. Tran SD, Sumita Y, Khalili S. Bone marrow-derived cells: A potential approach for the treatment of xerostomia. *Int J Biochem Cell Biol*. (2011) 43:5–9. doi: 10.1016/j.biocel.2010.10.010

10. Khalili S, Liu Y, Sumita Y, Maria OM, Blank D, Key S, et al. Bone marrow cells are a source of undifferentiated cells to prevent Sjögren's syndrome and to preserve salivary glands function in the non-obese diabetic mice. *Int J Biochem Cell Biol*. (2010) 42:1893–9. doi: 10.1016/j.biocel.2010.08.008

11. Kshitiz, Ellison DD, Suhail Y, Afzal J, Woo L, Kilic O, et al. Dynamic secretome of bone marrow-derived stromal cells reveals a cardioprotective biochemical cocktail. *Proc Natl Acad Sci U S A*. (2019) 116:14374–83. doi: 10.1073/pnas.1902598116

12. Ruiz EJ, Oeztuerk-Winder F, Ventura JJ. A paracrine network regulates the cross-talk between human lung stem cells and the stroma. *Nat Commun*. (2014) 5:3175. doi: 10.1038/ncomms4175

13. Yang Y, Zhao C, Yang Z, Du C, Chang Z, Wen X, et al. Myeloid-derived growth factor ameliorates dextran sodium sulfate-induced colitis by regulating macrophage polarization. *J Mol Med (Berl)*. (2024) 102:875-86. doi: 10.1007/s00109-024-02447-3

14. Meng B, Li Y, Ding Y, Xu X, Wang L, Guo B, et al. Myeloid-derived growth factor inhibits inflammation and alleviates endothelial injury and atherosclerosis in mice. *Sci Adv*. (2021) 7:eabe6903. doi: 10.1126/sciadv.abe6903

15. Ding Y, Xu X, Meng B, Wang L, Zhu B, Guo B, et al. Myeloid-derived growth factor alleviates non-alcoholic fatty liver disease alleviates in a manner involving IKKβ/NF-κB signaling. *Cell Death Dis*. (2023) 14:376. doi: 10.1038/s41419-023-05904-y

16. Shi H, Yu CQ, Xie LS, Wang ZJ, Zhang P, Zheng LY. Activation of TLR9-dependent p38MAPK pathway in the pathogenesis of primary Sjögren's syndrome in NOD/Ltj mouse. *J Oral Pathol Med*. (2014) 43:785–91. doi: 10.1111/jop.12209

17. Chivasso C, D'Agostino C, Parisis D, Soyfoo MS, Delporte C. Involvement of aquaporin 5 in Sjögren's syndrome. *Autoimmun Rev*. (2023) 22:103268. doi: 10.1016/j.autrev.2023.103268

18. Xu J, Liu O, Wang D, Wang F, Zhang D, Jin W, et al. *In vivo* generation of SSA/ro antigen-specific regulatory T cells improves experimental sjögren's syndrome in mice. *Arthritis Rheumatol*. (2022) 74:1699–705. doi: 10.1002/art.42244

19. Jang SI, Ong HL, Gallo A, Liu X, Illei G, Alevizos I. Establishment of functional acinar-like cultures from human salivary glands. *J Dent Res*. (2015) 94:304–11. doi: 10.1177/0022034514559251

20. Verstappen GM, Pringle S, Bootsma H, Kroese FGM. Epithelial-immune cell interplay in primary Sjögren syndrome salivary gland pathogenesis. *Nat Rev Rheumatol*. (2021) 17:333–48. doi: 10.1038/s41584-021-00605-2

21. Tian Y, Yang H, Liu N, Li Y, Chen J. Advances in pathogenesis of sjögren's syndrome. *J Immunol Res*. (2021) 2021:5928232. doi: 10.1155/2021/5928232

22. Chen X, Zhu L, Wu H. The role of M1/M2 macrophage polarization in primary Sjogren's syndrome. *Arthritis Res Ther*. (2024) 26:101. doi: 10.1186/s13075-024-03340-7

23. Ushio A, Arakaki R, Otsuka K, Yamada A, Tsunematsu T, Kudo Y, et al. CCL22-producing resident macrophages enhance T cell response in sjögren's syndrome. *Front Immunol*. (2018) 9:2594. doi: 10.3389/fimmu.2018.02594

24. Katsifis GE, Moutsopoulos NM, Wahl SM. T lymphocytes in Sjögren's syndrome: contributors to and regulators of pathophysiology. *Clin Rev Allergy Immunol*. (2007) 32:252–64. doi: 10.1007/s12016-007-8011-8

25. Nocturne G, Mariette X. B cells in the pathogenesis of primary Sjögren syndrome. *Nat Rev Rheumatol*. (2018) 14:133–45. doi: 10.1038/nrrheum.2018.1

26. Zong Y, Yang Y, Zhao J, Li L, Luo D, Hu J, et al. Characterisation of macrophage infiltration and polarisation based on integrated transcriptomic and histological analyses in Primary Sjögren's syndrome. *Front Immunol*. (2023) 14:1292146. doi: 10.3389/fimmu.2023.1292146

27. Stolp B, Thelen F, Ficht X, Altenburger LM, Ruef N, Inavalli V, et al. Salivary gland macrophages and tissue-resident CD8(+) T cells cooperate for homeostatic organ surveillance. *Sci Immunol*. (2020) 5:eaaz4371. doi: 10.1126/sciimmunol.aaz4371

28. Zhou D, Chen YT, Chen F, Gallup M, Vijmasi T, Bahrami AF, et al. Critical involvement of macrophage infiltration in the development of Sjögren's syndrome-associated dry eye. *Am J Pathol*. (2012) 181:753–60. doi: 10.1016/j.ajpath.2012.05.014

29. Aota K, Yamanoi T, Kani K, Nakashiro KI, Ishimaru N, Azuma M. Inverse correlation between the number of CXCR3(+) macrophages and the severity of inflammatory lesions in Sjögren's syndrome salivary glands: A pilot study. *J Oral Pathol Med*. (2018) 47:710–8. doi: 10.1111/jop.12756

30. Gnecchi M, Zhang Z, Ni A, Dzau VJ. Paracrine mechanisms in adult stem cell signaling and therapy. *Circ Res*. (2008) 103:1204–19. doi: 10.1161/circresaha.108.176826

31. Bortnov V, Annis DS, Fogerty FJ, Barretto KT, Turton KB, Mosher DF. Myeloid-derived growth factor is a resident endoplasmic reticulum protein. *J Biol Chem*. (2018) 293:13166–75. doi: 10.1074/jbc.AC118.002052

32. Xu J, Song Y, Ding S, Duan W, Xiang G, Wang Z. Myeloid-derived growth factor and its effects on cardiovascular and metabolic diseases. *Cytokine Growth Factor Rev*. (2024) 76:77–85. doi: 10.1016/j.cytogfr.2023.12.005

33. Korf-Klingebiel M, Reboll MR, Klede S, Brod T, Pich A, Polten F, et al. Myeloid-derived growth factor (C19orf10) mediates cardiac repair following myocardial infarction. *Nat Med*. (2015) 21:140–9. doi: 10.1038/nm.3778

34. Gao L, Li Z, Chang W, Liu Y, Zhang N. Myeloid-derived growth factor regulates high glucose-mediated apoptosis of gingival fibroblasts and induce AKT pathway activation and nuclear factor κB pathway inhibition. *J Dent Sci*. (2023) 18:636–44. doi: 10.1016/j.jds.2022.08.008

35. Ren M, Zhang J, Dai S, Wang C, Chen Z, Zhang S, et al. CX3CR1 deficiency exacerbates immune-mediated hepatitis by increasing NF-κB-mediated cytokine production in macrophage and T cell. *Exp Biol Med (Maywood)*. (2023) 248:117–29. doi: 10.1177/15353702221128573

36. Fu R, Guo H, Janga S, Choi M, Klinngam W, Edman MC, et al. Cathepsin S activation contributes to elevated CX3CL1 (fractalkine) levels in tears of a Sjögren's syndrome murine model. *Sci Rep*. (2020) 10:1455. doi: 10.1038/s41598-020-58337-4

frontiers | Frontiers in Immunology

TYPE Original Research
PUBLISHED 21 October 2024
DOI 10.3389/fimmu.2024.1448515

OPEN ACCESS

EDITED BY
Wai Po Chong,
Hong Kong Baptist University, China

REVIEWED BY
Lenin Pavón,
National Institute of Psychiatry Ramon de la Fuente Muñiz (INPRFM), Mexico
Julio César Flores González,
National Institute of Respiratory Diseases-Mexico (INER), Mexico

*CORRESPONDENCE
Elena V. Maryukhnich
maryukhnich@gmail.com
Leonid B. Margolis
leonidborisovichmargolis@gmail.com

†These authors have contributed equally to this work and share first authorship

‡These authors have contributed equally to this work and share senior authorship

RECEIVED 13 June 2024
ACCEPTED 25 September 2024
PUBLISHED 21 October 2024

CITATION
Vorobyeva DA, Potashnikova DM, Maryukhnich EV, Rusakovich GI, Tvorogova AV, Kalinskaya AI, Pinegina NV, Kovyrshina AV, Dolzhikova IV, Postnikov AB, Rozov FN, Sotnikova TN, Kanner DY, Logunov DY, Gintsburg AL, Vasilieva EJ and Margolis LB (2024) Cytokine production in an *ex vivo* model of SARS-CoV-2 lung infection. *Front. Immunol.* 15:1448515. doi: 10.3389/fimmu.2024.1448515

Cytokine production in an *ex vivo* model of SARS-CoV-2 lung infection

Daria A. Vorobyeva[1,2†], Daria M. Potashnikova[1,2†], Elena V. Maryukhnich[1,2*†], George I. Rusakovich[2], Anna V. Tvorogova[2], Anna I. Kalinskaya[1,2], Natalia V. Pinegina[1,2], Anna V. Kovyrshina[3], Inna V. Dolzhikova[3], Alexander B. Postnikov[4], Fedor N. Rozov[4], Tatiana N. Sotnikova[2], Dmitry Yu. Kanner[5], Denis Yu. Logunov[3], Alexander L. Gintsburg[3], Elena J. Vasilieva[1,2‡] and Leonid B. Margolis[6*‡]

[1]Laboratory of Atherothrombosis, Cardiology Department, Federal State Budgetary Educational Institution of Higher Education (FSBEI HE) "Russian University of Medicine" of the Ministry of Health of the Russian Federation, Moscow, Russia, [2]I.V. Davydovsky Moscow City Clinical Hospital, Moscow Department of Healthcare, Moscow, Russia, [3]Federal Government Budgetary Institution "The National Research Center for Epidemiology and Microbiology Named After Honorary Academician N.F. Gamaleya" of the Ministry of Health of the Russian Federation, Moscow, Russia, [4]HyTest Ltd, Turku, Finland, [5]Moscow City Oncology Hospital No 62, Moscow, Russia, [6]Faculty of Natural Sciences and Medicine, Ilia State University, Tbilisi, Georgia

Introduction: The mechanisms of the SARS-CoV-2-triggered complex alterations in immune cell activation and production of cytokines in lung tissue remain poorly understood, in part because of the limited use of adequate tissue models that simulate the structure and cell composition of the lung *in vivo*. We developed a novel *ex vivo* model of SARS-CoV-2 infection of lung explants, that maintains the intact tissue composition and the viral load for up to 7–10 days. Using this model, we studied cytokine production during SARS-CoV-2 infection.

Materials and methods: Lung tissue was monitored for viability and cell composition using flow cytometry and histological analysis. SARS-CoV-2 infection was verified immunohistochemically, viral loads in tissue and culture medium were monitored by qPCR. A panel of 41 cytokines was measured in culture medium using xMAP technology.

Results: The explant lung tissue was viable and maintained viral infection that influenced the cytokine production. Elevated concentrations of G-CSF, GM-CSF, GRO-a, IFN-g, IL-6, IL-8, IP-10, MCP-3, MIP-1a, PDGF-AA, and VEGF, and decreased IL-1RA concentration were observed in infected tissue compared to non-infected tissue.

Discussion: Our results generally reflect the data obtained in COVID-19 patients. GRO-a, IFN-g, IL-6, IL-8, MCP-1, MCP-3, and RANTES correlated with the viral

load, forming a distinct pro-inflammatory cluster. Thus, our lung *ex vivo* model faithfully reproduces some aspects of cytokine alterations in COVID-19 patients at an early disease stage, making the investigation of SARS-CoV-2 infection mechanisms more accessible and providing a potential platform for antiviral drug testing.

KEYWORDS

***ex vivo* model, lung explant *ex vivo* culture, SARS-CoV-2, COVID-19, cytokines, immune response, antiviral response**

1 Introduction

The new coronavirus disease COVID-19 has demonstrated a number of physiologic and metabolic abnormalities in the human organism that are associated with viral infection at both the systemic and the organ level. The systemic alterations, detected from blood plasma analysis, include a change in key metabolites and cytokine levels of the patients that might result in a cytokine storm syndrome – a severe systemic response to inflammation (1–4).

At the organ level, SARS-CoV-2 infection affects lung cells (especially type II alveolocytes), which show a high susceptibility to the SARS-CoV-2 both *in vivo* and *in vitro*, and probably constitute the primary trigger of inflammation (5–7). COVID-19 is often associated with pneumonia – a common inflammatory lung disease that has acquired a priority position in medical research as one of the main causes of death in severe COVID-19 cases (8). Pneumonia is characterized by damage to lung tissues that can occur both because of the direct virus action and of the excessive and uncontrolled immune response (9).

An immune response to SARS-CoV-2 *in vivo* includes a cooperative action of a wide range of immune cells, such as tissue-resident and infiltrating macrophages and dendritic cells that are responsible for phagocytosis and production of pro-inflammatory cytokines (10, 11), neutrophils that can produce NETs (neutrophil extracellular traps), trigger coagulation and thrombosis and participate in cytokine storm (12), and T cells that may boost the local inflammatory microenvironment and ensure persistent anti-viral protection *in situ* by IFNγ (13, 14). All of these cell types can facilitate virus eradication, but can lead to immune pathologies due to dysregulated immune responses (15). The effects of these cells are mediated by various stimuli, primarily cytokines, that have a prominent role in orchestrating cell populations in the inflammatory response to SARS-CoV-2 infection (16). Their action can both promote the resolution of disease and dysregulate the inflammation and stimulate life-threatening conditions (17, 18).

The mechanisms of the SARS-CoV-2-triggered complex alterations in immune cell activation, inactivation, production of cytokines, etc., have been poorly understood so far, in part because of the lack of adequate models that simulate the structure and cell composition of lung tissue *in vivo* and thus fail to faithfully reflect the complexity of the *in vivo* pathology. For instance, cell culture models provided important information regarding viral infection, but did not account for the 3D tissue organization and diverse cell content (19, 20). Organoid models were more physiological and diverse, yet they did not properly represent the lung immune microenvironment (21, 22). Animal models also did not faithfully represent some important aspects of human immune system and may not always allow to separate the local and the systemic immune responses (23). Hence, the lung explant models have several advantages, such as preserved organ structure, diversity of cell types, including the immune cells and a good potential to provide a relatively simple, cost-effective and accurate way to mimic the immune responses *in situ* observed during respiratory infections, such as COVID-19-associated pneumonia (24, 25). Here, we further developed a clinically relevant model of human lung explants that allows to mimic the initial events of SARS-CoV-2 infection and assess the viral effects on cytokine production.

2 Materials and methods

2.1 Ethics committee

The study was approved by the Moscow City Ethics Committee (protocol № 50/69_13.10.2020) of the Research Institute of the Organization of Health and Healthcare Management and performed according to the Declaration of Helsinki.

2.2 Specimens and reagents

We analyzed 18 post-mortem reference lung specimens obtained from individuals who died from COVID-19-associated pneumonia in April and May 2020. The clinical data on the patients are presented in Supplementary Table S1. The lung tissue specimens were stored in RNAlater RNA stabilization reagent (Qiagen, US) at -20°C for SARS-CoV-2 viral load assessment and as FFPE blocks for histological and immunohistochemical examination.

Lung tissue explants were obtained from the post-surgical material of 10 individuals with lung carcinoma who underwent lobectomy. The donors with primary lung carcinomas were used in this study. None of the individuals received treatment prior to surgery. Six specimens were obtained from NDRI (National Disease Research Interchange), four specimens were obtained in the Moscow City Clinical Hospital №62. The marginal part of the ectomized lung tissue was macroscopically intact, as assessed by the pathologist, and thus was excised for further tissue cultivation. The normal tissue morphology of the lung was additionally verified by histological examination of hematoxylin and eosin (H&E) tissue specimens on day 0 (tissue fixed on the day of surgery), thus the explants in the study corresponded to normal lung tissue.

The lung tissue of 6 individuals was used to set up the lung explant model, assess tissue viability and to analyze the immune cell content in cultured explants by flow cytometry.

The lung tissue of 4 individuals was used for SARS-CoV-2 infection experiments. The explant viability was monitored by lung tissue morphology on days 4, 7, and 10 of cultivation and compared to day 0. The viral infection was confirmed by qPCR and IHC. The cytokine concentrations were measured on beads using a commercial MILLIPLEX MAP Human kit (Merck Millipore).

All reagents used in the study are listed in Supplementary Table S2.

2.3 *Ex vivo* lung tissue

We delivered the lung tissue to the laboratory no later than 3 hours after surgery. We cut tissue under aseptic conditions into 2x2x2-mm blocks and randomly mixed them. Two blocks were fixed in 4% (v/v) formaldehyde (FA) for histological examination (day 0 of tissue culture). The rest of the tissue was cultured at the air–liquid interface on collagen rafts (Gelfoam, Pfizer, US). No fewer than 27 blocks of explants were placed into culture for each lung. The number of tissue blocks was 9 per 1/6 of gelfoam in a 6-well plate in culture medium containing RPMI-1640 (Gibco, Thermo Fisher Scientific, US), 15% (v/v) heat-inactivated FBS (HyClone, Cytiva, US); 1% (v/v) GlutaMAX (Gibco, Thermo Fisher Scientific); 1% (v/v) antibiotic/antimycotic (initial concentration 10,000 U/mL penicillin, 10,000 µg/mL streptomycin, 25 µg/ml amphotericin B, Gibco, Thermo Fisher Scientific); 1% (v/v) non-essential amino acids (Gibco, Thermo Fisher Scientific); 1% (v/v) sodium pyruvate (Gibco, Thermo Fisher Scientific). The tissue explants were cultured at 37°C in 5% CO_2.

2.4 Flow cytometry of lung tissue cells

Lung explants of 6 individuals were collected at day 4-5 of cultivation and digested with 5mg/ml collagenase IV and 40U/ml DNase 1 (Thermo Fisher, US) for 30 minutes on a thermomixer at 37°C, 800 rpm. Cells were released using a pestle and filtered through 40 µm strainers along with cells retained from the collagen raft. Cells were washed and centrifuged at 500g for 5 minutes and stained with Live-Dead fixable stain (AlexaFluor 350, Thermo Fisher, US) for 20 minutes at room temperature, washed and centrifuged. Cells were treated with a 1:100 dilution of Fc Block (BD Biosciences, US) in BD stain buffer for 10 minutes at room temperature, washed and centrifuged. Cells were incubated for 30 minutes at room temperature with the following mouse anti-human antibodies in a total volume of 100µl per condition in BD stain buffer: CD45-APC-R700, CD3-BV510, CD4-BUV661, CD8-BUV395, CD11c-PE-Cy7, CD14-BUV805, CD16-BUV737, CD56-BUV496, CD66b-AlexaFluor 647, CD123-PE, and HLA-DR-APC-Cy7 (all antibodies were produced by BD Biosciences). Cells were washed, centrifuged and resuspended in 250µl of 4% paraformaldehyde for 1 hour. Data acquisition was performed using a FACSymphony A5 instrument with FACSDiva 9.3.1 acquisition software (BD Biosciences). Compensation controls were used to calculate fluorescence spillover, fluorescence minus one controls were used for gating and data was analyzed with FlowJo 10.8.1 (BD Biosciences). The gating strategy involved exclusion of debris, setting singlet and live cell gates, defining the CD45+ leucocyte population, defining gates for monocytes/macrophages based on CD14 and CD16, dendritic cells based on HLA-DR, CD11c and CD123, granulocytes based on CD66b, and setting a lymphocyte gate followed by gates for CD3+CD4+ T helpers, CD3+CD8+ cytotoxic T cells, and CD3-CD56+ natural killer cells.

2.5 SARS-CoV-2 stock and infection

All experiments using infectious SARS-CoV-2 were performed in a biosafety level 3 (BSL3) laboratory. We used SARS-CoV-2 B.1.1.1 variant (GISAID EPI_ISL_421275) for lung explant infection. The viral stock solution contained 10^7 viral particles/mL as assessed from TCID50. The titration was performed on Vero E6 cell culture. The stock and its serial dilutions containing 10^6 and 10^5 particles/mL were used for infection.

After 24 h of cultivation, we replaced the culture medium to remove dead cells and cell debris, and infected the lung tissue with SARS-CoV-2 viral stock. We used serial stock dilutions of 10^5, 10^6, and 10^7 viral particles/mL and added 10 µL of viral stock on top of each tissue block. Therefore, we added 10^3, 10^4, and 10^5 viral particles on each lung explant. The number of blocks per collagen raft was 9; therefore, the total amount of viral particles in each well upon infection was $9x10^3$, $9x10^4$, or $9x10^5$. The tissue was incubated for 1 h at 37°C in 5% CO_2, and the culture medium was changed to the fresh medium without the virus. In parallel with infected tissue, we cultured the non-infected controls. Every 3 days of culture (days 4, 7, and 10), we fixed 2 blocks of tissue with 4% FA for further histological examination and immunohistochemistry analysis and 2 blocks with RNAlater RNA stabilization reagent (Qiagen, the Netherlands) for qPCR, and we collected and replaced the conditioned culture medium. The collected medium was centrifuged at 3,000 rpm for 15 min, aliquoted, and stored at -80°C prior to measurement of viral RNA load and cytokine concentrations. The study design is presented in Supplementary Figure S1.

2.6 Histology and immunohistochemistry

The lung tissue specimens, 2x2x2 mm in size (obtained on days 0; 4; 7 and 10 of cultivation) were fixed in 4% FA for further histological and immunohistochemical (IHC) examination. Specimens were dehydrated in 50%, 70%, 100% ethanol and toluene according to the standard procedure, cast in paraffin blocks, and used to make 4-µm paraffin sections stained with hematoxylin and eosin (H&E). The staining was performed according to the manufacturer's protocol; all dyes were provided by BioVitrum (Russia).

To confirm infection in cultured lung explants, we visualized SARS-CoV-2 N protein by immunohistochemistry on tissue sections. Anti-N protein antibodies (C706, rabbit monoclonal) were provided by HyTest (Finland) and used to detect SARS-CoV-2–infected cells. The preliminary step included incubation of the deparaffinized slides in 0.1% TritonX-100 for 1 h and blocking of the endogenous peroxidase using the Dual Endogenous Enzyme Block (Dako/Agilent, US) according to the manufacturer's instructions. We performed the rest of the staining procedure using the UltraVision detection HRP DAB kit (Thermo, US) according to the manufacturer's protocol. Additionally, anti-CD68 antibodies (mouse anti-human PG-M1; Talent Biomedical, China) were used to assess activated macrophages in the lung explants. The anti-CD68 staining was performed automatically using the Ventana BenchMark ULTRA system and reagents (Roche, Switzerland) according to the manufacturer's instructions. The nuclei in all IHC specimens were additionally stained with hematoxylin.

The stained specimens were dehydrated and mounted in Shandon-Mount medium (Thermo Fisher Scientific, US). We imaged the sections using a Leica DM2000 microscope and a Leica DFC7000 T camera (Leica, Germany).

2.7 RNA extraction

For total RNA extraction from lung tissue, two 2x2x2-mm cultured lung explants per each time point were stored at -20°C in RNAlater RNA stabilization reagent (Qiagen, Germany). We mechanically disrupted the tissue from RNAlater using a FastPrep homogenizer and 0.56–0.7-mm garnet flakes (MP Biomedicals, US) in 700 µL of RLT buffer (Qiagen, Germany) supplemented with 1% β-mercaptoethanol (Merck, Germany). The homogenized specimens were centrifuged at 10,000 g and the supernatants were processed according to the RNeasy mini kit protocol (Qiagen, Germany). Total RNA was eluted in 100 µL of nuclease-free water and stored at -20°C for further viral load estimation.

For total RNA extraction from the conditioned culture media, we used the RIBO-prep kit (AmpliSens, Russia) according to the manufacturer's protocol. Briefly, 100 µl of culture medium stored at -80°C was lysed, and nucleic acids were precipitated. The pellet obtained by centrifugation was washed and dissolved in 50 µL of nuclease-free water.

2.8 Reverse transcription qPCR

We detected SARS-CoV-2 RNA in the total RNA specimens of lung tissue and conditioned media using triple probe TaqMan real-time qPCR. We described the two sets of primers and probes for SARS-CoV-2 N2 and N3 detection previously (26) and used them simultaneously. We added the third primer/probe set for the *UBC* (ubiquitin C) gene as the internal normalization control. All primers and probes used for qPCR are listed in Supplementary Table S3.

The RNA solution (5 µL per well) was mixed with 5 µL of primer/probe mix and 10 µL of x2 OneTube RT-PCRmix (Sene, Russia). The PCR program was performed as follows: 20 min at 48°C for reverse transcription reaction followed by 5 min at 95°C, then 50 cycles, each comprising 20 s at 95°C, 20 s at 58°C, and 30 s at 72°C. All samples were analyzed in duplicates. For SARS-CoV-2 RNA copy number estimation, we generated the standard curve using 10-fold dilutions of synthetic DNA fragments containing N2 and N3 regions, as described previously (26).

2.9 Cytokine measurement

Forty-one cytokines in the culture medium were measured with a commercial kit MILLIPLEX MAP Human Cytokine/Chemokine Magnetic Bead Panel (Merck Millipore). The cytokine panel included interleukin-1α (IL-1α), IL-1β, IL-1RA (IL-1 receptor antagonist), IL-2, IL-3, IL-4, IL-5, IL-6, IL-7, IL-8, IL-9, IL-10, IL-12 (p40), IL-12 (p70), IL-13, IL-15, IL-17A, fractalkine (CX3CL1), growth-regulated alpha (GRO-α or CXCL1), interferon-γ-induced protein-10 (IP-10 or CXCL10), monocyte chemoattractant protein-1 (MCP-1 or CCL2), MCP-3 (CCL7), macrophage inflammatory protein-1α (MIP-1α or CCL3), MIP-1β (CCL4), regulated on activation normally T-cell expressed and secreted (RANTES or CCL5), eotaxin (CCL11), macrophage-derived chemokine (MDC or CCL22), soluble CD40-ligand (sCD40L), epidermal growth factor (EGF), fibroblast growth factor-2 (FGF-2), Fms-like tyrosine kinase 3 ligand (Flt-3L), vascular endothelial growth factor (VEGF), granulocyte colony-stimulating factor (G-CSF), granulocyte-macrophage colony-stimulating factor (GM-CSF), platelet-derived growth factor-AA (PDGF-AA), PDGF-AB/BB, transforming growth factor-α (TGF-α), interferon-α2 (IFN-α2), IFN-γ, tumor necrosis factor-α (TNF-α), and TNF-β.

The standard curve was built up from 8 standard dilutions in triplicates, with 1–3 standard dilutions with dilution factor 5 and 4–8 dilutions with dilution factor 4. We used culture medium to mimic the matrix effect on standard curves and blank wells. We used dilutions 1 and 1:50 with PBS (for cytokines with concentrations above the upper limit of detection).

Samples (25 µL) with dilutions 1 and 1:50, or standards and controls (25 µL), were diluted with 25 µL of assay buffer or with culture medium and incubated with 15 µL of 41-plex magnetic beads for 18 h at 4°C. Beads were washed twice manually with wash buffer on a magnet from the automatic magnetic washer ELx405 (Biotech) and incubated with detection antibodies for 1 h at 25°C.

Antibodies were diluted with wash buffer 1.93 times and added in the amount 25 µL per well. After incubation, we added 15 µL of streptavidin–PE solution to the wells and incubated for 30 min at 25°C. Beads were washed twice, fixed with 1% FA for 1 h at room temperature, washed, and resuspended in wash buffer and analyzed on a Luminex 200 instrument. We collected 50 beads per region. During the analysis, we used a 5PL fit for the standard curve.

Steps prior to bead fixation were performed at the BSL3 laboratory. Cytokine measurement on the Luminex 200 instrument was performed at the BSL2 laboratory.

2.10 Statistical analysis

Statistical analysis was performed with R 4.2.1 software. The expression values obtained in the present study were in most cases not normally distributed, according to the Shapiro-Wilk test. For group comparison, we used the Wilcoxon signed-rank test with continuity correction. In order to overcome errors from multiple comparisons we performed a Benjamini-Hochberg FDR correction with calculation of critical values for each comparison matched with corresponding *p*-values; we calculated adjusted *p* values and compared them with a critical value of 0.05, if not stated otherwise.

For the correlation analysis we used Spearman's correlation coefficients. The corresponding *p*-values with continuity correction for multiple comparisons were calculated. For calculation of Spearman's coefficient, correlations with $|R| \geq 0.5$ and p. adj.≤ 0.05 were treated as significant.

We performed cytokine clusterization by the K-medoids clustering (27) method, which is more robust to noises and outliers, instead of k-means. Elbow and Silhouette methods used to define the optimal number of clusters.

3 Results

3.1 Development of the *ex vivo* lung tissue model

3.1.1 Monitoring the lung tissue morphology using H&E sections

The normal morphology of intact lung tissue was confirmed by an experienced pathologist based on macroscopic evaluation and on H&E tissue sections analysis. A representative H&E stained lung tissue is provided in Supplementary Figure S2. The alveoli were not collapsed and retained normal morphology. The adjacent vessels contained a few erythrocytes and leucocytes. The cell nuclei remained intact, thus the non-stained part of the same lung specimen was considered normal and suitable for culturing.

To validate infected and non-infected lung explant viability, H&E staining was also employed. In the stained sections we assessed the collapsed vs. intact alveoli, tissue fibrosis and swelling, the presence of intact vs. lysed erythrocytes, cell karyolysis. The lung tissue morphology was mostly unaltered for up to day 7 of culture regardless of SARS-CoV-2 infection. We observed intact alveoli and cell nuclei (Supplementary Figures S3A–D). At day 10 we observed the collapse of the alveoli, in the specimens, the extracellular matrix was swollen and the erythrocytes were mostly lysed. However, the cells still contained intact nuclei with no karyolysis under all conditions (Supplementary Figures S3E, F). Thus, we concluded that the explants on the collagen rafts were generally viable up to day 10 of culture and thus were a suitable model for cytokine analysis.

3.1.2 Monitoring the immune cell content and viability by flow cytometry

Ex vivo lung tissue specimens of 6 individuals were analyzed for cell content and viability on day 4-5 of culture using flow cytometry. Figure 1A provides representative dot plots and the gating strategy for this analysis. The average amount of viable cells as evaluated by Live/Dead dye exclusion test on day 4-5 of culture was 81.8 ± 7.9% (Mean ± SEM). The average amount of CD45+ leucocytes recovered from digested lung explants and the underlying collagen raft, including both tissue-infiltrating cells and cells from the lung vessels was 47.5 ± 12.6% (Mean ± SEM). The average percentages of various leukocyte subpopulations are presented in Figure 1B. Thus the normal lung explants used for cultivation contained large amounts of viable diverse immune cells. The prevailing population of leukocytes were T helpers, followed by cytotoxic T cells. The intermediately represented populations were monocytes/macrophages and natural killer (NK) cells. The smallest populations observed were dendritic cells (DC) and granulocytes. The cytokine response provided by lung tissue with such immune cell content was further studied in SARS-CoV-2 infection experiments.

3.2 Immunohistochemical evaluation of infected lung tissue

The staining of 18 autopsy lung specimens with SARS-CoV-2-associated pneumonia was used to assess the frequency of infected cells during lung infection *in vivo*. The infected cells that were positive for SARS-CoV-2 N-protein were typically single or assembled in small groups within pneumonia autopsy lungs (Supplementary Figure S4). Similarly, we observed single SARS-CoV-2-positive cells or small cell groups in explants infected *ex vivo* on day 4 of culture. The non-infected control explants demonstrated no positive staining (Figures 2A, B). The infected explants also showed brighter staining for CD68 than the non-infected control explants (Figures 2C, D), probably reflecting macrophage activation in infected tissues. Thus, we used IHC staining to confirm the infection in the lung explants. The characteristic pattern of infected cells in the explants was similar to that in the autopsy pneumonia. However, we were not able to detect SARS-CoV-2-positive cells in infected lung explants on days 7 and 10 of culture (Supplementary Figure S5).

10.3389/fimmu.2024.1448515

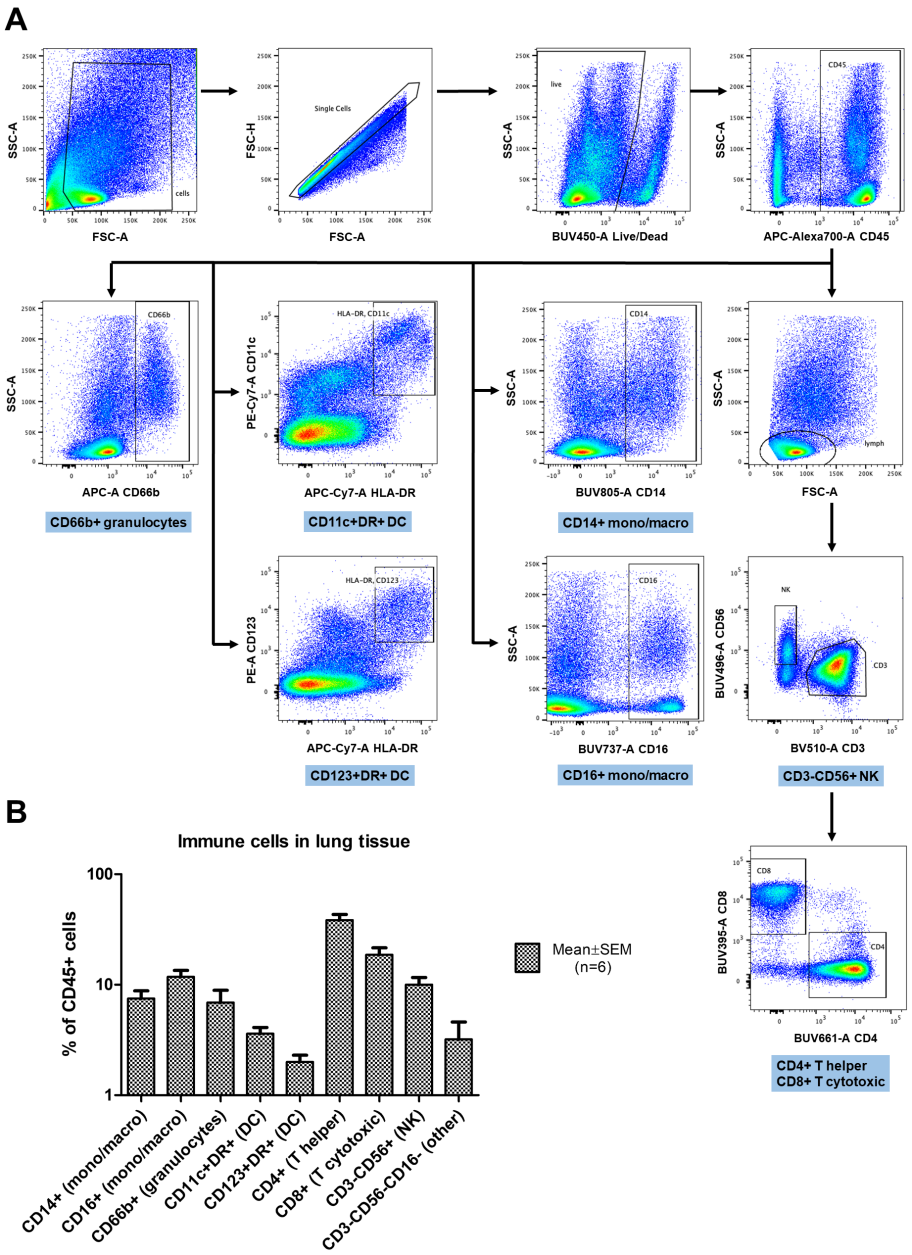

FIGURE 1
Flow cytometry analysis of immune cells in cultured lung explants enzymatically digested into cell suspensions. **(A)** The gating strategy: forward and side scatter (FSC, SSC) parameters were used to exclude debris and define single cell gates. Live cells were then identified and further limited to CD45+ leukocytes. Leukocyte subsets were defined based on expression of CD14 and CD16 (monocytes/macrophages); HLA-DR, CD11c, and CD123 (dendritic cells, DC); CD66b (granulocytes); CD3, CD4 and CD8 (T lymphocytes) or CD56 (natural killer cells, NK). **(B)** The percentages of leukocytes with specific subset markers in digested lung tissue (n=6), gated as shown in **(A)**. The data are presented as percentage of CD45+ cells (Mean ± SEM) in log scale.

3.3 SARS-CoV-2 RNA expression in lung *ex vivo* culture

To assess the SARS-CoV-2 RNA levels associated with COVID-19 pneumonia patient autopsies were used. In the 18 reference COVID-19-associated pneumonia autopsies the estimated viral load normalized by the *UBC* (ubiquitin C) reference gene mRNA varied in a broad range: the median normalized viral load in the sample set amounted to 0.0233 [0.0016; 0.2232] (Figure 3A). With the unknown infection efficiency, a large range of initial virus concentrations was proposed in the infection model: it was decided to test 3 viral particle concentrations to infect lung tissue explants; thus, tissue explants were inoculated with 10^5, 10^6, and 10^7 viral particles/mL. We then analyzed SARS-CoV-2 RNA content in tissue explants and in culture medium in dynamics. The *UBC*-normalized viral load in infected lung tissue explants fell in the same range as that in autopsy specimens (Figure 3A). *p* values for the comparisons of

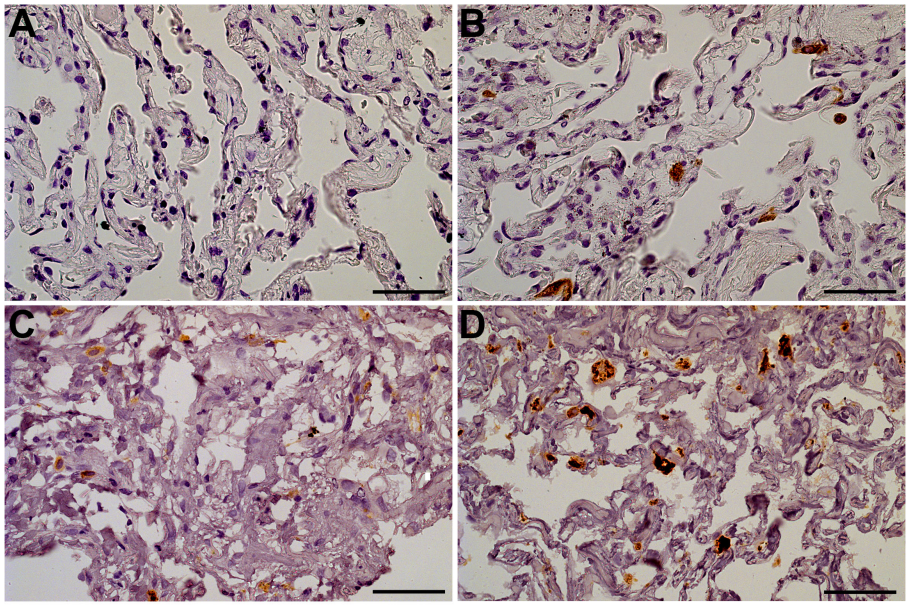

FIGURE 2
Lung tissue explants, day 4 of culture. The representative IHC stainings. **(A)** Anti-N-protein in a non-infected explant (specimen used as negative control); **(B)** Anti-N-protein in an explant infected with 10^7 viral particles/mL (specimen contains single positive cells); **(C)** Anti-CD68 in an non-infected explant (macrophages exhibit CD68-positive staining); **(D)** Anti-CD68 in an explant infected with 10^7 viral particles/mL (macrophages exhibit bright CD68-positive staining). Objective x40, scale bar 25 µm.

UBC-normalized viral load in autopsy specimens and tissue explants are presented in Supplementary Table S4.

The dynamics of viral RNA in the culture medium of infected tissue showed the presence of viral RNA during days 4, 7 and 10 of culture (Figure 3B). As viral load in tissue and culture medium in the infected lung *ex vivo* model was the highest after infection with 10^7 viral particles/mL, we used the culture medium of tissue infected at this concentration for further analysis of cytokines.

3.4 Cytokine production in infected tissue

For the values falling below LLOD (lower limit of detection, the concentration of the maximally diluted standard) or exceeding the ULOD (upper limit of detection, the concentration of the minimally diluted standard), the following imputation techniques were employed. Initially, the quantity of missing values was estimated for each cytokine, as depicted in the Supplementary Figure S6. IL-3

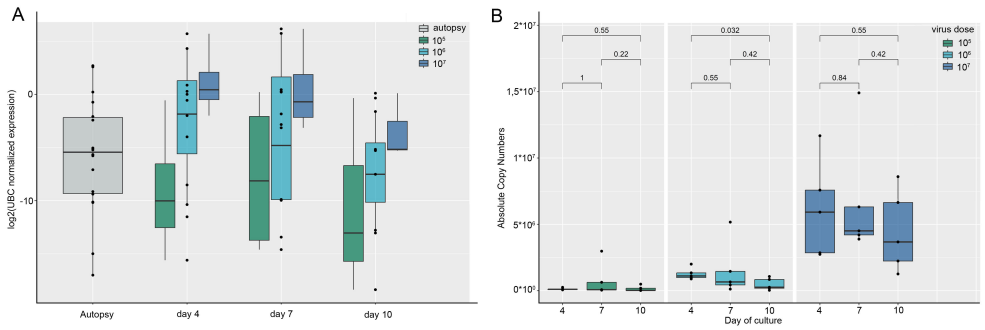

FIGURE 3
SARS-CoV-2 RNA expression in lung autopsy specimens compared to lung *ex vivo* culture. Presented are the results of individual experiments, medians and quartiles. **(A)** Tissue viral load. SARS-CoV-2 RNA tissue viral load normalized by the *UBC* reference gene in lung autopsy specimens and in lung tissue explants infected with SARS-CoV-2 during culture. The tissue viral load in the explants (except for 10^7 particles/mL on day 4) does not differ significantly from the autopsies. *p* values are presented in Supplementary Table S4; **(B)** Viral load in conditioned culture media. The dynamics of SARS-CoV-2 viral load expressed in RNA absolute copy numbers in the conditioned culture media of lung explants infected with different concentrations of SARS-CoV-2 viral particles. SARS-CoV-2 copy numbers were calculated as an average between N2 and N3 copy numbers.

had more than 40% missing and extrapolated values; therefore, we excluded it from the analysis. Conversely, the remaining cytokines had less than 40% missing or extrapolated values, rendering them eligible for further analysis. G-CSF, GRO-α, MCP-1, IL-6, and IL-8 were analyzed in dilution 1:50 because for these cytokines more than 40% of values were above the ULOD in dilution 1 and less than 40% of values were out of range in dilution 1:50. For the values below the LLOD, extrapolated values were used where available. Non-extrapolated cytokine concentrations below LLOD were replaced with the LLOD/2. Missed values above ULOD were replaced with ULOD.

We measured the concentrations of cytokines in the culture medium of lung tissue infected with 10^7 SARS-CoV-2 particles per mL and in the vehicle control. Culture medium was replaced 1 h after infection and then collected and replaced on days 4, 7, and 10. Measurement of cytokines was performed for each time-point separately; then the results for days 4, 7, and 10 were included in one sample and analyzed with the Wilcoxon signed-rank test. The final sample included 24 values (12 for infected tissue, 12 for non-infected tissue) for each cytokine. In infected tissue compared with control tissue, we found an elevation of G-CSF, GM-CSF, GRO-α, IFN-γ, IL-6, IL-8, IP-10, MCP-3, MIP-1α, PDGF-AA, and VEGF concentrations, and a decrease of the IL-1RA concentration (Figure 4). Prior to *p* adjustment, IL-10, MIP-1β, and TNF-α were also elevated in infected tissue. However, with *p* adjustment these cytokines had a trend for elevation and did not achieve statistical significance (Supplementary Table S5). Figure 4 shows cytokines differentially produced in infected vs. non-infected tissue. The results for all of the cytokines are presented in Supplementary Table S5. The dynamics of cytokine concentrations by time points during culture is presented in Supplementary Table S6.

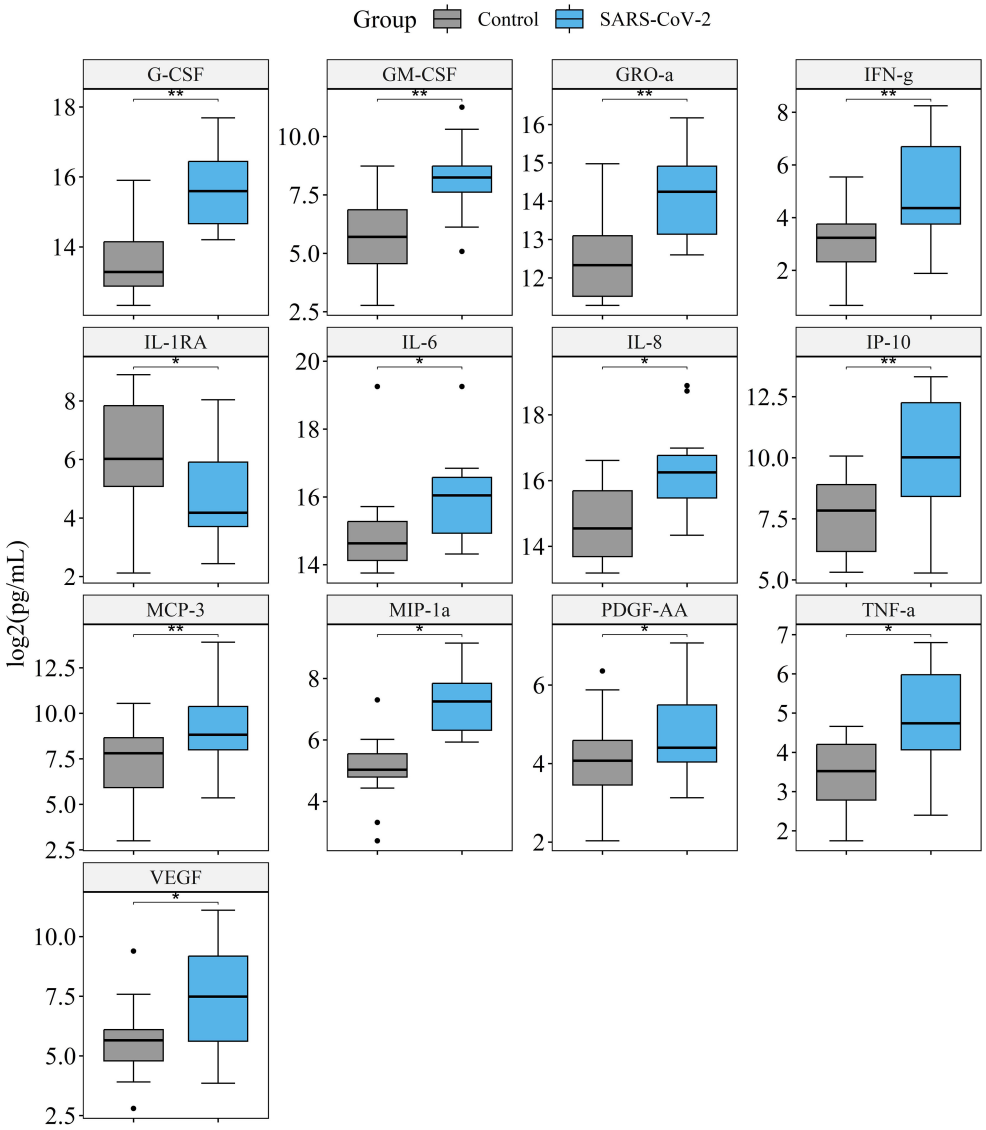

FIGURE 4
Comparison of cytokine production in the culture medium of lung tissue infected with 10^7 SARS-CoV-2 viral particles/mL, and vehicle control. Presented are the cytokines that significantly differ in infected vs. non-infected tissue. The final sample set included 12 values for infected tissue and 12 values for non-infected tissue were analyzed for each cytokine. *p. adj.<0.05, **p. adj.<0.01, Wilcoxon signed-rank test.

3.5 Correlations of cytokines with viral load

The correlation coefficients for cytokine levels for infected and non-infected tissue are provided in Figure 5 and Supplementary Figure S7 respectively. For infected tissue a correlation with viral load was also analyzed. We observed more positive correlations between cytokines in control (Supplementary Figure S7) than in infected tissue, which affected almost all measured cytokines. However, we found many new correlations (Spearman's correlation coefficient≥0.5, *p*. adj.≤0.05) for IL-1RA, IL-5, IP-10, and MIP-1α with other cytokines in the culture medium of infected tissue (Figure 5). We found 7 cytokines which correlated with viral load, namely: GRO-α, IFN-γ, IL-6, IL-8, MCP-1, MCP-3, and RANTES (Figure 5).

3.6 Clusterization of cytokines

We performed clusterization analysis of cytokines in infected (Figure 6A) and control tissue (Figure 6B) by K-medoids clustering method. The optimal number of clusters was calculated by Elbow and Silhouette methods.

We found three clusters of cytokines in infected tissues. Cluster 1 predominantly consisted of totally intercorrelated cytokines (Figure 6A). Cluster 1 contained only two cytokines that differed significantly in infected tissues and controls (GM-CSF and IL-1RA). Viral load and all of the cytokines which correlated with the viral load (GRO-α, IFN-γ, IL-6, IL-8, MCP-1, MCP-3, and RANTES) were included in cluster 2. Cytokines which differed between infected and control tissues were predominantly included in cluster 2 (G-CSF, GRO-α, IFN-γ, IL-6, IL-8, IP-10, MCP-3, and VEGF) and cluster 3 (MIP-1α, PDGF-AA, and trends for IL-10, MIP-1β, and TNF-α). Moreover, there were only three cytokines in clusters 2 and 3 which were not different in infected and non-infected tissues (IL-1α, IL-3, and MDC). Cytokines in cluster 3 had very few or no correlations.

Clusterization of cytokines in control tissues is shown in Figure 6B. Control tissues showed 5 clusters of cytokines; each cluster differed from clusters in infected tissues.

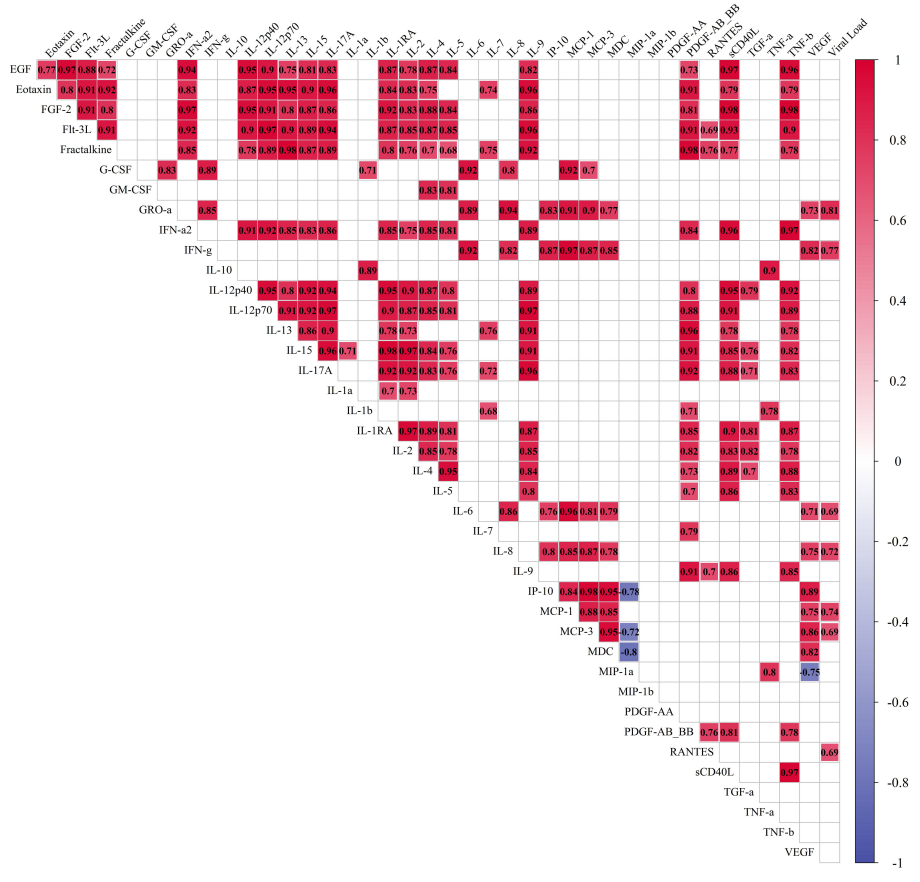

FIGURE 5
Correlations of cytokines in the culture medium of lung tissue infected with 10^7 viral particles of SARS-CoV-2 per mL. Measurement of cytokines was performed for each time point separately, and then the results for days 4, 7, and 10 were included in one sample. The final sample set included 12 values for each cytokine. Red: correlations with Spearman's correlation coefficient≥0.5, *p*. adj.≤0.05. Blue: correlations with Spearman's correlation coefficient≤-0.5, *p*. adj.≤0.05. The size of the filling of each cell corresponds to the value of the Spearman's correlation coefficient.

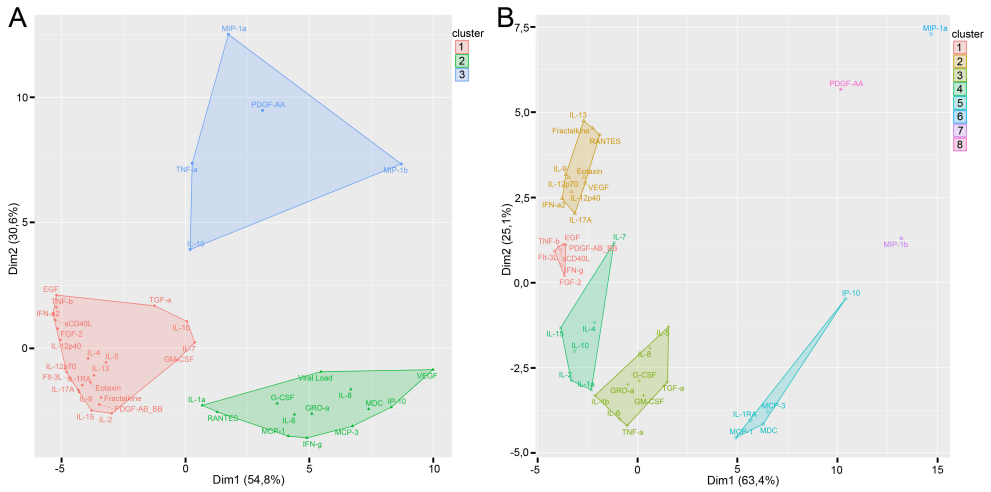

FIGURE 6
Clusterization of cytokines with K-medoids clustering method in infected tissue **(A)** and control tissue **(B)**. Optimal number of clusters was calculated by the Elbow and Silhouette methods.

4 Discussion

Many studies on SARS-CoV-2 infection are performed in animal models and cell cultures. Moreover, novel techniques are used, including transwell models, lung-on-a-chip systems, and lung organoids (28–35). However, more sophisticated models are needed to further reproduce the structure and complexity of human lung tissue. To study the immune response to SARS-CoV-2 under laboratory-controlled conditions, we developed an *ex vivo* model of SARS-CoV-2 infection based on our previous studies with other tissues including tonsil, placental, and atherosclerotic plaque cultures (36–38).

In our lung *ex vivo* model, we demonstrated cell viability and the predominance of T cells by flow cytometry and by lung tissue morphology similarly to other authors (39, 40). We confirmed that until day 10 we did not observe the collapse of the alveoli, extracellular matrix swelling and erythrocyte lysis in the specimens. Moreover, the nuclei remained intact even on day 10 of culture. The previous estimates of tissue viability (39) showed viable lung cells in cultured explants until days 10-17 even after the collapse of the alveoli.

Here, we showed that SARS-CoV-2 infection in our model occurred well within the tissue viability limits: We observed N-protein-positive cells on day 4 of culture but did not find them on days 7 and 10. We attribute the lack of infected cells after day 7 to their limited number in a small tissue block. Thus, all available cells in the model were infected within a short range of time and therefore the primary immune *in situ* response could be observed without contribution of the systemic host inflammatory response. We found that SARS-CoV-2-infected cells were disseminated within the lung explant similarly to the autopsy specimens and the viral load in our experiments was in the same range as in the COVID-19 autopsies. Thus, our *ex vivo* lung model and the used virus titers reflect some important aspects of patients' infection and allow to study *ex vivo* the initial stages of local cytokine response in the lung.

We hypothesized that since the architecture of the *ex vivo* lung tissue was largely preserved the cytokine profile in the SARS-CoV-2-infected model may correspond to the cytokine profile of infected lung tissue *in vivo*. To test this hypothesis, we measured the concentrations of 41 cytokines in the culture medium of infected and non-infected tissues using xMAP technology. We detected a significant elevation of G-CSF, GM-CSF, GRO-α, IFN-γ, IL-6, IL-8, IP-10, MCP-3, MIP-1α, PDGF-AA, and VEGF concentrations, and a reduction of the IL-1RA concentration in infected tissue. IL-10, MIP-1β, and TNF-α concentrations also tended to increase during SARS-CoV-2 infection. Most of the cytokines elevated in infected lung explants refer to pro-inflammatory response of innate and adaptive immunity and have been known to participate in lung inflammation of different types (41–54). Among the most prominent elevated cytokines we observed IL-6, a pleiotropic cytokine involved in host defense; its elevation may be a part of tissue response to viral infection and SARS-CoV-2-induced tissue injury (55). The elevation of IFN-γ may indicate the activation of antiviral response in the tissue. Interestingly, other authors who studied cytokines in lung explants reported interferon as missing in the anti-SARS-CoV-2 response (22, 56, 57) unlike the anti-H1N1 influenza or other coronaviruses. This apparent controversy may be due to the shorter culture period of the explants in these works. As our explants remained viable for 10 days, we were able to observe the cytokine response for longer and to detect the elevation of IFNγ in infected lung tissue.

Correlation and clusterization analyses revealed the cytokine pattern shift upon infection: three large clusters were formed upon SARS-CoV-2 infection, two of which contained the 11 upregulated cytokines. Moreover, we found GRO-α, IFN-γ, IL-6, IL-8, MCP-1, MCP-3, and RANTES to correlate with the viral load within a distinct cluster. These findings may indicate the cytokines in first line of involvement in SARS-CoV-2 infection.

We compared our results obtained in *ex vivo* culture with cytokine expression in COVID-19 patients in published studies

and found similarity in cytokine profiles. G-CSF, GRO-α, IFN-γ, IL-6, IL-8, IP-10, and MIP-1α, elevated in our study, were previously shown to be elevated in the blood of patients with COVID-19 (58–61). Moreover, G-CSF, IFN-γ, IL-6, IP-10, MCP-3, and MIP-1α were shown to be associated with the severity of COVID-19 (58, 59, 62–64). In our previous study, G-CSF, GM-CSF, IL-6, IL-8, MCP-3, MIP-1α, and VEGF were elevated in the total group of COVID-19 patients with short-term combined clinical endpoint (transfer to intensive care, high-flow oxygen therapy, lung ventilation, and in-hospital mortality). Among these cytokines IL-6 and G-CSF exhibited the strongest difference between patients with and without the clinical endpoint. Moreover, IL-6 had the highest prognostic value for prediction of clinical endpoint in COVID-19 patients (65). Thus, a number of early stage cytokines detected in the lung tissue *ex vivo* are essentially similar to the cytokines that drive the systemic host response *in vivo*.

Taken together, our lung *ex vivo* explants retain their viability and support SARS-CoV-2 infection importantly reproducing the tissue viral load and infection dissemination through the tissue as well as the early stage cytokine profile characteristic of COVID-19 patients. As we have previously shown on other explanted tissues, such models are suitable for drug testing (66, 67) and co-infection studies (68–70). The developed system provides a laboratory-controlled model to investigate the mechanisms of lung infection by SARS-CoV-2 and by other viruses and potentially may be used for pre-clinical antiviral drug testing.

Data availability statement

The data that support the findings of this study are openly available at https://github.com/GeorgeRusakovich/Cytokine-production-in-ex-vivo-model-of-SARS-CoV-2-lung-infection.

Ethics statement

The studies involving humans were approved by Moscow City Ethics Committee (protocol number; 50/69_13.10.2020) of the Research Institute of the Organization of Health and Healthcare Management and performed according to the Declaration of Helsinki. The studies were conducted in accordance with the local legislation and institutional requirements. The participants provided their written informed consent to participate in this study.

Author contributions

DV: Writing – original draft, Validation, Methodology, Investigation, Data curation, Conceptualization, Visualization. DP: Writing – review & editing, Writing – original draft, Visualization, Validation, Methodology, Investigation, Data curation, Conceptualization. EM: Writing – original draft, Validation, Methodology, Investigation, Data curation, Conceptualization. GR: Writing – original draft, Visualization, Validation, Methodology, Investigation, Formal analysis, Data curation. AT: Writing – original draft, Visualization, Methodology, Investigation. AK: Writing – review & editing, Project administration, Data curation, Conceptualization. NP: Writing – review & editing, Investigation. AK: Writing – review & editing, Methodology, Investigation. ID: Writing – review & editing, Methodology. AP: Writing – review & editing, Methodology. FR: Writing – review & editing, Methodology. TS: Writing – review & editing, Methodology, Investigation. DK: Writing – review & editing, Resources. DL: Writing – review & editing, Methodology. AG: Writing – review & editing, Resources, Methodology. EV: Writing – review & editing, Supervision, Project administration, Funding acquisition. LM: Writing – review & editing, Supervision.

Funding

The author(s) declare financial support was received for the research, authorship, and/or publication of this article. This study was funded by Moscow Center for Innovative Technologies in Healthcare. This research was funded by grant from the Moscow government (research project 0803-5/23).

Acknowledgments

We thank Wendy Fitzgerald and Christophe Vanpouille for their invaluable help and consulting in cytokine measurement and analysis. We thank Barry Alpher for his assistance in editing and improving English style.

Conflict of interest

Authors AP and FR were employed by HyTest Ltd.

The remaining authors declare that the research was conducted in the absence of any commercial or financial relationships that could be construed as a potential conflict of interest.

Publisher's note

Supplementary material

The Supplementary Material for this article can be found online at: https://www.frontiersin.org/articles/10.3389/fimmu.2024.1448515/full#supplementary-material

References

1. Yang L, Xie X, Tu Z, Fu J, Xu D, Zhou Y. The signal pathways and treatment of cytokine storm in COVID-19. *Signal Transduct Target Ther*. (2021) 6:255. doi: 10.1038/s41392-021-00679-0

2. Montazersaheb S, Hosseiniyan Khatibi SM, Hejazi MS, Tarhriz V, Farjami A, Ghasemian Sorbeni F, et al. COVID-19 infection: an overview on cytokine storm and related interventions. *Virol J*. (2022) 19:92. doi: 10.1186/s12985-022-01814-1

3. Zanza C, Romenskaya T, Manetti AC, Franceschi F, La Russa R, Bertozzi G, et al. Cytokine storm in COVID-19: immunopathogenesis and therapy. *Medicina (Kaunas)*. (2022) 58:144. doi: 10.3390/medicina58020144

4. Cron RQ. No perfect therapy for the imperfect COVID-19 cytokine storm. *Lancet Rheumatol*. (2022) 4:e308–10. doi: 10.1016/S2665-9913(22)00068-6

5. Rosa RB, Dantas WM, do Nascimento JCF, da Silva MV, de Oliveira RN, Pena LJ. *In vitro* and *in vivo* models for studying SARS-CoV-2, the etiological agent responsible for COVID-19 pandemic. *Viruses*. (2021) 13:379. doi: 10.3390/v13030379

6. Calkovska A, Kolomaznik M, Calkovsky V. Alveolar type II cells and pulmonary surfactant in COVID-19 era. *Physiol Res*. (2021) 70:S195–208. doi: 10.33549/physiolres.934763

7. Eling VA, Semenova NY, Bikmurzina AE, Kruglova NM, Rybalchenko OV, Markov AG. SARS-CoV-2-induced pathology-relevance to COVID-19 pathophysiology. *Pathophysiology*. (2022) 29:281–97. doi: 10.3390/pathophysiology29020021

8. Elezkurtaj S, Greuel S, Ihlow J, Michaelis EG, Bischoff P, Kunze CA, et al. Causes of death and comorbidities in hospitalized patients with COVID-19. *Sci Rep*. (2021) 11:4263. doi: 10.1038/s41598-021-82862-5

9. Alipoor SD, Jamaati H, Tabarsi P, Mortaz E. Immunopathogenesis of pneumonia in COVID-19. *Tanaffos*. (2020) 19:79–82.

10. Sefik E, Qu R, Junqueira C, Kaffe E, Mirza H, Zhao J, et al. Inflammasome activation in infected macrophages drives COVID-19 pathology. *Nature*. (2022) 606:585–93. doi: 10.1038/s41586-022-04802-1

11. García-Nicolás O, Godel A, Zimmer G, Summerfield A. Macrophage phagocytosis of SARS-CoV-2-infected cells mediates potent plasmacytoid dendritic cell activation. *Cell Mol Immunol*. (2023) 20:835–49. doi: 10.1038/s41423-023-01039-4

12. Zhu Y, Chen X, Liu X. NETosis and neutrophil extracellular traps in COVID-19: immunothrombosis and beyond. *Front Immunol*. (2022) 13:838011. doi: 10.3389/fimmu.2022.838011

13. Shakiba MH, Gemünd I, Beyer M, Bonaguro L. Lung T cell response in COVID-19. *Front Immunol*. (2023) 14:1108716. doi: 10.3389/fimmu.2023.1108716

14. Pieren DKJ, Kuguel SG, Rosado J, Robles AG, Rey-Cano J, Mancebo C, et al. Limited induction of polyfunctional lung-resident memory T cells against SARS-CoV-2 by mRNA vaccination compared to infection. *Nat Commun*. (2023) 14:1887. doi: 10.1038/s41467-023-37559

15. Sayahinouri M, Mashayekhi Firouz S, Ebrahimi Sadrabadi A, Masoudnia M, Abdolahi M, Jafarzadeh F, et al. Functionality of immune cells in COVID-19 infection: development of cell-based therapeutics. *Bioimpacts*. (2023) 13:159–79. doi: 10.34172/bi.2023.23839

16. Hasanvand A. COVID-19 and the role of cytokines in this disease. *Inflammopharmacology*. (2022) 30:789–98. doi: 10.1007/s10787-022-00992-2

17. Tang Y, Liu J, Zhang D, Xu Z, Ji J, Wen C. Cytokine storm in COVID-19: the current evidence and treatment strategies. *Front Immunol*. (2020) 11:1708. doi: 10.3389/fimmu.2020.01708

18. Coperchini F, Chiovato L, Ricci G, Croce L, Magri F, Rotondi M. The cytokine storm in COVID-19: Further advances in our understanding the role of specific chemokines involved. *Cytokine Growth Factor Rev*. (2021) 58:82–91. doi: 10.1016/j.cytogfr.2020.12.005

19. Pires De Souza GA, Le Bideau M, Boschi C, Wurtz N, Colson P, Aherfi S, et al. Choosing a cellular model to study SARS-CoV-2. *Front Cell Infect Microbiol*. (2022) 12:1003608. doi: 10.3389/fcimb.2022.1003608

20. Pizzorno A, Padey B, Julien T, Trouillet-Assant S, Traversier A, Errazuriz-Cerda E, et al. Characterization and treatment of SARS-CoV-2 in nasal and bronchial human airway epithelia. *Cell Rep Med*. (2020) 1:100059. doi: 10.1016/j.xcrm.2020.100059

21. Youhanna S, Wright SC, Lauschke VM. Organotypic human ex vivo models for coronavirus disease 2019 research and drug development. *Curr Opin Pharmacol*. (2021) 59:11–8. doi: 10.1016/j.coph.2021.04.006

22. Hui KPY, Ching RHH, Chan SKH, Nicholls JM, Sachs N, Clevers H, et al. Tropism, replication competence, and innate immune responses of influenza virus: an analysis of human airway organoids and ex-vivo bronchus cultures. *Lancet Respir Med*. (2018) 6:846–54. doi: 10.1016/S2213-2600(18)30236-4

23. Fan C, Wu Y, Rui X, Yang Y, Ling C, Liu S, et al. Animal models for COVID-19: advances, gaps and perspectives. *Signal Transduct Target Ther*. (2022) 7:220. doi: 10.1038/s41392-022-01087-8

24. Valenzi E, Tabib T, Lafyatis RA. Direct lung explant culture is an efficacious model for testing therapeutics in primary SSc-ILD tissue. *Am J Respir Crit Care Med*. (2024) 209:A2535. doi: 10.1164/ajrccm-conference.2024.A71

25. Xia JY, Zeng YF, Wu XJ, Xu F. Short-term ex vivo tissue culture models help study human lung infectionsA review. *Medicine*. (2023) 102:e32589. doi: 10.1097/MD.0000000000032589

26. Komissarov A, Molodtsov I, Ivanova O, Maryukhnich E, Kudryavtseva S, Mazus A, et al. High SARS-CoV-2 load in the nasopharynx of patients with a mild form of COVID-19 is associated with clinical deterioration regardless of the hydroxychloroquine administration. *PLoS One*. (2021) 16:e0246396. doi: 10.1371/journal.pone.0246396

27. Kaufman L, Rousseeuw PJ. *Finding Groups in Data: An Introduction to Cluster Analysis*. Hoboken: John Wiley & Sons, Inc. (1990) p. 68–125.

28. Heinen N, Klöhn M, Steinmann E, Pfaender S. *In vitro* lung models and their application to study SARS-CoV-2 pathogenesis and disease. *Viruses*. (2021) 13:792. doi: 10.3390/v13050792

29. Sun AM, Hoffman T, Luu BQ, Ashammakhi N, Li S. Application of lung microphysiological systems to COVID-19 modeling and drug discovery: a review. *Biodes Manuf*. (2021) 4:757–75. doi: 10.1007/s42242-021-00136-5

30. Zhang M, Wang P, Luo R, Wang Y, Li Z, Guo Y, et al. Biomimetic human disease model of SARS-CoV-2-induced lung injury and immune responses on organ chip system. *Adv Sci (Weinh)*. (2021) 8:2002928. doi: 10.1002/advs.202002928

31. Si L, Bai H, Rodas M, Cao W, Oh CY, Jiang A, et al. human-airway-on-a-chip for the rapid identification of candidate antiviral therapeutics and prophylactics. *Nat BioMed Eng*. (2021) 5:815–29. doi: 10.1038/s41551-021-00718-9

32. Tiwari SK, Wang S, Smith D, Carlin AF, Rana TM. Revealing tissue-specific SARS-CoV-2 infection and host responses using human stem cell-derived lung and cerebral organoids. *Stem Cell Rep*. (2021) 16:437–45. doi: 10.1016/j.stemcr.2021.02.005

33. Han Y, Yang L, Lacko LA, Chen S. Human organoid models to study SARS-CoV-2 infection. *Nat Methods*. (2022) 19:418–28. doi: 10.1038/s41592-022-01453-y

34. Kim J, Koo BK, Clevers H. Organoid studies in COVID-19 research. *Int J Stem Cells*. (2022) 15:3–13. doi: 10.15283/ijsc21251

35. Boroojerdi MH, Al Jabry T, Mirarefin SMJ, Albalushi H. Insights into organoid-based modeling of COVID-19 pathology. *Virol J*. (2023) 20:37. doi: 10.1186/s12985-023-01996-2

36. Introini A, Vanpouille C, Fitzgerald W, Broliden K, Margolis L. Ex vivo infection of human lymphoid tissue and female genital mucosa with human immunodeficiency virus 1 and histoculture. *J Vis Exp*. (2018) 140):57013. doi: 10.3791/57013

37. Fitzgerald W, Gomez-Lopez N, Erez O, Romero R, Margolis L. Extracellular vesicles generated by placental tissues ex vivo: A transport system for immune mediators and growth factors. *Am J Reprod Immunol*. (2018) 80:e12860. doi: 10.1111/aji.12860

38. Lebedeva A, Vorobyeva D, Vagida M, Ivanova O, Felker E, Fitzgerald W, et al. Ex vivo culture of human atherosclerotic plaques: A model to study immune cells in atherogenesis. *Atherosclerosis*. (2017) 267:90–8. doi: 10.1016/j.atherosclerosis.2017.10.003

39. Stoner GD. Explant culture of human peripheral lung. *Methods Cell Biol*. (1980) 21A:65–77. doi: 10.1016/s0091-679x(08)60758-x

40. Nicholas B, Staples KJ, Moese S, Meldrum E, Ward J, Dennison P, et al. A novel lung explant model for the ex vivo study of efficacy and mechanisms of anti-influenza drugs. *J Immunol*. (2015) 194:6144–54. doi: 10.4049/jimmunol.1402283

41. Aggarwal A, Baker CS, Evans TW, Haslam P.L. G-CSF. and IL-8 but not GM-CSF correlate with severity of pulmonary neutrophilia in acute respiratory distress syndrome. *Eur Respir J*. (2000) 15:895–901. doi: 10.1034/j.1399-3003.2000.15e14.x

42. Chen Y, Li F, Hua M, Liang M, Song C. Role of GM-CSF in lung balance and disease. *Front Immunol*. (2023) 14:1158859. doi: 10.3389/fimmu.2023.1158859

43. McCormick TS, Hejal RB, Leal LO, Ghannoum MA. GM-CSF: orchestrating the pulmonary response to infection. *Front Pharmacol*. (2022) 12:735443. doi: 10.3389/fphar.2021.735443

44. Villard J, Dayer-Pastore F, Hamacher J, Aubert JD, Schlegel-Haueter S, Nicod LP. GRO alpha and interleukin-8 in Pneumocystis carinii or bacterial pneumonia and adult respiratory distress syndrome GRO alpha and interleukin-8 in Pneumocystis carinii or bacterial pneumonia and adult respiratory distress syndrome. *Am J Respir Crit Care Med*. (1995) 152:1549–54. doi: 10.1164/ajrccm.152.5.7582292

45. Paudel S, Baral P, Ghimire L, Bergeron S, Jin L, DeCorte JA, et al. CXCL1 regulates neutrophil homeostasis in pneumonia-derived sepsis caused by Streptococcus pneumoniae serotype 3. *Blood*. (2019) 133:1335–45. doi: 10.1182/blood-2018-10-878082

46. Gomez JC, Yamada M, Martin JR, Dang H, Brickey WJ, Bergmeier W, et al. Mechanisms of interferon-γ production by neutrophils and its function during Streptococcus pneumoniae pneumonia. *Am J Respir Cell Mol Biol*. (2015) 52:349–64. doi: 10.1165/rcmb.2013-0316OC

47. Paats MS, Bergen IM, Hanselaar WE, Groeninx van Zoelen EC, Hoogsteden HC, Hendriks RW, et al. Local and systemic cytokine profiles in nonsevere and severe community-acquired pneumonia. *Eur Respir J*. (2013) 41:1378–85. doi: 10.1183/09031936.00060112

48. Yang Y, Shen C, Li J, Yuan J, Wei J, Huang F, et al. Plasma IP-10 and MCP-3 levels are highly associated with disease severity and predict the progression of COVID-19. *J Allergy Clin Immunol*. (2020) 146:119–127.e4. doi: 10.1016/j.jaci.2020.04.027

49. Chollet-Martin S, Montravers P, Gibert C, Elbim C, Desmonts JM, Fagon JY, et al. High levels of interleukin-8 in the blood and alveolar spaces of patients with pneumonia and adult respiratory distress syndrome. *Infect Immun*. (1993) 61:4553–9. doi: 10.1128/iai.61.11.4553-4559.1993

50. Standiford TJ, Kunkel SL, Greenberger MJ, Laichalk LL, Strieter RM. Expression and regulation of chemokines in bacterial pneumonia. *J Leukoc Biol*. (1996) 59:24–8. doi: 10.1002/jlb.59.1.24

51. Bhavsar I, Miller CS, Al-Sabbagh M. Macrophage inflammatory protein-1 alpha (MIP-1 alpha)/CCL3: as a biomarker. *Gen Methods biomark Res their Applications*. (2015), 223–49. doi: 10.1007/978-94-007-7696-8_27

52. Papaioannou AI, Kostikas K, Kollia P, Gourgoulianis KI. Clinical implications for vascular endothelial growth factor in the lung: friend or foe? *Respir Res*. (2006) 7:128. doi: 10.1186/1465-9921-7-128

53. Noskovičová N, Petřek M, Eickelberg O, Heinzelmann K. Platelet-derived growth factor signaling in the lung. From lung development and disease to clinical studies. *Am J Respir Cell Mol Biol*. (2015) 52:263–84. doi: 10.1165/rcmb.2014-0294TR

54. Verma N, Awasthi S, Pandey AK, Gupta P. Assessment of interleukin 1 receptor antagonist (IL-1RA) levels in children with and without community acquired pneumonia: a hospital based case-control study. *J Trop Pediatr*. (2023) 69:fmad040. doi: 10.1093/tropej/fmad040

55. Wang X, Tang G, Liu Y, Zhang L, Chen B, Han Y, et al. The role of IL-6 in coronavirus, especially in COVID-19. *Front Pharmacol*. (2022) 13:1033674. doi: 10.3389/fphar.2022.1033674

56. Alfi O, Yakirevitch A, Wald O, Wandel O, Izhar U, Oiknine-Djian E, et al. Human nasal and lung tissues infected ex vivo with SARS-CoV-2 provide insights into differential tissue-specific and virus-specific innate immune responses in the upper and lower respiratory tract. *J Virol*. (2021) 95:e0013021. doi: 10.1128/JVI.00130-21

57. Chu H, Chan JF, Wang Y, Yuen TT, Chai Y, Hou Y, et al. Comparative replication and immune activation profiles of SARS-CoV-2 and SARS-CoV in human lungs: an ex vivo study with implications for the pathogenesis of COVID-19. *Clin Infect Dis*. (2020) 71:1400–9. doi: 10.1093/cid/ciaa410

58. Huang C, Wang Y, Li X, Ren L, Zhao J, Hu Y, et al. Clinical features of patients infected with 2019 novel coronavirus in Wuhan, China. *Lancet*. (2020) 395:497–506. doi: 10.1016/S0140-6736(20)30183-5

59. Lucas C, Wong P, Klein J, Castro TBR, Silva J, Sundaram M, et al. Longitudinal analyses reveal immunological misfiring in severe COVID-19. *Nature*. (2020) 584:463–9. doi: 10.1038/s41586-020-2588-y

60. Ribeiro Dos Santos Miggiolaro AF, da Silva Motta Junior J, Busatta Vaz de Paula C, Nagashima S, Alessandra Scaranello Malaquias M, Baena Carstens L, et al. Covid-19 cytokine storm in pulmonary tissue: Anatomopathological and immunohistochemical findings. *Respir Med Case Rep*. (2020) 31:101292. doi: 10.1016/j.rmcr.2020.101292

61. Ronit A, Berg RMG, Bay JT, Haugaard AK, Ahlström MG, Burgdorf KS, et al. Compartmental immunophenotyping in COVID-19 ARDS: A case series. *J Allergy Clin Immunol*. (2021) 147:81–91. doi: 10.1016/j.jaci.2020.09.009

62. McElvaney OJ, McEvoy NL, McElvaney OF, Carroll TP, Murphy MP, Dunlea DM, et al. Characterization of the inflammatory response to severe COVID-19 illness. *Am J Respir Crit Care Med*. (2020) 202:812–21. doi: 10.1164/rccm.202005-1583OC

63. Liu Y, Zhang C, Huang F, Yang Y, Wang F, Yuan J, et al. Elevated plasma levels of selective cytokines in COVID-19 patients reflect viral load and lung injury. *Natl Sci Rev*. (2020) 7:1003–11. doi: 10.1093/nsr/nwaa037

64. Del Valle DM, Kim-Schulze S, Huang HH, Beckmann ND, Nirenberg S, Wang B, et al. An inflammatory cytokine signature predicts COVID-19 severity and survival. *Nat Med*. (2020) 26:1636–43. doi: 10.1038/s41591-020-1051-9

65. Lebedeva A, Molodtsov I, Anisimova A, Berestovskaya A, Dukhin O, Elizarova A, et al. Comprehensive cytokine profiling of patients with COVID-19 receiving tocilizumab therapy. *Int J Mol Sci*. (2022) 23:7937. doi: 10.3390/ijms23147937

66. Vanpouille C, Günaydın G, Jangard M, Clerici M, Margolis L, Broliden K, et al. The progestin medroxyprogesterone acetate affects HIV-1 production in human lymphoid tissue explants in a dose-dependent and glucocorticoid-like fashion. *Viruses*. (2021) 13:2303. doi: 10.3390/v13112303

67. Alexandrova L, Zicari S, Matyugina E, Khandazhinskaya A, Smirnova T, Andreevskaya S, et al. Dual-targeted anti-TB/anti-HIV heterodimers. *Antiviral Res*. (2017) 145:175–83. doi: 10.1016/j.antiviral.2017.07.011

68. Grivel J-C, Garcia M, Moss B, Margolis L. Measles virus inhibits HIV replication in human lymphoid issue ex vivo. *J Infect Dis*. (2005) 192:71–8. doi: 10.1086/430743

69. Lisco A, Grivel JC, Biancotto A, Vanpouille C, Origgi F, Malnati MS, et al. Viral inter actions in human lymphoid tissue: Human herpesvirus 7 suppresses the replication of CCR5-tropic human immunodeficiency virus type 1 via CD4 modulation. *J Virol*. (2007) 81:708–17. doi: 10.1128/JVI.01367-06

70. Andrei G, Lisco A, Vanpouille C, Introini A, Balestra E, van den Oord J, et al. Topical tenofovir, a microbicide effective against HIV, inhibits herpes simplex virus-2 replication. *Cell Host Microbe*. (2011) 10:379–89. doi: 10.1016/j.chom.2011.08.015

frontiers | Frontiers in Immunology

TYPE Original Research
PUBLISHED 13 November 2024
DOI 10.3389/fimmu.2024.1459616

OPEN ACCESS

EDITED BY
Huawei Mao,
Capital Medical University, China

REVIEWED BY
Kingsley Yin,
Rowan University School of Osteopathic Medicine, United States
Todd Bradley,
Children's Mercy Kansas City, United States

*CORRESPONDENCE
Jakob Hjorth Von Stemann
Jakob.hjorth.von.stemann@regionh.dk

†These authors share first authorship

‡These authors share last authorship

RECEIVED 04 July 2024
ACCEPTED 04 October 2024
PUBLISHED 13 November 2024

CITATION
Von Stemann JH, Dungu AM, Laguarda MV, Ryrsø CK, Hegelund MH, Faurholt-Jepsen D, Krogh-Madsen R, Hansen MB, Lindegaard B and Ostrowski SR (2024) Autoantibodies targeting interferons and GM-CSF are associated with adverse outcome risk, comorbidities, and pathogen in community-acquired pneumonia.
Front. Immunol. 15:1459616.
doi: 10.3389/fimmu.2024.1459616

Autoantibodies targeting interferons and GM-CSF are associated with adverse outcome risk, comorbidities, and pathogen in community-acquired pneumonia

Jakob Hjorth Von Stemann[1*†], Arnold Matovu Dungu[2†], Maria Vispe Laguarda[1], Camilla Koch Ryrsø[1,3], Maria Hein Hegelund[1], Daniel Faurholt-Jepsen[4,5], Rikke Krogh-Madsen[3,6,7], Morten Bagge Hansen[1,7‡], Birgitte Lindegaard[2,3,7‡] and Sisse Rye Ostrowski[1,6‡]

[1]Department of Clinical Immunology, Copenhagen University Hospital, Rigshospitalet, Copenhagen, Denmark, [2]Department of Pulmonary and Infectious Diseases, Copenhagen University Hospital, North Zealand, Denmark, [3]Centre for Physical Activity Research, Copenhagen University Hospital, Rigshospitalet, University of Copenhagen, Copenhagen, Denmark, [4]Department of Infectious Diseases, Copenhagen University Hospital, Rigshospitalet, Copenhagen, Denmark, [5]Department of Clinical Medicine, Copenhagen University Hospital, Rigshospitalet, Copenhagen, Denmark, [6]Department of Infectious Diseases, Copenhagen University Hospital, Hvidovre, Denmark, [7]Department of Clinical Medicine, Faculty of Health and Medical Sciences, University of Copenhagen, Copenhagen, Denmark

Introduction: Cytokine autoantibodies (c-aAb) have been associated with pulmonary diseases, including severe novel coronavirus disease 2019 (COVID-19) and pulmonary alveolar proteinosis. This study aimed to determine c-aAb association with community-acquired pneumonia (CAP) etiology (SARS-CoV-2, influenza, or bacteria) and c-aAb associations with CAP-related clinical outcomes and pulmonary comorbidities.

Methods: In a cohort of 665 patients hospitalized with CAP, c-aAb targeting interferon α (IFNα), IFNβ, IFNγ, interleukin-1α (IL-1α), IL-6, IL-10, and granulocyte-macrophage colony-stimulating factor (GM-CSF) were measured in plasma samples. Associations between c-aAb and baseline characteristics, pulmonary comorbidities, pathogen, intensive care unit (ICU) transferal, time to clinical stability, and mortality were estimated, with results stratified by sex.

Results: More men infected with SARS-CoV-2 were had high-titer type 1 IFN c-aAb compared to other pathogens. Among patients with CAP, asthma and bronchiectasis comorbidities were associated with high-titer GM-CSF c-aAb in men, and men with high-titer IFNβ c-aAb had increased odds for ICU transferal. High-titer IL-10 c-aAb were associated with faster clinical stability in women

Conclusion: In men with CAP, various c-aAb—including type 1 IFN and GM-CSF c-aAb—were associated with adverse clinical events and comorbidities, whereas c-aAb targeting an autoinflammatory cytokine were associated with a positive outcome in women. This suggests that the potentially immunomodulatory effects of c-aAb depend on pathogen, autoantibody specificity, comorbidity, and sex.

KEYWORDS

community-acquired pneumonia (CAP), coronavirus disease 2019, cytokine autoantibody, type 1 interferon, interleukin-10, granulocyte-macrophage colony stimulating factor

Introduction

Community-acquired pneumonia (CAP) is a significant global concern and responsible for a considerable amount of morbidity and mortality (1, 2). Pro- and anti-inflammatory cytokines modulate the immune response to CAP, with excessive or impaired cytokine responses associated with increased risk of CAP mortality (3–5).

High titers of neutralizing cytokine autoantibodies (c-aAb) are associated with autoimmunity and immunodeficiency, and increasingly recognized as risk factors for severe viral, bacterial, and mycotic infections in various patient cohorts (6). Furthermore, c-aAb may persist at high-titer levels for several years (7–9). High titers of neutralizing c-aAb targeting type I interferons (IFNs) disrupt antiviral immunity and predict the development of severe coronavirus disease 2019 (COVID-19) caused by the severe acute respiratory syndrome coronavirus 2 (SARS-CoV-2) and influenza virus pneumonia (10–15). Furthermore, c-aAb targeting IFNγ, interleukin (IL)-6, and granulocyte-macrophage colony-stimulating factor (GM-CSF) have been associated with increased susceptibility to various infections in humans such as non-tuberculosis mycobacteria, *Staphylococcus aureus*, and aspergillus (6, 16–18), and GM-CSF c-aAb are counted as a diagnostic factor for pulmonary alveolar proteinosis (PAP) (19). However, the relationship between c-aAb and CAP, including causal pathogens and clinical outcomes, remains undetermined. Additionally, whether c-aAb are associated with other chronic diseases common to CAP patients—such as chronic obstructive pulmonary disease (COPD) or asthma—has not been established (20).

Therefore, this exploratory study compared distributions of c-aAb targeting the cytokines IFNα, IFNβ, IFNγ, IL-1α, IL-6, IL-10, and GM-CSF in patients hospitalized with CAP with registered CAP etiology. We further assessed whether the presence of these c-aAb was associated with specific patterns of pulmonary comorbidities within the cohort (asthma, bronchiectasis, COPD, and fibrosis), as well as whether c-aAb served as predictors of clinical outcomes (including mortality, disease severity, time to readmission, admission to intermediary or intensive care, and time to clinical stability). As both c-aAb distribution and associations to disease outcome have been found to be highly sex-specific (11, 21), we stratified our investigations by sex.

Abbreviations: CAP, Community-acquired pneumonia; COVID-19, coronavirus disease 2019; c-aAb, cytokine autoantibody; GM-CSF, granulocyte-macrophage colony-stimulating factor; IMU, intermediary care; ICU, intensive care; IFNα, interferon α; IFNβ, interferon β; IFNγ, interferon γ; IL-1α, interleukin-1α; IL-6, interleukin-6; IL-10, interleukin-10; LUT, urinary antigen test for *Legionella pneumophila*; PUT, urinary antigen test for *Streptococcus pneumoniae*.

Methods

Study reporting

The Strengthening the Reporting of Observational Studies in Epidemiology (STROBE) guidelines for reporting observational cohort studies were used for this study (22).

Design and settings

This study included patients enrolled between January 2019 and November 2021 in the Surviving Pneumonia Study cohort, an ongoing observational, prospective cohort of patients hospitalized with CAP at Copenhagen University Hospital - North Zealand, Denmark (23, 24). The patients included in this study were followed for at least 1 year after being discharged or until death (Supplementary Table 1).

Participants

Inclusion criteria were age 18 years or older, clinical symptoms or signs consistent with a respiratory infection (e.g., coughing, production of sputum, fever or hypothermia, chest pain, difficulty breathing, and abnormal chest auscultation), and a new infiltrate on a chest x-ray or chest computed tomography scan. Eligible patients were enrolled within 24 h of being admitted to the hospital. The only exclusion criterion was a missing biobank sample, required to measure c-aAb.

Data collection

Clinical information, including radiology reports, vital signs at admission, comorbidities, microbiological test results, and disease outcomes, was obtained from the electronic medical record. The Charlson comorbidity index, which assigns a weight to 19 specific comorbidities, was used to assess the comorbidity burden (26). These comorbidities included myocardial infarction, congestive heart failure, peripheral vascular disease, cerebrovascular disease, dementia, rheumatic disease, peptic ulcer disease, diabetes without chronic complication, diabetes with chronic complication, hemiplegia or paraplegia, renal disease, any solid malignancy without metastasis, metastatic solid tumor, leukemia or lymphoma, mild liver disease, moderate or severe liver disease, and AIDS/HIV. In addition, data on chronic pulmonary diseases (asthma, bronchiectasis, COPD, and fibrosis) were also collected. Body mass index (BMI) was calculated from self-reported height and weight measured on an electric scale (Seca, Hamburg, Germany) within 48 h of admission. Vital signs included the first measurements of blood pressure, respiratory rate, and body temperature. CAP severity was assessed with the CURB-65 score, which is a risk-stratification tool that assigns one point each for confusion, urea >7 mmol/L, respiratory rate ≥30/min, systolic blood pressure <90 mm Hg or diastolic ≤60 mm Hg, and age ≥65 years. Scores are categorized as 0–1 for mild, 2 for moderate, and 3–5 for severe CAP (27). Plasma samples were prepared from venous blood collected in ethylene diamine tetraacetic acid (EDTA) tubes within 24 h of study enrollment and stored at −80°C until analysis.

Microbiological testing

Routine microbiological sampling and testing included blood cultures and culturing of respiratory samples (sputum and tracheal aspirate). Polymerase chain reaction testing of respiratory samples (sputum, tracheal aspirate, and oropharyngeal swabs) for causes of atypical pneumonia (*Legionella pneumophila, Mycoplasma pneumoniae*, and *Chlamydia pneumoniae*) and respiratory viruses [influenza A and B viruses, SARS-CoV-2, respiratory syncytial virus (RSV), rhinovirus, enterovirus, human metapneumovirus, parainfluenza virus, and adenoviruses] was also performed. Furthermore, urinary antigen tests for *Streptococcus pneumoniae* (PUT) and *L. pneumophila* (LUT) were performed on some patients. As microbiological testing was conducted at the discretion of the attending physician, the extent of microbiological testing differed between patients.

Cytokine autoantibody screening

An in-house assay was used to screen plasma samples for c-aAb targeting GM-CSF, IFNα, IFNβ, IFNγ, IL-1α, IL-6, and IL-10 according to a previously described protocol (28). Briefly, plasma samples were diluted 10-fold in a mix of assay buffer and seven different MagPlex microspheres, conjugated to recombinant, human molecules of the c-aAb relevant cytokines. Samples + beads were incubated with 800 rpm shaking for 1 h, followed by rounds of washing with assay buffer using manual magnetic plate inversion. Following a further 30-min incubation with PE-conjugated anti F(ab′)2 IgG, samples were washed again and read on a Luminex 200 system. The assay was performed using room temperature ingredients and shielded from light exposure as much as possible.

Patients were considered to have high titers of c-aAb if their mean fluorescence intensities (MFIs) were above the 90th or 95th percentiles at baseline or the earliest available sample for the seven individual c-aAb. This cutoff was considered to correspond to patients most likely to have functionally cytokine neutralizing c-aAb.

Outcomes

The outcomes of interest were differences in c-aAb across pathogen groups, baseline characteristics, clinical outcomes, and pre-existing comorbidities in patients. The clinical outcomes were mortality (within 30 or 180 days from admission), transferal to the intermediary or intensive care unit (IMU/ICU), readmission (within 30 or 180 days from discharge), disease severity, and time to clinical stability. Clinical stability was defined according to a modified version of Halm's criteria (29), which required meeting all of the following parameters concurrently: temperature ≤ 37.2°C, heart rate ≤ 100 beats/min, respiratory rate ≤ 24 breaths/min, systolic blood pressure ≥ 90 mm Hg, and oxygen saturation ≥ 90% without oxygen therapy. Time to clinical stability was measured in hours elapsed since admission.

Statistical analyses

C-aAb vs. baseline characteristics

Continuous variables were summarized as the median with interquartile range (IQR) and categorical variables were summarized as counts with percentages. Differences in c-aAb at admission between sexes in the cohort were compared with Wilcoxon rank sum test for the non-normally distributed c-aAb MFI values and the chi-squared test for comparing the number of cases above/below high-titer cutoffs in the cohort (90th or 95th percentile c-aAb MFI for men or women, respectively). Subsequent analyses were stratified by sex as indicated, as well as performed for men and women combined due to the limited sample size.

Differences in associations between c-aAb MFI and baseline characteristics were estimated with the Mann–Whitney *U* test for dichotomous, categorical variables and by Spearman's correlation coefficient for continuous variables, respectively, due to the nonparametric distribution of c-aAb. Based on these analyses, variables with significant associations to c-aAb, including age, sex, BMI, all forms of tobacco usage (defined as any prior or current usage of cigarettes, cigarillos, or pipe), and Charlson comorbidity index, were used as covariates in subsequent multivariate analyses.

C-aAb vs. pathogens

C-aAb differences between pathogen groups were estimated with the chi-squared test for categorical variables (high titers above the 90th percentile) and Kruskal–Wallis tests followed by Dunn's *post-hoc* test comparing overall c-aAb distribution between pathogen groups. Pathogen groups were defined as patients with bacterial infections, COVID-19 infection, or other viral infections. These general groupings were chosen in order to maximize *n* for subsequent analyses, especially considering they would also be stratified by sex. Patients with unknown etiology were excluded from these analyses, as well as cases with multiple different pathogen subtypes, such as patients with mixed bacterial and viral infections. Differences in baseline characteristics and vital parameters at admission between pathogen groups were estimated with the chi-squared test for categorical variables and the Kruskal–Wallis test for continuous variables. Subsequently, multivariate logistic regressions were performed with high-titer c-aAb as predictors, and age, BMI, tobacco usage, and Charlson comorbidity index as covariates, as well as sex when testing for the whole cohort.

C-aAb vs. clinical outcomes and comorbidities

The Mann–Whitney *U* test was used to estimate differences in general c-aAb MFI across binary clinical outcomes (readmissions within 30 or 180 days from discharge, mortality within 30 days, 180 days, 1 year, 2 years, or all-cause mortality following index admission, and admission to IMU/ICU) and comorbidity status. Chi-squared analyses used to test for high-titer c-aAb association to the aforementioned dependent variables. Analyses concerning clinical outcomes were limited to patients with follow-up spanning a minimum of 30 days, 180 days, etc. Owing to similar results, ultimately data from analyses spanning 180 days of follow-up were chosen to be reported. Multivariate logistic regressions were performed for c-aAb MFI/high-titer c-aAb as predictors for comorbidity status or clinical outcomes, adjusted for age, BMI, tobacco usage, and Charlson comorbidity index. Pathogen grouping was not included as a covariate, as we considered it a possible mediator of potential c-aAb-derived effects. Likewise, analyses were not stratified by pathogen to retain *n*. C-aAb as predictors of disease severity was assessed using an ordinal variable of mild, moderate, or severe CURB-65 score as the dependent variable in logistic regressions, with uni-/multivariate tests utilizing MFI/high-titer c-aAb and the aforementioned covariates as independent variables. As no regressions yielded significant results, we also elected to not include severity as a covariate in other clinical outcome analyses.

The association between c-aAb/high-titer c-aAb and time to death/clinical stability were investigated using the multivariate Cox proportional hazards model, adjusted for covariates as above, with c-aAb and high-titer c-aAb as predictors.

Statistical tests were two-sided, with $p < 0.05$ considered significant, and were conducted using STATA software v.18 (StataCorp, College Station, Texas, USA). Analyses were corrected for multiple testing using Bonferroni correction.

Results

Study population and microbiological findings

During the study period, 756 patients were enrolled in the Surviving Pneumonia Study cohort, with 91 excluded due to lack of a biobank sample (Figure 1). Patient characteristics of the included 665 patients are presented in Table 1. Based on the CURB-65 score, 369 (55%) patients presented with mild CAP, while 296 (45%) had moderate to severe CAP (Table 1). Of the total number of included patients, 85 (13%) had COVID-19, 39 (6%) had a non-COVID-19 virus, 151 (22%) had a bacterial infection, and 26 (4%) had a bacterial–viral co-infection (Supplementary Table 2). Among the 364 (55%) patients with no identified pathogen, 13 had no samples collected for microbiological testing (respiratory samples, blood cultures, or urine samples for LUT and PUT). Further details about this cohort have been published elsewhere (23, 24).

Men exhibited a higher median MFI of IL-1α-, IFNα-, and IFNγ-specific c-aAb and a lower MFI of IL-6 c-aAb compared to women among patients with CAP (Table 2). Subsequent c-aAb analyses were stratified by sex.

C-aAb distribution vs. patient pathogen

The distribution of c-aAb differed significantly across the pathogen groups for IFNα, IFNβ, and IFNγ c-aAb in the Surviving Pneumonia study cohort (Figures 2A–C), with the distribution skewed higher for the COVID-19 group in relation to the bacterial pathogen group. This was also observed for IFNα and IFNβ, specifically for men (Figures 2A, B).

Men with COVID-19 or other viral infections expressed more high-titer IFNα c-aAb (Table 3A) and IFNγ c-aAb (Table 3B), respectively, compared to patients with bacterial infection. In addition, high-titer IFNβ c-aAb presence was borderline significantly elevated in men with COVID-19 following multiple correction (Table 3C).

Association of C-aAb with pulmonary comorbidities and clinical outcomes

Regarding the pulmonary comorbidities of CAP patients (asthma, bronchiectasis, COPD, and fibrosis), we observed a higher likelihood for having asthma for high-titer GM-CSF c-aAb, both generally [OR = 2.78 (IQR: 1.41–5.47), $p = 0.012$] and for men specifically [OR = 3.92 (IQR: 1.34–11.26), $p = 0.044$]. Likewise, men with high-titer GM-CSF c-aAb had a significantly higher likelihood for bronchiectasis [OR = 8.89 (IQR: 2.05–38.49), $p = 0.012$, Table 4]. High-titer IL-6 c-aAb were associated with increased odds for pulmonary fibrosis diagnosis in men [OR = 8.90 (IQR: 1.65–48.18), $p = 0.040$]. No statistically significant trends were observed between c-aAb and non-pulmonary comorbidities.

In terms of clinical outcomes (mortality, readmission, IMU/ICU admission, and time to clinical stability), high-titer IFNβ c-aAb in men predicted increased odds of admission to the IMU or ICU [OR = 7.69 (95% CI: 2.80–21.12), $p < 0.001$, Figure 3]. When

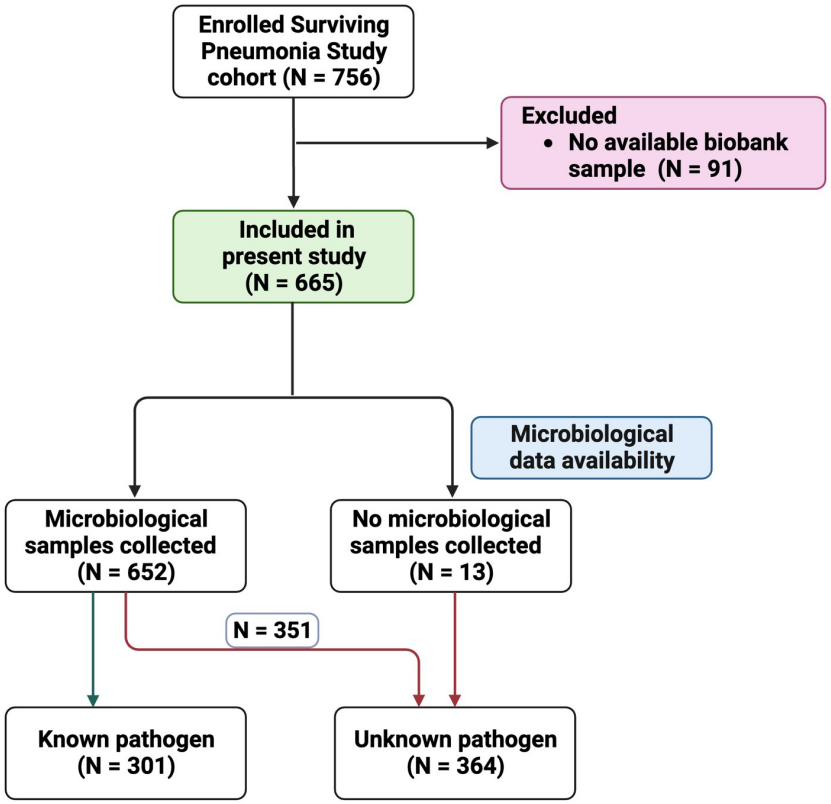

FIGURE 1
Flowchart of patient inclusion with illustration of patients with known vs. unknown pathogen.

TABLE 1 Baseline characteristics and epidemiologic overview of the Surviving Pneumonia Study cohort (*n* = 665).

Variable	Distribution
Epidemiological variables	
Age, median (IQR), yrs.	73 (63; 81)
Sex, n(%) - Female - Male	 314 (47%) 351 (53%)
Tobacco usage, n (%)	442 (66%)
BMI, median (IQR), kg/m^2	26 (22; 30)
Number of comorbidities	
0, n (%)	41 (6%)
1, n (%)	38 (6%)
≥2, n (%)	563 (88%)
Disease outcome	
IMU admission, n (%)	14 (2%)
ICU admission, n (%)	29 (5%)
Length of stay, median (IQR), days	5 (3;9)

(Continued)

TABLE 1 Continued

Variable	Distribution
Disease outcome	
30-day readmission, n (%)	133 (20%)
180-day readmission, n (%)	241 (36%)
30-day mortality, n (%)	62 (9%)
180-day mortality, n (%)	119 (18%)
1-year mortality, n (%)	148 (22%)
2-year mortality, n (%)	184 (28%)
All-course mortality, n (%)	186 (28%)
Death during hospital admission, n (%)	43 (6%)
Time to clinical stability, median (IQR), hrs.	97 (48; 177)
Achieved clinical stability, n of eligible (%)	444/572 (78%)
CURB-65 score	
0, n (%)	135 (20%)
1, n (%)	234 (35%)

(Continued)

10.3389/fimmu.2024.1459616

TABLE 1 Continued

Variable	Distribution
CURB-65 score	
2, n (%)	216 (32%)
3, n (%)	68 (10%)
≥4, n (%)	12 (2%)
Disease pathogen	
Bacterial infection, n (%)	141 (23%)
COVID-19 infection, n (%)	85 (13%)
Other viral infection, n (%)	39 (6%)
Bacterial/ COVID-19 infection, n (%)	12 (2%)
Bacterial/other viral infection, n (%)	14 (2%)
Unknown, n (%)	364 (52%)

subtracting one major pathogen group (including "Unknown") at a time from subsequent logistic analyses results, this finding for IFNβ c-aAb was largely unchanged upon exclusion of bacteria, virus, or COVID-19 infection as the cause, but became nonsignificant upon removal of the "Unknown" group (data not shown).

No other c-aAb presented significant associations to outcomes, including for severity, all-cause mortality, and readmission at any of the time points between 30 days and 2 years from baseline (hospital admission for mortality and discharge for readmission).

Finally, high-titer IL-10 c-aAb were associated with reduced time to clinical stability in women [HR = 1.93 (1.21; 3.08), p = 0.024, Figure 4].

Discussion

In this study, we screened for c-aAb targeting IFNα, IFNβ, IFNγ, IL-1α, IL-6, IL-10, and GM-CSF in the

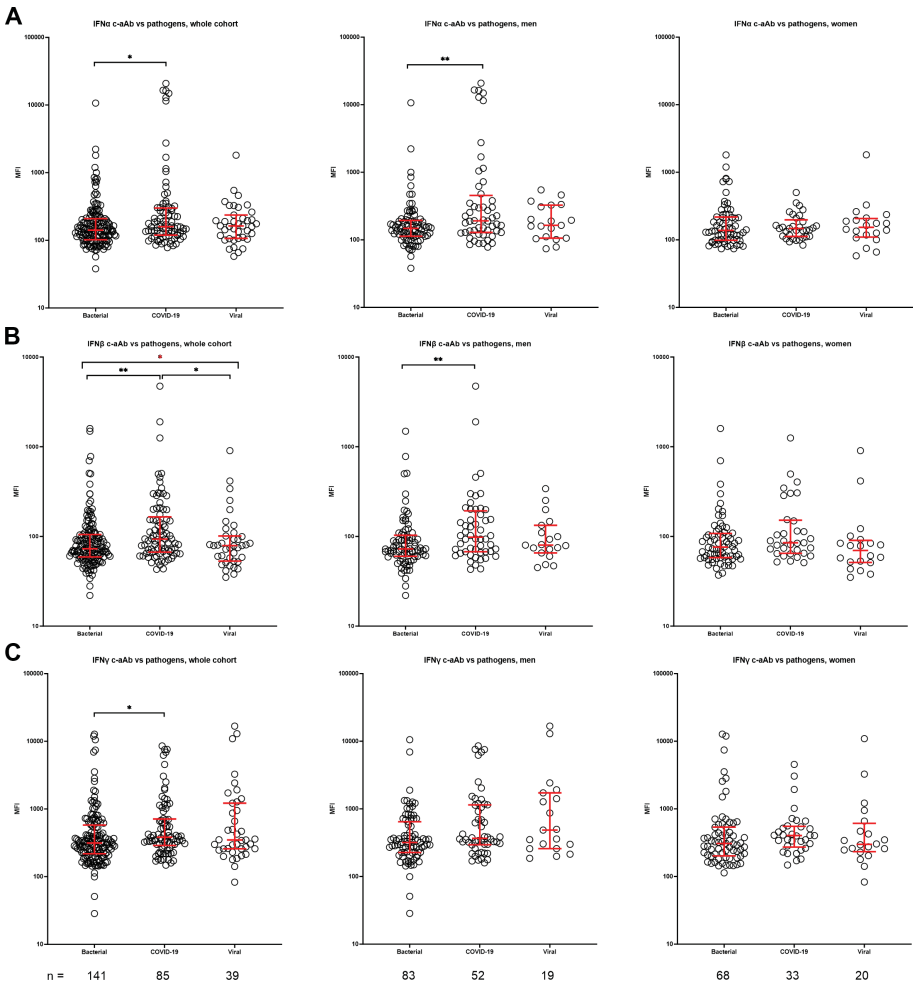

FIGURE 2
C-aAb in the Surviving Pneumonia Study cohort by pathogen in whole cohort, men and women. Distribution of IFNα **(A)**, IFNβ **(B)** and IFNγ **(C)** specific c-aAb in specific pathogen groups was compared to the rest of cohort using Kruskal–Wallis test, followed by Dunn's post-hoc test. Red lines indicate median with IQR. * Indicates adjusted $p < 0.05$, $^{**}p < 0.01$; Red * indicates Kruskal–Wallis test results.

TABLE 2 Sex differences in c-aAb.

C-aAb specificity	Distribution	Men (n =351)	Women (n = 314)	p-value
IL-1α	C-aAb, median (IQR), net MFI	156 (113; 272)	143 (102; 229)	0.045*
	90th percentile cutoff (n), net MFI	620 (35)	436 (31)	0.068 **
	95th percentile cutoff (n), net MFI	1,389 (18)	795 (16)	0.075***
IFNβ	C-aAb, median (IQR), net MFI	78 (61; 119)	75 (57; 111)	0.116*
	90th percentile cutoff (n), net MFI	224 (35)	274 (31)	0.725 **
	95th percentile cutoff (n), net MFI	497 (18)	405 (16)	0.281 ***
IFNγ	C-aAb, median (IQR), net MFI	356 (245; 719)	306 (213; 472)	<0.001*
	90th percentile cutoff (n), net MFI	1,572 (35)	1,120 (31)	0.232 **
	95th percentile cutoff (n), net MFI	3,287 (18)	3,054 (16)	0.710 ***
IFNα	C-aAb, median (IQR), net MFI	299 (141; 1248)	186 (110; 624)	<0.0001*
	90th percentile cutoff (n), net MFI	6,313 (35)	3,490 (31)	0.015**
	95th percentile cutoff (n), net MFI	9,451 (18)	6,882 (16)	0.153***
IL-6	C-aAb, median (IQR), net MFI	399 (247; 822)	518 (257; 1216)	0.006*
	90th percentile cutoff (n), net MFI	2,463 (35)	3,760 (31)	0.101**
	95th percentile cutoff (n), net MFI	4,895 (18)	6,394 (16)	0.739***
IL-10	C-aAb, median (IQR), net MFI	89 (67; 139)	90 (60; 129)	0.312*
	90th percentile cutoff (n), net MFI	270 (35)	223 (31)	0.180**
	95th percentile cutoff (n), net MFI	521 (18)	471 (16)	0.710***
GM-CSF	C-aAb, median (IQR), net MFI	74 (53; 154)	75 (51; 127)	0.540*
	90th percentile cutoff (n), net MFI	446 (35)	582 (31)	0.260**
	95th percentile cutoff (n), net MFI	2,481 (18)	2,007 (16)	0.469***

*Wilcoxon rank sum test comparing non-normally distributed variables between sexes.
**Chi-squared test comparing testing for c-aAb distribution above/below the full cohort 90th percentile between sexes.
***Chi-squared test comparing testing for c-aAb distribution above/below the full cohort 95th percentile between sexes.

TABLE 3A MR Analysis of the Mediation Role of Immune Cells in the Relationship between Gut Microbiota and Coagulation Defects, Purpura, and Other Hemorrhagic.

Group and test			Bacterial/ Not bacterial	COVID-19/ No COVID-19	Virus/no virus (excl. COVID-19)
Whole cohort	C-Ab high-titer Distribution*	Pathogen cases	12/151 (8.00%)	14/97 (14.4%)	<5/26 (<19%)
		Non cases	14/124 (11.3%)	17/223 (7.6%)	37/249 (14.9%)
	Test**	Odds Ratio	0.99	1.87	0.33
		p value	0.190	0.186	0.295
		Multiple testing adjusted *p* value	0.570	0.558	0.885
Women	C-Ab high-titer Distribution*	Pathogen cases	17/68 (10.3%)	<5/39 (<12.5%)	<5/20 (<25%)
		Non cases	<5/53 (<10%)	8/93 (8.6%)	7/101 (6.9%)
	Test**	Odds Ratio	(All cases are high-titer)	0.28	(No cases are high-titer)
		p value		*0.264*	
		Multiple testing adjusted *p* value		0.792	
Men	C-Ab high-titer Distribution*	Pathogen cases	5/83(6%)	13/58 (22.4%)	<5/19 (<25%)

(Continued)

TABLE 3A Continued

Group and test			Bacterial/ Not bacterial	COVID-19/ No COVID-19	Virus/no virus (excl. COVID-19)
		Non cases	13/71(18%)	7/111 (6.3%)	17/135 (12.6%)
	Test**	Odds Ratio	0.20	4.30	0.67
		p value	0.067	0.016	0.718
		Multiple testing adjusted *p* value	0.201	0.048	1

Binary high-titer/non- high-titer c-aAb (MFI over/under 90th percentile) variables used as predictors for having each pathogen compared to rest of cohort.
* Distribution = n & percentage of high-titer individuals within/outside of pathogen group (case/non case)
** Multivariate regression = logistic regression, with pathogen/non pathogen as outcome, and high-titer c-aAb status as predictor. Age, BMI, tobacco usage, and comorbidity score were used as covariate predictors, as well as sex in the non-stratified analyses. Odds ratio, unadjusted *p* values and multiple testing adjusted *p* values are listed.

Surviving Pneumonia Study cohort, comprising 665 patients with CAP caused by COVID-19, influenza virus, bacteria, or unknown pathogen.

Beyond various autoimmune diseases (6), the currently most well-documented instances of naturally occurring c-aAb as predictors for pathologies are those between GM-CSF c-aAb and PAP and IFNα c-aAb and COVID-19 (11, 19). Numerous observational studies have demonstrated a positive association between the presence of high titers of c-aAb that target type I IFNs, particularly IFNα, and severe disease in patients with COVID-19 or influenza virus pneumonia, with men in particular being at risk (10–13, 30, 31). In PAP, GM-CSF c-aAb-associated macrophage dysfunction can lead to the accumulation of mucus in the airways, and in COVID-19, IFNα c-aAb attenuates the type 1

TABLE 3B High-titer IFNβ c-aAb vs. pathogen.

Group and test			Bacterial/ Not bacterial	COVID-19/ No COVID-19	Virus/no virus (excl. COVID-19)
Whole cohort	C-Ab high-titer Distribution*	Pathogen cases	11/151 (7.3%)	16/97 (16.5%)	<5/30 (<17%)
		Non cases	19/124 (15.3%)	19/223 (8.5%)	35/245 (14.3%)
	Test**	Odds Ratio	0.34	2.63	0.67
		p value	0.034	0.035	0.614
		Multiple testing adjusted *p* value	0.102	0.115	1
Women	C-Ab high-titer Distribution*	Pathogen cases	5/68 (7.4%)	7/39 (18%)	<5/20 (<25%)
		Non cases	9/53 (17%)	8/93 (8.6%)	12/101 (11.9%)
	Test**	Odds Ratio	0.39	1.58	1.32
		p value	0.218	0.153	0.753
		Multiple testing adjusted *p* value	0.654	0.459	1
Men	C-Ab high-titer Distribution*	Pathogen cases	6/83 (7.2%)	9/58 (15.5%)	<5/19 (<25%)
		Non cases	10/71 (14.1%)	9/111 (8.1%)	14/135 (10.4%)
	Test**	Odds Ratio	0.31	4.63	(No cases are high-titer)
		p value	0.086	0.017	
		Multiple testing adjusted *p* value	0.258	0.051	

Binary high-titer/non- high-titer c-aAb (MFI over/under 90th percentile) variables used as predictors for having each pathogen compared to rest of cohort.
* Distribution = n & percentage of high-titer individuals within/outside of pathogen group (case/non case)
** Multivariate regression = logistic regression, with pathogen/non pathogen as outcome, and high-titer c-aAb status as predictor. Age, BMI, tobacco usage, and comorbidity score were used as covariate predictors, as well as sex in the non-stratified analyses. Odds ratio, unadjusted *p* values and multiple testing adjusted *p* values are listed.

TABLE 3C High-titer IFNγ c-aAb vs. pathogen.

Group and test			Bacterial/ Not bacterial	COVID-19/ No COVID-19	Virus/no virus (excl. COVID-19)
Whole cohort	C-Ab high-titer Distribution*	Pathogen cases	11/151 (7.3%)	13/97 (13.4%)	7/30 (23.3%)
		Non cases	19/124 (15.3%)	19/204 (9.3%)	32/245 (13.1%)
	Test**	Odds Ratio	0.42	1.15	2.89
		p value	0.088	0.770	0.048
		Multiple testing adjusted *p* value	0.264	1	0.136
Women	C-Ab high-titer Distribution*	Pathogen cases	<5/83 (<6%)	<5/39 (<12.5%)	<5/20 (<25%)
		Non cases	14/71 (19.7%)	10/93 (10.8%)	11/101 (10.9%)
	Test**	Odds Ratio	0.51	1.24	2.04
		p value	0.342	0.766	0.354
		Multiple testing adjusted *p* value	1	1	1
Men	C-Ab high-titer Distribution*	Pathogen cases	<5/83 (<6%)	9/58 (15.5%)	5/19 (26.3%)
		Non cases	14/71 (19.7%)	9/111 (8.1%)	12/135 (8.9%)
	Test**	Odds Ratio	0.22	0.83	6.45
		p value	0.071	0.792	0.005
		Multiple testing adjusted *p* value	0.213	1	0.015

Binary high-titer/non- high-titer c-aAb (MFI over/under 90th percentile) variables used as predictors for having each pathogen compared to rest of cohort.
* Distribution = n & percentage of high-titer individuals within/outside of pathogen group (case/non case)
** Multivariate regression = logistic regression, with pathogen/non pathogen as outcome, and high-titer c-aAb status as predictor. Age, BMI, tobacco usage, and comorbidity score were used as covariate predictors, as well as sex in the non-stratified analyses. Odds ratio, unadjusted *p* values and multiple testing adjusted *p* values are listed.

IFN-mediated antiviral response. Both c-aAb have been detected in bronchiolar lavage (14, 32). This led us to further investigate c-aAb in the context of acute pulmonary disease in our Surviving Pneumonia Study cohort and, furthermore, to look for associations between levels of c-aAb and pulmonary disease-associated comorbidities in CAP patients.

In line with the existing literature, our study found a positive association between IFNα c-aAb titers and patients with COVID-19 infection in comparison to other pathogens, as well as a smaller, less significant association for IFNβ. High-titer IFNγ c-aAb were also more prominent specifically in men with non-COVID-19 viral infection, showcasing that different c-aAb are linked to different pathologies.

The higher MFI levels of c-aAb targeting IL-1α in men compared to women in our study, as well as their association with age, also align with previous studies of Danish blood donors (21). This includes positive associations of IFNα c-aAb and male sex—also documented in COVID-19 studies—as well as a positive association of IL-6 c-aAb and female sex (21, 33, 34).

It is our general hypothesis that high-titer c-aAb may inhibit the functionality of target cytokines and thus modulate any cytokine-associated disease risk and outcomes. Within this study, we found c-aAb targeting IFNβ in men exclusively to be associated with adverse outcomes, namely, increased odds of being admitted to the IMU/ICU. It is unclear what renders IFNβ c-aAb specifically relevant in this context, but IFNβ c-aAb have been found to be associated with critical disease course independently of IFNα c-aAb previously, such as for infection with *S. pneumoniae* (11, 35). In our study, this association to clinical outcomes was not reliant on the COVID-19-infected subset of the cohort, indicating that type 1 IFN targeting c-aAb may be relevant in contexts beyond COVID-19.

In contrast to these findings, we found IL-10 c-aAb to be associated with reduced time to clinical stability for women, the lone case of a c-aAb being associated with a preferable outcome. This is in line with prior findings of IL-10 c-aAb being associated with reduced infection risk in Danish blood donors (36), which we speculate is due to the anti-inflammatory role of IL-10, where c-aAb-mediated inhibition may result in a more active immune system. Conversely, we have also found IL-10 c-aAb to be associated with increased risk of cardiovascular disease in a cohort of kidney transplant recipients, again emphasizing the highly context-specific impact of c-aAb (37).

While GM-CSF c-aAb levels were not associated with clinical outcomes, we observed that men had significant associations of high-titer GM-CSF c-aAb to diagnosed asthma and bronchiectasis. We believe that we are the first to describe these associations.

It has been suggested that tissues expressing high cytokine levels may yield potentially immunogenic alternative cytokine-analogs, due to some post-transcriptional and translationally modified cytokine-analogs escaping negative selection in the thymus (38). Such scenarios might include pulmonary diseases, as GM-CSF is, for instance, highly expressed in bronchoalveolar lavage and sputum of patients with

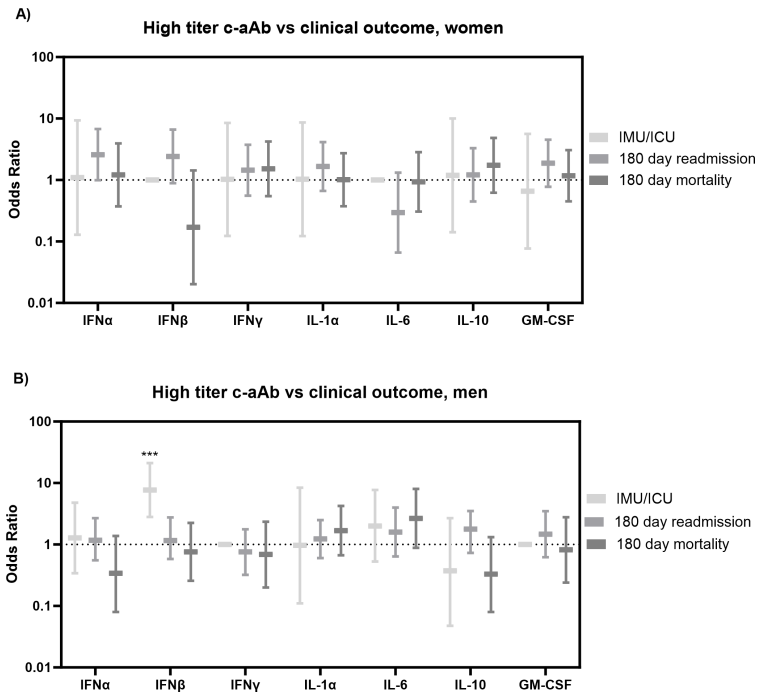

FIGURE 3
Clinical outcomes vs. high-titer c-aAb in the Surviving Pneumonia Study cohort. Logistic regression with IMU/ICU transferal, 180 days readmission, or mortality (180 days) as outcomes for women **(A)** and men **(B)**. Covariates were age, BMI, sex, tobacco, Charlson comorbidity index. *** indicates p <0.001.

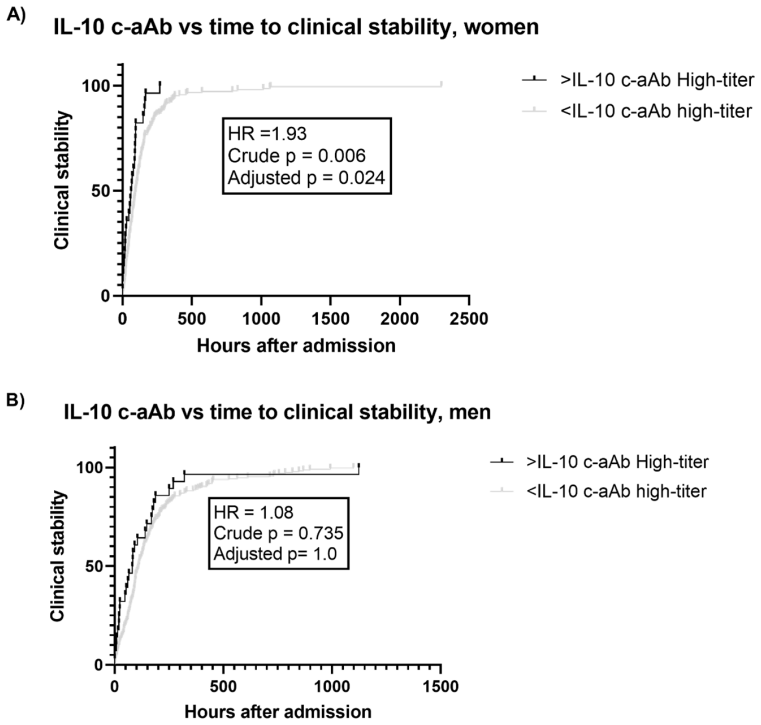

FIGURE 4
IL-10 c-aAb vs. time to clinical stability in the Surviving Pneumonia Study cohort. Survival curves for time to clinical stability (hours after admission) for individuals with or without high-titer IL-10 c-aAb (90th percentile) for women **(A)** or men **(B)** with time to stability data (572/665). Tested for difference using Cox regression, adjusted for age, BMI, tobacco usage, and Charlson comorbidity index, hazard ratio (HR), crude p-value, and multiple testing adjusted p-value (×4 for four different clinical outcomes investigated) listed.

10.3389/fimmu.2024.1459616

TABLE 4 GM-CSF c-aAb vs. pulmonary comorbidities.

Group and test				Asthma (n= 87/665)	Bronchiectasis (n= 21/665)	COPD (n= 221/663)	Fibrosis (n= 16/665)
Whole cohort	Continuous c-aAb MFI*	Distribution	Comorbidity cases	75.5 (50, 236)	73 (53, 271)	72 (50, 132)	74.25 (51.75, 157)
			Non cases	73.72 (52, 134)	74.75 (52, 138)	76 (53, 146)	74.25 (52, 138)
		Test	Odds ratio	1.13 (1.02; 1. 23)	0.88 (0.56; 1.39)	1.02(0.91; 1.14)	0.99(0.76; 1.30)
			p value	0.018	0.608	0.748	0.978
			Multiple testing adjusted p value	0.072	1	1	1
	High-titer c-aAb**	Distribution	Comorbidity cases	17/87(19,5%)	<5/21(24%)	22/221(9,9%)	<5/16(<31%)
			Non cases	50/578(8.7%)	63/644(9.8%)	45/442(10.2%)	64/649(9.9%)
		Test	Odds ratio	2.78(1.41; 5.47)	2.49(0.77; 8.04)	1.10(0.54; 2.24)	1.21 (0.25; 5.89)
			p value	0.003	0.128	0.792	0.815
			Multiple testing adjusted p value	0.012	0.384	1	1
Women	Continuous c-aAb MFI*	Distribution	Comorbidity cases	74.5 (51, 118)	53.5 (40, 66)	67 (46, 132)	78.5 (47, 91)
			Non cases	75.5 (50, 236)	76 (51.5, 130)	76.5 (55, 126.5)	75 (51, 130)
		Test	Odds ratio	1.13 (0.99; 1. 29)	0.00003 (2.14e-13; 6447)	1.06(0.87; 1.30)	0.01(3.21e-09; 33992)
			p value	0.149	0.292	0.512	0.551
			Multiple testing adjusted p value	0.447	0.876	1	1
	High-titer c-aAb**	Distribution	Comorbidity cases	9/57(15.8%)	0/10(0%)	13/108(12%)	0/6(0%)
			Non cases	22/257(8.6%)	<5/11(<45,5%)	18/204(8.8%)	31/308(10.1%)
		Test	Odds ratio	2.43(0.96; 6.15)	(No cases are high-titer)	0.71 (0.25; 2.02)	(No cases are high-titer)
			p value	0.060		0.525	
			Multiple testing adjusted p value	0.180		1	
Men	Continuous c-aAb MFI*	Distribution	Comorbidity cases	76 (50, 197)	271 (72, 868)	73 (54, 128)	74.25 (53, 978)
			Non cases	73 (53, 149)	73 (52.5, 147.5)	75 (52, 165.2)	74 (53, 149)
		Test	Odds ratio	1.12 (0.99; 1. 25)	0.99 (0.69; 1.38)	0.99 (0.86; 1.15)	1.03 (0.81; 1.31)
			p value	0.089	0.910	0.998	0.788
			Multiple testing adjusted p value	0.384	1	1	1
	High-titer c-aAb**	Distribution	Comorbidity cases	6/30(20%)	<5/11(<45,5%)	8/113(7.1%)	<5/10(50%)
			Non cases	29/321(9%)	31/340(9.1%)	27/238(11.3%)	32/341(9.4%)
		Test	Odds ratio	3.92 (1.34; 11.26)	8.89 (2.05; 38.49)	1.34(0.49; 3.71)	2.78(0.47; 16.62)
			p value	0.011	0.003	0.564	0.261
			Multiple testing adjusted p value	0.044	0.012	1	0.783

* C-aAb MFI/1000 used as independent variable. Distribution = median + IQR in case/non-case groups, test = logistic regression, with age, BMI, tobacco usage and comorbidity score as covariates, as well as sex in the non-stratified analyses. ** C-aAb high-titer status (>90th percentile) used as independent variable. Distribution = n & percentage of high-titer individuals within/outside of comorbidity group (case/non case), test = logistic regression, with age, BMI, tobacco usage and comorbidity score as covariates, as well as sex in the non-stratified analyses. Outcome was Odds Ratio with 95% Confidence interval. Unadjusted as well as multiple testing adjusted p values are listed.

COPD compared to healthy controls (39, 40). It is possible that our association of high-titer GM-CSF c-aAb to asthma and bronchiectasis in our cohort might reflect such a breach of tolerance. Future studies may investigate whether GM-CSF c-aAb influence disease severity for these specific comorbidities, as seen in a murine study where neutralizing GM-CSF-specific antibodies ameliorated inflammation caused by exposure to cigarette smoke, the primary risk factor for COPD (41). Conversely, both asthma and bronchiectasis have been known to feature accumulation of mucus, a key feature of PAP, which could thus also be partially GM-CSF c-aAb derived in these diseases (42, 43). A case with both bronchiectasis and GM-CSF c-aAb-derived PAP has been described (44), yet none of the patients in the cohort featured diagnosed PAP. Thus, based on our findings, we speculate that pulmonary diseases linked causally to high-titer c-aAb—including PAP or similar pathologies—may be overlooked and labeled with other diagnoses, and our study suggests the merit of c-aAb in more full-fledged cohorts for the comorbidities in question. Finally, autoantibody Ig subclass has recently been found correlated to COVID-19 severity (45), and future studies could thus assess the potential links of c-aAb subclasses to clinical outcomes.

To our knowledge, this is the first study to investigate this wide range of c-aAb in the context of CAP and its wider associated pulmonary comorbidities. That our findings are generally in line with previously observed age/sex patterns of c-aAb distribution and disease associations, and seem coherent with the functionality of the targeted cytokines all corroborate our results. Weaknesses of the study include the comparatively small sample sizes of the patients with specific diagnosed comorbidities and the lack of direct neutralization assays for the seven c-aAb screened in our cohort. Another limitation is that the patients being attended to by different physicians may have caused variation in the level of microbiological testing performed, as this was decided at the discretion of the attending physician.

In conclusion, our study underlines the relevance of type 1 IFN targeting c-aAb for COVID-19 patients and shows IFNβ c-aAb in men being specifically associated with unfavorable infectious disease outcomes outside of a COVID-19 context. Conversely, c-aAb targeting the anti-inflammatory cytokine IL-10 were associated with faster clinical stability in women, and GM-CSF-specific c-aAb were found to be associated with asthma and bronchiectasis in men. Taken together, these findings, including their high degree of sex dependency, emphasize that the influence of c-aAb may be highly tied to specific contexts and cytokine functionality, and suggest multiple avenues for future c-aAb studies, including association to multiple pulmonary clinical phenotypes.

Data availability statement

The datasets presented in this article are not readily available because the datasets used for the current study are not publicly available. However, pseudonymised data can be provided by the corresponding author upon a reasonable request. Requests to access the datasets should be directed to jakob.hjorth.von.stemann@regionh.dk.

Ethics statement

The Surviving Pneumonia Study cohort was approved by the scientific Ethics Committee at the Capital Region of Denmark (H-18024256), registered on ClinicalTrials.gov (NCT03795662), and conducted according to the Declaration of Helsinki (25). Written informed consent was obtained from all competent study participants before enrollment in the Surviving Pneumonia Study. If a potential participant was deemed incapacitated at enrollment, written informed consent was obtained from a legal guardian or next of kin and an independent physician not affiliated with the study, according to the guidelines of the Ethics Committee at the Capital Region of Denmark.

Author contributions

JS: Conceptualization, Formal analysis, Investigation, Methodology, Project administration, Resources, Visualization, Writing – original draft, Writing – review & editing. AD: Conceptualization, Data curation, Investigation, Methodology, Project administration, Resources, Validation, Writing – original draft, Writing – review & editing. ML: Conceptualization, Formal analysis, Investigation, Writing – review & editing. CR: Conceptualization, Methodology, Project administration, Resources, Writing – review & editing, Funding acquisition. MH: Conceptualization, Methodology, Writing – review & editing, Funding acquisition, Project administration. DF-J: Conceptualization, Methodology, Project administration, Resources, Writing – review & editing, Funding acquisition, Supervision. RK-M: Conceptualization, Methodology, Project administration, Resources, Writing – review & editing, Funding acquisition, Supervision. MH: Conceptualization, Methodology, Project administration, Resources, Supervision, Writing – review & editing. BL: Conceptualization, Funding acquisition, Methodology, Project administration, Resources, Supervision, Writing – review & editing. SO: Conceptualization, Funding acquisition, Methodology, Project administration, Resources, Supervision, Writing – review & editing.

Funding

The author(s) declare financial support was received for the research, authorship, and/or publication of this article. The Surviving Pneumonia study was supported by grants from the Research Council at Copenhagen University Hospital – North Zealand, Hillerød, Denmark; Grosserer L. F. Foghts Fond; Fru Olga Bryde Nielsens Fond; Helen Rudes Fond; Kaptajnløjtnant Harald Jensens og Hustrus Fond; and Fonden til Lægevidenskabens Fremme. The funding sources were not involved in the study design, data collection, data analysis, interpretation of data, writing of the paper, or decision to submit the report for publication.

Conflict of interest

The authors declare that the research was conducted in the absence of any commercial or financial relationships that could be construed as a potential conflict of interest.

Publisher's note

All claims expressed in this article are solely those of the authors and do not necessarily represent those of their affiliated organizations, or those of the publisher, the editors and the reviewers. Any product that may be evaluated in this article, or claim that may be made by its manufacturer, is not guaranteed or endorsed by the publisher.

Supplementary material

The Supplementary Material for this article can be found online at: https://www.frontiersin.org/articles/10.3389/fimmu.2024.1459616/full#supplementary-material

References

1. Torres A, Cilloniz C, Niederman MS, Menéndez R, Chalmers JD, Wunderink RG, et al. Pneumonia. *Nat Rev Dis Primers*. (2021) 7:25. doi: 10.1038/s41572-021-00259-0

2. Vos T, Lim SS, Abbafati C, Abbas KM, Abbasi M, Abbasifard M, et al. Global burden of 369 diseases and injuries in 204 countries and territories, 1990-2019: a systematic analysis for the Global Burden of Disease Study 2019. *Lancet*. (2020) 396:1204–22. doi: 10.1016/S0140-6736(20)30925-9

3. Alagarasu K, Kaushal H, Shinde P, Kakade M, Chaudhary U, Padbidri V, et al. TNFA and IL10 polymorphisms and IL-6 and IL-10 levels influence disease severity in influenza A(H1N1)pdm09 virus infected patients. *Genes (Basel)*. (2021) 12. doi: 10.3390/genes12121914

4. Hu H, Pan H, Li R, He K, Zhang H, Liu L. Increased circulating cytokines have a role in COVID-19 severity and death with a more pronounced effect in males: A systematic review and meta-analysis. *Front Pharmacol*. (2022) 13:802228. doi: 10.3389/fphar.2022.802228

5. Kellum JA, Kong L, Fink MP, Weissfeld LA, Yealy DM, Pinsky MR, et al. Understanding the inflammatory cytokine response in pneumonia and sepsis: results of the Genetic and Inflammatory Markers of Sepsis (GenIMS) Study. *Arch Intern Med*. (2007) 167:1655–63. doi: 10.1001/archinte.167.15.1655

6. Knight V. Immunodeficiency and autoantibodies to cytokines. *J Appl Lab Med*. (2022) 7:151–64. doi: 10.1093/jalm/jfab139

7. Galle P, Svenson M, Bendtzen K, Hansen MB. High levels of neutralizing IL-6 autoantibodies in 0.1% of apparently healthy blood donors. *Eur J Immunol*. (2004) 34:3267–75. doi: 10.1002/eji.200425268

8. de Lemos RC, Galle P, Pedersen BK, Hansen MB. A state of acquired IL-10 deficiency in 0.4% of Danish blood donors. *Cytokine*. (2010) 51:286–93. doi: 10.1016/j.cyto.2010.06.009

9. Jouvenne P, Fossiez F, Banchereau J, Miossec P. High levels of neutralizing autoantibodies against IL-1 alpha are associated with a better prognosis in chronic polyarthritis: a follow-up study. *Scand J Immunol*. (1997) 46:413–8. doi: 10.1046/j.1365-3083.1997.d01-139.x

10. Eto S, Nukui Y, Tsumura M, Nakagama Y, Kashimada K, Mizoguchi Y, et al. Neutralizing type I interferon autoantibodies in Japanese patients with severe COVID-19. *J Clin Immunol*. (2022) 42:1360–70. doi: 10.1007/s10875-022-01308-3

11. Bastard P, Gervais A, Le Voyer T, Rosain J, Philippot Q, Manry J, et al. Autoantibodies neutralizing type I IFNs are present in ~4% of uninfected individuals over 70 years old and account for ~20% of COVID-19 deaths. *Sci Immunol*. (2021) 6. doi: 10.1126/sciimmunol.abl4340

12. Zhang Q, Pizzorno A, Miorin L, Bastard P, Gervais A, Le Voyer T, et al. Autoantibodies against type I IFNs in patients with critical influenza pneumonia. *J Exp Med*. (2022) 219. doi: 10.1084/jem.20220514

13. Wang EY, Mao T, Klein J, Dai Y, Huck JD, Jaycox JR, et al. Diverse functional autoantibodies in patients with COVID-19. *Nature*. (2021) 595:283–8. doi: 10.1038/s41586-021-03631-y

14. Philippot Q, Fekkar A, Gervais A, Le Voyer T, Boers LS, Conil C, et al. Autoantibodies neutralizing type I IFNs in the bronchoalveolar lavage of at least 10% of patients during life-threatening COVID-19 pneumonia. *J Clin Immunol*. (2023) 43:1–11. doi: 10.1007/s10875-023-01512-9

15. Su HC, Jing H, Zhang Y, Casanova JL. Interfering with interferons: A critical mechanism for critical COVID-19 pneumonia. *Annu Rev Immunol*. (2023) 41:561–85. doi: 10.1146/annurev-immunol-101921-050835

16. Arango-Franco CA, Migaud M, Ramírez-Sánchez IC, Arango-Bustamante K, Moncada-Vélez M, Rojas J, et al. Anti-GM-CSF neutralizing autoantibodies in Colombian patients with disseminated cryptococcosis. *J Clin Immunol*. (2023) 43:1–12. doi: 10.1007/s10875-023-01451-5

17. Wang SY, Lo YF, Shih HP, Ho MW, Yeh CF, Peng JJ, et al. Cryptococcus gattii infection as the major clinical manifestation in patients with autoantibodies against granulocyte-macrophage colony-stimulating factor. *J Clin Immunol*. (2022) 42:1730–41. doi: 10.1007/s10875-022-01341-2

18. Krisnawati DI, Liu YC, Lee YJ, Wang YT, Chen CL, Tseng PC, et al. Functional neutralization of anti-IFN-γ autoantibody in patients with nontuberculous mycobacteria infection. *Sci Rep*. (2019) 9:5682. doi: 10.1038/s41598-019-41952-1

19. Ataya A, Knight V, Carey BC, Lee E, Tarling EJ, Wang T. The role of GM-CSF autoantibodies in infection and autoimmune pulmonary alveolar proteinosis: A concise review. *Front Immunol*. (2021) 12:752856. doi: 10.3389/fimmu.2021.752856

20. Torres A, Peetermans WE, Viegi G, Blasi F. Risk factors for community-acquired pneumonia in adults in Europe: a literature review. *Thorax*. (2013) 68:1057–65. doi: 10.1136/thoraxjnl-2013-204282

21. von Stemann JH, Rigas AS, Thorner LW, Rasmussen DGK, Pedersen OB, Rostgaard K, et al. Prevalence and correlation of cytokine-specific autoantibodies with epidemiological factors and C-reactive protein in 8,972 healthy individuals: Results from the Danish Blood Donor Study. *PloS One*. (2017) 12:e0179981. doi: 10.1371/journal.pone.0179981

22. von Elm E, Altman DG, Egger M, Pocock SJ, Gøtzsche PC, Vandenbroucke JP. The Strengthening the Reporting of Observational Studies in Epidemiology (STROBE) statement: guidelines for reporting observational studies. *Lancet*. (2007) 370:1453–7. doi: 10.1016/S0140-6736(07)61602-X

23. Ryrsø CK, Dungu AM, Hegelund MH, Jensen AV, Sejdic A, Faurholt-Jepsen D, et al. Body composition, physical capacity, and immuno-metabolic profile in community-acquired pneumonia caused by COVID-19, influenza, and bacteria: a prospective cohort study. *Int J Obes (Lond)*. (2022) 46:817–24. doi: 10.1038/s41366-021-01057-0

24. Hegelund MH, Glenthøj A, Ryrsø CK, Ritz C, Dungu AM, Sejdic A, et al. Biomarkers for iron metabolism among patients hospitalized with community-acquired pneumonia caused by infection with SARS-CoV-2, bacteria, and influenza. *Apmis*. (2022) 130:590–6. doi: 10.1111/apm.v130.9

25. World Medical Association. Declaration of Helsinki: ethical principles for medical research involving human subjects. *Jama*. (2013) 310:2191–4. doi: 10.1001/jama.2013.281053

26. Charlson ME, Pompei P, Ales KL, MacKenzie CR. A new method of classifying prognostic comorbidity in longitudinal studies: development and validation. *J Chronic Dis*. (1987) 40:373–83. doi: 10.1016/0021-9681(87)90171-8

27. Capelastegui A, España PP, Quintana JM, Areitio I, Gorordo I, Egurrola M, et al. Validation of a predictive rule for the management of community-acquired pneumonia. *Eur Respir J*. (2006) 27:151–7. doi: 10.1183/09031936.06.00062505

28. Guldager DK, von Stemann JH, Larsen R, Bay JT, Galle PS, Svenson M, et al. A rapid, accurate and robust particle-based assay for the simultaneous screening of plasma samples for the presence of five different anti-cytokine autoantibodies. *J Immunol Methods*. (2015) 425:62–8. doi: 10.1016/j.jim.2015.06.010

29. Menéndez R, Martinez R, Reyes S, Mensa J, Polverino E, Filella X, et al. Stability in community-acquired pneumonia: one step forward with markers? *Thorax*. (2009) 64:987–92. doi: 10.1136/thx.2009.118612

30. Troya J, Bastard P, Planas-Serra L, Ryan P, Ruiz M, de Carranza M, et al. Neutralizing autoantibodies to type I IFNs in >10% of patients with severe COVID-19 pneumonia hospitalized in Madrid, Spain. *J Clin Immunol*. (2021) 41:914–22. doi: 10.1007/s10875-021-01036-0

31. Goncalves D, Mezidi M, Bastard P, Perret M, Saker K, Fabien N, et al. Antibodies against type I interferon: detection and association with severe clinical outcome in COVID-19 patients. *Clin Transl Immunol*. (2021) 10:e1327. doi: 10.1002/cti2.v10.8

32. Kitamura T, Tanaka N, Watanabe J, Uchida, Kanegasaki S, Yamada Y, et al. Idiopathic pulmonary alveolar proteinosis as an autoimmune disease with neutralizing antibody against granulocyte/macrophage colony-stimulating factor. *J Exp Med*. (1999) 190:875–80. doi: 10.1084/jem.190.6.875

33. Hansen MB, Svenson M, Abell K, Varming K, Nielsen HP, Bertelsen A, et al. Sex- and age-dependency of IgG auto-antibodies against IL-1 alpha in healthy humans. *Eur J Clin Invest*. (1994) 24:212–8. doi: 10.1111/j.1365-2362.1994.tb00991.x

34. Bastard P, Rosen LB, Zhang Q, Michailidis E, Hoffmann HH, Zhang Y, et al. Autoantibodies against type I IFNs in patients with life-threatening COVID-19. *Science*. (2020) 370. doi: 10.1126/science.abd4585

35. Parker D, Martin FJ, Soong G, Harfenist BS, Aguilar JL, Ratner AJ, et al. Streptococcus pneumoniae DNA initiates type I interferon signaling in the respiratory tract. *mBio*. (2011) 2:e00016–11. doi: 10.1128/mBio.00016-11

36. von Stemann JH, Pedersen OB, Hjalgrim H, Erikstrup C, Ullum H, Thørner LW, et al. Cytokine autoantibodies are associated with infection risk and self-perceived health: results from the Danish blood donor study. *J Clin Immunol*. (2020) 40:367–77. doi: 10.1007/s10875-020-00744-3

37. Lund KP, von Stemann JH, Eriksson F, Hansen MB, Pedersen BK, Sorensen SS, et al. IL-10-specific autoantibodies predict major adverse cardiovascular events in kidney transplanted patients - a retrospective cohort study. *Transpl Int*. (2019) 32:933–48. doi: 10.1111/tri.13425

38. de Lemos RC, Galle P, Hansen MB. Characterization and potential clinical applications of autoantibodies against cytokines. *Cytokine Growth Factor Rev*. (2009) 20:61–75. doi: 10.1016/j.cytogfr.2009.01.003

39. Vlahos R, Bozinovski S, Hamilton JA, Anderson GP. Therapeutic potential of treating chronic obstructive pulmonary disease (COPD) by neutralising granulocyte macrophage-colony stimulating factor (GM-CSF). *Pharmacol Ther*. (2006) 112:106–15. doi: 10.1016/j.pharmthera.2006.03.007

40. Saha S, Doe C, Mistry V, Siddiqui S, Parker D, Sleeman M, et al. Granulocyte-macrophage colony-stimulating factor expression in induced sputum and bronchial mucosa in asthma and COPD. *Thorax*. (2009) 64:671–6. doi: 10.1136/thx.2008.108290

41. Vlahos R, Bozinovski S, Chan SP, Ivanov S, Lindén A, Hamilton JA, et al. Neutralizing granulocyte/macrophage colony-stimulating factor inhibits cigarette smoke-induced lung inflammation. *Am J Respir Crit Care Med*. (2010) 182:34–40. doi: 10.1164/rccm.200912-1794OC

42. Verna R, Proietti S, Spiga A, Unfer V, Bizzarri M. Nebulized myo-inositol increases mucus clearance in patients with Bronchiectasis: a retrospective study. *Eur Rev Med Pharmacol Sci*. (2023) 27:6876–81. doi: 10.26355/eurrev_202307_33159

43. Evans CM, Kim K, Tuvim MJ, Dickey BF. Mucus hypersecretion in asthma: causes and effects. *Curr Opin Pulm Med*. (2009) 15:4–11. doi: 10.1097/MCP.0b013e32831da8d3

44. Asami-Noyama M, Ito K, Harada M, Hisamoto Y, Kunihiro Y, Ikeda E, et al. A case of development of autoimmune pulmonary alveolar proteinosis during the treatment of hypersensitivity pneumonitis. *Respir Med Case Rep*. (2023) 44:101862. doi: 10.1016/j.rmcr.2023.101862

45. Geanes ES, McLennan R, LeMaster C, Bradley T. Autoantibodies to ACE2 and immune molecules are associated with COVID-19 disease severity. *Commun Med (Lond)*. (2024) 4:47. doi: 10.1038/s43856-024-00477-z

frontiers | Frontiers in Immunology

TYPE Review
PUBLISHED 09 January 2025
DOI 10.3389/fimmu.2024.1497026

OPEN ACCESS

EDITED BY
Jian Zheng,
University of Louisville, United States

REVIEWED BY
Luis Castro-Sánchez,
University of Colima, Mexico
Federico Diaz-Gonzalez,
University of La Laguna, Spain
Andrey Elchaninov,
Avtsyn Research Institute of Human Morphology of FSBI "Petrovsky National Research Centre of Surgery", Russia
Shrabanti Chowdhury,
Icahn School of Medicine at Mount Sinai, United States

*CORRESPONDENCE
Xiaoyu Li
lixiaoyu05@163.com

RECEIVED 16 September 2024
ACCEPTED 11 December 2024
PUBLISHED 09 January 2025

CITATION
Guo S, Zhang Q, Guo Y, Yin X, Zhang P, Mao T, Tian Z and Li X (2025) The role and therapeutic targeting of the CCL2/CCR2 signaling axis in inflammatory and fibrotic diseases. *Front. Immunol.* 15:1497026. doi: 10.3389/fimmu.2024.1497026

The role and therapeutic targeting of the CCL2/CCR2 signaling axis in inflammatory and fibrotic diseases

Shan Guo, Qi Zhang, Yingjie Guo, Xiaoyan Yin, Peng Zhang, Tao Mao, Zibin Tian and Xiaoyu Li*

Department of Gastroenterology, The Affiliated Hospital of Qingdao University, Qingdao, China

CCL2, a pivotal cytokine within the chemokine family, functions by binding to its receptor CCR2. The CCL2/CCR2 signaling pathway plays a crucial role in the development of fibrosis across multiple organ systems by modulating the recruitment and activation of immune cells, which in turn influences the progression of fibrotic diseases in the liver, intestines, pancreas, heart, lungs, kidneys, and other organs. This paper introduces the biological functions of CCL2 and CCR2, highlighting their similarities and differences concerning fibrotic disorders in various organ systems, and reviews recent progress in the diagnosis and treatment of clinical fibrotic diseases linked to the CCL2/CCR2 signaling pathway. Additionally, further in-depth research is needed to explore the clinical significance of the CCL2/CCR2 axis in fibrotic conditions affecting different organs.

KEYWORDS

CCL2, CCR2, inflammation, fibrosis, immune regulation, clinical diagnosis and treatment

Introduction

Chemokines are a large family of small proteins that play a crucial role in regulating cell movement (1), particularly in guiding leukocyte migration (2), which is central to maintaining immune system balance (3). In 2000, chemokines were systematically classified into four families: CXC, CC, CX3C, and C (4). Among these, CC chemokine ligand 2 (CCL2), also known as monocyte chemotactic protein-1 (MCP-1), is a key regulator in immune response. Discovered in 1989, CCL2 is primarily anchored to endothelial cell membranes (5) and is most abundantly expressed in monocytes, macrophages, and lymphocytes (6). Other cells, such as smooth muscle cells, endothelial cells, and fibroblasts, can also secrete CCL2 (7), particularly in response to cytokines like interleukin (IL)-6, tumor necrosis factor-α (TNF-α), and transforming growth factor-β (TGF-β) (8).

CCL2 exerts its effects mainly by binding to the receptor CCR2 (9), which has the highest affinity for CCL2 due to its specific structural characteristics (10). This binding

activates various downstream pathways (Figure 1), resulting in diverse chemotactic responses, particularly in monocytes. The CCL2-CCR2 interaction not only promotes cell migration but also regulates cell adhesion and macrophage chemotaxis. Upon ligand binding, CCR2 experiences conformational changes that initiate the activation of phospholipase C (PLC). This activation leads to an increased release of Ca^{2+} ions and the subsequent activation of protein kinase C (PKC) and phosphoinositide 3-OH kinase (PI3K). These processes further activate signaling molecules such as protein kinase B (PKB, Akt) and mitogen-activated protein kinase (MAPK). This signaling pathway is crucial for the regulation of central transduction mechanisms within the cell (11–13). Additionally, it plays a significant role in cancer progression by activating pathways such as p38-MAPK (14, 15) and PI3K/AKT/mTOR (16–18), which enhance tumor cell invasion, migration, and survival.

CCL2 is extensively involved in disease regulation, particularly in inflammation, fibrosis, and cancer. It mobilizes monocytes from the bone marrow into the bloodstream and directs their migration to sites of inflammation (19), underscoring its essential role in immune defense (20). Beyond inflammation, CCL2 contributes to fibrosis development in various organs like the liver, pancreas, and kidneys (Figure 2). It also plays a role in cancer biology, known as the "tumor chemokine" (21), aiding in tumor initiation, growth, and metastasis (22, 23). Tumor-associated macrophages secrete CCL2 (24), which aids in the progression of cancers like breast (25) and pancreatic cancers (26, 27). CCL2 expression in the tumor microenvironment, involving various cell types, highlights its significance in cancer pathology (28) and its potential as a therapeutic target.

Chemokine receptors have been targeted in therapeutic strategies, and recent years have seen promising results from CCL2/CCR2 antagonists in treating inflammatory and fibrotic diseases (29) and cancer immunotherapy (30, 31). This review explores the mechanisms and the diagnostic and therapeutic potentials of the CCL2/CCR2 axis in inflammatory and fibrotic diseases. These conditions are characterized by chronic inflammation leading to fibrosis, where prolonged immune responses cause excessive extracellular matrix deposition, tissue scarring, and organ dysfunction. Understanding the role of the CCL2/CCR2 axis in fibrosis will provide a basis for developing novel therapies.

Mechanisms of the CCL2/CCR2 axis in inflammatory and fibrotic diseases

CCL2 plays a pivotal role in fibrogenesis in the liver, pancreas, and intestine by attracting immune cells such as monocytes and macrophages to fibrotic areas, promoting inflammatory responses and matrix remodeling. In viral hepatitis, CCL2 helps create an immunosuppressive microenvironment that facilitates fibrosis progression and favors viral infection. In liver fibrosis, CCL2 synergizes with TGF-β to activate hepatic stellate cells (HSCs) and promote matrix deposition. In intestinal fibrosis, CCL2 works with intestinal-specific factors like IL-17. In pancreatic fibrosis, CCL2 leads to M2-like polarization of macrophages after attracting immune cells to the tissue.

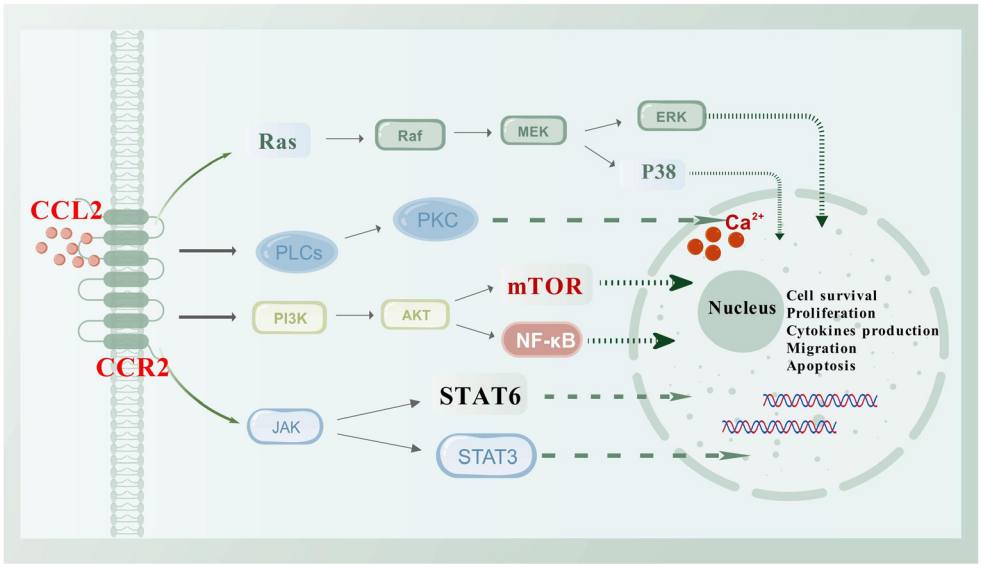

FIGURE 1
Schematic diagram of the CCL2/CCR2 axis and its associated signaling pathways. CCR2, a classic G protein-coupled receptor, activates a variety of downstream signaling pathways upon binding to its ligand CCL2, such as PI3K/Akt, JAK/STAT, and P38/MAPK. Activation of these pathways leads to the regulation of various transcription factors and genes involved in cell survival, proliferation, cytokine production, migration, and apoptosis. This figure was created with biogdp.com.

Hepatic fibrosis diseases

CCL2 is crucial in liver diseases such as acute and chronic liver injury, cirrhosis, and tumor progression (32). Liver inflammation often coexists with fibrosis, driven by the recruitment and polarization of macrophages, particularly through hepatic stellate and Kupffer cell activation (33, 34). Key pathways like hedgehog (35) and TGF-β (36) are involved in these processes, contributing to conditions like non-alcoholic steatohepatitis (NASH) and hepatocellular carcinoma (HCC) (37).

NASH

NASH results from excessive fat accumulation in the liver, causing hepatocyte damage and triggering inflammation. This inflammatory state activates HSCs, leading to fibrosis, cirrhosis, or liver cancer. Studies have shown that increased expression of CCL2 is a hallmark of NASH, promoting the infiltration of monocyte-derived macrophages through CCL2-mediated chemotaxis.

CCL2 is implicated in NASH progression through several mechanisms. Li et al. (38) identified methyltransferase 3 (METTL3) as a key negative regulator, loss of Mettl3 accelerates NASH by enhancing CD36-dependent fatty acid uptake and CCL2-driven inflammation. The absence of CX3CR1 promotes a shift from M1 to M2 macrophages, slowing NASH progression. CCL2 deficiency in *Cx3cr1*$^{-/-}$ mice reduces macrophage infiltration and supports M2 dominance in the liver, alleviating NASH (39). Recent research has indicated that the activation of Notch signaling pathways in hepatocytes is crucial for the advancement of liver fibrosis linked to NASH (40). Additionally, existing literature has underscored the role of Notch signaling in hepatocytes, which further facilitates the infiltration of macrophages dependent on CCL2, thereby exacerbating fibrosis (41).

Autophagy in liver sinusoidal endothelial cells is also involved in NASH. Insufficient autophagy increases the expression of CCL2, CCL5, and CD68, exacerbating fibrosis in high-fat diet-fed mice (42). $CD11c^{+}CD206^{+}$ cells, which express high levels of CCR2, show increased CCL2 expression in NASH, correlating with disease severity. Inhibition of CCR2 reduces the infiltration of $CD11b^{+}CD11c^{+}F4/80^{+}$ monocytes and improves liver inflammation and fibrosis in NASH models (43).

Multiple signaling pathways are implicated in steatohepatitis, with the CCL2/CCR2 axis playing a key role. Gasdermin D, involved in programmed necrosis, promotes the secretion of pro-inflammatory cytokines IL-1β and CCL2 and activates the NF-κB pathway, driving NASH progression (44). The NLRP3-IL-1β pathway also contributes to inflammation and obesity-related comorbidities. Inhibition of NLRP3 inflammasome reduces lipopolysaccharide-induced inflammation by down-regulating CCL2 mRNA levels (45). Suppressing the IL-33 signaling pathway can inhibit NASH progression by down-regulating CCL2 and α-SMA expression (46), while activating IL-19 signaling reduces HSC migration by down-regulating CCL2 expression, alleviating liver fibrosis (47).

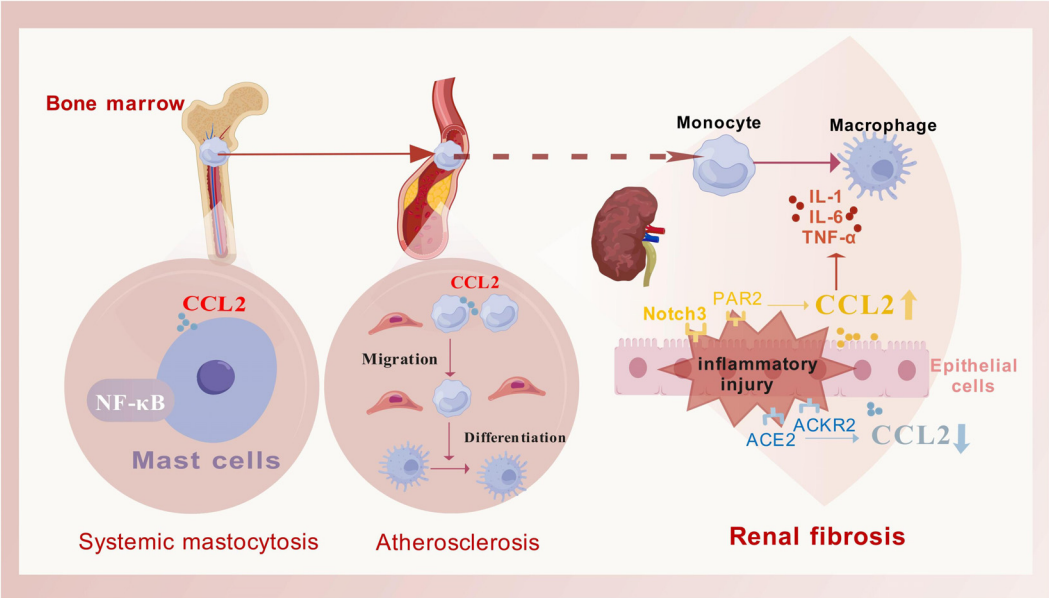

FIGURE 2
The primary role process of CCL2 in fibrotic diseases. CCL2 facilitates the mobilization of monocytes from the bone marrow into the bloodstream and guides their migration to targeted inflammatory fibrotic areas. Once there, these monocytes differentiate into macrophages to address tissue damage (as exemplified by atherosclerotic plaques), this process is frequently associated with the activation of the NF-κB signaling pathway (as exemplified by systemic mastocytosis). Additionally, the regulation of CCL2 secretion is often influenced by various receptors, which in turn modulate the release of inflammatory mediators (as seen in fibrosis associated with chronic kidney disease). This figure was created with biogdp.com.

Viral hepatitis

CCL2 plays a specific role in immune evasion during hepatitis B virus (HBV) infection. Chronic HBV infection, a major risk factor for liver diseases such as HCC, can persist for decades. HBV evades immune response by downregulating CCL2 (48), reducing inflammatory monocyte and macrophage recruitment to the liver. In chronic HBV cases complicated by cirrhosis, plasma CCL2 levels tend to decrease (49). Additionally, HBeAg can promote HSC proliferation, movement, and contraction in a macrophage-dependent manner, inducing CCL2 production that activates HSCs and worsens liver fibrosis (50).

Hepatitis C virus (HCV)-mediated hepatitis is also a significant global health issue, particularly in the United States. Studies show that HCV-infected individuals can downregulate specific microRNAs, such as miRNA-107 and miRNA-449a, to regulate CCL2 expression by targeting the interleukin-6 receptor (IL-6R) complex (51), suggesting potential therapeutic avenues. A novel pathway involving the HCV core protein interacting with gC1qR has been identified, leading to CCL2 and CXCL10 secretion in macrophages via the NF-κB signaling pathway (52).

Other hepatic fibrotic diseases

Analysis of the liver fibrosis expression dataset GSE84044 from the GEO database identified 10 key genes in the protein interaction network, including CCL2, highlighting its importance in fibrosis and inflammation (53). Glucocorticoid-induced leucine zippers (GILZ), encoded by the *Tsc22d3* gene in mice, mimic glucocorticoids' anti-inflammatory effects. Mice deficient in GILZ show increased CCL2 production and pro-inflammatory leukocyte infiltration in early liver fibrosis, accelerating its progression (54). Moreover, sphingosine kinase 1 (SPHK1) levels were significantly higher in fibrotic compared to normal human livers. SPHK1 knockout in Kupffer cells reduced CCL2 secretion, while its knockout in HSCs decreased CCR2 expression (55).

CCL2 also has a role in pediatric liver fibrosis. A recent study identified *FOCAD* germline recessive mutation in pediatric liver cirrhosis. In a zebrafish model with *FOCAD* deficiency, liver injury was accompanied by increased CCL2 expression, suggesting that targeting the CCL2/CCR2 axis could be a new approach for treating pediatric liver cirrhosis (56).

Inflammatory bowel disease

Inflammatory bowel disease (IBD) is a chronic autoimmune inflammatory disease affecting the gastrointestinal tract, with two main subtypes: ulcerative colitis (UC) and Crohn's disease (CD). The dextran sodium sulfate (DSS)-induced colitis model, which activates the classic NF-κB signaling pathway, is widely used to study UC. In intestinal tissues, CCL2 responds to diverse signals. Inflammatory damage triggers monocytes to secrete CCL2, recruiting white blood cells or macrophages to injury sites, ultimately leading to intestinal fibrosis.

In early intestinal inflammation, Ly6c high-expressing cells markedly enhance the expression of *CCL2* and *CCR2* genes through the activation of STAT1 signaling, in contrast to Ly6c intermediate-expressing cells. Additionally, inhibiting the CCR2 pathway can mitigate colonic damage in models of acute colitis (57). PC3-secreted microproteins (PSMP) upregulate phosphorylated ERK levels via the CCR2 pathway (58), driving $CCR2^{+}$ monocyte migration to inflamed colonic tissue. PSMP attracts $Ly6c^{hi}$ monocytes in a CCR2-dependent manner, aided by Dectin-1 on myeloid cells (59, 60), while cobalt protoporphyrin IX (CoPP) reduces the migration of $CCR2^{+}$ $Ly6c^{hi}$ monocytes to the inflamed colon (61).

As inflammation reaches the muscle layer, $Ly6c^{+}$ monocytes infiltrate, adopting a unique transcriptional state and promoting muscle inflammation. They alter the microenvironment, promoting more monocyte infiltration, which then differentiates into anti-inflammatory $CD206^{+}$ macrophages through CCL2 (62). Bone marrow-derived mesenchymal stromal cells (BM-MSCs) secrete CCL2, influencing colitis development, while IL-10 in MSCs polarizes resident macrophages (63). During chronic inflammation, $CCR2^{+}$ monocytes and fibrocytes infiltrate the colon, promoting fibrosis by inhibiting collagen degradation (64).

CCL2 promotes intestinal fibrosis by activating pro-inflammatory factors, notably IL-6, a process reversible with CCR2 antagonist RS102895 (65). Antisense IL-7 (IL-7-AS) accelerates inflammation by upregulating IL-6 and CCL2 (66). Poly(rC)-binding protein 1 (PCBP1) deficiency reduces CCL2 and IL-6 production in colitis macrophages (67). Additionally, in colitis models, CCR2 and CD30L expression in monocytes are positively correlated; CD30L drives monocyte homing and differentiation via the CCL2/CCR2 axis and NF-κB pathway, enhancing inflammation (68).

CCL2 is also involved in hyperoxia-induced intestinal injury. IL-17D, a member of the IL-17 family, promotes CCL2 expression in intestinal epithelial cells under hyperoxic conditions, leading to chronic intestinal inflammation (69).

Chronic pancreatitis

Chronic pancreatitis (CP) is characterized by progressive, irreversible inflammation and fibrosis, with pancreatic stellate cells (PSCs) playing a key role in this process (70). Studies in CP patients have shown that prostaglandin E2 mediates CCL2 synthesis in PSCs via TNF-α regulation, and inhibiting cyclooxygenase (COX)-2 activity can slow the progress of pancreatitis and fibrosis (71).

Research on CCL2's role in CP progression is limited. Interestingly, alternatively activated macrophages (M2) secrete PDGF and TGF-β, which activate PSCs and promote fibrosis—a key factor in CP development (72). This contrasts with the immune microenvironment in NASH (39), highlighting the plasticity of macrophages and suggesting that CCL2 regulates immune cells differently across organs. Additionally, during chronic pancreatic inflammation, CCL2 secretion and NF-κB pathway activation persist (73).

Cardiovascular fibrotic diseases

Cardiovascular diseases remain a leading cause of morbidity and mortality worldwide (74). Recent studies highlight the inflammatory immune response as a central mechanism in their pathogenesis (75). Among the key mediators, CCL2 plays a crucial role in regulating leukocyte migration and infiltration in various cardiovascular diseases. Consequently, CCL2/CCR2 inhibitors are being explored as novel therapeutic targets for inflammation-related cardiovascular conditions (76).

Myocardial infarction

During the healing process of Myocardial infarction (MI), macrophages undergo dynamic polarization. CCL2 is differentially expressed in LPS-induced M1 and IL-4-induced M2 macrophages (77). Unlike in the liver and pancreas, CCL2 deficiency in the heart results in reduced total macrophage and M1 macrophage numbers in the infarcted area, while M2 macrophages increase (78). This suggests that CCL2 is a pivotal regulator of macrophage polarization during MI healing, both *in vivo* and *in vitro*, and it specifically promotes M1 polarization. The organ-specific and environment-dependent nature of CCL2's role likely explains these differential effects.

The repair process following MI is critical for cardiac recovery. In response to acute myocardial ischemia-reperfusion (MIR), macrophages infiltrate damaged heart tissue and shift their polarization to manage acute inflammation and subsequent fibrotic remodeling. Studies indicate that CCL2/CCR2 signaling in macrophages facilitates the transition from acute injury to chronic fibrosis in MIR in mice through the NLRP3 inflammatory pathway and phenotypic changes (79). Furthermore, IL-34 enhances CCL2 expression by maintaining NF-κB pathway activation, aggravating cardiac remodeling and fibrosis after reperfusion injury (80).

Other cardiovascular inflammatory diseases

A meta-analysis by Georgakis et al. demonstrated that circulating CCL2 levels, synonymous with CCL2, are strongly associated with cardiovascular mortality (81). Elevated CCL2 levels in atherosclerotic plaques correlate with increased plaque vulnerability, and persistently high circulating CCL2 levels heighten the risk of adverse outcomes following plaque removal (82). Moreover, circulating CCL2 levels appear genetically influenced; higher levels are linked to a greater risk of stroke, suggesting that CCL2-targeted therapies might reduce stroke incidence (83).

CCL2 is also implicated in the regulation of circadian rhythms during atherosclerosis progression. Winter et al. (84) revealed that CCL2 is a key chemokine at atherosclerotic sites and that the chronic inflammation of large blood vessels depends on the rhythmic release of CCL2, which peaks in the early stage and declines later. This discovery opens new avenues for chronotherapy targeting the CCL2-CCR2 axis in atherosclerosis treatment.

Mast cells (MCs), known for their roles in allergy and parasitic infections, are also pivotal in inflammation and fibrosis. CCL2 acts as an activator of MCs (85). Luo et al. (86) highlighted that early MC-fibroblast interaction and the stem cell factor/mast cell/CCL2/monocyte/macrophage axis are critical for initiating myocardial fibrosis. Additionally, hypoxia, which can be both a cause and a result of heart failure, induces CCL2 expression in both right ventricle (RV) and left ventricle (LV) of mice, potentially contributing to cardiac inflammation, fibrosis, and ventricular dysfunction (87).

Pulmonary fibrotic diseases

Pulmonary inflammatory lesions tend to progress to fibrosis more consistently than in other organ systems, with CCL2 playing a significant role in this process. Pulmonary fibrosis is a multicellular phenomenon involving alveolar epithelial cells (AECs), recruited monocytes/macrophages, and fibroblasts. Several cell types, including AECs, produce CCL2, which promotes fibrosis via CCR2 activation (88). CCR2 signaling is therefore crucial for the development and progression of pulmonary fibrosis.

Idiopathic pulmonary fibrosis

Idiopathic pulmonary fibrosis (IPF) is a progressive interstitial lung disease characterized by chronic inflammation, AEC damage, and excessive deposition of extracellular matrix proteins, with myofibroblasts acting as the main effector cells (89). In mouse models of bleomycin-induced pulmonary fibrosis, transcriptional analysis has shown a significant increase in CCL2 expression (90, 91). FoxF1, an endothelial transcription factor, has also been implicated in pulmonary fibrosis. *In vitro*, studies reveal that FoxF1-deficient endothelial cells enhance lung fibroblast proliferation, invasion, activation, and macrophage migration by secreting chemokines such as CCL2, collectively contributing to fibrosis (92). Moreover, IL-33 treatment increases CCL2 and CXCL2 production in $NFATc3^{+/+}$ macrophages, but not in $NFATc3^{+/-}$ mice, suggesting that NFATc3 regulates pulmonary fibrosis by regulating CCL2 and CXCL2 expression in macrophages (93).

Myofibroblasts play a central role in IPF pathogenesis. Single-cell RNA sequencing (scRNA-seq) data from IPF patients indicates that the CCL2/CCR2 axis is essential for M1 macrophage polarization (94). Pathogenesis varies among IPF subgroups, with ligand-receptor analysis suggesting a monocyte-macrophage chemotactic axis, potentially involving CCL2-CCR2, particularly in cilia-rich subgroups (95). Immunohistochemical analysis of human lung tissues has shown that activated IPF fibroblasts possess high contractile forces and produce abundant CCL2 (96), with the NF-κB signaling pathway contributing to CCL2 production and release in these fibroblasts (97). Another study on acute exacerbation of IPF found significantly higher CCL2 concentrations in bronchoalveolar lavage fluid compared to serum, indicating a localized inflammatory response (98).

Radiation-induced pulmonary fibrosis

Radiation exposure to the lungs triggers a damage response, including the release of cytokines and chemotactic mediators, signaling the recruitment of immune cells for inflammation and wound healing. A recent study has reported significantly elevated CCL2 expression in macrophages of irradiated lungs, which potentially stimulates the fibrotic phenotype in lung fibroblasts (99). Following radiation, bone marrow-derived inflammatory monocytes migrate to the lungs, where $CCR2^{+}$ monocyte-derived macrophages infiltrate and may play a critical role in the development of Radiation-induced pulmonary fibrosis (RIPF) (100).

Other pulmonary fibrotic diseases

CCL2 also contributes to receptor-mediated pulmonary fibrosis progression. Adhesion G Protein-Coupled Receptor F5 (ADGRF5) is a key regulator of lung surfactant homeostasis in type II alveolar cells. Research has shown that ADGRF5 can regulate *CCL2* gene expression, maintaining its potential role in lung immune homeostasis. Disruption of ADGRF5 results in airway inflammation mediated by type 2 immune response and CCL2-induced inflammation (101). In a mouse model of pulmonary fibrosis, Leucine-Rich Repeat Kinase 2 (LRRK2) expression is significantly reduced in alveolar type II epithelial (ATII) cells, and LRRK2-deficient ATII cells exhibit an enhanced ability to recruit profibrotic macrophages via the CCL2/CCR2 axis. This recruitment triggers extensive macrophage-associated profibrotic responses and progressive pulmonary fibrosis (102).

Additionally, while IL-17 is known for its pro-inflammatory role in the intestine, it also contributes to parenchymal fibrosis in chronic pulmonary graft-versus-host disease (cpGVHD). Blocking IL-17A leads to reduced CCL2 expression in cpGVHD-related pulmonary fibrosis (103), though this effect is not observed in kidney diseases (104).

Renal fibrotic diseases

During kidney injury, CCL2 recruits immune cells such as macrophages and T cells to the site of injury, activating them and triggering the release of additional inflammatory mediators. These mediators not only worsen kidney damage but also promote fibrosis. Proteomic analysis of an *in vitro* model of renal fibrosis identified CCL2 as a key factor contributing to collagen deposition in the kidney (105).

Unilateral ureteral obstruction

Unilateral ureteral obstruction (UUO) can lead to renal interstitial fibrosis and is a potential precursor to chronic kidney disease (CKD), promoting extensive research into the underlying mechanisms. As mentioned earlier, activation of the Notch signaling pathway is known to upregulate CCL2 expression, contributing to fibrosis in organs like the liver (41). Recent animal studies have shown that Notch3 is newly expressed in damaged renal epithelium at early stages of CKD. Notably, systemic deficiency of Notch3 prevents leukocyte invasion and organ fibrosis, suggesting that targeting Notch3 may protect the epithelial epithelium and interrupt pro-inflammatory signaling, thereby alleviating kidney injury (106). Brandt et al. (107) utilized chimeric mice with Notch3 deficiency in hematopoietic cells and/or resident histiocytes to analyze renal fibrosis and inflammation following UUO. Their results indicated that a pro-inflammatory environment is characterized by upregulation of CCL2 and CCL5, which are regulated in a Notch3-dependent manner.

A recent study identified increased Twist1 expression in both the UUO mouse model and IgA nephropathy. Knockout of Twist1 in macrophages partially inhibited CCL2-mediated macrophage chemotaxis and suppressed M2 macrophage polarization, thereby mitigating fibrosis progression (108). Conversely, IL-15 has been shown to reduce CCL2 expression in the UUO mouse model, alleviating fibrosis and decreasing the likelihood of progression to CKD (109). Nicotinamide exhibits similar effects (110).

Other renal fibrotic diseases

In CKD patients, angiopoietin-1 has been found to reduce the expression of chemokine CCL2 in fibrotic renal endothelial cells. In contrast, angiopoietin-2 induces CCL2 expression in endothelial cells, which promotes macrophage infiltration and increases apoptosis in fibrotic renal endothelial cells. This process negatively impacts the renal survival rate in CKD patients (111). Consistently, angiotensin-converting enzyme 2 (ACE2), which is inversely correlated with CCL2 expression, is strongly associated with CKD and is known to limit renal fibrosis (112). Another important factor is protease-activated receptor 2 (PAR2), which is involved in renal inflammation and fibrosis. Activation of PAR2 in cultured renal tubular epithelial cells triggers extracellular signal-regulated kinase signaling and CCL2 secretion, contributing to tubulointerstitial inflammation and fibrosis (113).

Abnormal immune system activation is also implicated in CKD development. Wilkening et al. (114) analyzed glomerular CCR2 expression in focal segmental glomerulosclerosis (FSGS) and demonstrated that macrophages expressing CCR2 contribute to kidney damage and fibrosis remodeling in conditions such as glomerulonephritis and diabetic nephropathy. In contrast, atypical chemokine receptor 2 (ACKR2), also known as D6, degrades CCL2, limiting the recruitment of immune cells and myofibroblasts to renal mesenchymal cells. This degradation inhibits renal inflammation and fibrosis remodeling in glomerulonephritis (115).

Kashyap et al. (116)reported that CCL2 deficiency protects against chronic kidney damage in a mouse model of renovascular hypertension caused by renal artery stenosis (RAS). The deficiency leads to reduced monocyte infiltration and lower expression of CCR2 and CD206, suggesting that CCL2 is a key mediator of kidney injury in renovascular hypertension.

Bone marrow fibrotic diseases

Myelofibrosis (MF) is a prominent clinical feature observed in patients with myeloproliferative neoplasms (MPN). Prior research has established a correlation between the progression of MF and the aberrant expression of cytokines (117). Within the context of myeloproliferative disorders, CCL2 and its associated signaling pathways may play a critical role. CCL2 is thought to be involved in both the proliferation and differentiation of fibrosis-associated cells, thereby impacting the bone marrow microenvironment.

MPN

A recent investigation revealed that among the MPN cohort, the proportion of $CCR2^+$ cells is significantly associated with the severity of myelofibrosis in patients, and CCR2 expression on $CD34^+$ cells correlates with higher-risk classifications in MF and the presence of circulating blast cells (118). Additionally, polymorphisms in the CCL2 gene have been shown to influence the bone marrow microenvironment in MPN, with homozygosity for the CCL2 rs1024611 SNP linked to diminished survival in individuals with primary myelofibrosis (119). The -2518 A/G SNP of CCL2 has emerged as a potential susceptibility marker for MPN and myelofibrosis (120).

Systemic mastocytosis

As noted in the aforementioned myeloproliferative neoplasms, there is also a frequent elevation in the production of profibrotic and angiogenic cytokines in Systemic mastocytosis (SM), which contributes to alterations in the bone marrow microenvironment. A defining characteristic of SM is the abnormal accumulation of neoplastic MCs harboring the activating KIT mutation D816V within the bone marrow. Recent studies indicate that KIT D816V enhances CCL2 expression in abnormal MCs via the classical NF-κB signaling pathway. Furthermore, it has been demonstrated that CCL2 derived from MCs facilitates the migration of endothelial cells in SM, both *in vitro* and *in vivo*, thereby modifying the tumor microenvironment to favor fibrosis and angiogenesis. Serum CCL2 levels are markedly elevated in SM patients, with significantly higher concentrations observed in individuals with advanced SM compared to asymptomatic SM patients and those with cutaneous mastocytosis. Importantly, CCL2 levels exhibit only a moderate correlation with MCs infiltration in the bone marrow and instances of myelofibrosis (121).

Acute myeloid leukemia

Literature indicates that the CCL2/CCR2 axis may be implicated in cell migration in acute AML. However, plasma CCL2 levels in Acute myeloid leukemia (AML) patients are reported to be lower than those in healthy donors (122). This finding contrasts with earlier observations made by Manzur et al. (123), highlighting the need for further investigation.

Other fibrotic diseases

Fibrosis of the skin and internal organs is a hallmark of systemic sclerosis (SSc), with monocytes playing a crucial role in the skin's inflammatory response (124). Studies have shown that CCL2 expression is significantly higher in SSc mouse models compared to normal mice (125), and CCL2 holds significant promise as a valuable biological marker for SSc (126). Additionally, knockout of STAT6 in SSc mouse models significantly reduces the expression of CCL2 and CD206, indicating that CCL2 is involved in the immune response that drives skin and organ fibrosis (127).

Experimental autoimmune orchitis (EAO) serves as an animal model for studying chronic testicular inflammation and fibrosis, replicating pathogenic changes similar to those seen in humans. During EAO, there is an increase in pro-inflammatory CCL2 expression, which coincides with leukocyte infiltration into the testicular parenchyma. Elevated levels of activin A are correlated with the severity of EAO, while high CCL2 levels mediate leukocyte transport and the recruitment of macrophages through its receptor, CCR2. These findings suggest that both CCR2 and activin A promote fibrosis in testicular inflammation by regulating macrophage function (128).

CCL2/CCR2 axis as a diagnostic marker for fibrotic diseases

Renal diseases

Urine is an easily obtainable sample that can reflect the severity of kidney disease, making it a focus for studying CCL2 levels as a diagnostic tool and for predicting prognosis. Urrego-Callejas et al. (129) included 120 systemic lupus erythematosus (SLE) patients and found that serum anti-C1Q antibody and urinary ceruloplasmin levels were associated with CCL2 activity in chronic injury. Similarly, in 125 patients with active lupus nephritis (LN), urinary CCL2 levels were positively correlated with interstitial inflammation, glomerulosclerosis, interstitial fibrosis, and tubular atrophy based on kidney biopsies (130). Standard LN therapies, like mycophenolate and rapamycin, improve glomerular sclerosis by downregulating CCL2 and reducing fibrosis-related proteins (131).

Studies have shown that excessive cisplatin administration induces renal interstitial fibrosis in C57BL/6 mice, and CCL2 serves as a marker of renal injury in this model (132). Additionally, high urinary CCL2 and low urinary epidermal growth factor (EGF) levels are associated with renal tubulointerstitial fibrosis (133), suggesting that urinary CCL2 could be a useful diagnostic marker for CKD patients.

Identifying early prognostic markers in high-risk renal transplant recipients can help optimize immunosuppressive therapy and improve outcomes. The ratio of CCL2 to creatinine (CCL2:Cr) has been shown to predict BK nephropathy; however, the diagnostic value of CCL2 for BKV infection in immunocompromised transplant recipients still needs further investigation (134).

Cardiovascular disease

Macrophages drive vasculopathy changes in Takayasu arteritis (TA) through phenotypic transformation. Peripheral CCL2 levels fluctuate at different disease stages, suggesting CCL2 as a potential biomarker for disease activity (135). In human atria, markers of leukocyte infiltration and matrix degradation indicate severe inflammation—a key factor in atrial fibrillation—linked to CCL2 (136). In a study of 131 patients undergoing aortic valve replacement, CCL2 was identified as an inflammatory marker for aortic remodeling (137). In diabetic cardiomyopathy (DCM), both serum CCL2 and myocardial CCL2 mRNA levels are elevated (138).

IBD

An interesting study of 33 children with IBD found that blood CCL2 levels were significantly higher in patients with CD compared to those with UC at all stages of the disease (139). This suggests that CCL2 could serve as a diagnostic biomarker for CD and help differentiate subtypes of pediatric IBD. However, it remains unclear if the same pattern is present in adult IBD patients. Given that both heart failure and IBD have immune-related pathogenesis, a study identified 34 genes associated with immune diseases, including CCL2, through Gene Ontology (GO) and Kyoto Encyclopedia of Genes and Genomes (KEGG) analysis (140).

IPF

As an inflammation-related gene, *CCL2* may help predict the prognosis of IPF (141). While combined detection of CCL2, KL-6, and CXCL13 improves diagnostic accuracy for idiopathic interstitial pneumonia (IIP), it does not effectively differentiate among lung fibrosis diseases (142). Interestingly, serum CCL2 levels may help distinguish between IPF and fibrotic hypersensitivity pneumonitis (fHP), two conditions that are often difficult to differentiate (143).

CCL2 as a therapeutic target for fibrotic diseases

Recent research has identified CCL2 as a key therapeutic target for treating fibrotic diseases across various organs. Its significance in fibrosis pathogenesis has led to the development of diverse treatment strategies, including traditional Chinese medicines (TCM), chemical agents, and application of nanotechnology. The broad potential of targeting CCL2 underscores the need for further research to fully leverage its role in creating effective antifibrotic therapies. CCR2 antagonists show significant potential for treating fibrotic diseases by specifically blocking CCR2 receptors. These antagonists have demonstrated positive effects in various conditions, including liver, lung, and renal fibrosis. Studies suggest that CCR2 antagonists reduce inflammatory cell infiltration, inhibit profibrotic gene expression, and slow fibrosis progression by modulating relevant signaling pathways.

Liver diseases

In addition to the previously mentioned GILZ and SPHK1 that play a role in regulating CCL2 expression and thereby affecting liver fibrosis progression (54, 55), several pharmacological agents can also mitigate liver fibrosis by targeting the CCL2/CCR2 signaling pathway. Moreover, recent developments in nanotechnology have shown promise in the treatment of liver fibrosis through the modulation of CCL2 levels.

A recent investigation has introduced an innovative strategy involving the silencing of CCR2 through small interfering RNA (siCcr2) encapsulated within tetrahedron framework DNA nanostructure (tFNA) vehicle (tFNA-siCcr2). This method effectively overcomes the challenges associated with the *in vivo* efficacy of siCcr2 by facilitating targeted delivery to the liver, and resulting in improved therapeutic effects for liver fibrosis (144). Additionally, genetic engineering is being explored to create transgenic nano decoys that interfere with liver fibrosis. These decoys, engineered to overexpress CCR2 on their surface, can neutralize CCL2 levels. When loaded with curcumin and delivered to the liver, this combined therapy effectively reduces macrophage infiltration, offering promising therapeutic outcomes (145).

TCM formulations like Dahuang Zhizhu Pill, Tianhuang formula, and Fu-Gan-Wan have been shown to reduce the expression of CCL2 and its receptor CCR2 in the liver, particularly targeting $CCR2^{+}$ macrophages (146–148). Similarly, Fuzheng Huayu (FZHY) modulates macrophage recruitment and polarization via CCL2 and CX3CL1, providing anti-inflammatory and antifibrotic effects. The Ganxianfang formula exhibits comparable benefits and may offer superior protective effects compared to FZHY (149). These findings suggest that TCM's antifibrotic effects primarily result from inhibiting CCL2-induced macrophage recruitment to fibrotic sites, though the exact mechanisms—direct or indirect—remain unclear.Cenicriviroc (CVC) has gained attention for its therapeutic value in liver diseases. Krenkel et al. (150) conducted studies in NAFLD patients and C57BL/6 mice, demonstrating that CVC is effective and safe. CVC also enhances the therapeutic effect of fibroblast growth factor 21 on NASH, primarily by reducing liver fibrosis (151). In a mouse model of liver fibrosis induced by CCL4 and using Ccr2 knockout ($Ccr2^{-/-}$) mice, Guo et al. (152) showed that CVC treatment was effective in both mice and human liver samples. Yu et al. (153) further demonstrated that CVC was effective in treating cholestatic liver injury in bile duct-ligated rats and Mdr2 ($Abcb4^{-/-}$) mouse models. Additionally, Mbade et al. (154) found that CVC could prevent liver injury and steatosis in an alcoholic liver disease mouse model.

Bile duct diseases

The CCL2/CCR2 axis's chemotactic effect on monocytes and macrophages is a key driver of primary sclerosing cholangitis (PSC)

progression. Studies have shown a positive correlation between serum CCL2 levels and fibrosis severity in primary biliary cholangitis (PBC) patients (155). In acute sclerosing cholangitis mouse models treated with the apoptosis-inhibiting BV6 inhibitor, both CVC treatment and CCR2 deletion were found to reduce macrophage accumulation, liver damage, and biliary fibrosis (156). Similarly, Reuveni et al. (157) observed improvements in primary biliary cholangitis models using *Cx3cr1*$^{gfp/+}$ and *Ccr2*$^{-/-}$*Cx3cr1*$^{gfp/+}$ mice following intraperitoneal CVC injection.

Intestinal diseases

In the treatment of IBD, agonists or inhibitors targeting specific factors or receptors have been developed. For example, SARI, commonly used as a colon cancer inhibitor, has been found to increase CCL2 production when deficient, whereas knocking out CCR2 can block this effect, thereby reducing colitis symptoms (158). Dimethyl itaconate decreases CCL2 production in epithelial cells, reduces macrophage recruitment to the tumor microenvironment, alleviates the hyperinflammatory state of UC, and lowers the risk of colitis-associated cancer (159).

Several other drugs directly target the CCL2/CCR2 axis. Luteolin and homoharringtonine both exhibit strong anti-inflammatory effects by inhibiting NF-κB signaling and reducing CCL2 production in colonic tissues (160, 161). Nobiletin reduces CCL2 expression and collagen deposition in colitis-induced mice (162), while berberine and geniposide show similar effects in chronic colitis (163, 164).

Pulmonary diseases

Excessive inflammation in silicosis is triggered by silica exposure. Research has shown that the Caspase-1 inhibitor VX-765 reduces the infiltration of inflammatory M1 alveolar macrophages and decreases CCL2 expression, thereby mitigating the inflammatory response (165). TAS-115, a novel polytyrosine kinase inhibitor, has been found to inhibit the phosphorylation of the macrophage colony-stimulating factor receptor c-FMS in mouse bone marrow-derived macrophages, both *in vivo* and *in vitro*. This inhibition reduces CCL2 production, highlighting CCL2 as a key molecule in pulmonary fibrosis development (166).

Pancreatic diseases

Oxidative stress is a major pathway in pancreatitis pathogenesis. Hydroxytyrosol has anti-inflammatory and antioxidant effects, reducing CCL2 release in pancreatic and colon tissues (167). Additionally, the classic TCM formulation known as Dahuang Chaihu Decoction has been shown to lower the levels of CCL2 in the pancreas, which in turn reduces macrophage infiltration and fibrosis associated with CP (168).

Renal diseases

In a glomerulosclerosis model, the use of a CCR2 antagonist (CCR2A) can inhibit renal macrophage accumulation and enhance the effects of conventional treatments like angiotensin-converting enzyme inhibitors (ACEi) (169). CKD often leads to complications such as salt-sensitive (SS) hypertension. Daily intraperitoneal administration of a CCR2 antagonist (RS 102895) during active disease stages has been shown to reduce renal leukocyte infiltration, kidney injury, and hypertension incidence (170). Additionally, bladder outlet obstruction (BOO) causes bladder remodeling, affecting its structure and function. Wang et al. (171) demonstrated that treatment with a CCR2 antagonist (RS504393) may offer a therapeutic strategy for managing bladder remodeling in such conditions.

Clinical applications of CCL2/CCR2 antagonists

In recent years, a considerable number of clinical studies focusing on adult patients have been conducted to explore the effects of CCL2/CCR2 antagonists (Figure 3). Currently, significant advancements have been made in clinical research concerning the treatment of NASH-related liver fibrosis using CVC, with clinical trials advancing to Phase III. It is widely acknowledged that the medication shows good tolerability, with a safety profile similar to that of a placebo (172). Initial results from ongoing trials indicate that CVC may offer additional benefits for patients suffering from advanced fibrosis (173, 174). However, the combination of CVC with Tropifexor did not yield improved therapeutic efficacy (175). Although the Phase III clinical trial demonstrated good therapeutic efficacy, it still lacks histological data from clinical studies to confirm its efficacy in the treatment of liver fibrosis (176).

Primary sclerosing cholangitis (PSC) is a chronic cholestatic condition that can result in liver fibrosis. A multicenter clinical trial conducted with adult patients diagnosed with PSC revealed that after 24 weeks of treatment with CVC, there was a moderate decrease in the surrogate marker of serum alkaline phosphatase (ALP), and the therapy was well tolerated by the participants (177).

In addition to fibrotic diseases, there has been notable advancement in clinical trials involving CCL2/CCR2 antagonists for other conditions, including pancreatic ductal adenocarcinoma (PDAC) (178, 179) and coronary stent restenosis (180). Future exploration of larger clinical studies in these domains is warranted (Table 1).

Conclusions and future perspectives

Recent research underscores the crucial role of the CCL2/CCR2 axis in the development and progression of inflammatory and fibrotic diseases across various organs (Table 2). While the mechanisms by which CCL2 mediates cell interactions differ slightly between organs (Figure 4), its primary role in most fibrotic conditions is to recruit macrophages to sites of tissue

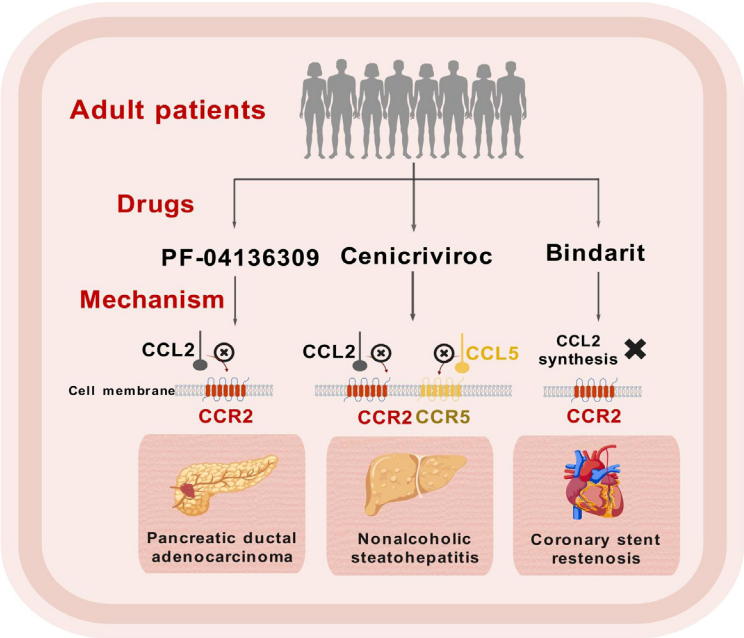

FIGURE 3
Schematic representation of clinical trials for CCL2/CCR2 inhibitors. This figure was created with biogdp.com.

TABLE 1 Clinical trials of CCR2/CCL2 antagonists in treating inflammatory and fibrotic diseases.

Drug(s)	Mechanism	Disease	Research Stage	Efficacy and safety	Trial identification	Authors (year) [reference]
CVC; Tropifexor (TXR)	TXR, a potent nonbile acid FXR agonist	NASH	IIb	Combination therapy safety similar to monotherapy; no significant improvement in efficacy.	NCT03517540	Anstee et al. (2023) (175)
CVC	CCR2/5 dual antagonist	NASH	II	While overall safety remains satisfactory, the patient's condition has not improved significantly.	NCT03059446	.Francque et al. (2024) (172)
			IIb	Safe and improves liver fibrosis in some patients.	NCT02217475	Friedman et al. (2018) (173)
			III	Good efficacy and tolerability; significant effect on advanced fibrosis.	NCT02217475	Ratziu et al. (2020) (174)
			III	Safe, but did not meet histological efficacy criteria.	NCT03028740	Anstee et al. (2024) (176)
		PSC	II	Demonstrated good efficacy and safety.	NCT02653625	Eksteen et al. (2021) (177)
PF-04136309	PF-04136309(CCR2 antagonist) in combination with FOLFIRINOX	PDAC	Ib	Good tolerance, most patients experienced remission.	NCT01413022	Nywening et al. (2016) (178)
PF-04136309	PF-04136309 in combination with nab-paclitaxel/gemcitabine	PDAC	Ib	High incidence of lung toxicity; combination therapy showed no better efficacy than monotherapy.	NCT02732938	Noel et al. (2020) (179)
Bindarit	Selective inhibitor of CCL2	Coronary stent restenosis	II	Showed therapeutic effect with good tolerability; did not reach a primary endpoint.	NCT01269242	Colombo et al. (2016) (180)

CVC, Cenicriviroc; NASH, Nonalcoholic steatohepatitis; PSC, Primary sclerosing cholangitis; PDAC, Pancreatic ductal adenocarcinoma.

damage. An exception is viral hepatitis, where CCL2 expression is downregulated in liver cells, contributing to an immunosuppressive environment that allows viral persistence, a key early step in the disease's pathogenesis.

In pancreatic fibrosis, the role of the CCL2/CCR2 axis is less understood. It remains unclear whether CCL2 is the primary chemokine driving macrophage infiltration in the pancreas or which genes trigger its activation during fibrosis. Recent evidence

TABLE 2 The role of CCL2/CCR2 axis in organ fibrosis.

Disease	Main role of CCL2/CCR2 axis in fibrosis	Reference
Hepatic fibrosis	The CCL2/CCR2 axis not only attracts chemotactic macrophages to the liver but also promotes M1 polarization of macrophages, activating hepatic stellate cells (HSCs) via inflammatory factors like IL-1β and TNF-α and signaling pathways such as NF-κB.	(39, 41, 43)
Intestinal fibrosis	In intestinal tissues, the CCL2/CCR2 axis attracts chemotactic monocytes/macrophages to fibrotic regions, induces M2 polarization, and participates in inflammation-mediated fibrosis through factors like IL-6 and IL-17.	(57, 59, 60, 62, 65, 67, 69)
Cardiovascular fibrosis	The CCL2/CCR2 axis recruit leukocytes to inflammatory areas and promotes monocyte differentiation into macrophages, where M1-type macrophages aid in myocardial healing.	(77, 78)
Pulmonary fibrosis	In pulmonary fibrosis, alveolar epithelial cells and macrophages are primary sources of CCL2. They release IL-4 and IL-13 upon inflammatory stimulation, which activates myofibroblasts and promotes fibrosis progression.	(94–97)
Renal fibrosis	In kidney injury, various cells such as renal tubular epithelial cells, macrophages, and fibroblasts release CCL2. Binding to CCR2 recruits chemotactic monocytes to the damaged site, releasing TGF-β and IL-6.	(106–108)

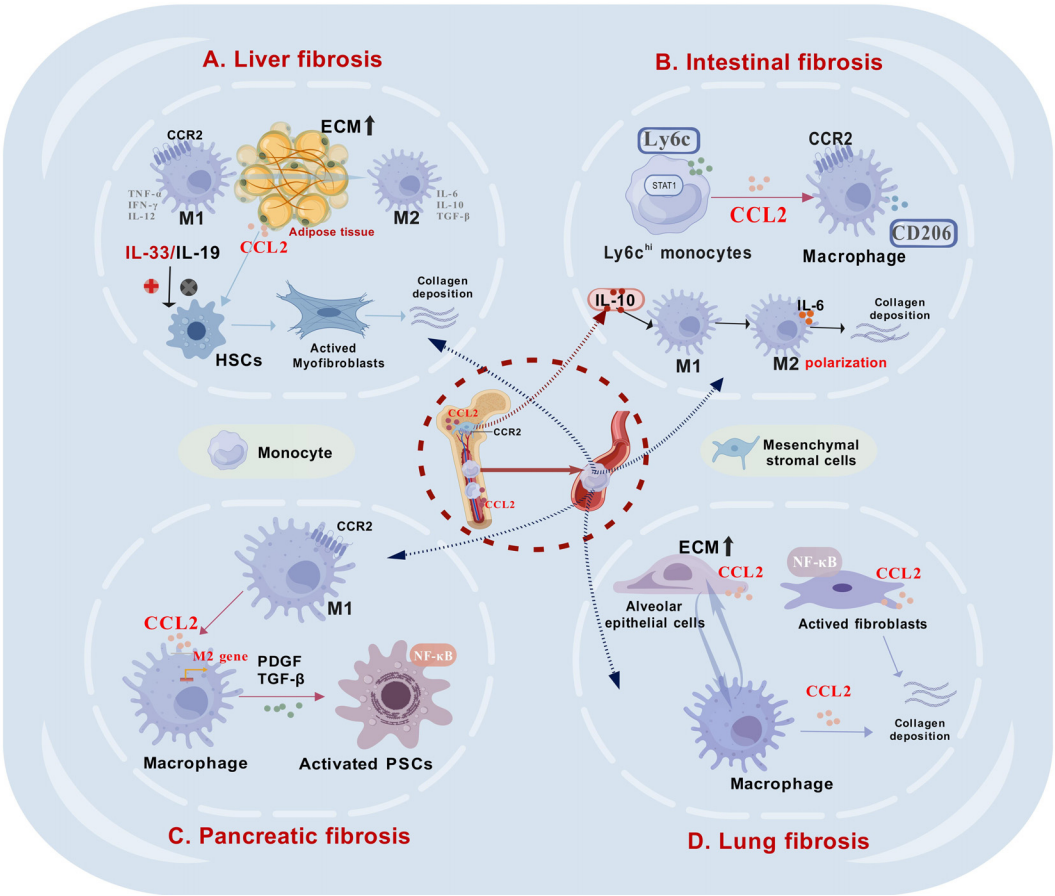

FIGURE 4
The role of CCL2 in mediating intercellular interactions within fibrotic tissues in various organs. **(A)**. In liver fibrosis, CCL2 plays a critical role by recruiting macrophages to the fibrotic regions and facilitating their M2 polarization, which subsequently activates hepatic stellate cells (HSCs) and promotes collagen deposition. **(B)**. In intestinal fibrosis, Ly6C^{hi} monocytes are predominant, and an increase in their proportion significantly enhances the expression of CCL2. Bone marrow-derived mesenchymal stromal cells (BM-MSCs) can release IL-10, which facilitates the M2 polarization of intestinal macrophages, subsequently contributing to the development of fibrosis. **(C)**. In pancreatic fibrosis, M2 macrophages secrete pro-fibrotic factors that activate pancreatic stellate cells (PSCs), a process similar to that in liver fibrosis. **(D)**. In lung fibrosis, alveolar epithelial cells (AECs) exhibit increased CCL2 production, facilitating macrophage recruitment to fibrotic regions. Additionally, activated fibroblasts release significant amounts of CCL2 via NF-κB signaling, contributing to collagen accumulation. This figure was created with biogdp.com.

suggests that SPHK1 is critical in promoting fibrosis in CP models (181). Given SPHK1's regulatory effect on CCL2 in liver fibrosis, it is worth investigating if a similar mechanism occurs in SPHK1-induced pancreatic fibrosis.

Another area needing exploration is the role of CCL2 in pain associated with fibrotic diseases. Emerging studies have linked CCL2 to pancreatic tumor growth, neural invasion, and pancreatic cancer-related pain (182, 183). Since pain is a common, debilitating symptom in many inflammatory and fibrotic conditions, such as CP (184), understanding how CCL2 contributes to neural invasion and pain mechanisms could reveal new research and treatment avenues.

The therapeutic potential of targeting the CCL2/CCR2 axis is promising. Various strategies, including natural compounds, chemical agents, and traditional Chinese medicine, have been explored to modulate this pathway in treating fibrotic diseases, highlighting its clinical translation potential. Beyond inflammatory and fibrotic conditions, targeting CCL2 could also enhance cancer treatment, particularly immunotherapy in cancers such as esophageal squamous cell carcinoma (185, 186) and breast cancer (187). Circulating CCL2 levels may also serve as biomarkers for predicting the onset, progression, and prognosis of various cancers, including liver and prostate cancers. Further research is needed to determine if CCL2 has similar predictive value in other cancers and its potential to improve chemotherapy outcomes.

Clinical trials of CCL2/CCR2 antagonists are ongoing for various diseases. In conclusion, recent studies investigating the role of CCR2 antagonists in treating fibrotic diseases have shown promising safety profiles, with the majority of participants reporting significant symptom relief. However, there is an urgent necessity for more sophisticated assessment methodologies to rigorously evaluate the effectiveness of CCL2/CCR2 inhibitors in various fibrotic conditions. Notwithstanding these challenges, CCL2 is anticipated to undergo further evaluation as a viable therapeutic target for a broader spectrum of organ-related diseases, potentially providing patients with innovative and effective treatment alternatives.

Author contributions

SG: Writing – original draft, Conceptualization, Software, Visualization. QZ: Conceptualization, Writing – review & editing. YG: Formal Analysis, Writing – review & editing. XY: Software, Writing – review & editing. PZ: Software, Writing – review & editing. TM: Methodology, Writing – review & editing. ZT: Supervision, Writing – review & editing. XL: Funding acquisition, Resources, Supervision, Writing – review & editing.

Funding

The author(s) declare financial support was received for the research, authorship, and/or publication of this article. National Natural Science Foundation of China (Grant No.: 82270676); Taishan Young Scholars Program of Shandong Province (NO. tsqn202306395); 2023 Qingdao Technology Benefiting Demonstration Project (Grant No.: 23–2-8-smjk-8-nsh); 2021 Shandong Province Graduate Education and Teaching Reform Research Project (SDYJG21110); Qingdao Chinese Medicine Technology Project (Grant No.: 2021-zyym26).

Conflict of interest

The authors declare that there are no commercial or financial relationships that could be construed as a potential conflict of interest in the conduct of this research.

Publisher's note

References

1. Hughes CE, Nibbs RJB. A guide to chemokines and their receptors. *FEBS J.* (2018) 285:2944–71. doi: 10.1111/febs.2018.285.issue-16

2. Ono SJ, Nakamura T, Miyazaki D, Ohbayashi M, Dawson M, Toda M. Chemokines: roles in leukocyte development, trafficking, and effector function. *J Allergy Clin Immunol.* (2003) 111:1185–99. doi: 10.1067/mai.2003.1594

3. Sokol CL, Luster AD. The chemokine system in innate immunity. *Cold Spring Harb Perspect Biol.* (2015) 7(5):a016303. doi: 10.1101/cshperspect.a016303

4. Murphy PM, Baggiolini M, Charo IF, Hébert CA, Horuk R, Matsushima K, et al. International union of pharmacology. XXII. Nomenclature for chemokine receptors. *Pharmacol Rev.* (2000) 52:145–76.

5. Matsushima K, Larsen CG, DuBois GC, Oppenheim JJ. Purification and characterization of a novel monocyte chemotactic and activating factor produced by a human myelomonocytic cell line. *J Exp Med.* (1989) 169:1485–90. doi: 10.1084/jem.169.4.1485

6. Van Coillie E, Van Damme J, Opdenakker G. The MCP/eotaxin subfamily of CC chemokines. *Cytokine Growth Factor Rev.* (1999) 10:61–86. doi: 10.1016/S1359-6101(99)00005-2

7. Standiford TJ, Kunkel SL, Phan SH, Rollins BJ, Strieter RM. Alveolar macrophage-derived cytokines induce monocyte chemoattractant protein-1 expression from human pulmonary type II-like epithelial cells. *J Biol Chem.* (1991) 266:9912–8. doi: 10.1016/S0021-9258(18)92905-4

8. Gschwandtner M, Derler R, Midwood KS. More than just attractive: how CCL2 influences myeloid cell behavior beyond chemotaxis. *Front Immunol.* (2019) 10:2759. doi: 10.3389/fimmu.2019.02759

9. Huma ZE, Sanchez J, Lim HD, Bridgford JL, Huang C, Parker BJ, et al. Key determinants of selective binding and activation by the monocyte chemoattractant proteins at the chemokine receptor CCR2. *Sci Signal.* (2017) 10(480):eaai8529. doi: 10.1126/scisignal.aai8529

10. Bhusal RP, Foster SR, Stone MJ. Structural basis of chemokine and receptor interactions: Key regulators of leukocyte recruitment in inflammatory responses. *Protein Sci.* (2020) 29:420–32. doi: 10.1002/pro.v29.2

11. Ren J, Wang Q, Morgan S, Si Y, Ravichander A, Dou C, et al. Protein kinase C-δ (PKCδ) regulates proinflammatory chemokine expression through cytosolic interaction with the NF-κB subunit p65 in vascular smooth muscle cells. *J Biol Chem.* (2014) 289:9013–26. doi: 10.1074/jbc.M113.515957

12. Chiu HY, Sun KH, Chen SY, Wang HH, Lee MY, Tsou YC, et al. Autocrine CCL2 promotes cell migration and invasion via PKC activation and tyrosine phosphorylation of paxillin in bladder cancer cells. *Cytokine*. (2012) 59:423–32. doi: 10.1016/j.cyto.2012.04.017

13. Jiménez-Sainz MC, Fast B, Mayor F Jr., Aragay AM. Signaling pathways for monocyte chemoattractant protein 1-mediated extracellular signal-regulated kinase activation. *Mol Pharmacol*. (2003) 64:773–82. doi: 10.1124/mol.64.3.773

14. Hao Q, Vadgama JV, Wang P. CCL2/CCR2 signaling in cancer pathogenesis. *Cell Commun Signal*. (2020) 18:82. doi: 10.1186/s12964-020-00589-8

15. Arefieva TI, Kukhtina NB, Antonova OA, Krasnikova TL. MCP-1-stimulated chemotaxis of monocytic and endothelial cells is dependent on activation of different signaling cascades. *Cytokine*. (2005) 31:439–46. doi: 10.1016/j.cyto.2005.06.016

16. Yasui H, Kajiyama H, Tamauchi S, Suzuki S, Peng Y, Yoshikawa N, et al. CCL2 secreted from cancer-associated mesothelial cells promotes peritoneal metastasis of ovarian cancer cells through the P38-MAPK pathway. *Clin Exp Metastasis*. (2020) 37:145–58. doi: 10.1007/s10585-019-09993-y

17. Roca H, Varsos Z, Pienta KJ. CCL2 protects prostate cancer PC3 cells from autophagic death via phosphatidylinositol 3-kinase/AKT-dependent survivin up-regulation. *J Biol Chem*. (2008) 283:25057–73. doi: 10.1074/jbc.M801073200

18. Li D, Ji H, Niu X, Yin L, Wang Y, Gu Y, et al. Tumor-associated macrophages secrete CC-chemokine ligand 2 and induce tamoxifen resistance by activating PI3K/Akt/mTOR in breast cancer. *Cancer Sci*. (2020) 111:47–58. doi: 10.1111/cas.14230

19. Charo IF, Ransohoff RM. The many roles of chemokines and chemokine receptors in inflammation. *N Engl J Med*. (2006) 354:610–21. doi: 10.1056/NEJMra052723

20. Griffith JW, Sokol CL, Luster AD. Chemokines and chemokine receptors: positioning cells for host defense and immunity. *Annu Rev Immunol*. (2014) 32:659–702. doi: 10.1146/annurev-immunol-032713-120145

21. Nagarsheth N, Wicha MS, Zou W. Chemokines in the cancer microenvironment and their relevance in cancer immunotherapy. *Nat Rev Immunol*. (2017) 17:559–72. doi: 10.1038/nri.2017.49

22. Morein D, Erlichman N, Ben-Baruch A. Beyond cell motility: the expanding roles of chemokines and their receptors in Malignancy. *Front Immunol*. (2020) 11:952. doi: 10.3389/fimmu.2020.00952

23. Xu M, Wang Y, Xia R, Wei Y, Wei X. Role of the CCL2-CCR2 signalling axis in cancer: Mechanisms and therapeutic targeting. *Cell Prolif*. (2021) 54:e13115. doi: 10.1111/cpr.13115

24. Ozga AJ, Chow MT, Luster AD. Chemokines and the immune response to cancer. *Immunity*. (2021) 54:859–74. doi: 10.1016/j.immuni.2021.01.012

25. Lee S, Lee E, Ko E, Ham M, Lee HM, Kim ES, et al. Tumor-associated macrophages secrete CCL2 and induce the invasive phenotype of human breast epithelial cells through upregulation of ERO1-α and MMP-9. *Cancer Lett*. (2018) 437:25–34. doi: 10.1016/j.canlet.2018.08.025

26. Hou P, Kapoor A, Zhang Q, Li J, Wu CJ, Li J, et al. Tumor microenvironment remodeling enables bypass of oncogenic KRAS dependency in pancreatic cancer. *Cancer Discovery*. (2020) 10:1058–77. doi: 10.1158/2159-8290.CD-19-0597

27. Dey P, Li J, Zhang J, Chaurasiya S, Strom A, Wang H, et al. Oncogenic KRAS-driven metabolic reprogramming in pancreatic cancer cells utilizes cytokines from the tumor microenvironment. *Cancer Discovery*. (2020) 10:608–25. doi: 10.1158/2159-8290.CD-19-0297

28. Yoshimura T. The chemokine MCP-1 (CCL2) in the host interaction with cancer: a foe or ally? *Cell Mol Immunol*. (2018) 15:335–45. doi: 10.1038/cmi.2017.135

29. Proudfoot AE. Chemokine receptors: multifaceted therapeutic targets. *Nat Rev Immunol*. (2002) 2:106–15. doi: 10.1038/nri722

30. Vilgelm AE, Richmond A. Chemokines modulate immune surveillance in tumorigenesis, metastasis, and response to immunotherapy. *Front Immunol*. (2019) 10:333. doi: 10.3389/fimmu.2019.00333

31. Saxena S, Singh RK. Chemokines orchestrate tumor cells and the microenvironment to achieve metastatic heterogeneity. *Cancer Metastasis Rev*. (2021) 40:447–76. doi: 10.1007/s10555-021-09970-6

32. Marra F, Tacke F. Roles for chemokines in liver disease. *Gastroenterology*. (2014) 147:577–594.e1. doi: 10.1053/j.gastro.2014.06.043

33. Li S, Zhou B, Xue M, Zhu J, Tong G, Fan J, et al. Macrophage-specific FGF12 promotes liver fibrosis progression in mice. *Hepatology*. (2023) 77:816–33. doi: 10.1002/hep.32640

34. Chen Y, Wang J, Zhou N, Fang Q, Cai H, Du Z, et al. Protozoan-derived cytokine-transgenic macrophages reverse hepatic fibrosis. *Adv Sci (Weinh)*. (2024) 11:e2308750. doi: 10.1002/advs.202308750

35. Guillen-Sacoto MJ, Martinez AF, Abe Y, Kruszka P, Weiss K, Everson JL, et al. Human germline hedgehog pathway mutations predispose to fatty liver. *J Hepatol*. (2017) 67:809–17. doi: 10.1016/j.jhep.2017.06.008

36. Giannelli G, Chieti A, Cigliano A, Mancarella S, Dituri F. TGF-β as multifaceted orchestrator in HCC progression: signaling, EMT, immune microenvironment, and novel therapeutic perspectives. *Semin Liver Dis*. (2018) 39:053–69. doi: 10.1055/s-0038-1676121

37. Zhuang H, Cao G, Kou C, Liu T. CCL2/CCR2 axis induces hepatocellular carcinoma invasion and epithelial-mesenchymal transition *in vitro* through activation of the Hedgehog pathway. *Oncol Rep*. (2018) 39:21–30. doi: 10.3892/or.2017.6069

38. Li X, Yuan B, Lu M, Wang Y, Ding N, Liu C, et al. The methyltransferase METTL3 negatively regulates nonalcoholic steatohepatitis (NASH) progression. *Nat Commun*. (2021) 12:7213. doi: 10.1038/s41467-021-27539-3

39. Ni Y, Zhuge F, Ni L, Nagata N, Yamashita T, Mukaida N, et al. CX3CL1/CX3CR1 interaction protects against lipotoxicity-induced nonalcoholic steatohepatitis by regulating macrophage migration and M1/M2 status. *Metabolism*. (2022) 136:155272. doi: 10.1016/j.metabol.2022.155272

40. Yu J, Zhu C, Wang X, Kim K, Bartolome A, Dongiovanni P, et al. Hepatocyte TLR4 triggers inter-hepatocyte Jagged1/Notch signaling to determine NASH-induced fibrosis. *Sci Transl Med*. (2021) 13(599):eabe1692. doi: 10.1126/scitranslmed.abe1692

41. Kang J, Postigo-Fernandez J, Kim K, Zhu C, Yu J, Meroni M, et al. Notch-mediated hepatocyte MCP-1 secretion causes liver fibrosis. *JCI Insight*. (2023) 8:e165369. doi: 10.1172/jci.insight.165369

42. Hammoutene A, Biquard L, Lasselin J, Kheloufi M, Tanguy M, Vion AC, et al. A defect in endothelial autophagy occurs in patients with non-alcoholic steatohepatitis and promotes inflammation and fibrosis. *J Hepatol*. (2020) 72:528–38. doi: 10.1016/j.jhep.2019.10.028

43. Parker R, Weston CJ, Miao Z, Corbett C, Armstrong MJ, Ertl L, et al. CC chemokine receptor 2 promotes recruitment of myeloid cells associated with insulin resistance in nonalcoholic fatty liver disease. *Am J Physiol Gastrointest Liver Physiol*. (2018) 314:G483–93. doi: 10.1152/ajpgi.00213.2017

44. Xu B, Jiang M, Chu Y, Wang W, Chen D, Li X, et al. Gasdermin D plays a key role as a pyroptosis executor of non-alcoholic steatohepatitis in humans and mice. *J Hepatol*. (2018) 68:773–82. doi: 10.1016/j.jhep.2017.11.040

45. Unamuno X, Gómez-Ambrosi J, Ramírez B, Rodríguez A, Becerril S, Valentí V, et al. NLRP3 inflammasome blockade reduces adipose tissue inflammation and extracellular matrix remodeling. *Cell Mol Immunol*. (2021) 18:1045–57. doi: 10.1038/s41423-019-0296-z

46. Wakamatsu S, Jojima T, Hashiguchi M, Kishi H, Niitani T, Sakurai S, et al. Inhibition of IL-33 signaling ameliorate hepatic fibrosis with decreasing MCP-1 in a mouse model of diabetes and non-alcoholic steatohepatitis; comparison for luseogliflozin, an SGLT2 inhibitor. *J Diabetes Complications*. (2024) 38:108650. doi: 10.1016/j.jdiacomp.2023.108650

47. Ono N, Fujita T, Miki M, Nishiyama K, Izawa T, Aoyama T, et al. Interleukin-19 gene-deficient mice promote liver fibrosis via enhanced TGF-β Signaling, and the interleukin-19-CCL2 axis is important in the direction of liver fibrosis. *Biomedicines*. (2023) 11(7):2064. doi: 10.3390/biomedicines11072064

48. Duriez M, Mandouri Y, Lekbaby B, Wang H, Schnuriger A, Redelsperger F, et al. Alternative splicing of hepatitis B virus: A novel virus/host interaction altering liver immunity. *J Hepatol*. (2017) 67:687–99. doi: 10.1016/j.jhep.2017.05.025

49. Barathan M, Riazalhosseini B, Iyadorai T, Vellasamy KM, Vadivelu J, Chang LY, et al. Comparative expression of pro-inflammatory and apoptotic biosignatures in chronic HBV-infected patients with and without liver cirrhosis. *Microb Pathog*. (2021) 161:105231. doi: 10.1016/j.micpath.2021.105231

50. Xie X, Lv H, Liu C, Su X, Yu Z, Song S, et al. HBeAg mediates inflammatory functions of macrophages by TLR2 contributing to hepatic fibrosis. *BMC Med*. (2021) 19:247. doi: 10.1186/s12916-021-02085-3

51. Sarma NJ, Tiriveedhi V, Crippin JS, Chapman WC, Mohanakumar T, Williams B. Hepatitis C virus-induced changes in microRNA 107 (miRNA-107) and miRNA-449a modulate CCL2 by targeting the interleukin-6 receptor complex in hepatitis. *J Virol*. (2014) 88:3733–43. doi: 10.1128/JVI.03060-13

52. Song X, Gao X, Wang Y, Raja R, Zhang Y, Yang S, et al. HCV core protein induces chemokine CCL2 and CXCL10 expression through NF-κB signaling pathway in macrophages. *Front Immunol*. (2021) 12:654998. doi: 10.3389/fimmu.2021.654998

53. Bai YM, Liang S, Zhou B. Revealing immune infiltrate characteristics and potential immune-related genes in hepatic fibrosis: based on bioinformatics, transcriptomics and q-PCR experiments. *Front Immunol*. (2023) 14:1133543. doi: 10.3389/fimmu.2023.1133543

54. Flamini S, Sergeev P, Viana de Barros Z, Mello T, Biagioli M, Paglialunga M, et al. Glucocorticoid-induced leucine zipper regulates liver fibrosis by suppressing CCL2-mediated leukocyte recruitment. *Cell Death Dis*. (2021) 12:421. doi: 10.1038/s41419-021-03704-w

55. Lan T, Li C, Yang G, Sun Y, Zhuang L, Ou Y, et al. Sphingosine kinase 1 promotes liver fibrosis by preventing miR-19b-3p-mediated inhibition of CCR2. *Hepatology*. (2018) 68:1070–86. doi: 10.1002/hep.29885

56. Moreno Traspas R, Teoh TS, Wong PM, Maier M, Chia CY, Lay K, et al. Loss of FOCAD, operating via the SKI messenger RNA surveillance pathway, causes a pediatric syndrome with liver cirrhosis. *Nat Genet*. (2022) 54:1214–26. doi: 10.1038/s41588-022-01120-0

57. Kii S, Kitamura H, Hashimoto S, Ikeo K, Ichikawa N, Yoshida T, et al. STAT1-mediated induction of Ly6c-expressing macrophages are involved in the pathogenesis of an acute colitis model. *Inflammation Res*. (2022) 71:1079–94. doi: 10.1007/s00011-022-01620-z

58. Pei X, Sun Q, Zhang Y, Wang P, Peng X, Guo C, et al. PC3-secreted microprotein is a novel chemoattractant protein and functions as a high-affinity ligand for CC

chemokine receptor 2. *J Immunol*. (2014) 192:1878–86. doi: 10.4049/jimmunol.1300758

59. Pei X, Zheng D, She S, Ma J, Guo C, Mo X, et al. The PSMP-CCR2 interactions trigger monocyte/macrophage-dependent colitis. *Sci Rep*. (2017) 7:5107. doi: 10.1038/s41598-017-05255-7

60. Rahabi M, Jacquemin G, Prat M, Meunier E, AlaEddine M, Bertrand B, et al. Divergent roles for macrophage C-type lectin receptors, dectin-1 and mannose receptors, in the intestinal inflammatory response. *Cell Rep*. (2020) 30:4386–4398.e5. doi: 10.1016/j.celrep.2020.03.018

61. Schaefer REM, Callahan RC, Atif SM, Orlicky DJ, Cartwright IM, Fontenot AP, et al. Disruption of monocyte-macrophage differentiation and trafficking by a heme analog during active inflammation. *Mucosal Immunol*. (2022) 15:244–56. doi: 10.1038/s41385-021-00474-8

62. Stakenborg M, Abdurahiman S, De Simone V, Goverse G, Stakenborg N, van Baarle L, et al. Enteric glial cells favor accumulation of anti-inflammatory macrophages during the resolution of muscularis inflammation. *Mucosal Immunol*. (2022) 15:1296–308. doi: 10.1038/s41385-022-00563-2

63. Giri J, Das R, Nylen E, Chinnadurai R, Galipeau J. CCL2 and CXCL12 derived from mesenchymal stromal cells cooperatively polarize IL-10+ Tissue macrophages to mitigate gut injury. *Cell Rep*. (2020) 30:1923–1934.e4. doi: 10.1016/j.celrep.2020.01.047

64. Kuroda N, Masuya M, Tawara I, Tsuboi J, Yoneda M, Nishikawa K, et al. Infiltrating CCR2(+) monocytes and their progenies, fibrocytes, contribute to colon fibrosis by inhibiting collagen degradation through the production of TIMP-1. *Sci Rep*. (2019) 9:8568. doi: 10.1038/s41598-019-45012-6

65. Cao Q, Lin Y, Yue C, Wang Y, Quan F, Cui X, et al. IL-6 deficiency promotes colitis by recruiting Ly6C(hi) monocytes into inflamed colon tissues in a CCL2-CCR2-dependent manner. *Eur J Pharmacol*. (2021) 904:174165. doi: 10.1016/j.ejphar.2021.174165

66. Liu X, Lu Y, Zhu J, Liu M, Xie M, Ye M, et al. A long noncoding RNA, antisense IL-7, promotes inflammatory gene transcription through facilitating histone acetylation and switch/sucrose nonfermentable chromatin remodeling. *J Immunol*. (2019) 203:1548–59. doi: 10.4049/jimmunol.1900256

67. Yang X, Yabe-Wada T, Han J, Saito F, Ogasawara C, Yamada S, et al. PCBP1 acts as a regulator of CCL2 expression in macrophages to induce recruitment of monocyte-derived macrophages into the inflamed colon. *Int Immunol*. (2023) 35:287–99. doi: 10.1093/intimm/dxad003

68. Mei C, Meng F, Wang X, Yan S, Zheng Q, Zhang X, et al. CD30L is involved in the regulation of the inflammatory response through inducing homing and differentiation of monocytes via CCL2/CCR2 axis and NF-κB pathway in mice with colitis. *Int Immunopharmacol*. (2022) 110:108934. doi: 10.1016/j.intimp.2022.108934

69. Li T, Liu Y, Yu X, Wang P, Sun S, Liu D. IL-17D affects the chemokines and chemokine receptors of intestinal epithelial cells under hyperoxia. *Int Immunopharmacol*. (2022) 113:109386. doi: 10.1016/j.intimp.2022.109386

70. Mews P, Phillips P, Fahmy R, Korsten M, Pirola R, Wilson J, et al. Pancreatic stellate cells respond to inflammatory cytokines: potential role in chronic pancreatitis. *Gut*. (2002) 50:535–41. doi: 10.1136/gut.50.4.535

71. Sun LK, Reding T, Bain M, Heikenwalder M, Bimmler D, Graf R. Prostaglandin E2 modulates TNF-alpha-induced MCP-1 synthesis in pancreatic acinar cells in a PKA-dependent manner. *Am J Physiol Gastrointest Liver Physiol*. (2007) 293:G1196–204. doi: 10.1152/ajpgi.00330.2007

72. Xue J, Sharma V, Hsieh MH, Chawla A, Murali R, Pandol SJ, et al. Alternatively activated macrophages promote pancreatic fibrosis in chronic pancreatitis. *Nat Commun*. (2015) 6:7158. doi: 10.1038/ncomms8158

73. Wu N, Xu XF, Xin JQ, Fan JW, Wei YY, Peng QX, et al. The effects of nuclear factor-kappa B in pancreatic stellate cells on inflammation and fibrosis of chronic pancreatitis. *J Cell Mol Med*. (2021) 25:2213–27. doi: 10.1111/jcmm.16213

74. Vos T, Lim SS, Abbafati C, Abbas KM, Abbasi M, Abbasifard M, et al. Global burden of 369 diseases and injuries in 204 countries and territories, 1990–2019: a systematic analysis for the Global Burden of Disease Study 2019. *Lancet*. (2020) 396:1204–22. doi: 10.1016/S0140-6736(20)30925-9

75. Liberale L, Badimon L, Montecucco F, Lüscher TF, Libby P, Camici GG. Inflammation, aging, and cardiovascular disease: JACC review topic of the week. *J Am Coll Cardiol*. (2022) 79:837–47. doi: 10.1016/j.jacc.2021.12.017

76. Weber C, Noels H. Atherosclerosis: current pathogenesis and therapeutic options. *Nat Med*. (2011) 17:1410–22. doi: 10.1038/nm.2538

77. Chen L, Pan D, Zhang Y, Zhang E, Ma L. C-C motif chemokine 2 regulates macrophage polarization and contributes to myocardial infarction healing. *J Interferon Cytokine Res*. (2024) 44:68–79. doi: 10.1089/jir.2023.0132

78. Cheng Y, Luo D, Zhao Y, Rong J. N-Propargyl caffeate amide (PACA) prevents cardiac fibrosis in experimental myocardial infarction by promoting pro-resolving macrophage polarization. *Aging (Albany NY)*. (2020) 12:5384–98. doi: 10.18632/aging.102959

79. Shen SC, Xu J, Cheng C, Xiang XJ, Hong BY, Zhang M, et al. Macrophages promote the transition from myocardial ischemia reperfusion injury to cardiac fibrosis in mice through GMCSF/CCL2/CCR2 and phenotype switching. *Acta Pharmacol Sin*. (2024) 45:959–74. doi: 10.1038/s41401-023-01222-3

80. Zhuang L, Zong X, Yang Q, Fan Q, Tao R. Interleukin-34-NF-κB signaling aggravates myocardial ischemic/reperfusion injury by facilitating macrophage recruitment and polarization. *EBioMedicine*. (2023) 95:104744. doi: 10.1016/j.ebiom.2023.104744

81. Georgakis MK, de Lemos JA, Ayers C, Wang B, Björkbacka H, Pana TA, et al. Association of circulating monocyte chemoattractant protein-1 levels with cardiovascular mortality: A meta-analysis of population-based studies. *JAMA Cardiol*. (2021) 6:587–92. doi: 10.1001/jamacardio.2020.5392

82. Georgakis MK, van der Laan SW, Asare Y, Mekke JM, Haitjema S, Schoneveld AH, et al. Monocyte-chemoattractant protein-1 levels in human atherosclerotic lesions associate with plaque vulnerability. *Arterioscler Thromb Vasc Biol*. (2021) 41:2038–48. doi: 10.1161/ATVBAHA.121.316091

83. Georgakis MK, Gill D, Rannikmäe K, Traylor M. Genetically determined levels of circulating cytokines and risk of stroke. *Circulation*. (2019) 139:256–68. doi: 10.1161/CIRCULATIONAHA.118.035905

84. Winter C, Silvestre-Roig C, Ortega-Gomez A, Lemnitzer P, Poelman H, Schumski A, et al. Chrono-pharmacological targeting of the CCL2-CCR2 axis ameliorates atherosclerosis. *Cell Metab*. (2018) 28:175–182.e5. doi: 10.1016/j.cmet.2018.05.002

85. Singh S, Anshita D, Ravichandiran V. MCP-1: Function, regulation, and involvement in disease. *Int Immunopharmacol*. (2021) 101:107598. doi: 10.1016/j.intimp.2021.107598

86. Luo Y, Zhang H, Yu J, Wei L, Li M, Xu W. Stem cell factor/mast cell/CCL2/monocyte/macrophage axis promotes Coxsackievirus B3 myocarditis and cardiac fibrosis by increasing Ly6C(high) monocyte influx and fibrogenic mediators production. *Immunology*. (2022) 167:590–605. doi: 10.1111/imm.13556

87. Chouvarine P, Legchenko E, Geldner J, Riehle C, Hansmann G. Hypoxia drives cardiac miRNAs and inflammation in the right and left ventricle. *J Mol Med (Berl)*. (2019) 97:1427–38. doi: 10.1007/s00109-019-01817-6

88. Yang J, Agarwal M, Ling S, Teitz-Tennenbaum S, Zemans RL, Osterholzer JJ, et al. Diverse injury pathways induce alveolar epithelial cell CCL2/12, which promotes lung fibrosis. *Am J Respir Cell Mol Biol*. (2020) 62:622–32. doi: 10.1165/rcmb.2019-0297OC

89. Scotton CJ, Chambers RC. Molecular targets in pulmonary fibrosis: the myofibroblast in focus. *Chest*. (2007) 132:1311–21. doi: 10.1378/chest.06-2568

90. Zhao T, Wu X, Zhao X, Yao K, Li X, Ni J. Identification and validation of chemokine system-related genes in idiopathic pulmonary fibrosis. *Front Immunol*. (2023) 14:1159856. doi: 10.3389/fimmu.2023.1159856

91. Hult EM, Gurczynski SJ, O'Dwyer DN, Zemans RL, Rasky A, Wang Y, et al. Myeloid- and epithelial-derived heparin-binding epidermal growth factor-like growth factor promotes pulmonary fibrosis. *Am J Respir Cell Mol Biol*. (2022) 67:641–53. doi: 10.1165/rcmb.2022-0174OC

92. Bian F, Lan YW, Zhao S, Deng Z, Shukla S, Acharya A, et al. Lung endothelial cells regulate pulmonary fibrosis through FOXF1/R-Ras signaling. *Nat Commun*. (2023) 14:2560. doi: 10.1038/s41467-023-38177-2

93. Nie Y, Zhai X, Li J, Sun A, Che H, Christman JW, et al. NFATc3 promotes pulmonary inflammation and fibrosis by regulating production of CCL2 and CXCL2 in macrophages. *Aging Dis*. (2023) 14:1441–57. doi: 10.14336/AD.2022.1202

94. Li C, Feng X, Li S, He X, Luo Z, Cheng X, et al. Tetrahedral DNA loaded siCCR2 restrains M1 macrophage polarization to ameliorate pulmonary fibrosis in chemoradiation-induced murine model. *Mol Ther*. (2024) 32:766–82. doi: 10.1016/j.ymthe.2024.01.022

95. Karman J, Wang J, Bodea C, Cao S, Levesque MC. Lung gene expression and single cell analyses reveal two subsets of idiopathic pulmonary fibrosis (IPF) patients associated with different pathogenic mechanisms. *PloS One*. (2021) 16:e0248889. doi: 10.1371/journal.pone.0248889

96. Walsh SMW, Worrell JC, Fabre A, Hinz B, Kane R, Keane MP. Novel differences in gene expression and functional capabilities of myofibroblast populations in idiopathic pulmonary fibrosis. *Am J Physiol-Lung C*. (2018) 315:L697–710. doi: 10.1152/ajplung.00543.2017

97. Hadjicharalambous MR, Roux BT, Feghali-Bostwick CA, Murray LA, Clarke DL, Lindsay MA. Long non-coding RNAs are central regulators of the IL-1β-induced inflammatory response in normal and idiopathic pulmonary lung fibroblasts. *Front Immunol*. (2018) 9:2906. doi: 10.3389/fimmu.2018.02906

98. Gui X, Qiu X, Tian Y, Xie M, Li H, Gao Y, et al. Prognostic value of IFN-γ, sCD163, CCL2 and CXCL10 involved in acute exacerbation of idiopathic pulmonary fibrosis. *Int Immunopharmacol*. (2019) 70:208–15. doi: 10.1016/j.intimp.2019.02.039

99. Su L, Dong Y, Wang Y, Wang Y, Guan B, Lu Y, et al. Potential role of senescent macrophages in radiation-induced pulmonary fibrosis. *Cell Death Dis*. (2021) 12:527. doi: 10.1038/s41419-021-03811-8

100. Groves AM, Johnston CJ, Williams JP, Finkelstein JN. Role of infiltrating monocytes in the development of radiation-induced pulmonary fibrosis. *Radiat Res*. (2018) 189:300–11. doi: 10.1667/RR14874.1

101. Kubo F, Ariestanti DM, Oki S, Fukuzawa T, Demizu R, Sato T, et al. Loss of the adhesion G-protein coupled receptor ADGRF5 in mice induces airway inflammation and the expression of CCL2 in lung endothelial cells. *Respir Res*. (2019) 20:11. doi: 10.1186/s12931-019-0973-6

102. Tian Y, Lv J, Su Z, Wu T, Li X, Hu X, et al. LRRK2 plays essential roles in maintaining lung homeostasis and preventing the development of pulmonary fibrosis. *Proc Natl Acad Sci U.S.A*. (2021) 118(35):e2106685118. doi: 10.1073/pnas.2106685118

103. Martinu T, McManigle WC, Kelly FL, Nelson ME, Sun J, Zhang HL, et al. IL-17A contributes to lung fibrosis in a model of chronic pulmonary graft-versus-host disease. *Transplantation*. (2019) 103:2264–74. doi: 10.1097/TP.0000000000002837

104. Rosendahl A, Kabiri R, Bode M, Cai A, Klinge S, Ehmke H, et al. Adaptive immunity and IL-17A are not involved in the progression of chronic kidney disease after 5/6 nephrectomy in mice. *Br J Pharmacol*. (2019) 176:2002–14. doi: 10.1111/bph.14509

105. Zhou S, Yin X, Mayr M, Noor M, Hylands PJ, Xu Q. Proteomic landscape of TGF-β1-induced fibrogenesis in renal fibroblasts. *Sci Rep*. (2020) 10:19054. doi: 10.1038/s41598-020-75989-4

106. Kavvadas P, Keuylian Z, Prakoura N, Placier S, Dorison A, Chadjichristos CE, et al. Notch3 orchestrates epithelial and inflammatory responses to promote acute kidney injury. *Kidney Int*. (2018) 94:126–38. doi: 10.1016/j.kint.2018.01.031

107. Brandt S, Ballhause TM, Bernhardt A, Becker A, Salaru D, Le-Deffge HM, et al. Fibrosis and immune cell infiltration are separate events regulated by cell-specific receptor notch3 expression. *J Am Soc Nephrol*. (2020) 31:2589–608. doi: 10.1681/ASN.2019121289

108. Wu Q, Sun S, Wei L, Liu M, Liu H, Liu T, et al. Twist1 regulates macrophage plasticity to promote renal fibrosis through galectin-3. *Cell Mol Life Sci*. (2022) 79:137. doi: 10.1007/s00018-022-04137-0

109. Devocelle A, Lecru L, Ferlicot S, Bessede T, Candelier JJ, Giron-Michel J, et al. IL-15 prevents renal fibrosis by inhibiting collagen synthesis: A new pathway in chronic kidney disease? *Int J Mol Sci*. (2021) 22(21):11698. doi: 10.3390/ijms222111698

110. Zheng M, Cai J, Liu Z, Shu S, Wang Y, Tang C, et al. Nicotinamide reduces renal interstitial fibrosis by suppressing tubular injury and inflammation. *J Cell Mol Med*. (2019) 23(6):3995–4004. doi: 10.1111/jcmm.14285

111. Chang FC, Liu CH, Luo AJ, Tao-Min Huang T, Tsai MH, Chen YJ, et al. Angiopoietin-2 inhibition attenuates kidney fibrosis by hindering chemokine C-C motif ligand 2 expression and apoptosis of endothelial cells. *Kidney Int*. (2022) 102 (4):780–97. doi: 10.1016/j.kint.2022.06.026

112. Maksimowski N, Williams VR, Scholey JW. Kidney ACE2 expression: Implications for chronic kidney disease. *PloS One*. (2020) 15:e0241534. doi: 10.1371/journal.pone.0241534

113. Ma FY, Han Y, Ozols E, Chew P, Vesey DA, Gobe GC, et al. Protease-activated receptor 2 does not contribute to renal inflammation or fibrosis in the obstructed kidney. *Nephrol (Carlton)*. (2019) 24:983–91. doi: 10.1111/nep.13635

114. Wilkening A, Krappe J, Mühe AM, Lindenmeyer MT, Eltrich N, Luckow B, et al. C-C chemokine receptor type 2 mediates glomerular injury and interstitial fibrosis in focal segmental glomerulosclerosis. *Nephrol Dial Transplant*. (2020) 35:227–39. doi: 10.1093/ndt/gfy380

115. Bideak A, Blaut A, Hoppe JM, Müller MB, Federico G, Eltrich N, et al. The atypical chemokine receptor 2 limits renal inflammation and fibrosis in murine progressive immune complex glomerulonephritis. *Kidney Int*. (2018) 93:826–41. doi: 10.1016/j.kint.2017.11.013

116. Kashyap S, Osman M, Ferguson CM, Nath MC, Roy B, Lien KR, et al. Ccl2 deficiency protects against chronic renal injury in murine renovascular hypertension. *Sci Rep*. (2018) 8:8598. doi: 10.1038/s41598-018-26870-y

117. Hasselbalch HC. The role of cytokines in the initiation and progression of myelofibrosis. *Cytokine Growth Factor Rev*. (2013) 24:133–45. doi: 10.1016/j.cytogfr.2013.01.004

118. Pozzi G, Carubbi C, Gobbi G, Tagliaferri S, Mirandola P, Vitale M, et al. Tracking fibrosis in myeloproliferative neoplasms by CCR2 expression on CD34(+) cells. *Front Oncol*. (2022) 12:980379. doi: 10.3389/fonc.2022.980379

119. Masselli E, Carubbi C, Pozzi G, Percesepe A, Campanelli R, Villani L, et al. Impact of the rs1024611 polymorphism of CCL2 on the pathophysiology and outcome of primary myelofibrosis. *Cancers (Basel)*. (2021) 13(11):2552. doi: 10.3390/cancers13112552

120. Masselli E, Carubbi C, Cambò B, Pozzi G, Gobbi G, Mirandola P, et al. The -2518 A/G polymorphism of the monocyte chemoattractant protein-1 as a candidate genetic predisposition factor for secondary myelofibrosis and biomarker of disease severity. *Leukemia*. (2018) 32:2266–70. doi: 10.1038/s41375-018-0088-y

121. Greiner G, Witzeneder N, Berger A, Schmetterer K, Eisenwort G, Schiefer AI, et al. CCL2 is a KIT D816V-dependent modulator of the bone marrow microenvironment in systemic mastocytosis. *Blood*. (2017) 129:371–82. doi: 10.1182/blood-2016-09-739003

122. Macanas-Pirard P, Quezada T, Navarrete L, Broekhuizen R, Leisewitz A, Nervi B, et al. The CCL2/CCR2 axis affects transmigration and proliferation but not resistance to chemotherapy of acute myeloid leukemia cells. *PloS One*. (2017) 12: e0168888. doi: 10.1371/journal.pone.0168888

123. Mazur G, Wróbel T, Butrym A, Kapelko-Słowik K, Poreba R, Kuliczkowski K. Increased monocyte chemoattractant protein 1 (MCP-1/CCL-2) serum level in acute myeloid leukemia. *Neoplasma*. (2007) 54:285–9.

124. Haub J, Roehrig N, Uhrin P, Schabbauer G, Eulberg D, Melchior F, et al. Intervention of inflammatory monocyte activity limits dermal fibrosis. *J Invest Dermatol*. (2019) 139:2144–53. doi: 10.1016/j.jid.2019.04.006

125. Park MJ, Park Y, Choi JW, Baek JA, Jeong HY, Na HS, et al. Establishment of a humanized animal model of systemic sclerosis in which T helper-17 cells from patients with systemic sclerosis infiltrate and cause fibrosis in the lungs and skin. *Exp Mol Med*. (2022) 54:1577–85. doi: 10.1038/s12276-022-00860-7

126. Jin J, Liu Y, Tang Q, Yan X, Jiang M, Zhao X, et al. Bioinformatics-integrated screening of systemic sclerosis-specific expressed markers to identify therapeutic targets. *Front Immunol*. (2023) 14:1125183. doi: 10.3389/fimmu.2023.1125183

127. Huang J, Puente H, Wareing NE, Wu M, Mayes MD, Karmouty-Quintana H, et al. STAT6 suppression prevents bleomycin-induced dermal fibrosis. *FASEB J*. (2023) 37:e22761. doi: 10.1096/fj.202200994R

128. Peng W, Kepsch A, Kracht TO, Hasan H, Wijayarathna R, Wahle E, et al. Activin A and CCR2 regulate macrophage function in testicular fibrosis caused by experimental autoimmune orchitis. *Cell Mol Life Sci*. (2022) 79:602. doi: 10.1007/s00018-022-04632-4

129. Urrego-Callejas T, Álvarez SS, Arias LF, Reyes BO, Vanegas-García AL, González LA, et al. Urinary levels of ceruloplasmin and monocyte chemoattractant protein-1 correlate with extra-capillary proliferation and chronic damage in patients with lupus nephritis. *Clin Rheumatol*. (2021) 40:1853–9. doi: 10.1007/s10067-020-05454-0

130. Pérez-Arias AA, Méndez-Pérez RA, Cruz C, Zavala-Miranda MF, Romero-Diaz J, Márquez-Macedo SE, et al. The first-year course of urine MCP-1 and its association with response to treatment and long-term kidney prognosis in lupus nephritis. *Clin Rheumatol*. (2023) 42:83–92. doi: 10.1007/s10067-022-06373-y

131. Zhang C, Chan CCY, Cheung KF, Chau MKM, Yap DYH, Ma MKM, et al. Effect of mycophenolate and rapamycin on renal fibrosis in lupus nephritis. *Clin Sci (Lond)*. (2019) 133:1721–44. doi: 10.1042/CS20190536

132. Sears SM, Sharp CN, Krueger A, Oropilla GB, Saforo D, Doll MA, et al. C57BL/6 mice require a higher dose of cisplatin to induce renal fibrosis and CCL2 correlates with cisplatin-induced kidney injury. *Am J Physiol Renal Physiol*. (2020) 319:F674–85. doi: 10.1152/ajprenal.00196.2020

133. Chanrat E, Worawichawong S, Radinahamed P, Sathirapongsasuti N, Nongnuch A, Assanatham M, et al. Urine epidermal growth factor, monocyte chemoattractant protein-1 or their ratio as predictors of complete remission in primary glomerulonephritis. *Cytokine*. (2018) 104:1–7. doi: 10.1016/j.cyto.2018.01.015

134. Gniewkiewicz MS, Czerwińska M, Gozdowska J, Czerwińska K, Sadowska A, Dęborska-Materkowska D, et al. Urinary levels of CCL2 and CXCL10 chemokines as potential biomarkers of ongoing pathological processes in kidney allograft: an association with BK virus nephropathy. *Pol Arch Intern Med*. (2019) 129:592–7. doi: 10.20452/pamw.14926

135. Kong X, Xu M, Cui X, Ma L, Cheng H, Hou J, et al. Potential role of macrophage phenotypes and CCL2 in the pathogenesis of takayasu arteritis. *Front Immunol*. (2021) 12:646516. doi: 10.3389/fimmu.2021.646516

136. Aguiar CM, Gawdat K, Legere S, Marshall J, Hassan A, Kienesberger PC, et al. Fibrosis independent atrial fibrillation in older patients is driven by substrate leukocyte infiltration: diagnostic and prognostic implications to patients undergoing cardiac surgery. *J Transl Med*. (2019) 17:413. doi: 10.1186/s12967-019-02162-5

137. Sequeira Gross TM, Lindner D, Ojeda FM, Neumann J, Grewal N, Kuntze T, et al. Comparison of microstructural alterations in the proximal aorta between aortic stenosis and regurgitation. *J Thorac Cardiovasc Surg*. (2021) 162:1684–95. doi: 10.1016/j.jtcvs.2020.03.002

138. Wang L, Wu H, Deng Y, Zhang S, Wei Q, Yang Q, et al. FTZ ameliorates diabetic cardiomyopathy by inhibiting inflammation and cardiac fibrosis in the streptozotocin-induced model. *Evidence-Based Complementary Altern Med*. (2021) 2021:1–16. doi: 10.1155/2021/5582567

139. Ott A, Tutdibi E, Goedicke-Fritz S, Schöpe J, Zemlin M, Nourkami-Tutdibi N. Serum cytokines MCP-1 and GCS-F as potential biomarkers in pediatric inflammatory bowel disease. *PloS One*. (2023) 18:e0288147. doi: 10.1371/journal.pone.0288147

140. Luo X, Wang R, Zhang X, Wen X, Deng S, Xie W. Identification CCL2,CXCR2, S100A9 of the immune-related gene markers and immune infiltration characteristics of inflammatory bowel disease and heart failure via bioinformatics analysis and machine learning. *Front Cardiovasc Med*. (2023) 10:1268675. doi: 10.3389/fcvm.2023.1268675

141. Yin YQ, Peng F, Situ HJ, Xie JL, Tan L, Wei J, et al. Construction of prediction model of inflammation related genes in idiopathic pulmonary fibrosis and its correlation with immune microenvironment. *Front Immunol*. (2022) 13:1010345. doi: 10.3389/fimmu.2022.1010345

142. Xue M, Guo Z, Cai C, Sun B, Wang H. Evaluation of the diagnostic efficacies of serological markers KL-6, SP-A, SP-D, CCL2, and CXCL13 in idiopathic interstitial pneumonia. *Respiration*. (2019) 98:534–45. doi: 10.1159/000503689

143. d'Alessandro M, Bergantini L, Cameli P, Lanzarone N, Perillo F, Perrone A, et al. BAL and serum multiplex lipid profiling in idiopathic pulmonary fibrosis and fibrotic hypersensitivity pneumonitis. *Life Sci*. (2020) 256:117995. doi: 10.1016/j.lfs.2020.117995

144. Tian T, Zhao C, Li S, Huang Z, Guo Y, Dai W, et al. Liver-targeted delivery of small interfering RNA of C-C chemokine receptor 2 with tetrahedral framework nucleic acid attenuates liver cirrhosis. *ACS Appl Mater Interfaces*. (2023) 15:10492–505. doi: 10.1021/acsami.2c22579

145. Du Y, Ding H, Chen Y, Gao B, Mao Z, Wang W, et al. A genetically engineered biomimetic nanodecoy for the treatment of liver fibrosis. *Adv Sci (Weinh)*. (2024) 11 (40):e2405026. doi: 10.1002/advs.202405026

146. Lan T, Chen B, Hu X, Cao J, Chen S, Ding X, et al. Tianhuang formula ameliorates liver fibrosis by inhibiting CCL2-CCR2 axis and MAPK/NF-κB signaling pathway. *J Ethnopharmacol*. (2024) 321:117516. doi: 10.1016/j.jep.2023.117516

147. Chen C, Yao X, Xu Y, Zhang Q, Wang H, Zhao L, et al. Dahuang Zhechong Pill suppresses colorectal cancer liver metastasis via ameliorating exosomal CCL2 primed pre-metastatic niche. *J Ethnopharmacol*. (2019) 238:111878. doi: 10.1016/j.jep.2019.111878

148. Shi H, Duan X, Dong J, Tao Y, Lei Y. RNA-seq combined network pharmacology reveals that Fu-Gan-Wan (FGW) inhibits liver fibrosis via NF-κB/CCL2/CCR2 and lipid peroxidation via Nrf2/HMOX1 signaling pathway. *J Ethnopharmacol*. (2024) 326:117963. doi: 10.1016/j.jep.2024.117963

149. Liu Z, Xiang H, Xiang D, Xiao S, Xiang H, Xiao J, et al. Revealing potential anti-fibrotic mechanism of Ganxianfang formula based on RNA sequence. *Chin Med*. (2022) 17:23. doi: 10.1186/s13020-022-00579-7

150. Krenkel O, Puengel T, Govaere O, Abdallah AT, Mossanen JC, Kohlhepp M, et al. Therapeutic inhibition of inflammatory monocyte recruitment reduces steatohepatitis and liver fibrosis. *Hepatology*. (2018) 67:1270–83. doi: 10.1002/hep.29544

151. Puengel T, Lefere S, Hundertmark J, Kohlhepp M, Penners C, Van de Velde F, et al. Combined therapy with a CCR2/CCR5 antagonist and FGF21 analogue synergizes in ameliorating steatohepatitis and fibrosis. *Int J Mol Sci*. (2022) 23(12):6696. doi: 10.3390/ijms23126696

152. Guo Y, Zhao C, Dai W, Wang B, Lai E, Xiao Y, et al. C-C motif chemokine receptor 2 inhibition reduces liver fibrosis by restoring the immune cell landscape. *Int J Biol Sci*. (2023) 19:2572–87. doi: 10.7150/ijbs.83530

153. Yu D, Cai SY, Mennone A, Vig P, Boyer JL. Cenicriviroc, a cytokine receptor antagonist, potentiates all-trans retinoic acid in reducing liver injury in cholestatic rodents. *Liver Int*. (2018) 38:1128–38. doi: 10.1111/liv.13698

154. Ambade A, Lowe P, Kodys K, Catalano D, Gyongyosi B, Cho Y, et al. Pharmacological inhibition of CCR2/5 signaling prevents and reverses alcohol-induced liver damage, steatosis, and inflammation in mice. *Hepatology*. (2019) 69:1105–21. doi: 10.1002/hep.30249

155. Bauer A, Rawa T. Circulating monocyte chemoattractant protein-1 (MCP-1) in patients with primary biliary cholangitis. *Int J Mol Sci*. (2024) 25. doi: 10.3390/ijms25021333

156. Guicciardi ME, Trussoni CE, Krishnan A, Bronk SF, Lorenzo Pisarello MJ, O'Hara SP, et al. Macrophages contribute to the pathogenesis of sclerosing cholangitis in mice. *J Hepatol*. (2018) 69:676–86. doi: 10.1016/j.jhep.2018.05.018

157. Reuveni D, Gore Y, Leung PSC, Lichter Y, Moshkovits I, Kaminitz A, et al. The critical role of chemokine (C-C motif) receptor 2-positive monocytes in autoimmune cholangitis. *Front Immunol*. (2018) 9:1852. doi: 10.3389/fimmu.2018.01852

158. Dai L, Liu Y, Cheng L, Wang H, Lin Y, Shi G, et al. SARI attenuates colon inflammation by promoting STAT1 degradation in intestinal epithelial cells. *Mucosal Immunol*. (2019) 12:1130–40. doi: 10.1038/s41385-019-0178-9

159. Wang Q, Li XL, Mei Y, Ye JC, Fan W, Cheng GH, et al. The anti-inflammatory drug dimethyl itaconate protects against colitis-associated colorectal cancer. *J Mol Med (Berl)*. (2020) 98:1457–66. doi: 10.1007/s00109-020-01963-2

160. Xue L, Jin X, Ji T, Li R, Zhuge X, Xu F, et al. Luteolin ameliorates DSS-induced colitis in mice via suppressing macrophage activation and chemotaxis. *Int Immunopharmacol*. (2023) 124:110996. doi: 10.1016/j.intimp.2023.110996

161. Liu J, Shi L, Huang W, Zheng Z, Huang X, Su Y. Homoharringtonine attenuates dextran sulfate sodium-induced colitis by inhibiting NF-κB signaling. *Mediators Inflammation*. (2022) 2022:3441357. doi: 10.1155/2022/3441357

162. Hagenlocher Y, Gommeringer S, Held A, Feilhauer K, Köninger J, Bischoff SC, et al. Nobiletin acts anti-inflammatory on murine IL-10(-/-) colitis and human intestinal fibroblasts. *Eur J Nutr*. (2019) 58:1391–401. doi: 10.1007/s00394-018-1661-x

163. Zhou Z, Lin Y, Gao L, Yang Z, Wang S, Wu B. Circadian pharmacological effects of berberine on chronic colitis in mice: Role of the clock component Rev-erbα. *Biochem Pharmacol*. (2020) 172:113773. doi: 10.1016/j.bcp.2019.113773

164. Yu Y, Bian Y, Shi JX, Gu Y, Yuan DP, Yu B, et al. Geniposide promotes splenic Treg differentiation to alleviate colonic inflammation and intestinal barrier injury in ulcerative colitis mice. *Bioengineered*. (2022) 13:14616–31. doi: 10.1080/21655979.2022.2092678

165. Tao H, Zhao H, Mo A, Shao L, Ge D, Liu J, et al. VX-765 attenuates silica-induced lung inflammatory injury and fibrosis by modulating alveolar macrophages pyroptosis in mice. *Ecotoxicol Environ Saf*. (2023) 249:114359. doi: 10.1016/j.ecoenv.2022.114359

166. Koyama KG, Goto H, Morizumi S, Kagawa K, Nishimura H, Sato S, et al. The tyrosine kinase inhibitor TAS-115 attenuates bleomycin-induced lung fibrosis in mice. *Am J Resp Cell Mol*. (2019) 60:478–87. doi: 10.1165/rcmb.2018-0098OC

167. Fusco R, Cordaro M, Siracusa R, D'Amico R, Genovese T, Gugliandolo E, et al. Biochemical evaluation of the antioxidant effects of hydroxytyrosol on pancreatitis-associated gut injury. *Antioxidants (Basel)*. (2020) 9(9):781. doi: 10.3390/antiox9090781

168. Duan LF, Xu XF, Zhu LJ, Liu F, Zhang XQ, Wu N, et al. Dachaihu decoction ameliorates pancreatic fibrosis by inhibiting macrophage infiltration in chronic pancreatitis. *World J Gastroenterol*. (2017) 23:7242–52. doi: 10.3748/wjg.v23.i40.7242

169. Tesch GHP, Pullen N, Jesson MI. Combined inhibition of CCR2 and ACE provides added protection against progression of diabetic nephropathy in Nos3-deficient mice. *Am J Physiol-Renal*. (2019) 317:F1439–49. doi: 10.1152/ajprenal.00340.2019

170. Alsheikh AJ, Dasinger JH, Abais-Battad JM, Fehrenbach DJ. CCL2 mediates early renal leukocyte infiltration during salt-sensitive hypertension. *Am J Physiol-Renal*. (2020) 318:F982–93. doi: 10.1152/ajprenal.00521.2019

171. Wang W, Ai J, Liao B, Xiao K, Lin L, Chen H, et al. The roles of MCP-1/CCR2 mediated macrophage recruitment and polarization in bladder outlet obstruction (BOO) induced bladder remodeling. *Int Immunopharmacol*. (2021) 99:107947. doi: 10.1016/j.intimp.2021.107947

172. Francque SM, Hodge A, Boursier J, Younes ZH, Rodriguez-Araujo G, Park GS, et al. Phase 2, open-label, rollover study of cenicriviroc for liver fibrosis associated with metabolic dysfunction-associated steatohepatitis. *Hepatol Commun*. (2024) 8(2):e0335. doi: 10.1097/HC9.0000000000000335

173. Friedman SL, Ratziu V, Harrison SA, Abdelmalek MF, Aithal GP, Caballeria J, et al. A randomized, placebo-controlled trial of cenicriviroc for treatment of nonalcoholic steatohepatitis with fibrosis. *Hepatology*. (2018) 67:1754–67. doi: 10.1002/hep.29477

174. Ratziu V, Sanyal A, Harrison SA, Wong VW, Francque S, Goodman Z, et al. Cenicriviroc treatment for adults with nonalcoholic steatohepatitis and fibrosis: final analysis of the phase 2b CENTAUR study. *Hepatology*. (2020) 72:892–905. doi: 10.1002/hep.31108

175. Anstee QM, Lucas KJ, Francque S, Abdelmalek MF, Sanyal AJ, Ratziu V, et al. Tropifexor plus cenicriviroc combination versus monotherapy in nonalcoholic steatohepatitis: Results from the phase 2b TANDEM study. *Hepatology*. (2023) 78:1223–39. doi: 10.1097/HEP.0000000000000439

176. Anstee QM, Neuschwander-Tetri BA, Wai-Sun Wong V, Abdelmalek MF, Rodriguez-Araujo G, Landgren H, et al. Cenicriviroc lacked efficacy to treat liver fibrosis in nonalcoholic steatohepatitis: AURORA phase III randomized study. *Clin Gastroenterol Hepatol*. (2024) 22:124–134.e1. doi: 10.1016/j.cgh.2023.04.003

177. Eksteen B, Bowlus CL, Montano-Loza AJ, Lefebvre E, Fischer L, Vig P, et al. Efficacy and safety of cenicriviroc in patients with primary sclerosing cholangitis: PERSEUS study. *Hepatol Commun*. (2021) 5:478–90. doi: 10.1002/hep4.1619

178. Nywening TM, Wang-Gillam A, Sanford DE, Belt BA, Panni RZ, Cusworth BM, et al. Targeting tumour-associated macrophages with CCR2 inhibition in combination with FOLFIRINOX in patients with borderline resectable and locally advanced pancreatic cancer: a single-centre, open-label, dose-finding, non-randomised, phase 1b trial. *Lancet Oncol*. (2016) 17:651–62. doi: 10.1016/S1470-2045(16)00078-4

179. Noel M, O'Reilly EM, Wolpin BM, Ryan DP, Bullock AJ, Britten CD, et al. Phase 1b study of a small molecule antagonist of human chemokine (C-C motif) receptor 2 (PF-04136309) in combination with nab-paclitaxel/gemcitabine in first-line treatment of metastatic pancreatic ductal adenocarcinoma. *Invest New Drugs*. (2020) 38:800–11. doi: 10.1007/s10637-019-00830-3

180. Colombo A, Basavarajaiah S, Limbruno U, Picchi A, Lettieri C, Valgimigli M, et al. A double-blind randomised study to evaluate the efficacy and safety of bindarit in preventing coronary stent restenosis. *EuroIntervention*. (2016) 12:e1385–94. doi: 10.4244/EIJY15M12_03

181. Wang D, Han S, Lv G, Hu Y, Zhuo W, Zeng Z, et al. Pancreatic acinar cells-derived sphingosine-1-phosphate contributes to fibrosis of chronic pancreatitis via inducing autophagy and activation of pancreatic stellate cells. *Gastroenterology*. (2023) 165:1488–1504.e20. doi: 10.1053/j.gastro.2023.08.029

182. Pausch TM, Aue E, Wirsik NM, Freire Valls A, Shen Y, Radhakrishnan P, et al. Metastasis-associated fibroblasts promote angiogenesis in metastasized pancreatic cancer via the CXCL8 and the CCL2 axes. *Sci Rep*. (2020) 10:5420. doi: 10.1038/s41598-020-62416-x

183. Wang X, Istvanffy R, Ye L, Teller S, Laschinger M, Diakopoulos KN, et al. Phenotype screens of murine pancreatic cancer identify a Tgf-α-Ccl2-paxillin axis driving human-like neural invasion. *J Clin Invest*. (2023) 133(21):e166333. doi: 10.1172/JCI166333

184. Kempeneers MA, Issa Y, Verdonk RC, Bruno M, Fockens P, van Goor H, et al. Pain patterns in chronic pancreatitis: a nationwide longitudinal cohort study. *Gut*. (2021) 70:1724–33. doi: 10.1136/gutjnl-2020-322117

185. Yang H, Zhang Q, Xu M, Wang L, Chen X, Feng Y, et al. CCL2-CCR2 axis recruits tumor associated macrophages to induce immune evasion through PD-1 signaling in esophageal carcinogenesis. *Mol Cancer*. (2020) 19:41. doi: 10.1186/s12943-020-01165-x

186. Higashino N, Koma YI, Hosono M, Takase N, Okamoto M, Kodaira H, et al. Fibroblast activation protein-positive fibroblasts promote tumor progression through secretion of CCL2 and interleukin-6 in esophageal squamous cell carcinoma. *Lab Invest*. (2019) 99:777–92. doi: 10.1038/s41374-018-0185-6

187. Brummer G, Fang W, Smart C, Zinda B, Alissa N, Berkland C, et al. CCR2 signaling in breast carcinoma cells promotes tumor growth and invasion by promoting CCL2 and suppressing CD154 effects on the angiogenic and immune microenvironments. *Oncogene*. (2020) 39:2275–89. doi: 10.1038/s41388-019-1141-7

frontiers | Frontiers in Immunology

TYPE Original Research
PUBLISHED 15 January 2025
DOI 10.3389/fimmu.2024.1493306

OPEN ACCESS

EDITED BY
Jian Zheng,
University of Louisville, United States

REVIEWED BY
Chiara Colarusso,
University of Salerno, Italy
Ruangang Pan,
The University of Iowa, United States

*CORRESPONDENCE
Gilles Kaplanski
gilles.kaplanski@ap-hm.fr

RECEIVED 08 September 2024
ACCEPTED 11 December 2024
PUBLISHED 15 January 2025

CITATION
Cambon A, Guervilly C, Delteil C, Potere N, Bachelier R, Tellier E, Abdili E, Leprince M, Giani M, Polidoro I, Albanese V, Ferrante P, Coffin L, Schiffrin M, Arnaud L, Lacroix R, Roque S, Forel J-M, Hraiech S, Daniel L, Papazian L, Dignat-George F and Kaplanski G (2025) Caspase-1 activation, IL-1/IL-6 signature and IFNγ-induced chemokines in lungs of COVID-19 patients.
Front. Immunol. 15:1493306.
doi: 10.3389/fimmu.2024.1493306

Caspase-1 activation, IL-1/IL-6 signature and IFNγ-induced chemokines in lungs of COVID-19 patients

Audrey Cambon[1], Christophe Guervilly[2,3], Clémence Delteil[4], Nicola Potere[5], Richard Bachelier[1], Edwige Tellier[1], Evelyne Abdili[1,6], Marine Leprince[7], Marco Giani[5], Ildo Polidoro[8], Valentina Albanese[8], Paolo Ferrante[8], Laurence Coffin[9], Michael Schiffrin[9], Laurent Arnaud[6], Romaric Lacroix[1,6], Sandrine Roque[7], Jean-Marie Forel[2,3], Sami Hraiech[2,3], Laurent Daniel[10], Laurent Papazian[11], Françoise Dignat-George[1,6] and Gilles Kaplanski[1,7]*

[1]Aix-Marseille Université, INSERM, INRAE, C2VN, Marseille, France, [2]Centre d'Etudes et de Recherches sur les Services de Santé et qualité de vie EA 3279, Aix-Marseille Université, Marseille, France, [3]Service de Médecine Intensive Réanimation, Hôpital Nord, Assistance Publique- Hôpitaux de Marseille, Chemin des Bourrely, Marseille, France, [4]Département de Médecine légale, Hôpital de la Timone, Assistance Publique-Hôpitaux de Marseille, Marseille University, Marseille, France, [5]School of Medicine and Health Sciences, "G. d'Annunzio" University of Chieti-Pescara, Chieti, Italy, [6]Service d'Hématologie et de Biologie vasculaire, CHU La Timone, APHM, Marseille, France, [7]Service de Médecine interne et d'Immunologie clinique, Assistance Publique - Hôpitaux de Marseille, Hôpital La Conception, Marseille, France, [8]Unit of Legal Medicine, "Santo Spirito" Hospital, Local Health Authority of Pescara, Pescara, Italy, [9]AB2 Bio, Lausanne, Switzerland, [10]Service d'Anatomopathologie, APHM, Aix Marseille University, Marseille, France, [11]Service de Réanimation, Centre Hospitalier de Bastia, Bastia, France

Rationale: COVID-19-associated acute-respiratory distress syndrome (C-ARDS) results from a direct viral injury associated with host excessive innate immune response mainly affecting the lungs. However, cytokine profile in the lung compartment of C-ARDS patients has not been widely studied, nor compared to non-COVID related ARDS (NC-ARDS).

Objectives: To evaluate caspase-1 activation, IL-1 signature, and other inflammatory cytokine pathways associated with tissue damage using post-mortem lung tissues, bronchoalveolar lavage fluids (BALF), and serum across the spectrum of COVID-19 severity.

Methods: Histological features were described and activated-caspase-1 labeling was performed in 40 post-mortem biopsies. Inflammatory cytokines were quantified in BALF and serum from 19 steroid-treated-C-ARDSand compared to 19 NC-ARDS. Cytokine concentrations were also measured in serum from 128 COVID-19 patients at different severity stages.

Measurements and main results: Typical "diffuse alveolar damage" in lung biopsies were associated with activated caspase-1 expression and vascular lesions. Soluble Caspase-1p20, IL-1β, IL-1Ra, IL-6 and at lower level IFNγ and CXCL-10, were highly elevated in BALF from steroid-treated-C-ARDS as well as in NC-ARDS. IL-1β appeared concentrated in BALF, whereas circulating IL-6 and

IL-1Ra concentrations were comparable to those in BALF and correlated with severity. TNFα, TNFR1 and CXCL8 however, were significantly higher in NC-ARDS compared to C-ARDS, treated by steroid.

Conclusions: In the lungs of C-ARDS, both caspase-1 activation with a predominant IL-1β/IL-6 signature and IFNγ -associated chemokines are elevated despite steroid treatment. These pathways may be specifically targeted in ARDS to improve response to treatment and to limit alveolar and vascular lung damage.

KEYWORDS

acute respiratory distress syndrome, vasculopathy, caspase-1, cytokines, bronchoalveolar fluid, COVID-19

Highlights

Caspase-1 activation and a predominant IL-1/IL-6 signature associated with IFNγ-induced chemokines remain highly detectable in the BALF of steroid-resistant COVID-19-ARDS, arguing for new multi-targeted therapeutics in COVID-19-ARDS. Lung biopsies from deceased COVID-19 patients show Diffuse Alveolar Damage and vasculopathy associated with activated-caspase-1. In the lungs of C-ARDS and NC-ARDS, a predominant caspase-1-induced IL-1β/IL-6 signature and IFNγ -induced chemokines persist.

Introduction

Coronavirus-disease-2019 (COVID-19), caused by severe-acute-respiratory-syndrome-coronavirus-2 (SARS-CoV-2) is associated with dysregulation of host immune responses (1). In severe forms, COVID-19 causes bilateral pneumonia, that rapidly progresses to acute-respiratory-distress-syndrome (ARDS) and death (1). Immunothrombosis is one of the main complications arising in severe forms of COVID-19, due to the combined hyperactivation of the immune and coagulation systems (2–5). Multiple immune pathways have been shown to play a role in the immunopathogenesis of COVID-19. Type I interferons (IFN) promote the activation of antiviral effector mechanisms and induce the production of pro-inflammatory cytokines (6, 7). Conversely, the impaired type III-IFN response observed in severe cases of COVID-19 may promote innate immunity with hyperinflammation and immunothrombosis (2, 8–10). Increased circulating levels of pro-inflammatory cytokines have been detected in patients with severe COVID-19, as well as increased activation of nuclear-factor-kappa-light chain enhancer of activated B cells (NF-kB) (11). Inflammasomes markers such as the NACHT, LRR, pyrin domain (PYD) domains-containing protein 3 (NLRP3) and the absent-in-melanoma-2 (AIM2) are also activated during COVID-19 (12). Danger-associated molecular patterns (DAMPs) and pathogen-associated molecular patterns (PAMPS) released upon tissue injury are detected by NLRP3, a cytoplasmic protein which is in turn, activated into a macromolecular complex called NLRP3-inflammasome (13, 14). The activated NLRP3-inflammasome engages through the PYD domain of ASC (apoptosis-associated speck-like protein containing a caspase recruitment domain [CARD]) pro-caspase-1, which then undergoes autocatalytic activation to caspase-1. Activated caspase-1 (Casp1p20) is then responsible for transforming pro-IL-1β and pro-IL-18 into biologically active IL-1β and IL-18, two major pro-inflammatory and pro-coagulant cytokines of the IL-1 family. Casp1p20 also cleaves gasdermin-D, which forms cytoplasmic membrane pores and triggers pyroptosis (15). During COVID-19, strong activation of the NLRP3-inflammasome and caspase-1 is induced with subsequent release of IL-1β and IL-18, although these cytokines remain difficult to detect in patient's blood (14, 16). Although controversial, caspase-1-induced pyroptotic cell death also appears to occur following SARS-CoV-2

Abbreviations: COVID, Coronavirus Disease-2019; DAMPS, Danger-associated molecular patterns; PAMPS, Pathogen-associated molecular patterns; BALF, Bronchoalveolar lavage fluids; IL-, Interleukin; IFN-γ, interferon-gamma; CXCL-, Chemokines; HMGB1, High–mobility group box 1; Il-1Ra, Interleukin- Receptor antagonist; TNFR-1, Tumor necrosis factor receptor 1; ARDS, Acute-respiratory-distress-syndrome; NF-kB, Nuclear factor kappa-light-chain; NACTH, NAIP, CIITA, HET-E et TEP1 *NTPases implicated in apoptosis and MHC transcription activation*"; *LRR*, Leucine-Rich Repeat; PYD, Pyrin Domain; NLRP3, NOD-like receptor family, pyrin domain containing 3; AIM2, Absent-In-Melanoma-2; ASC, Apoptosis-associated speck-like *protein*; CARD, Caspase Recruitment Domain; CD, Cluster Differenciation; IgG, Immunoglobin G; ECMO, Extracorporeal Membrane Oxygenation; ICU, Intensive Care Unit; IMV, Invasive Mechanical Ventilation; ARDS, Acute-Respiratory-Distress-Syndrome; RT-PCR, Reverse Transcriptase Polymerase Chain Reaction; HES, Hematoxylin, Eosin and Saffron; ELISA, Enzyme-linked Immunosorbent assay; TNF-a, Tumor necrosis factor-a; DAD, Diffuse Alveolar Damage; PBMC, Peripheral Blood Mononuclear Cells; ACE, Angiotensin-Converting Enzyme; ORF3, Open reading frame; RNA, Ribonucleic acid; Ab, antibody; PANapotosis, Pyrosis, Apoptosis, Necroptosis.

infection of mononuclear cells *in vitro* (15, 17–19). Furthermore, in humanized mice expressing the human ACE2 receptor, SARS-CoV-2 infects macrophages by binding of anti-spike IgG to CD16, resulting in NLRP3-inflammasome activation, IL-1β and IL-18 production, and pyroptosis (19–21). Both pyroptosis and necrosis play an important role in hyperinflammatory syndromes, mainly through a significant release of DAMPs, notably IL-1α, which maintains an upward inflammatory loop (20, 22–24). IL-1α induces inflammasome activation and IL-1β production and, like IL-1β, is mediated through the IL-1 receptor. Despite their central role in amplifying the innate immune response, the role of DAMPs in COVID-19 is poorly understood to date. Moreover, the specific contribution of NLRP3 inflammasome activation and IL-1 signaling to COVID-19 immunopathogenesis remains unclear. In the present study of three prospective cohorts of COVID-19-patients, we investigated caspase-1 activation and IL-1 signature using post-mortem lung tissue, bronchoalveolar lavage fluid (BALF), and serum across the spectrum of COVID-19 severity. We also investigated the hypothetical role of other important inflammatory pathways and DAMPs in COVID-19 immunopathogenesis.

Methods

Patients characteristics and samples

This prospective multicenter study was approved by the Medical Ethics Committee of Aix-Marseille-University (CPP # 1123 HPS1) and by the Assistance Publique de Marseille digital data protection delegate (RGPD2020-47). Patients were divided into three different cohorts (Supplementary Figure S1). All patients underwent a nasopharyngeal swab to confirm SARS-CoV-2 infection with RT-PCR.

Cohort A, consisted of post-mortem lung samples from 40 patients admitted to the public hospitals of Marseille (France) and "Santo Spirito" hospital in Pescara (Italy) with ARDS and SARS-CoV-2 infection who died of respiratory failure. For comparison, we used lung samples from 10 patients with ARDS and a negative RT-PCR SARS-CoV-2, who died from other causes than COVID-19: drowning, thoracic traumatism, epiglottitis, bladder perforation, aortic dissection, congenital cardiopathy and unexplained death.

Cohort B, consisted of 38 patients enrolled between July 1st, 2019 and April 23rd, 2021 in two tertiary university extracorporeal membrane oxygenation (ECMO) centers in Marseille (Hôpital Nord) and Paris (Pitié-Salpétrière). We included intubated and mechanically ventilated (IMV) adults with severe ARDS receiving veno-venous-ECMO for less than 24 hours. 19 patients were RT-PCR confirmed SARS-CoV-2 infected (C-ARDS) and 19 patients were COVID-19 free, with negative RT-PCR for SARS-CoV-2 (NC-ARDS). All C-ARDS patients received dexamethasone 6 mg intravenously for 10 days as standard treatment according to the RECOVERY protocol (17) and anticoagulation. All ARDS-patients underwent BAL and blood sampling within 48 hours of ECMO cannulation and baseline characteristics as well as clinical outcomes were recorded. BALF and serum were collected and stored at -80°C prior to analysis. BALF from 12 patients diagnosed with lung cancer were used as controls. We chose to use these controls because these patients were in diagnostic phasis. All patients had early-stage lung cancer and early-stage lung cancer is a disease with very low systemic and bronchoalveolar inflammation. Of these, 9 patients had non-small-cell lung cancer and 3 patients had small-cell lung cancer.

Cohort C, consisted of 128 patients with COVID-19 pneumonia confirmed by positive RT-PCRand lung computed tomodensitometry, admitted to public hospitals of Marseille, between March 20th, 2020 and April 14th, 2020. Patients were classified according to their clinical manifestations and severity, like in the protocol for novel coronavirus pneumonia (25). 37 patients were hospitalized in intensive care unit with critical COVID-19 and required invasive mechanical ventilation (IMV), were categorized as IMV-COVID-19 patients, (n=37); 21 patients were hospitalized in medical units with severe COVID-19 and required supplemental O_2 >6L/min to achieve peripheral oxygen saturation (SpO_2) ≥95% (severe COVID-19, n=21), 70 patients were hospitalized in medical units with COVID-19 not meeting the criteria for severe or IMV-COVID-19 and therefore categorized as moderate COVID-19 (n=70). Baseline clinical data and clinical outcomes were recorded for all patients. Serum was collected within 48 hours of hospitalization and stored at -80°C. Serum was also collected from 11 healthy volunteers COVID-19 free, with a negative RT-PCR for SARS-CoV2.

Post-mortem lung tissue sampling and characterization

The autopsies were performed by experienced forensic pathologists in accordance with published recommendations (26). The organs were studied both *in situ* and individually on the dissection table. Lungs were biopsied transparietally (pleura and lung parenchyma samples), in the posterior region and inferior lobar. Pathologic examination was performed on each organ fixed in 10% buffered formalin. Microscopic examinations of the lungs were performed on the central and peripheral areas of each inferior lobe, using 4µm sections stained with hematoxylin, eosin and saffron (HES). The most representative lung samples were analyzed by immunohistochemistry. Slides were incubated overnight at 4°C with a rabbit polyclonal antibody (Ab) anti-activated-caspase-1 (1:100; Merck, St-Louis, USA), followed by an secondary rabbit antibody and HRP-DAB. Images were acquired with the NanoZoomer S360 (Hamamatsu, Massy, France) using a 10×objective (×100 magnification) for HES and for immunohistochemistry.

Cytokine assays

Soluble Caspase-1 p20 (sCasp1p20) and human IL-1 receptor antagonist (IL-Ra) concentrations were evaluated by

QUANTIKINE ELISA assays (Bio-Techne Minneapolis, USA), IL-1α by ProQuantum Human IL-1α immunoassay (Thermo Fisher Scientific, Waltham, USA), HMGB1 by ELISA kit (Bio-Techne), IL-33 by ELISA kit (Abcam, Cambridge, UK), IL-1β by human IL-1β High-Sensitivity ELISA kit (Thermo Fisher Scientific) and soluble sNLRP3, C-X-C motif chemokine ligand (CXCL)10, IL-6, and IL-18 using specific ELISA assays (BD Biosciences, San Jose, USA). IFNγ concentration was quantified by Luminex kit (Thermo Fisher Scientific), and tumor necrosis α (TNFα), soluble tumor necrosis factor receptor-1 (sTNFR-1) and CXCL8 by Luminex kits from Merck (St-Louis, USA).

Statistical analysis

GraphPad-Prism V.9.2.0 software (GraphPad Software Inc., San Diego, USA) was used for statistical analysis. Values are presented as median with interquartile range (25%-75% percentile) for the indicated number of dosages. Comparisons between groups were performed using Mann-Whitney test for quantitative variables. Before carrying out these statistical tests, we performed a one-factor ANOVA test to highlight any significant differences between the groups. The ANOVA test with a $p<0.05$ value prompted us to perform a Mann-Whitney test, comparing the groups 2 by 2.

Associations between continuous variables were analysed using Spearman-correlation-test. Statistical significance was defined as $p<0.05$.

Results

Caspase-1 activation is mostly associated with vasculopathy in lungs with C-ARDS

We first examined pathologic findings and *in situ* caspase-1 activation in C-ARDS-related lung injury using postmortem lung samples from 40 deaths (Table 1). Typical features of alveolar injury (Figure 1A, left panel) were observed in 72.5% of cases among which 23 had diffuse alveolar damage (DAD) (Figure 1Bc). Evidence of vasculopathy was present in 34 cases distributed as follows: 8/34 with thrombo-embolisms (Figure 1Bb), 8/34 with thrombotic microangiopathy (Figure 1Bc), 6/34 with endothelitis (Figure 1Bd) and 26/34 with intimal lesions (Figures 1Bd, Be). In 20/40 of the cases, interstitial inflammation was present, mainly consisting in the presence of mononuclear cells in inflammatory lesions. We then performed immunohistochemistry on lung sections using specific anti-Casp1p20 Ab (Figure 1C). Caspase-1 activation was detected in 14 of 29 (48.2%) lung biopsies presenting with alveolar lesions, in 10/23 (43.4%) of those presenting DAD (Figure 1C, left panel), but in only in 1/10 (10%) among controls. Moreover, Casp1p20 labelling was mostly associated with endoalveolar macrophages (15/20) rather than with interstitial inflammatory cells (4/20) or pneumocytes (1/20). Casp1p20 labelling associated with vascular lesions in 90% of cases (18/20), with alveolar lesions in 70% (14/20) and with interstitial lesions in 45% (9/20).

TABLE 1 Histological analysis of lung sections from 40 patients who died of COVID-19 ARDS: frequency of alveolar, interstitial, vascular lesions and Casp1p20 expression.

TOTAL LUNG SAMPLE	40
Alveolar+Interstitial+Vascular lesions	**14/40 (35%)**
Alveolar lesions	**29/40 (72.5%)**
Casp1p20 +	*14/29*
DAD	*23/29*
DAD Casp1p20 +	*10/23*
Interstitial inflammation	**20/40 (50%)**
Casp1p20 +	9/20
Vascular lesions	**34/40 (85%)**
Casp1p20 +	18/34
Isolated TE	8/34
Isolated TMA	*8/34*
TE and TMA	*1/34*
Thrombotic lesions	***17/34 (50%)***
Endothelitis	*6/34*
Endothelitis+Intimal lesions	*10/34*
Intimal fibrosis	*14/34*
Intimal edema	*6/34*
Intimal edema+ fibrosis	*6/34*
Inflammatory lesions	***26/34 (76.4%)***
Thrombotic + inflammatory lesions	***14/34 (41.1%)***
Total Casp1p20 positive biopsies	**20/40 (50%)**
Casp1p20+ endoalveolar macrophages	*15/20 (75%)*
Casp1p20+ other inflammatory cells	*4/20*
Casp1p20+ pneumocytes *Casp1p20+ vascular lesions* *Casp1p20+ alveolar lesions* *Casp1p20+ interstitial lesions*	*1/20* *18/20 (90%)* *14/20 (70%)* *9/20 (45%)*

DAD, Diffuse Alveolar Damage; TE, Thromboembolism; TMA, Thrombotic microangiopathy. The bold/italicized values mean number/total (percent).

Elevated sNLRP3 and caspase-1 levels in BALF and serum of COVID-19 patients

First, we examined the activation of the NLRP3-inflammasome signaling pathway. sNLRP3 was significantly increased in BALF from C-ARDS and NC-ARDS patients compared to controls ($p<0.0001$, respectively; Figure 2A). Similar results were obtained when sCasp1p20 was measured in BALF (Figure 2B). sNLRP3 was also significantly increased in the serum of C-ARDS and NC-ARDS patients compared to controls ($p<0.05$ and $p<0.0001$ respectively; Figure 2A), as was sCasp1p20 in the serum of C-ARDS and NC-ARDS patients compared to controls ($p<0.001$ and $p<0.0001$, respectively; Figure 2B). However, no significant difference was found, when comparing sNLRP3 and sCasp1p20 levels in BALF from C-ARDS versus NC-ARDS patients

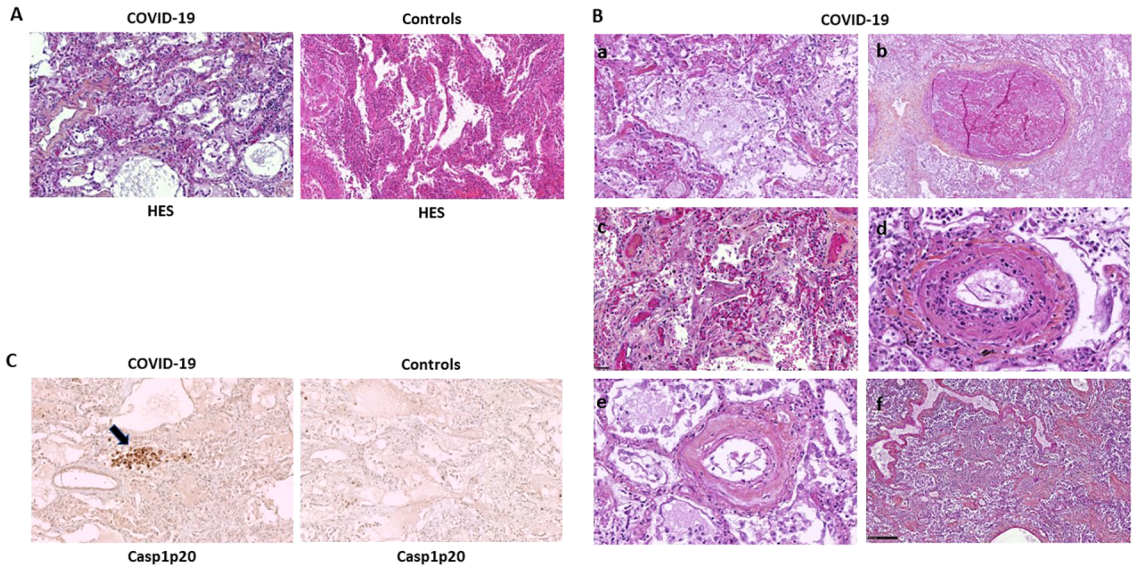

FIGURE 1
Caspase-1 activation is mostly associated with vascular lesions in C-ARDS lung samples. Paraffine-embedded lung sections (4µm) from patients who died of COVID-19 (**A**, left panel and **B**) or controls (**A**, right panel) stained by hematoxylin-eosin-saffron (HES) coloration (original magnification x100). Microscopic aspect of lesions such as Diffuse Alveolar Damage (DAD) with desquamation of alveolar epithelium (**A**, left panel and **B**a), thrombosis (**B**b), intra-alveolar fibrin deposits (**B**c), endothelitis (**B**d and **B**e) and interstitial infiltration by mononuclear inflammatory cells (**B**f). Activated Caspase-1 (Casp1p20) expression in lung sections of patients who died of COVID-19 (**C**, left panel) or controls (**C**, right panel), was analyzed by anti-Casp1p20 immunostaining of macrophages and desquamative pneumocytes (original magnification x100). Scale bar = 250µm.

(p=0.66 and p=0.16, respectively; Figures 2A, B). Importantly, sNLRP3 levels were significantly higher in BALF from C-ARDS patients compared to serum from the same patients (p<0.001; Figure 2A), while this was not true for sCasp1p20 (p>0.05, Figure 2B).

We then assessed circulating sNLRP3 and sCasp1p20 levels in relation to disease severity (Figures 2C, D). Overall, serum sNLRP3 levels were significantly increased in COVID-19 patients compared to controls at all disease stages (Figure 2C; Table 2). Similar results were obtained for sCasp1p20 levels (Figure 2D; Table 2). When stratified, sCasp1p20 levels were significantly higher in patients with severe versus moderate COVID-19 (p<0.01; Figure 2D).

Activation of the IL-1β/ IL-6 pathway in C-ARDS

To assess the consequences of NLRP3-inflammasome and caspase-1 activation in COVID-19 patients, we measured the levels of IL-1β, IL-1Ra and IL-6 in both BALF and serum of C-ARDS or NC-ARDS patients and in control subjects. Despite inter-individual variability, IL-1β (p<0.0001 and p<0.0001, respectively; Figure 3A), IL-1Ra (p<0.0001 and p<0.0001, respectively; Figure 3B) and IL6 (p<0.001 and p<0.001 respectively; Figure 3C) concentrations were significantly increased in BALF from C-ARDS and NC-ARDS patients compared to controls. In serum, IL-1β was detectable at very low concentrations but was significantly higher in C-ARDS and NC-ARDS patients compared to controls (p<0.0001 and p<0.0001, respectively; Figure 3A). In contrast, the concentrations of IL-1Ra (p<0.0001 and p<0.0001, respectively; Figure 3B) and IL-6 concentrations (p<0.0001 and p<0.0001, respectively; Figures 3C) were well detectable in the serum and significantly higher in C-ARDS and NC-ARDS than in controls. We also evaluated whether cytokine concentrations in BALF and serum differed between C-ARDS and NC-ARDS. We found no significant differences in IL-1β, IL-Ra and IL-6 concentrations in subjects with C-ARDS versus NC-ARDS in either BALF or serum (Figures 3A–C). Interestingly, IL-1β levels, from subjects with C-ARDS, were significantly higher in BALF than in serum (p<0.0001; Figure 3A), unlike IL-1Ra and IL-6 (p>0.05 and p>0.05; respectively; Figures 3B, C).

We then assessed serum IL-1β, IL-1Ra and IL-6 concentrations in COVID-19 patients according to disease severity. Serum IL-1β was increased in all COVID-19 patients compared to healthy subjects (Table 2, Figure 3D) as was IL-1Ra. (Table 2, Figure 3E), and IL-6 (Table 2, Figure 3F). Intriguingly). Interestingly, circulating IL-1β levels were lower in patients with IMV-COVID-19 compared to severe or moderate COVID-19 (Table 2, Figure 3D), while no difference was observed for IL-1Ra (p>0.05; Figure 3E). Moreover, circulating IL-6 levels were significantly higher in patients with IMV-COVID compared to severe or moderate COVID-19 (Table 2, Figure 3F).

Activation of the IL-18/IFNγ pathway in C-ARDS

Since production of IL-18/IFNγ can also be affected by NLRP3-inflammasome and caspase-1 activation, we assessed IL-18, IFNγ, and CXCL10 levels in BALF and serum of patients with C-ARDS or NC-ARDS and of control subjects. In BALF, IL-18 was elevated in both C-ARDS and NC-ARDS patients compared to the controls

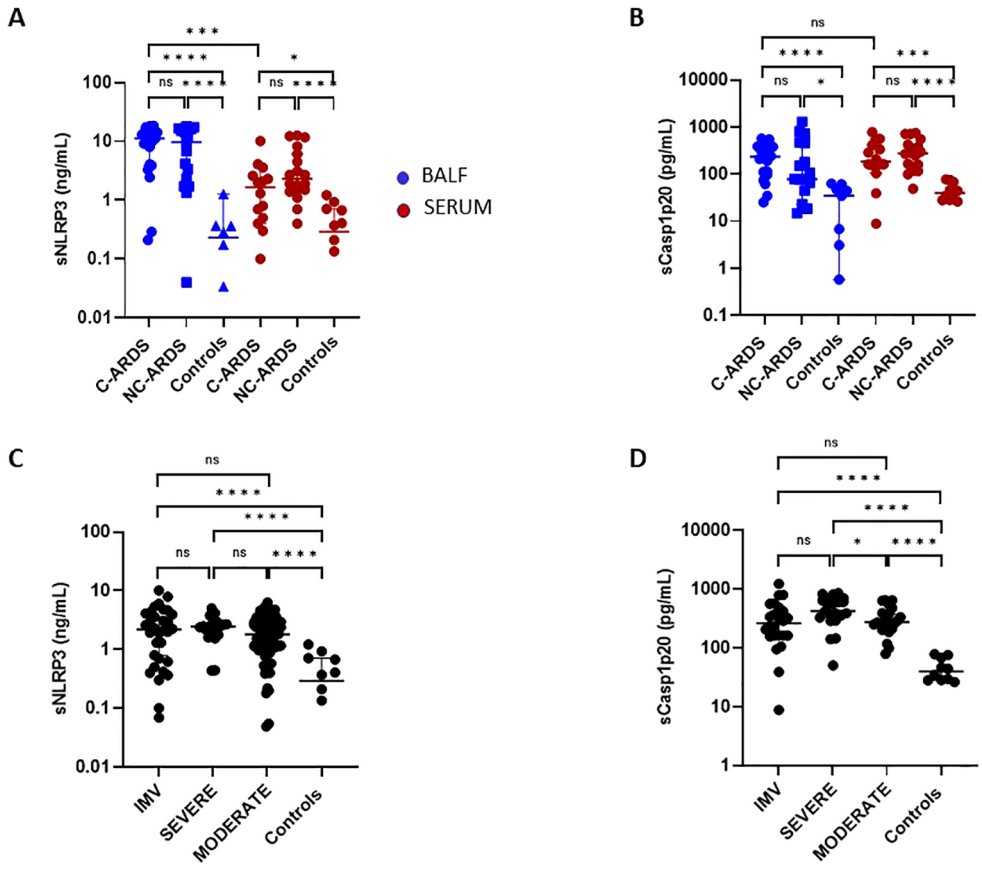

FIGURE 2
Elevated sNLRP3 and sCasp1p20 concentrations in C-ARDS and in NC-ARDS. sNLRP3 **(A)** and sCasp1p20 **(B)** proteins concentrations were measured by ELISA in the BALF (blue) from patients with COVID-19 ARDS (C-ARDS, n=19), non-COVID-19 ARDS (NC-ARDS, n=19) or with lung cancer as respective controls (Controls, n=8). Concentrations of the same proteins were measured in the serum (red) from patients with C-ARDS (n=14), NC-ARDS (n=19) or healthy donors as respective controls (n=12). sNLRP3 **(C)** proteins concentrations were measured in the serum from COVID-19 patients (**C**: n=122) and sCasp1p20 **(D)** proteins concentrations were measured in the serum from COVID-19 patients (**D**: n=69) and from healthy donors as respective controls (n=10). COVID patients were classified in IMV forms (**C**: n=32 and **D**: 24 respectively), severe forms (**C** n= 20 and **D**: n=21 respectively) and moderate forms (**C**: n= 70 and **D**: 24 respectively) and compared to controls. Numbers of patients tested for cytokines assays could varied in each cohort, according to technical difficulties. Each dot represents the value from a single individual (*p<0.05, ***p<0.001, ****p<0.0001). ns, no statistically significant.

(p<0.05 and p<0.01, respectively; Figure 4A) but detectable at very low concentrations. IL-18 was considerably higher in serum than in BALF from C-ARDS patients (p<0.0001, Figure 4A) and in serum of C-ARDS and NC-ARDS patients than in controls (p<0.001 and p<0.01 respectively; Figure 4A).

IFNγ levels in BALF were significantly higher in both C-ARDS and NC-ARDS than in controls (p<0.05 and p<0.001, respectively; Figure 4B). Conversely, serum INFγ concentrations from C-ARDS and NC-ARDS patients were not different from controls (p>0.05 respectively; Figure 4B). CXCL10 was increased in BALF from C-ARDS and NC-ARDS compared to controls (p<0.001 and p<0.05, respectively; Figure 4C) and in serum from C-ARDS and NC-ARDS compared to controls (p<0.0001 and p<0.0001, respectively; Figure 4C). However, no significant differences of CXCL10 concentrations were observed when comparing BALF from C-ARDS versus NC-ARDS (p=0.98; Figure 4C).

When stratifying according to disease severity, serum IL-18 was overall increased in all COVID-19 subgroups compared to controls (Table 2, Figure 4D). Circulating IL-18 was slightly higher in severe compared to moderate COVID-19 (p<0.05; Figure 4D), but lower in IMV-COVID-19 compared to severe COVID-19 (p<0.05; Figure 4D). Serum CXCL10 was increased in all COVID-19 patients compared to controls, (Table 2, Figure 4E). Plasma). Serum levels of CXCL10 appeared to increase with the severity of COVID-19 (Table 2, Figure 4E).

To define predictive biomarkers of severity, we then explored the correlation between serum cytokine levels and widely used scores reflective of patient clinical status. Circulating IL-1Ra and IL-6 positively correlated with SOFA score (p<0.01, respectively; Supplementary Figures S2A, B), whereas sNLRP3 concentrations positively correlated with SAPS2 score (p<0.05; Supplementary Figure S2C).

Elevated DAMPS in BALF from C-ARDS

To evaluate the pathogenic contribution of DAMPs in C-ARDS, we measured IL-1α and HMGB1 levels in BALF of C-ARDS or NC-ARDS patients and of control subjects. Both IL-1α and HMGB1 levels were detectable and significantly higher in BALF from C-ARDS and NC-ARDS patients than from controls (for IL-1α, $p<0.0001$ and $p<0.001$, respectively; Figure 5A and for HMGB1, $p<0.001$ and $p<0.0001$, respectively; Figure 5B). However, no difference was observed between patients with C-ARDS and with NC-ARDS concerning IL-1α or HMGB1 concentrations in BALF ($p=0.20$ and $p=0.3$, respectively; Figures 5A, B).

Lower TNFα, sTNFR-1 and CXCL8 concentrations in C-ARDS

To determine the contribution of other inflammatory cytokines to the immunopathogenesis of C-ARDS, we measured TNFα, TNF-R1 and CXCL8 in BALF and serum of patients with C-ARDS, NC-ARDS and of controls. Surprisingly, concentrations of TNFα, sTNFR-1 and CXCL8 in BALF of C-ARDS were significantly lower than in NC-ARDS (Table 3, Figures 5C–E), but significantly higher than in controls for sTNFR-1 and CXCL8 (Table 3, Figures 5D, E). Similarly, serum levels of TNFα, sTNFR-1 and CXCL8 in C-ARDS were significantly lower than in NC-ARDS (Table 3, Figures 5C–E) and serum levels of sTNFR-1 was higher than in controls ($p<0.0001$; Figure 5D).

Discussion

In this prospective multicenter study, we used several approaches such as histopathological and immunohistochemical analyses on post-mortem tissues from subjects with fatal C-ARDS, and immune profiling of BALF and serum from patients across the COVID-19 severity spectrum to provide information on NLRP3-inflammasome activation and the involvement of IL-1 signaling in COVID-19 patients.

Consistent with previous reports (27–30), DAD was present in almost 60% of subjects with fatal COVID-19-ARDS, and interstitial mononuclear cell inflammation in half of them. Inflammatory vascular lesions, including endothelitis, were detected in the vast majority (>80%) of subjects died of COVID-19 disease. In the same time, pulmonary thromboembolism and thrombotic microangiopathy were also frequent (>40%), confirming the idea that vasculopathy, coagulopathy and immunothrombosis contribute centrally to the pathogenesis of refractory ARDS in patients with COVID-19 (2, 29, 31–34).

Expression and localization of Casp1p20, an indicator of NLRP3-inflammasome activation, were assessed in the lungs of patients with refractory C-ARDS. Interestingly, intense Casp1p20 expression was also detected in abundance (>90%) at sites of vascular injury and vessel thrombosis, indicating a spatial association between NLRP3-inflammasome activation and COVID-19-associated vasculopathy.

In agreement with autopsy findings, increased levels of sNLRP3 and sCasp1p20 were observed in both BALF and serum from C-

TABLE 2 Associations of cytokines and pro-inflammatory proteins with COVID-19 severity.

	PLASMA										
	Median concentration (pg/ml) [CI]				p values						
	(a) IMV	(b) SSevere	(c) Moderate	(d) Healthy Donors	(a) vs (d)	(b) vs (d)	(c) vs (d)	(a) vs (b)	(a) vs (c)	(b) vs (c)	(a)+(b) +(c) vs (d)
IL-1β	0.278 [0.128-0.908]	0.4150 [0.186-0.77]	0.166 [0.1-0.297]	0.004 [0.00-0.005]	p<0.0001	p<0.0001	p<0.0001	p<0.01	p<0.01	p>0.05	p<0.0001
IL-1Ra	2446 [1567-4792]	2021[1227-7128]	1726 [592.1-4482]	240.2 [202.6-397.5]	p<0.0001	p<0.0001	p<0.0001	p=0.066	p>0.05	p>0.05	p<0.0001
IL-6	62.32 [34.39-147.1]	24.08 [13.46-67.38]	25 [14.68-46.51]	0.38 [0.00-2.50]	p<0.0001	p<0.0001	p<0.0001	p<0.001	p<0.0001	p>0.05	p<0.0001
IL-18	478.5 [404.8-798.3]	801.5 [553.5-1283]	590.5 [438.3-715]	394 [316-475]	p<0.001	p<0.0001	p<0.001	p<0.05	p>0.05	p<0.05	p<0.001
CXCL10	214.3 [125.1-339.5]	2146 [74.87-407.3]	106.4 [53.85-209.6]	15.14 [11.63-19.51]	p<0.0001	p<0.0001	p<0.0001	p<0.01	p<0.0001	p<0.01	p<0.0001
NLRP3 (ng/ml)	2.17 [0.64-4.06]	2.46[1.74-2.90]	1.79 [1.01-2.93]	0.29[0.00-0.70]	p<0.0001	p<0.0001	p<0.0001	p>0.05	p>0.05	p>0.05	p<0.0001
Casp1p20	261.1 [161.1-468.6]	421.4 [309.4-666.7]	273.3 [216.9-386.0]	39.58 [28.27-69.75]	p<0.0001	p<0.0001	p<0.0001	p>0.05	p>0.05	p<0.01	p<0.0001

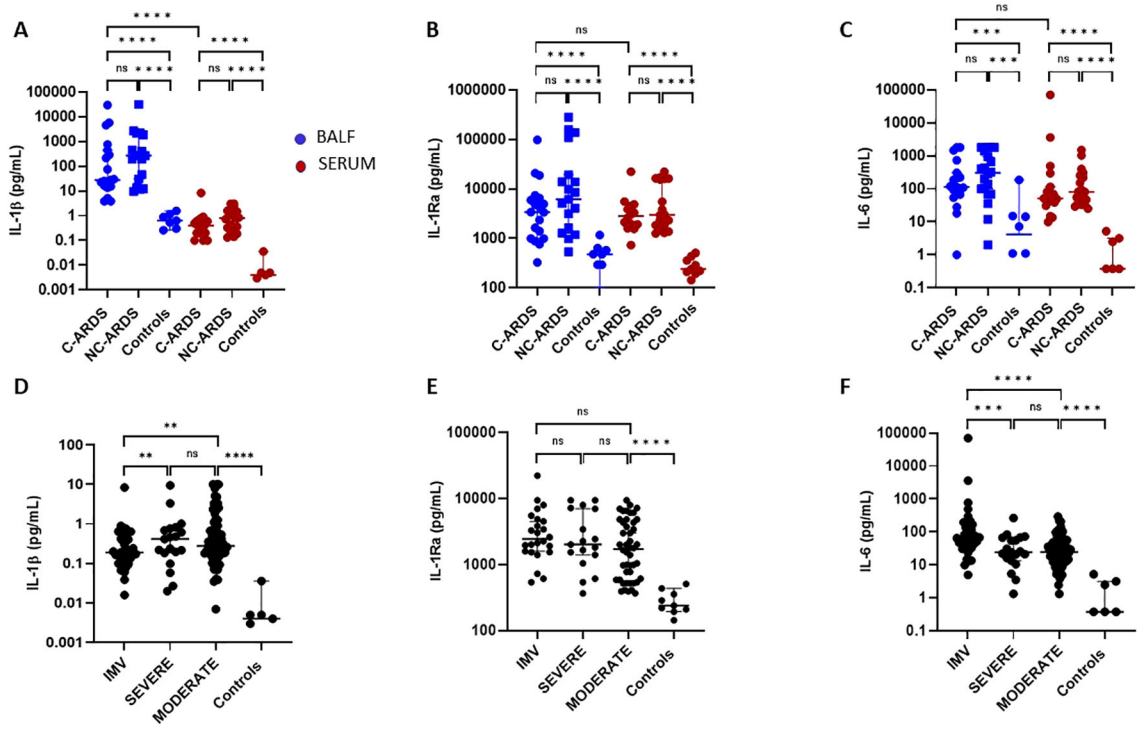

FIGURE 3
Activation of the IL-1β/IL-6 pathway in C-ARDS and in NC-ARDS. IL-1β **(A)**, IL-1Ra **(B)**, and IL-6 **(C)** concentrations were measured in the BALF (blue) from patients with C-ARDS (n=19), NC-ARDS (n=19) or with lung cancer as specific controls (Controls, n=8). Concentrations of the same proteins were measured in serum (red) from patients with C-ARDS (n=19), NC-ARDS (n=19) or healthy donors as specific controls (n=9). IL-1β **(D)**, IL-1Ra **(E)**, and IL-6 **(F)** concentrations were measured in the serum from COVID-19 patients (n=128) and healthy donors as respective controls (n=8). COVID patients were classified in IMV (**D**: n=37, **E**: n=24 and **F**: n=37 respectively), severe (**D**: n= 21, **E**: n=17 and **F**: n=21 respectively) and moderate forms (**D**: n =70, **E**: n= 46 and **F**: n=70 respectively) and compared to controls. Numbers of patients tested for cytokines assays could varied in each cohort, according to technical difficulties. Each dot represents the value from a single individual (ns: p>0.05, **p<0.01, ***p<0.001, ****p<0.0001).

ARDS, with sNLRP3 concentrations considerably higher in BALF than in serum. The lung is thus a major site of inflammasome assembly and activation during C-ARDS. In addition, serum levels of sNLRP3 and sCasp1p20 were globally increased in all COVID-19 patients, with Casp1p20 concentrations higher in severely ill compared to moderate ill patients. This suggests the involvement of caspase-1 in hyperinflammatory responses. Collectively, these findings are consistent with activation of the NLRP3-inflammasome pathway in both lungs and blood and also corroborate previous observations showing elevated Casp1p20 levels in COVID-19 patients and inflammasome activation in patient-derived PBMCs and in $CD14^{+}$ macrophages resident in COVID-19 lung tissue (17, 29, 35, 36). NLRP3-inflammasome activation can be directly triggered by multiple SARS-CoV-2-derived proteins, including spike protein and ORF3a, which act as PAMPs (19).

Activation of the NLRP3-inflammasome and subsequent cleavage of caspase-1 are responsible for the processing of IL-1β and IL-18 precursors into biologically active cytokines. In turn, IL-1β induces IL-6 synthesis, as well as the production of IL-1Ra, a natural endogenous inhibitor of IL-1. IL-18, in combination with IL-12, is a major inducer of IFNγ production (37). Due to its extremely short half-life, IL-β is usually detected at very low concentrations in the bloodstream, even in disorders typically driven by IL-1β. As expected, we observed low serum IL-β concentrations in COVID-19 patients, which were, however, significantly higher than controls. Interestingly, we found high concentrations of IL-1β (reaching >10,000pg/ml in some individuals) in BALF, indicating intense activation of the pulmonary NLRP3-inflammasome and IL-1β production during COVID-19 disease. These observations corroborate and extend data from single-cell RNA transcriptomic analyses suggesting increased IL-1β in BALF of smaller cohorts of COVID-19 patients (38–40). In contrast to IL-1β, IL-1Ra and IL-6 are generally secreted at higher concentrations and appeared elevated in both BALF and serum of COVID-19 patients. In our study, serum IL-6 correlates with the severity of COVID-19, as previously shown by others (41, 42). Our results, showing abundant expression of activated caspase-1 associated with pulmonary vascular injury and thrombosed vessels, as well as elevated levels of NLRP3, caspase-1, IL-1β and IL-6 in the pulmonary microenvironment, confirm the role of the NLRP3-inflammasome pathway in COVID-19-associated immunothrombosis, as we previously suggested (14).

IL-18 was increased in BALF but especially in the serum of C-ARDS patients compared to controls, showing a positive association with disease severity as previously described (17, 43). However, serum IL-18 levels remained lower than those observed in other hyperinflammatory syndromes (44). We found low but detectable concentrations of IFNγ in C-ARDS patients, which in BALF appeared

10.3389/fimmu.2024.1493306

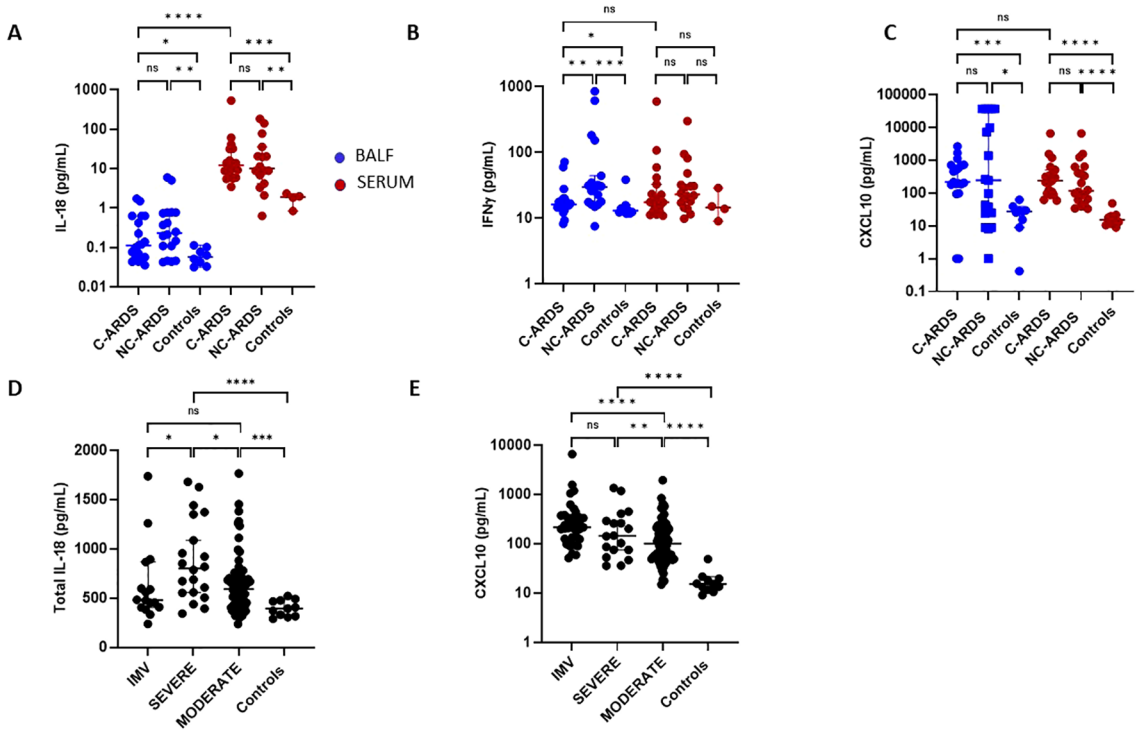

FIGURE 4
Activation of the IL-18/IFNγ pathway in C-ARDS and in NC-ARDS. IL-18 **(A)**, IFNγ **(B)** and CXCL10 **(C)** concentrations were measured in the BALF (blue) from patients with C-ARDS (n=19), NC-ARDS (n=18) and with lung cancer as specific controls (n=8). Concentrations of the same proteins were measured in serum (red) from patients with C-ARDS, (n=19), NC-ARDS, (n=19) and healthy donors as controls (**A**: n=4, **B**: n= 4 and **C**: n=11 respectively). IL-18 **(D)** and CXCL10 **(E)** concentrations were measured in serum from COVID-19 patients (n= 127) and from healthy donors as respective controls (n=11). COVID patients were classified in IMV (**D**: n=16 and **E**: n= 37, respectively), severe (n=20) and moderate forms (n= 70) and compared to controls. Numbers of patients tested for cytokines assays could varied in each cohort, according to technical difficulties. Each dot represents the value from a single individual (*p<0.05, **p<0.01, ***p<0.001, ****p<0.0001). ns, no statistically significant.

higher in C-ARDS and NC-ARDS than in controls. However, an IFNγ-induced signature is probably present in COVID-19, since CXCL10 (in common with CXCL9), an important IFNγ-induced chemokine, is highly detectable, as previously observed in several IFNγ-mediated syndromes (45). CXCL10 levels were elevated in BALF and serum of C-ARDS patients and correlated with disease severity. Several other reports have shown an elevated CXCL10 signature during COVID-19, including in BALF (39, 40, 46) and CXCL10 is a good circulating marker of disease severity (43, 47), consistent with the fact that a Th-1 signature can develop over time during severe COVID-19 (43, 48).

Inflammasome-dependent caspase-1 activation can also trigger pyroptosis with subsequent release of intracellular contents (49, 50). Increased levels of intracellular proteins such as NLRP3 and Casp1p20 observed in BALF and serum from C-ARDS patients suggest widespread cell death resulting from direct viral cytotoxicity or inflammatory damage. Consequently, we also found detectable levels of DAMPs such as IL-1α and HMGB1 in BAL of C-ARDS patients. These intranuclear proteins are released after cell death. They probably originate from injured cells of respiratory tractus, although the nature of these cells (bronchial epithelial, alveolar or endothelial…) remains uncertain. The specific contribution of DAMPs to COVID-19 immunopathogenesis remains incompletely understood, but the role of DAMPS is investigated in the review by Land et al. When viral load is too high, for example, in the respiratory tract, authors suppose a "forcing" of many virus-infected host cells to decide to commit "suicidal" regulated cell death (e.g., necroptosis, pyroptosis) associated with release of large amounts of DAMPs. Ironically, although the aim of this "suicidal" cell death is to save and restore organismal homeostasis, the intrinsic release of excessive amounts of DAMPs leads to those dysregulated hyperinflammatory responses—as typically involved in the pathogenesis of acute respiratory distress syndrome and systemic inflammatory response syndrome in respiratory viral infections (21). DAMPS could be released as a direct consequence of SARS-CoV-2 cytotoxicity, triggering cell necrosis, or indirectly because of the excessive inflammatory response, leading to necroptosis or pyroptosis associated with the release of large amounts of DAMPs. The excessive emission of DAMPS thus released into the extracellular environment could promote dysregulated hyperinflammatory responses, and pro-inflammatory programs, such as the activation of inflammasomes, notably the NLRP3 inflammasome (21, 51–53). In response to NLRP3 inflammasome activation, Caspase-1 is cleaved, resulting in pyroptosis. Moreover, IL-1ß and IL-18 released after cleavage by activated Caspase-1 belong to DAMPS. DAMPS could therefore participate in a positive feedback loop of the innate immune response induced by SARS-CoV-2 infection. The authors defined

10.3389/fimmu.2024.1493306

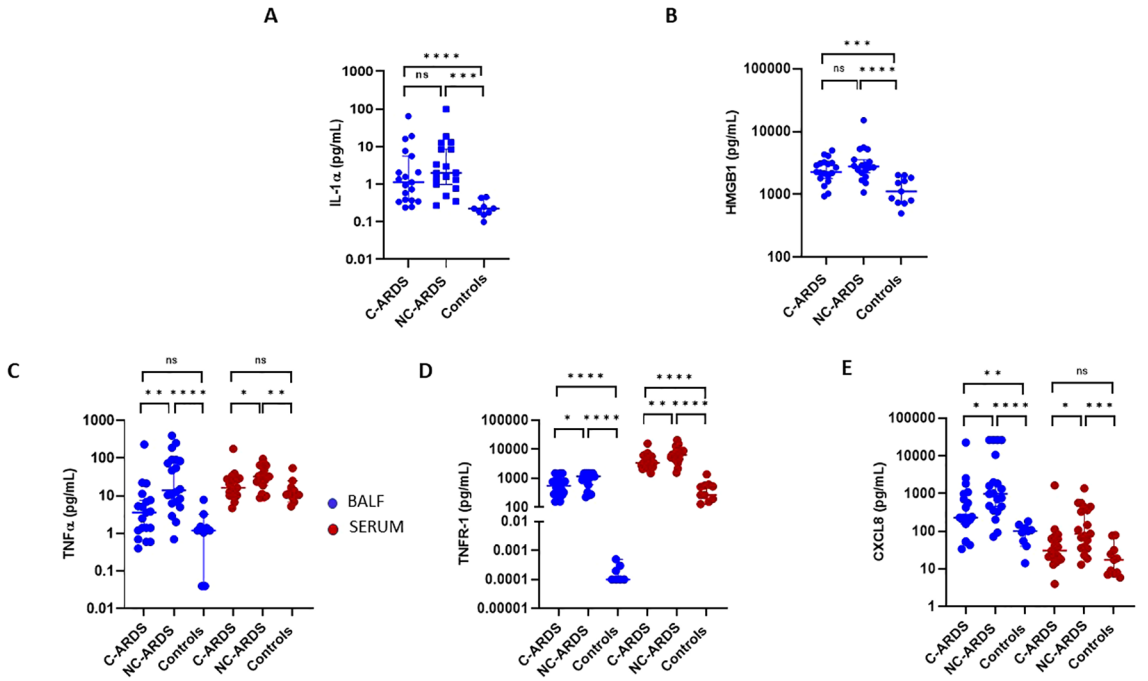

FIGURE 5
Elevated DAMPS concentrations in BALF of C-ARDS, and TNFα, sTNFR-1, CXCL8 concentrations in C-ARDS and NC-ARDS. IL-1α **(A)** and HMGB1 **(B)** concentrations were measured in the BALF from patients with C-ARDS (n=19), NC-ARDS (n=18) and with lung cancer as respective controls (n=11). TNFα **(C)**, TNFR-1 **(D)**, CXCL8 **(E)** concentrations were measured in the BALF (blue) from patients with C-ARDS (n=19), NC-ARDS, (n=19) and with lung cancer as controls (n=8). Concentrations of the same proteins were measured in serum (red) from patients C-ARDS, NC-ARDS and healthy donors as controls (n=10). Numbers of patients tested for cytokines assays could varied in each cohort, according to technical difficulties. Each dot represents the value from a single individual (*p<0.05, **p<0.01, ***p<0.001, ****p<0.0001). ns, no statistically significant.

different classes of activating DAMPS in the event of cell lysis, and suppressor DAMPS or compensatory SAMPS in the initiation of controlled defense responses favoring, depending on their balance, either inflammation or resolution of inflammation in the event of infection (21). Two studies have reported elevated circulating concentrations of HMGB1 and calprotectin (S100A8/A9, a marker of neutrophil activation) in serum from COVID-19 patients (54, 55). In a study by Renieris et al., mice injected with serum from COVID-19 patients showed elevated pulmonary expression of pro-inflammatory molecules, including TNFα, IL-6 and CXCL10 resembling human COVID-19. Treatment of these mice with anakinra (which blocks both IL-1α and IL-1β signaling) or with antibodies selectively targeting IL-1α significantly attenuated COVID-19-like pulmonary immunopathology, potentially identifying IL-1α as a mediator of inflammation and tissue-specific injury (54, 56). Taken together, these observations may help to explain the limited efficacy of the anti-IL-1β monoclonal antibody, canakinumab, compared to anakinra in COVID-19 (57–61). Aware of the limitations of these observations, we plan to pursue this work by characterizing and specifically targeting DAMPS and eventually SAMPS in BALF and serum from ARDS patients.

We found that NLRP3-inflammasome activation and concentrations of IL-1α, IL-β, IL-6, IL-1Ra or CXCL10 were broadly similar in C-ARDS and NC-ARDS. However, concentrations of TNFα, sTNF-R1 and CXCL8 both in BALF and serum, were significantly higher in NC-ARDS than in C-ARDS, suggesting that inflammatory pathways involving NF-kB could be probably more up-regulated in NC-ARDS than in C-ARDS. A more likely explanation of these results may be due to the different use of steroids, which are well-known inhibitors of NF-kB-induced gene transcription. Glucocorticoids act by modulating the gene expression of several proteins involved in the inflammatory response. The reduced transcriptional activity of NF-κB is key to the anti-inflammatory effects of glucocorticoids. As expression of many of the pro-inflammatory cytokines implicated in COVID-19 is NF-κB-dependent, including IL-6, TNFα, and CXCL10 among others (62). Indeed, all C-ARDS subjects included in this study received steroids as a part of standard and recommended treatment, whereas NC-ARDS subjects were steroids free. It should be noted that all C-ARDS patients included in this study were in fact refractory to this steroid therapy, experiencing severe clinical deterioration despite well-conducted treatment, and that in these patients, steroids demonstrated almost a poor biological inhibitory effect on IL-1α, IL-β, IL-6, IL-1Ra or CXCL10 levels (62). The deterioration of COVID-19 patients is inextricably linked to immunopathological phenomena rather than viral load. The aggressive inflammatory responses in COVID-19 result in damage to the airways, termed ARDS, which may lead to respiratory failure and death. Corticosteroid treatment reduced mortality, but subsequent meta-analyses have again highlighted the importance of timing when considering corticosteroid

TABLE 3 Cytokine concentrations in BALF and plasma from COVID-19/non-COVID-19 ARDS patients and respective controls.

	BALF						PLASMA					
	Median concentration (pg/ml) [CI]			p values			Median concentration (pg/ml) [CI]			p values		
	(a) C-ARDS	(b) NC-ARDS	(c) Cancer controls	(a) vs (c)	(b) vs (c)	(a) vs (b)	(d) C-ARDS	(e) NC-ARDS	(f) Healthy donors	(d) vs (f)	(e) vs (f)	(d) vs (e)
IL-1α	1.130 [0.37-5.58]	2 [0.94-9.51]	0.224 [0.16-0.34]	p<0.0001	p<0.0001	p>0.05	–	–	–	–	–	–
HMGB-1	2288 [1808-3178]	2785 [2131-4002]	1119 [738.1-1850]	p<0.001	p<0.0001	p>0.05	–	–	–	–	–	–
NLRP3 (ng/ml)	11210 [3.91-15.94]	9630 [1.84-16.37]	230 [0.008-0.37]	p<0.0001	p<0.0001	p>0.05	1650 [470-2850]	2850 [1470-6620]	290 [0.00-700]	p<0.05	p<0.0001	p>0.05
Casp1p20	234 [97.26-379,8]	78.43 [21.79-458.8]	34.59 [1.83-53.99]	p<0.0001	p<0.05	p>0.05	184.6 [143.5-452.6]	275.3 [122.9-455.3]	39.58 [28.27-69.75]	p<0.001	p<0.0001	p>0.05
IL-1β	27.55 [15.43-447.6]	270.3 [22.39-2028]	0.6390 [0.3048-1.165]	p<0.0001	p<0.0001	p>0.05	0.4 [0.20-0.60]	0.80 [0.326-1.59]	0.004 [0.000-0.005]	p<0.0001	p<0.0001	p=0.07
IL-1Ra	3404 [995.6-6518]	6213 [1283-19384]	478.4 [146.8-606.1]	p<0.0001	p<0.0001	p>0.05	1666 [956.8-3817]	3001 [1754-16 000]	240.2 [202.6-397.5]	p<0.0001	p<0.0001	p>0.05
IL-6	114.0 [67.00-307.0]	303.0 [77.0-1275]	4.15 [0.27-14.88]	p<0.001	p<0.001	p>0.05	51.83 [38.55-114.9]	81.02 [40.36-254.3]	0.38 [0.00-2.50]	p<0.0001	p<0.0001	p>0.05
IL-18	0.1129 [0.053-0.63]	0.23 [0.09-0.77]	0.057 [0.035-0.09]	p<0.05	p<0.01	p>0.05	12.22 [6.83-31.40]	10.11 [4.85-31.80]	1.91 [1.09-2.25]	p<0.01	p<0.001	p>0.05
IFNγ	16.14 [14.53-19.76]	29.67 [17.15-71.13]	12.98 [012.14-14.43]	p<0.05	p<0.001	p<0.01	17.48 [12.78-32.64]	23.00 [16.41-36.08]	14.46 [10.22-25.37]	p>0.05	p>0.05	p>0.05
IP10	218 [181-711]	171.0 [12.75-30219]	27.29 [12.17-34.26]	p<0.001	p>0.05	p>0.05	239.0 [98.21-6509.4]	116.2 [63.27-571.4]	15.14 [11.63-48.74]	p<0.0001	p<0.0001	p>0.05
TNFα	3.6 [1.20-7.70]	13.90 [6.45-88.88]	1.19 [0.54-2.38]	p=0.07	p<0.0001	p<0.01	16.4 [10.3-27.8]	32.5 [19.0-64.1]	11.02 [8.98-16.55]	p>0.05	p<0.01	p<0.05
TNFR-1	554.0 [285.0-800.0	1186 [598.0-1500]	0.000 [0.0001-0.0003]	p<0.0001	p<0.0001	p<0.05	3402.0 [2577.0-5775.0]	6452 [4586-8868]	266.7 [156.0-570.5]	p<0.0001	p<0.0001	p<0.01
CXCL8	232.0 [156.0-987.0]	996.0 [382.5-8460]	101.3 [48.10-134.5]	p=0.0051	p<0.0001	p<0.05	31.0 [18.00-64.00]	86 [36- 442]	17.49 [7.51-31.81]	p=0.08	p<0.001	p<0.05

10.3389/fimmu.2024.1493306

administration, as corticosteroid use was associated with increased viral load. NLRP3 inflammasome activation is strongly correlated with COVID-19 severity and part of dexamethasone's clinical effect in COVID-19 may be via NLRP3 inhibition (63). But our results suggest that these inflammatory cytokines,IL-1α, IL-β, IL-6, IL-1Ra or CXCL10, may be poorly targeted by steroids and may require to be specifically targeted in C-ARDS patients with poor response to steroids (64–66). Thus, in pursuit of this work, we aim to assess and analyze some of the anti-inflammatory cytokines, dependent from NLRP3 inflammasome pathway or from NF-κB pathway, to show how the balance between pro- and anti-inflammatory cytokines is affected in C-ARDS, NC-ARDS and control pulmonary vasculopathies, before and after steroid treatment. Furthermore, data showing similar IL-1/IL-6 cytokine profiles in C-ARDS and NC-ARDS patients suggest that these cytokine pathways may be highly activated in all types of ARDS, leading to the conclusion that ARDS should be considered as an hyperinflammatory state with DAD and severe prognosis in which novel anti-inflammatory strategies targeting these cytokines merit further mechanistic investigation (30). Specific NLRP3 inhibitors are currently undergoing clinical trials for the treatment of COVID-19 (63).

This study is limited in terms of power and clinical significance. Our control patients represented an imperfect control, since they were patients who might have incipient bronchopulmonary cancer. Bronchopulmonary cancer develops in inflammatory tumor microenvironment, which may involve the NLRP3 pathways. Tumor cell-intrinsic mechanisms of NLRP3 activation in the tumor microenvironment has been described by Tengesdal. et al (67). Aberrant activation of NLRP3 within the tumor microenvironment results in increased IL-1β and IL-18 secretion. Dysregulation of these cytokines induce tumor promoting mechanisms, such as angiogenesis, immunosuppression and metastasis. NLRP3 activation therefore represents a key immune checkpoint within the tumor microenvironnement, acting as a master switch for inflammation-mediated tumor progression. Nevertheless, according to our results from controls, ELISA protein expression levels of the inflammatory cytokines from the IL-1 family, and dependent from NLRP3 pathway, were significantly lower in BAL and in serum than in the other groups studied. Moreover, NLRP3 activation in cancer remains controversial. The role of the NLRP3 inflammasome therefore appears to be secondary in this inflammatory tumor microenvironment, after Transforming growth factor β (TGF-β). The article by Zhao et al. characterizes the tumor microenvironment in relation to carcinogenesis, and the predominant role of TGF-ß/SMAD4 signaling in cancer. TGF-β signaling pathway plays important roles in many biological processes, including cancer initiation and progression (68). Another predominantly inflammatory pathway, is interferon persistent signaling. Mathew et al. described the persistent IFN signaling as a potent immunoregulatory effect, promoting carcinogenesis. In cancer cells and immune cells, chronic IFN-I signaling is linked with cancer resistance in humans. IFN signaling thus appears to be involved in the carcinogenesis process, and argue to using combined JAK inhibition and PD-1 immunotherapy for non-small cell lung cancer patients (69). It seemed ethically difficult to propose another group controls totally asymptomatic.

Limitations of our study lie in the small number of patients in the study groups, and the missing data, resulting from mainly technical reasons, like insufficient quantity of samples or poor preservation of samples.

Finally, these results are therefore not generalizable but raise the hypothesis of an IL-1/IL-6 and IFNγ/IL-18 cytokine signature in ARDS BAL, in response to activation of the NLRP3 inflammasome in lung cells. These results are preliminary data to support clinical trials for new NLRP3 inhibitors, anti-IL-1 and anti-IL-6 therapies or JAK ½ inhibitors in COVID-ARDS and in ARDS.

As a conclusion, the results of this study support a role for the NLRP3-inflammasome activation and IL-1 in the immunopathogenesis of COVID-19. The presence of increased plasma levels of sNLRP3, sCasp1p20 and IL-1 cytokines (IL-1β, IL-18) was demonstrated in hospitalized patients across the spectrum of COVID-19 severity. Upregulation of this pro-inflammatory IL-1β/IL-6 pathway was also observed in both BALF and plasma obtained from critically ill patients with steroid-refractory-C-ARDS, but predominantly in BALF, better reflecting the inflammatory alveolar microevironment. Consistent with NLRP3-inflammasome activation, caspase-1 activation was detected on post-mortem lung tissues and mainly registered with lung-residing macrophages, localizing predominantly at the areas of alveolar injury and foremost-injured vasculature and thrombosis, hence supporting NLRP3-inflammasome activation as a putative mechanism contributing to immunothrombosis in COVID-19. IL-18/IFNγ-induced pathways also appeared to play a role in patients with steroid-resistant C-ARDS and may be insufficiently targeted by steroid therapy alone, arguing for new multi-target strategies in COVID-ARDS.

Data availability statement

The raw data supporting the conclusions of this article will be made available by the authors, without undue reservation.

Ethics statement

This prospective multicenter study was approved by the Medical Ethics Committee of Aix-Marseille-University (CPP # 1123 HPS1) and by the Assistance Publique de Marseille digital data protection delegate (RGPD2020-47). The studies were conducted in accordance with the local legislation and institutional requirements. The participants provided their written informed consent to participate in this study.

Author contributions

AC: Conceptualization, Data curation, Formal analysis, Funding acquisition, Investigation, Methodology, Project

administration, Resources, Software, Supervision, Validation, Visualization, Writing – original draft, Writing – review & editing. CG: Conceptualization, Data curation, Formal analysis, Funding acquisition, Investigation, Methodology, Project administration, Resources, Software, Supervision, Validation, Visualization, Writing – review & editing. CD: Formal analysis, Methodology, Writing – review & editing. NP: Methodology, Project administration, Resources, Supervision, Writing – review & editing. RB: Data curation, Formal analysis, Funding acquisition, Investigation, Methodology, Project administration, Resources, Supervision, Validation, Writing – review & editing. ET: Formal Analysis, Funding acquisition, Investigation, Methodology, Project administration, Resources, Visualization, Writing – review & editing. EA: Data curation, Formal analysis, Investigation, Methodology, Writing – review & editing. ML: Data curation, Investigation, Software, Writing – review & editing. MG: Data curation, Methodology, Writing – review & editing. IP: Data curation, Investigation, Methodology, Writing – review & editing. VA: Data curation, Investigation, Methodology, Writing – review & editing. PF: Data curation, Investigation, Methodology, Writing – review & editing. LC: Formal analysis, Resources, Writing – review & editing. MS: Formal Analysis, Methodology, Resources, Writing – review & editing. LA: Data curation, Formal analysis, Investigation, Methodology, Validation, Writing – review & editing. RL: Data curation, Methodology, Supervision, Validation, Visualization, Writing – review & editing. SR: Formal analysis, Methodology, Writing – review & editing. J-MF: Data curation, Formal analysis, Methodology, Writing – review & editing. SH: Data curation, Formal Analysis, Investigation, Methodology, Writing – review & editing. LD: Writing – review & editing. LP: Writing – review & editing. FD-G: Conceptualization, Resources, Writing – review & editing. GK: Conceptualization, Data curation, Formal analysis, Funding acquisition, Investigation, Methodology, Project administration, Resources, Software, Supervision, Validation, Visualization, Writing – original draft, Writing – review & editing.

Funding

The author(s) declare that no financial support was received for the research, authorship, and/or publication of this article.

Acknowledgments

To AB2 Bio EPFL Innovation Park Building B, Lausanne, Switzerland.

Conflict of interest

Authors LC and MS were employed by the company AB2 Bio. Author NP has received a training fellowship from the International Society on Thrombosis and Haemostasis ISTH, and a research grant from the International Network of VENous Thromboembolism Clinical Research Networks INVENT, outside of the present work. Author CG reported personal consulting fees from Xenios FMC outside the submitted work.

The remaining authors declare that the research was conducted in the absence of any commercial or financial relationships that could be construed as a potential conflict of interest.

Publisher's note

Supplementary material

The Supplementary Material for this article can be found online at: https://www.frontiersin.org/articles/10.3389/fimmu.2024.1493306/full#supplementary-material

SUPPLEMENTARY FIGURE 1
Flowchart of the study design including 3 cohorts of COVID-19 patients.

SUPPLEMENTARY FIGURE 2
Circulating IL-6, IL-1Ra and sNLRP3 concentrations correlated with clinical severity in C-ARDS. Correlations between circulating IL-1Ra **(A)**, IL-6 **(B)** and SOFA, or between soluble sNLRP3 and SAPS2 **(C)** in C-ARDS patients. SOFA, Sequential-Organ-Failure-Assessment; SAPS2, Simplified-Acute-Physiology-Score-2. Spearman R correlation coefficients are indicated.

References

1. Jin Y, Yang H, Ji W, Wu W, Chen S, Zhang W, et al. Virology, epidemiology, pathogenesis, and control of COVID-19. *Viruses*. (2020) 12:372. doi: 10.3390/v12040372

2. Bonaventura A, Vecchié A, Dagna L, Martinod K, Dixon DL, Van Tassell BW, et al. Endothelial dysfunction and immunothrombosis as key pathogenic mechanisms in COVID-19. *Nat Rev Immunol*. (2021) 21:319–29. doi: 10.1038/s41577-021-00536-9

3. Vallier L, Bouriche T, Bonifay A, Judicone C, Bez J, Franco C, et al. Increasing the sensitivity of the human microvesicle tissue factor activity assay. *Thromb Res*. (2019) 182:64–74. doi: 10.1016/j.thromres.2019.07.011

4. Choi D, Waksman O, Shaik A, Mar P, Chen Q, Cho DJ, et al. Association of blood viscosity with mortality among patients hospitalized with COVID-19. *J Am Coll Cardiol*. (2022) 80:316–28. doi: 10.1016/j.jacc.2022.04.060

5. Ranucci M, Ballotta A, Dedda UD, Baryshnikova E, Poli MD, Resta M, et al. The procoagulant pattern of patients with COVID-19 acute respiratory distress syndrome. *J Thromb Haemostasis*. (2022) 18:1747. doi: 10.1111/jth.14854

6. McNab F, Mayer-Barber K, Sher A, Wack A, O'Garra A. Type I interferons in infectious disease. *Nat Rev Immunol*. (2015) 15:87–103. doi: 10.1038/nri3787

7. Hadjadj J, Yatim N, Barnabei L, Corneau A, Boussier J, Smith N, et al. Impaired type I interferon activity and inflammatory responses in severe COVID-19 patients. *Science*. (2020) 369:718–24. doi: 10.1126/science.abc6027

8. Mizurini DM, Hottz ED, Bozza PT, Monteiro RQ. Fundamentals in covid-19-associated thrombosis: molecular and cellular aspects. *Front Cardiovasc Med 17 dèc*. (2021) 8:785738. doi: 10.3389/fcvm.2021.785738

9. Tang L, Yin Z, Hu Y, Mei H. Controlling cytokine storm is vital in COVID-19. *Front Immunol 30 nov*. (2020) 11:570993. doi: 10.3389/fimmu.2020.570993

10. Zhang F, Mears JR, Shakib L, Beynor JI, Shanaj S, Korsunsky I, et al. IFN-γ and TNF-α drive a CXCL10+ CCL2+ macrophage phenotype expanded in severe COVID-19 lungs and inflammatory diseases with tissue inflammation. *Genome Med 20 avr*. (2021) 13:64. doi: 10.1186/s13073-021-00881-3

11. Su C, Rousseau S, Emad A. Identification of transcriptional regulatory network associated with response of host epithelial cells to SARS-CoV-2. *Sci Rep 14 déc*. (2021) 11:23928. doi: 10.1038/s41598-021-03309-5

12. Vora SM, Lieberman J, Wu H. Inflammasome activation at the crux of severe COVID-19. *Nat Rev Immunol*. (2021) 21:694–703. doi: 10.1038/s41577-021-00588-x

13. Jo EK, Kim JK, Shin DM, Sasakawa C. Molecular mechanisms regulating NLRP3 inflammasome activation. *Cell Mol Immunol*. (2016) 13:148–59. doi: 10.1038/cmi.2015.95

14. Potere N, Del Buono MG, Caricchio R, Cremer PC, Vecchié A, Porreca E, et al. Interleukin-1 and the NLRP3 inflammasome in COVID-19: Pathogenetic and therapeutic implications. *eBioMedicine*. (2022) 85:104299. doi: 10.1016/j.ebiom.2022.104299

15. Silva CMS, Wanderley CWS, Veras FP, Gonçalves AV, Lima MHF, Toller-Kawahisa JE, et al. Gasdermin-D activation by SARS-CoV-2 triggers NET and mediate COVID-19 immunopathology. *Crit Care*. (2022) 26:206. doi: 10.1186/s13054-022-04062-5

16. Bertoni A, Penco F, Mollica H, Bocca P, Prigione I, Corcione A, et al. Spontaneous NLRP3 inflammasome-driven IL-1-β secretion is induced in severe COVID-19 patients and responds to anakinra treatment. *J Allergy Clin Immunol*. (2022) 150:796–805. doi: 10.1016/j.jaci.2022.05.029

17. Rodrigues TS, de Sá KSG, Ishimoto AY, Becerra A, Oliveira S, Almeida L, et al. Inflammasomes are activated in response to SARS-CoV-2 infection and are associated with COVID-19 severity in patients. *J Exp Med*. (2020) 218:e20201707. doi: 10.1084/jem.20201707

18. Ferreira AC, Soares VC, de Azevedo-Quintanilha IG, Dias S da SG, Fintelman-Rodrigues N, Sacramento CQ, et al. SARS-CoV-2 engages inflammasome and pyroptosis in human primary monocytes. *Cell Death Discovery 1 mars*. (2021) 7:43. doi: 10.1038/s41420-021-00428-w

19. Junqueira C, Crespo Â, Ranjbar S, Ingber J, Parry B, Ravid S, et al. SARS-CoV-2 infects blood monocytes to activate NLRP3 and AIM2 inflammasomes, pyroptosis and cytokine release. *medRxiv [Preprint]*. (2021) 8:2021.03.06.21252796. doi: 10.1101/2021.03.06.21252796

20. Cicco S, Cicco G, Racanelli V, Vacca A. Neutrophil extracellular traps (NETs) and damage-associated molecular patterns (DAMPs): two potential targets for COVID-19 treatment. *Mediators Inflamm*. (2020) 2020:7527953. doi: 10.1155/2020/7527953

21. Land WG. Role of DAMPs in respiratory virus-induced acute respiratory distress syndrome—with a preliminary reference to SARS-CoV-2 pneumonia. *Genes Immun*. (2021) 22:141–60. doi: 10.1038/s41435-021-00140-w

22. Karki R, Sharma BR, Tuladhar S, Williams EP, Zalduondo L, Samir P, et al. Synergism of TNF-α and IFN-γ Triggers inflammatory cell death, tissue damage, and mortality in SARS-coV-2 infection and cytokine shock syndromes. *Cell*. (2021) 184:149–168.e17. doi: 10.1016/j.cell.2020.11.025

23. Xu H, Akinyemi IA, Chitre SA, Loeb JC, Lednicky JA, McIntosh MT, et al. SARS-CoV-2 viroporin encoded by ORF3a triggers the NLRP3 inflammatory pathway. *Virology*. (2022) 568:13–22. doi: 10.1016/j.virol.2022.01.003

24. Shen X, He L, Cai W. Role of lipopolysaccharides in the inflammation and pyroptosis of alveolar epithelial cells in acute lung injury and acute respiratory distress syndrome. *J Inflammation Res*. (2024) 17:5855–69. doi: 10.2147/JIR.S479051

25. Wei PF. Diagnosis and treatment protocol for novel coronavirus pneumonia (Trial version 7). *Chin Med J (Engl)*. (2020) 133(9):1087–95. doi: 10.1097/CM9.0000000000000819

26. Hanley B, Lucas SB, Youd E, Swift B, Osborn M. Autopsy in suspected COVID-19 cases. *J Clin Pathol*. (2020) 73:239–42. doi: 10.1136/jclinpath-2020-206522

27. Delorey TM, Ziegler CGK, Heimberg G, Normand R, Yang Y, Segerstolpe Å, et al. COVID-19 tissue atlases reveal SARS-CoV-2 pathology and cellular targets. *Nature*. (2021) 595:107–13. doi: 10.1038/s41586-021-03570-8

28. Wichmann D, Sperhake JP, Lütgehetmann M, Steurer S, Edler C, Heinemann A, et al. Autopsy findings and venous thromboembolism in patients with COVID-19: A prospective cohort study. *Ann Intern Med*. (2020) 173(4):268–77. doi: 10.7326/M20-2003

29. Barton LM, Duval EJ, Stroberg E, Ghosh S, Mukhopadhyay S. COVID-19 autopsies, Oklahoma, USA. *Am J Clin Pathol*. (2020) 153(6):725–33. doi: 10.1093/ajcp/aqaa062

30. Serdaroglu E, Kesici S, Bayrakci B, Kale G. Diffuse alveolar damage correlation with clinical diagnosis of pediatric acute respiratory distress syndrome. *J Pediatr Intensive Care*. (2021) 10:052–7. doi: 10.1055/s-0040-1714127

31. Xu G, Qi F, Li H, Yang Q, Wang H, Wang X, et al. The differential immune responses to COVID-19 in peripheral and lung revealed by single-cell RNA sequencing. *Cell Discovery*. (2020) 6:73. doi: 10.1038/s41421-020-00225-2

32. Flaumenhaft R, Enjyoji K, Schmaier AA. Vasculopathy in COVID-19. *Blood*. (2022) 140:222–35. doi: 10.1182/blood.2021012250

33. Hottz ED, Martins-Gonçalves R, Palhinha L, Azevedo-Quintanilha IG, de Campos MM, Sacramento CQ, et al. Platelet-monocyte interaction amplifies thromboinflammation through tissue factor signaling in COVID-19. *Blood Adv*. (2022) 6:5085–99. doi: 10.1182/bloodadvances.2021006680

34. Paul O, Tao JQ, West E, Litzky L, Feldman M, Montone K, et al. Pulmonary vascular inflammation with fatal coronavirus disease 2019 (COVID-19): possible role for the NLRP3 inflammasome. *Respir Res*. (2022) 23:25. doi: 10.1186/s12931-022-01944-8

35. Aymonnier K, Ng J, Fredenburgh LE, Zambrano-Vera K, Münzer P, Gutch S, et al. Inflammasome activation in neutrophils of patients with severe COVID-19. *Blood Adv*. (2022) 6:2001–13. doi: 10.1182/bloodadvances.2021005949

36. Courjon J, Dufies O, Robert A, Bailly L, Torre C, Chirio D, et al. Heterogeneous NLRP3 inflammasome signature in circulating myeloid cells as a biomarker of COVID-19 severity. *Blood Adv*. (2021) 5:1523–34. doi: 10.1182/bloodadvances.2020003918

37. Kaplanski G. Interleukin-18: Biological properties and role in disease pathogenesis. *Immunol Rev*. (2018) 281:138–53. doi: 10.1111/imr.2018.281.issue-1

38. Xu Z, Shi L, Wang Y, Zhang J, Huang L, Zhang C, et al. Pathological findings of COVID-19 associated with acute respiratory distress syndrome. *Lancet Respir Med*. (2020) 8:420–2. doi: 10.1016/S2213-2600(20)30076-X

39. Liao M, Liu Y, Yuan J, Wen Y, Xu G, Zhao J, et al. Single-cell landscape of bronchoalveolar immune cells in patients with COVID-19. *Nat Med*. (2020) 26:842–4. doi: 10.1038/s41591-020-0901-9

40. Zhou Z, Ren L, Zhang L, Zhong J, Xiao Y, Jia Z, et al. Heightened innate immune responses in the respiratory tract of COVID-19 patients. *Cell Host Microbe*. (2020) 27:883–890.e2. doi: 10.1016/j.chom.2020.04.017

41. Bivona G, Agnello L, Ciaccio M. Biomarkers for prognosis and treatment response in COVID-19 patients. *Ann Lab Med*. (2021) 41:540–8. doi: 10.3343/alm.2021.41.6.540

42. Broman N, Rantasärkkä K, Feuth T, Valtonen M, Waris M, Hohenthal U, et al. IL-6 and other biomarkers as predictors of severity in COVID-19. *Ann Med*. (2021) 53:410–2. doi: 10.1080/07853890.2020.1840621

43. Lucas C, Wong P, Klein J, Castro TBR, Silva J, Sundaram M, et al. Longitudinal analyses reveal immunological misfiring in severe COVID-19. *Nature*. (2020) 584:463–9. doi: 10.1038/s41586-020-2588-y

44. Kessel C, Hedrich CM, Foell D. Innately adaptive or truly autoimmune: is there something unique about systemic juvenile idiopathic arthritis? *Arthritis Rheumatol*. (2020) 72:210–9. doi: 10.1002/art.41107

45. Prencipe G, Bracaglia C, Caiello I, Pascarella A, Francalanci P, Pardeo M, et al. The interferon-gamma pathway is selectively up-regulated in the liver of patients with secondary hemophagocytic lymphohistiocytosis. *PloS One*. (2019) 14:e0226043. doi: 10.1371/journal.pone.0226043

46. Zaid Y, Doré É, Dubuc I, Archambault AS, Flamand O, Laviolette M, et al. Chemokines and eicosanoids fuel the hyperinflammation within the lungs of patients with severe COVID-19. *J Allergy Clin Immunol août*. (2021) 148:368–380.e3. doi: 10.1016/j.jaci.2021.05.032

47. Diorio C, Henrickson SE, Vella LA, McNerney KO, Chase J, Burudpakdee C, et al. Multisystem inflammatory syndrome in children and COVID-19 are distinct presentations of SARS-CoV-2. *J Clin Invest*. (2020) 130:5967–75. doi: 10.1172/JCI140970

48. Basheer M, Saad E, Kananeh M, Asad L, Khayat O, Badarne A, et al. Cytokine patterns in COVID-19 patients: which cytokines predict mortality and which protect against? *Curr Issues Mol Biol*. (2022) 44(10):4735–47. doi: 10.3390/cimb44100323

49. Kelley N, Jeltema D, Duan Y, He Y. The NLRP3 inflammasome: an overview of mechanisms of activation and regulation. *Int J Mol Sci 6 juill*. (2019) 20:3328. doi: 10.3390/ijms20133328

50. Pan P, Shen M, Yu Z, Ge W, Chen K, Tian M, et al. SARS-CoV-2 N protein promotes NLRP3 inflammasome activation to induce hyperinflammation. *Nat Commun*. (2021) 12:4664. doi: 10.1038/s41467-021-25015-6

51. Silva-Lagos LA, Pillay J, van Meurs M, Smink A, van der Voort PHJ, de Vos P. DAMPening COVID-19 severity by attenuating danger signals. *Front Immunol*. (2021) 12:720192. doi: 10.3389/fimmu.2021.720192/full

52. Fan X, Song JW, Wang SY, Cao WJ, Wang XW, Zhou MJ, et al. Changes of damage associated molecular patterns in COVID-19 patients. *Infect Dis Immun*. (2021) 1:20–7. doi: 10.1097/01.ID9.0000733572.40970.6c

53. Parthasarathy U, Martinelli R, EH V, Best K, Therien AG. The impact of DAMP-mediated inflammation in severe COVID-19 and related disorders. *Biochem Pharmacol janv*. (2022) 195:114847. doi: 10.1016/j.bcp.2021.114847

54. Renieris G, Karakike E, Gkavogianni T, Droggiti DE, Stylianakis E, Andriopoulou T, et al. IL-1 mediates tissue-specific inflammation and severe respiratory failure in COVID-19. *J Innate Immun*. (2022) 14:643–56. doi: 10.1159/000524560

55. Shi H, Zuo Y, Yalavarthi S, Gockman K, Zuo M, Madison JA, et al. Neutrophil calprotectin identifies severe pulmonary disease in COVID-19. *J Leukoc Biol*. (2021) 109:67–72. doi: 10.1002/JLB.3COVCRA0720-359R

56. Silvin A, Chapuis N, Dunsmore G, Goubet AG, Dubuisson A, Derosa L, et al. Elevated calprotectin and abnormal myeloid cell subsets discriminate severe from mild COVID-19. *Cell 17 sept*. (2020) 182:1401–1418.e18. doi: 10.1016/j.cell.2020.08.002

57. Kyriazopoulou E, Panagopoulos P, Metallidis S, Dalekos GN, Poulakou G, Gatselis N, et al. An open label trial of anakinra to prevent respiratory failure in COVID-19. *Elife. 8 mars.* (2021) 10:e66125. doi: 10.7554/eLife.66125

58. Caricchio R, Abbate A, Gordeev I, Meng J, Hsue PY, Neogi T, et al. Effect of canakinumab vs placebo on survival without invasive mechanical ventilation in patients hospitalized with severe COVID-19: A randomized clinical trial. *JAMA.* (2021) 326(3):230–9. doi: 10.1001/jama.2021.9508

59. Kyriazopoulou E, Poulakou G, Milionis H, Metallidis S, Adamis G, Tsiakos K, et al. Early treatment of COVID-19 with anakinra guided by soluble urokinase plasminogen receptor plasma levels: a double-blind, randomized controlled phase 3 trial. *Nat Med.* (2021) 27(10):1752–60. doi: 10.1038/s41591-021-01499-z

60. Cauchois R, Koubi M, Delarbre D, Manet C, Carvelli J, Blasco VB, et al. Early IL-1 receptor blockade in severe inflammatory respiratory failure complicating COVID-19. *Proc Natl Acad Sci U.S.A.* (2020) 117:18951–3. doi: 10.1073/pnas.2009017117

61. Audemard-Verger A, Le Gouge A, Pestre V, Courjon J, Langlois V, Vareil MO, et al. Efficacy and safety of anakinra in adults presenting deteriorating respiratory symptoms from COVID-19: A randomized controlled trial. *PloS One.* (2022) 17:e0269065. doi: 10.1371/journal.pone.0269065

62. De Bosscher K, Vanden Berghe W, Haegeman G. The interplay between the glucocorticoid receptor and nuclear factor-kappaB or activator protein-1: molecular mechanisms for gene repression. *Endocr Rev.* (2003) 24(4):488–522. doi: 10.1210/er.2002-0006

63. Hooftman A, O'Neill LAJ. Can NLRP3 inhibitors improve on dexamethasone for the treatment of COVID-19? *Curr Res Pharmacol Drug Discovery.* (2021) 2:100048. doi: 10.1016/j.crphar.2021.100048

64. Forsyth CB, Zhang L, Bhushan A, Swanson B, Zhang L, Mamede JI, et al. The SARS-coV-2 S1 spike protein promotes MAPK and NF-kB activation in human lung cells and inflammatory cytokine production in human lung and intestinal epithelial cells. *Microorganisms.* (2022) 10:1996. doi: 10.3390/microorganisms10101996

65. Olajide OA, Iwuanyanwu VU, Lepiarz-Raba I, Al-Hindawi AA. Induction of exaggerated cytokine production in human peripheral blood mononuclear cells by a recombinant SARS-coV-2 spike glycoprotein S1 and its inhibition by dexamethasone. *Inflammation.* (2021) 44:1865–77. doi: 10.1007/s10753-021-01464-5

66. Colás-Algora N, Muñoz-Pinillos P, Cacho-Navas C, Avendaño-Ortiz J, de Rivas G, et al. Simultaneous targeting of il-1-signaling and il-6-trans-signaling preserves human pulmonary endothelial barrier function during a cytokine storm-brief report. *Arterioscler Thromb Vasc Biol.* 43(11):2213–22. doi: 10.1161/ATVBAHA.123.319695.

67. Tengesdal IW, Dinarello CA, Marchetti C. NLRP3 and cancer: pathogenesis and therapeutic opportunities. *Pharmacol Ther nov.* (2023) 251:108545. doi: 10.1016/j.pharmthera.2023.108545

68. Zhao M, Mishra L, Deng CX. The role of TGF-β/SMAD4 signaling in cancer. *Int J Biol Sci.* (2018) 14:111–23. doi: 10.7150/ijbs.23230

69. Mathew D, Marmarelis ME, Foley C, Bauml JM, Ye D, Ghinnagow R, et al. Combined JAK inhibition and PD-1 immunotherapy for non–small cell lung cancer patients. *Sci (New York NY).* (2024) 384:eadf1329. doi: 10.1126/science.adf1329

Frontiers in Immunology

Explores novel approaches and diagnoses to treat immune disorders.

The official journal of the International Union of Immunological Societies (IUIS) and the most cited in its field, leading the way for research across basic, translational and clinical immunology.

Discover the latest Research Topics

See more →

Frontiers

Avenue du Tribunal-Fédéral 34
1005 Lausanne, Switzerland
frontiersin.org

Contact us

+41 (0)21 510 17 00
frontiersin.org/about/contact